A0 4190

RECORD COPY

REPORT NO. GDC-DAA70-004 (VOL. III) COPY NO. 001

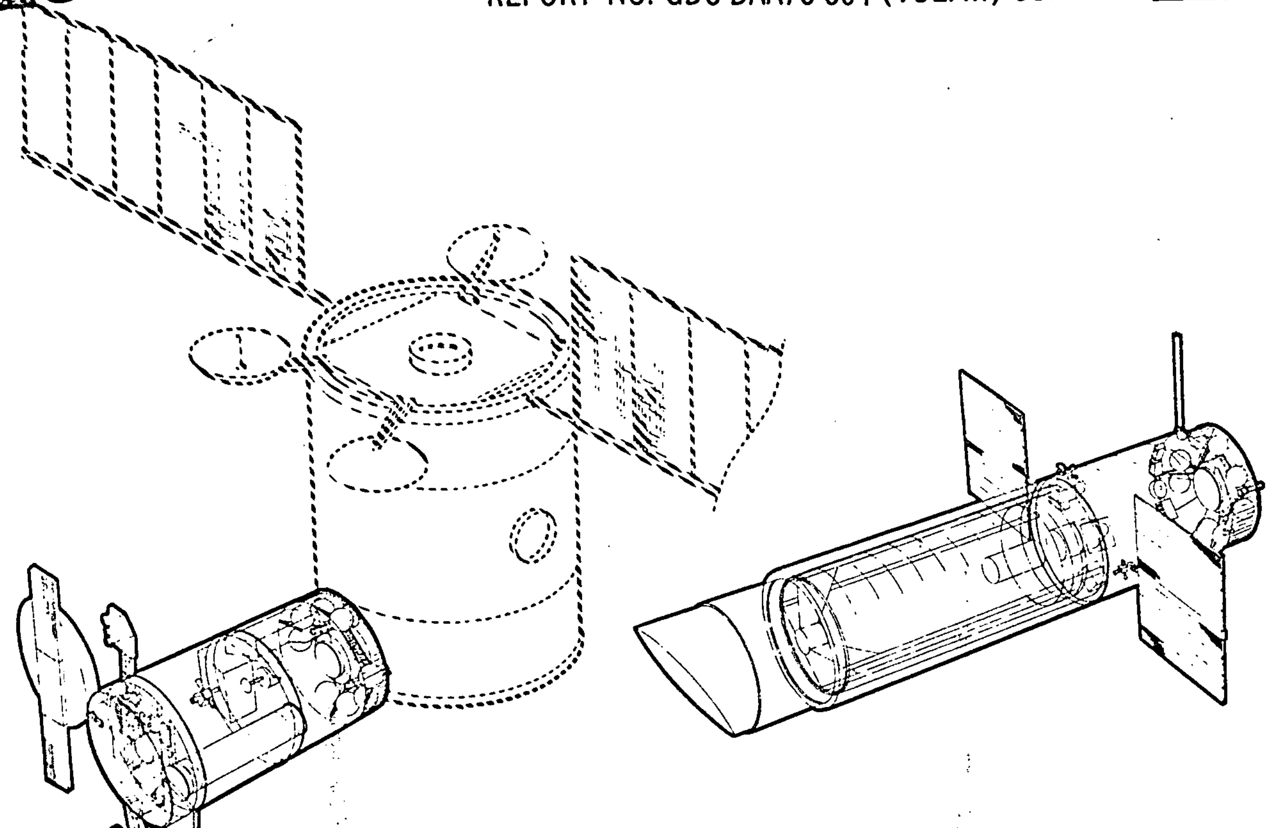

EXPERIMENT MODULE CONCEPTS STUDY

FINAL REPORT

VOLUME III · MODULE AND SUBSYSTEM DESIGN

October 1970

Prepared for
GEORGE C. MARSHALL SPACE FLIGHT CENTER
Huntsville, Alabama
Contract NAS8-25051

Advanced Space Systems, Research and Engineering
CONVAIR AEROSPACE DIVISION OF GENERAL DYNAMICS
San Diego, California

N72-14893 (NASA-CR-117656) EXPERIMENT MODULE CONCEPTS STUDY. VOLUME 3: MODULE AND SUBSYSTEM DESIGN Final Report J.R. Hunter, et al (General Dynamics/Convair) Oct. 1970 497 p CSCL 22B G3/31

Unclas
12046

Rpt-64612

INDEX OF FUNCTIONAL PROGRAM ELEMENTS

FPE NO.	TITLE	BASIC STUDY ASSIGNMENT
5.1	Grazing Incidence X-Ray Telescope	Module
5.2A	Stellar Astronomy Module	Module
5.3A	Solar Astronomy Module	Module
5.4	UV Stellar Survey	Space Station
5.5	High Energy Stellar Astronomy	Module
5.6	Space Physics Airlock Experiments	Space Station
5.7	Plasma Physics & Environmental Perturbations	Module
5.8	Cosmic Ray Physics Laboratory	Module
5.9	Small Vertebrates (Bio D)	Module
5.10	Plant Specimens (Bio E)	Module
5.11	Earth Surveys	Module
5.12	Remote Maneuvering Subsatellite	Module
5.13	Biomedical & Behavioral Research	Space Station
5.14	Man/System Integration	Space Station
5.15	Life Support & Protective Systems	Space Station
5.16	Materials Science & Processing	Module
5.17	Contamination Measurements	Module
5.18	Exposure Experiments	Module
5.19	Extended Space Structure Development	Space Station
5.20	Fluid Physics in Microgravity	Module
5.21	Infrared Stellar Survey	Space Station
5.22	Component Test & Sensor Calibration	Module
5.23	Primates (Bio A)	Module
5.24	MSF Engineering & Operations	Space Station
5.25	Microbiology (Bio C)	Space Station
5.26	Invertebrates (Bio F)	Space Station
5.27	Physics & Chemistry Laboratory	Module

GDC-DAA70-004
Contract NAS8-25051

EXPERIMENT MODULE CONCEPTS STUDY

FINAL REPORT

VOLUME III

MODULE AND SUBSYSTEM DESIGN

October 1970

Prepared by:
J. R. Hunter
D. J. Chiarappa

Approved by: D. J. Powell
D. J. Powell, Study Manager

W. W. Withee
W. W. Withee, Director
Advanced Space Systems
Research and Engineering

Prepared for
GEORGE C. MARSHALL SPACE FLIGHT CENTER
Huntsville, Alabama
Contract NAS8-25051

Advanced Space Systems, Research and Engineering
CONVAIR AEROSPACE DIVISION OF GENERAL DYNAMICS
San Diego, California

FOREWORD

This final report is submitted in accordance with the requirements of Appendix 3 — Reports and Visual Aids Requirements, Statement of Work, Experiment Module Concepts Study, Contract NAS8-25051, as amended by Amendment No. 2 dated 9 March 1970.

It comprises the following documents:

Volume I — Management Summary
Volume II — Experiments & Mission Operations
Volume III — Module & Subsystem Design
Volume IV — Resource Requirements
Volume V — Book 1 Appendix A Shuttle-Only Task
Book 2 Appendix B Commonality Analysis
Appendix C Maintenance Analysis

The study was conducted under the program and technical direction of Max E. Nein and Jean R. Olivier, PD-MP-A, of the George C. Marshall Space Flight Center, National Aeronautics and Space Administration. Dr. Rodney W. Johnson, OMSF (Code MF), as study sponsor furnished valuable guidance and assistance.

Other NASA centers and offices made significant contributions of advice, consultation, and documentation to the performance of the tasks, the results of which are reported here. Personnel from OMSF, OSSA, OART, MSFC, MSC, GSFC, LeRC, and Ames RC took part in periodic reviews during the study.

Convair Aerospace Division of General Dynamics was assisted by TRW Systems Group, Redondo Beach, California, in the performance of this contract. Personnel of both companies who contributed to this report are listed in Vol. I, Management Summary.

Comments or requests for additional information should be directed to the following:

M. E. Nein, PD-MP-A
J. R. Olivier, PD-MP-A
National Aeronautics and Space Administration
George C. Marshall Space Flight Center
Alabama 35812
Telephone: (205) 453-3427

D. J. Powell
Convair Aerospace Division of
General Dynamics
P.O. Box 1128, Mail Zone 501-10
San Diego, California 92112
Telephone: (714) 277-8900, Ext. 1941

OBJECTIVES AND GROUND RULES

OBJECTIVES

The primary objectives of this study are:

- To define the minimum number of standardized module concepts that will satisfy the NASA Candidate Experiment Program for Manned Space Stations at least cost.
- To define the module interfaces with other elements of the manned space program such as the space station, space shuttle, ground stations, and the experiments themselves.
- To define the total experiment module program resource and test requirements including SRT-ART.
- To determine the effect on experiment program implementation of shuttle-only operations.

GROUND RULES

The ground rules listed here evolved during the course of the study from the set provided at initiation of effort. They illustrate the reference framework within which results were developed.

General

Primary consideration will be given to the development of the minimum number of basic module concepts that through reasonable modification will be capable of accommodating all of the candidate experiment groups at least cost.

Experiments

1. NHB 7150.XX, "Candidate Experiment Program for Manned Space Stations" (Blue Book) will be used as an illustrative program of experiments to be integrated into the space station core module or into separately launched experiment/laboratory modules to assure that the system has the inherent capabilities to support those specific experiments and other experiments not yet identified.

2. Where not otherwise stated, the Blue Book period of experiment implementation will be two years.

3. All experiment equipment shall be assumed to have self-contained calibration capability.

Mission and Operations

1. The modules shall be capable of operating in conjunction with a space station in an orbit of 55 degrees inclination and 200-300 n.mi. altitude. The modules will not necessarily operate in this altitude range and inclination.

2. For a limited number of experiment groups the preferred alternate missionof sun synchronous (polar) orbit at an altitude of 200 n.mi. may be specified.

3. Experiment/laboratory modules may be operated in free-flying, docked, or permanently attached modes and may or may not be manned during their operation. However, all experiment modules operating in detached mode will be unmanned.

4. NASA will specify the operating mode and servicing mode for each experiment group. In some cases, concepts for particular experiment groups may be required for more than one operating and/or servicing mode.

5. Modules that operate in a free-flying mode and do not require the frequent attention of man for operation should have the capability of command and control by a station or logistics spacecraft and from the ground.

6. Modules docked to the space station for servicing or operation should be assumed to be docked to a zero gravity station or a non-rotating hub of an artificial gravity station.

7. Unless a space tug is available, all modules designed for detached operation shall have the inherent capability of returning to and docking with the space station.

8. Rendezvous operations bring the module within 3000 feet of the space station with a maximum relative velocity of 5 ft/sec. Docking operations continue from there to contact. Automatic docking will be the preferred mode.

9. Attached modules shall have the capability of changing docked position on the space station once during a two-year period.

10. All detached modules shall operate depressurized.

Configurations

1. Where practical from a payload standpoint, the modules should be compatible with manned logistics systems consisting of Saturn IB-Modified CSM, Titan III - Big Gemini, S-IC/S-IVB-Modified CSM, and S-IC/S-IVB Big Gemini. Consideration should also be given to launching the modules in an unmanned mode on the above launch vehicles. The possibility of transporting the modules in an advanced logistics system should also be examined.

2. To the extent practical, experiment/laboratory modules will be designed to be compatible for launch on both expendable and reusable launch vehicles.

3. Modules and equipment will be designed for the axial and lateral accelerations associated with the launch vehicle specified.

4. Experiment equipment and module subsystems will be completely assembled/installed on the ground and checked out prior to launch. Assembly in space will be avoided. However, to permit flexibility in updating equipment (and meeting maintenance requirements) designs should provide the capability for equipment replacement both on the ground and in orbit.

5. When docked to the space station, the modules will derive, for the most part, the electrical power, communications support, environmental control and life support, data processing facilities, and crew sytems needs (food preparation, hygiene, sleeping quarters) from the main space station. Careful attention should be given to the definition of the support required from the station and/or manned logistics spacecraft for each module and the module-station, module-logistics spacecraft, and module-experiment interfaces.

6. The experiment/laboratory modules will be designed for efficient utilization of the support services that the space station and the logistics systems can provide. The experiment/laboratory modules will supply services or supplement services that are inadequate (e.g., the space station cannot accept rejected heat).

7. All fluid interfaces with the space station may be assumed to be umbilical at the docking port.

8. A means will be provided to jettison modules from the space station as an emergency measure in event of a major hazard (fire, overpressure, etc.).

9. Modules shall be designed for a nominal two-year mission, with refurbishment in space at end of two years to extend life up to 10 years.

10. Servicing and maintenance of the modules and their experiments will be accomplished without EVA and in a shirtsleeve environment to the maximum practical extent. Possible exception to this would be the inspection and maintenance of externally mounted subsystems such as solar panels and RCS motors.

11. Means will be provided to accomplish inspection, servicing, repair and/or replacement of all equipment items not accessible from the module interior.

12. Modules will be designed for crew servicing, maintenance, and updating in a docked or hangared mode or by on-site repair from a docked tug.

13. Appropriate safety features (such as high voltage protection, adequate ingress/egress provisions, non-toxic and non-flammable materials, protrusion protection, etc.) will be incorporated into the design and maintenance aspects of each module concept. A crew safety analysis will be conducted to identify potential safety problems associated with the operation, servicing and maintenance of each module concept.

14. For the baseline module system no electronic data storage capability will be provided aboard modules. Centralized facilities on the space station/ground will be used. Over-the-horizon capability for detached modules will be studied as a modular add-on subsystem and costs.

15. Optical surfaces will be protected during the firing of RCS thrusters.

16. Leakage from pressurized modules will be assumed as follows:

0.08 lb per day per linear foot of breakable seal

0.04 lb per day per linear foot of static seal

0.0001 lb per day per square foot of pressurized surface area.

Shuttle-Only Mode

Ground rules peculiar to this task are given in Volume V, Appendix A.

TABLE OF CONTENTS

PRECEDING PAGE BLANK NOT FILMED

TABLE OF CONTENTS, Contd

TABLE OF CONTENTS, Contd

TABLE OF CONTENTS, Contd

LIST OF FIGURES

LIST OF FIGURES, Contd

LIST OF FIGURES, Contd

LIST OF FIGURES, Contd

LIST OF FIGURES, Contd

LIST OF FIGURES, Contd

LIST OF TABLES

LIST OF TABLES, Contd

LIST OF TABLES, Contd

LIST OF TABLES, Contd

SECTION 1

CONFIGURATIONS

1.1 BASELINE COMMON MODULES

An early task in the study of experiment modules was the conceptual design of customized modules for the various experiment groups. This group of concepts provided the basis for the subsequent commonality analysis that determined the experiment program cost effects of assigning various experiment groups to common modules. This analysis is described in detail in Appendix B of Volume V.

The commonality analysis objective was to examine the custom module concepts to determine if experiment program costs could be minimized through the use of common modules. A common module is defined as one whose configuration and subsystems permit it to accommodate any one of a group of FPEs considered in its synthesis. Thus, the degree of commonality ranges from a single concept to accommodate all FPEs to custom-designed modules for each FPE. The high cost for custom-designed modules is due to the nonrecurring costs associated with multiple development programs. A single module concept minimizes nonrecurring costs, but results in cost penalties associated with the excess capabilities of oversized and/or overdesigned subsystems. The commonality analysis procedure identified a minimum in the curve between these two points. The analysis shown in Figure 1-1 consisted of four major activities:

a. Common Module Synthesis — A procedure wherein concept data was analyzed to determine commonality trends in module subsystem requirements. Engineering analysis and cost guidelines were used to synthesize sets of common modules.

b. Design Verification — A procedure whereby each common module defined above was subjected to detailed design and subsystem analyses to ensure the feasibility of the module to accommodate each FPE assigned.

c. Candidate Selection — A cost analysis of each set of verified common modules was made to determine the least-cost set of modules of each set size. Minimization of experiment program costs was the primary criterion used in candidate selection.

d. Sensitivity Analyses — The initial least-cost solution was examined to determine sensitivity to interfaces, ground rules, abnormal experiment requirements, and experiment reassignments.

Conclusions resulting from the commonality analysis were:

a. The minimum cost group contains two to four common modules.

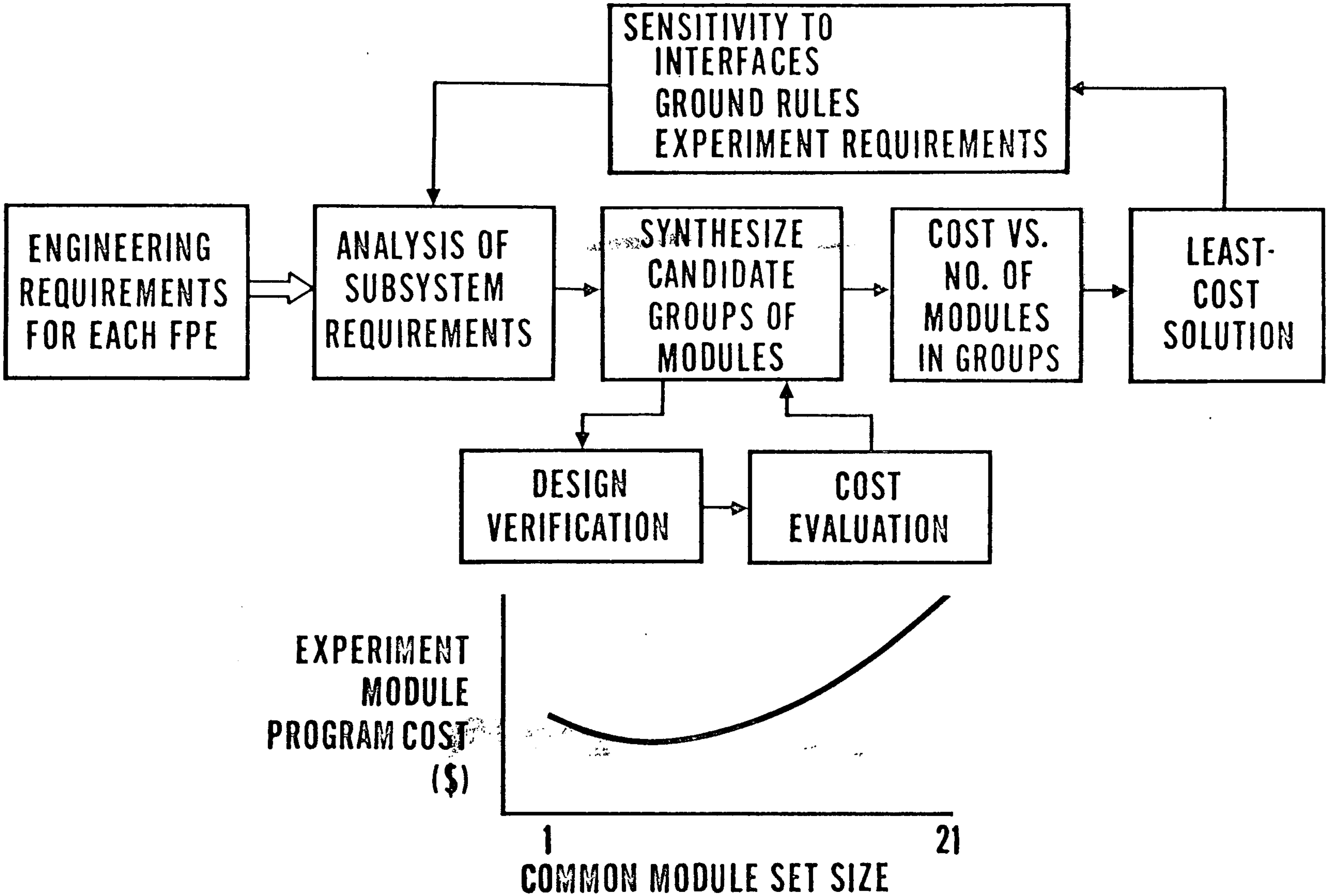

Figure 1-1. Commonality Approach

b. Variation of total program cost is relatively small for two to five common modules, but increases rapidly for more than five common modules.

c. Further design optimization of groups will not affect location of the minimum.

d. A total program cost saving of about 50% is achievable by implementing the module commonality approach.

The original derived common module set has been subjected to continuing re-examination and trade studies aimed at reducing cost and effecting operational improvements. This has resulted in considerable refinement of the common modules during the study, and this evolution is illustrated in Figure 1-2. The final common module set exhibiting wide commonality is depicted in Figure 1-3. They consist of three types of modules: one free-flying module and two modules that operate attached to the space station. A propulsion unit is attached to the CM-1 module for performance of experiments requiring low but sustained accelerations. The experiment allocations are listed in Table 1-1. Implementation of the total experiment program requires thirteen common modules as illustrated in Figure 1-4. Five CM-1, five CM-3 and three CM-4 modules are required. Experiments and experiment-peculiar equipment and structure are shaded.

It can be seen that the CM-1 pressure bulkheads are experiment-peculiar. A common flat pressure bulkhead is used on all CM-3 and two CM-4 modules. It would be a "leave-off" item for the FPE 5.11, Earth Surveys, CM-4.

These common module designs provide for the experiment program as defined. Experiment-peculiar systems include two centrifuges, a cosmic ray instrumentation bay, and fluid physics test tankage. The feasibility, economy, and practicality of these modules hinges on factors that do not affect the approach or results of the commonality process, but are important to the validity of the common module concepts. They are:

a. The degree to which the common module design has been impacted by very stringent requirements of a single or only a few experiments.

b. The degree to which modules can accommodate growth in the defined experiments.

d. The compatibility of modules with launch vehicles and the degree to which this compatibility may be improved to permit less expensive launches, including use of the shuttle.

d. The flexibility of the modules to accommodate experiment programs currently assigned as integral to the space station, such as the Biomedical/Behavioral group of FPEs.

ORIGINAL COMMON MODULE SET

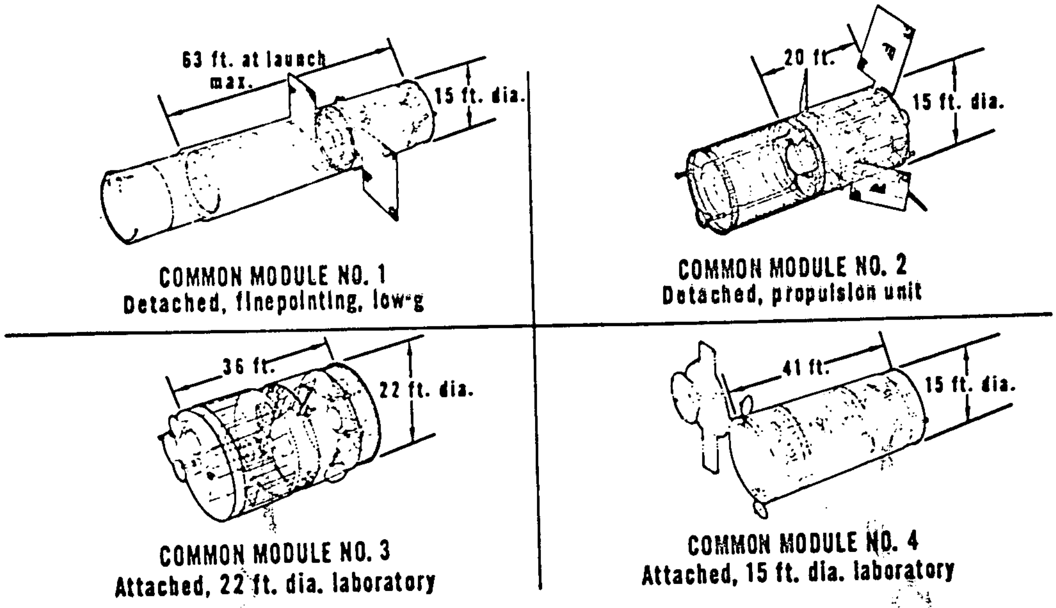

REVISED COMMON MODULE SET

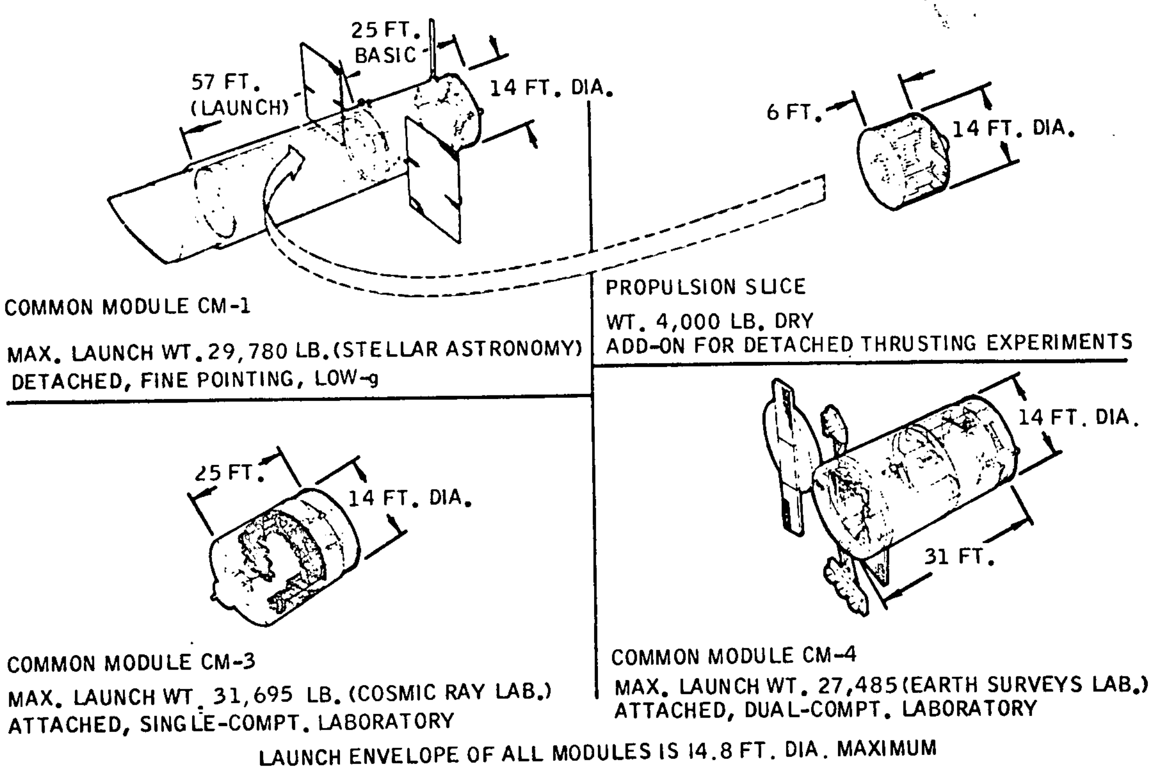

Figure 1-2. Evolution of Common Modules

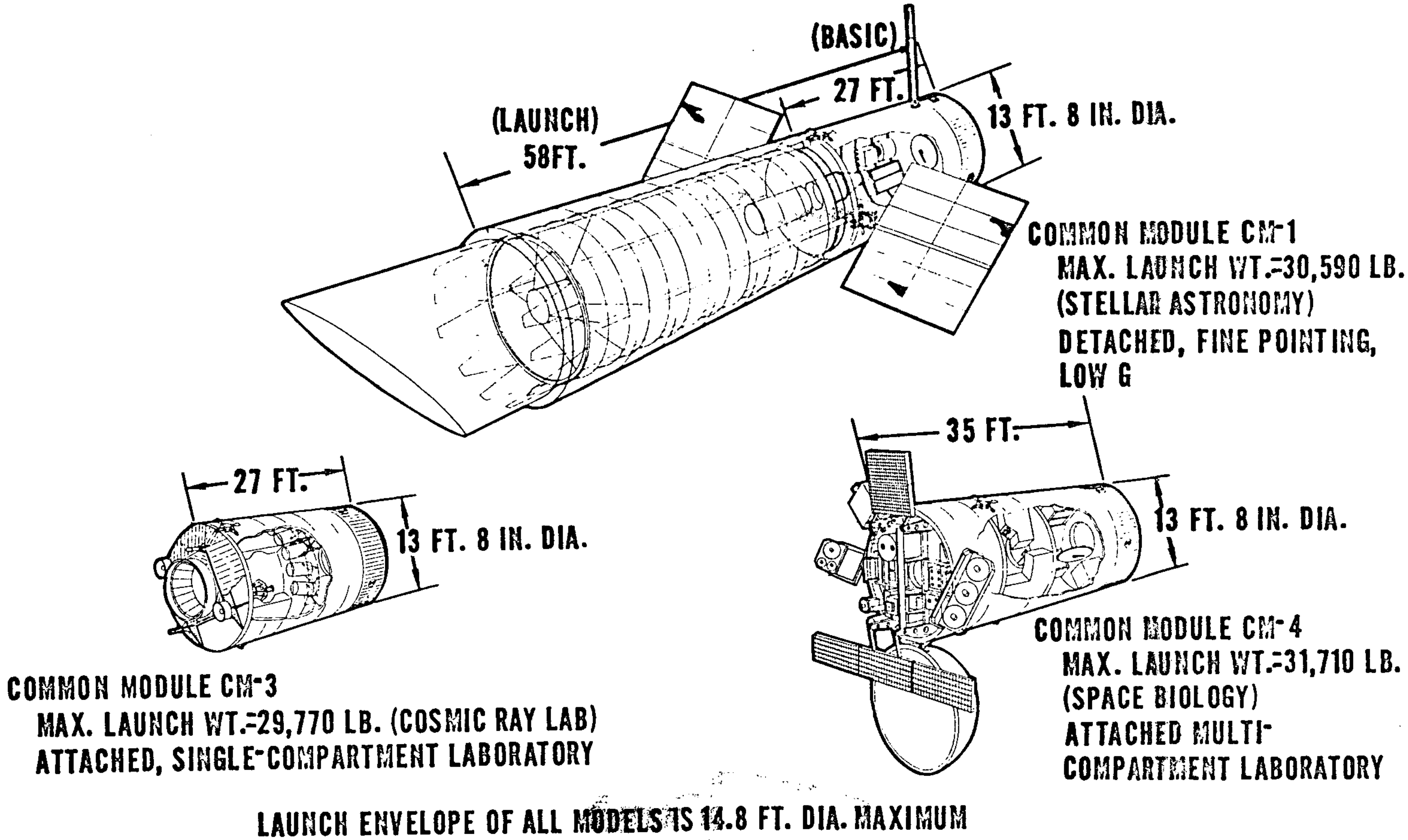

Figure 1-3. Baseline Common Module Set

Table 1-1 Common Module FPE Allocations

FPE		CM-1	CM-3	CM-4	Experiment Peculiar Requirements
5.1	X-Ray	X			
5.2A	Stellar	X			
5.3A	Solar	X			
5.5	Hi-Energy	X			
5.7, 5.12	Plasma Physics		X		
5.8	Cosmic Ray		X		Sensor Bay
5.9, 5.10, 5.23	Biology			X	Centrifuge
5.11A	Earth Survey			X	End Dome
5.13C	Centrifuge				Centrifuge
5.16	Materials Science		X		
5.20	Fluid Physics	X	X		Propulsion Slice, 2 Tanks
5.22	Component Test			X	
5.27	Physics/Chemistry		X		
Subtotal Modules		5	5	3	
Total Modules			13		
Total Experiment Peculiar			7		
TOTAL			20		

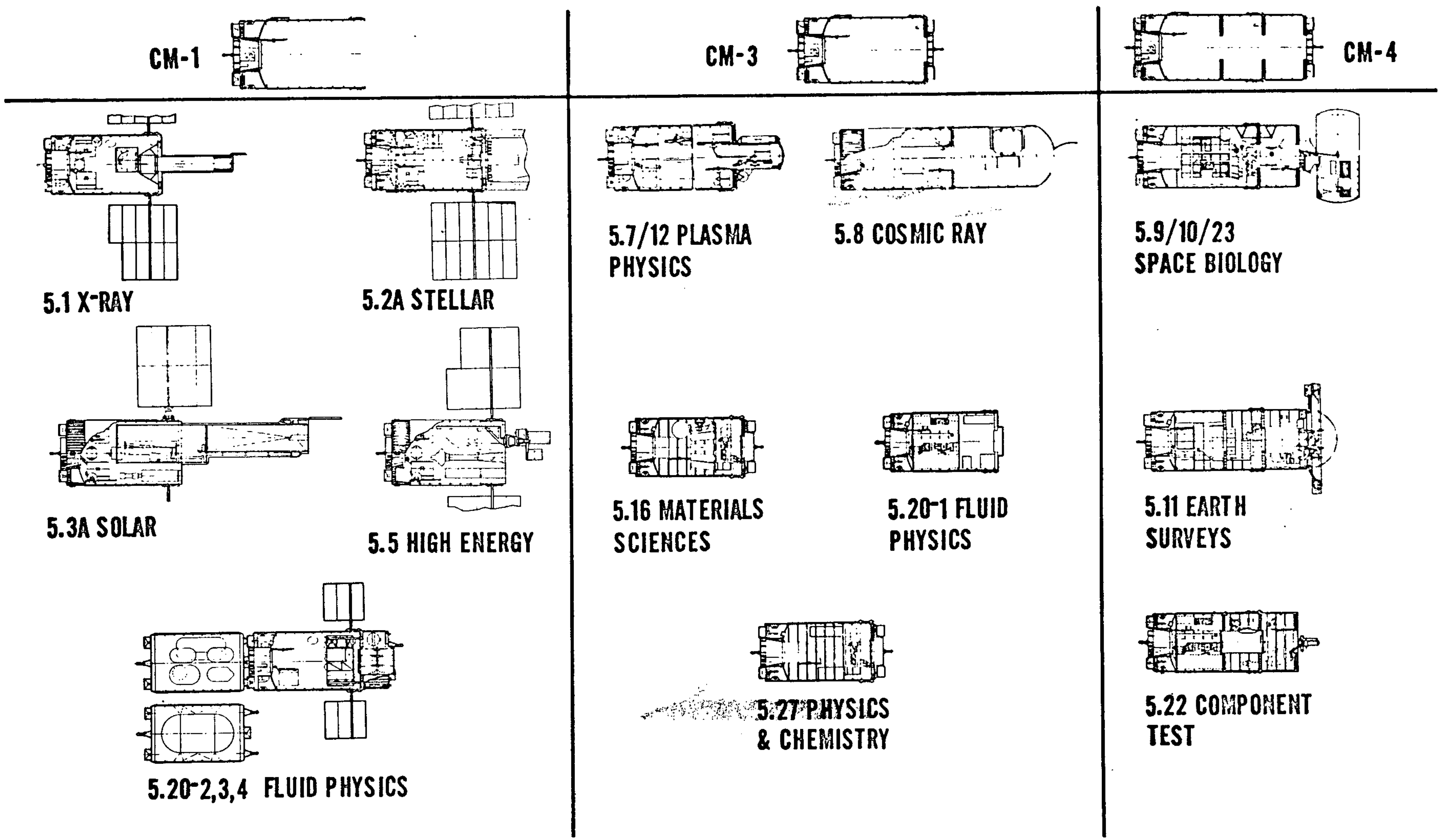

Figure 1-4. Total Program Commonality

During the commonality analysis, experiments were assigned to particular modules based on individual subsystem requirements and other indications of common usage of a single module design. These assignments were reviewed for their relative impact on the resultant module design to determine if some of these more stringent experiment requirements should be provided as experiment-peculiar equipment rather than in a common module. Also considered was whether they were more compatible with a different module than the initial assignment.

The experiments not compatible with mounting in a common module were removed from the assigned common module and provided as experiment equipment. Examples of this are the removal of the two centrifuges from the attached module thereby permitting a diameter of 13 feet 8 inches, which is compatible with the shuttle cargo bay size.

As illustrated in Figure 1-5, common modules CM-1, CM-3, and CM-4 have identical structures with respect to pressure wall, frame spacing, docking structure, end bulkhead, hatch, RCS mount, and launch vehicle attachment. The exterior radiator panels are the same for CM-1 and CM-3 at 600 square feet. The additional length of CM-4 adds 250 square feet.

CM-3 is similar to CM-1 except that a flat pressure bulkhead is added. The bolt-and-weld seal attachment of all pressure bulkheads would be similar. Common module CM-4, with three pressure bulkheads, can provide three pressurizable compartments.

A maximum effort has been expended to gain the economic advantage of subsystem commonality among the free-flyer CM-1 and the attached modules CM-3 and CM-4. This is illustrated in Figure 1-6. The thermal control system uses a two-fluid system (water inside, freon outside) with exchanger at the pressure shell plus a water evaporator backup. A common external radiator panel design is used for all modules essentially covering all available external area. The additional length of CM-4 relative to CM-1 and CM-3 affords the additional 250 square feet of radiator area. The difference in the electrical power subsystem is that the free-flyer has solar panels, whereas the attached module obtains power from the space station supply.

The difference in the communication/data/checkout subsystem is the communication portion. The free-flyer requires a wideband data RF transmission link, whereas the attached module uses a hardline connection to the space station. The lesser data transmission capability for the free-flyer relative to the attached module reflects the desire to minimize radiated power and bandwidth in the interest of economy.

The R&D guidance and navigation system is the same for the attached and the free-flyer. For attached modules, the system is used for initial delivery and subsequent docking port change. A special provision is the addition of a laser radar sensor for the fluid physics (5.20-1) experiment installation in CM-3 to permit the docking of another experiment module.

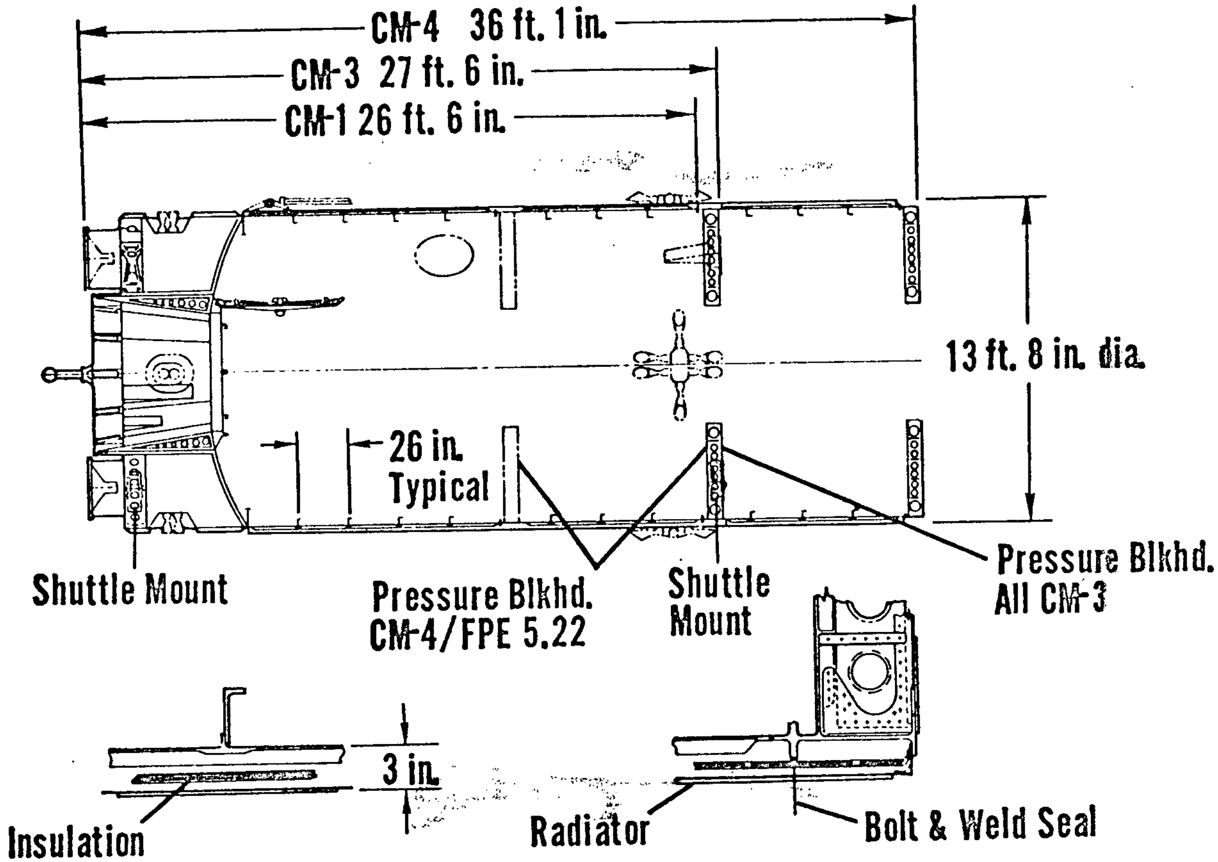

Figure 1-5. Structural Commonality

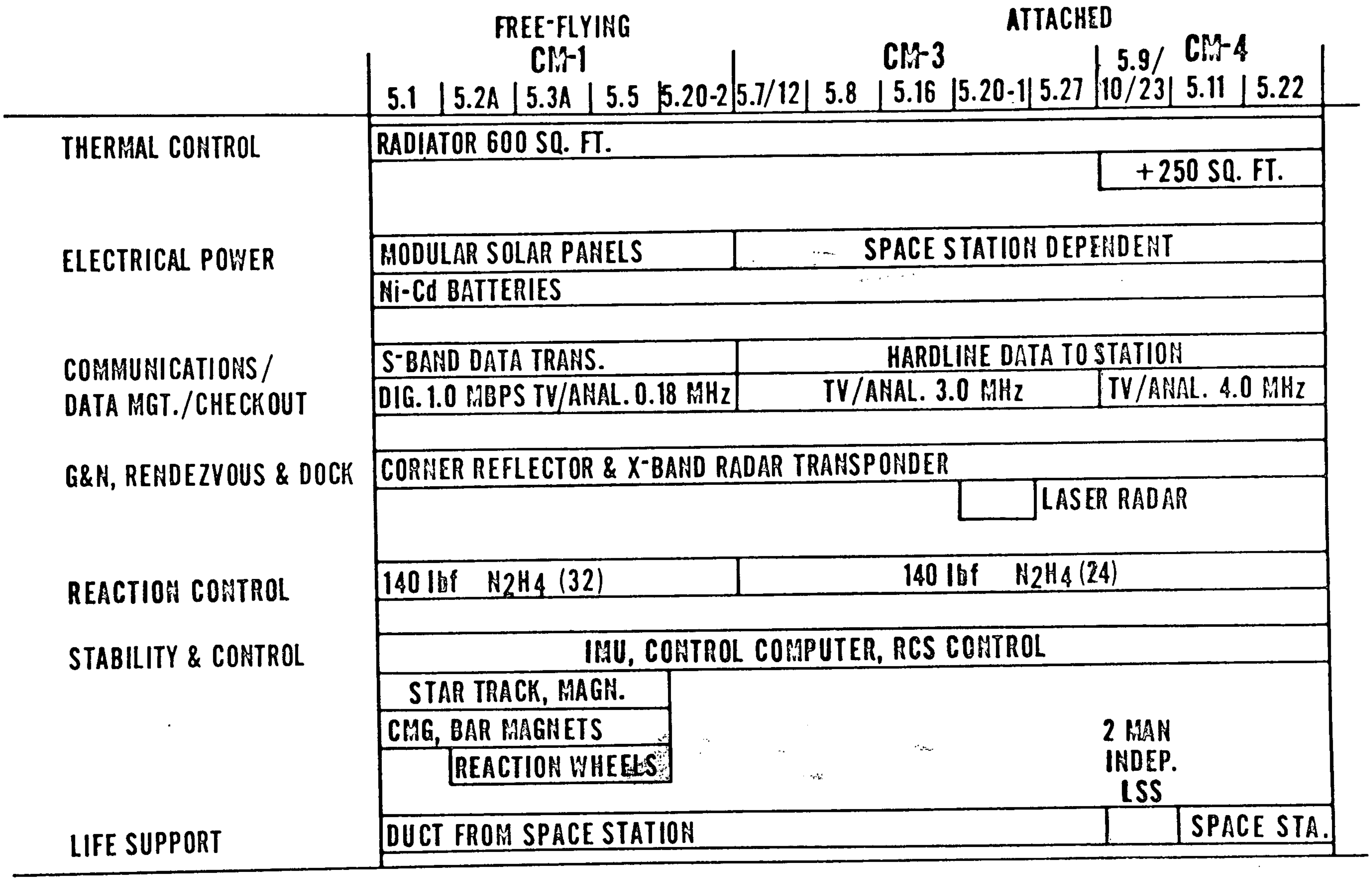

Figure 1-6. Subsystems Commonality

The reaction control subsystem is identical for all modules except that eight thrusters of the free-flyer 32-thruster system are left off of the attached module. The stability and control subsystem is essentially identical for the free-flyer and attached modules in regard to RCS control. A momentum actuator-dumping system is added to all the astronomy experiment free-flyers. A fine point capability via reaction wheels is added to all astronomy free flyers except 5.1, where module arc-second stability is not currently required. The environment control/life support system is identical for all modules except the space biology FPE 5.9/10/23, in which a separate two-man independent system is added to isolate the experiment subject compartment from the space station. For all other experiments, the life support subsystem is simple since it derives most of the support from the space station.

1.1.1 COMMON MODULE CM-1. The free-flying common module CM-1 shown in Figure 1-7 will accommodate any of the five experiment groups listed. All of these experiments are mounted on the experiment peculiar end pressure bulkhead. Subsystems are mounted adjacent to the docking bulkhead and are thermally shielded from the experiment components as required.

Basic structural shell, hatches, docking system, and bulkhead attachments are similar to the other two common modules. Manned IVA access to critical subsystems components is inherent to the maintenance design approach.

Modularization of some of the subsystems listed in Table 1-2 allows the matching of performance capabilities with experiment requirements. In the case of the three-meter telescope shown, a stringent complement of module subsystems is required.

The thermal control subsystem is sized by the heat rejection requirements for the growth version of the three-meter telescope (FPE 5.2A). The system is capable of dissipative 9720 Btu/hr heat load. The total heat is transferred out of the module through liquid transport loops to external radiators.

The electrical power subsystem major components are two two-degree-of-freedom solar cell wings and NiCd batteries. Sun-line orientation is maintained by rotation about the wing roll axis in conjunction with roll about the module longitudinal axis. The other degree-of-freedom of the wing is used for initial erection, retraction for clearance during docking operations, and total retraction for possible return to earth in the shuttle bay. The NiCd batteries were chosen because they satisfy the high cycle life requirement of low earth orbit.

The communication/data management digital data rate of 1×10^6 bps is the current system sizing. The 0.2 MHz video bandwidth analog channel is for a TV signal used to verify module experiment pointing. Film is used for all other wideband data.

The space station is the primary location for the rendezvous and docking equipment. Module on-board equipment includes a laser reflector for docking and a transponder for stationkeeping guidance and navigation data.

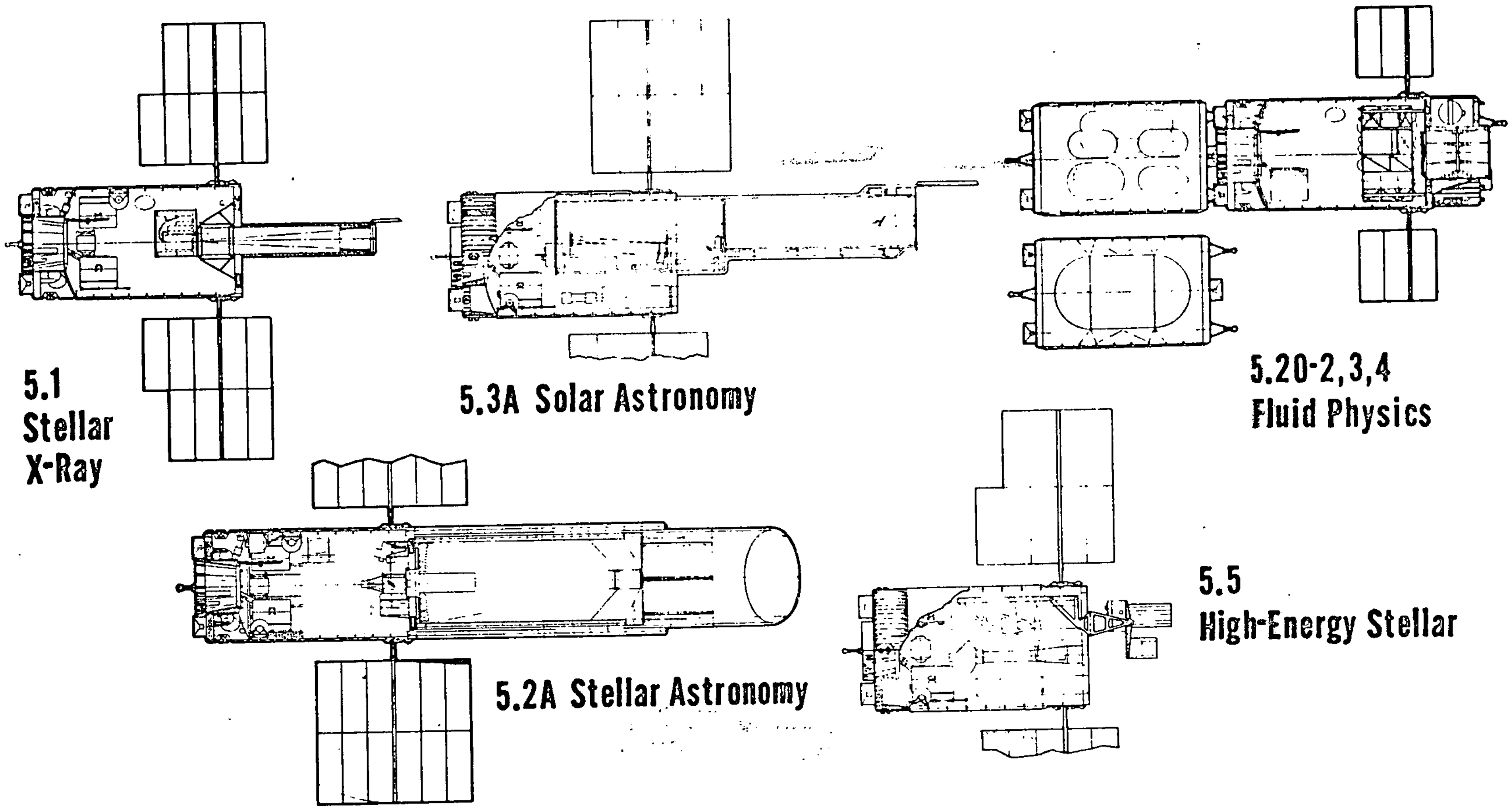

Figure 1-7. Common Module CM-1

CM-1 ITEM LIST

1. SKIRT SECTION, CM-1
2. SHUTTLE PICK-UP RECEPTACLES, PITCH LOADS (2)
3. SHUTTLE PICK-UP RECEPTACLES, YAW LOADS (1)
4. RCS ENGINES, PITCH/YAW
5. RCS ENGINES, TRUST/ROLL
6. ANTENNA, X-BAND OMNI-DIRECTIONAL (3)
7. ANTENNA, S-BAND OMNI-DIRECTIONAL (3)
8. STAR TRACKER, NO. 1
9. STAR TRACKER, NO. 2
10. CORNER REFLECTOR
11. COARSE SUN SENSOR
12. PRIMARY SECTION, CM-1, 164 IN. DIA.
13. PRESSURE SKIN, INTERNAL, 158 IN. DIA.
14. METEOROID SKIN/EXTERNAL RADIATOR
15. SOLAR CELL ARRAY, STOWED
16. SOLAR CELL ARRAY, ERECTED, 330 SQ. FT.
17. EXPERIMENT PECULIAR BULKHEAD MECHANICAL INTERFACE
18. SHUTTLE PICK-UP TRUNIONS, LONGITUDINAL AND PITCH LOADS
19. SHUTTLE PICK-UP TRUNION, YAW LOADS
20. BAR MAGNET STOWED
21. BAR MAGNET ERECTED, TWO D.O.F. (STA 96)
22. EVA HAND RAILS, 4 FIXED
23. HYDRAZINE (N_2H_4) BOTTLES, 4 @ 10.25 CU. FT. EA.
24. HELIUM (He) BOTTLES, 4 @ 1.9 CU. FT. EA.
25. ENTRANCE HATCH, 60 IN. DIA.
26. EMERGENCY ESCAPE HATCH, 30 IN. DIA.
27. SUIT CIRCUITS (2)
28. POWER RECEPTACLE
29. PUMP DOWN LINE
30. ATMOSPHERE INTAKE DUCT
31. ATMOSPHERE EXHAUST DUCT
32. DECOMPRESSION VALVE
33. THERMAL CONTROL CABINET: COMM., DATA, S&C
34. THERMAL CONTROL CABINET, ELECT. POWER
35. THERMAL CONTROL CABINET, STAB & CONTROL
36. RISER DUCT, ATMOSPHERE INTAKE
37. RISER DUCT, ATMOSPHERE EXHAUST
38. REACTION WHEEL (3)
39. CONTROL MOMENT GYROS (2)
40. INSULATION, ENTIRE HULL
41. DOCKING PROBE (2)
42. DOCKING DROGUE (2)
43. ATMOSPHERE MONITORING LINE
44. EVA INSPECT/COMPONENT REPLACEMENT DOOR-OPEN

FPE 5.2A ITEM LIST

50. QUARTZ ROD SPACER/SUPPORTS (4)
51. PRIMARY MIRROR, 3 METER (118.11 IN. DIA.)
52. PRIMARY (CASSEGRAIN) FOCAL POINT (f3) -354.33 IN.
53. SECONDARY REFLECTOR, 0.661 METER (26 IN. DIA.)
54. SECONDARY FOCAL POINT (f14), 364 IN.
55. TERTIARY FOCAL POINTS (f15), (5 PLACES)
56. ROTATABLE 45 DEG MIRROR
57. SPECTROGRAPH
58. ALIGNMENT AUTOCOLLIMATOR
59. 225 mm CAMERA
60. 70 mm CAMERA
61. HINGED 45 DEG MIRROR
62. VIDEO GRAPH
63. MIRROR BOOST SUPPORT BLADDER-TOROIDAL
64. STRAY LIGHT TUBE
65. CRUCIFORM SUPPORT - SECONDARY REFLECTOR
66. CONTAMINATION/IRIS DOORS OPEN
67. CONTAMINATION/IRIS DOORS CLOSED
68. WAVE FRONT 3 METER APERTURE (CLEAR)
69. SUN SHADE SECTION - OUTER (100 IN. EXTENSION)
70. SUN SHADE SECTION - INNER 45 DEG TERMINUS (130 IN. EXTENSION)
71. GROUND QUARTZ APERTURE, 10 IN. DIA. - HINGED
72. EXPERIMENT ACCESS PRESSURE DOOR, 40 IN. DIA.
73. TRACKS - EXTENDABLE SUN SHADE SECTION
74. EXPERIMENT SECTION - 5.2A - 164 IN. DIA.

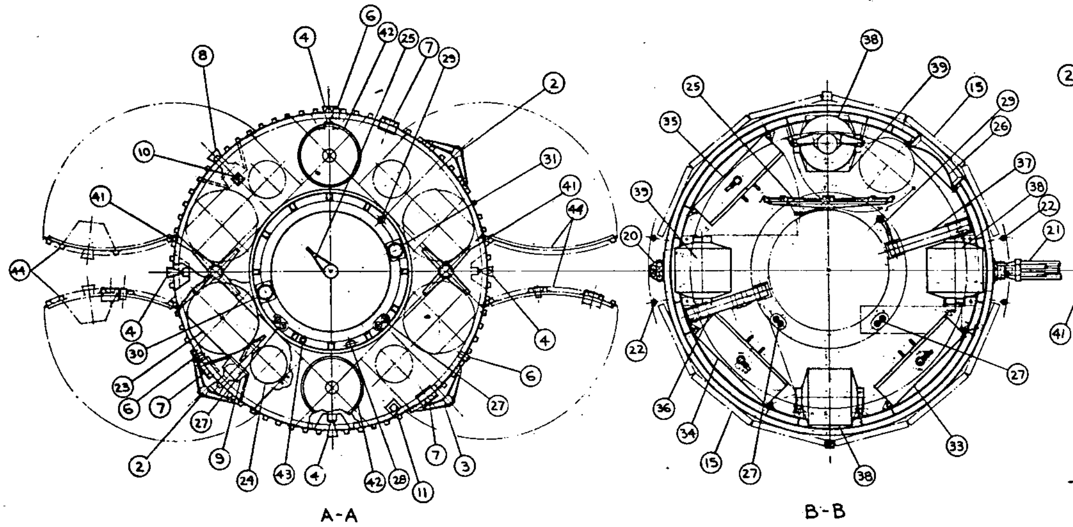

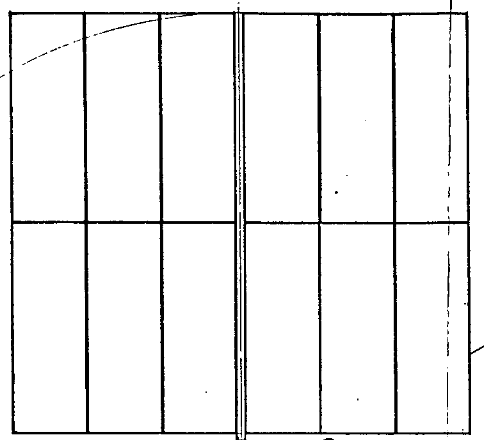

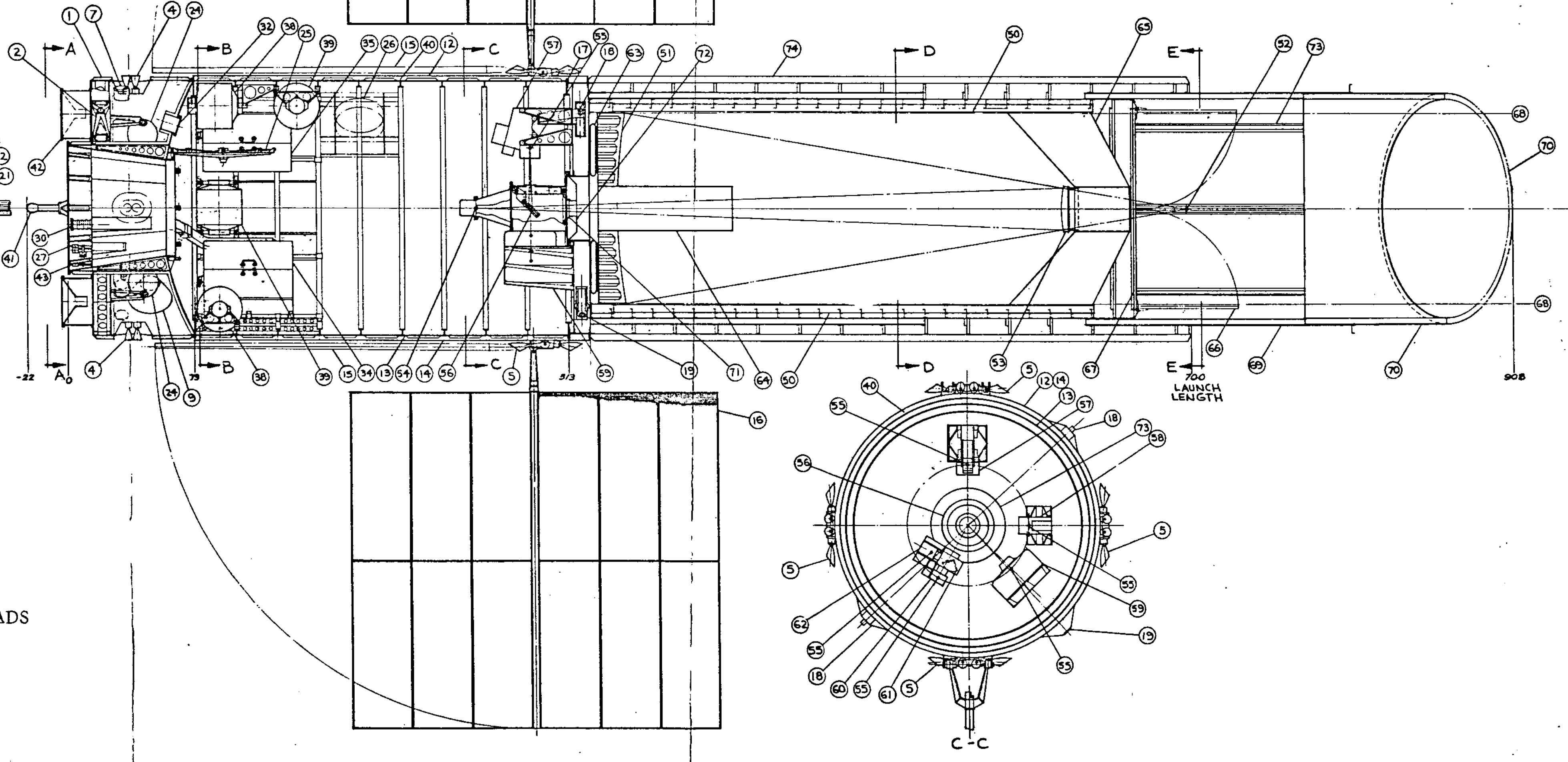

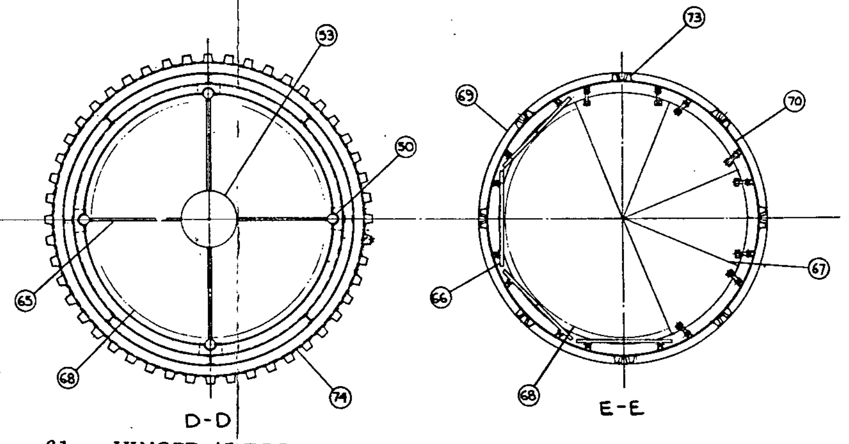

FOLDOUT FRAME 1

PRECEDING PAGE BLANK NOT FILMED

FOLDOUT FRAME 2

FOLDOUT FRAME 3

Figure 1-8. Inboard Profile, CM-1/FPE 5.2A

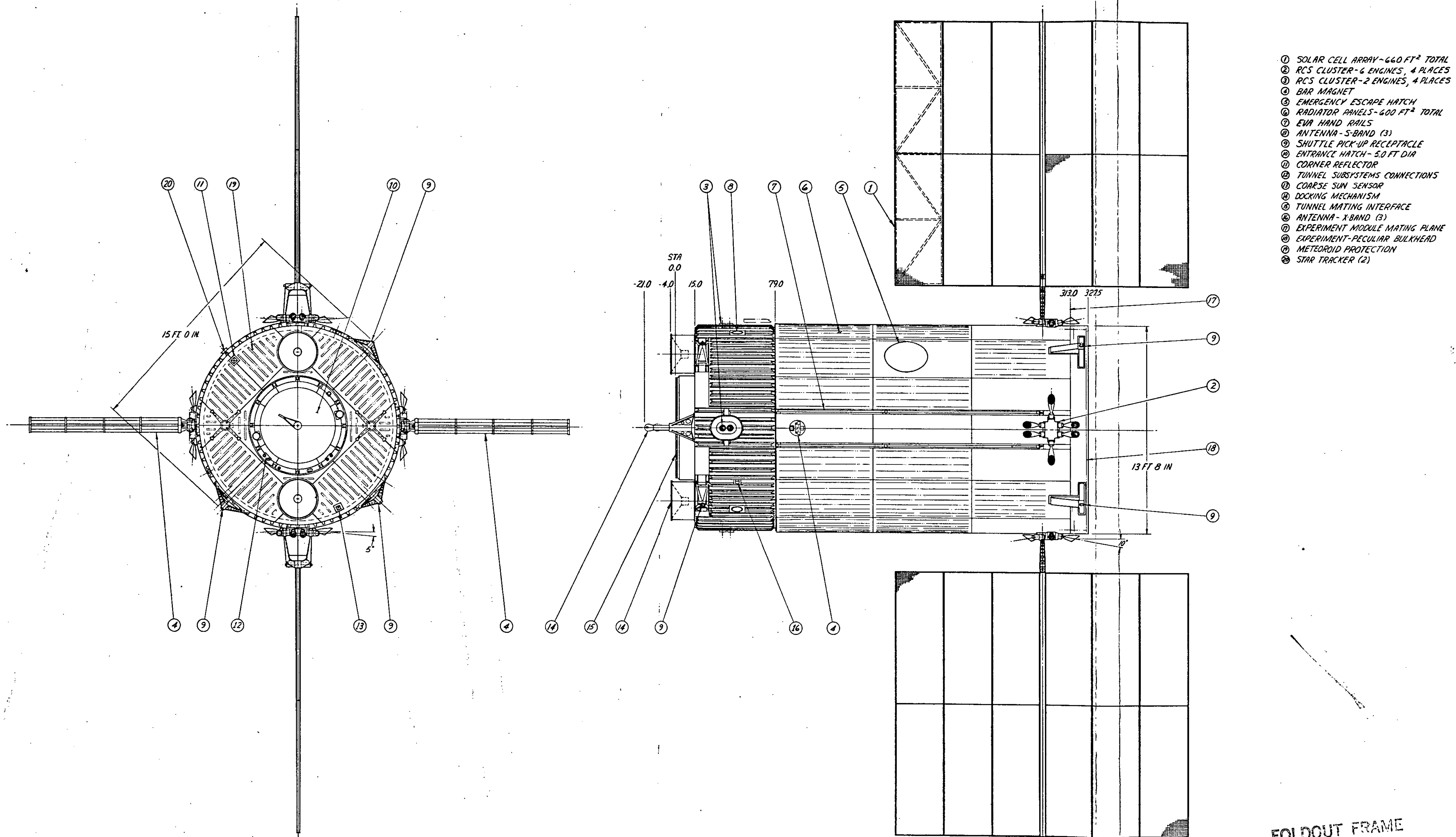

Figure 1-9. External Arrangement, Free-Flying Common Module CM-1

The basic module is 13 feet 8 inches in diameter over the meteoroid protection panels with a 13-foot 2-inch diameter pressure hull. The pressure hull constant section length is 19 feet 6 inches with an overall basic module length of 27 feet 10 inches.

The common module structure is comprised of a pressure hull of integrally stiffened skin panels and frames closed at one end by a curved bulkhead and docking tunnel and at the other end by a flat experiment peculiar bulkhead which is tailored structurally to suit the experiment to be installed. The pressure skin is protected from meteoroid puncture by the thermal radiator skin panels under which is mounted a blanket of insulation material for passive thermal control of the module interior. A 64-inch-long aft skirt houses the star trackers, the RCS propellant, and pressurization gas bottles together with the docking mechanism and structure.

All subsystems components are located around the module wall in the aft end of compartment.

Power for detached operation is furnished by two two-degree-of-freedom solar cell wings. Each wing has 330 square feet of active area divided into 12 panels of 27.5 square feet. Panels are added or removed as required by the mission power profile. For experiments such as fluid physics which do not demand accurate pointing of the star trackers, CMGs and reaction wheels together with their associated components are removed. Access doors in the skirt section allow removal and replacement of the propellant system and thermal control components.

External components would be protected during boost on an expendable launch vehicle by jettisonable fairings. These fairings are not required if launched with a shuttle type vehicle.

The expendable booster structural interface is at the base of the 64-inch skirt section. It is anticipated that the skirt will take axial boost loads in a launch by Titan III.

Weight summaries for the CM-1 module are provided in Section 2.

1.1.2 <u>COMMON MODULE CM-3.</u> The CM-3 common module shown in Figure 1-10 is a single-compartment lab module that docks and remains attached to the space station, which provides electrical power and environment gases to the module through the interface. The primary structure is identical to the CM-1 common modules except that a flat pressure bulkhead is added in place of the experiment-peculiar bulkhead of the CM-1.

The CM-3 utilizes docking mechanisms at both ends of the module to accommodate the free-flying fluid physics modules and the growth potential of a free-flying material science casting facility.

In the case of the cosmic ray module this main laboratory is housed in the CM-3 while the experiment bay is an experiment-peculiar structure permanently fastened to the CM-3 module.

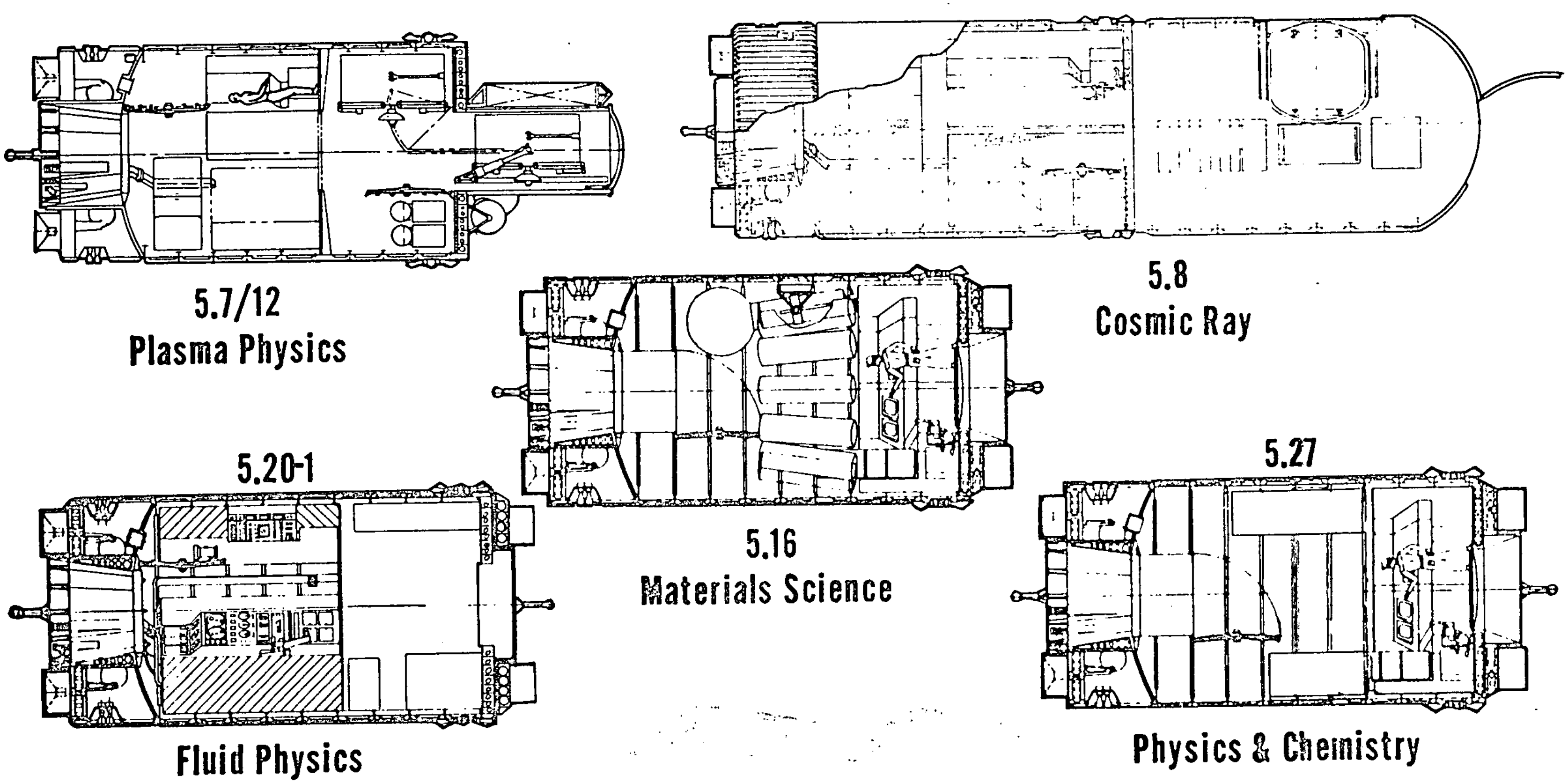

Figure 1-10. Common Module CM-3

Table 1-3. Common Module CM-3 Subsystems Summary

Subsystem	Description	Typical Parameters
Thermal Control	600 sq ft of Radiator Panels	12,600 Btu/hr. Maximum
Electrical Power	Space Station Dependent	3.7 kW Average 5.3 kW Peak
Communication/Data Management	Hardlines Data to Space Station	3 MHz Bandwidth
G&N, Rendezvous/ Dock	Corner Reflector & Transponder Laser Radar	±4 in Accuracy
RCS	Monopropellant System for Rendezvous/Docking	I_{sp} = 225 sec 24 Thrusters at 140 lbf
Stabilization & Control	Autopilot for Rendezvous/ Docking	210 lb, 295 W

The experiment operating mode is attached. However, initial delivery from an expendable launch vehicle and change in space station docking port require short-term detached operations. The RCS, SCS, and electrical power subsystems reflect this mode.

The thermal control subsystem transports heat to the module heat rejection system via a liquid coolant loop.

Module electrical power is derived from the station. The requirement shown is the maximum, corresponding to the support of cosmic ray lab experiments (FPE 5.8). For detached operations mentioned above, batteries provide subsystem standby and operating power.

The given communication/data management digital data rate is the maximum experiment requirement. The 3 MHz bandwidth analog channel is for TV experiment monitoring. Transmission to the ground is via the space station.

The space station is the primary location for the rendezvous (one-time only) and docking control equipment. However, a laser radar is also provided on-board to enable docking of additional experiment modules to CM-3 during fluid physics (5.20) experiments.

A hydrazine monopropellant RCS is provided for circularization, docking, and change in station docking port detached operations.

The SCS receives angle and ΔV instructions from the space station and directs RCS firings for maneuvering. For the short-term detached operations, the SCS uses a minimum autopilot.

The CM-3 module and FPE 5.16 are shown on Figure 1-11. It is a single compartment module operating attached to the space station and may be used with other modules to perform discrete functions of a particular FPE. This module constitutes the command/control and data handling center for the FPE-related, detached modules. Operationally, in the case of fluid physics, the CM-3 modules are an intermediate vehicle between the detached mode vehicles and the space station, providing storage, workshop areas, and services. These services include the transfer of fluids, gases, and cryogens onto a docked module. Additionally, many experiments of the associated FPE are conducted within the module when the space station environment is tolerable to the experiments.

The pressure compartment is 13 feet 2 inches in diameter with the constant section 19 feet 6 inches long. Diameter over the meteoroid protection panels is 13 feet 8 inches. Overall length is 31 feet 10 inches in the usual configuration, having a docking bulkhead at the experiment interface. The cosmic ray application of CM-3 results in a length of 50 feet 6 inches for the combined CM-3 and experiment peculiar instrument bay.

The module basic structure is of the same construction and size as described for CM-1. The basic subsystem components are located around the internal periphery of the pressure hull for a length of approximately three feet adjacent to the space station docking port.

Weight summaries of the CM-3 module are provided in Section 2.

1.1.3 <u>COMMON MODULE CM-4.</u> The CM-4 Module shown in Figure 1-12 is similar in diameter and construction to the other two common modules. It is a multi-compartment lab module which docks and remains attached to the space station. The four experiment groups accommodated include the alternate biomedical group of experiments. These experiment groups have larger volume requirements than those accommodated in CM-3.

A major configuration driver for CM-4 is the Component Test and Sensor Calibration experiment group. This experiment group results in the requirement for a tunnel airlock leading to two test chambers and a five-foot-diameter hatch in the end compartment. Volumetric requirements for the earth surveys experiments are another major driver.

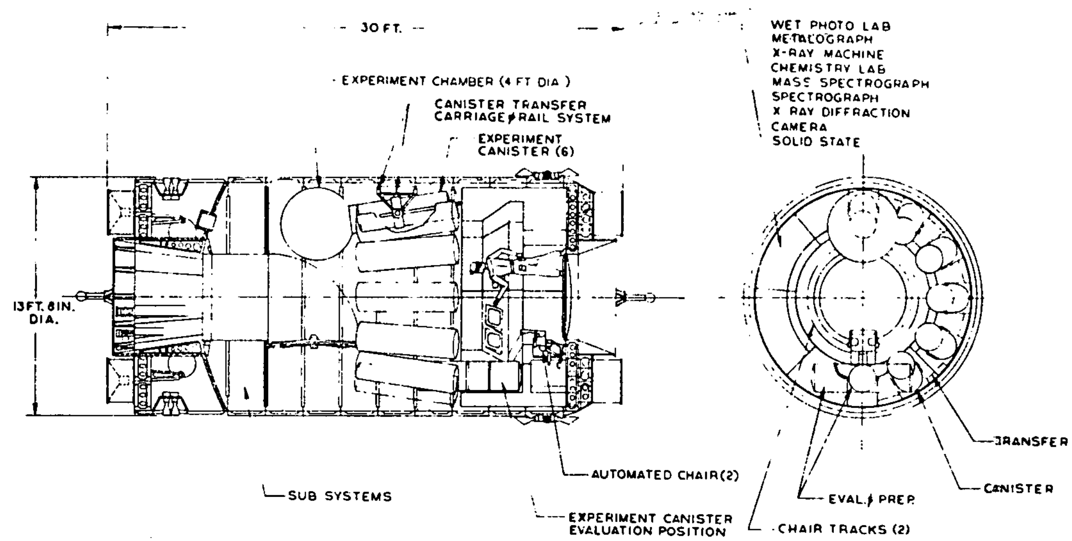

Figure 1-11. Common Module CM-3/FPE 5.16

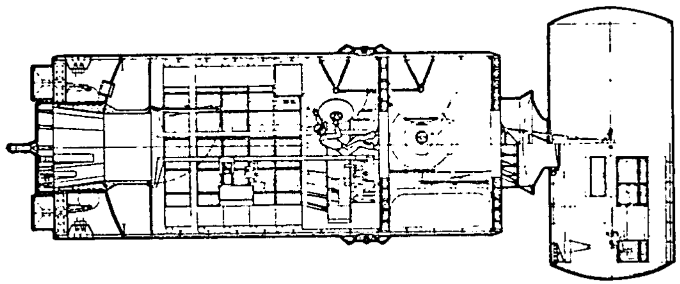

FPE 5.9/10/23 Space Biology Lab

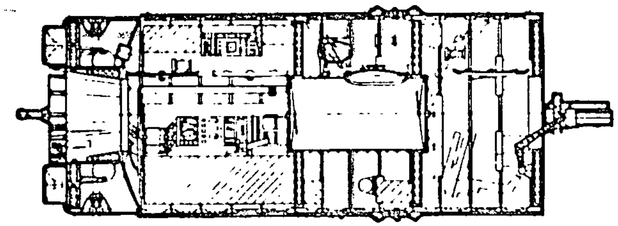

FPE 5.22 Components Test Lab

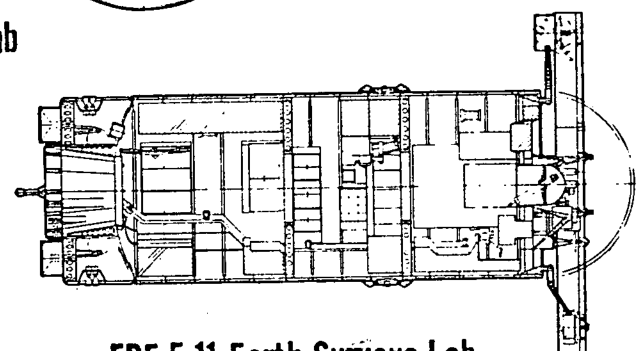

FPE 5.11 Earth Surveys Lab

Figure 1-12. Common Module CM-4

CM-4 subsystems listed in Table 1-4 are identical to those on CM-3 except as follows:

The on-board docking radar is deleted because no dockings to CM-4 are anticipated.

The electrical power distribution requirements are for higher power.

A two-man life support system is provided for the Space Biology Lab for contaminant and CO_2 removal and atmosphere replenishment.

The CM-4 module is shown in Figure 1-13. This common module features three compartments separated by flat bulkheads, permitting independent pressurization if pressure bulkheads are used. The compartments are 11, 8, and 8 feet long. The 11-foot

Table 1-4. Common Module CM-4 Subsystems Summary

Subsystem	Description	Typical Parameters
Thermal Control	850 sq ft of radiator panels	17,700 Btu/hr. Maximum
Electrical Power	Space Station Dependent	5.2 kW Average 7 kW Peak
Communication/Data Management	Hardlines Data to Space Station	4 MHz Bandwidth
Guidance & Navigation, Rendezvous/Dock	Corner Reflector & Transponder	—
RCS	Monopropellant System for Docking	I_{sp} = 225 sec 24 Thrusters at 140 lbf.
Stabilization & Control	Autopilot for Rendezvous/ Docking	210 lb, 295 W
Life Support Systems	Contaminent Removal CO_2 Removal Atmosphere Replenishment	2-Man Capacity for Biology Lab

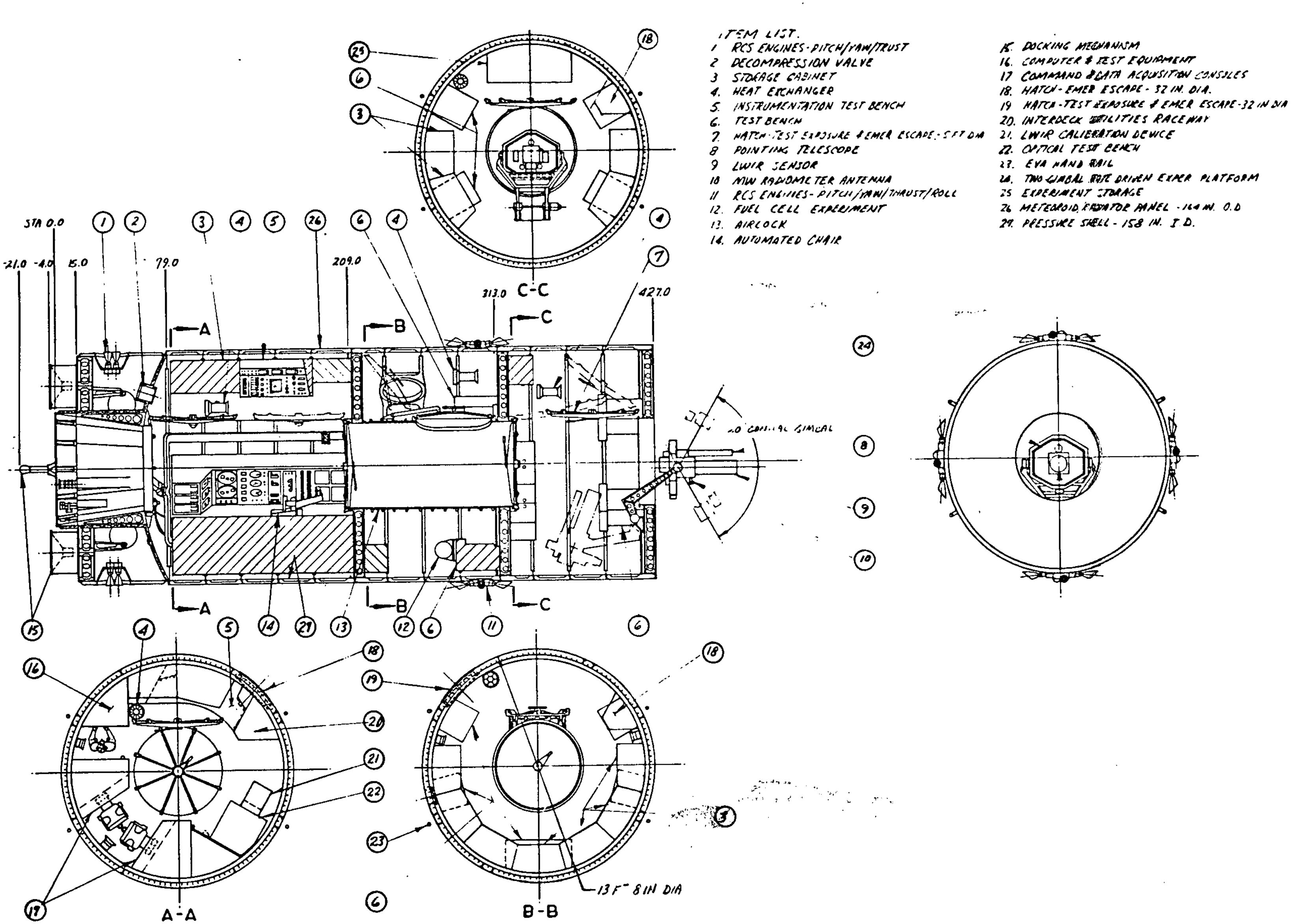

Figure 1-13. Component Test and Sensor Calibration, CM-4/FPE 5.22

compartment is adjacent to the space station and contains the basic subsystem components around the internal periphery for a length of approximately three feet. This compartment generally serves as the control and services center. An experiment-peculiar interdeck tunnel, 60 inches in diameter, is used on the FPE 5.22 (Component Test & Sensor Calibration).

The CM-4 module is used in conjunction with the two centrifuge modules. The centrifuge modules are experiment peculiar and not a derivative of a common module.

Dimensionally and structurally the CM-4 module is identical to the CM-1 or CM-3, except for length.

Weight summaries of the CM-4 module are provided in Section 2.

1.2 EXPERIMENT IMPLEMENTATION

Table 1-5 provides a summary of the recommended experiment operational modes for implementation of each assigned experiment (FPE). A basis for these mode selections is explained in brief. The task of FPE implementation into a complement of common modules necessitated varying extents of deviation from the vehicle geometric shapes, sizes, volumes, and arrangements as implied by the FPE definition contained within the Candidate Experiment Program document (Blue Book). However, the common modules, as conceived and constrained by the ground rules, will fulfill the requirements of each experiment program. Additionally, these modules possess sufficient capability to adapt to experiment programs yet to be defined.

Detailed study of methods to accomplish each experiment objective have revealed several areas where special approaches are presumed in order to assure feasibility or practicality. These areas, Table 1-6, are subject to NASA and scientific panel review and approval in order to avoid any compromise of experiment objectives.

1.2.1 <u>LABORATORY APPROACH TO COMMON MODULES.</u> Although it is virtually impossible to predict all of the user requirements for the next 10 to 15 years, three general categories may be assumed:

a. General laboratory

b. Permanent research facility (e.g., astronomy)

c. Special purpose experiments (e.g., remote maneuvering subsatellite)

Table 1-5. Selection of Operating Mode

FPE No.	Experiment	Selected Mode of Operation	Basis for Selected Mode
5.1	X-Ray	Detach	Contam. & Radiation, viewing
5.2A	3-M Stellar	Detach	Stab. & Control, viewing, contam.
5.3A	Solar	Detach	Stab. & Control, contam., viewing
5.5	High Energy	Detach	Contam. & Radiation, viewing
5.7	Plasma	Attach/Detach	Experiment Operation
5.8	Cosmic Ray	Attach	Station Compatible (1)
5.9	Vertebrates (Bio D)	Attach/Ctrfge.	Station Compatible (2)
5.10	Plants (Bio E)	Attach/Ctrfge/Isol.	Station Compatible (2)
5.11	Earth Surveys	Attach	Power, Exper. Oper.
5.12	RMS	Attach/Detach	Experiment Operation (3)
5.13C	Centrifuge	Attach/Ctrfge.	Station Compatible
5.16	Materials Processing	Attach	Station Compatible
5.17	Contamination	Attach *	Contam. Required
5.18	Exposure	Detach *	Contam. & Radiation
5.20	Fluid Physics	Attach	Station Compatible
5.20-2, -3, -4	Fluid Physics	Detach/Prop.	Sustained Acceleration Required
5.22	Component Test	Attach	Station Compatible
5.23	Primates (Bio A)	Attach	Station Compatible
5.27	Physics & Chemistry	Attach	Station Compatible

* Suitcase experiments

(1) Assumes use of substitute for nuclear emulsions.
(2) Assumes located at adequate distance from power generator.
(3) Housed in attached mode.

Table 1-6. Variations From Blue Book Implementation Methods

FPE	Title	Variation	Reason
5.3A	Solar Astronomy	Propose use of photographic imaging for several sensors.	Data rates during periods of solar activity exceed projected capabilities for RF transmission.
5.8	Cosmic Ray	Propose reduction in laboratory diameter from 22 ft to 13 ft 8 in.	Reduced for compatibility with shuttle.
		Propose replacement of nuclear emulsions with electronic methods.	Use of nuclear emulsions limited to short periods (days) at station altitudes.
5.9 5.10	Bio D (Vert.) Bio E (Plants)	Propose different centrifuge configuration.	Reduced to less than 15 ft cylinder for compatibility with shuttle, yet maintain 10 ft radius arm.
5.13C	Centrifuge	Propose different exterior configuration.	Reduced to less than 15 ft cylinder for compatibility with shuttle, yet maintain 10 ft radius arm.
5.27	Physics & Chemistry	Solar furnace not in baseline module design.	Defined as not usable in inclined orbit. Can be accommodated if desired.

The general laboratory concept is envisioned as a laboratory area adequately fitted for general disciplines such as chemistry, biology, materials science, physics, or equipment test experimentation. The principal investigator sends or brings test specimens and experiment-unique equipments to earth orbit, and is allocated time and space in the laboratory. Several of the currently designed module laboratories fall into this category:

FPE 5.9/10	Biology, including FPE 5.23
FPE 5.11	Earth Surveys
FPE 5.16	Materials Science and Processing
FPE 5.20	Fluid Physics
FPE 5.22	Component Test and Sensor Calibration
FPE 5.27	Chemistry

Viewing these modules as general purpose labs will help to define their requirements for growth, complete their laboratory equipment requirements definition, and better define the activities of the crew conducting experiments in these labs.

Two key areas in pursuing this approach to general purpose laboratories are:

a. The role of man as associated with various experiments, skills involved, and degree of flexibility needed between specialized areas within a discipline.

b. Commonality of equipment that exists between disciplines that might use a single lab.

1.2.2 EXPERIMENT EQUIPMENT COMMONALITY. Two categories of commonality within the experiment equipment have been identified. One type uses experiment equipment such as a sensor to collect data usable by another experiment discipline or principal investigator. The other type is multiple use of experiment supporting equipment. Three example cases of this second type have been identified in the present program:

a. FPE 5.1 (Grazing Incidence X-Ray Telescope) and FPE 5.5 (High-Energy Stellar Astronomy) both contain grazing incidence telescopes but of different size and for different purposes. Present launch schedules indicate that both modules will be operating in the detached mode at the same time. It is therefore possible that equipment designed for maintenance and support could be shared.

b. FPE 5.27 (Physics and Chemistry) incorporates microscopes and X-ray equipment. FPE 5.16 (Materials Science and Processing) also utilizes equipment of the same nature. The planned on-orbit evaluation phase of the materials experiments might be enhanced by the presence of chemistry equipment.

c. FPE 5.22 (Components Test and Sensor Calibration) contains laboratory type photographic and test equipment which could be considered as candidate support equipment for common usage by other FPEs.

1.2.3 EXPERIMENT IMPLEMENTATION STUDIES. Experiment module concepts for implementing certain experiments required special studies of experiment requirements to arrive at feasible and low cost concepts. These special studies included the following:

FPE 5.5, High Energy Stellar

FPE 5.8, Cosmic Ray Lab

FPE 5.10, Plants (Bio E)

FPE 5.16, Materials Science & Processing

FPE 5.20, Fluid Physics

The results of the investigations and conclusions on implementation requirements are shown in Table 1-7. (See Volume V, Appendix A.)

1.3 EXPERIMENT INTEGRATION

1.3.1 EXPERIMENT-PECULIAR INTEGRATION HARDWARE. Major experiment-peculiar hardware items required for the experiment program as defined in this study are shown in Figure 1-14. These consist of two centrifuges, a propulsion slice, and two cryogenic tanks for the fluid physics experiments.

Since the spin radius experiments for the biomedical and space biology centrifuges require a length of 20 feet, they cannot be mounted to rotate within the 15-foot-diameter common modules. To meet space shuttle payload dimension restrictions, the centrifuge proper is encased in a small-diameter can and the whole is rotated on an external bearing. In orbit, these centrifuges would be attached to the end of common modules. Longitudinal mounting within the shuttle cargo bay would allow simultaneous launch with the related module. Retraction mechanisms would then position the centrifuges for operation.

The free-flying CM-1 is coupled with a propulsion slice to conduct the entire series of sustained g fluid physics tests. The cryogenic sustained g tests are conducted by in-orbit coupling to experiment-peculiar tank units, two similar units being required to fulfill all of the cyrogenic tests.

Experiment integration equipment is required to adapt the experiment hardware to the common module and its subsystems. Table 1-8 identifies several items or sets of

Table 1-7. Experiment Implementation Requirements

FPE No.	Title	Experiment Requirements Affecting Implementation	Effect of Requirement on Implementation Concepts	Conclusion - Implementation Requirements
5.5	High Energy Stellar Astronomy	1. Gamma ray deflections are sensitive to space station nuclear power source radiation.	1. It is desirable to oper- gamma ray deflectors at a distance from nuclear power source greater than attached mode will permit.	1. Combine with high energy X-ray instruments in same module resulting in cost saving of one common module.
5.8	Cosmic Ray Lab	1. Use of nuclear emulsions sensitive to trapped radiation.	1. Avoiding fogging of emulsion requires either short exposure times or operations at lower altitude.	1. Assume the development of electronic devices to replace nuclear emulsions.
		2. Diameter of lab.	2. Lab diameter of 22 ft incompatible with probable advanced logistic system cargo diameter.	2. Retain basic aperture geometry in 15 ft diameter for lab as currently defined.
		3. Use of high field strength magnet.	3. Magnet reacts with earth's magnetic field creating high torque potentials.	3. Potential for torque to be accommodated in attached operating mode.

Table 1-7. (Continued)

FPE No.	Title	Experiment Requirements Affecting Implementation	Effect of Requirement on Implementation Concepts	Conclusion - Implementation Requirements
5.10	Plants (Bio E)	1. Isolation of some plant growth experiments from noise, vibration, and other disturbances above 10^{-6}g. 2. Isolation of plants from cyclic disturbances or "cues."	1. Complete confidence in isolation from all disturbances above threshold of sensitivity in detached mode. 2. Requires separation from source, or random programming of source outputs.	1. Design of plant accommodations in lab to provide required isolation in attached mode. 2. All potential cyclic inputs must be programmed for random occurrence.
5.16	Materials Processing	1. Retain containerless casting molten mat'ls. for up to 1 hr. duration w/o application of excessive retention forces.	1. Relative motion between experiment and module in attached mode requires forces which are considered to adversely affect internal mixing and external shape of molten mass.	1. Provide means for eliminating relative motion potential for containerless casting experiments.
5.20	Fluid Physics	1. ±10% g level stability tolerance.	1. Requires variable thrust engines to hold g levels due to mass changes.	1. Use fixed thrust engines. Considerable cost savings result. Four of 10 experiments will be out of tolerance. Sense resulting levels and correlate.

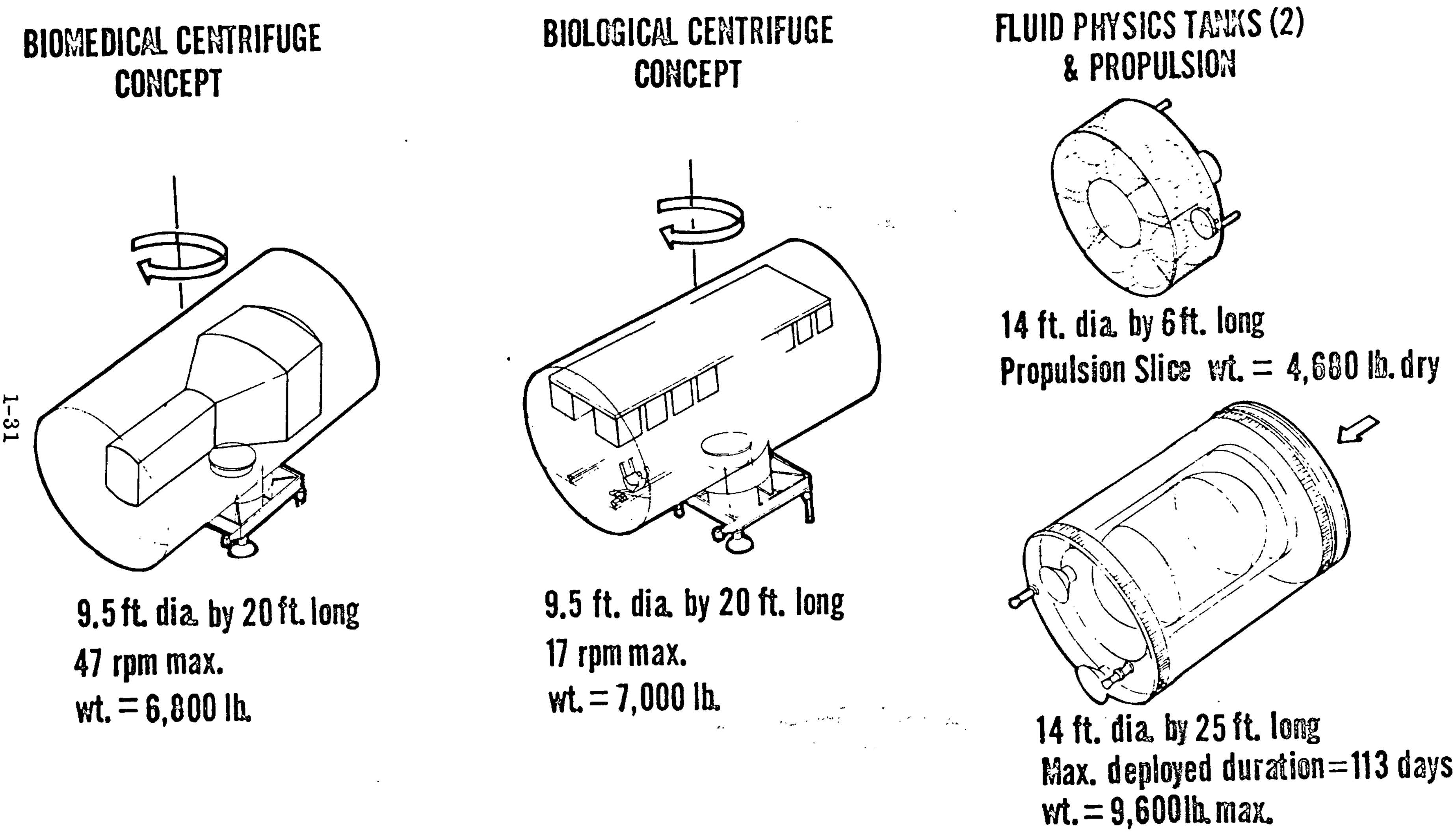

Figure 1-14. Major Experiment-Peculiar Integration Hardware

Table 1-8. Major Experiment Integration and Unique Equipment

Common Module -1	-3	-4	FPE NO.	1.0 Complete Experiment Housing										2.0 Experiment Mount. & Opr. Struct.						
				1.1 Housing Structure	1.2 Housing Attachment/Dock Mech.	1.3 Housing G&N	1.4 Housing RCS	1.5 Housing Elec.	1.6 Housing Stab. & Control	1.7 Housing Radiator	1.8 Centrifuge Depl. Mech.	1.9 Mount Struct/Brackets	1.10 Propulsion Slice	2.1 Bulkhead/Partition	2.2 Thermal/Meteor Shroud	2.3 Viewing Hatch	2.4 Equip. Mount Struct/Bracket	2.5 Sunshade	2.6 Tunnel	2.7 Airlock
X			5.1											X	X	X	X			
X			5.2A											X	X	X	X	X		
X			5.3A											X	X	5	X			
X			5.5											X		3	X			
	X		5.7											X			X			
	X		5.8	X(4)						X		X				7	X			
		X	5.9/10/23											X			X			
Exp. Unique Cent. Arm			5.9/10(7)	X	X						X	X					X		X	
		X	5.11A											X		X	X			
		(6)	5.12																	X
Exp. Unique Cent. Arm			5.13C(8)	X	X	X	X	X	X			X					X/SS			
	X		5.16														X			
	X		5.20-1														X			
X			5.20-										X	X			X			
Exp. Unique			-3 Exp.	X	X	X						X		X						
Exp. Unique			-4 Exp.	X	X	X						X		X						
		X	5.22														X			X
	X		5.27														X			
Suitcase			5.17/5.18														SS/MOD			

FPE NO.	3.0 Experiment Operations & Deployment Mech.								4.0 Experiment Support Equipment								
	3.1 Dewar Rails & Mech.	3.2 Viewing Hatch Mech.	3.3 Sunshade Deploy. Mech.	3.4 Radiometer Deploy. Mech.	3.5 Radar Imager Deploy Mech.	3.6 Satellite Deploy. Mech.	3.7 Experiment Deploy. Mech./Rail	3.8 Exp. Gimbal Mech.	4.1 Cryogenic Control	4.2 Prop. Control/Fueling	4.3 Gas Control	4.4 Vacuum Control	4.5 Subsystems Interface	4.6 Cabinets (Storage)	4.7 2 Man EC/LSS	4.8 Magnetic/Radiation Shielding	4.9 Emulsion Storage/Process
5.1		X							X		X		X			X	
5.2A		X	X								X		X			X	
5.3A		5						X			X		X			X	
5.5		3					X		X		X		X			X	X
5.7																	
5.8		7							X		X			X		X	X
5.9/10/23											X			X	X		
5.9/10(7)																	
5.11A		X		X	X				X		X	X		X			
5.12						X			X(1)	X	X	X		X			
5.13C(8)																	
5.16											X	X		X			
5.20-1									X	X	X	X		X			
5.20-									X	X	X		X				
-3 Exp.																	
-4 Exp.																	
5.22							X		X(2)		X	X		X			
5.27											X	X		X			
5.17/5.18							SS/MOD										

FPE NO.	5.0 Electro/Mech. Experiment Support										6.0 Experiment Support Electronics			
	5.1 Cryo. Valves	5.2 Cryo. Plumbing	5.3 Prop. Valves	5.4 Prop. Plumbing	5.5 Gas Valves	5.6 Gas Plumbing	5.7 Vacuum Valves	5.8 Vacuum Plumbing	5.9 EVA Suit Control Valves	5.10 EVA Suit Control Lines	6.1 Operations Sequencing (5)	6.2 Contam. Monitor (Equip.)	6.3 Hatch/Shroud Sensors	6.4 Subsystem Interface (5)
5.1	X	X			X	X			X	X	X	X	X	X
5.2A					X	X			X	X	X	X	X	X
5.3A					X	X			X	X	X	X	X	X
5.5	X	X			X	X			X	X	X	X	X	X
5.7														X
5.8	X	X			X	X							X	X
5.9/10/23					X	X					X			X
5.9/10(7)														
5.11A	X	X			X	X	X	X	X	X	X		X	X
5.12	X(1)	X(1)	X	X	X	X	X	X						X
5.13C(8)														
5.16					X	X	X	X	X	X				X
5.20-1	X	X	X	X	X	X	X	X						X
5.20-			X	X	X	X			X	X	X			X
-3 Exp.														
-4 Exp.														
5.22	X(2)	X(2)			X	X	X	X	X	X		X		X
5.27					X	X	X	X	X	X				X
5.17/5.18									SS/MOD	SS/MOD				SS/MOD

(1) Oxygen and hydrogen.
(2) Oxygen, hydrogen and nitrogen.
(3) Assumes delivery to space station by experiment module.

(4) Includes ~ 7' hatch for magnet dewar removal/replacement.
(5) Module to experiment integration equip. interface, and subsystem to experiment interface (e.g., command, control, data, power).
(6) The RMS and satellite hangar are combined with FPE 5.7.

(7) Assumes delivery with 5.9/10/23 module.
(8) Assumes autonomous delivery of experiment unique centrifuge.
(9) SS/MOD denotes location on either space station or experiment module.

FOLDOUT FRAME 1

FOLDOUT FRAME 2

FOLDOUT FRAME 3

experiment integration equipment not specificially accounted for in either experiment or common module definition in the following categories:

a. Complete experiment housing
b. Experiment mounting structure
c. Experiment operating/deployment mechanisms
d. Experiment support equipment
e. Electro/mechanical experiment support
f. Experiment support astrionics

Experiment integration equipment is developed in an iterative manner, with only preliminary results shown in Table 1-8. It is expected that future studies and analyses will indicate that some of the items should be redefined as part of the common module or experiment. For example, sets of gas control equipment (Table 1-8, Item 4.3), gas valves and plumbing (Items 5.5 and 5.6) are frequently needed for gas purging of experiment equipment and test setups. Specific gas requirements vary with each FPE as installed in the common module. For example, nitrogen purge is required for portions of telescope or sensor optics to prevent contamination or condensation when detached modules are docked for service. Physics modules use helium purges around superinsulated cryogenic storage tanks.

Other presently identified experiment integration equipment could be redefined as applicable to only one or perhaps two of the three common module types with modularity incorporated wherever possible.

Within certain classes of integration equipment, commonality can produce development cost savings. For example, the thermal meteoroid shroud (Table 1-8, Item 2.2) for the X-ray telescope (FPE 5.1) might be made common with the Solar Astronomy (FPE 5.3A) shroud thereby requiring only one development program.

1.3.2 EXPERIMENT INTEGRATION IN DETACH COMMON MODULE CM-1. Common Module CM-1 accommodates a wide range of experiment disciplines. The following experiments are accommodated:

FPE 5.1	0.5 Meter Grazing Incidence X-ray Telescope
FPE 5.2A	3 Meter UV-Visible IR Advanced Stellar Astronomy Telescope
FPE 5.3A	1-1/2 Meter UV-Visible and Other Solar Telescopes
FPE 5.5	Grazing Incidence and Venetian Blind X-ray Telescope Gamma Ray Detectors
FPE 5.20	Non-Cryogenics Fluid Physics

The integration of these experiments into the five required CM-1 modules is shown in Figure 1-7. FPE 5.2A is shown in Figure 1-8.

Additionally, an alternate, detached version of FPE 5.11 (Earth Surveys) utilizing a CM-1 is discussed in Section 1.4.3.

In the case of the astronomy modules, the experiment integration is accomplished through the use of an experiment peculiar bulkhead that provides the structural interface between the common module structural shell and the experiment hardware. No experiment hardware attachment is required to the common module structure for these experiments except for the gamma ray detector track supports of FPE 5.5.

The fluid physics experimentation is accomplished through the use of one CM-1 module in conjunction with one CM-3 module. A discussion of these experiments is provided in Section 1.3.2.5. CM-1 provides the power, navigation, and docking capability for the fluid physics experiments.

The CM-1 subsystems have been modularized to accommodate the wide range of performance demands imposed upon them by the various experiment integrations.

The solar cell wings are designed to accommodate up to 24 modularized panels of 27.5 square feet each. Stabilization of the astronomy modules is aided by the use of two clusters of bar magnets, each containing five elements 8.2 feet long. Elements are added or removed to suit the mass moment of inertia of the various modules.

Various subsystems components, such as the star trackers, inertia wheels and CMG units, are used only for the astronomy applications. These are removed for all other experimentation. The propellant tanks (four hydrazine and four helium) are accessible through hinged panels around the skirt periphery.

1.3.2.1 <u>FPE 5.1, Grazing Incidence X-ray Telescope.</u> This application of the CM-1 module, Figure 1-15, contains a telescope system for the purpose of measuring X-ray radiation from stellar objects. The module is operated in a detached mode for observations, and is docked to the space station for crew servicing. It therefore contains the necessary subsystems of propulsion, attitude control, communications, guidance, and power.

The telescope system consists of three primary elements: a 1000 cm^2 collecting area, grazing incidence, multi-segment lens assembly; an instrument section containing four recording instruments; and a truss structure that maintains the proper geometric relationship between the lens assembly and the recording instruments. The truss structure and lens assembly are enclosed in an insulated shroud to minimize

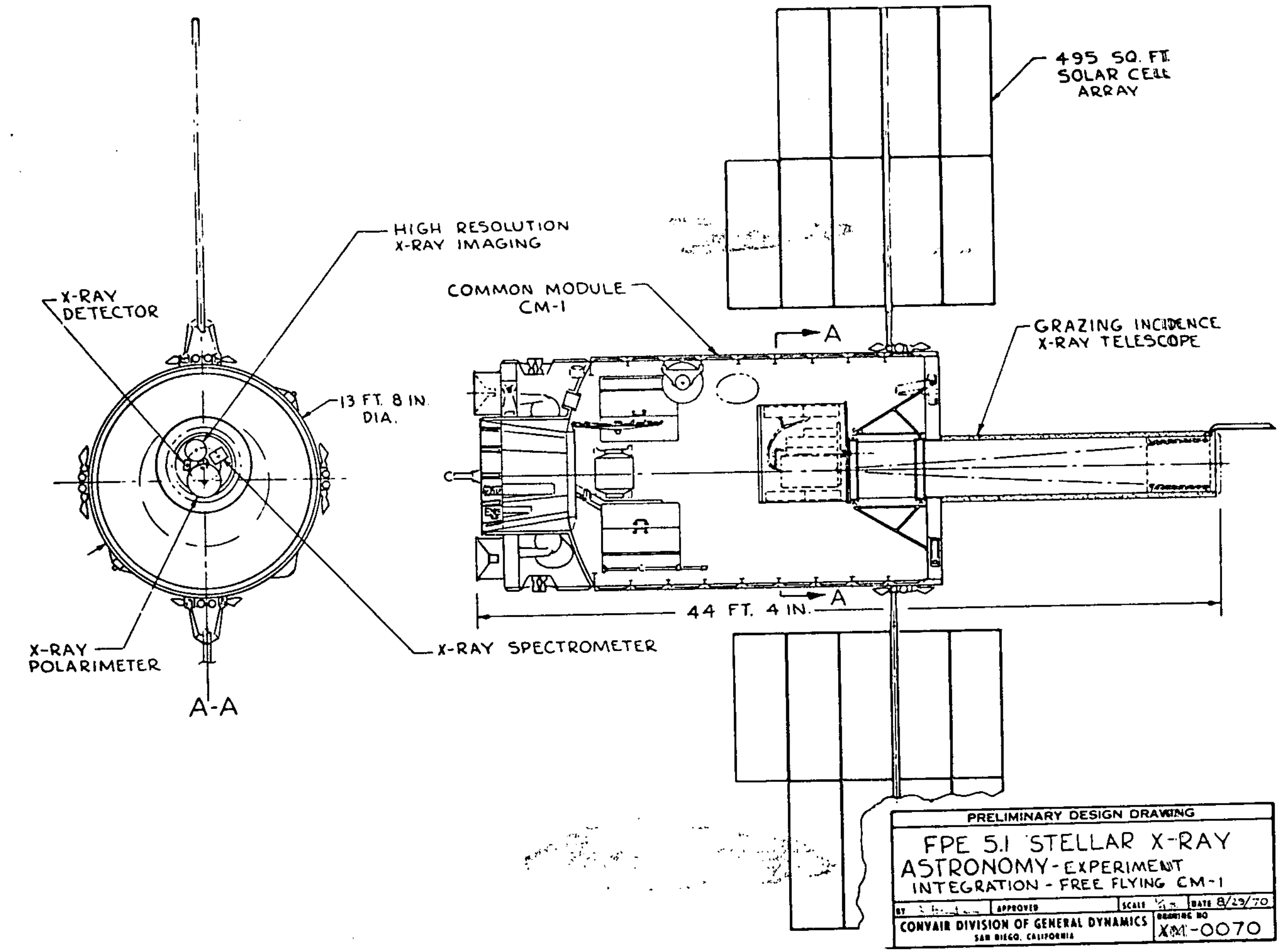

Figure 1-15. FPE 5.1 — Stellar X-Ray Astronomy, Experiment Integration, Free-Flying CM-1

thermally induced distortions. The entire telescope system is rotatable through ±90° to satisfy the polarimeter experiment. The four instruments are turret-mounted within the instrument section, and upon command are rotated into the receiving position at the prime focus. These instruments consist of:

a. Polarimeter 12.4 Å to 3.1 Å

b. Crystal spectrometer 25 Å to 1.5 Å

c. Imaging spectrometer 62 Å to 3.1 Å

d. Solid state detector 25 Å to 3.0 Å

Normal operation when attached utilizes the space station systems to provide a shirt-sleeve environment, although operation is essentially "closed door" due to the presence of the instrument cryostat. Within the instrument section a small pressure door ahead of the prime focus is closed at time of cabin pressurization. Additionally, this internal bulkhead of the instrument section seals at the telescope bearing nearest the section. Rotation of the telescope is borne by two bearing surfaces spread approximately four feet apart and outboard of the pressure boundary.

The telescope insulated shroud has an automatically operable door at the extreme end which closes when the telescope is pointed within 45° (90° cone) of the sun or earth. This door is also commanded to close prior to and during docked operations to prevent contamination of the lens assembly.

The primary power system is generated from a two-wing solar cell array of 495 square feet total. The modular CM-1 array is reduced to this area by removing three panels from each wing of the full size array.

All functions of stabilization, environment control, data management, attitude control and propulsive maneuvers are handled via the appropriate CM-1 subsystems. The entire telescope system is mounted to the experiment-peculiar bulkhead. Special control equipment and overboard dump valves, plumbing, tankage, and safety equipment are also mounted to this bulkhead.

1.3.2.2 FPE 5.2A, Stellar Astronomy. The integration of this experiment was the major configuration driver for the development of the CM-1 module. Also, the gross sizing of subsystems was generally forced by the requirements of this experiment. An inboard profile of FPE 5.2A integrated into CM-1 is shown in Figure 1-8.

The dominating features governing the configuration and its size are those of the telescope optical geometry, the instrument cabin, and the design for thermal stability.

The cabin provides crew access to the instruments and subsystems in a shirtsleeve environment. The primary optics are of a fixed geometry and do not require erection in orbit. Within the cabin the instruments are mounted on a common, thermally isolated bulkhead. Change of observing instrument is by rotationally indexing a remotely controlled optical flat, permitting observation of the same celestial body with different instruments. Sufficient volume exists for updating or adding instruments.

The optical system is a Ritchey-Chretien modified cassegrainian having a system focal ratio of f/15 at an effective focal length of 1848 inches. The primary mirror is 118.11 inches (3 meters) in diameter at f/3. Light blockage due to the secondary mirror and housing is 5%.

Design of the primary structure is dictated by boost conditions and on-orbit thermal stability. Careful attention is given to decoupling the telescope optics and supports from the outer thermal protective shell. The instrument mounting flat bulkhead forms the structural backbone of the telescope system. It is attached to the CM-1 shell by low thermal conductive supports. The cabin walls and environment control shrouds are also isolated from the bulkhead. The primary mirror is suspended within a baffle tube by three point tangent straps designed to minimize heat shorts. Support of the primary mirror through the boost phase is provided by an inflatable bladder system.

An extendable, irreversible barrel with an earth/sun/contamination shutter provides protection and thermal isolation to the telescope optics.

The secondary mirror and control cell are mounted on four fixed quartz rods. Lateral and torsional support of these rods are provided by the lower baffle tube. At launch the secondary mirror and cell are borne by the extendable barrel, so the rods support only their own weight. The control cell provides fine axis automated control for aligning the secondary mirror.

Power is provided by 660 square feet of solar cell arrays arranged in two diametrically opposite wings. Each wing possesses two degrees of freedom.

Gross maneuvering is performed by a reaction control system (RCS) of 32 hydrazine motors arranged in eight clusters around the vehicle shell. The module is maneuvered in attitude or coarse pointing by control moment gyros. Subsequently, control is shifted to a boresighted or experiment derived sensor driving three inertia wheels for fine point stability. Inertia wheel momentum dumping is provided by a two-axis pivoted bar electromagnet reacting against the earth's magnetic field.

The cabin life support functions are provided by interconnection to the space station systems (open door). An active environmental control system is provided via 600 square feet of external radiator integral with the meteoroid bumper. A removable pressure door at the telescope bulkhead permits access to the internal regions of the telescope barrel. This allows a space-suited crewman access to this area in event servicing is required and for inspection of the primary and secondary reflectors.

A major design problem of this FPE concerns the control of the primary mirror figure. This reflector surface can be distorted by very minute thermal variations. Reflector materials of nearly zero coefficients of expansion possess this characteristic at very low temperatures and it then becomes necessary to operate and maintain the optics at that temperature. However, producing and checking the reflector must consider the practical aspects of the time and hand craftsmanship involved. Some optical manufacturers believe the telescope system should be operated at a temperature equal to that of final figuring, possibly 70°F. Further argument for this lies in the need to keep the recording film at a similar temperature. To determine the configuration for operating at 70°F, the concept of Figure 1-16 was developed. It was necessary to add 420 square feet of solar array to generate sufficient additional thermal energy to operate the reflector at 70°F. This array is peculiar to the experiment in this operational mode.

1.3.2.3 FPE 5.3A Solar Astronomy. The following telescopes are included in the solar astronomy CM-1 free-flying module:

a. 1-1/2 meter UV-visible telescope

b. 0.25 meter spectroheliograph

c. 0.5 meter grazing incidence X-ray telescope

d. 1-6 solar radii coronagraph

e. 5-30 solar radii coronagraph

The module shown in Figure 1-17 will be unpressurized during free-flying operation. While docked to the station the module, including the 1-1/2 meter telescope aft of the primary mirror, is pressurized. The 1-1/2 meter telescope penetrates the experiment-peculiar mounting bulkhead and is protected with external insulation and a contamination shield, which closes during rendezvous and docking. Access into the interior is provided at the end of the telescope. The remaining solar telescopes are mounted entirely within the module. Pressure hatches in the experiment-peculiar bulkhead are opened automatically prior to viewing.

Accommodation of the telescopes within the 13 foot 2 inch diameter pressure shell utilizes the full volume of CM-1 for instrument access. The viewing angle of the coronagraph has a minimum clearance of the 1-1/2 meter telescope. Twenty solar cell panels provide 2 kW of electrical power. For solar observations the array could be fixed in the position shown, allowing removal of the orientation drive.

1.3.2.4 FPE 5.5 High Energy Stellar Astronomy. The periment equipment consists of an intermediate size X-ray telescope, a "venetian blind" X-ray telescope/

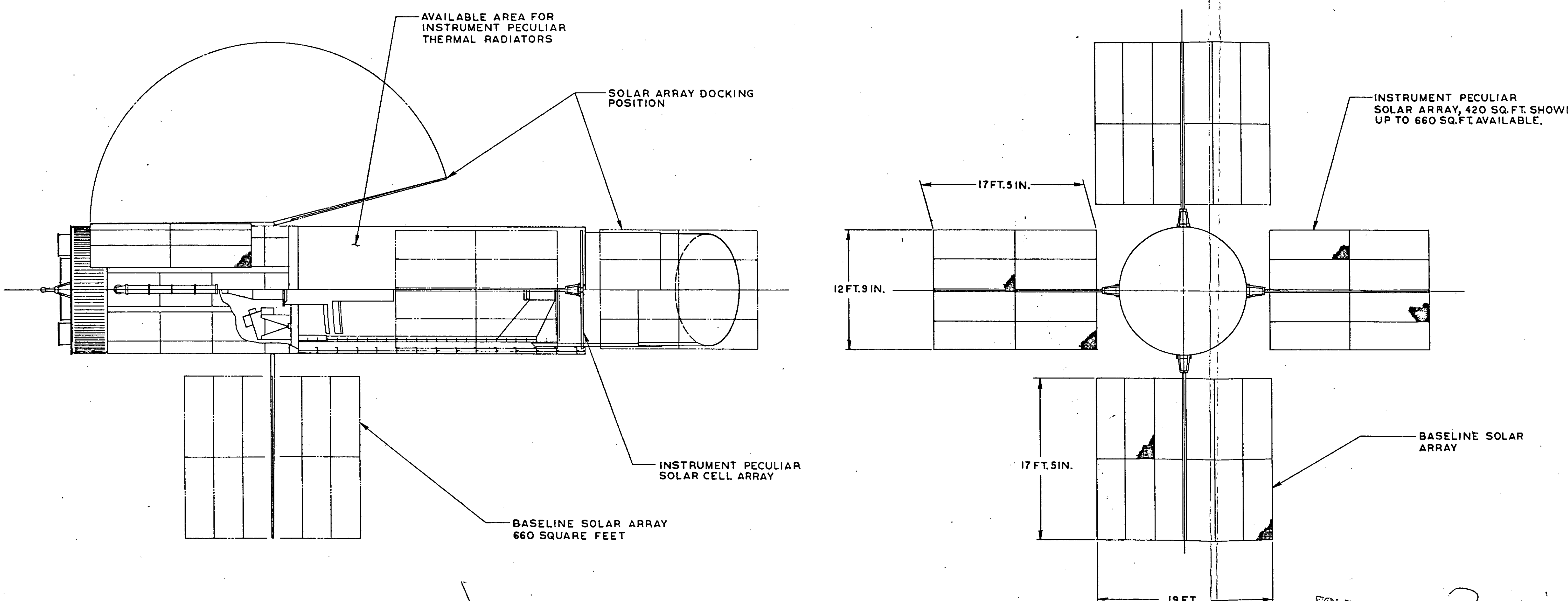

FOLDOUT FRAME 1

FOLDOUT FRAME 2

Figure 1-16. FPE 5.2A/CM-1—Modifications for Operating 70°F Mirror

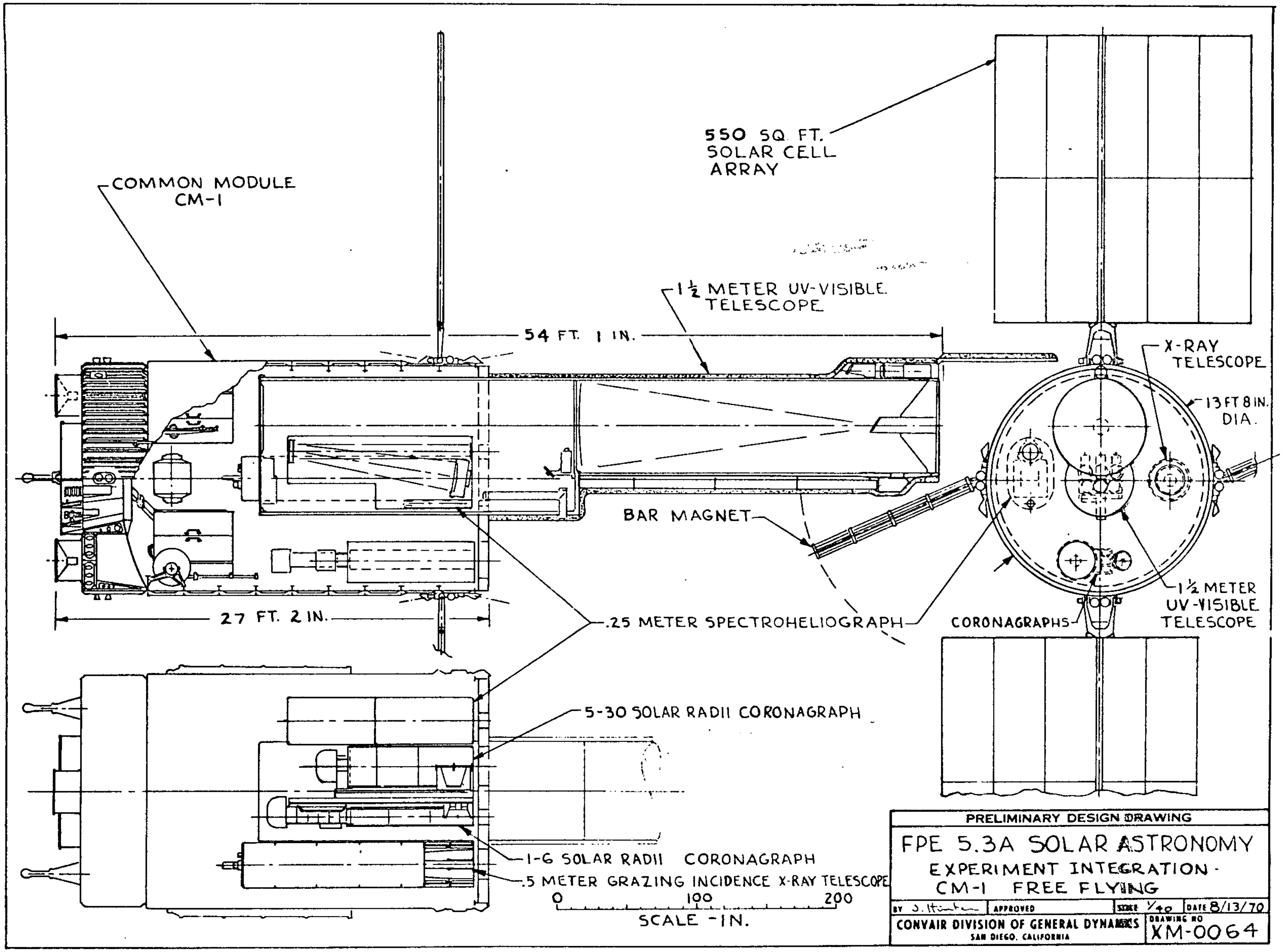

Figure 1-17. FPE 5.3A — Solar Astronomy, Experiment Integration, CM-1

spectrometer, a nuclear gamma ray spectrometer, and a high-energy gamma-ray astronomy spark chamber detection system.

The arrangement of experiments within the free flying CM-1 module is shown in Figure 1-18. During operation the module is unpressurized and viewing hatches in the experiment-peculiar bulkhead are automatically opened.

The two X-ray telescopes are rigidly mounted to the module with pointing accomplished by orientation of the spacecraft. In order to permit concurrent viewing of different sources with the gamma-ray instruments, these are gimbal mounted to a rail extension system which allows the deployment of the gamma-ray spectrometer and spark chamber through the forward bulkhead. A gimbal angle of ±50 to 75 degrees should be possible, depending upon solar cell array orientation.

The solar cell arrays (18 panels) provide 1.8 kW of electrical power. Because of the low moment of inertia of the module, only two bar magnets are required for momentum unloading.

1.3.2.5 FPE 5.20 Fluid Physics. One CM-1 module is used to conduct that portion of the fluid physics experiment which require sustained levels of g force. It provides the power, attitude control, thermal control, navigation, data relay, and experiment housing. This module must work in conjunction with a space-station-based CM-3 module outfitted to contain the command and control center and the remainder of the fluid physics experiments. To provide the low level thrusting, a unit designated the propulsion slice is attached to the CM-1 module at the usual experiment peculiar bulkhead.

The fluid physics experiments have been subdivided into subgroups for purposes of identification of requirements, due to major differences in one or more requirements. These divisions are:

a. 5.20-1 include experiments with acceleration limits of 10^{-3} and 10^{-4}g. (assigned to CM-3, attached module)

b. 5.20-2 includes a group of noncryogenic experiments at controlled acceleration levels from 10^{-3} to 10^{-6}g.

c. 5.20-3 includes a group of cryogenic experiments at controlled acceleration levels from 10^{-3} to 10^{-6}g.

d. 5.20-4 includes one long term cryogenic storage experiment at controlled acceleration levels from 10^{-3} to 10^{-6}g.

The 5.20-2, -3 and -4 experiments are accomplished by use of the CM-1 module, Figure 1-19. The operational scheme for the fluid physics experiments is shown on Figure 1-20.

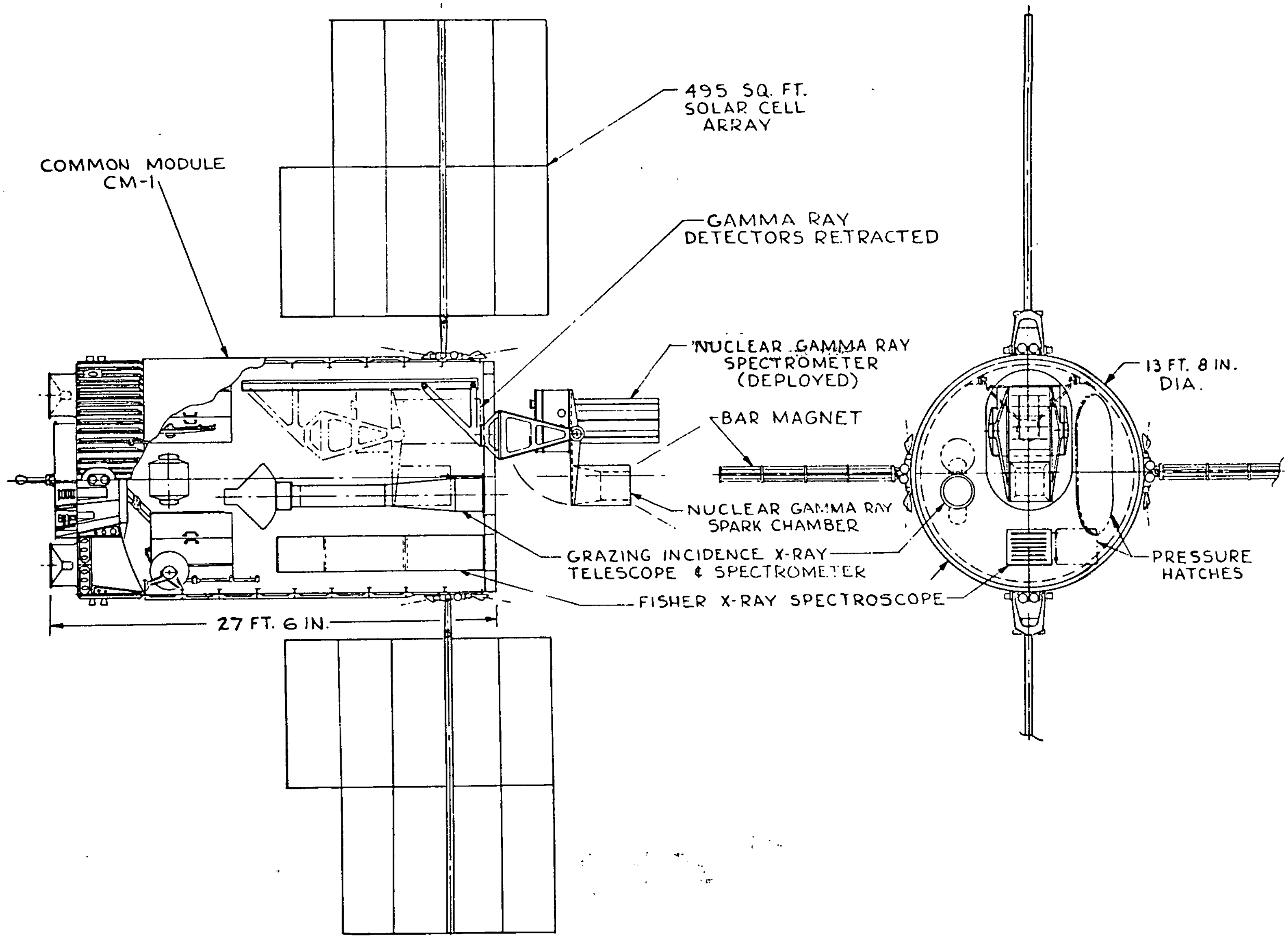

Figure 1-18. FPE 5.5—High Energy Stellar Astronomy, Equipment Integration, CM-1

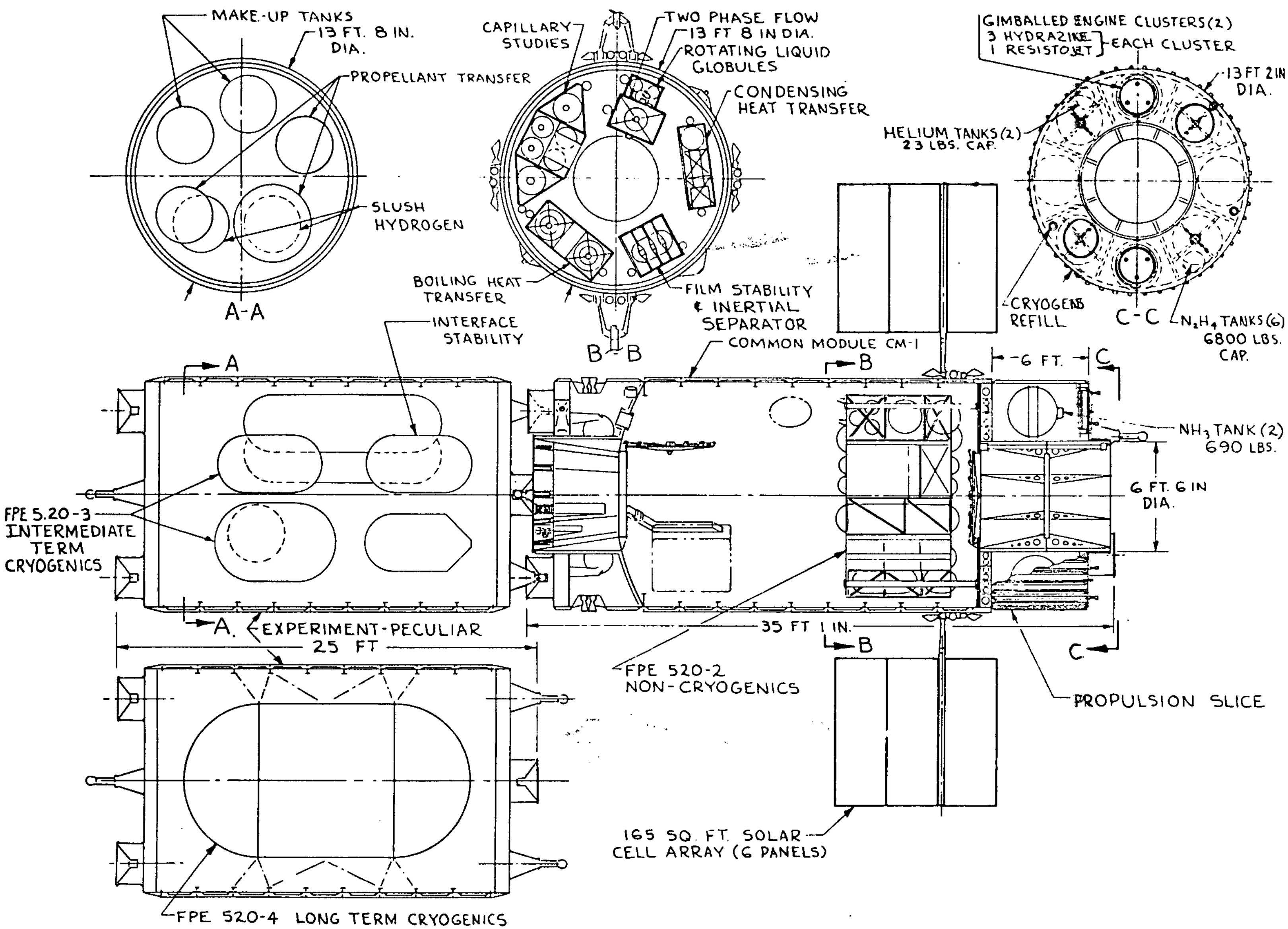

Figure 1-19. FPE 5.20-2, -3, -4—Fluid Physics, Experiment Integration, Free-Flying CM-1

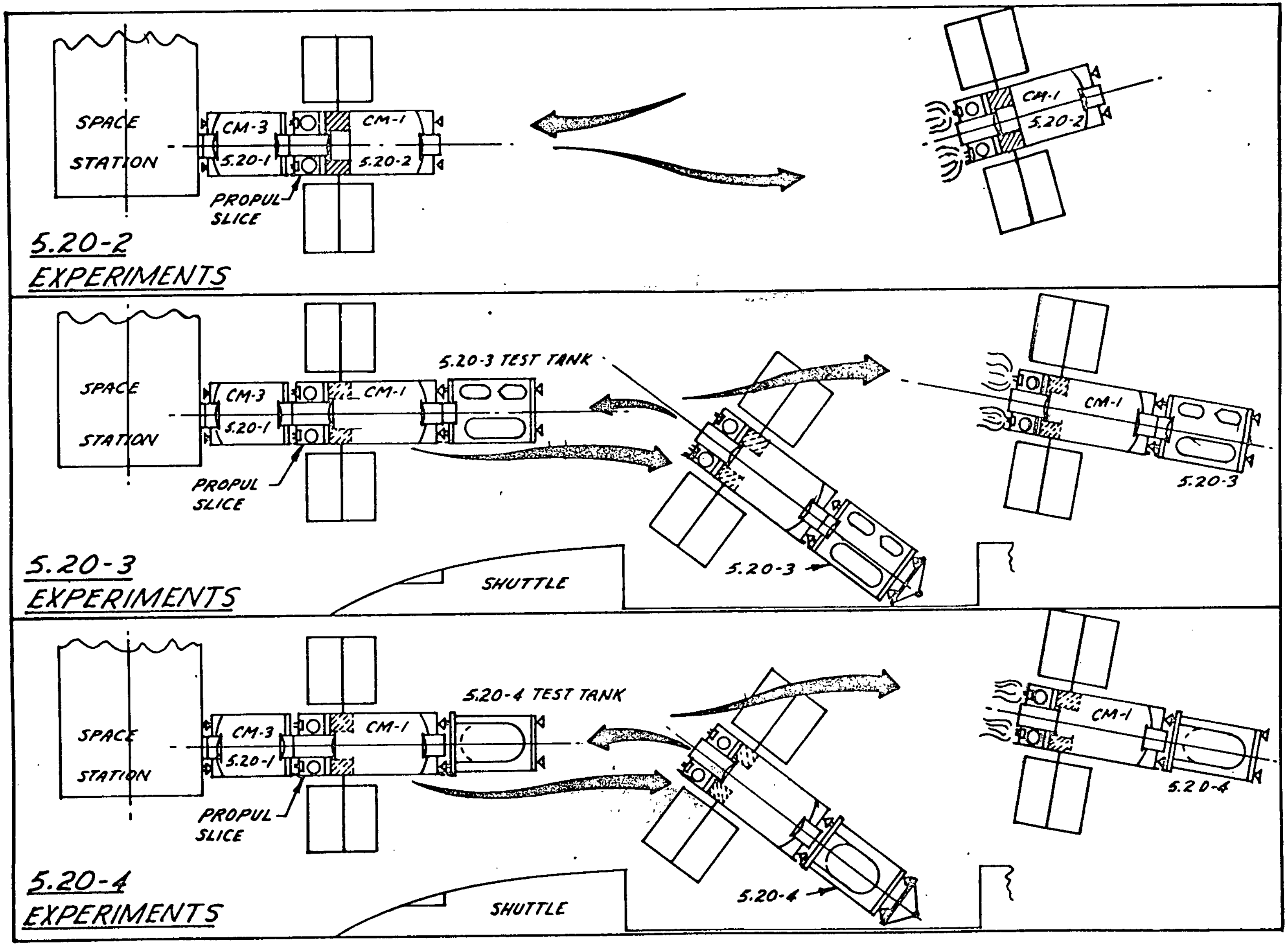

Figure 1-20. Fluid Physics Operational Concept

1.3.2.5.1 Propulsion Slice. The propulsion slice is a bolt-on experiment-peculiar item which is used with a CM-1 module for conducting fluid physics experiments (see Figure 1-21). The CM-1 module is equipped with an experiment-peculiar pressure bulkhead that interfaces with the propulsion slice. The bulkhead is removable for changing the experiment equipment on the ground.

The propulsion slice is used to provide axial acceleration to the CM-1 module for conducting fluid physics experiments. The standard CM-1 module RCS is used for docking maneuvers, etc. The propulsion slice contains thrusters that will result in axial accelerations of 10^{-3}, 10^{-4}, 10^{-5}, and 10^{-6}g. These are nominal levels and the actual levels may vary ± 25% above or below the desired nominal levels. However, the acceleration level of a given run will not vary more than ± 10% from the average level during that run.

The worst case individual single flight requirement is for a $\Delta V = 2590$ fps for experiment No. 10. The worst case ΔV segment for experiment No. 10 is 774 fps at 10^{-4}g. The next limiting case is for $\Delta V = 1090$ fps at 10^{-3}g for experiment No. 2. Directional thrust control is provided to overcome the effects of center of gravity offset due to experiment equipment and expending test fluids and propellant. The propulsion slice incorporates instrumentation for housekeeping information and for on-board checkout. Resupply of propellants and pressurant gases is from the space station.

1.3.2.5.2 Fluid Physics Integration. The conceptual approach provides a system that does not require return of the CM-1-based 5.20 experiments to earth for reapplying the next experiment. This requires in-orbit add-on experiment tankage for the 5.20-3 and 5.20-4 experiments.

The 5.20-2 experiments require a shirtsleeve environment and room temperature. These experiments are changed considerably between tests and therefore require man's participation. Many experiments of a varied nature are in this group.

The experiments of 5.20-3 require a minimum of servicing, mostly to retrieve film. Due to the presence of cryogens, a pressurized environment is undesirable. Shirtsleeve access to the experiments and cameras is probably not mandatory.

The experiment of 5.20-4 requires a minimum of servicing, mostly to retrieve film. This experiment was always considered non-serviceable internally, requiring EVA.

Experiments 5.20-3 and 5.20-4 require replenishment of test cryogens to complete tests. The slush hydrogen tests of 5.20-3 cannot be resupplied from the space station due to the nature of making slush hydrogen.

It is desirable that the 5.20-4 experiment be flexible in regards to the tank size such that subsequent tests could be run of the same nature, but of larger or different shape tanks.

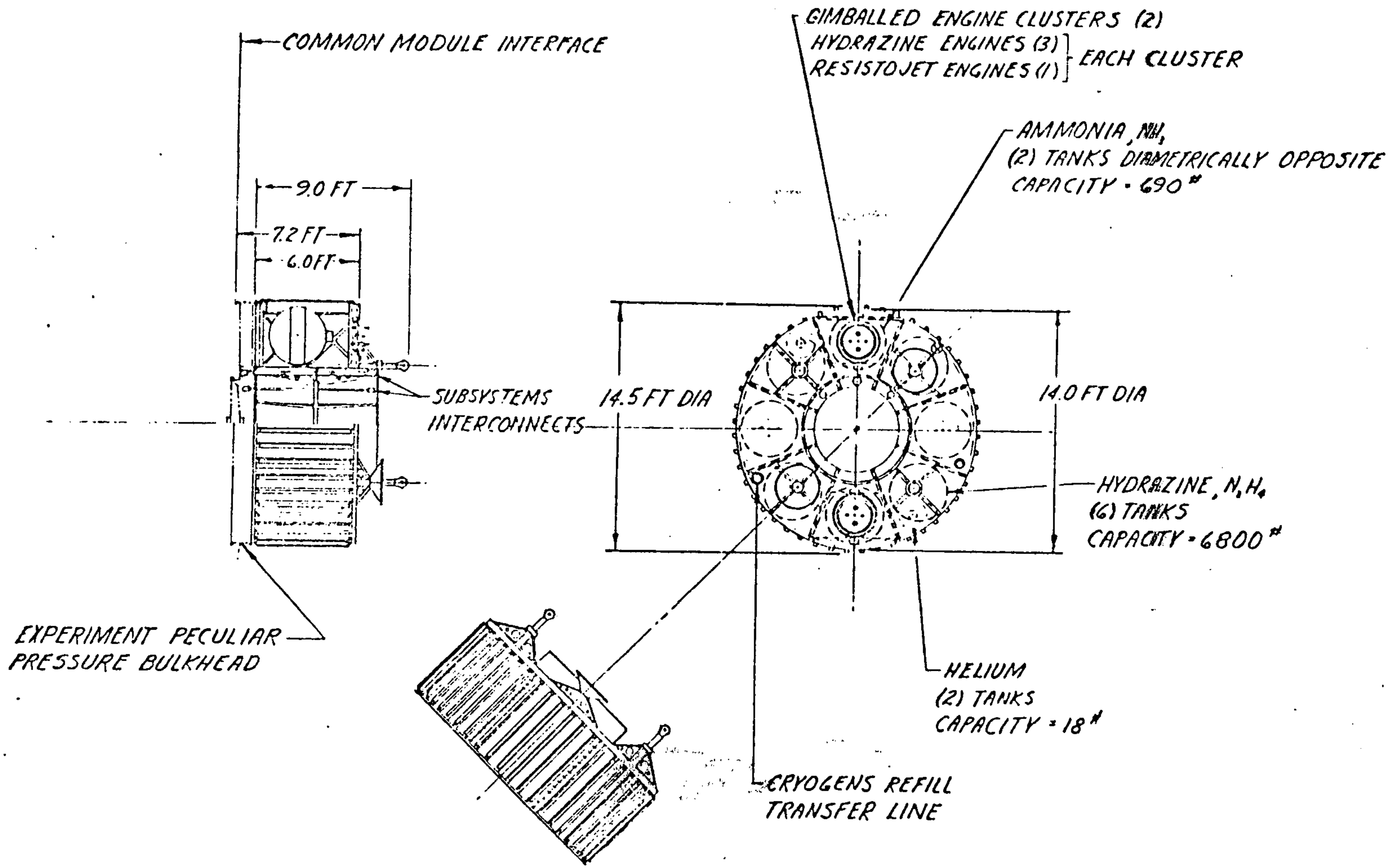

Figure 1-21. Propulsion Slice (FPE 5.20)

Operational Concept (see Figure 1-20): Experiments 5.20-2 are installed to the pressure bulkhead and attached to the propulsion slice, internal to the CM-1 module. To run the 5.20-3 tests, all expendables are expelled from 5.20-2 experiments to lighten the module. The 5.20-3 "test tank module" is docked onto the CM-1 at the end normally docked to the space station. Cryogen transfer lines must be added to the CM-1. One end of the test tank module contains a docking bulkhead to mate to the CM-1. The other end does not contain a docking bulkhead, but perhaps a partial docking system for mounting in the shuttle and erecting to position for CM-1 docking and extraction. The same procedure and design features are used for the 5.20-4 tests.

1.3.3 EXPERIMENT INTEGRATION IN ATTACHED COMMON MODULE CM-3

1.3.3.1 FPE 5.7/12 Plasma Physics Lab. The Plasma Physics Lab shown in Figure 1-22 utilizes a CM-3 common module that rendezvous and docks with the space station and remains attached during experiment operations. A floor partitions the module into two compartments. The compartment adjacent to the station dock houses the control station for the remote maneuvering subsatellites and antenna orientation. Also included in this compartment are data, VLF transmitter/receiver, wake body storage, and some growth volume for FPE 5.6 Space Physics experiments.

The second compartment provides for storage, servicing, and checkout of two large and four small RMSs. A BI-STEM type device would also be stowed in this area. Attached to the flat pressure bulkhead is a 5 foot diameter by 10 foot long experiment peculiar airlock. This airlock is used for the deployment, launch, retrieval and refueling of RMSs. Assuming a maximum ΔV of 600 fps, sufficient hydrazine is available for eight refuelings of the large RMS. Based on a ΔV of 100 fps for the small RMSs, sufficient N_2 is available for seven repressurizations. The propellant and cold gas storage tanks are mounted on the exterior of the pressure bulkhead.

Also mounted on this bulkhead are the gimballed acceleration/inverter with batteries and the stowed VLF antenna. This antenna would be extended 50 feet from the module prior to deployment of the 40 foot by 60 foot antenna dipoles. Deployment would be automatic with manned initiation and control.

An alternate use of the airlock would be to extend experiments out into the space environment by attaching these experiments to the BI-STEM device mounted in the airlock.

1.3.3.2 FPE 5.8 Cosmic Ray Lab. The Cosmic Ray Lab utilizes a CM-3 common module with a large experiment-peculiar compartment added to house the sensors. As depicted in Figure 1-23, this segregates the module into two compartments. The compartment adjacent to the station dock houses the experiment controls and work and storage areas.

As discussed in Volume II, the cosmic ray sensors depicted are projected growth versions of the initial experiment definitions.

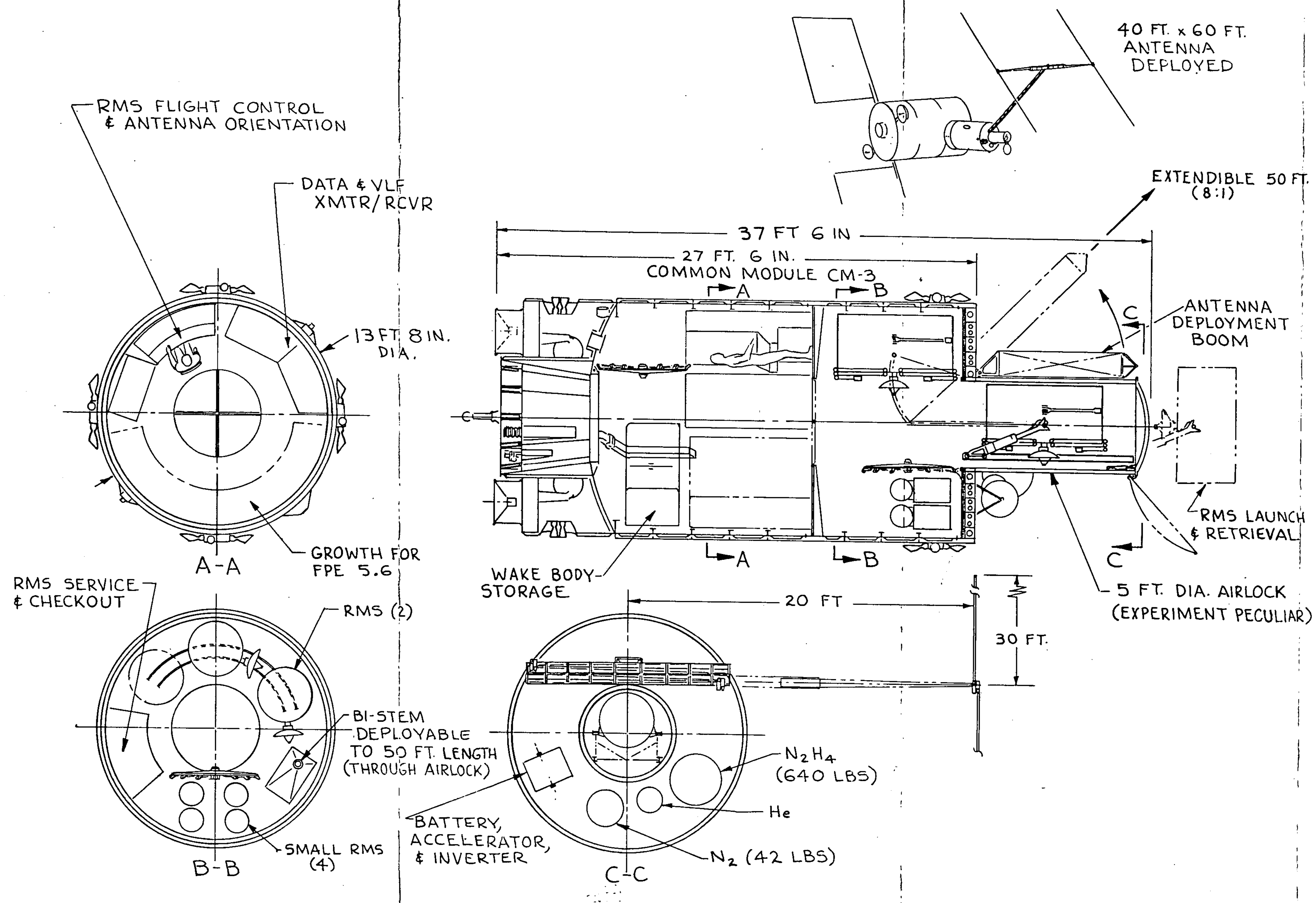

Figure 1-22. FPE 5.7/5.12 Plasma Physics Lab

FOLDOUT FRAME 1

FOLDOUT FRAME 2

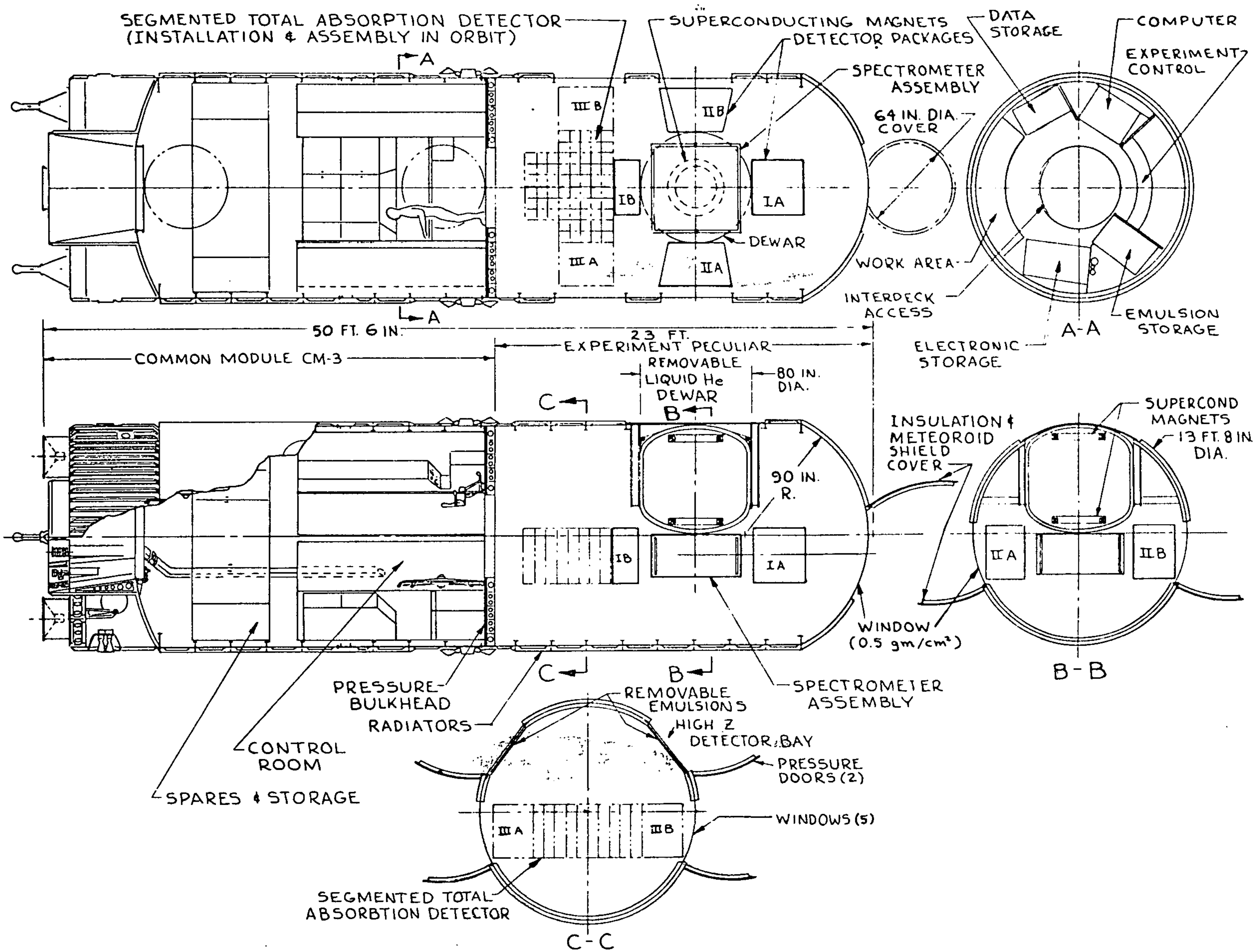

Figure 1-23. FPE 5.8 Cosmic Ray Lab, Attached CM-3, Experiment Integration

Construction of the experiment-peculiar compartment is similar to the common modules with respect to pressure wall diameter, stiffening, and frame spacing. However, modifications include cutouts for the high Z detector bay doors and for removal of the 80-inch-diameter liquid helium dewar. Replacement of the dewar is anticipated about once a year. If this is accomplished in orbit, it is expected that a sizable manipulator would be required on the space station for the 3000-pound dewar.

It may also be necessary to deploy the insulation/meteoroid protection from in front of the five detector windows in order to reduce the wall mass to no more than 0.5 gm/cm^2.

The sensor compartment will operate at 14.7 psi. Space is provided in this compartment for the in-orbit installation of a segmented total absorption detector. Although the total weight of this detector is 24,000 pounds, it may be installed in 350-pound segments. Emulsion plates would be manually installed and sealed around the high Z bays prior to opening the pressure doors.

1.3.3.3 FPE 5.16 Experiment Integration. The space manufacturing experiment and facilities are incorporated into a single CM-3 attached module. Docking provisions are provided to accommodate a future version of a free flying zero drag module.

The experiment integration as shown in Figure 1-11 provides work facilities for experiment preparation and analysis, spectrograph facilities, X-ray facilities and a chemistry laboratory; special equipment such as a metalograph, cameras, and photo laboratory items are also included. These facilities are located on a common deck at the end of the module away from the space station.

Also located in the module is the 4-foot-diameter sphere in which the zero drag casting and forming experiments are performed. Also mounted on a 360° track system are the 20-inch diameter by 72 inch long canisters which contain the various experiments for the spherical chamber. The experiment canisters are controlled remotely to rotate into place, raise into the sphere to conduct the experiment, then lower onto the evaluation facility for examination of the completed experiment.

1.3.3.4 FPE 5.20 Fluid Physics. One CM-3 module is utilized to conduct those fluid physics experiments that require limiting accelerations between 10^{-3} and 10^{-4}g. Also these experiments are non-cryogenic and are suited for direct man participation.

This module is also the command and control center for the other fluid physics experiments operating in a free-flying mode. It has been designated 5.20-1 and is illustrated in Figure 1-24. The particular experiments of this module are mounted onto the flat bulkhead and present no problems of integration into the module. There is sufficient volume to increase the quantity or scope of experiments of a like nature. There are problems of integration, however, in the provisions that this module must possess to be capable of servicing the free-flying module. These problems are predominantly

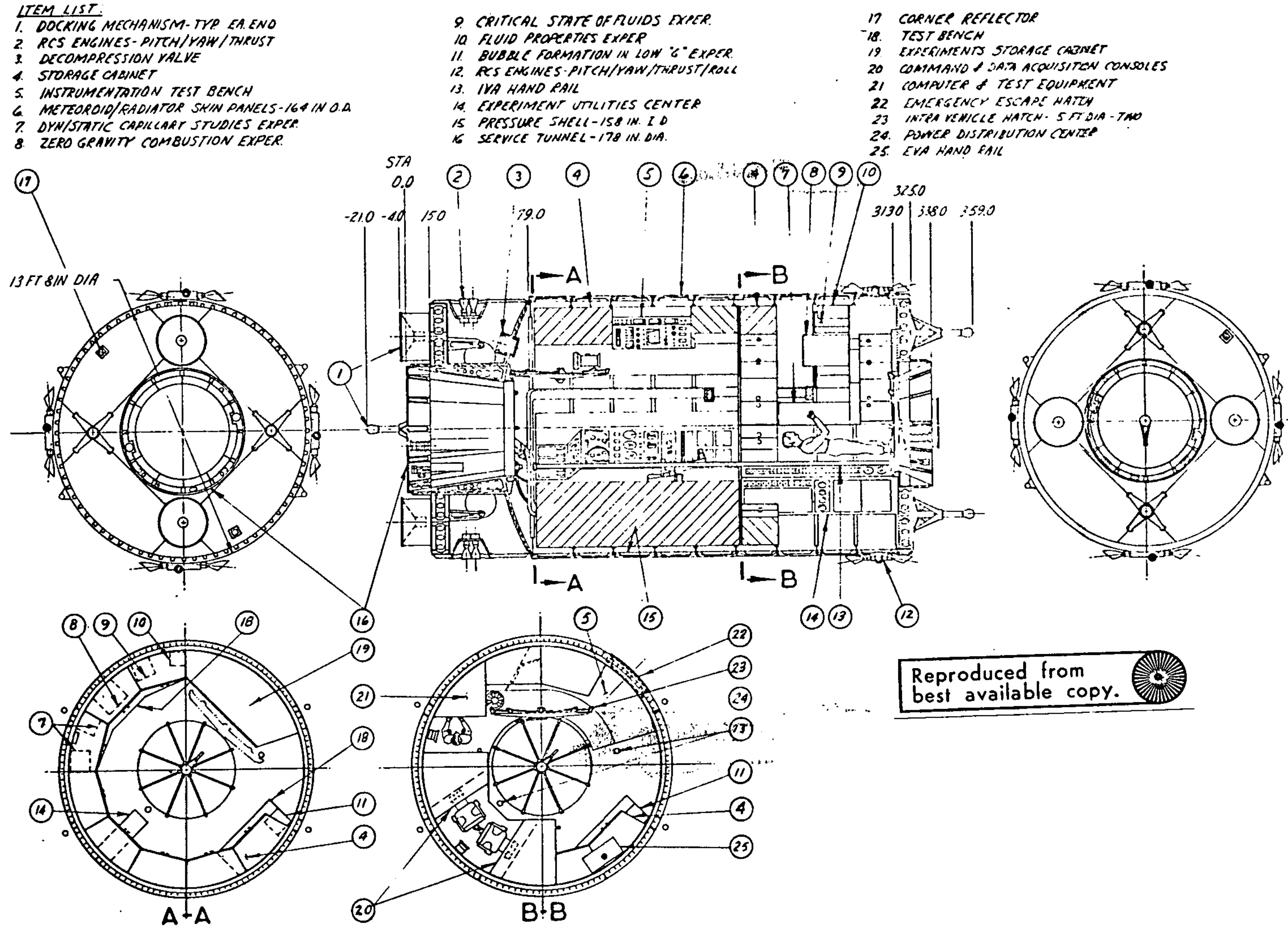

Figure 1-24. FPE 5.20-1—Fluid Physics, CM-3

those of fluid transfer to refill cryogenics and propellants. There is also the possibility that these service-station activities will be a function performed by the space station.

1.3.3.5 FPE 5.27 Experiment Integration. The physics and chemistry laboratory experiment equipment has been integrated into a CM-3 module as shown in Figure 1-25. This laboratory module operates attached to the space station utilizing the module airlock between the experiment equipment area and the space station to prevent possible contamination of the space station.

The laboratory floor area is located at the remote end of the module from the space station. The various experiment areas are accessible to the astronaut through the use of a track-mounted automated chair.

The facilities provided include a chemistry lab, metallographic apparatus, X-ray diffraction machine, and a mass spectrograph. Also provided is an induction furnace and air lock chamber similar to that used in FPE 5.16 which is vented to outer space for conduction of the artificial meteoroid experiments. Fluid and film storage facilities are also provided.

The experimentation packages are stored in a locker until such time that a package is removed and placed into the appropriate bench facility.

1.3.4 EXPERIMENT INTEGRATION IN ATTACHED COMMON MODULE CM-4

1.3.4.1 FPE 5.9, 5.10, and 5.23 Experiment Integration. The space biology experiments are incorporated into a single CM-4 module and an experiment peculiar centrifuge. The configuration may be seen in Figure 1-26.

The facility work areas consisting of a data management area, a specimen preparation and return area, and four specialized research facilities located at the remote end of the module from the space station. Work at the various facilities is accomplished through the use of an automated chair that is horizontally adjustable and is mounted to a pole that rotates around the interior of the module on tracks located at each end of the module. Above the facilities area are 65 holding racks mounted around the module wall. The racks provide holding capability for lower vertebrate, higher plant, invertebrate culture, cell tissue, microbiology experiments, and small and large mammals. Also provided are two freezers, two refrigerators, and two chemical storage racks. Access to the cages is through the use of an automated laminar flow bench used in conjunction with the above mentioned chair. The laminar flow bench is capable of moving up and down the rail mounted pole as well as radially via movement of the pole on the tracks.

Also provided are the large primate holding containers consisting of four 4 foot 10 inch spherical containers. Access to the container is through a 30-inch hatch in the sphere.

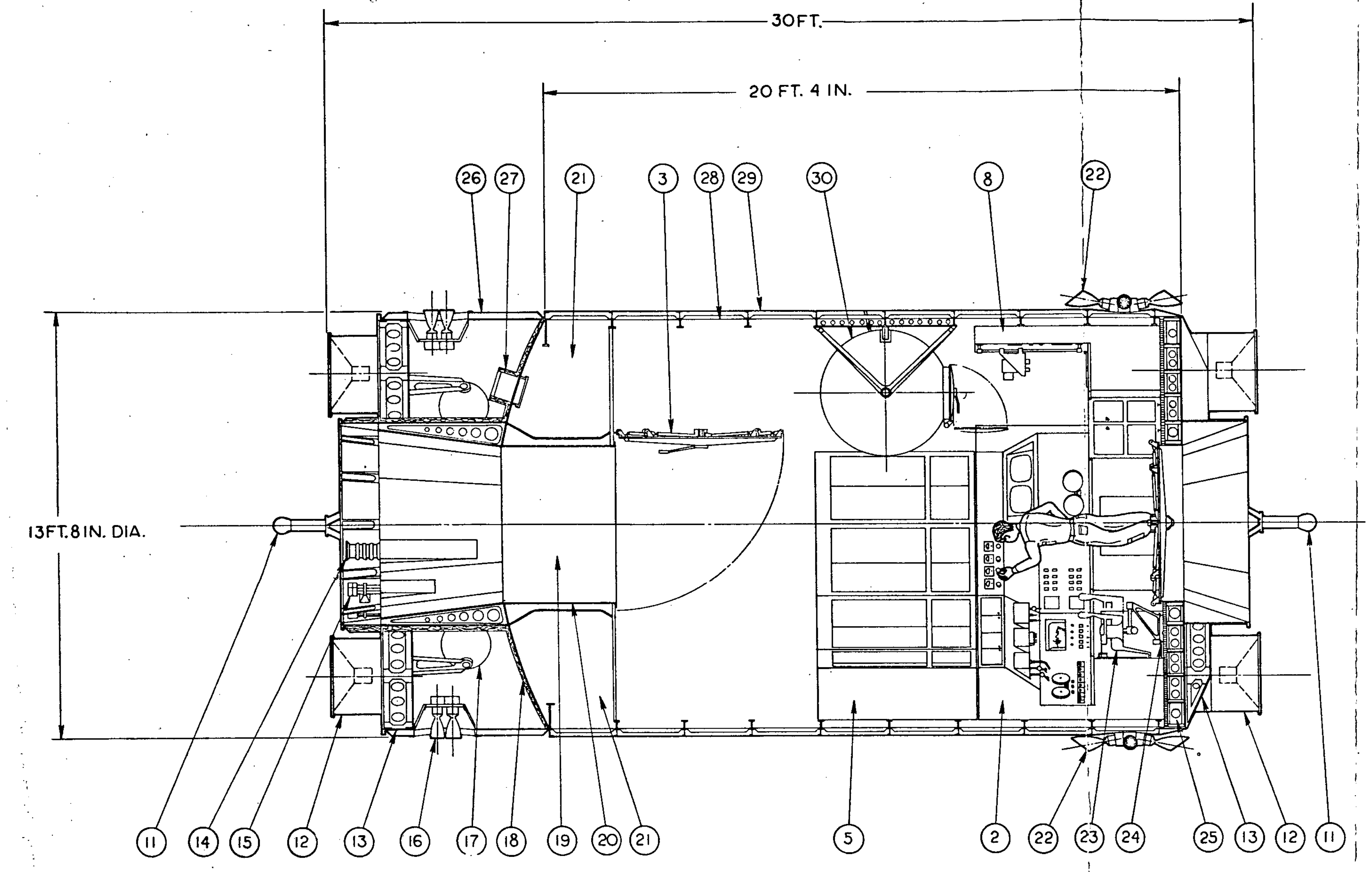

21 COMMON SUBSYSTEMS COMPARTMENT
22 RCS ENGINES - THRUST/ROLL
23 AUTOMATED CHAIR
24 CHAIR RAILS
25 PRESSURE BULKHEAD
26 SKIRT SECTION
27 PRESSURE RELIEF VALVE
28 PRESSURE SKIN
29 METEOROID PROTECTION/RADIATOR PANELS
30 EXPERIMENT CHAMBER

11 DOCKING PROBE
12 DOCKING DROUGE
13 DOCKING BEAM STRUCTURE
14 CREW LIFE SUPPORT DUCT
15 SYSTEMS INTERFACE
16 RCS ENGINES - PITCH/YAW
17 HELIUM TANKS (4)
18 INSULATION
19 AIRLOCK
20 79/60 INCH DIA. TUNNEL

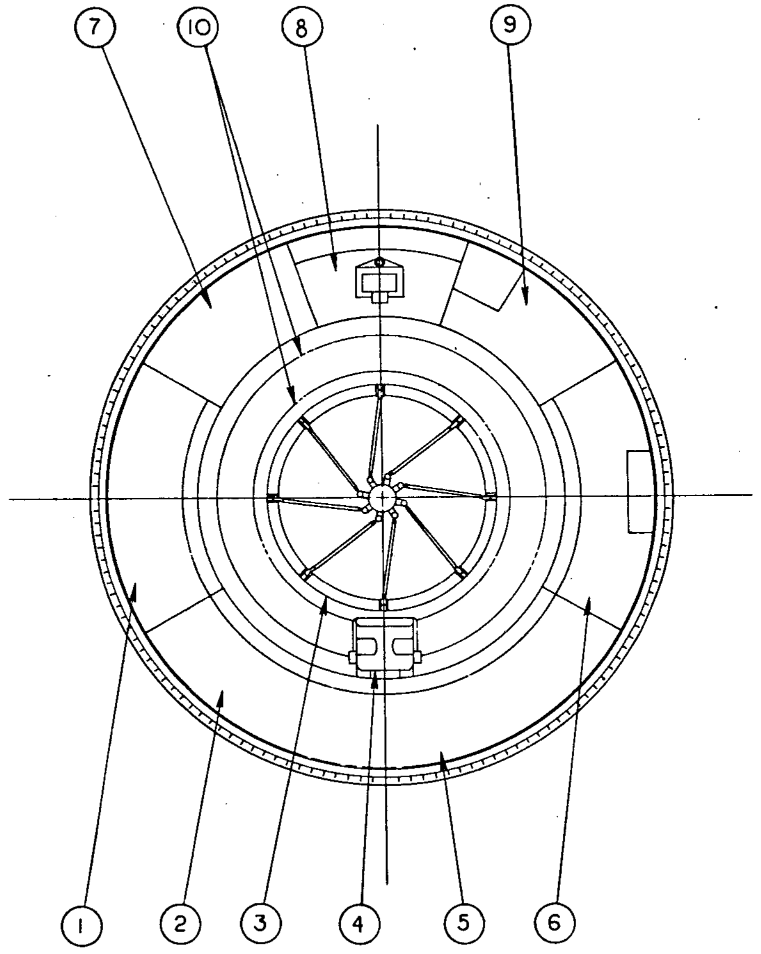

1 DATA MANAGEMENT
2 CHEMISTRY LABORATORY
3 60 INCH DIA. HATCH
4 AUTOMATED CHAIR
5 STORAGE
6 METALOGRAPH
7 FILM STORAGE
8 CAMERA FACILITIES
9 MASS SPECTROMETER
10 CHAIR RAILS

Figure 1-25. Common Module CM-3/FPE 5.27

FOLDOUT FRAME 1

FOLDOUT FRAME 2

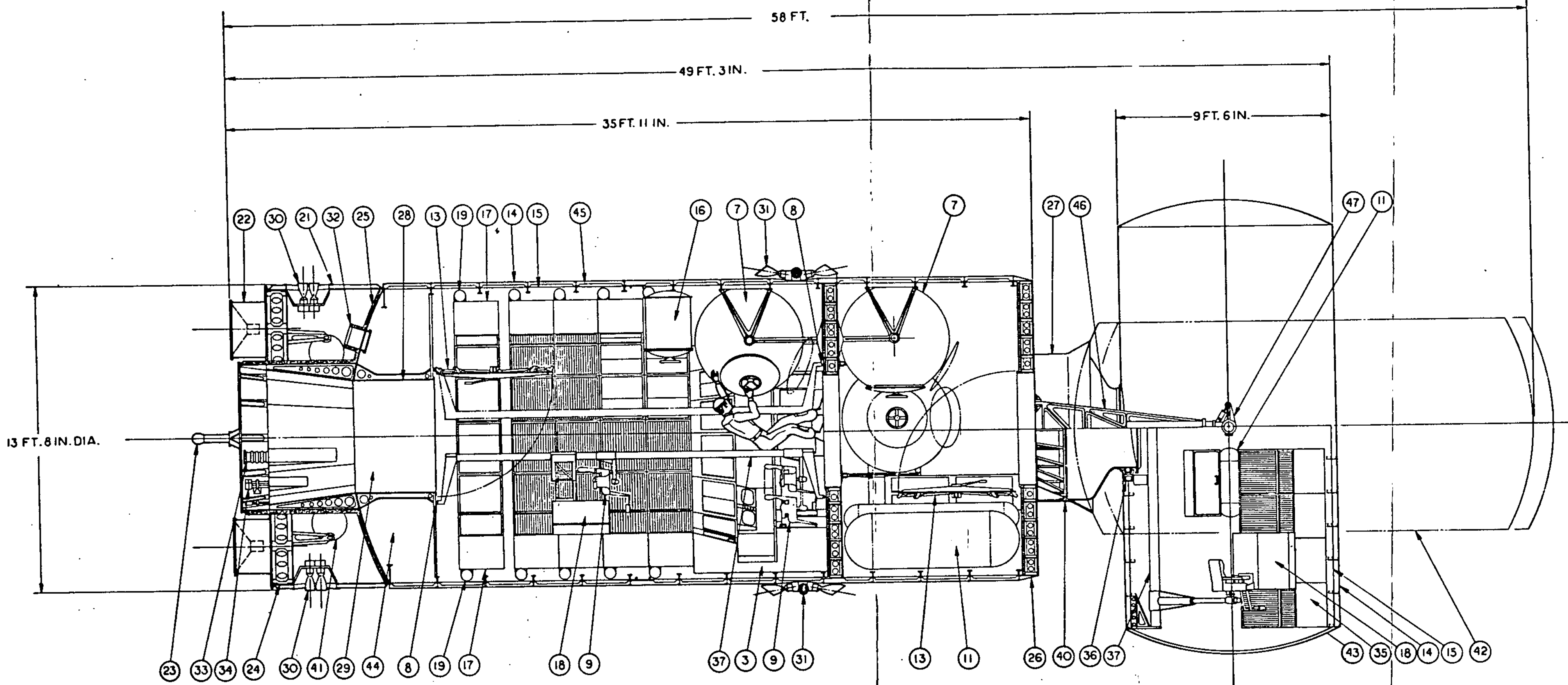

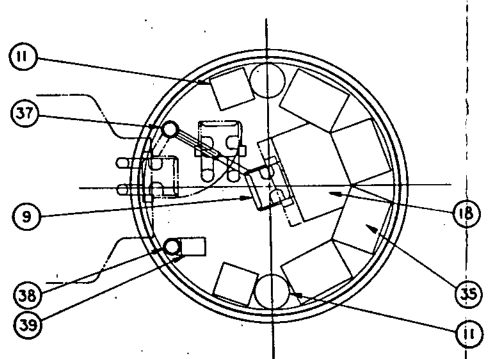

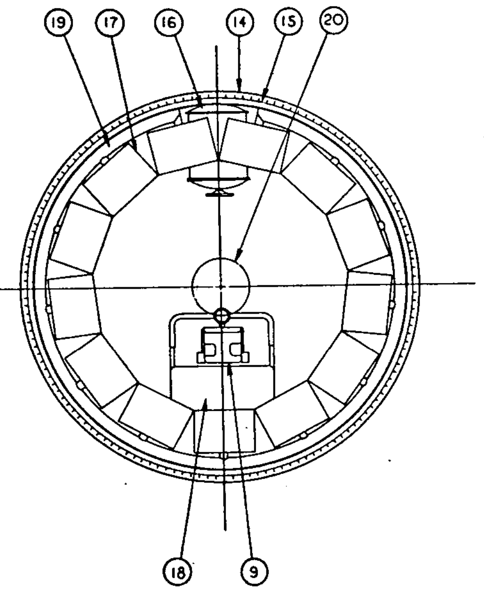

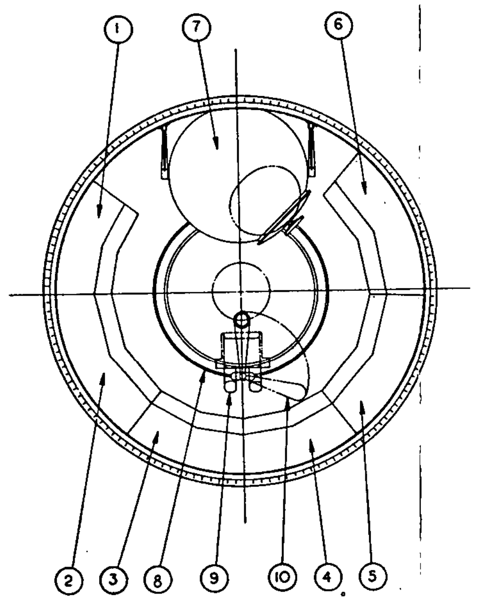

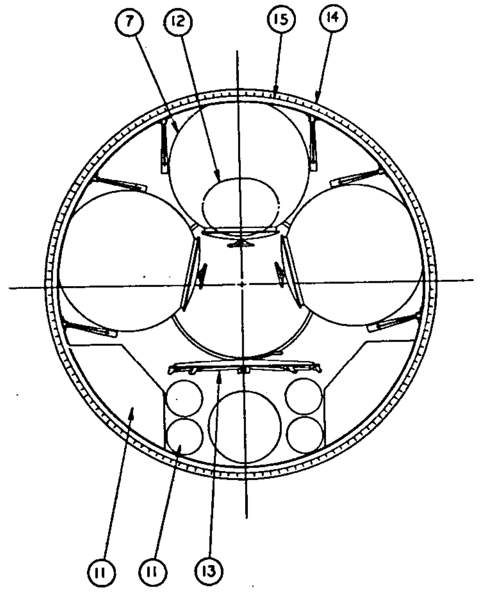

35 HOLDING FACILITIES (32)
36 CENTRIFUGE BEARING, SEAL / DRIVE
37 AUTOMATED EQUIPMENT POLE
38 COUNTERBALANCE POLE
39 COUNTERBALANCE
40 MATING SEAL INTERFACE
41 HELIUM TANKS (4)
42 CENTRIFUGE LAUNCH POSITION
43 CENTRIFUGE OPERATIONAL POSITION
44 COMMON SUB SYSTEMS COMPARTMENT
45 INSULATION
46 CENTRIFUGE ERECTION MECHANISM
47 RELEASE MECHANISM

21 SKIRT SECTION
22 DOCKING DROUGE (2)
23 DOCKING PROBE (2)
24 DOCKING BEAM STRUCTURE
25 FORWARD PRESSURE BULKHEAD
26 AFT PRESSURE BULKHEAD
27 79/42 INCH TUNNEL
28 79/60 INCH TUNNEL
29 9 FOOT AIRLOCK
30 RCS ENGINES - PITCH/YAW
31 RCS ENGINES - THRUST/ROLL
32 PRESSURE RELIEF VALVE
33 CREW LIFE SUPPORT DUCT
34 SYSTEMS INERFACE

16 AUTOCLAVE
17 HOLDING FACILITIES (65)
LOWER VERTEBRATE
HIGHER PLANT
INVERTEBRATE CULTURE
CELL, TISSUE / MICROBIOLOGY
SMALL MAMMEL
LARGE MAMMEL
FREEZERS (2)
REFRIGERATORS (2)
CHEMICAL STORAGE (2)
18 LAMINAR FLOW BENCH
19 ATMOSPHERE CONTROL DUCTS
20 LOCUS OF POLE ROTATION

1 PREPARATION / SPECIMEN RETURN
2 DATA MANAGEMENT
3 PHYSIOLOGICAL RESEARCH
4 MICROBIOLOGY, HYSTOLOGY / CYTOLOGY
5 VISUAL RECORDS / MICROBIOLOGY
6 CHEMICAL / PHYSICAL ANALYSIS / RADIOBIOLOGY
7 LARGE PRIMATE HOLDING FACILITY (4)
8 POLE TRACTION RAILS
9 AUTOMATED CHAIR
10 POLE RETRACTED POSITION

11 EXPERIMENT LIFE SUPPORT
12 PRIMATE HOLDING FACILITY DOOR OPEN
13 60 INCH HATCH
14 METEOROID PROTECTION / RADIATOR PANELS
15 INTEGRALY STIFFENED PRESSURE SKIN

Figure 1-26. Common Module CM-4 and FPE 5.9/10/23

FOLDOUT FRAME 1

FOLDOUT FRAME 2

FOLDOUT FRAME 3

centrifuge provides for mounting of 32 holding racks and a laminar flow bench and chair similar to the main lab.

1.3.4.2 FPE 5.11 Earth Surveys. The baseline concept for earth surveys experiments is accommodated in one CM-4 module, shown in Figure 1-27. The module consists of four sections: (1) the laboratory work section, (2) command and data acquisitional section, (3) sensor test section, and (4) external sensor bay. Sections 1, 2, and 3 are interconnected as one pressure compartment. Section 4 is pressurizable when all extended sensors have been retracted and the dome closed and latched. Section 4 is then accessible through a 32-inch-diameter hatch for servicing the sensors.

That portion of the module from Station 417 to 521 is considered experiment peculiar, including the sensor bulkhead. The earth surveys equipment of Sections 1, 2, and 3 is attached to the non-pressure flat bulkheads or the shell circumferential rings.

This concept is predicated upon specific sensors, their envelope size, pointing direction, degree of articulation and fields of view as outlined in the FPE for nineteen instruments plus three supporting sensors. Because of large dimensions, articulation and view angles, and the desirability for access to these instruments within a shirt-sleeve atmosphere, physical clearances and viewing interferences do not allow much latitude in a rearrangement, substitution or enlargement of sensors. This problem of integration is a geometric progression, and with a starting point of 22 sensors introducing a new variable has a snowballing effect upon the physical arrangement and incompatibilities.

The earth surveys FPE presents a unique problem of integration because of the operational anomalies. A nadir orientation is required in all cases coupled with a ground track flight path, and corresponding changes in altitude are desired for conducting some observations. These operational anomalies seriously impact upon the space station operations if the module is attached. Additional requirements for experiment growth specifies an operational need to provide 60° half-angle conical pointing for all sensors. This is primarily to engage truth sites during each path across the North American continent. The baseline shown per Figure 1-27 does not possess this capability. Such maneuvers depend on the space station and this constitutes a severe penalty.

Various methods of achieving the 60° half-angle conical pointing, were briefly investigated. The geometric problems of integration noted previously require a depth of investigation beyond the time allocation of this study. However, these investigations were sufficient to show that an extendible, gimballed platform system that would retain the capability for shirtsleeve access to the sensors would add approximately 20 feet to the module length with an attendant weight increase. This total facility would then exceed the 60-foot shuttle cargo bay. Additionally, the mechanical complexity was considered impractical and although platform gimballing through a conical 60° half-angle is possible, one quadrant was not available due to presence of the pressurizable

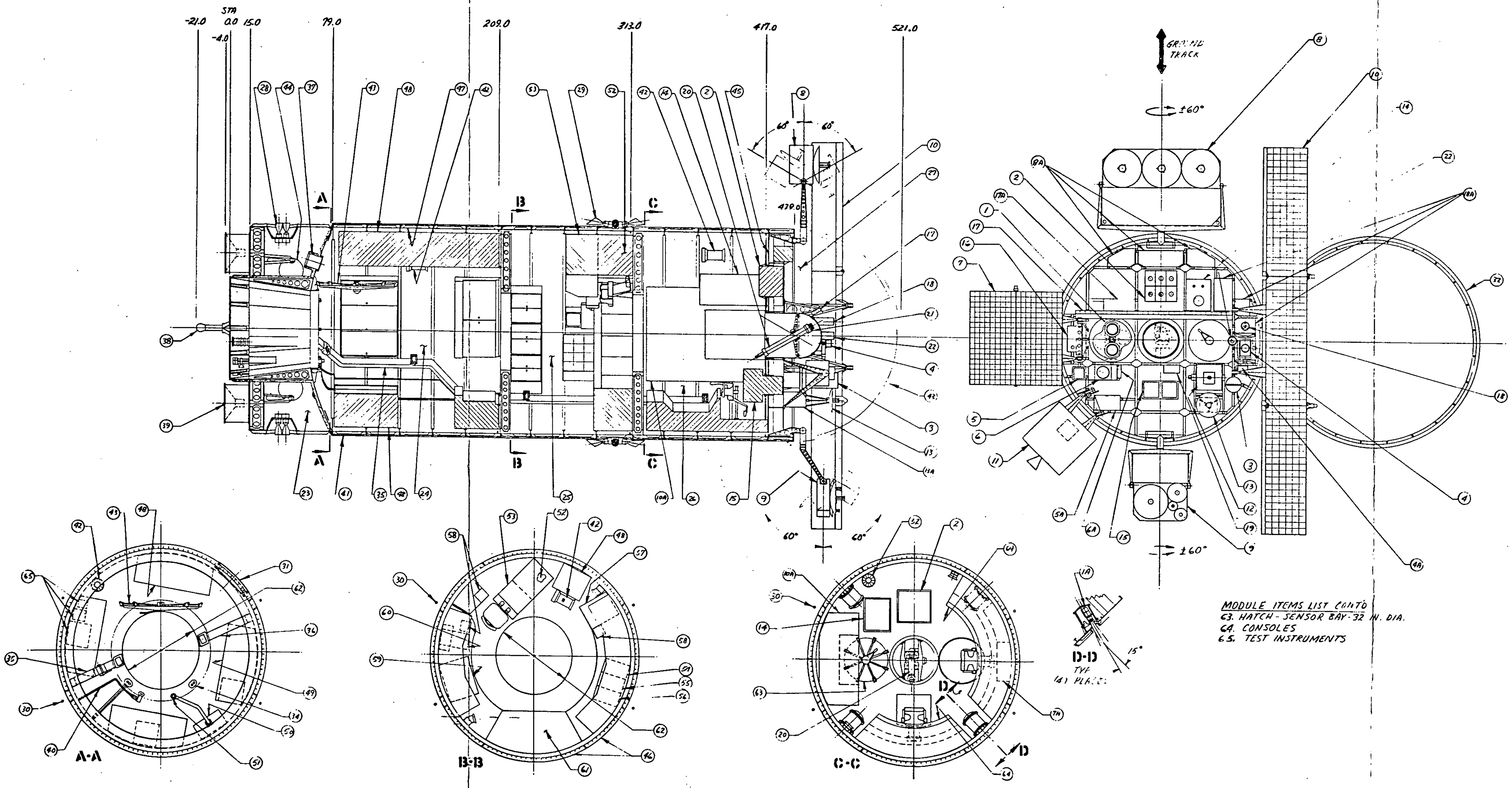

MODULE ITEMS LIST CONT'D
63. HATCH - SENSOR BAY - 32 IN. DIA.
64. CONSOLES
65. TEST INSTRUMENTS

FPE 5.11 SENSORS LIST
1 METRIC CAMERA - 2
1A. STELLAR CAMERA - 4 (METRIC CAMERA REF)
2. MULTI-SPECTRAL CAMERA
3 MULT-SPECTRAL IR SCANNER
4 IR INTERFEROMETER SPECTROMETER
4A. IR INTERFEROMETER SPECTROMETER ELECTRONICS
5. IR ATMOSPHERIC SOUNDER
5A. IR ATMOSPHERIC SOUNDER ELECTRONICS
6 IR SPECTROMETER/RADIOMETER
6A. IR SPECTROMETER/RADIOMETER ELECTRONICS
7. MW SCANNER
7A MW SCANNER ELECTRONICS
8 MULTI-FREQUENCY MW RADIOMETER
8A MULTI-FREQUENCY MW RADIOMETER ELECTRONICS
9. MW ATMOSPHERIC SOUNDER
10 RADAR IMAGER
10A RADAR IMAGER ELECTRONICS
11. ACTIVE/PASSIVE MW RADIOMETER
12. VISIBLE WAVELENGTH POLARIMETER
13. UHF SFERICS
13A UHF SFERICS ELECTRONICS
14. ABSORPTION SPECTROMETER
15 LASER ALTIMETER
16 UV IMAGER/SPECTROMETER
17 RADAR ALTIMETER/SCATTEROMETER
17A RADAR ALTIMETER/SCATTEROMETER ELECTRONICS
18 PHOTO-IMAGING CAMERA
18A PHOTO-IMAGING CAMERA ELECTRONICS
19 DATA COLLECTION
20 TRACKING TELESCOPE } SUPPORT SENSORS
21 INDEXING CAMERA } SUPPORT SENSORS
22 DAY/NIGHT TELEVISION CAMERA } SUPPORT SENSORS

MODULE ITEMS LIST
23 SKIRT SECTION
24 LABORATORY WORK SECTION
25 COMMAND & DATA ACQUISITION SECTION
26 SENSOR TEST SECTION
27 EXTERNAL SENSOR BAY
28 RCS ENGINES - PITCH/YAW/THRUST
29 RCS ENGINES - PITCH/YAW/THRUST/ROLL
30 EVA HAND RAILS
31 EMERGENCY ESCAPE HATCH
32 SENSOR BAY PRESSURE DOME - OPEN
33 SENSOR BAY PRESSURE DOME - CLOSED
34 SUIT CIRCUITS - TWO
35 ATMOSPHERE INTAKE DUCT
36 ATMOSPHERE EXHAUST DUCT
37 DECOMPRESSION VALVE
38 DOCKING PROBE - TWO
39 DOCKING DROGUE - TWO
40 ATMOSPHERE MONITORING LINES
41 INSULATION
42 HEAT EXCHANGER
43 ENTRANCE HATCH
44 HELIUM TANKS - FOUR
45 EXPERIMENT PECULIAR BULKHEAD
46 METEOROID/RADIATOR SKIN PANELS - 164 IN. O.D.
47 PRESSURE SKIN - 158 IN. I.D.
48 STORAGE CABINET
49 WORK BENCH/STORAGE CABINETS OVER - 3 PLACES
50 POWER DISTRIBUTION BOX
51 POWER RECEPTACLE
52 FILM PROCESSOR
53 STEREO-COMPARATOR
54 GROUND TRACK TV
56 SENSOR FOV TV
57 DISPLAY STORAGE TV
57 STEREOSCOPE
58 KEY BOARD
59 MICRODENSITOMETER
60 DISPLAY STORAGE
61 TEST AREA
62 60 INCH PASSAGE WAY

Figure 1-27. Inboard Profile—Attached CM-4 Earth Surveys dome. To place the dome out of view would require another complex extension mechanism (more weight) and increased radiator shadowing.

Another gimballed concept considered use of a CM-3 containing the sensors only, with a gimbal mechanism between the CM-4 and CM-3. This approach results in a gross waste of both modules volumetrically, adds one CM-3 to the program and is mechanically unsound due to the large mass outside of the gimbal pivot planes. Also, the opened dome would limit the necessary gimbal angle.

A promising gimballed concept is shown in Figure 1-28. It resolves the dome limitations on gimbal angles, increases module length and weight slightly but within the space shuttle limits, does not shadow the radiator, and has favorable mass distribution relative to gimbal pivots.

Detached modes of operation are described in Section 1.4.4.3.

1.3.4.3 FPE 5.22 Component Test and Sensor Calibration. The integration of this FPE into a CM-4 module is shown on Figure 1-29. This integration results in four separately pressurizable compartments: (1) the control/data center and calibration area, (2) test cell No. 1, (3) test cell No. 2, and (4) an interconnect airlock. All circular hatches are five feet in diameter. The airlock side hatch is 32 inches by 54 inches.

Test cell No. 1 is depressurizable to space vacuum and has a 30-inch side hatch for emergency escape. This hatch can also be used for exposure of test items to space. An arrangement of five test benches are shown although this is only a postulated arrangement. Flexibility of test operations can be enhanced by provision of movable and erector type benches.

Test cell No. 2 is depressurizable and contains a standard five-foot hatch through which the rate stabilized platform is extended for test purposes. This platform provides 120° conical viewing. The LWIR, a tracking telescope and microwave radiometer, are shown mounted on the platform.

The control center contains two primary operating consoles with two automated chairs mounted to vertical poles. The optical bench is located in this compartment but due to the basic dimensions of the module the bench is 132 inches in length rather than the 150 inches specified in the FPE. A test bench and instrumentation are also in this compartment.

1.4 EXPERIMENT MODULE/LAUNCH VEHICLE INTEGRATION

The experiment modules have been designed to be compatible for launch operations in either an expendable type launch vehicle or the reusable shuttle orbiter vehicle.

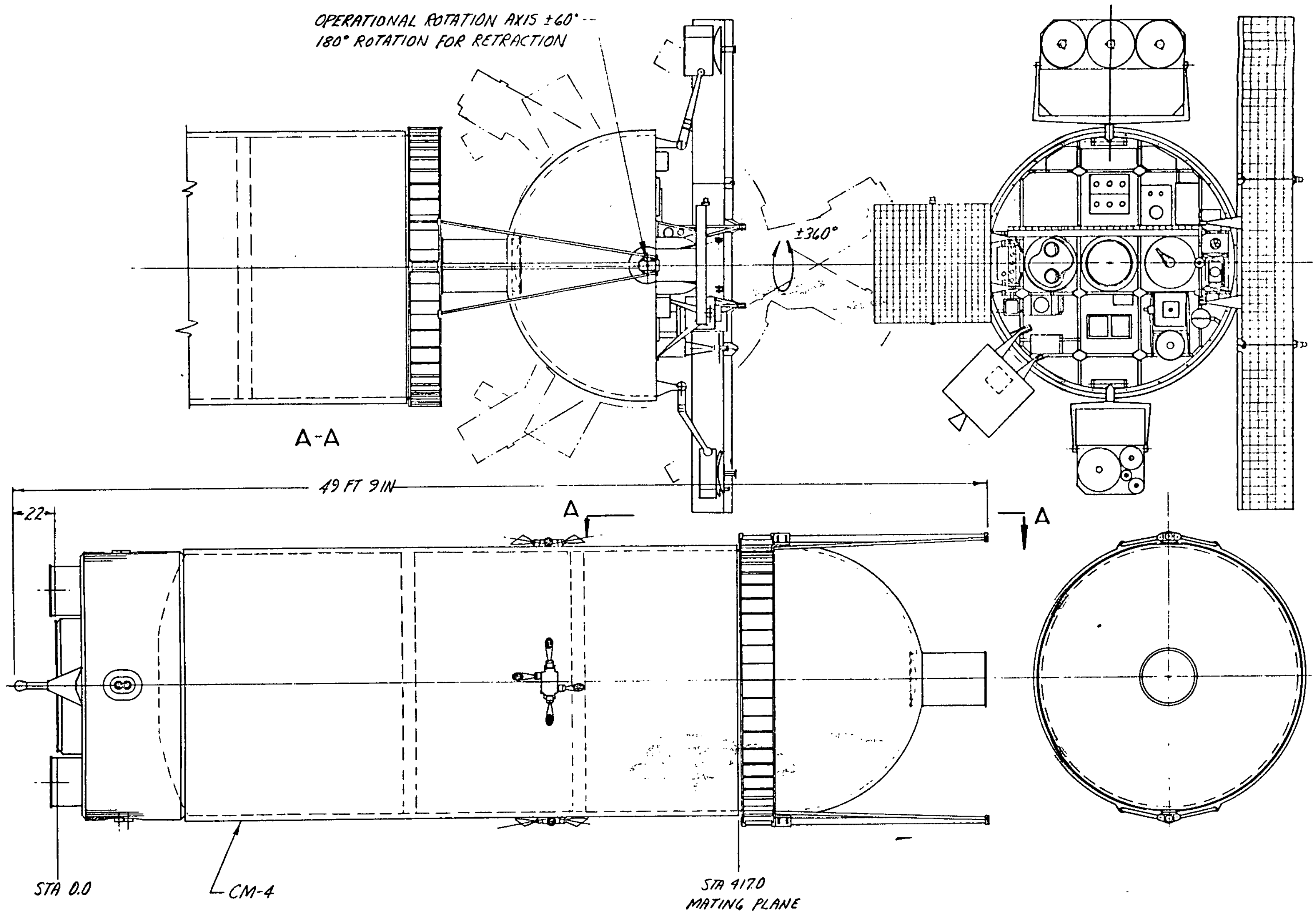

Figure 1-28. FPE 5.11— Earth Surveys, Attached, Two Axis Control, CM-4

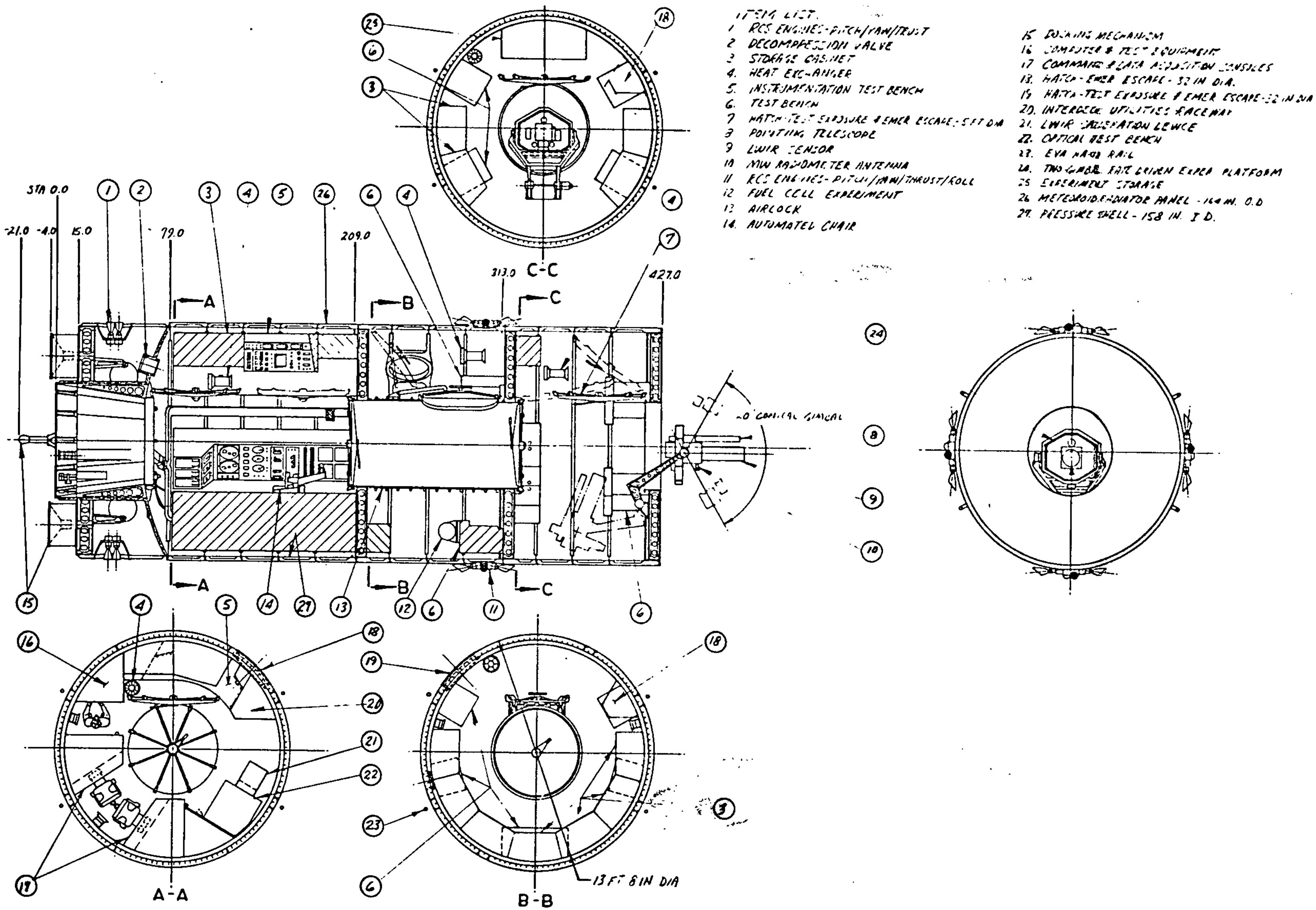

Figure 1-29. Component Test and Sensor Calibration, CM-4

1.4.1 EXPENDABLE LAUNCH VEHICLE INTEGRATION. In the case of expendable launch vehicles such as Titan IIIC and IIIF, Saturn IB, and Saturn Intermediate 20, the experiment modules must be entirely enclosed in a jettisonable shroud as a protective measure during boost operation. The shroud configuration for both the astronomy and laboratory type modules is shown in Figure 1-30. Sufficient clearance must be maintained between the fairing and the module payload to allow for any sway motion. The shrouds protect the solar arrays, radiators, and thermal coatings from contamination and thermal damage during launch.

1.4.2 SHUTTLE ORBITER VEHICLE INTEGRATION. The primary structural tiedown interface between the experiment module payload and the shuttle orbital payload compartment is through a system of six tiedown pins, four of which are located on two sides of the module and two at the bottom (see Figure 1-31).

Longitudinal loads are taken by the two horizontal pins located nearest the module center of gravity; vertical loads are reacted by all four of the horizontal fittings. Lateral or torsional loads are reacted by all six of the fittings.

Auxiliary sway fittings will be required for some of the longer experiment configurations such as the three-meter stellar telescope and the 1-1/2 meter UV solar telescope.

A possible method of shuttle launch and retrieval of experiment modules is shown in Figure 1-35. In this case a rotatable docking pallet is provided on the shuttle to which the module is docked. After the docking operation is completed, the pallet with the docked module is rotated into the payload bay. The module is then translated forward into the hard hold-down fittings and also mated with the five-foot-diameter tunnel leading to the shuttle cabin. The payload bay doors are closed and retrieval is complete. Manned access to the module is through the shuttle tunnel into the pressurized module. Deployment operation is the reverse of the retrieval operation.

The end view of the CM-1 baseline module, shown in Figure 1-32, illustrates the accommodation within a shuttle payload bay having a circular envelope of 15 feet. The 13-foot 2-inch dimension is the pressure shell inside diameter. Exterior to this shell is the insulation, meteoroid bumper, radiator panels, solar cell arrays, RCS engines, and magnetic torquing bars.

The solar cells arrays, RCS engines, and magnetic torquing bars have been configured for launch stowage within the eight-inch annulus. The solar cell arrays wrap around the module exterior and are secured against the meteoroid bumper. The five-element bar magnet is arranged in a flat configuration of two rows to lower the stowed profile. The elevation and azimuth drive mechanisms are also configured to maintain a low profile.

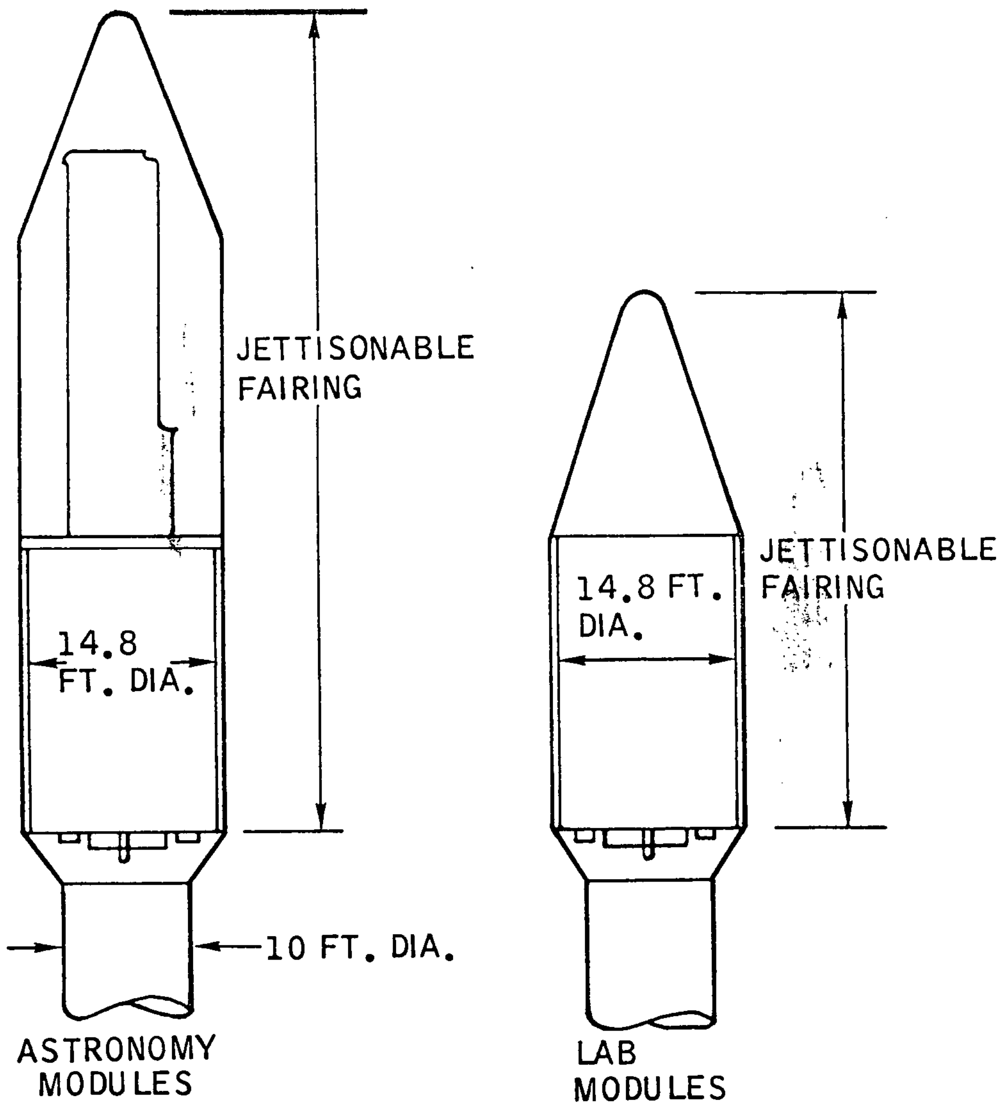

Figure 1-30. Expendable Launch Vehicles/Module Interface

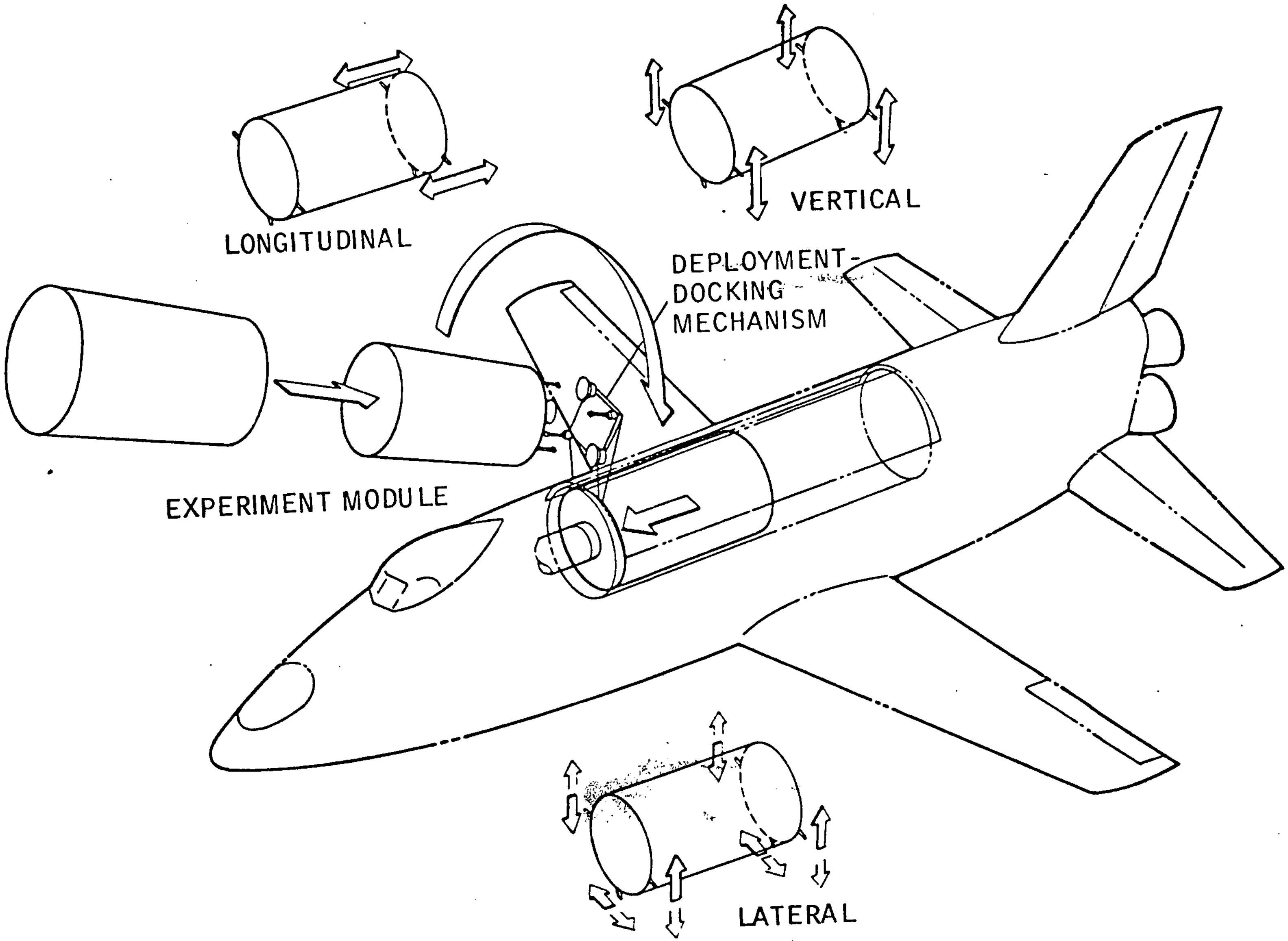

Figure 1-31. Shuttle Attachment, Deployment, Launch, and Retrieval of Experiment Modules

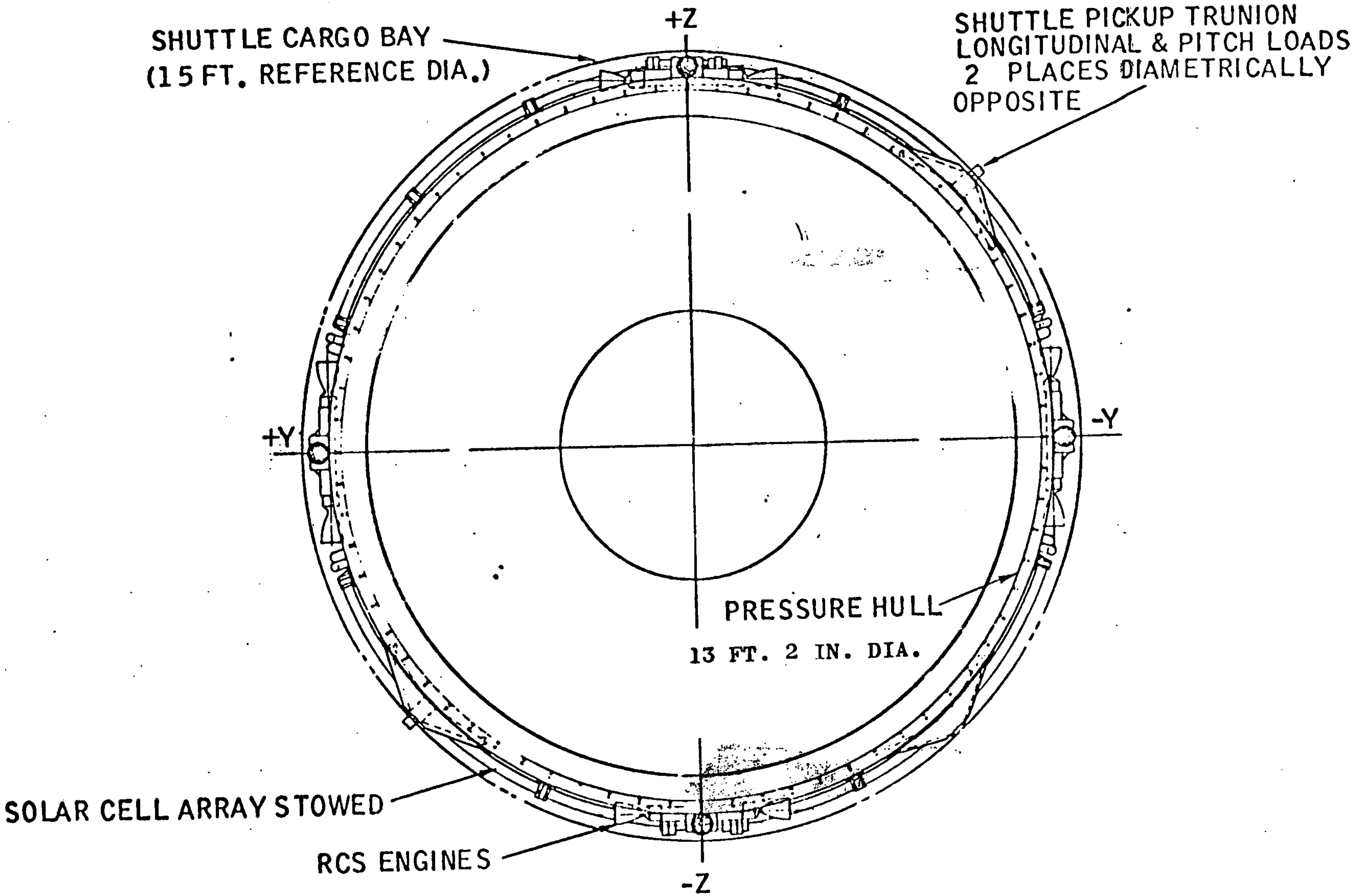

Figure 1-32. Baseline Module Clearance, Shuttle Cargo Bay

The module-to-shuttle support fittings project to the extremes of the 15-foot-diameter payload bay.

1.5 CONFIGURATION STUDIES

1.5.1 BIOMEDICAL/BEHAVIORAL/MAN-SYSTEM AND LIFE SUPPORT/PROTECTIVE SYSTEMS EXPERIMENTS COMPATIBILITY WITH THE COMMON MODULE. The common module design criteria was developed during earlier tasks without including the requirements imposed by biomedical FPEs, since these experiments are currently assigned as integral experiments in the space station. Compatibility of the modules with the following biomedical FPEs was examined on a preliminary basis:

a. FPE 5.13 Biomedical and Behavioral

b. FPE 5.14 Man/System Integration

c. FPE 5.15 Life Support and Protective Systems

A preliminary outline of the primary objectives and requirements for these experiments is shown in Tables 1-9 through 1-11. Values in parentheses are preliminary estimates where none are available from the above FPE descriptions.

Examination of the compatibility of common modules with these FPEs is to be made based on the following assumption: All requirements are to be provided by the module(s) except as follows:

a. 5.13, 5.14, 5.15 – Space station will provide power, data transmission, and environmental control.

b. 5.14 – Man System Integration – The space station will provide living quarters including movable partitions for crew quarters habitability tests.

c. 5.15 – Space station will provide food preparation test area.

It is assumed that experiments that could use common test chambers, pumps, EVA access, etc. will be programmed to prevent need for dual capabilities.

A potential arrangement of the biomedical experiments in the attached common module CM-4 is shown in Figure 1-33. Although the concept is based on an early common module CM-4 design, the arrangement will not change significantly for the final CM-4 common module. Life support and protective systems are located in the compartment adjacent to the space station. The second compartment is partitioned into two compartments, the first containing the IMBLMS console and isolation chamber and the second containing additional biomonitoring and test equipment, including the manned centrifuge control station. The manned centrifuge could be attached to the end of the common module as shown. The 60-inch-diameter airlock, which is provided in the

Table 1-9. FPE 5.13 Biomedical and Behavioral Research

OBJECTIVES

1. To extend man's capabilities in manned space flight by determining the effects, time course, mechanisms, predictability, severity and prevention of effects of space flight on man.
2. To obtain scientific information of value to conventional research.

EXPERIMENT EQUIPMENT:	Weight	Volume
IMBLMS	1300 lb	350 ft^3
Peripheral equipment including:		
Bicycle ergometer	(300)	(50)
Rotating litter chair	265	38
Lower body negative pressure	33	5
Body mass measuring device	38	28
Specimen mass measuring device	14	.3
On-Board centrifuge — manned	--	--

STATION SUPPORT:

Power — Avg 500 W, Peak 1000 W, Standby 50W*

Data — 100 KBPS plus TV and films

Thermal — 1000 Btu/Hr oper., 100 Btu/Hr standby

MODULE FEATURES REQUIRED:

EVA access with connections to IMBLMS

20 ft. clear run for IVA restraint tests

*Not including manned centrifuge.

Table 1-10. FPE 5.14 Man/System Integration

OBJECTIVE:

1. Quantify man's capabilities to perform physical and mental tasks.
2. Develop methods for crew selection and training.
3. Determine man's individual and group behavior.
4. Develop crew equipment and technology for transfer, assembly and maintenance internal and external to station.
5. Develop technology for habitable living areas.

EXPERIMENT EQUIPMENT:

	Weight	Volume
IMBLMS (Use 5.13 equipment)	--	--
Isolated work area — visual and acoustic	--	600 ft^3
Space station operational and living areas	--	--
EVA equipment (2 suits and biopacks)	(300)	(10)
Leakage detection and repair equipment	(200)	(20)
RCS installation	(100)	(30)
On-board centrifuge — manned	--	--
On-board simulator — (e.g., manual reentry)	(200)	(100)
IVA locomotion aids	(100)	(10)
Tethered mobility and hand-held thruster	(200)	(20)

STATION SUPPORT:

Power — (IMBLMS: 500 W avg., 1000 W peak)
Data — (IMBLMS: 100 KBPS)
Thermal — (1000 Btu/Hr)
Other — movable partitions and test areas in station

MODULE FEATURES REQUIRED:

EVA access with tethered reel — in device and view port.
Visual and acoustically isolated chamber.
20 ft. clear run for IVA transfer tests.
Environmental controlled chamber for leak repair test, RCS replacement simulating EVA, and EVA simulated pointing of large optical system.

Table 1-11. FPE 5.15 Life Support and Protective Systems

OBJECTIVES:

1. Investigation of basic chemical and physical phenomena in "g" sensitive LS/PS components.
2. Evaluate and flight qualify advanced LS/PS components.
3. Investigate man/system/vehicle interfaces and demonstrate man's ability to perform maintenance and repair. (Note: Items 1 and 3 appear to have been largely deleted as duplicating other experiment areas)

EXPERIMENT EQUIPMENT:	Wt(lb)	Vol. (ft^3)	Pwr Watts
1. LS/PS components installed in parallel with space station system per crew member in station	450	75	500
2. Zero g shower (30" × 80")	247	48	30
3. Protective clothing and EVA equipment	86	8	200
4. Fire prevention	80	7	150
5. Leak detection	5	.5	10

STATION SUPPORT:

Power — 300 Watts per crew member (electrolysis)
Data — (assume 100 KBPS max.)
Thermal — (assume 1000 Btu's - equiv. 300 W)
Other — parallel LS/PS connections capability
— shower water reclamation

MODULE FEATURES REQUIRED:

Capability to operate, checkout, measure, test, repair and evaluate performance of LS/PS components prior to switchover to space station supply mode.
EVA access and view port.
Chamber to simulate EVA for suit and biopac tests.
Chamber to simulate evacuated area for leak detection and repair.
Chamber to isolate hazard of fire detection tests.
Capability to install heat rejection test devices.
Isolation of pressurized gas storage vessels and other hazardous components.

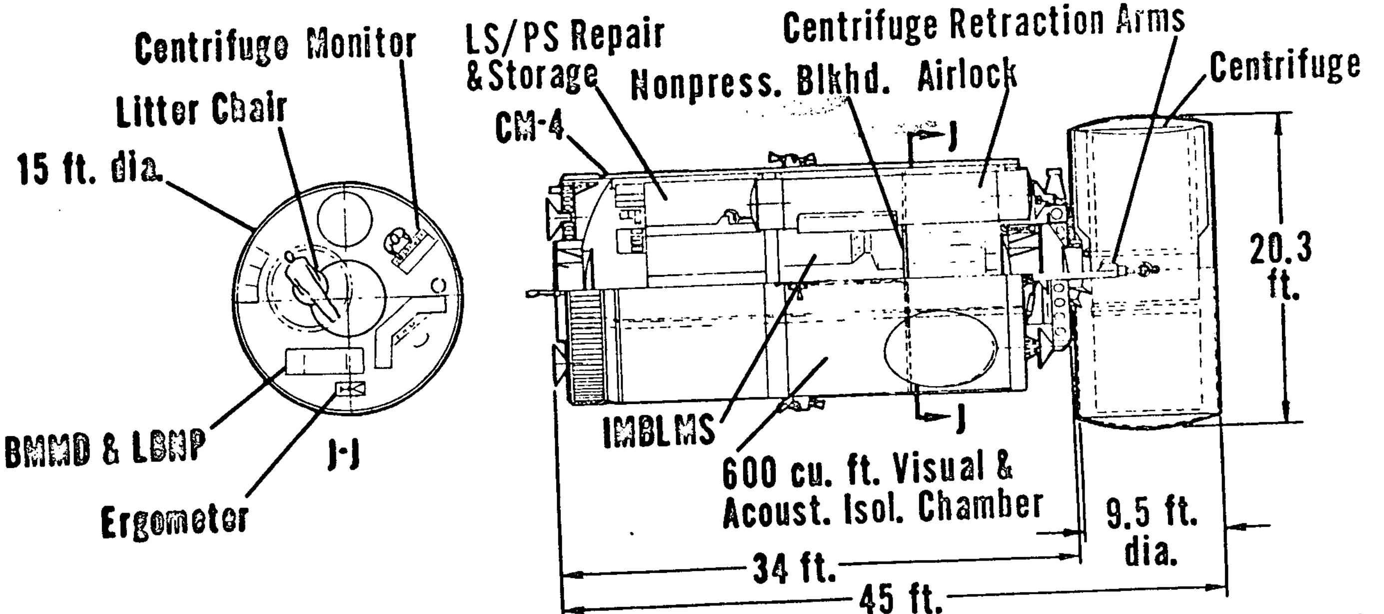

	WEIGHT (lb.)
Max. Gross	29,390
Experiment	4,300
Exper. Integr.	8,350

	WEIGHT (lb.)
Structure	11,650
Subsystems	4,800
Propellant	290

Figure 1-33. Biomedical Accommodation, Biomedical Experiments/Onboard Centrifuge (FPE 5.13, 5.14, 5.15/FPE 5.13C Attached)

common module, is utilized for EVA. This tunnel airlock can also be used to provide a clear run of greater than 20 feet by opening the hatch into the end compartment.

Animals required to accomplish experiment objectives could be accommodated in the Space Biology Laboratory. These animals include:

a. Rats and mice

b. Mini swine or dogs

c. Monkeys (2) — Rhesus or Spider

d. Rhesus primates (2) — closed EC/LSS

e. Guinea pigs

f. Chickens

g. Microbes

1.5.2 FPE 5.11D - EARTH SURVEYS, DUAL. An investigation of the sensitivity of reassignment of Earth Survey FPE 5.11 to another common module operating in the detached mode was conducted. The earth surveys experiments involve many sensors, each with its own peculiar viewing angle. The FPE describes various operational aspects associated with each sensor, some of which entail manned participation. Although several conflicts are immediately evident, two requirements are dominant. These are:

a. Orientation to the nadir and module alignment to a ground track (or velocity vector).

b. High peak power demand on the order of 7 kilowatts.

The first requirement imposes severe penalties on the space station in the attached mode. The second requirement is a demand on the power system far beyond the demands of any other detached experiment. The area of solar array required is considered undesirable, geometrically, for detached operation. The output of the commonality analysis and verification placed the earth surveys experiments into the attached common module CM-4. This attached version is discussed in Section 1.3.4.2. The operational penalties were imposed upon the space station, although the experiments conceivably were not compromised.

An investigation was made to conceptually integrate the earth surveys experiments into a detached CM-1 module. This version is shown on Figure 1-34. In the detached mode, the module is unmanned with the greatest power demand occurring when the sensors are all activated at a fly-over of truth sites. The power demands at this time are on the order of 4.5 kilowatts. To resolve the power demand, an operational restriction must be imposed. Interferences of the solar arrays with the deploying

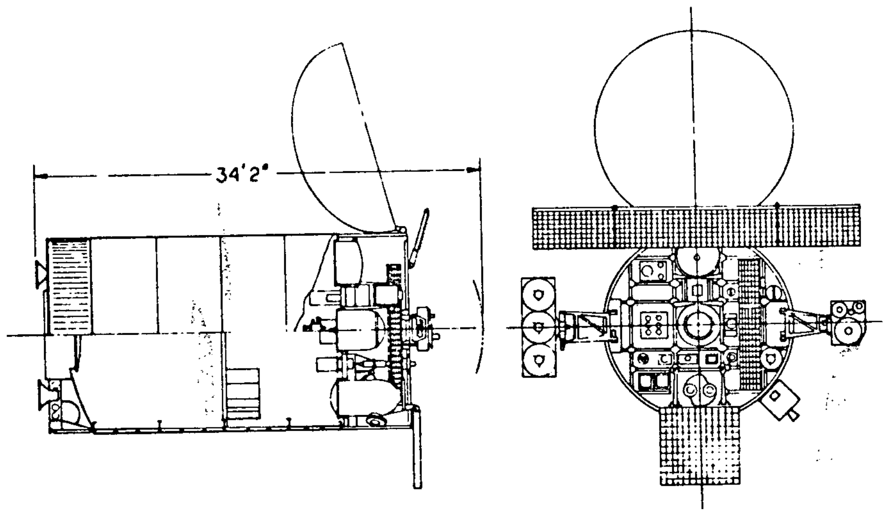

Figure 1-34. Earth Surveys Detached Mode, CM-1

elliptical bulkhead, in conjunction with the high power demand, were resolved by removing the arrays, installing rechargeable battery packs, and requiring redocking for charging on an approximate 24-hour sortie time. Additionally, the large inertia of this vehicle is unfavorable since considerable maneuvering is necessary to obtain the equivalent of 120° conical pointing.

The dual mode operation does show decided promise, especially if the sensors are integrated into a vehicle configuration designed to obtain favorable inertias and can cope with the power demand. A CM-3 or CM-4 would serve as the command/control, work, and test facility and the free-flyer would be experiment peculiar. Two candidate configurations of the free-flyer are shown in Figures 1-35 and 1-36.

1.5.3 TRANSPORTER MODULES. Preliminary concepts of manned and unmanned transporters have been developed. The space transporter vehicle has two basic types of interfaces:

a. Interfaces with other system elements; e.g., space station, shuttle, or other delivery vehicle.

b. Interfaces between the space transporter and experiment modules.

Only the experiment module interfaces are discussed in this section.

1.5.3.1 Unmanned Transporter Mission Interface with Experiment Modules. The following candidate missions are defined for the unamnned space transporter:

a. Transport modules from shuttle to space station.

b. Deploy and retrieve free-flying modules.

c. Provide orbit maintenance for free-flying modules.

d. Relocate modules from one station dock to another.

e. Retrieve disabled free-flying modules.

Interface guidelines between the space transporter and the module related to the candidate missions are:

a. The transporter will be unmanned while operating in the detached mode and could be manned while docked to the space station for servicing and maintenance.

b. The transporter provides physical docking mechanisms compatible with common modules.

c. The transporter provides manned access to the module to which it is attached.

d. The transporter provides automatic docking guidance capability equipment to the space station.

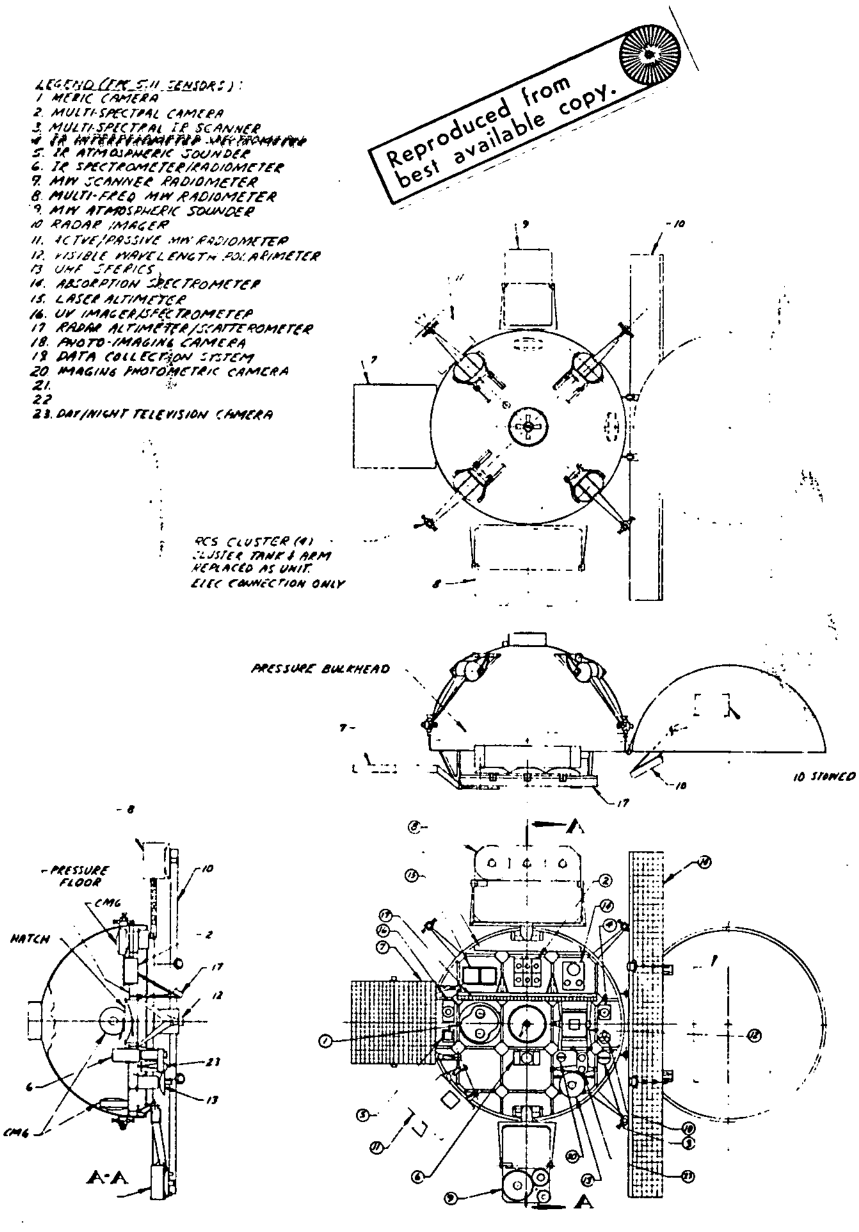

Figure 1-35. Earth Surveys, Detached Mode, Experiment-Peculiar Module

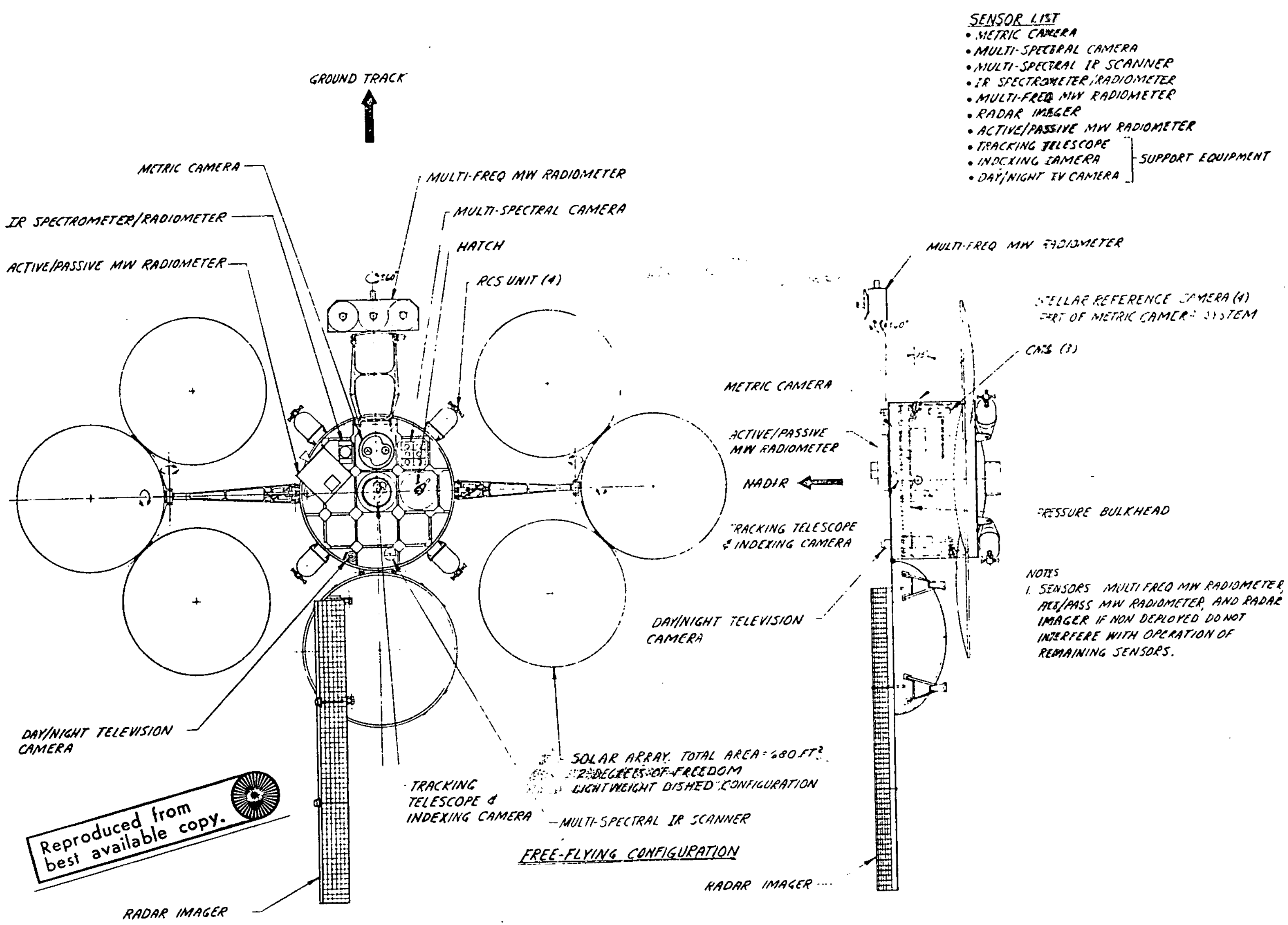

Figure 1-36. Dual Mode Earth Surveys Concept

e. Round trip delivery or complete payload repositioning cycle ΔV requirements related to the reference missions are provided by the transporter. Transporter limiting round trip ΔV requirements are 240 ft/sec for providing orbit maintenance to a single free-flying module located 100 n.mi. ahead of the space station and 425 ft/sec for five modules, assuming that the transporter remains at the remote distance until all five module orbit adjustments are completed.

f. The transporter will provide propellant or other fluid transfer capability, power, data, and atmosphere transfer to the experiment module for conditions where it is "sandwich" docked between the space station and the module.

g. The transporter will provide sufficient performance to accommodate delivery or retrieval of the heaviest detached common module configuration.

h. For certain module failure modes, the transporter could be required to provide power or commands to a disabled module.

i. Experiment modules, when considered as payloads, are assumed to remain physically attached to the payload delivery vehicle until the transporter has completed payload docking.

1.5.3.2 Candidate Operations. A representative list of experiment module operations and performance parameters was developed as the basis for formulating five alternative design solutions. This list is shown in Table 1-12. The operational capabilities of the unmanned and manned transporter versions are indicated.

a. The transporter is unamnned while operating in the detached mode, and could be manned while docked to the space station for servicing and maintenance.

b. The normal CM-1 subsystems are employed; e.g., electrical, RCS, data and communication, thermal control, etc., although unneeded items (e.g., inertia wheels) would not be installed.

c. An automatic docking system is required which will give the transporter a docking guidance capability equivalent to the space station; e.g., ITT laser radar, computer, or RF link to space station computer, and RF communication link to payload or payload delivery vehicle.

d. Transporter payloads are equipped with docking adapters as required so that the transporter can dock the payloads to the space station docking ports in their normal mode.

e. Transporter payloads remain physically attached to the payload delivery vehicle until the transporter has docked with the payload.

f. The transporter will normally be docked to a space station providing utility services and resupply as required.

Table 1-12. Transporter Module Candidate Operations

Operation	Maximum ΔV (FPS)	Transporter Version	
		Unmanned	Manned
1. Transport Modules From Shuttle to Space Station and Return.	250.	X	X
2. Deploy, Retrieve, and Stationkeep Astronomy Modules.	250.	X	X
3. Relocate Attached Modules to Another Docking Port	100.	X	X
4. Transport Maintenance Crew to Detached Module for In-situ Servicing.	250.	–	X
5. Transport Astronomy Modules to Drag-Free Altitude.	4,600.	(Space Tug)	(Space Tug)
6. Provide Sustained "g" for Fluid Physics Experiments.	1,450.	(Propulsion Slice)	(Propulsion Slice)
7. Retrieve Disabled Detached Modules.	250.	X	X

g. Transporter mission life $\leq$ 5 years. Refurbishment at intervals $\leq$ 2 years, on the ground.

h. Transporter will be compatible with the space shuttle — round trip.

Missions. The unmanned transporter missions and ΔV requirements are summarized in Table 1-13. The missions are described as follows:

Transporter accepts payload from space shuttle, flys to space station, and docks payload to space station docking port. ΔV requirements per mission = 250 fps.

Payloads are:

Module	FPE
CM-3	5.7/12
CM-3	5.8
CM-3	5.16
CM-3	5.20-1
CM-3	5.27
CM-4	5.11
CM-4	5.9/10/23
CM-4	5.22

Experiment Peculiar Payloads

Centrifuge Arm	5.9/10
Centrifuge Arm	5.13C

1.5.3.3 Unmanned Transporter Module. The configurations shown in Figure 1-37 varies somewhat from the existing CM-1 concept as the current CM-1 is a few iterations beyond the concept used in the transporter study. This does not alter the validity of the study.

Operational and Design Requirements

a. This transporter module consists of a CM-1 module equipped with a pressure bulkhead with a docking adapter and hatch.

b. Module Recovery. Transporter flies out to disabled detached-type module, docks with it, flies back to station, and docks itself to the space station, sandwiched

Table 1-13. Unmanned Transporter Missions — 5 Year Span

Module	Experiment Payload	Initial Delivery		Module Recovery		Repositioning		Payload Return		Redelivery	
		No.	ΔV (fps)	No.	ΔV (fps)	No.	ΔV (fps)	No.	ΔV (fps)	No.	ΔV (fps)
CM1	5.1			1	≤250						
CM1	5.2A			1							
CM1	5.3A-1			1							
CM1	-2, -3			1							
CM1	5.5			1							
CM1	5.16-2			1							
CM1	5.20-2, -3, -4			1							
CM3	5.8-1	1	≤250			1	≤100				
CM3	5.8-2	1				1					
CM4	5.9/10-1, -3	1				1					
None	5.9/10-2	1				1					
None	5.13C	1				1					
CM3	5.16-1	1				1		5	≤250	5	≤250
CM3	5.20-1	1				1					
CM4	5.11A	1				1					
CM3	5.12/7	1				1					
CM4	5.22	1				1					

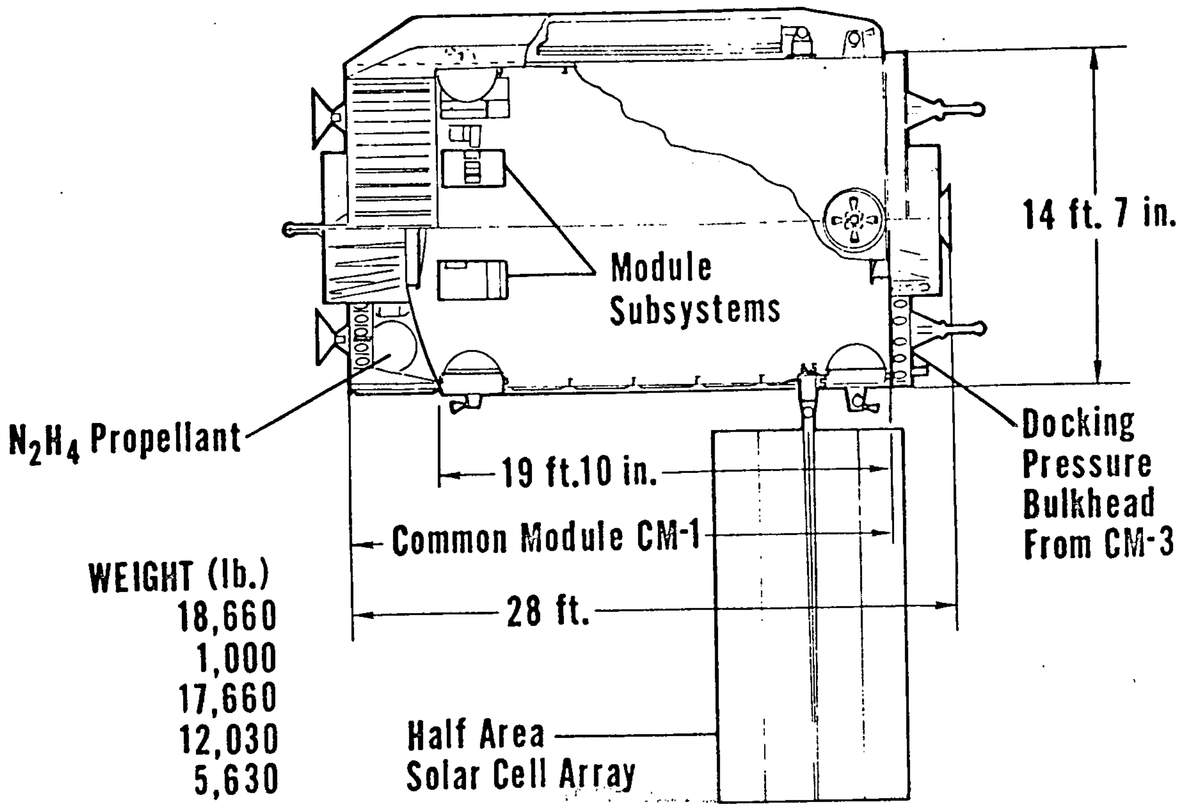

	WEIGHT (lb.)
Max. Gross	18,660
Propellant	1,000
Module Dry	17,660
Structure	12,030
Subsystems	5,630

Figure 1-37. Unmanned Transporter Concept Derived from Common Module CM-1

between the module and the station. The module is then entered for servicing through the transporter. ΔV requirements per mission = 250 fps.

c. Payload Repositioning. Transporter moves any of payloads listed in a above from one space station port to another. ΔV requirement per mission = 100 fps.

d. Payload Return. Transporter returns any attached type module or experiment payload to shuttle for return to earth. ΔV requirement per mission ≤ 250 fps.

e. Total mission ΔV requirement ≤ 450 fps (includes orbit maintenance for free flying modules).

f. Time interval between payload deliveries is:

Nominal:	3 months
Closest Scheduled:	1 month

g. Span of scheduled payload deliveries is 48 months.

h. Attached type modules are repositioned once during the five-year mission (assumed).

i. Each detached type module requires recovery once during the five-year mission (assumed).

j. Unscheduled return to the ground of any of the attached-type modules will be required once per year on the average over the five-year mission (assumed). After repair or updating, the modules will be relaunched in the shuttle and redelivered to the space station by the tug.

k. Mission time is 14 days of operation on any one mission.

Design Characteristics

The following changes would be made to the CM-1 baseline design:

a. Revise existing RCS to increase thrust.

b. Delete digital data system associated with experiment data.

c. Delete inertia wheels, CMG and magnetic torquers.

d. Add laser docking and computer from space station.

e. Delete active thermal control elements and radiator.

f. Delete one-half of CM-1 solar panel area.

g. Add a pressure bulkhead and docking port from CM-3 and mounting provisions for a laser docking radar.

Based on a full propellant capacity of 3,600 pounds, the performance capability varies from a ΔV of 500 fps (FPE 5.2A) to 1,300 fps unloaded.

1.5.3.4 Manned Transporter Module. Operational requirements for the manned transporter shown in Figure 1-38 are the same as those for the unamnned transporter except for the following:

a. The module shall be operable manned or unmanned.

b. The module shall be capable of transporting maintenance personnel and equipment to a free-flying module for in-situ servicing, and providing EC/LSS and other supporting functions during the servicing period.

c. The module shall provide EC/LSS and other crew support for a two-man crew, five days.

Design Characteristics. The manned transporter characteristics are listed in Table 1-14. It is a derivative of the CM-1 module and, with the exception of crew provisions, is similar to the unmanned transporter version.

Table 1-14. Transporter Module Characteristics — Five-Day Mission, Two-Man Crew

Performance:	ΔV = 350 fps (FPE 5.2A) to 890 fps unloaded
Rendezvous & Dock:	CM-1, system plus monitor & manual override
Structure:	CM-1 plus docking bulkhead & windows
Power:	CM-1 less 6 panels, each array
EC/LSS:	Heat rejection: CM-1 radiator
	CO_2 removal: LiOH
	No O_2 recovery, No H_2O recovery
	Waste storage & dump to space station
	O_2 storage: 295 lb
	N_2 storage: 355 lb
	H_2O storage: 150 lb

The module consists of a single pressurized volume partitioned into three areas: (1) subsystems, (2) living and control area, and (3) a workshop and cargo area. Manned docking stations are provided at each pressure bulkhead. The station at the domed bulkhead has the greater visual restriction due to the recessed depth within the skirt.

One quarter of the total propellant tankage is removed to obtain the visual sighting station through the domed bulkhead.

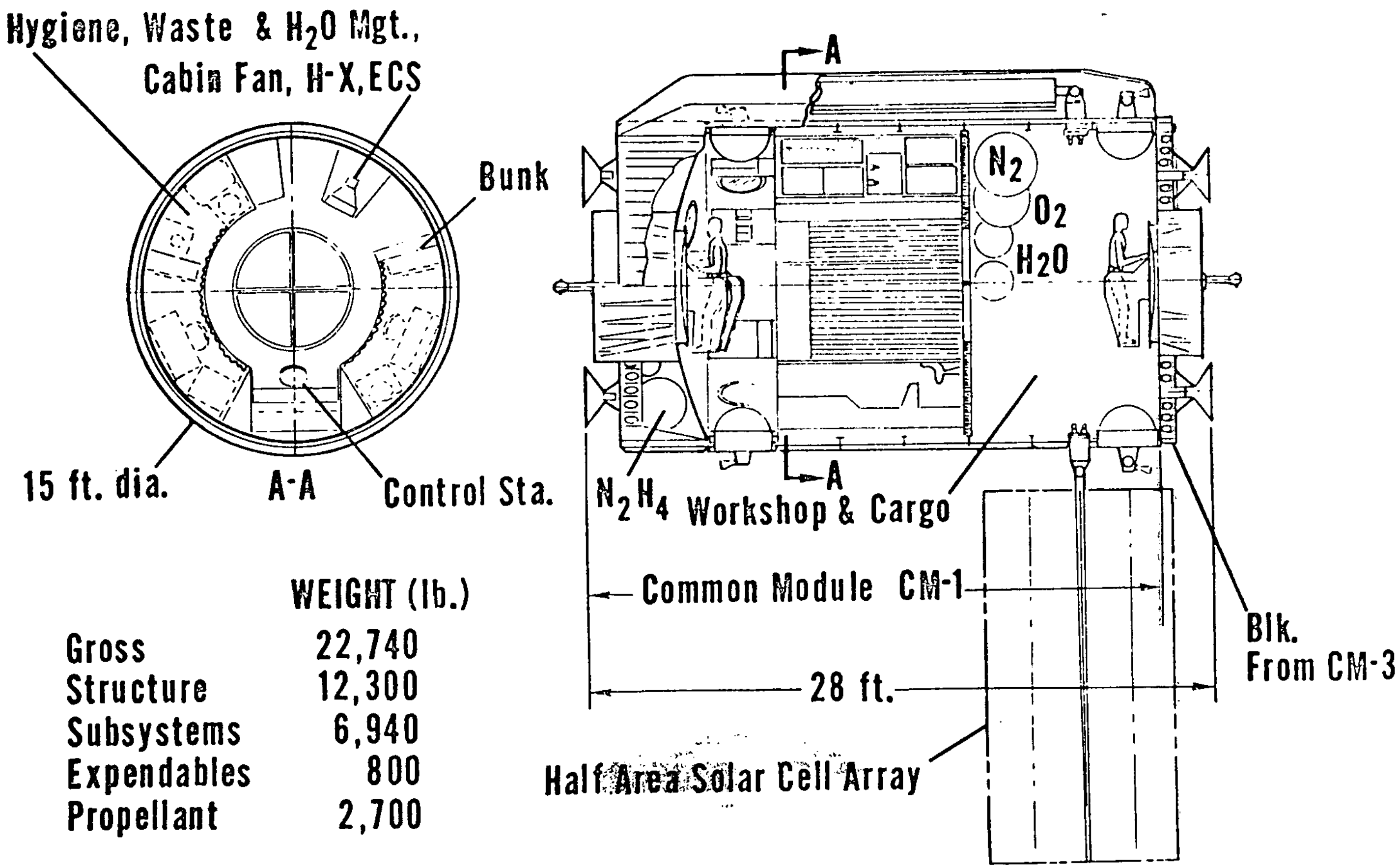

	WEIGHT (lb.)
Gross	22,740
Structure	12,300
Subsystems	6,940
Expendables	800
Propellant	2,700

Figure 1-38. Manned Transporter Concept, Derived from CM-1

To further the flexibility of the transporter concept, these features are or can be provided:

a. Star tracker ports converted to windows to provide lateral vision.

b. All components of the internal conversion to living quarters can be sized to conform to passage through the five-foot hatches, permitting refurbishment in orbit for extended or varied capabilities.

c. An airlock can be adapted to the flat bulkhead ingress/egress port.

The ΔV performance of the manned transporter is about 75% that of the unmanned transporter, due to reduced propellant capacity.

1.5.4 REDUCED MODULE DIAMETER EFFECTS. As previously noted, the baseline diameter of the common modules, 13-1/2 feet, is the largest diameter that can be mounted in the 15-foot diameter shuttle cargo bay considering the module external appendages such as solar cell panels, RCS, and bar magnets.

In considering the possibility of a smaller diameter shuttle cargo bay, a study was performed to determine the effects of a reduced diameter on the module and accommodation of experiments.

In order to establish module length requirements for each experiment group, the pressurized interior of the module has been allocated into three volumes: (1) subsystems, (2) access/passageway, and (3) experiment installation, as shown in Figure 1-39.

The subsystems volume required for installation and access for maintenance and replacement of components is the greatest for the astronomy mission modules. The 6-foot diameter passageway provides clearance for opening the hatch and crew locomotion with cargo diameters up to 5 feet.

The module length required for experiment accommodation is a function of access required and either experiment volume or length.

Each of the free-flying experiment arrangements were studied for accommodation within modules of 13.5-, 12-, 10-, and 8-foot diameter. See Figure 1-40. All experiment groups are accommodated with the 13.5-foot diameter module. As the diameter is reduced to 12 feet, solar astronomy group FPE 5.3A will no longer fit and an additional module is required. The minimum structural diameter for mounting and thermal isolation of the 3-meter primary mirror of the FPE 5.2A stellar astronomy telescope is 11 to 12 feet.

A minimum-diameter common module that will accommodate all of the FPE 5.5 high-energy sensors is about 11 feet. Below this diameter a second module is required.

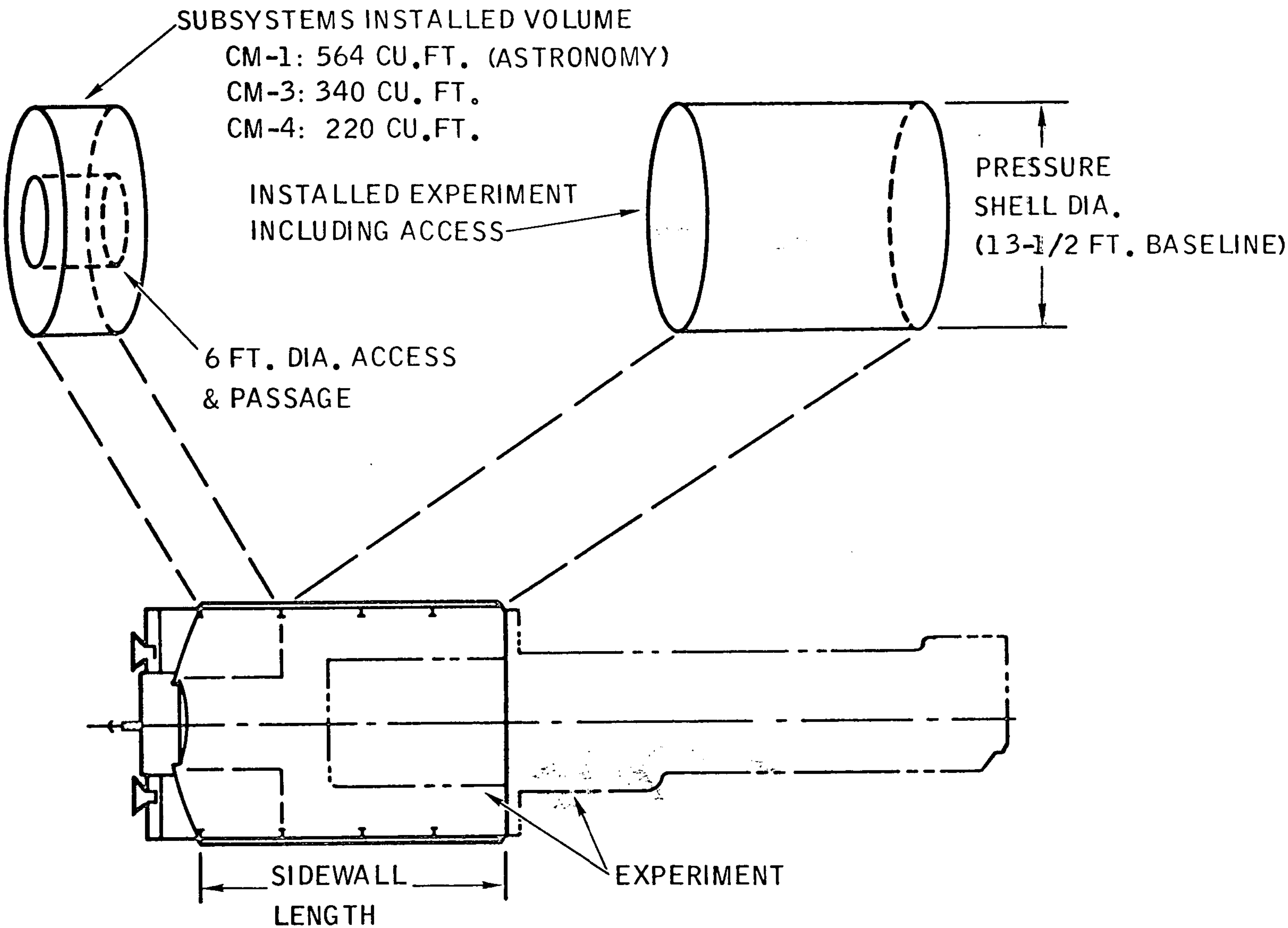

Figure 1-39. Pressurized Volume Allocations

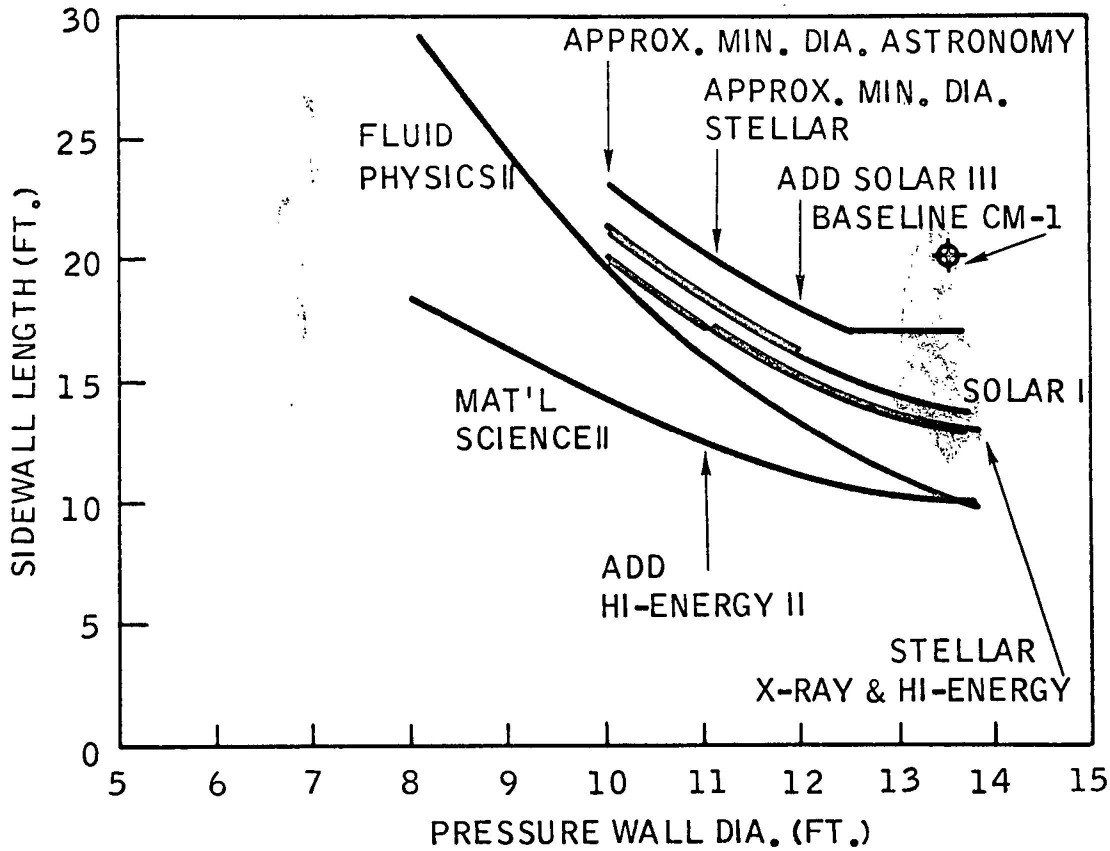

Figure 1-40. Pressure Shell Sidewall Length vs. Diameter, CM-1 Experiments

An approximate minimum module diameter for the stellar X-ray, solar, and high-energy astronomy experiments is 10 feet.

Equipment arrangements for the various experiment groups assigned to attached common module CM-3 were studied to determine the effect of reduced module diameters on module length and on the feasibility of accommodating the experiments as defined. See Figure 1-41.

The previous common module CM-3 baseline had a sidewall length of 15 feet. Recent studies have shown this module volume to be marginal. At the current CM-1 baseline diameter of 13.5 feet, a sidwall length of at least 17 feet is required. It appears desirable to utilize the CM-1 common module structure for the CM-3 experiments. This would provide some growth volume because of the 20-foot long sidewall.

Approximate minimum diameters for the defined cosmic ray and space biology experiments are 13 and 10 feet.

The three experiment groups assigned to the larger attached common module CM-4 were examined for compatibility with module diameters of 13.5, 12, 10 and 8 feet. See Figure 1-42. Total sidewall length required at 13.5-foot diameter is the same for each experiment group at 25 feet. This sidewall must provide attachments for two intermediate pressure bulkheads since the FPE 5.22 Components Test experiments require three pressurizable compartments.

The complement and arrangement of the FPE 5.11 Earth surveys sensors would be compromised by a module diameter less than 13.5 feet. See Figure 1-43. Minimum diameters for the FPE 5.12 Remote Maneuvering Subsatellite and the Component Test modules are 12 and 10 feet.

A summary of reduced module diameter effects on experiments is presented in Figure 1-44. Upper limit sidewall lengths required for CM-1, CM-3, and CM-4 experiments are also shown. The current baseline diameter of 13.5 feet is considered a minimum for earth surveys and cosmic ray experiments. The baseline 13.5 foot diameter CM-1 structure with 20-foot long sidwall appears properly sized for the CM-3 experiment groups. A diameter of 12 feet would eliminate or change these experiments and add one additional common module for solar astronomy. A further reduction to 10 feet would eliminate or change the RMS and 3-meter stellar telescope and add one additional common module CM-1 for high energy astronomy. A further reduction in diameter affects all experiment group sizing.

The effects of reduced diameter on module structure weight are discussed in Section 3.4.1.

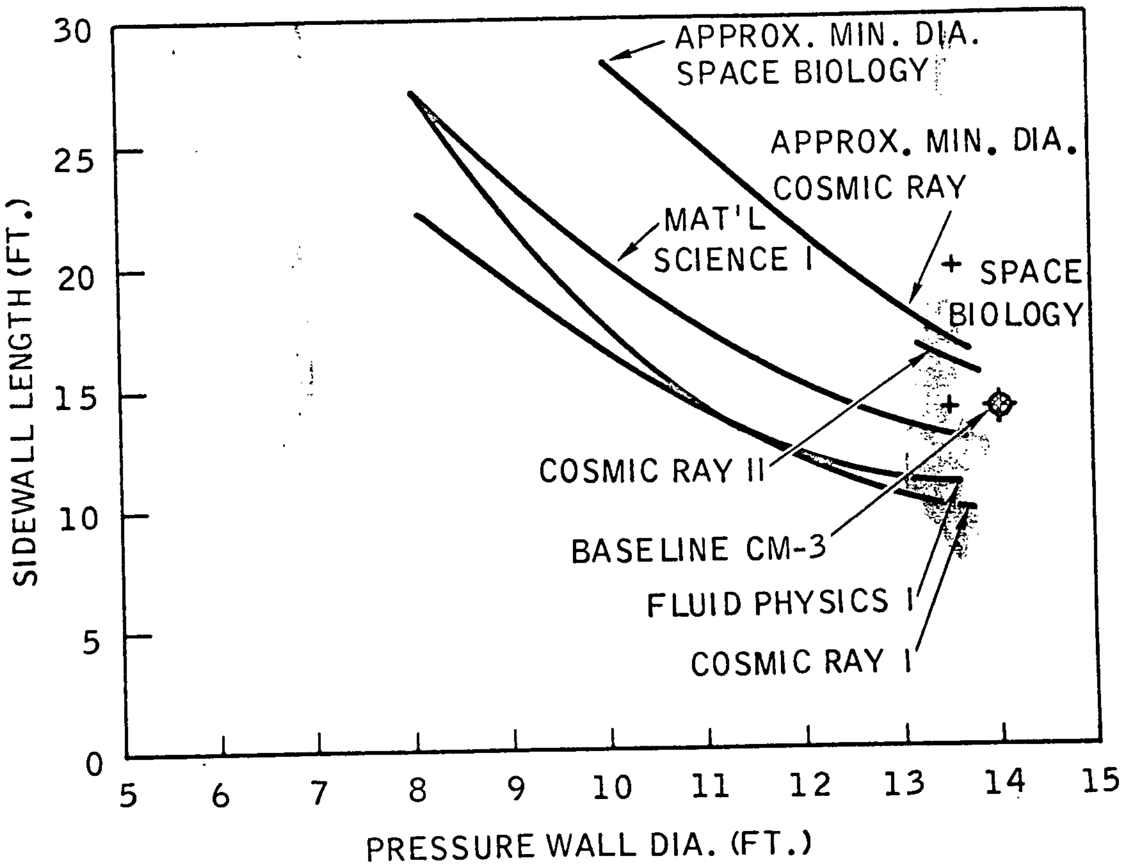

Figure 1-41. Pressure Shell Sidewall Length vs. Diameter, CM-3 Experiments

34

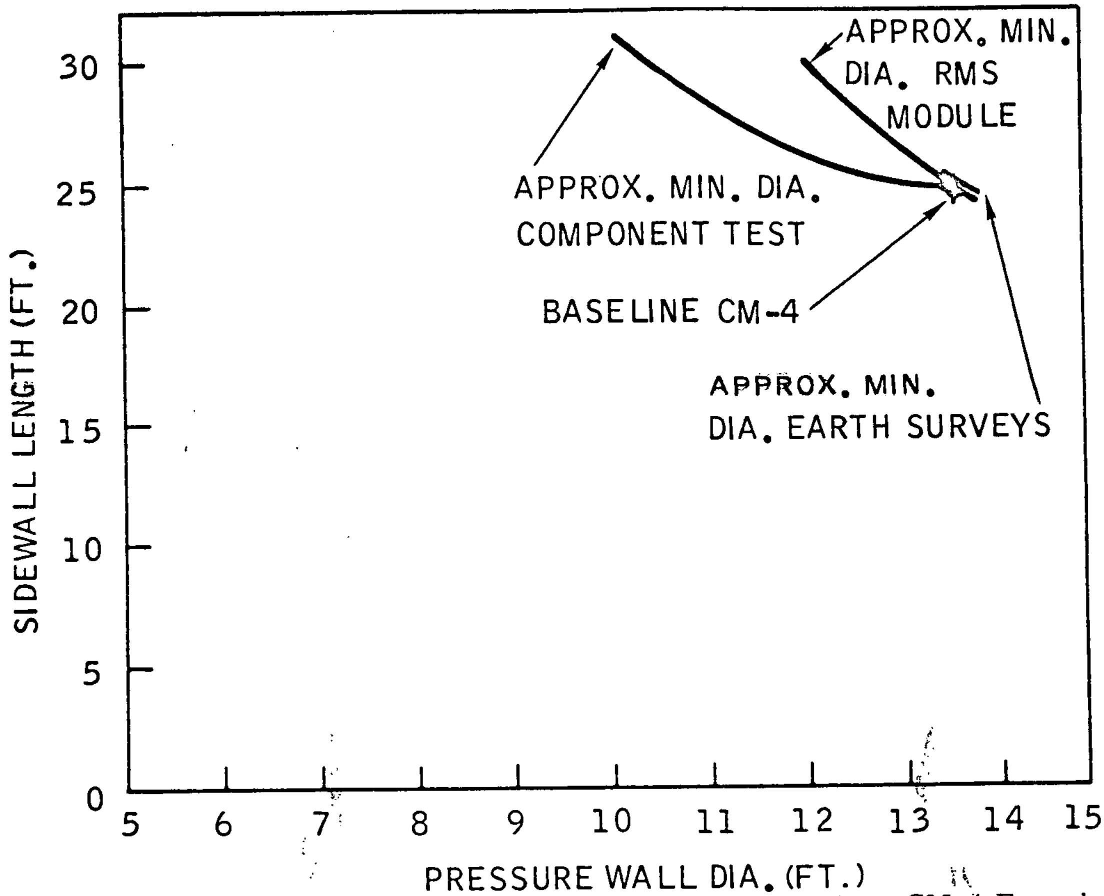

Figure 1-42. Pressure Shell Sidewall Length vs. Diameter, CM-4 Experiments

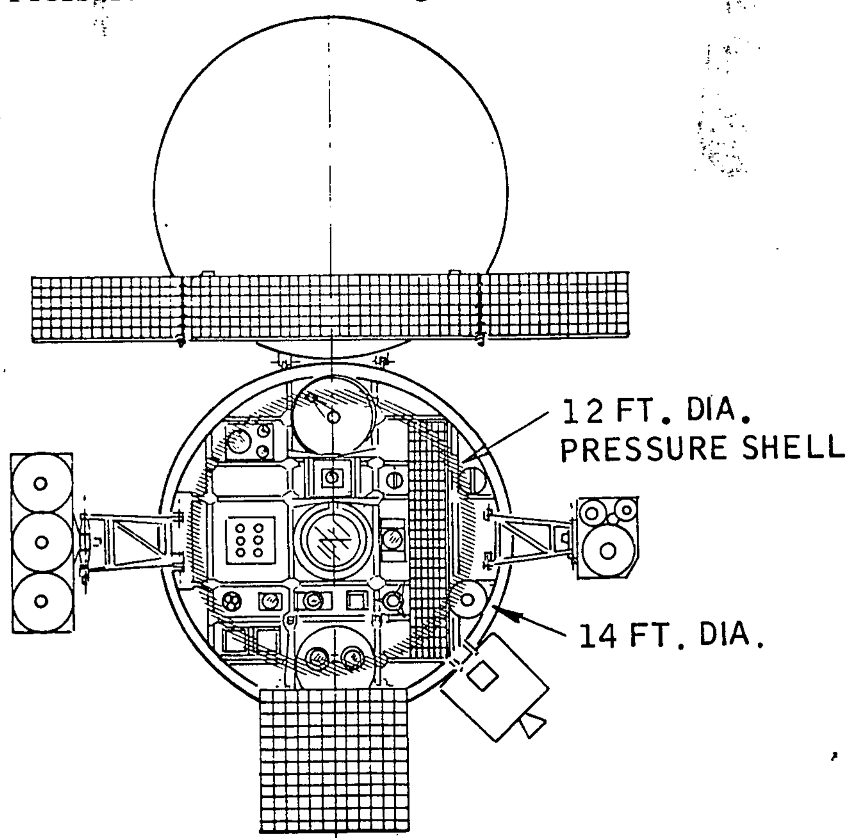

Figure 1-43. Earth Surveys Lab

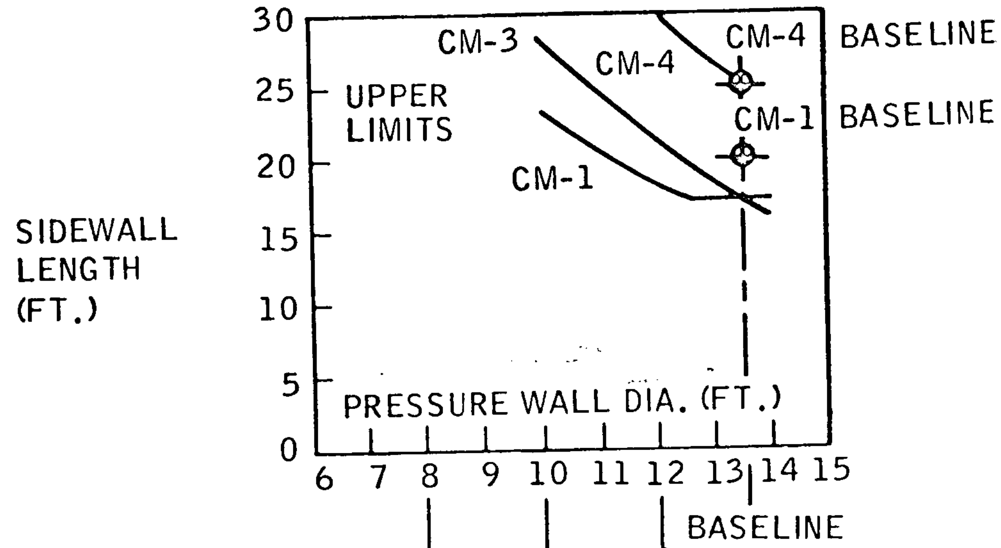

8 ft:
- REDUCE SIZE OF ALL EXPERIMENTS &/OR REVISE CONCEPTUAL APPROACH TO COMMON MODULE DESIGN

10 ft:
- REDUCE SIZE OR MAKE COSMIC RAY, EARTH SURVEYS, REMOTE MANEUV. SUBSATELLITES, & 3-METER TELESCOPE EXPERIMENT PECULIAR
- ADD ONE SOLAR ASTRONOMY MODULE
- ADD ONE HI-ENERGY ASTRONOMY MODULE

12 ft:
- REDUCE SIZE OR MAKE COSMIC RAY & EARTH SURVEYS EXPERIMENT PECULIAR
- ADD ONE SOLAR ASTRONOMY MODULE
- 3-METER TELESCOPE MARGINAL

Baseline:
- EARTH SURVEYS & COSMIC RAY MARGINAL

Figure 1-44. Reduced Module Diameter Effects on Experiments

SECTION 2

EXPERIMENT MODULE MASS PROPERTIES

Mass properties data have been developed for all experiment module concepts considered in this study. Mass properties for final Phase A configurations are included in this section.

Table 2-1 describes the basis for weight estimates. Tables 2-2, 2-13, and 2-24 depict critical mass properties characteristics for in-orbit operating conditions for each of the common module/FPE configurations. It should be noted that maximum in-orbit operational mass properties assume fill-up of all propulsion/RCS tankage, a maximum complement of experiment equipment (including expendables) and deployment of solar panels, retractable shrouds, and other articulating items. This results in plausible worst-case conditions for sizing of control systems.

Tables 2-3, 2-14, and 2-25 summarize weights for the major systems and the total dry modules. Launch vehicle interface equipment and minimum shuttle and expendable payload launch weights are identified in Section 3.1.

Tables 2-12, 2-23, and 2-34 summarize the total experiment equipment weight by FPE grouping showing the major identifiable equipment items or categories. These data represent only the type of components that might be required by the various experiments such that realistic total weight values can be derived. Experiment peculiar structure and support subsystems components are included in the other tables.

Weight summaries for the propulsion slice and transporter module concepts are provided in Tables 2-35 through 2-37.

Table 2-38 depicts common module (CM-1) weight sensitivity to launch mode (expendable versus shuttle). It should be noted that the baseline modules incorporate the worst case/highest weight values for each item resulting in vehicles compatible with both launch modes.

The remaining tables itemize weights for components in each major system for each module/FPE configuration.

It should be noted that weight values for the various equipment items reflect estimates of the "installed" hardware that are nominally greater than catalogue or "off-the-shelf" weight values listed in other sections of this report.

Table 2-1. Basis for Weight Estimates

Subsystem/Item	Basis for Estimate
Experiment	NASA Blue Book, June, 1970.
Structure	
Press Cyl Shell	Semimonocoque, skin thickness = 0.060, plus integral stiffeners, frames @ 26 in. spacing, "smeared" thickness = 0.115 in., plus 15% for cutouts, hatches, and other non-optimum features. 2219 Al.
Bulkhead — Common	Spherical, 168 in. radius, web thickness = 0.055 in., plus cutouts, hatch, and other non-optimum features.
Bulkhead — Flat	Experiment peculiar — continuous beam (egg crate) — experiment peculiar removable panels.
Other Structure	Estimated from preliminary structural analysis.
Propulsion & Reaction Control	Based on similar state-of-the-art components — includes 10% contingency and 15% installation and structural supports.
Electrical Power	Modularized solar arrays @ 1.1 lb./sq. ft. plus supports. State-of-the-art battery power conditioning and distribution components — includes 10% contingency and 15% installation and structural supports (except batteries).
Guidance & Navigation	Based on similar state-of-the-art components.
Stabilization & Control	Modularized pivoted bar electro-magnets, other state-of-the-art components — includes 10% contingency and installation.
Communications & Data Management	Based on weights of similar state-of-the-art components, includes 10% contingency and 15% installation and structural supports (except data storage, displays and consoles).
Environmental Control & LSS	Based on weights of similar state-of-the-art components, includes 10% contingency and 15% installation and structural supports.

Table 2-1. Basis for Weight Estimates (continued)

Subsystem/Item	Basis for Estimate
Thermal Control and Environmental Protection	
Meteoroid Shell	Thickness = 0.016, 2024 Al, Fiberglass standoffs.
Radiators	Externally mounted aluminum tubing, 1.0 inch O.D., 0.125 wall thickness, 1.0 lb./sq. ft. additive to meteoroid shell.
Insulation	Aluminized mylar covering press. compt. @ 0.15 lb./sq. ft.
Active System	Based on weights of similar state-of-the-art components; includes 10% contingency and 15% installation and structural supports.

Table 2-2. Experiment Module Mass Properties Summary, CM-1

Item Condition	FPE 5.1 X-Ray	FPE 5.2A, 3-Meter Stellar	FPE 5.3A Solar	FPE 5.5, High Energy Stellar	FPE 5.20-2, Fluid Physics — Non-Cryogenics	FPE 5.20-3, Fluid Physics — Intermediate Term Cryogenics	FPE 5.20-4, Fluid Physics Long Term Cryogenics
Nominal Dry Weight (Table 2-3)	18,299	27,900	24,247	23,368	22,266	26,455	27,939
Operating Propellant & Service Items	2,560	2,560	2,560	2,560	9,360(1)	9,360(1)	9,360(1)
Nominal Operating Weight, Lb.	20,859	30,460	26,807	25,928	31,626	35,815	37,299
Roll Inertia, Slug-Ft.^{2}/1,000	26.3	42.7	34.0	25.4	29.3	36.3	37.0
Pitch/Yaw Inertia, Slug-Ft.^{2}/1,000	88.0	318.9	170.1	69.9	175.8	283.7	327.4
Nominal C.G. — Experiment Module Station, feet (2)	15.6	23.3	18.6	15.5	22.9	35.8	34.3
Nominal C.P. — Experiment Module Station, feet — Max Solar Array View (2)	21.0	31.9	22.6	20.6	18.6	31.8	31.8
Nominal C.P. — Experiment Module Station, feet — Min Solar Array View (2)	16.7	36.7	19.9	15.7	17.0	28.8	28.8

Notes: (1) Includes 6800 lb propulsion slice fuel.

(2) Station, feet from mating interface with space station. See Figure 1-8.

Table 2-4. Experiment Module Weight Summary, CM-1 Structure

Item Condition	FPE 5.1 X-Ray	FPE 5.2A, 3-Meter Stellar	FPE 5.3A Solar	FPE 5.5, High Energy Stellar	FPE 5.20-2, Fluid Physics — Non-Cryogenics	FPE 5.20-3, Fluid Physics — Intermediate Term Cryogenics	FPE 5.20-4, Fluid Physics Long Term Cryogenics
Shell Skin	1,014	1,014	1,014	1,014	1,014	1,014	1,014
Frames	129	129	129	129	129	129	129
Longerons	324	324	324	324	324	324	324
Crack Stoppers 8 Frame Mounting Lands	275	275	275	275	275	275	275
Aft Skirt Assembly	626	626	626	626	626	626	626
Domed Bulkhead Assembly	1,112	1,112	1,112	1,112	1,112	1,112	1,112
Docking Structure & Equipment	451	451	451	451	451	451	451
Aft External Subsystems Supports & Tunnel	350	350	350	350	350	350	350
Launch Support Fittings (Shuttle)	400	400	400	400	400	400	400
Subtotal	(4,681)	(4,681)	(4,681)	(4,681)	(4,681)	(4,681)	(4,681)

Table 2-4. Experiment Module Weight Summary, CM-1 Structure (Continued)

Item Condition	FPE 5.1 X-Ray	FPE 5.2A, 3-Meter Stellar	FPE 5.3A Solar	FPE 5.5, High Energy Stellar	FPE 5.20-2, Fluid Physics — Non-Cryogenics	FPE 5.20-3, Fluid Physics — Intermediate Term Cryogenics	FPE 5.20-4, Fluid Physics Long Term Cryogenics
Flat Bulkhead — Experiment Peculiar	2,530	2,530	2,530	2,530	1,898	1,898	1,898
Telescope Contamination Shroud	380	1,900	1,518	—	—	—	—
Sunshade Installation	—	506	—	—	—	—	—
Shroud Hatch	158	1,012	433	—	—	—	—
Experiment Deployment Equipment	—	—	—	700	—	—	—
Experiment Housing Assembly	—	—	—	—	—	3,400	3,400
Subtotal — Experiment Integration Structure	(3,068)	(5,948)	(4,481)	(3,230)	(1,898)	(5,298)	(5,298)
Total	7,749	10,629	9,162	7,911	6,579	9,979	9,979

Table 2-5. Experiment Module Weight Summary, CM-1 Reaction Control

Item Condition	FPE 5.1 X-Ray	FPE 5.2A, 3-Meter Stellar	FPE 5.3A Solar	FPE 5.5, High Energy Stellar	FPE 5.20-2, Fluid Physics — Non-Cryogenics	FPE 5.20-3, Fluid Physics — Intermediate Term Cryogenics	FPE 5.20-4, Fluid Physics Long Term Cryogenics
Propellant Tanks (4)	160	160	160	160	160	160	160
Gas Pressure Vessels (4)	333	333	333	333	333	333	333
Thruster Assemblies (32)	612	612	612	612	612	612	612
Fuel Distribution	56	56	56	56	56	56	56
Total	(1,161)	(1,161)	(1,161)	(1,161)	(1,161)	(1,161)	(1,161)

Table 2-6. Experiment Module Weight Summary, CM-1 Electrical Power

Item Condition	FPE 5.1 X-Ray	FPE 5.2A, 3-Meter Stellar	FPE 5.3A Solar	FPE 5.5, High Energy Stellar	FPE 5.20-2, Fluid Physics — Non-Cryogenics	FPE 5.20-3, Fluid Physics — Intermediate Term Cryogenics	FPE 5.20-4, Fluid Physics Long Term Cryogenics
Solar Array Assembly (1)	675	900	750	675	225	225	225
Deployment & Restraints	235	235	235	235	235	235	235
Batteries	616	616	616	616	770	924	616
Power Conditioning & Distribution	333	333	333	333	289	289	289
Total	1,859	2,084	1,934	1,859	1,519	1,673	1,365

Table 2-7. Experiment Module Weight Summary, CM-1 Guidance and Navigation

Item Condition	FPE 5.1 X-Ray	FPE 5.2A, 3-Meter Stellar	FPE 5.3A Solar	FPE 5.5, High Energy Stellar	FPE 5.20-2, Fluid Physics — Non-Cryogenics	FPE 5.20-3, Fluid Physics — Intermediate Term Cryogenics	FPE 5.20-4, Fluid Physics Long Term Cryogenics
Corner Reflector	2	2	2	2	2	2	2
Diplexer	1	1	1	1	1	1	1
OMNI Antenna	4	4	4	4	4	4	4
Target Stadiu Instl.	6	6	6	6	6	6	6
Transponder (2)	22	22	22	22	22	22	22
Installation Structure	10	10	10	10	10	10	10
Total	45	45	45	45	45	45	45

Table 2-8. Experiment Module Weight Summary, CM-1 Stabilization and Control

Item Condition	FPE 5.1 X-Ray	FPE 5.2A, 3-Meter Stellar	FPE 5.3A, Solar	FPE 5.5, High Energy Stellar	FPE 5.20-2, Fluid Physics — Non-Cryogenics	FPE 5.20-3, Fluid Physics — Intermediate Term Cryogenics	FPE 5.20-4, Fluid Physics Long Term Cryogenics
Momentum Unloading System	427	955	691	251	—	—	—
Control Moment Gyro (2)	215	215	215	215	—	—	—
Reaction Wheel (3)	—	528	528	528	—	—	—
Control Computer	293	348	348	348	216	216	216
Star Tracker (2)	44	44	44	44	—	—	—
Sun Sensor	3	3	3	3	6	6	6
Horizon Scanner	10	10	10	10	20	20	20
Magnetometer	10	10	10	10	—	—	—
Inertia Measuring Unit (2)	59	59	59	59	43	43	43
Total	1,061	2,172	1,908	1,468	285	285	285

Table 2-9. Experiment Module Weight Summary, CM-1 Communications and Data Management.

Item Condition	FPE 5.1 X-Ray	FPE 5.2A, 3-Meter Stellar	FPE 5.3A Solar	FPE 5.5, High Energy Stellar	FPE 5.20-2, Fluid Physics — Non-Cryogenics	FPE 5.20-3, Fluid Physics — Intermediate Term Cryogenics	FPE 5.20-4, Fluid Physics Long Term Cryogenics
Receiver (3)	56	56	56	56	56	56	56
Computer (3)	30	30	30	30	30	30	30
TV Camera	6	6	6	6	6	6	6
Data Formatter (3)	12	12	12	12	12	12	12
Command Decoder	8	8	8	8	8	8	8
OMNI Antenna System	13	13	13	13	13	13	13
TT&C Wideband Transmitter	29	29	29	29	29	29	29
Remodulator & Multicoupler	11	11	11	11	11	11	11
Switch & Bus	38	38	38	38	38	38	38
Data Storage/Displays & Consoles	140	140	140	140	140	140	140
Analog Video R/W Recorder	—	—	38	—	—	—	—
Total	343	343	381	343	343	343	343

Table 2-10. Experiment Module Weight Summary, CM-1 Environmental Control and Life Support

Item Condition	FPE 5.1 X-Ray	FPE 5.2A, 3-Meter Stellar	FPE 5.3A Solar	FPE 5.5, High Energy Stellar	FPE 5.20-2, Fluid Physics — Non-Cryogenics	FPE 5.20-3, Fluid Physics — Intermediate Term Cryogenics	FPE 5.20-4, Fluid Physics Long Term Cryogenics
Lights	12	12	12	12	12	12	12
Fire Equipment	12	12	12	12	12	12	12
Emergency Decompression Valves	25	25	25	25	25	25	25
Suit Lines & Fittings	30	30	30	30	30	30	30
Heat Exchanger	30	30	30	30	30	30	30
Ducting & Distribution	68	68	68	68	68	68	68
Total	177	177	177	177	177	177	177

Table 2-11. Experiment Module Weight Summary - CM-1 Thermal Control and Environmental Protection

Item Condition	FPE 5.1 X-Ray	FPE 5.2A, 3-Meter Stellar	FPE 5.3A Solar	FPE 5.5, High Energy Stellar	FPE 5.20-2, Fluid Physics — Non-Cryogenics	FPE 5.20.3, Fluid Physics — Intermediate Term Cryogenics	FPE 5.20-4, Fluid Physics Long Term Cryogenics
Meteoroid Bumper Shell	379	379	379	379	379	379	379
Radiators (Delta Value)	600	600	600	600	600	600	600
Outer Shell Supports	140	140	140	140	140	140	140
Thermal Insulation	150	150	150	150	150	150	150
Pumps, Lines, and Coolant	610	610	610	610	610	610	610
Subsystem Thermal Cabinets	725	725	725	725	725	725	725
Total	2604	2604	2604	2604	2604	2604	2604

Table 2-12. Experiment Module Weight Summary - CM-1 Experiment Weight by FPE Groupings

FPE Item		Weight (lb)
FPE 5.1		(3,300)
X-Ray Polarimeter (Novick)		350
X-Ray Spectrometer (Clark)		100
High Resolution X-Ray Scope (Giacconi)		200
X-Ray Detector (Boldt)		30
X-Ray Mirrors		300
Telescope Tube		400
Insulation	*	100
Telescope Drive Mechanism	*	150
Detector Housing Assy	*	350
Sensor Turret Installation	*	600
Miscellaneous Structural Supports	*	420
Miscellaneous Experiment Support Equipment	*	300
FPE 5.2A		(8,685)
Primary Mirror (Blue Book = 1700, Growth = 2300)		4,000
Primary Mirror Supports	*	500
Insulation	*	310
Telescope Trusswork	*	3,000
Secondary Mirror	*	150
Secondary Mirror Supports	*	240
Video	*	100
Flip Mirror	*	100
Photometer	*	30
Polarimeter	*	30
Spectographs		65
Cameras (2)		160
FPE 5.3A		(6,875)
1.5M Photoheliograph (including sensors)		4,075
Sensors		380
0.25 M Spectroheliograph		660
1 to 6 Solar Radii Coronagraph		660
5 to 30 Solar Radii Coronagraph		220
0.5 M Solar Telescope		880

*GDC Estimates, other values derived from bluebook

Table 2-12. Experiment Module Weight Summary - CM-1 Experiment Weight by FPE Groupings

FPE Item	Weight (lb)
FPE 5.5	(7,800)
X-Ray Spectroscope (Fisher)	800
X-Ray Telescope	515
Gamma Ray Spectrometer (Gibbons)	5,000
Gamma Ray Spark Chamber	1,485
FPE 5.20-2	(5,141)
Interface Stability	935
Capillary Studies	2,850
Condensing Heat Transfer	476
Rotating Liquid Globules	320
Two Phase Flow Regimes	460
Film Stability and Inertial Separator	100
FPE 5.20-3	(3,460)
Boiling Heat	600
Propellant Transfer	1,430
Slush Hydrogen	1,430
FPE 5.20-4	(5,252)
Long Term Storage of Cryogenics	5,252

Table 2-13. Experiment Module Mass Properties Summary - CM-3

Item Condition	FPE 5.7/12, Plasma Physics	FPE 5.8, Cosmic Ray Physics	FPE 5.16, Material Science and Proc.	FPE 5.20-1, Fluid Physics Lab	FPE 5.27, Physics and Chemistry Lab
Nominal Dry Weight (Table 2-14)	18,181	51,157	18,008	13,248	18,648
Operating Propellant and Service Items	2,560	2,560	2,560	2,560	2,560
Nominal Operating Weight, lb	20,741	53,717	20,568	15,808	21,208
Roll Inertia, Slug-ft^2/1000	22.7	33.6	20.0	16.2	20.2
Pitch/Yaw Inertia, Flug-ft^2/1000	88.5	249.5	53.5	49.4	55.9
Nominal C.G. - Experiment Module Station, feet (1)	17.7	28.0	13.2	13.5	14.0
Nominal C.P. - Experiment Module Station, feet (1)	15.8	24.3	14.8	14.8	14.8

Notes: (1) Feet from mating interface with space station.

Table 2-14. Experiment Module Weight Summary - CM-3 Systems Summary and Nominal Dry Weight

Item Condition	FPE 5.7/12, Plasma Physics	FPE 5.8, Cosmic Ray Physics	FPE 5.16, Material Science and Proc.	FPE 5.20-1, Fluid Physics Lab	FPE 5.27, Physics & Chemistry Lab
Experiment - Cargo	5,004	34,180	5,580	785	6,220
Structure	8,411	12,211	7,662	7,662	7,662
Reaction Control - Dry	1,008	1,008	1,008	1,008	1,008
Electrical Power	697	697	697	697	697
Guidance and Navigation	45	45	45	80	45
Stabilization and Control	262	262	262	262	262
Communications and Data Management	451	451	451	451	451
Environmental Control and LSS	271	271	271	271	271
Thermal Control & Environmental Protection	2,032	2,032	2,032	2,032	2,032
Total	18,181	51,157	18,008	13,248	18,648

Table 2-15. Experiment Module Weight Summary - CM-3 Structure

Item Condition	FPE 5.7/12, Plasma Physics	FPE 5.8, Cosmic Ray Physics	FPE 5.16, Material Science and Proc.	FPE 5.20-1, Fluid Physics Lab	FPE 5.27, Physics & Chemistry Lab
Shell Skin	1,014	1,014	1,014	1,014	1,014
Frames	129	129	129	129	129
Longerons	324	324	324	324	324
Crack Stoppers & Frame Mntg Lands	275	275	275	275	275
Aft Skirt Assembly	626	626	626	626	626
Domed Bulkhead Assembly	1,112	1,112	1,112	1,112	1,112
Docking Structure and Equipment	451	451	902	902	902
Aft External Subsystems Supports and Tunnel	350	350	350	350	350
Launch Support Fittings (Shuttle)	400	400	400	400	400
Fwd Flat Bulkhead Assembly	2,530	2,530	2,530	2,530	2,530
Subtotal - Basic Module Structure	7,211	7,211	7,662	7,662	7,662
Airlock and Deployment Mech	1,200	—	—	—	—
Experiment Peculiar Compartment/Housing	—	3,000	—	—	—
Experiment Assembly & Support Structure	—	2,000	—	—	—
Subtotal - Experiment Integration Structure			—	—	—
Total Module Structure	8,411	12,211	7,662	7,662	7,662

Table 2-16. Experiment Module Weight Summary - CM-3 Reaction Control

Item Condition	FPE 5.7/12, Plasma Physics	FPE 5.8, Cosmic Ray Physics	FPE 5.16, Material Science and Proc.	FPE 5.20-1, Fluid Physics Lab	FPE 5.27, Physics & Chemistry Lab
Propellant Tanks (4)	160	160	160	160	160
Gas Pressure Vessels (4)	333	333	333	333	333
Thruster Assemblies (24)	459	459	459	459	459
Fuel Distribution	56	56	56	56	56
Total-Reaction Control-Dry	1008	1008	1008	1008	1008

Table 2-17. Experiment Module Weight Summary - CM-3 Electrical Power

Item Condition	FPE 5.7/12, Plasma Physics	FPE 5.8, Cosmic Ray Physics	FPE 5.16, Material Science and Proc.	FPE 5.20-1, Fluid Physics Lab	FPE 5.27, Physics & Chemistry Lab
Batteries (3)	462	462	462	462	462
Battery Charger (3)	66	66	66	66	66
Regulator	44	44	44	44	44
Inverter (3)	59	59	59	59	59
Power Control & Distribution	66	66	66	66	66
Total	697	697	697	697	697

Table 2-18. Experiment Module Weight Summary - CM-3 Guidance and Navigation

Item Condition	FPE 5.7/12, Plasma Physics	FPE 5.8, Cosmic Ray Physics	FPE 5.16, Material Science and Proc.	FPE 5.20-1, Fluid Physics Lab	FPE 5.27, Physics & Chemistry Lab
Corner Reflector	2	2	2	2	2
Diplexer	1	1	1	1	1
Omni Antenna	4	4	4	4	4
Target Stadiu Installation	6	6	6	6	6
Transponder (2)	22	22	22	22	22
Installation Structure	10	10	10	10	10
Laser Docking System	-	-	-	35	-
Total	45	45	45	80	45

Table 2-19. Experiment Module Weight Summary-CM-3 Stabilization and Control

Item Condition	FPE 5.7/12, Plasma Physics	FPE 5.8, Cosmic Ray Physics	FPE 5.16, Material Science and Proc.	FPE 5.20-1, Fluid Physics Lab	FPE 5.27, Physics & Chemistry Lab
Inertia Measuring Unit	43	43	43	43	43
Control Computer	193	193	193	193	193
Sun Sensor (2)	6	6	6	6	6
Horizon Scanner (2)	20	20	20	20	20
Total	262	262	262	262	262

Table 2-20. Experiment Module Weight Summary-CM-3
Communications and Data Management

Item Condition	FPE 5.7/12, Plasma Physics	FPE 5.8, Cosmic Ray Physics	FPE 5.16, Material Science and Proc.	FPE 5.20-1, Fluid Physics Lab	FPE 5.27, Physics & Chemistry Lab
Receiver (3)	56	56	56	56	56
Computer	10	10	10	10	10
TV Camera	6	6	6	6	6
Data Formatter	9	9	9	9	9
Command Decoder	8	8	8	8	8
Omni Antenna System	13	13	13	13	13
TT&C and Wideband Transmitter	39	39	39	39	39
Remodulator & Multicoupler	14	14	14	14	14
Switch and Bus	38	38	38	38	38
TV Monitor	63	63	63	63	63
Data Storage/Displays & Consoles	195	195	195	195	195
Total	451	451	451	451	451

Table 2-21. Experiment Module Weight Summary-CM-3
Environmental Control and Lift Support

Item Condition	FPE 5.7/12, Plasma Physics	FPE 5.8, Cosmic Ray Physics	FPE 5.16, Material Science and Proc.	FPE 5.20-1, Fluid Physics Lab	FPE 5.27, Physics & Chemistry Lab
Lights	12	12	12	12	12
Fire Equipment	12	21	21	21	21
Emergency Decompression Valves	25	25	25	25	25
Suit Lines and Fittings	33	33	33	33	33
Heat Exchanger	30	30	30	30	30
Ducting and Distribution	150	150	150	150	150
Total	271	271	271	271	271

Table 2-22. Experiment Module Weight Summary-CM-3
Thermal Control and Environmental Protection

Item Condition	FPE 5.7/12, Plasma Physics	FPE 5.8, Cosmic Ray Physics	FPE 5.16, Material Science and Proc.	FPE 5.20-1, Fluid Physics Lab	FPE 5.27, Physics & Chemistry Lab
Meteoroid Bumper Shell	379	379	379	379	379
Radiators (Delta Value)	600	600	600	600	600
Outer Shell Supports	140	140	140	140	140
Thermal Insulation	150	150	150	150	150
Pumps Lines and Coolant	635	635	635	635	635
Subsystem Thermal Cabinets	128	128	128	128	128
Total	2032	2032	2032	2032	2032

Table 2-23. Experiment Module Weight Summary-CM-3
Experiment Weight by FPE Groupings

FPE - ITEM	WEIGHT - LBS
FPE 5.7 & 5.12	(5004)
Plasma Physics Measurement Equipment (including Antenna)	1800
RMS Control Center Equipment	500
Large RMS (2)	880
Small RMS (4)	424
RMS Fuel & Tankage	900
RMS Fueling and Service Equipment	500
FPE 5.8	(34180)
Total Absorption Detectors (TAD)	24000(1)
TAD Photo Multipliers	910
Total Absorption Shower Counter (TASC)	3000
TASC Photo Multipliers	280
Magnet-Dewar Assembly	3000
Liquid Cerenkov	1000
Spectrometer Assembly	200
Detector Bays	400
Spare Detectors	150
Emulsion Storage	100
Emulsion Processing	100
Control Console	200
Computer with Microflim Recorder	500
Microfilm Storage	20
Spare Photo Multipliers (Unshielded)	120
Spare Electronic Boards	200
FPE 5.20-1	(785)
Fluid Properties	100
Zero Gravity Combustion	60
Consoles, Flight Control and Data Displays	*625

*Convair Estimates, Other Values Derived from Blue Book
(1) Initial Logistics Items

Table 2-23. Experiment Module Weight Summary-CM-3
Experiment Weight by FPE Groupings (Continued)

FPE - ITEM	WEIGHT - LBS
FPE 5.16	(5580)
Thin Film	285
Glass Casting	215
Spherical Casting	185
Single Crystals	165
Composite Casting	215
Variable Density Casting	215
X-Ray Diffraction Measurement	* 1650
Electron Diffraction Measurement	* 210
Refraction Meter	* 400
2 Color Pyrometers	* 20
Materials Testing Machine	* 200
X-Ray Machine	* 200
Metallograph Machine	* 100
Chemical Lab	* 200
Mass Spectrograph	* 300
Furnace	* 1000
Spectroscope	* 20
FPE 5.27	(6220)
Artifical Meteoroids	200
Capillary Studies	200
Ultrapure Metals	165
Critical State Studies	100
Bubble Formation in Zero 6	935
Dynamics of Liquid Drops	320
X-Ray Diffraction Measurement	* 1650
Electron Diffraction Measurement	* 210
Refraction Meter	* 400
Two-Color Pyrometers	* 20
Materials Testing Machine	* 200
X-Ray Machine	* 200
Metallograph Machine	100
Chemical Lab	200
Mass Spectrograph	300
Furnace	1000
Spectroscope	* 20

*Convair Estimates, Other Values Derived from Blue Book
(1) Initial Logistics Items

Table 2-24. Experiment Module Mass Properties Summary, CM-4

Item Condition	FPE 5.9/10/23, Biology	FPE 5.11, Earth Surveys	FPE 5.22, Component Test & Calibration
Nominal Dry Weight (Table 2-25)	29,797	21,521	24,383
Operating Propellant & Service Items	2,560	2,560	2,560
Nominal Operating Weight, lb	32,357	24,081	26,943
Roll Inertia, Slug-ft^2/1000	29.8	19.4	24.8
Pitch/Yaw Inertia, Slug-ft^2/1000	209.0	151.7	120.2
Nominal c.g. – Experimental Module Station, feet (1)	23.3	21.7	19.3
Nominal c.p. — Experimental Module Station, feet (1)	26.4	20.5	18.8

Notes: (1) Feet from mating interface with space station.

Table 2-25. Experiment Module Weight Summary — CM-4 Systems Summary and Nominal Dry Weight

Item Condition	FPE 5.9/10/23, Biology	FPE 5.11, Earth Surveys	FPE 5.22, Component Test & Calibration
Experiment — Cargo	12,846	4,602	5,601
Structure	10,848	11,281	13,145
Reaction Control – Dry	1,008	1,008	1,008
Electrical Power	697	697	697
Guidance & Navigation	45	45	45
Stabilization & Control	314	314	314
Communications & Data Management	451	451	451
Environmental Control & LSS	841	415	414
Thermal Control & Environmental Protection	2,747	2,708	2,708
Total	29,797	21,521	24,383

Table 2-26. Experiment Module Weight Summary - CM-4 Structure

Item Condition	FPE 5.9/10/23 Biology	FPE 5.11, Earth Surveys	FPE 5.22, Component Test & Calibration
Shell Skin	1,470	1,470	1,470
Frames	187	187	187
Longerons	469	469	469
Crack Stoppers & Frame Mounting Lands	403	403	403
Aft Skirt Assembly	626	626	626
Docking Structure & Equipment	451	451	902
Aft External Subsystems Supports & Tunnel	350	350	350
Launch Support Fittings (Shuttle)	400	400	400
Flat End Bulkhead Assembly	2,530	2,530	2,530
Fwd Intermediate Blkhd Assembly	—	—	1,898
Aft Intermediate Blkhd Assembly	—	—	1,898
Domed Aft Bulkhead Assembly	1,112	1,112	1,112
Subtotal - Basic Module Structure	(7,998)	(7,998)	(12,245)
Interior Airlock Installation	—	—	500
Forward Domed/Hinged Bulkhead	—	1,950	—
Experiment Canisters	—	380	—
Experiment Deployment	—	253	400
Floor-Non-Pressurizable	350	700	—
Centrifuge Connecting Structure	1,500	—	—
Centrifuge Outer Shell	1,000	—	—
Subtotal - Exp. Peculiar Structure	(2,850)	(3,283)	(900)
Total - Module Structure	(10,848)	(11,281)	(13,145)

Table 2-27. Experiment Module Weight Summary CM-4 Reaction Control

Item Condition	FPE 5.9/10/23 Biology	FPE 5.11, Earth Surveys	FPE 5.22, Component Test & Calibration
Propellant Tanks (4)	160	160	160
Gas Pressure Vessels (4)	333	333	333
Thruster Assemblies (24)	459	459	459
Fuel Distribution	56	56	56
Total	1,008	1,008	1,008

Table 2-28. Experiment Module Weight Summary CM-4 Electrical Power

Item Condition	FPE 5.9/10/23 Biology	FPE 5.11, Earth Surveys	FPE 5.22, Component Test & Calibration
Batteries (3)	462	462	462
Battery Charger (3)	66	66	66
Regulator	44	44	44
Inverter (3)	59	59	59
Power Control & Distribution	66	66	66
Total - Electrical Power	697	697	697

Table 2-29. Experiment Module Weight Summary
CM-4 Guidance and Navigation

Item Condition	FPE 5.9/10/23 Biology	FPE 5.11, Earth Surveys	FPE 5.22, Component Test & Calibration
Corner Reflector	2	2	2
Diplexer	1	1	1
Omni Antenna	4	4	4
Target Stadiu Installation	6	6	6
Transponder (2)	22	22	22
Installation Structure	10	10	10
Total	45	45	45

Table 2-30. Experiment Module Weight Summary
CM-4 Stabilization and Control

Item Condition	FPE 5.9/10/23 Biology	FPE 5.11, Earth Surveys	FPE 5.22, Component Test & Calibration
Inertia Measuring Unit	43	43	43
Control Computer	245	245	245
Sun Sensor (2)	6	6	6
Horizon Scanner (2)	20	20	20
Total	314	314	314

Table 2-31. Experiment Module Weight Summary - CM-4
Communications and Data Management

Item Condition	FPE 5.9/10/23, Biology	FPE 5.11, Earth Surveys	FPE 5.22, Component Test & Calibration
Receiver (3)	56	56	56
Computer	10	10	10
TV Camera	6	6	6
Data Formatter	9	9	9
Command Decoder	8	8	8
Omni Antenna System	13	13	13
TT&C and Wideband Transmitter	39	39	39
Remodulator and Multicoupler	14	14	14
Switch and Bus	38	38	38
TV Monitor	63	63	63
Data Storage/Displays and Consoles	195	195	195
Total	451	451	451

Table 2-32. Experiment Module Weight Summary - CM-4 Environmental Control and Life Support

Item Condition	FPE 5.9/10/23, Biology	FPE 5.11, Earth Surveys	FPE 5.22, Component Test & Calibration
Lights	24	24	24
Fire Equipment	21	21	21
Emergency Decompression Valves	25	25	25
Suit Lines and Fittings	62	62	62
Heat Exchanger	60	60	75
Molecular Sieve	110	—	—
Oxidizer System	43	—	—
Condenser/Separator	44	—	—
Charcoal Filters	143	—	—
Waste Storage	50	—	—
Water System	68	—	—
Ducting and Distribution	191	223	207
Total	841	415	414

Table 2-33. Experiment Module Weight Summary - CM-4 Thermal Control and Environmental Protection

Item Condition	FPE 5.9/10/23, Biology	FPE 5.11, Earth Surveys	FPE 5.22, Component Test & Calibration
Meteoroid Bumper Shell	550	550	550
Radiators (delta value)	850	850	850
Outer Shell Supports	217	217	217
Thermal Insulation	232	232	232
Pumps, Lines and Coolant	730	730	730
Subsystem Thermal Cabinets	168	129	129
Total	2747	2708	2708

Table 2-34. Experiment Module Weight Summary - CM-4
Experiment Weight by FPE Grouping

FPE Item	Weight (lb)
FPE 5.9/5.10/5.23	(12,846)
Centrifuge Compartment Subtotal	(3,855)
Centrifuge	800
Laminar Flow Bench	1,200
Instruments	110
Specimens and Cages - Vertebrates	945
Specimens and Cages - Plants	800
Experimental Module Lab Compartment Subtotal	(8,991)
Specimens and Cages - Vertebrates	530
EC/LS (including back-up) - Vertebrates	800
Atmosphere Monitoring - Vertebrates	162
Laminar Flow Bench	1,200
Specimens and Housings - Plants	327
EC/LS (including back-up) - Plants	800
Atmosphere Monitoring - Plants	162
Ancillary Research Equipment - Plants	110
Acceleration Isolation Equipment - Plants *	400
Monkeys and Facilities	1,500
Chimpanzees and Facilities	3,000
FPE 5.22	(5,601)
Multi-Instrument Work Bench	200
Computer/Console	75
Optical Work Bench	100
IR Calibration Source	75
Microwave Radiometer	45
Fuel Cell	100
Fluid/Gas Components	50
Heat Exchanger/Pipes	75
Air Bearings	25
Microwave Sensor	5
Pointing Telescope Optics	15
LWIR Sensor	150
Film Developing Subsystems	150
Space Welding Gun	10
Developmental Flowmeter	5
Ancillary Research Equipment	571
Reactants and Cryogenics - Experiments	3,950(1)

* GDC Estimates, other values derived from bluebook.
(1) Initial logistics items.

Table 2-34. Experiment Module Weight Summary - CM-4
Experiment Weight by FPE Grouping (Continued)

FPE Item		Weight (lb)
FPE 5.11		(4,602)
Metric Camera		360
Multispectral Camera		185
Multispectral IR Scanner		150
IR Interferometer Spectrometer		66
IR Atmospheric Sounder		45
IR Spectrometer/Radiometer		65
MW Scanner		76
Multifrequency MW Radiometer		50
MW Atmospheric Sounder		80
Radar Imager		620
Active-Passive MW Radiometer		100
Visible Wavelength Polarimeter		50
UHF Sferics		22
Absorption Spectrometer		95
Laser Altimeter		371
UV Imager Spectrometer		150
Radar Altimeter/Scatterometer		75
Photo-Imaging Camera		145
Data Collection		11
Imaging Spectrometer Camera	*	30
Tracking Telescope	*	250
Indexing Camera	*	30
Day/Nite TV	*	50
Ancillary Research and Support Equipment	*	1,525

* GDC Estimates, other values derived from bluebook.

Table 2-35. Experiment Module Weight Summary Propulsion Slice

Item - System	Weight (lb)
Cylinder - Skin	304
Frames	49
Frame Mounting Lands	32
Radial Crack Stoppers	50
Longerons	97
Aft Flange	198
Fwd Flange	198
Docking Structure and Equipment	880
Center Tunnel	235
Miscellaneous Equipment Support Structure	300
Fore/Aft Contamination Covering	150
Motors - Gimballed	110
Tanks - Ammonia	640
Tanks - Hydrazine	280
Tanks - Helium	720
Fuel Distribution System	169
Total Dry Weight	4,412
Fuel	6,800
Total Operating Weight	11,212

Table 2-36. Experiment Module Weight Summary - Manned Transporter Module

Item - System	Weight (lb)
Cylindrical Shell (Window Penalty = 165 lb)	2,295
Aft Bulkhead w/Kick Ring and Hatch	750
Aft Skirt/Adapter	410
Aft Docking Structure and Equipment	750
Aft External Subsystems Supports and Tunnel	525
Forward Bulkhead - Flat	2,000
Forward Docking Structure and Equipment	750
Multi-purpose Structural Supports - 15%	1,120
Contingency - 10%	860
Future Growth Allowance - 30%	2,840
Subtotal - Structure	(12,300)
Reaction Control System - Dry	950
Electrical Power System	1,030
Guidance and Navigation System	75
Stability and Control System	350
Communications and Data Management	240
Environmental Control and Life Support System	1,900
Personnel Provisions (Including Expendables)	1,055
Crew	400
Propellant	2,700
Total Operating Weight	21,000

Table 2-37. Experiment Module Weight Summary - Unmanned Transporter Module

Item - System	Weight (lb)
Cylindrical Shell	2,130
Aft Bulkhead w/Kick Ring and Hatch	750
Aft Skirt Adapter	450
Aft Docking Structure and Equipment	750
Aft External Subsystems Supports and Tunnel	525
Forward Bulkhead - Flat	2,000
Forward Docking Structure and Equipment	750
Multi-purpose Structural Supports - 15%	1,100
Contingency - 10%	840
Future Growth Allowance - 30%	2,775
Subtotal - Structure	(12,030)
Reaction Control System - Dry	1,050
Electrical Power System	1,030
Guidance and Navigation System	75
Stability and Control System	350
Communications and Data Management	240
Environmental Control and Life Support System	1,170
Propellant	3,600
Total Operating Weight	19,545

Table 2-38. Experiment Module Weight Sensitivity - Shuttle Versus Expendable Vehicle Launch Modes - CM-1

Item	Weight (lb)		
	Shuttle Launch	Expendable Launch	Optional Launch
Skin (t = 0.065 vs. 0.060)	780	1,014	1,014
Frames (A = 0.25 vs. 0.22)	113	129	129
FR/Skin Pads	146	107	107
Radial Crack Stoppers	168	168	168
Aft Skirt (Interstage Adapter)	428	428	428
Aft Skirt Flange	175	198	198
Aft Bulkhead - Spherical	1,112	1,112	1,112
Aft Docking Beams and Equipment	451	451	451
Aft External Subsystems Structure	200	200	200
Aft Tunnel	150	150	150
Longerons	130	324	324
Shuttle Launch Fittings and Doublers	400	—	400
Total - Basic Module Structure	4,253	4,281	4,681

SECTION 3

STRUCTURE SUBSYSTEM

In order to provide realistic predictions of module characteristics a structural arrangement has been conceived. Major elements of structure, such as the skirt, dock, hatch, bulkheads, and side wall construction are identical for all three common modules. The difference occurs in the number of side wall ring segments, which determines the module length and volume.

In addition to the base-line structural arrangement described below, several alternate configurations were considered for the side wall structure. Relative costs for the various alternates were estimated. Several bulkhead configurations were investigated and their effects on module weight were determined.

A detailed analysis of the side wall joint design was made.

A preliminary structural analysis of the shell for meteoroid protection, launch, and pressure loads has been performed. First mode natural frequencies of the solar cell arrays have also been determined.

3.1 LOADS CRITERIA

The loads criteria for the experiment modules are concerned with two basic conditions. Those loads and environmental conditions associated with placing the module into orbit and those loads and environmental conditions associated with orbital service.

Two launch vehicles have been assumed in determining boost phase loads. The base line structure was designed assuming launch by space shuttle with the possibility of launch by a Titan III type expendable launch vehicle.

For space shuttle launch the limit load factors are 4g in any direction (longitudinal, lateral and transverse) combining with 1g in the other two directions.

For the Titan III launch case the loads are based on a preliminary Centaur-Titan III D hammerhead payload configuration and are more realistic than the Titan III loads initially used for analysis.

The design compressive load intensity (N_ϕ) for the module wall in compression is based on launch by a Titan III C booster. Lacking launch trajectories and flight loads at this time, tentative design requirements are based on critical values taken from the Titan III C/Centaur configuration using the "hammerheaded" payload setup shown in Figure 3-1.

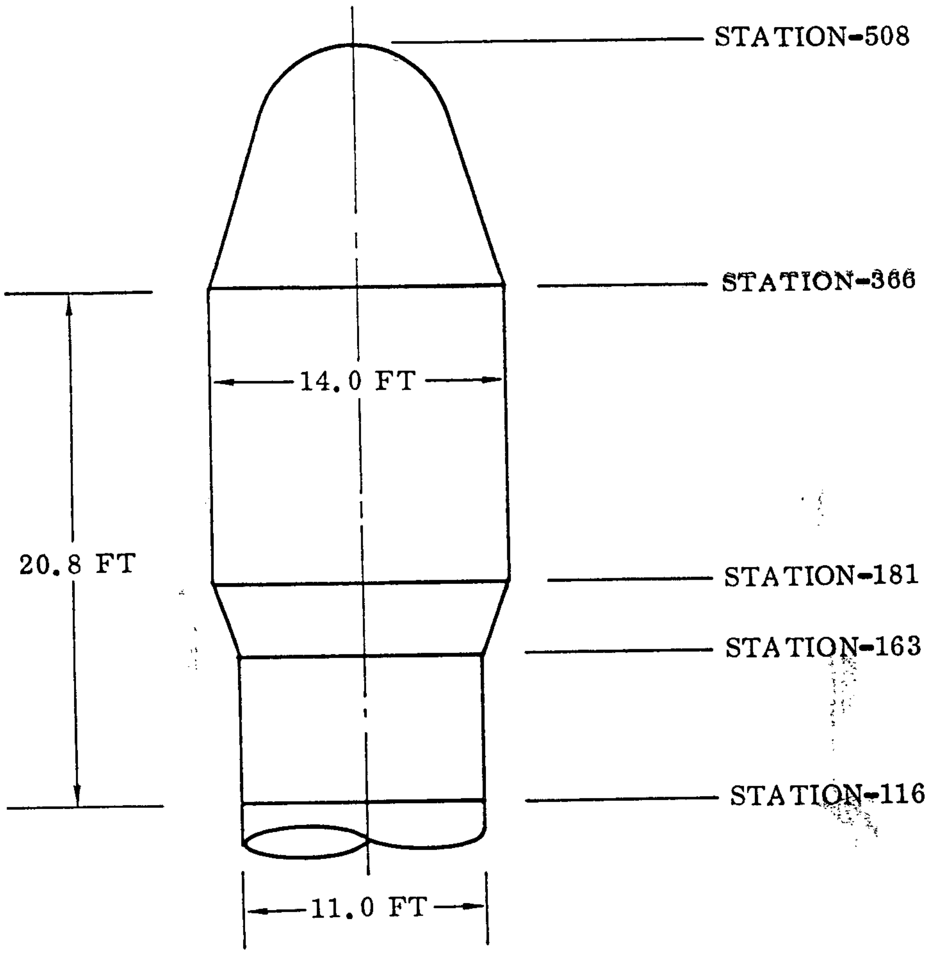

Figure 3-1. "Hammerhead" Payload Setup

Station -116.0 was selected for design loads since it most closely represented the typical module length of 20 feet. The N_ϕ load was based on a 14.0 feet diameter, as shown in Figure 3-1, instead of the slightly smaller baseline diameter. This is considered valid since the N_ϕ value would be about the same for either case.

$$N_\phi = \frac{M(R)(t)}{\pi R^3(t)} + \frac{P}{2\pi R} = \frac{M}{\pi R^2} + \frac{P}{2\pi R}$$

Equivalent Axial Load = $P_{EQ} = 2\pi R(N_\phi)$

$$P_{EQ} + 2\pi R\ (M/\pi R^2 + P/2\pi R) = (2M/R + P)$$

Thus, the highest P_{EQ} will produce the design compression N_ϕ.

The loads given in Table 3-1 were obtained from: NAS3-8718, Letter Report, Preliminary TIII/Centaur Maximum Airloads Study, (SA-14), dated December 1969. The conditions are not described here beyond giving the table number in the above document from which they were obtained and the Mach number where ultimate load values were given in a particular table.

Table 3-1. Loads Criteria

Condition Table	$10^{-6}M$ (in-lb)	$10^{-3}V$ (lb)	$10^{-3}P$ (lb)	10^{-3} (2M/R)* (lb)	$10^{-3}P_{EQ}$ (lb)	Mach No.
18	8.91	31.6	75.6	212.1	287.7	1.52
19	8.93	31.8	76.8	212.6	289.4	1.60
20	9.61	29.5	19.8	228.8	248.6	0.80
22	9.38	31.5	70.1	223.3	293.4	1.20
24	8.91	31.6	75.6	212.1	287.7	1.52
25	8.94	31.8	76.8	212.9	289.7	1.60
35	11.06	34.4	19.8	263.3	283.1	0.80
36	10.54	33.8	37.5	251.0	288.5	1.00
37	9.94	33.6	70.1	236.7	306.8 Critical	1.20

(*2/R = 2.0/(14.0/2)12 - 2.0/84.0 = 0.0238)

$$N_{\phi_{CRIT}} = P_{EQ_{CR}}/2\pi R = (306.8 \times 10^3/168.0\pi) = \frac{581.0 \text{ lb/in Limit}}{(\text{Use } 581.0 \times 1.10 = 640.0)}$$

$N_{\phi_{CR}}$ - Ultimate - 1.4 (640.0) = 900.0 lb/in

The structural criteria for the experiment modules is summarized below.

a. Meteoroid damage: 90% probability of no penetration in 10 years.

b. Leak before break: Flaws will grow through skin thickness before critical propagation length is reached.

c. Pressure: May vary from 0 to 14.7 ±2.0 psig. No pressure during launch.

d. Factors of safety: Manned cabin
Ult = 2.0
Proof = 1.33
Yield - 1.46 - 1.10 × Proof
Space loads: Ultimate - 1.4
Limit = 1.0

3.2 STRUCTURAL DESCRIPTION

The primary structure of each common module is comprised of a segmented barrel section, a constant radius dome closure, an aft skirt and docking structure, and an experiment peculiar bulkhead which is tailored to fit the various experiment requirements.

The barrel section in the case of CM-1 is comprised of four skin segments and eight frames. The skin sections are integrally stiffened panels with the stiffeners located on the external surface to provide a smooth inner surface for meteoroid damage repair. Longitudinal butt welding is used to join the panels into a completed ring. The frames are stretch formed aluminum sheet metal sections mechanically fastened to integrally machined stub frames inside the skin panels. See Figure 3-2.

The aft skirt is typical skin, frame, stringer type of semimonocoque construction.

The docking structure is comprised of four beams arranged in egg crate fashion in the aft skirt. The docking beams pick up the docking loads from the two probes and two drogues at the intersection of the beams and transfer the load to the aft skirt. The aft skirt distributes this load into the barrel section.

The meteoroid protection skin panels surround the barrel section with a three-inch gap enclosing the passive thermal protection system. The meteoroid panels are in ring segments overlayed at the structural ring stations. Support is furnished by Z frames attached to integral lug attachments of the primary structure frame. See Figure 3-3.

For most of the modules, space radiators will be substituted for the meteoroid shield and will serve as meteoroid bumper as well as radiators. The radiator panels will consist of aluminum tubes diffusion bonded to aluminum panels. Joints and manifolds will be provided to interconnect the coolant passages of the various radiator panels.

3.3 CYLINDER PRESSURE WALL

3.3.1 DESIGN APPROACH. The design of the module cylinder walls was based on several functional requirements. It must (1) withstand the internal pressures listed in Section 3.1, (2) react the boost flight loads of the space shuttle, and (3) protect against meteoroid penetration for 10 years with a 90% probability of no penetration. In addition to this criteria, two other requirements were established for the design of the pressure hull walls. First, it is desirable to provide a smooth, uninterrupted inner hull surface for the detection and repair of meteoroid damage. Second, it is desirable to provide as part of the basic structure, some means for the attachment of the various subsystem components contained within each module.

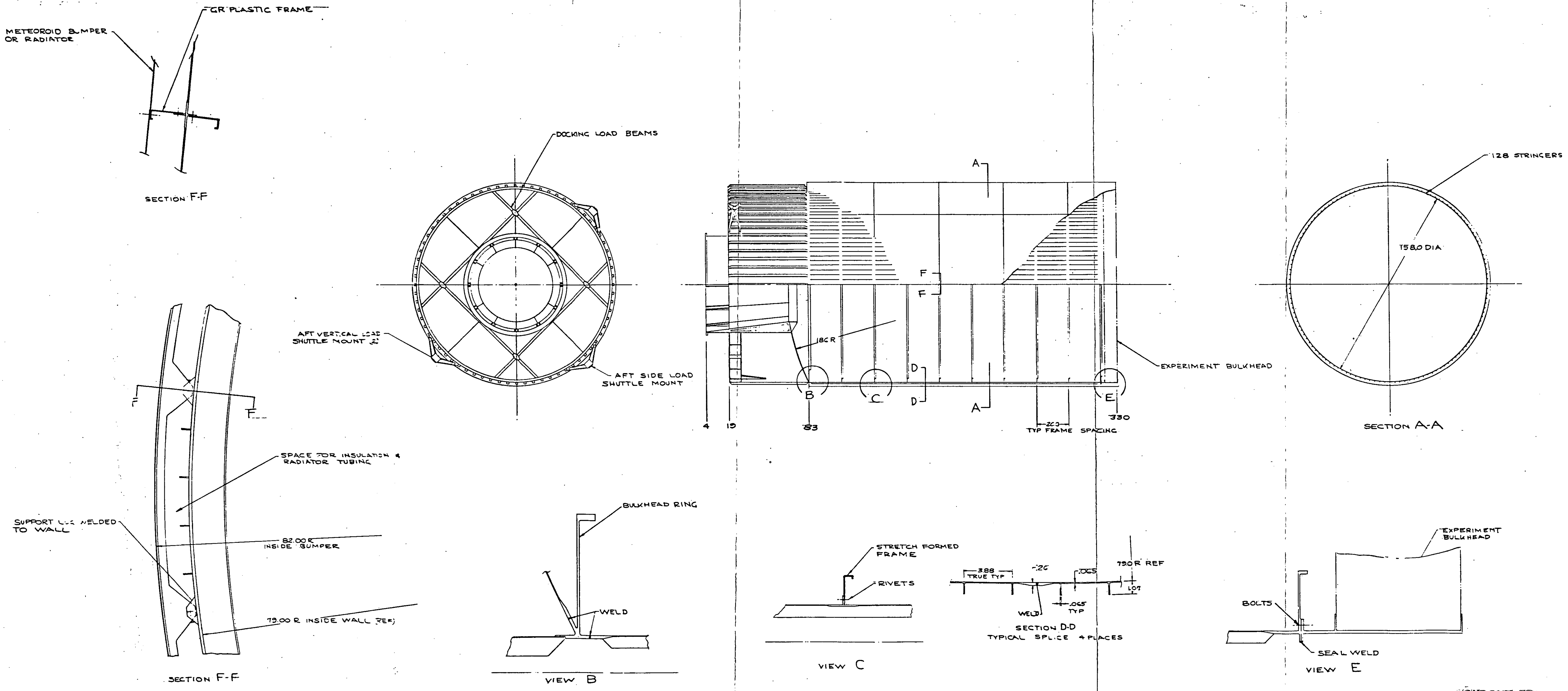

Figure 3-2. CM-1 Basic Structural Arrangement

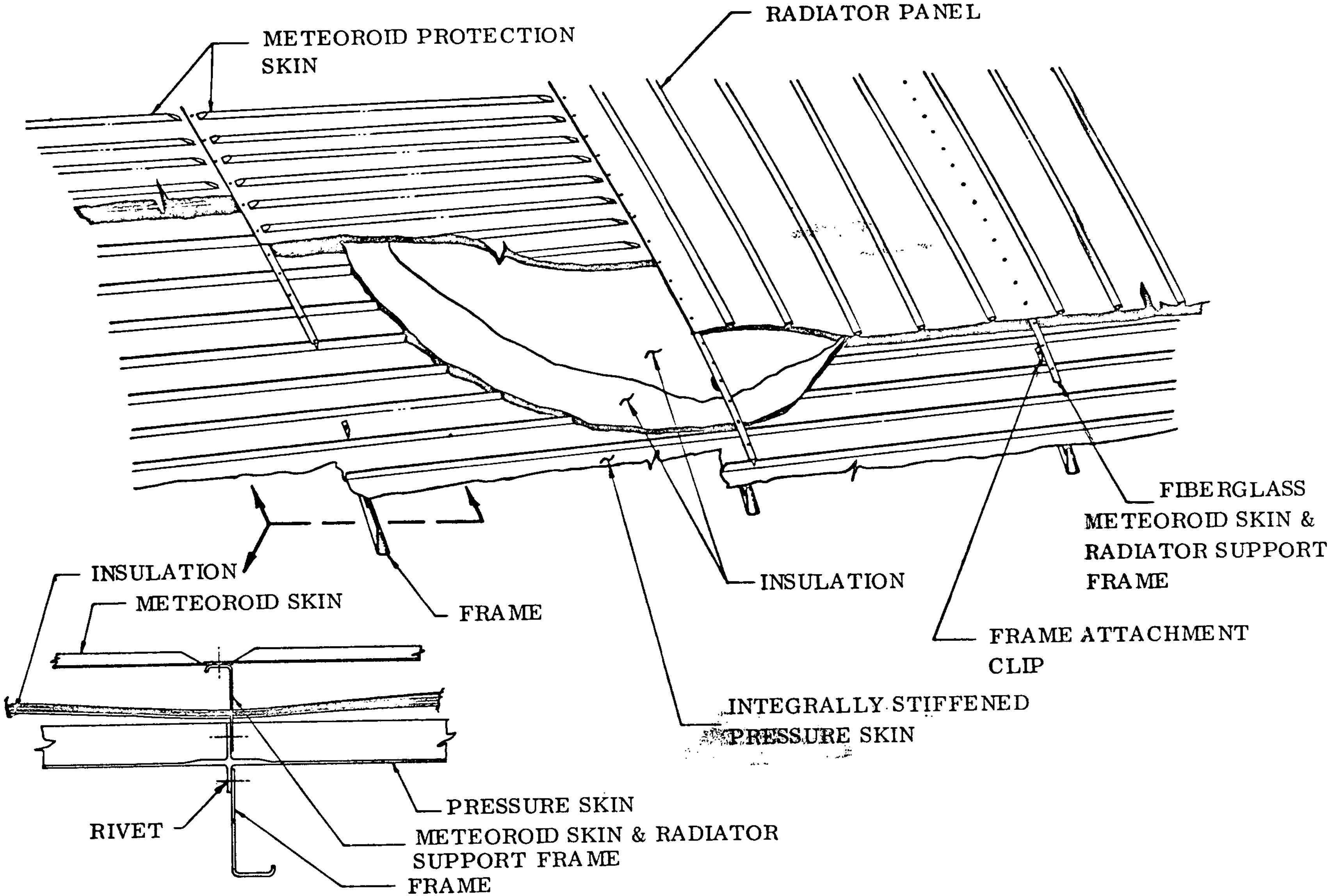

Figure 3-3. Pressure Shell and Meteoroid Protection Structure

Several configurations and design approaches were used in the evaluation of the module side walls. A computer program described in Report GDC-DCB70-001, Structural Sizing and Costing Analysis System for an Advanced Staging Vehicle – Computer Documentation, was used to help size the shell walls, stiffeners, and rings.

The shell walls were sized both for shuttle-only loads and for launch by Titan III expendable launch vehicle. Initially the program was used to provide data to evaluate the structural weight of modules of varying diameter. Three types of construction were then evaluated: monocoque, waffled skin, and skin-stringer. Several stringer and ring spacings were also evaluated.

The results of this work are summarized briefly as follows:

a. The skin stringer construction tends to provide the lightest structure for either space shuttle or expendable launch vehicle loads.

b. A frame spacing of approximately 26 inches tends to produce a minimum weight structure for the diameter finally selected (158 inches).

c. Structural weight decreases as the number of stringers increases (within the limits selected).

Because it is potentially the lightest weight, the skin stringer-frame method of construction was chosen as the structural baseline. The type of construction selected is shown in Figure 3-4. The stringers are external to provide a smooth inner surface and the frames internal to provide mounting provisions for equipment.

Several detail design approaches were investigated. Figure 3-5 illustrates some of the side wall frame details that were investigated. Each of these was considered for ease of manufacture, structural acceptability, and the degree to which it met the other design requirements. Three types were chosen for more detailed study. These were Type 2 (the baseline), Type 5 (shown in earlier reports as the baseline), and Type 7. Type 7 was included because it represents a typical pressurized aircraft fuselage structure which could potentially show a cost saving.

The cost estimates considered fabrication of the cylindrical walls only, omitting insulation, meteoroid bumpers, and end closures. Tooling costs were prorated over 17 units.

If the cost of fabricating the baseline is assigned a value of 1.00, the cost of fabrication for the two alternates is 1.50 for the aircraft type construction and 1.70 for Type 5.

The trade studies treated the cylinder as a simple structure without cutouts. This is an oversimplification as each module will require an emergency hatch in the side wall as well as certain experiment peculiar openings.

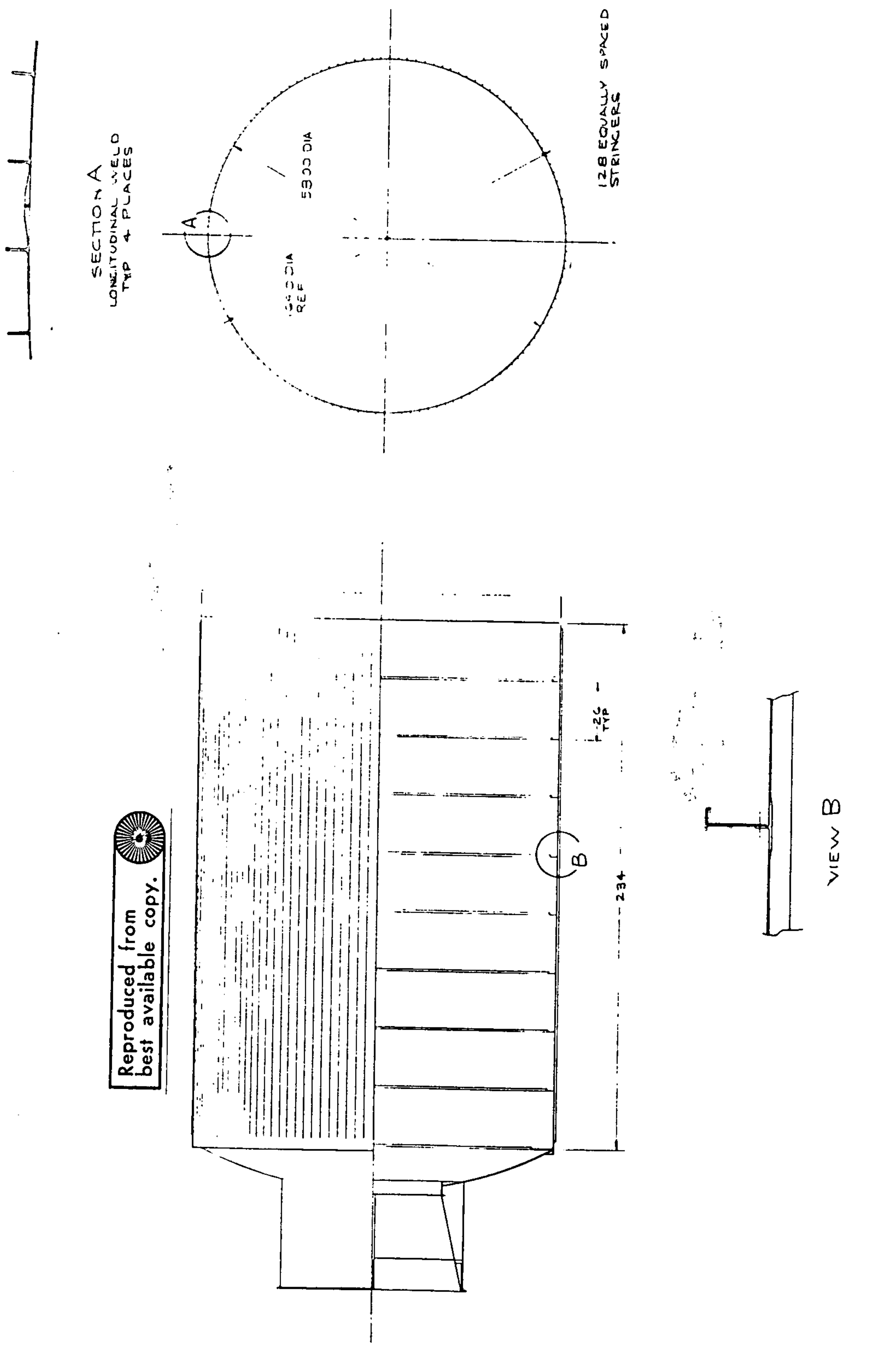

Figure 3-4. Baseline Pressure Hull Configuration

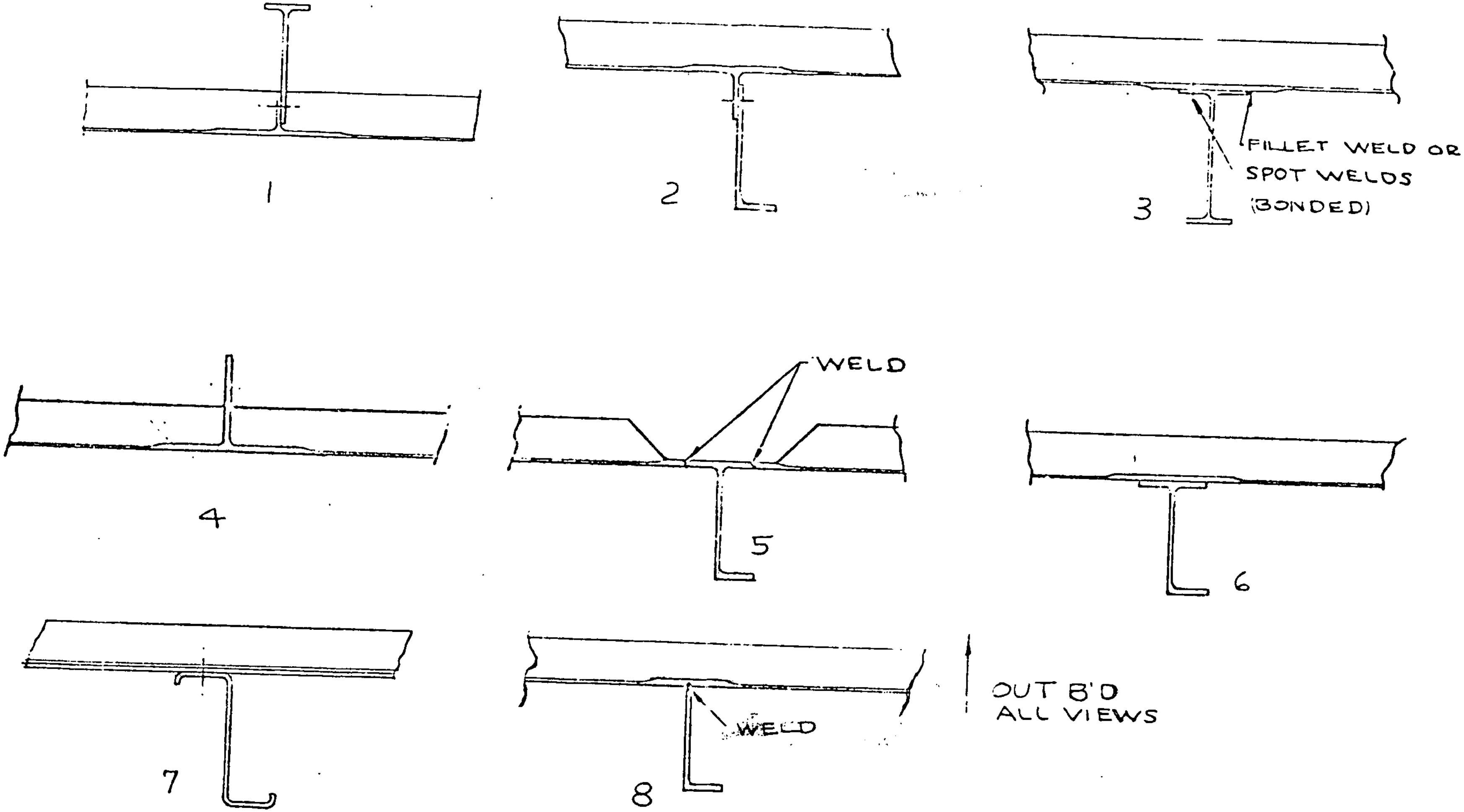

Figure 3-5. Side Wall Frame Details

Figure 3-6 shows one approach for an emergency hatch port in the side wall structure. This hatch would be common to all modules and be provided in one of the side wall panels.

One additional area considered but not investigated in depth is the question of hull wall damage due to impact by moving equipment. The relatively thin wall (0.065 in.) can be damaged by the impact of some sharp edged object being propelled by an astronaut. One possibility would be to place an energy absorbing blanket over the inner hull wall. This would, of course, be in conflict with the requirement to provide ready access for hull wall inspection. An alternate solution would be to design all movable equipment and tools with well-rounded corners and edges to minimize the possibility of hull damage. Another alternative would be to place the additional weight of the energy absorbing blanket in an increase in skin gage which would be more resistant to damage. This question deserves more consideration in future studies.

3.3.2 DESIGN ANALYSIS. The material selected was aluminum 2219-T851. This material has good strength and weight properties and is weldable. Past studies of pressure vessel designs at Convair have selected this material as having characteristics desirable for this type application (high tensile and yield strength, good toughness, resistance to stress corrosion, not particularly sensitive to strain direction, etc.).

Using Al 2219-T851 alloy for the shell, which is operating at room temperature:

$$\left.\begin{array}{lll} F_{tu} = 62.0 \text{ ksi} & : & E = 10.5 \times 10^6 \text{ psi} \\ F_{ty} = 46.0 \text{ ksi} & : & E_c = 10.8 \times 10^6 \text{ psi} \\ F_{cy} = 47.0 \text{ ksi} & : & \mu = 0.33 \\ F_{su} = 36.0 \text{ ksi} & : & \omega = 0.102 \text{ lb/in.}^3 \end{array}\right\} \text{MIL-HDBK-5 "A" values for plate} \leq 2.00 \text{ in. thick}$$

The computer program described in Report GDC-DCB70-001, Structural Sizing and Costing Analysis of an Expendable Tankage System for an Advanced Staging Vehicle — Computer Program Documentation, January 1970, was used to size the shell wall frames and stringers. The results obtained from several of the program runs are given in Table 3-2. In all cases the frame spacing was set at 26.0 inches, with the stringer blade and shell skin thickness minimum gage set at 0.065 inch. Varying blade spacings were then employed to arrive at overall requirements and unit weights.

Table 3-2. Sizing Program Results

Run No.	No. of Blades	b_s (in.)	t_s (in.)	$A_{str.}$ (in^2)	t_B (In.)	H_B (in.)	A_{fr} (in^2)	Wt (lb/ft^2)
1	96	5.17	0.081	0.072	0.065	1.114	0.1562	1.476
2	120	4.14	0.068	0.071	0.065	1.099	0.1562	1.339
3	128	3.88	0.065	0.070	0.065	1.077	0.1562	1.302

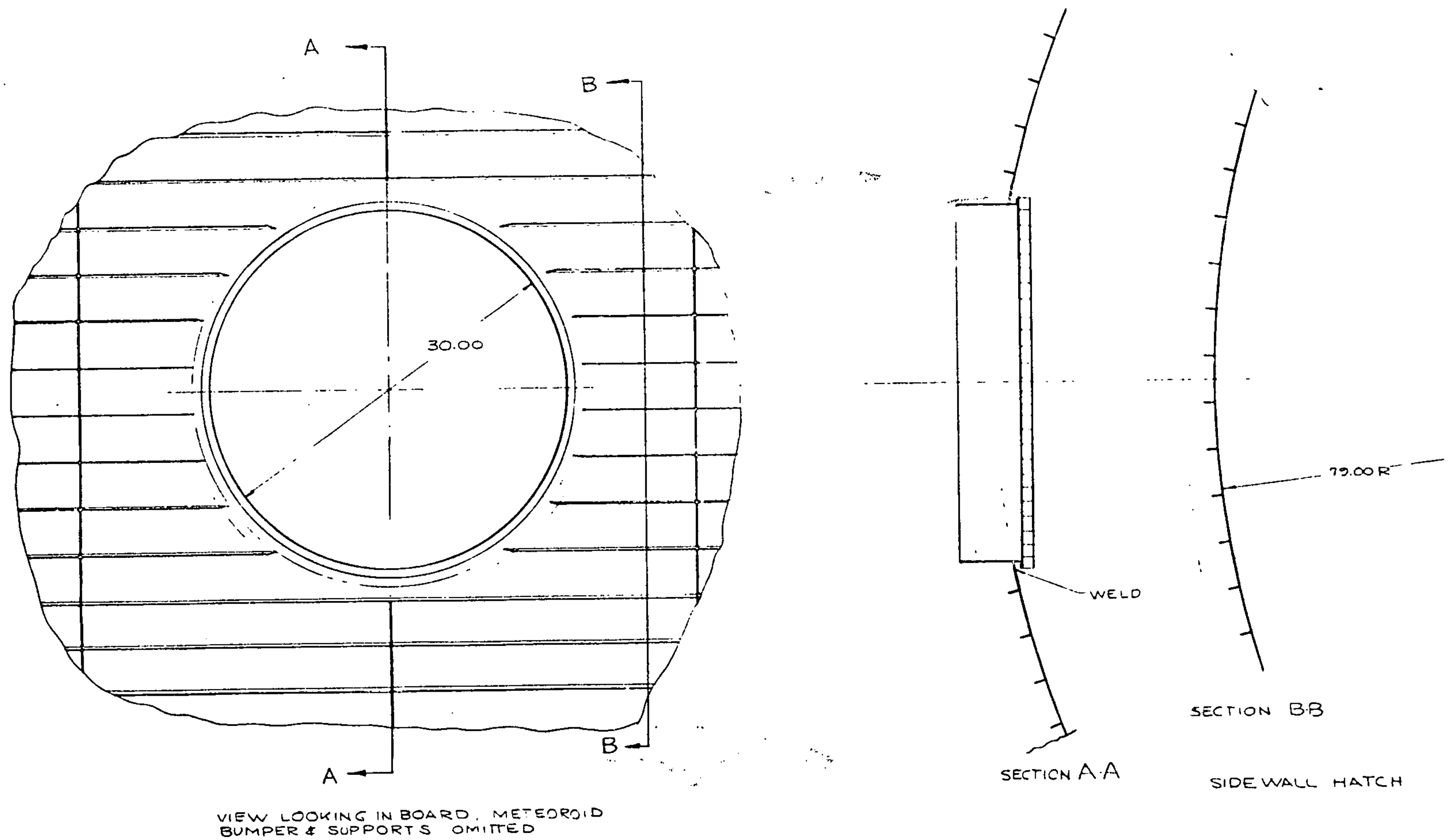

Figure 3-6. Emergency Hatch Port

The $I_{required}$ for the frame is given by the Shanley equation:

$$I_{req} = \frac{C_f \, M \, D^2}{E \, (L)}$$

where

$C_f = 0.0000625$

$L = 26.0$ in.

D = Diameter of cylinder = 158.0 in.

$M = N_{\phi_{cr}} \, (D^2)(\pi/4)$

The frame area thus required is given by:

$$A_{f_{req}} = \sqrt{\frac{C_f \times M \times 4R^2}{L \times F_F \times E}} = \sqrt{\frac{I_{req}}{F_F}}$$

where

F_F = a form factor = 4.0 for this case

$$A_{f_{req}} = \sqrt{I_{req}/4} = \sqrt{I_{req}}/2$$

Since $A_{f_{req}} = 0.1562 \text{ in}^2$, then

$$I_{req} = (2 \times 0.1562)^2 = 0.0976 \text{ in}^4$$

Checking the shell for internal pressure:

$p_U = 33.4$ psig

Effective skin thickness for hoop stress is: $t_S = 0.065$ (disregard frames due to wide spacing.)

$$\sigma_{hoop} = \sigma_H = 33.4\,(79.0)/0.065 = 40,600 \text{ psi Ultimate}$$

The effective unit area for the longitudinal stress is:

$$t_L = t_S + (A_{str}/b_S) = 0.065 + (0.070/3.88) = 0.065 + 0.018 = 0.083 \text{ Ultimate}$$

Then, $\sigma_L = 33.4\ (79.0)/2(0.083) = 15,900$ psi Ultimate

Checking the margin of safety using the Hencky-von Mises Theory of Failure:

$$M.S. = (1.0/R) - 1.0$$

where

$$R = (\sigma_H/\sigma_U)^2 - (\sigma_H/\sigma_U)(\sigma_L/\sigma_U) + (\sigma_L/\sigma_U)^2$$

σ_U = ultimate allowable tensile stress = F_{tu} = 62.0 ksi

$$R = (40.6/62.0)^2 - (40.6/62.0)(15.9/62.0) + (15.9/62.0)^2$$

$$= 0.429 - 0.168 + 0.066 = 0.327$$

$$M.S. = (1.0/0.327) - 1.0 = 3.06 - 1.00 = +2.06$$

Meteoroid protection analysis shows that the probability of a meteoroid penetrating the modules is a function of time in orbit and surface area. Figure 3-7 shows the thickness required as a function of exposed surface area for 0.9 and 0.95 probability of failure. The largest module (CM-4) requires a wall thickness of 0.060 in.

Figure 3-7 also summarizes the shell wall thickness requirements. Shown are the minimum gages for burst strength and for meteoroid protection. The minimum practical manufacturing gage is shown.

$$\left(\frac{21.56}{30.0}\right)^2 - \frac{(21.56)(15.9)}{(30.0)^2} + \left(\frac{15.9}{30.0}\right)^2 = 0.516 - 0.381 + 0.281 = 0.416$$

$$M.S. = (1.0/0.416) - 1.0 = +1.40$$

This margin may be a little on the high side, however. Use K = 4.0, i.e., $t_w = 4.0\ t_S$

$$t_w = 4.0\ (0.065) = 0.260$$

For weld taper length

$$L \geqq 4.0\ (0.260 - 0.065)$$

$$L \geqq 0.78 \text{ in. (Use 0.80 in.)}$$

The situation is somewhat different at the circumferential splices that have to handle the longitudinal pressure and compression loading as well as the resulting discontinuity problems. The same weld land thickness will be used in determining the discontinuity stresses at both intermediate and end rings. Figure 3-8 shows the setup for an intermediate frame.

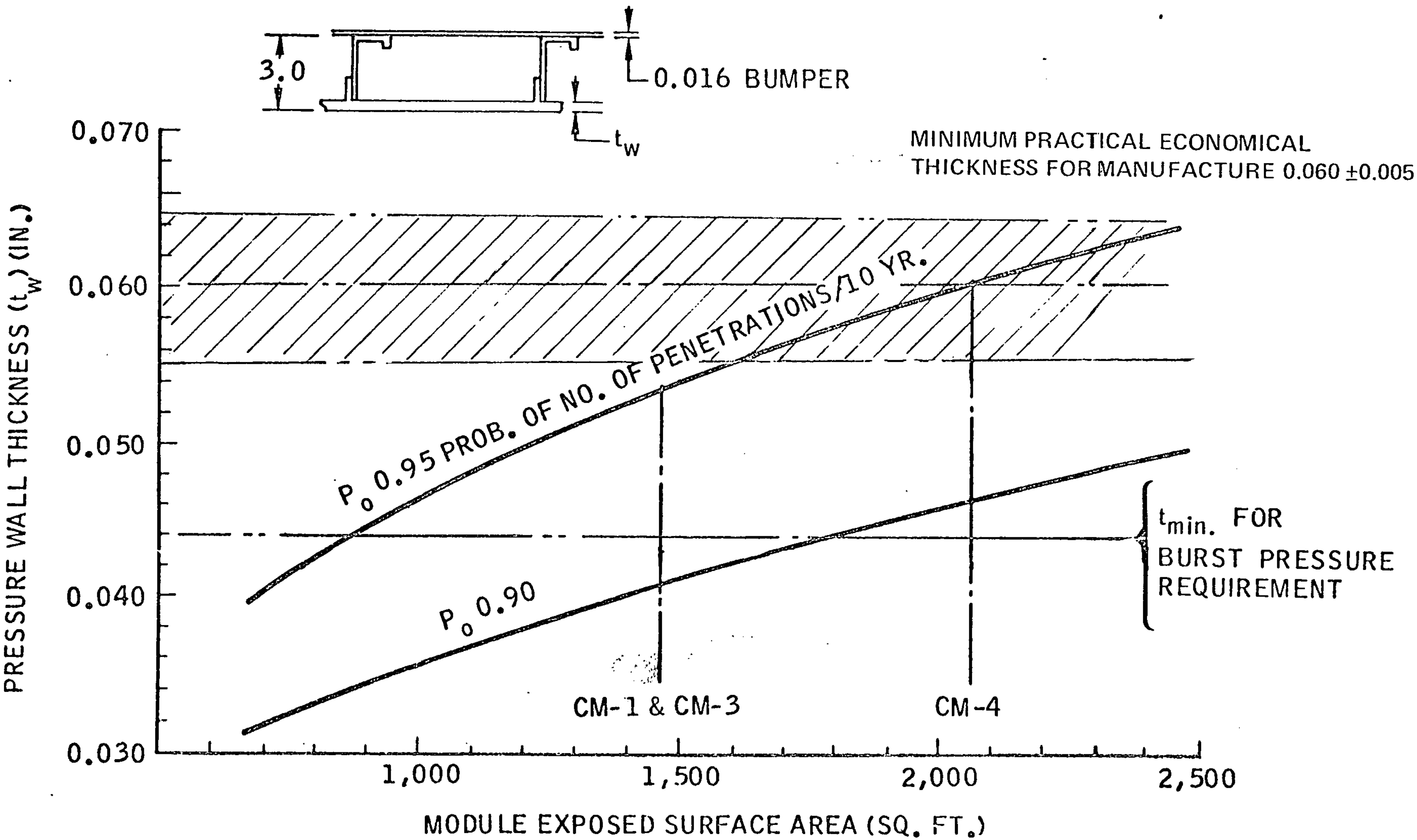

Figure 3-7. Thickness as a Function of Exposed Area

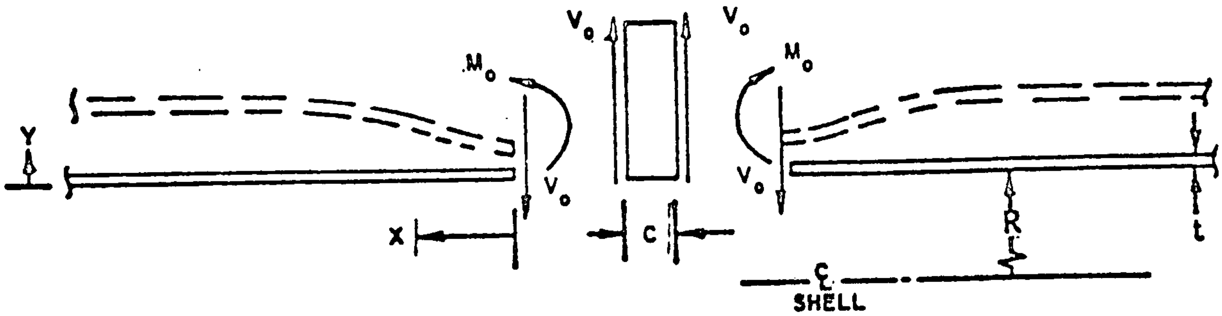

Figure 3-8. Intermediate Frame Setup

Using Roark's Formulas for Stress and Strain, Third Edition, page 271:

For uniform internal pressure

$$M_0 = 0.304\ pRt \left[\frac{A - Ct}{A + 1.56t\sqrt{Rt}}\right] = 0.304\ pRt\,(B)$$

$$V_0 = 0.78\ p(\sqrt{Rt})\left[\frac{A - Ct}{A + 1.56t\sqrt{Rt}}\right] = \frac{2.56\,(M_0)}{\sqrt{Rt}}$$

The maximum longitudinal stress is:

$$\sigma_L = \sigma_{bend} + \sigma_{axial}$$

Using the Run No. 3 section shown in Figure 3-9,

$$I_{xx} = 0.0217199 + 0.0057028 - (0.3180)(0.144)^2 = 0.0274227 - 0.0065940$$

$$I_{xx} = 0.02083 : (\bar{y}/I)_{tens.} = (0.144/0.02083) = 6.91$$

Then

$$\sigma_L = 3.88\left[(M_0)(6.91) + pR/2(0.318)\right]$$

$$\sigma_L = 3.88pR\left[0.304\,(6.91)(0.065)(B) + 1.572\right]$$

$$= 3.88\,(33.4)(79.0)\left[0.1365B + 1.572\right]$$

$$\sigma_L = 1397B + 16{,}090$$

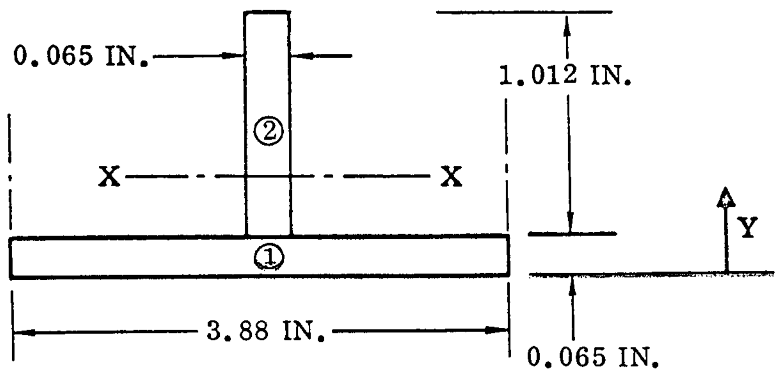

SECT.	A	Y	AY	AY^2	I_0
1	0.2522	0.0325	0.008197	0.0002664	0.0000888
2	0.0658	0.571	0.037572	0.0214535	0.0056140
TOTALS	0.3180	Y=0.144	0.045769	0.0217199	0.0057028

Figure 3-9. Run No. 3 Section

where

$B = \left[(A - Ct)/(A + 1.56t\sqrt{Rt})\right]$

A = area of frame plus land

$= 0.5938 + (1.00 + 1.00)^{\dagger}(0.260 - 0.125) + \frac{2(0.80)^{\ddagger}}{2}(0.195 - 0.125)$

$A = 0.5938 + 2(0.135) + 0.80(0.070) = 0.5938 + 0.270 + 0.056 + 0.920$

C = effective land width $= 2(1.00 + 0.80/2) = 2.8$

$t = t_S = 0.065$ (since a function of hoop stiffness)

$R \approx R_i = 79.0$

$(A - Ct) = 0.920 - 2.8(0.065) = 0.920 - 0.182 = 0.738$

$(A + 1.56t\sqrt{Rt}) = 0.920 + 1.56(0.065)\sqrt{79.0(0.065)} = 0.920 + 0.1014\sqrt{5.14}$

$(A + 1.56t\sqrt{Rt}) = 0.920 + 0.230 = 1.150$

† full land; ‡ taper

$$B = (0.738/1.150) = 0.642$$

$$\sigma_L = 1397\,(0.642) + 16,090 = 900 + 16,090 = 16,990 \text{ psi}$$

Since cracks or flaws present in the shell may propagate under the stresses resulting from internal pressure, particularly under repeated pressurization cycles, some consideration must be given in the design to the use of operating stresses that will enable the detection of cracks of critical size during the inspection and proof testing phase. The use of crack arrestors represents a design possibility where this can be done for a reasonably small weight penalty.

The critical crack length equation is

$$K_{I_c} = 1.10\,\sigma_0 \sqrt{\pi}\,(a/Q)^{1/2} \quad \text{(Partial crack)}$$

where

K_{I_c} = critical stress intensity factor, ksi $\sqrt{\text{inches}}$: for 2219-T851 = 34.0 for 2219 as welded = 28.0 ksi $\sqrt{\text{in}}$.

A review of the as-welded properties of 2219-T851 indicates that the joints are critical in tension yield and that the efficiency, based on the appropriate yield-to-ultimate ratios involved here, is given by:

$$\sigma_{w_{ult}} = \left(\sigma_{w_{yield}}\right) \times \left(\frac{p_{ult}}{p_{yield}}\right)$$

$$\sigma_{w_{ult}} = (22.0 \times 10^3) \times (33.4/24.4) = 30.1 \times 10^3 \text{ psi}$$

$$e = (\sigma_{w_{ult}}) / (\sigma_{ult}) = (30.1 \times 10^3/60.0 \times 10^3) = 0.502$$

Use e = 50%.

Disregarding maintenance of the same margins of safety in both the basic shell and the welded section, check using K = 4.0 in conjunction with the Hencky-von Mises criteria noted earlier for the welded section.

$$\left(\frac{\sigma_H}{30.0}\right)^2 - \frac{(\sigma_H)(\sigma_L)}{(30.0)^2} + \left(\frac{\sigma_L}{30.0}\right)^2 = R$$

where

$$\sigma_L = 15.90 \text{ ksi}$$

40

$\sigma_{H_{max}} = 21.56$ ksi

σ_0 = operating stress = 16.7 × 79.033/0.065 = 20.3 ksi

a = half crack length, inches

$Q = \left[\Phi^2 - (0.212)(\sigma/\sigma_y)^2\right]$

$(a/Q)_{cr} = (K_{I_c})^2/(1.10)^2(\pi)(\sigma_0)^2 = (K_{I_c}/\sigma_0)^2/3.80$

$(a/Q)_{cr} = (34.0/20.3)^2/(3.80) = 0.738$ (partial crack)

For a through-crack:

$(a/Q)_{cr} = (34.0/20.3)^2/(1.0)^2(\pi) = 0.893$ (through crack)

$\sigma_0/\sigma_y = (20.3/46.0) = 0.441$

The smallest critical flaw size occurs when Q_{cr} is minimum, which occurs when a/2c is a minimum. See Figure 3-10.

For $a/2c \approx 0$: $Q_{cr} \cong 1.0$

Then, for the partial crack:

$a_{cr} = 0.738(1.0) = 0.738$ in.

For a through crack:

$2(a_{cr}) = 2(0.893)(1.0) = 1.786$ in.

The critical flaw sizes are of sufficient magnitude that they would be detected in the inspection process. In any event, the shell would leak before any bursting and detection of a significant flaw could occur during proof testing. This recognizes the fact that some flaw growth occurs as a result of the pressure cycling; however, since a small number (on the order of 100) of cycles is anticipated, this growth is small.

In certain cases it may be desirable to use the leak-before-burst philosophy in the design approach to ensure that flaws exceeding a certain size are detected either prior to or during proof testing. This approach is worthwhile if:

a. Structure is expensive or irreplaceable.

b. Weight is not a prime design consideration.

c. Fabrication and inspection time must be reduced to minimize costs.

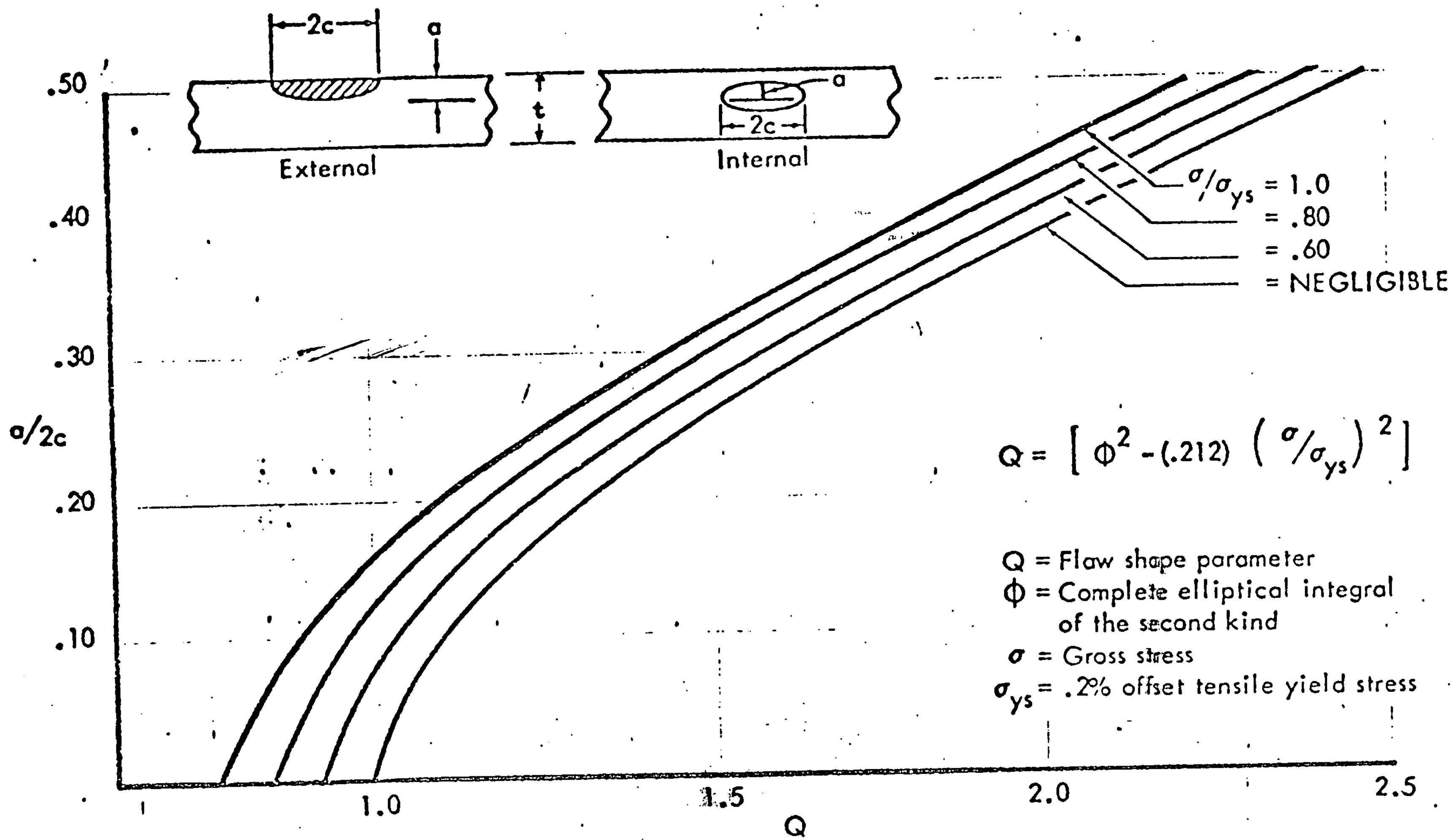

FLAW SHAPE PARAMETER CURVES FOR SURFACE AND INTERNAL CRACKS

Figure 3-10. Flaw Shape Parameter Curves for Surface and Internal Cracks

For a leak to occur in the case of a partial crack:

$$a_{min} \geq t$$

$$a_{min} = (K_{Ic})^2_{min} \,(Q_{min})/(1.10)^2 \pi \sigma_0^2$$

Using $a_{min} = t$

$$\sigma_0^2 = (K_{Ic})^2 \,(Q_{min}/t)/1.21\,\pi$$

$$Q_{min} = \left[\Phi^2 - 0.212\,(\sigma/\sigma_y)\right]$$

For $a/2c = 0$ and $\sigma/\sigma_y = 1$, $Q_{min} = 0.80$, which is somewhat unrealistic.

$$(\sigma_0)^2 = (34.0)^2\,(0.8/1.21\,\pi)/t = 243.3/t$$

Since

$$\sigma_0 \leq \sigma_{ys}, \text{ let } \sigma_0 = \sigma_p = \sigma_{ys} = 46.0 \text{ ksi}$$

Then

$$(46.0)^2 = 243.3/t, \text{ and}$$

$$t_{req} = 0.115 \text{ in.}$$

The above is the absolute minimum shell thickness that would have permitted leak-before-burst proof testing. If, as specified before, $\sigma_{ys} = 1.10\,\sigma_p$,

$$t_{req} = 243.3\,(1.10)^2/(46.0)^2 = 0.139 \text{ in.}$$

Since, in either case, this thickness requirement for leak-before-burst testing is on the order of twice the presently proposed basic thickness, and since the critical flaw size is sufficiently large that detection poses no problems, it is impractical from a weight standpoint to specify this test as a design requirement.

In view of the long-life design requirements and the possibility of damage occurring to the shell wall, a study of crack stopper designs was made in the interests of crew safety. Considered was a stainless steel strap bonded to the pressure wall on the inside in the hoop direction at each of the frames. Following the approach taken in Fracture Mechanics Guidelines for Aircraft Structural Applications, by D. P. Wilhelm, Technical Report AFFDL-TR-69-111, dated February 1970, the critical stress for a crack length equal to the frame spacing was determined. This critical stress was 12,880 psi. As might be anticipated, the critical operating stress for arrest of a crack that has reached this size is low. Another solution to this problem is the addition of more stoppers to reduce the spacing of the straps.

The possibility of using straps at both the frame center lines and the midpoints offers a solution since the normal operating hoop stress is 20,300 psi.

It was determined, however, that the incremental weight of these straps would nearly equal the unit weight of the basic proposed structure, and would result in a structure with a unit weight of 2.496 lb/ft^2. Since the computer runs indicated that the wall thickness required is only 0.188 in. for a monocoque shell and has a unit weight of 2.761 lb/ft^2, this approach would be preferable to the strap design from both a fabrication and cost standpoint. The monocoque design would have a minimum critical crack length of 6.15 in., which was arrived at as follows:

$$(a/Q)_{cr} = (34.0/\sigma_0)^2/(3.80) = (304.0/\sigma_0^2) \quad \text{(partial crack)}$$

where $Q_{cr} = 1.0$

$$\sigma_0 = p_0 R/t = 16.7\ (79.094)/0.188 = 7,030 \text{ psi} = 7.03 \text{ ksi}$$

$$a_{cr_{min}} = (1.0)(304.0)/(7.03)^2 = 6.15 \text{ in.}$$

Obviously, the monocoque design would require no new inspection techniques and could possibly incorporate a leak-before-burst proof test for some additional safety.

Insofar as design recommendations are concerned, however, the basic shell using the 0.065 in. wall thickness with 128 longitudinal machined stringers at 3.88 in. spacing and omitting the crack arrest straps is believed to have sufficient structural integrity to handle all aspects of the mission. The minimum critical crack length is of sufficient size that present inspection techniques are more than adequate to detect such a flaw prior to launch. Further, the penetrating meteoroid mass is of insufficient magnitude to produce a crack in the basic shell of any size approaching the critical crack length.

The only instance in which crack arresters such as the straps might be needed would occur as a result of damage to the shell wall caused by equipment impact, etc. An assessment of this problem would have to be made and a tradeoff between the mission performance risks involved and the weight penalty resulting for reduction of these risks would have to be made prior to any final conclusions on this aspect of the design.

3.4 PRESSURE BULKHEADS

3.4.1 DESIGN APPROACH. The weight of the end closures for the experiment module can be a significant portion of the total structural weight as indicated by Figure 3-11. The total structural weight shown for various diameters and a fixed volume includes the sidewall, one pressure bulkhead, docking structure, and miscellaneous attachments. The sidewall length is 19 ft 6 in. and its diameter is 13 ft 2 in. (equivalent to a CM-1 module). The total weight does not include the experiment peculiar pressure bulkhead, which is shown in phantom. A six-point shuttle attachment is assumed. It can be seen

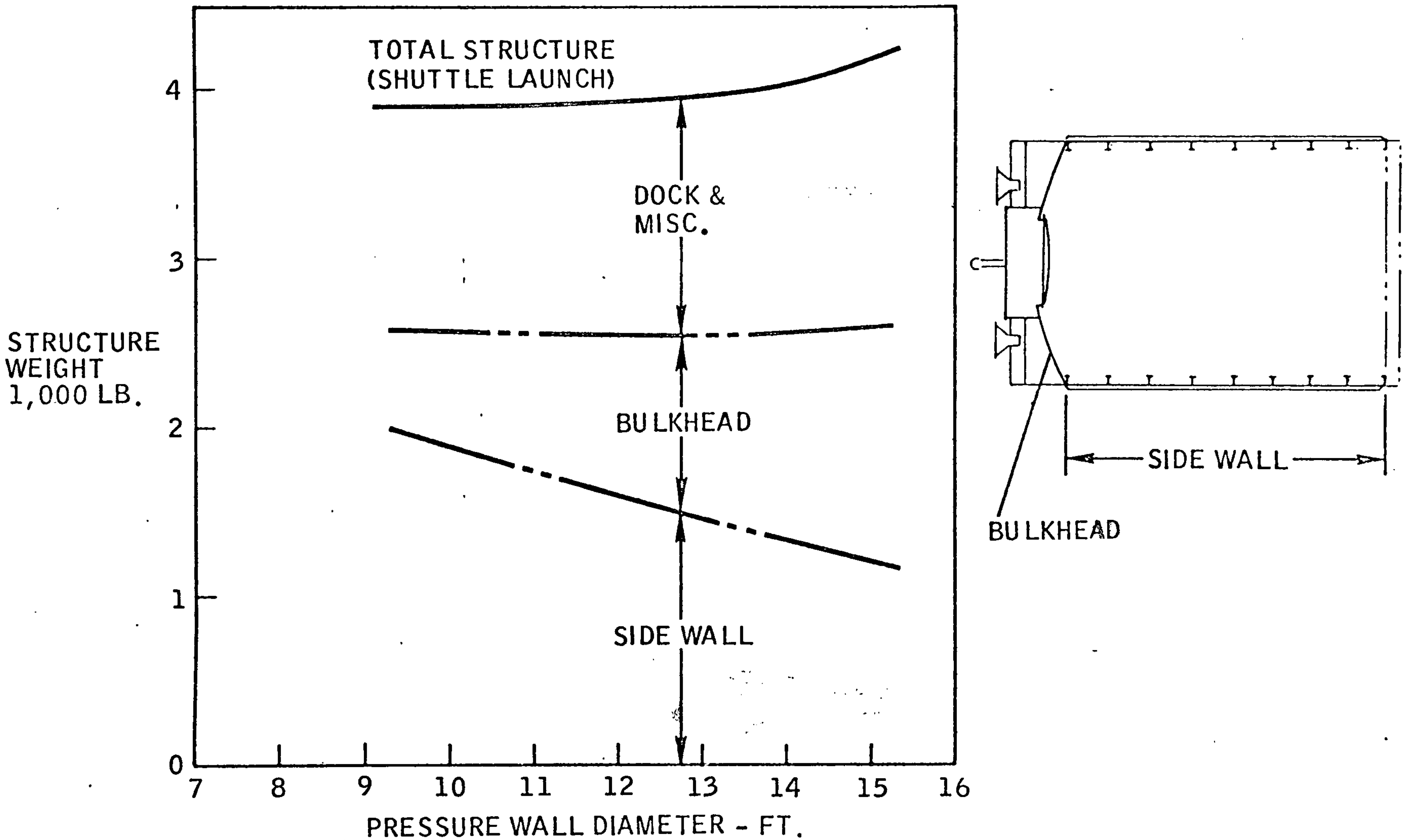

Figure 3-11. Structure Weight vs. Diameter

that the sidewall stiffening weight increases for the longer slender modules as the pressure bulkhead weight decreases. Pressure bulkhead weights become increasingly significant at the larger diameters. The addition of a second pressure bulkhead to the total structure weight would increase the slope of the total weight curve, making it desirable to reduce module diameter as limited by experiment compatibility.

In addition to the consideration of weight the space occupied by the bulkhead is an important factor in the selection of bulkhead configurations. The use of spherical or ellipsoidal bulkheads limits the cylindrical length for a given total length and wastes packaging space.

Four types of bulkheads were investigated and considered as being candidates for the experiment module. These are (1) spherical segment, (2) conical, (3) flat beam, and (4) flat sandwich.

In addition to the weights and space considerations the following functional requirements were considered.

Astronomy Modules. Spherical and flat bulkhead configurations, shown in Figure 3-12, are for use with the astronomy modules. In the case of a spherical bulkhead the instruments must protrude through the bulkhead and be mounted to the module sidewall with the bulkhead pressure-sealed around the instrument. In the case of a multi- instrument module, this approach could pose sealing problems considering the flexibility of the spherical bulkhead.

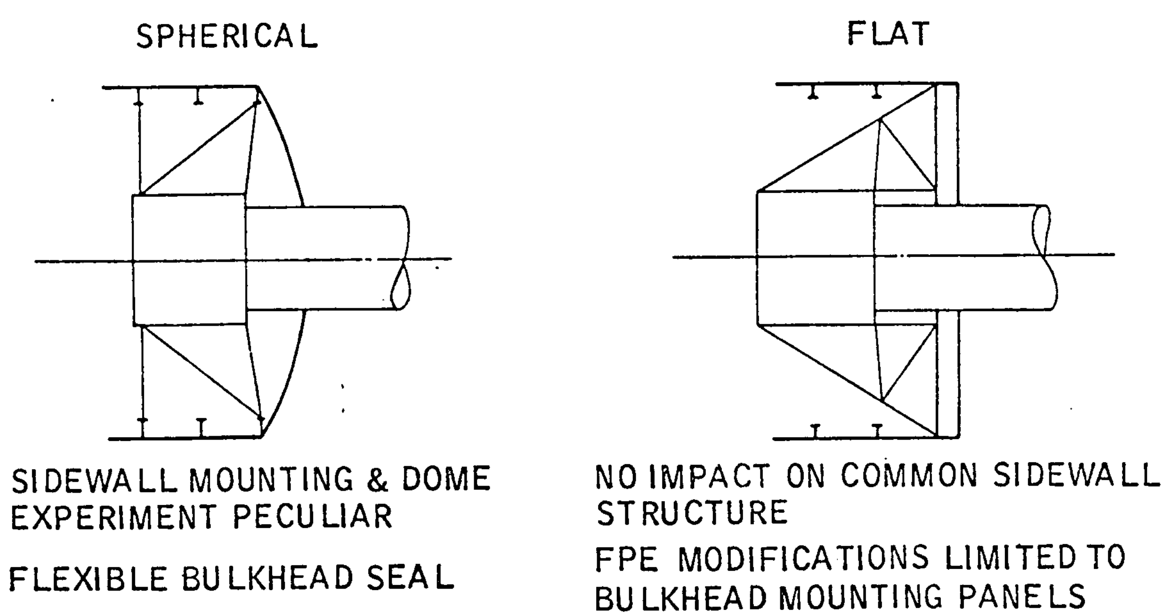

Figure 3-12. Bulkheads for Astronomy Applications

Laboratory Modules. The two types of bulkheads shown in Figure 3-13 are for application to laboratory type modules, the spherical with an auxiliary floor and the integral flat bulkhead, which also serves as the laboratory floor.

While the spherical bulkhead adds slightly to the overall module length, the use of the auxiliary floor in this configuration allows modification of floor-mounted equipment without causing modification to the primary structure as in the case of the integral floor. Floor panels are also removable for access to equipment mounted under the floor.

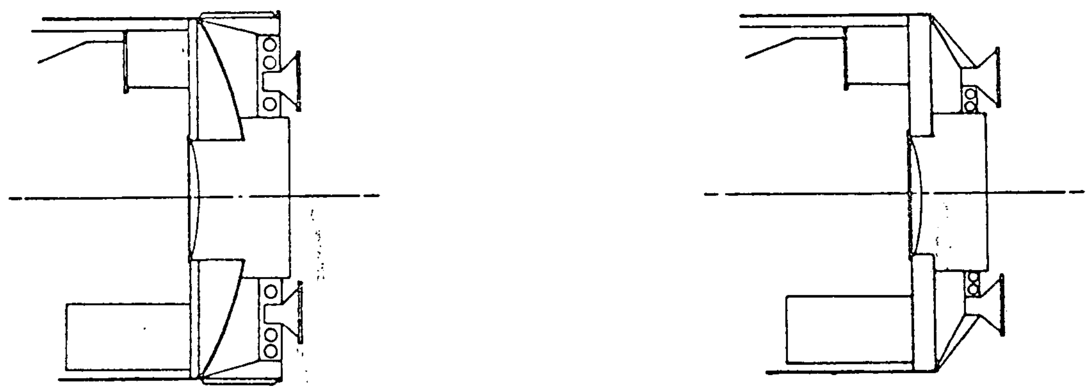

Figure 3-13. Bulkheads for Laboratory Applications

3.4.2 FLAT BULKHEAD CONFIGURATIONS. Three flat bulkhead configurations were studied: a radial ring concept (Figure 3-14), a continuous beam or egg-crate design (Figure 3-15), and a sandwich panel design.

The geometry of the radial beam concept does not lend itself to use as an experiment mounting bulkhead, but it could be used as a docking hatch bulkhead. The continuous beam bulkhead is the most desirable geometry for use as an instrument mounting structure. A wide variety of experiment equipment may be recommended through the use of three experiment-peculiar panels on the bulkhead (cross hatched area).

Two auxiliary bulkhead support systems were also studied for application to the two flat bulkhead concepts shown. In one concept a system of four tension rods is used to limit bulkhead deflections. The system requires the use of two flat bulkheads to provide end fixity for both ends of the rods. The rod system does not lend itself well to use in the free-flying astronomy modules since it restricts astronaut access to the instruments. Use in the lab modules is also marginal due to interference with lab equipment such as the experiment sphere of FPE 5.16 and the laminal flow bench tracks of FPE 5.9/10/23.

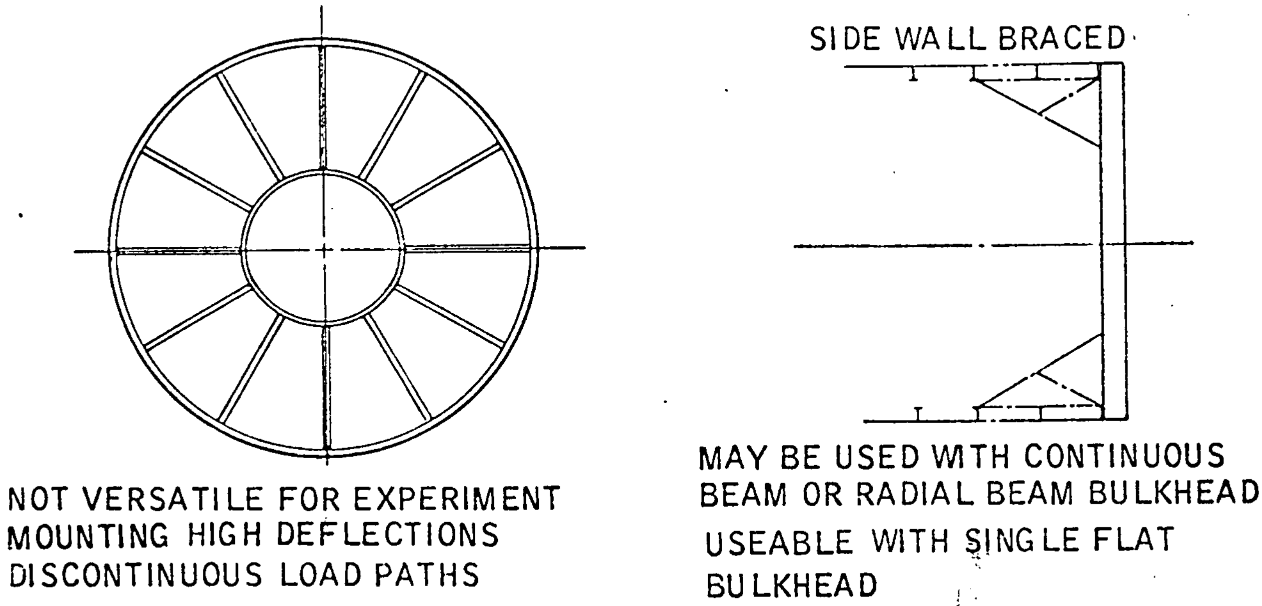

Figure 3-14. Radial Beam Bulkhead

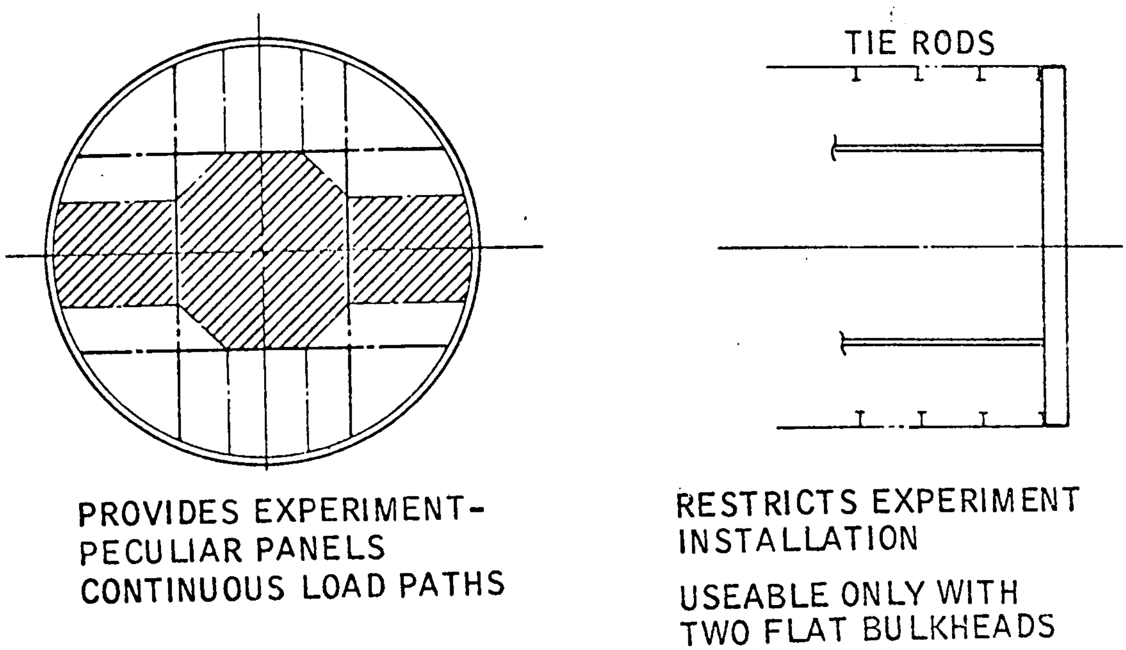

Figure 3-15. Continuous Beam Bulkhead

The corner brace system could be used with either bulkhead or with a single flat bulkhead and does not restrict access to the equipment or interfaces with equipment installation.

The sandwich panel flat bulkhead can be fabricated at a lower total weight than either the radial beam type or the continuous beam type. In the smaller diameter the weight can be competitive with the spherical segment type. For use as an experiment bulkhead it does not provide the flexibility of using experiment-peculiar panels as does the continuous beam design.

3.4.3 SPHERICAL SEGMENT BULKHEAD. One method of reducing the weight of the bulkhead is to carry the load as a membrane. This is accomplished in the spherical bulkhead. In order to reduce the overall length and to eliminate the wasted space at the intersection of the sphere and the cylinder, the spherical segment was investigated.

This type of bulkhead requires a ring at the intersection of the dome and the cylinder to react the radial component of the dome stresses.

Inasmuch as the minimum gage for meteoroid protection is in the range of 0.055 to 0.060 inch, the spherical bulkhead was sized by determining the spherical radius that would result in satisfactory membrane stresses for a constant thickness of 0.055 inch.

A radius of 168 inches was selected which produces a relatively flat bulkhead, thus saving on space.

The internal ring was sized to minimize discontinuity stresses between the dome and cylindrical section, and the bulkhead weight given includes this ring.

As a result of the relatively low weight predicted for the spherical segment bulkhead, it was selected as the baseline for the docking end bulkhead.

3.4.4 CONICAL BULKHEAD. In view of the fact that the spherical segment bulkhead is relatively flat and its tangent approaches a conical shape, it was decided to investigate the use of a truncated cone bulkhead with the same relative height as the spherical bulkhead.

The conical bulkhead is easier to manufacture than the spherical segment as it requires no forming of double curved surfaces. To achieve optimum weight, however, it is necessary to taper the skins.

The weight of the conical bulkhead is somewhat higher than the spherical. In the geometries being studied here, weight difference is not large and economic considerations might make the conical bulkhead the best choice.

The weights for the various types of bulkheads studied are summarized in Figure 3-16, which gives the bulkhead weight plotted for various module diameters.

3.5 SOLAR CELL ARRAY

The cantilevered solar panel array shown in Figure 3-17 was examined for minimum frequency of vibration. The structure was idealized and modeled in a finite element general purpose multi-dimensional vibration analysis program.

The centerline of the mast is also a line of symmetry; consequently, by imposing appropriate boundary conditions, only one-half of the total array need be modeled.

The solar cells and substrate were represented by an equivalent homogeneous isotropic plate with the following properties:

Shear Modulus	9×10^3 psi
Young's Modulus	1×10^7 psi
Plate Thickness	0.181 in.
Poisson's Ratio	0.3
Density	0.02 lb/in^3

Triangular plate bending finite elements were used to represent this equivalent plate.

Node points were located at the stiffener intersections. The stiffeners themselves were permitted to bend out of plane and twist only. The thickness of the mast was included in the array geometry, but no attempt was made to account for the stiffener-plate c.g. offset. This latter simplification results in a conservative estimate of bending stiffness of the system as the contribution of direct stresses in the plate to bending resistance is ignored. The stiffener depth was assumed to be 2.5 inches. The root cross section of the mast was used over its entire length. The mass of the plate was uniformly distributed over its area; the masses of the stiffeners were uniformly distributed along their lengths.

The analysis indicates a lowest symmetric mode at 1.5 Hz and a lowest anti-symmetric mode at 2.3 Hz. Further analysis of astronomy stability requirements will establish panel stiffness requirements.

3.6 SPACE RADIATORS

Most of the experiments require the dissipation of sizable quantities of heat. Several configurations of radiators were considered to dissipate this heat.

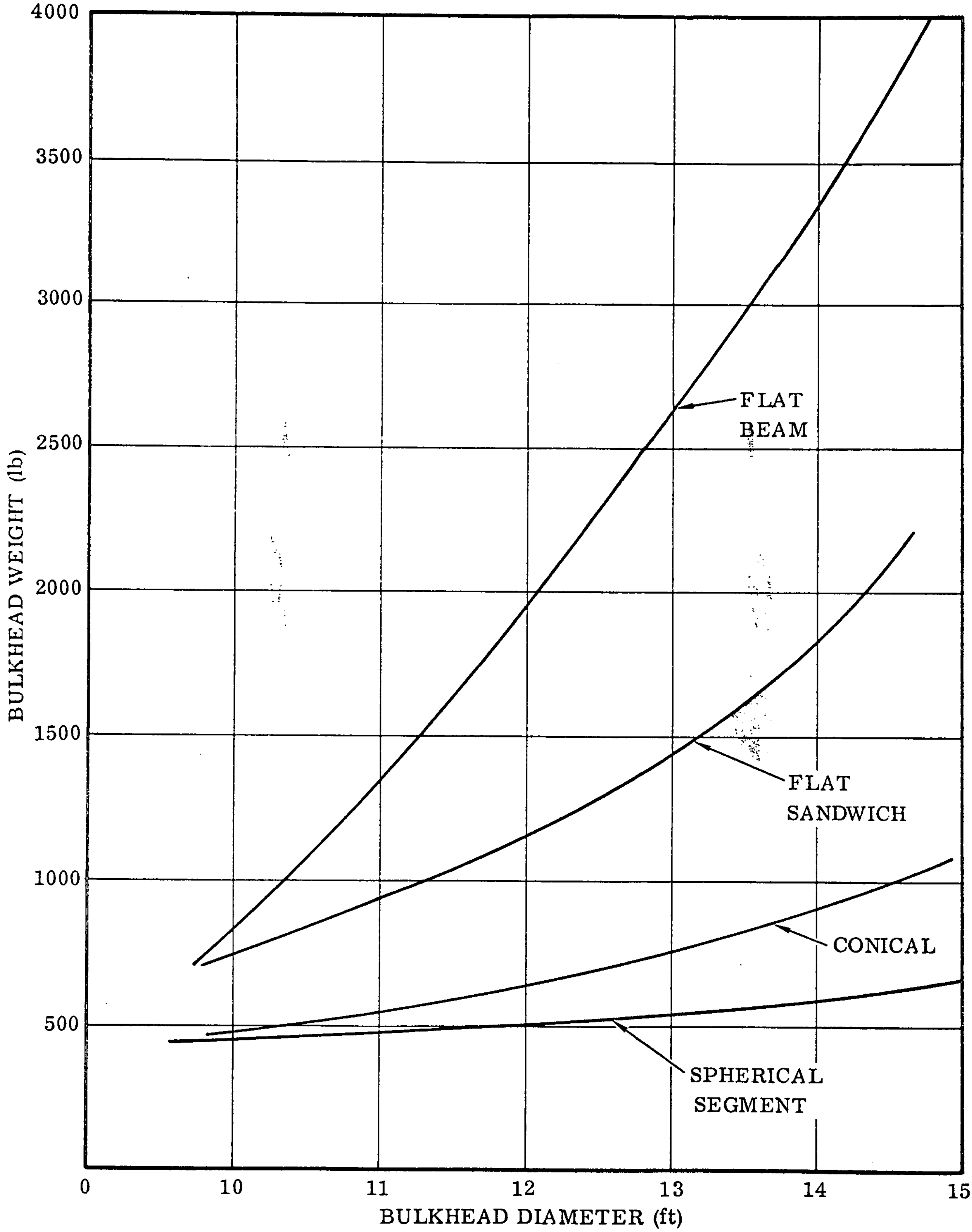

Figure 3-16. Experiment Module Bulkhead Weights

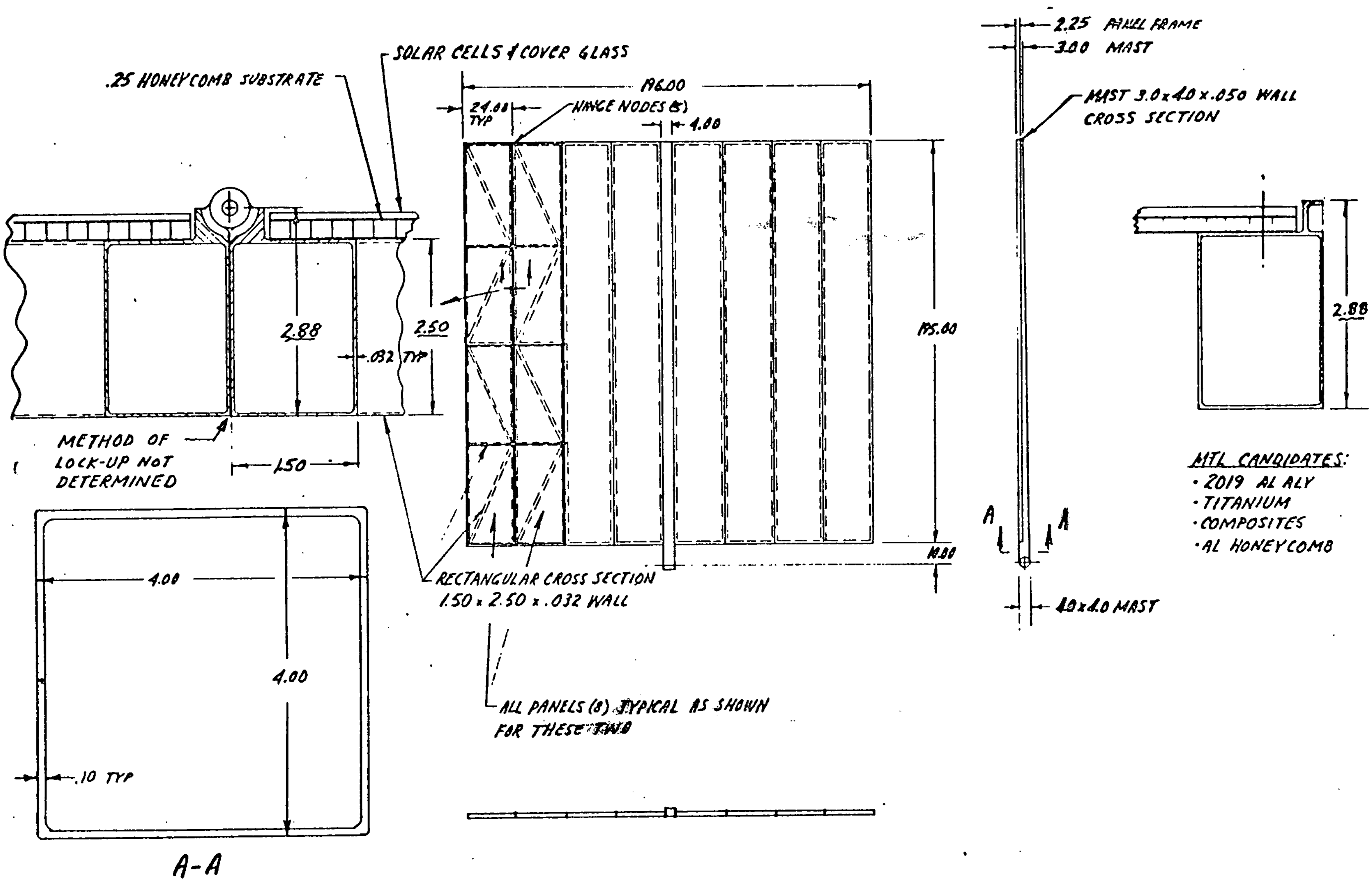

Figure 3-17. Solar Cell Array Configuration

The cylindrical surface area of the modules is large enough to radiate the heat loads presently envisioned. An appreciable increase in the heat load would probably require the use of deployable radiator panels.

For the integral radiator configuration, radiators are substituted for the meteoroid skin panels as shown in Figure 3-3. The radiator skin also serves as a meteoroid skin.

Several methods of constructing meteoroid panels were considered. The type selected for study was the external tube type. Figure 3-18 illustrates the radiator panel. The radiator consists of aluminum tubes diffusion bonded to the thin aluminum sheet. The stiffening effect of the tubes is sufficient to stabilize the skin without the need for beading or other stiffeners.

Calculations were made to determine the tubing wall thickness necessary to provide the desired probability of no meteoroid penetration. These calculations are summarized in Figures 3-19 through 3-21. These figures include curves on probabilities (P_0) of 0.60 and 0.75 in addition to the desired 0.90 in ten years. These were included to simplify trade studies on radiator systems.

The baseline configuration has the radiator tubes exposed and requires relatively heavy walled tubing (0.18) when a P_0 of 0.90 is used. Several compromises are available and should be considered in future studies. These are (1) use a lower probability, P_0, and provide redundant tubing circuits, (2) assume a period of operation shorter than ten years and provide redundant paths or provide replacement panels, (3) move the tubing to the inside of the panels, which is less efficient but will reduce the wall thickness somewhat, and (4) consider another radiator system that might be less susceptible to meteoroid puncture.

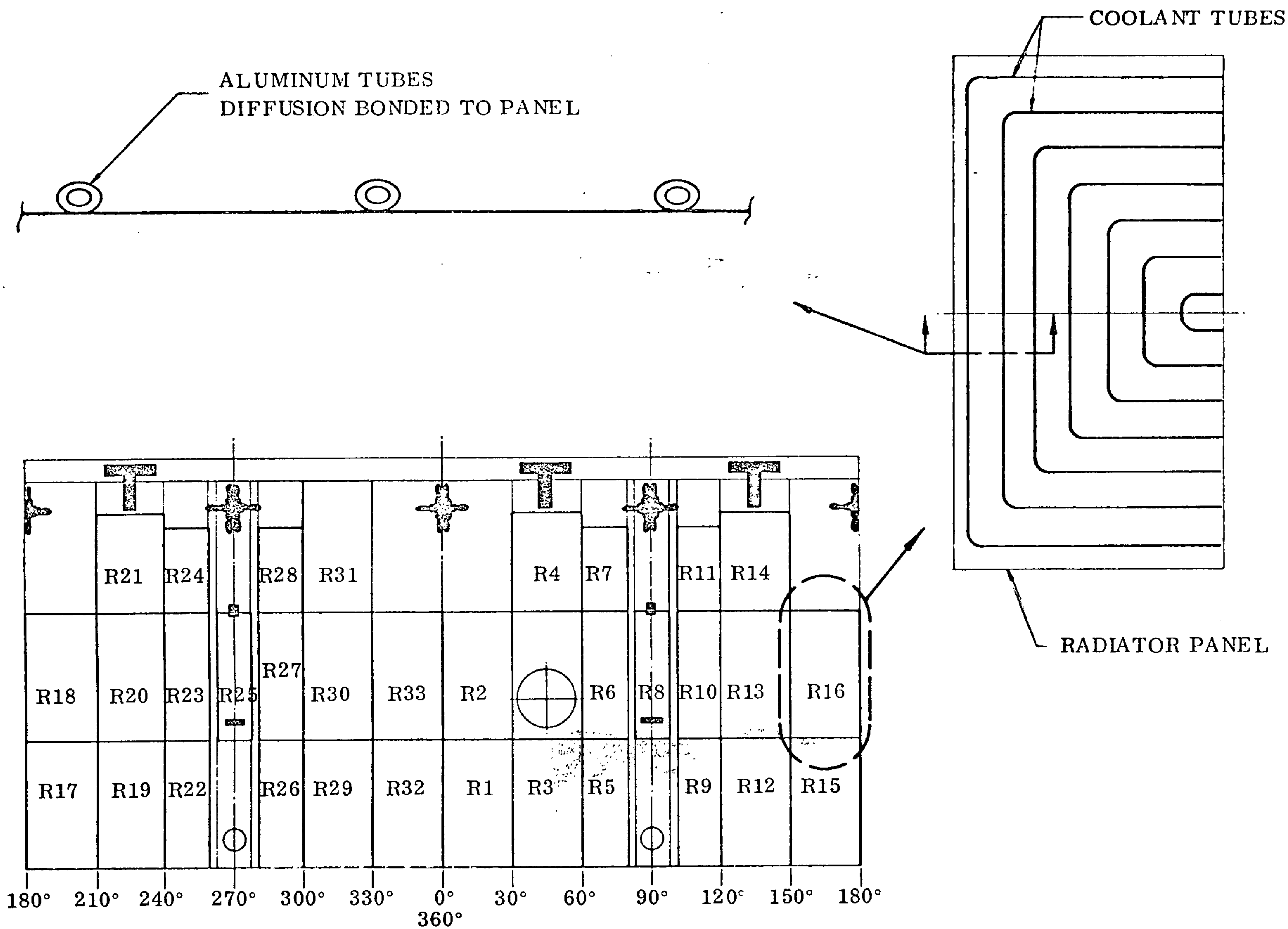

Figure 3-18. CM-1 Radiator Panels Flat Development

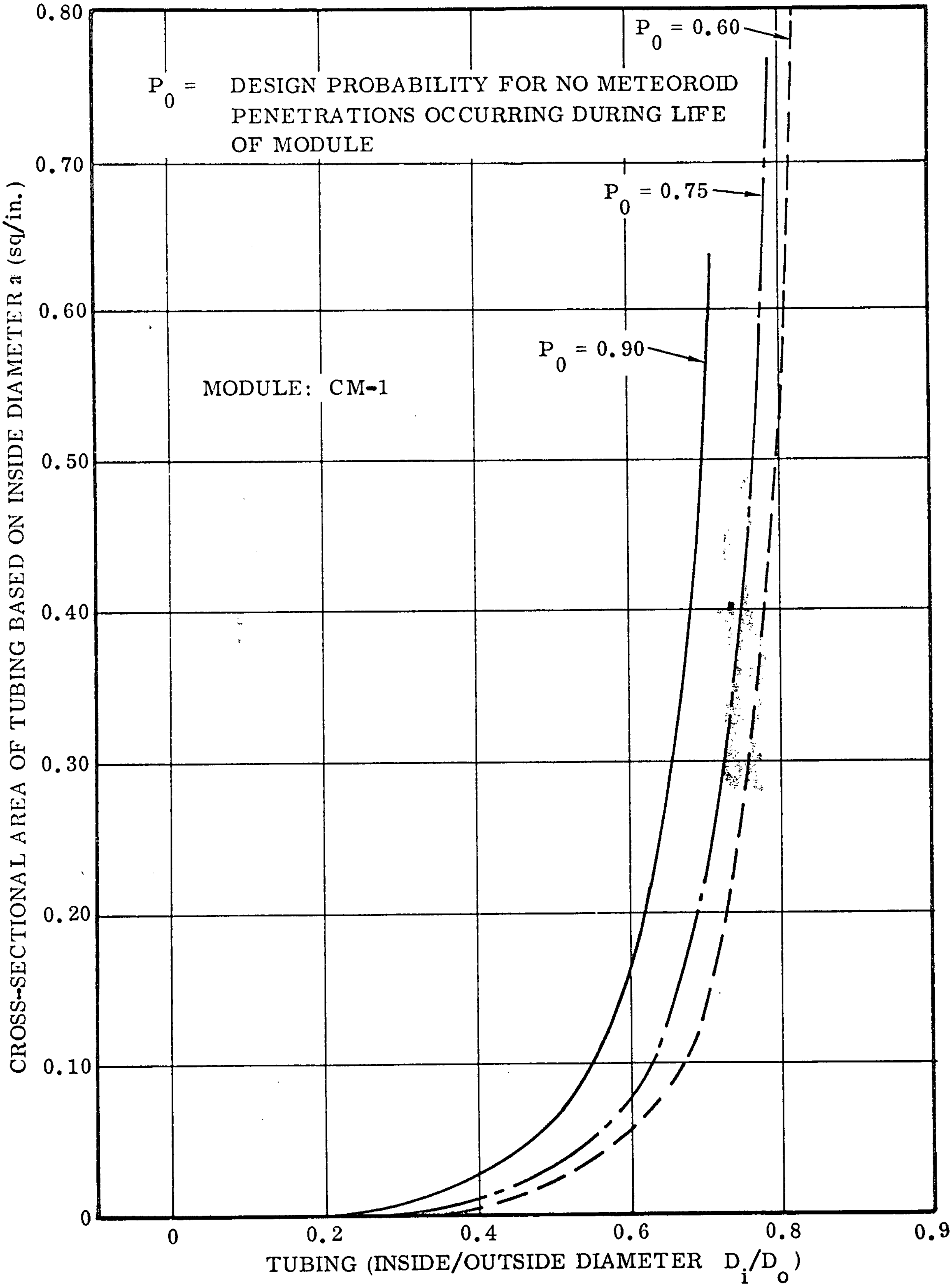

Figure 3-19. Tubing Area vs. Tubing Diameter Ratio, CM-1

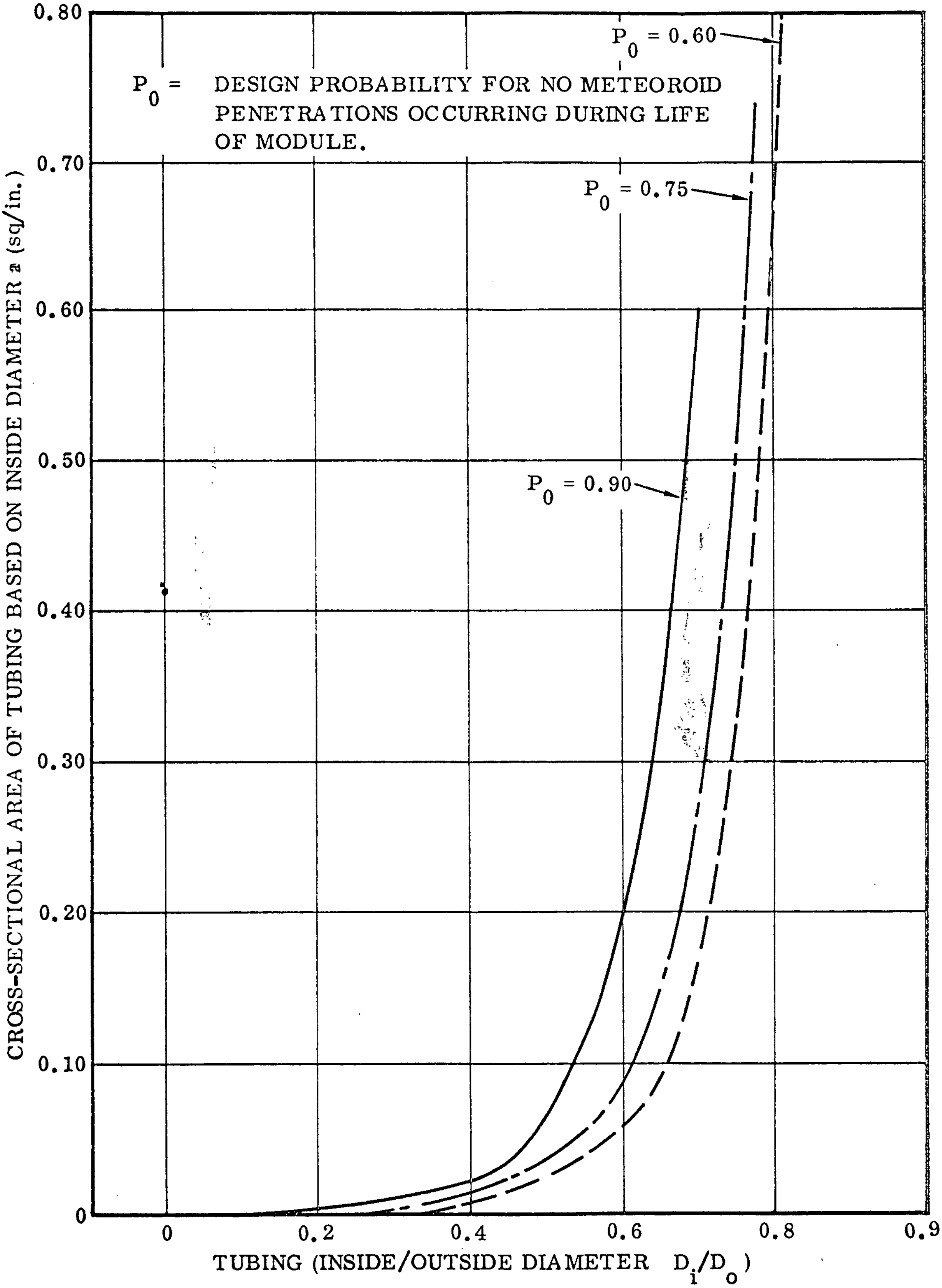

Figure 3-20. Tubing Area vs. Tubing Diameter Ratio, CM-3

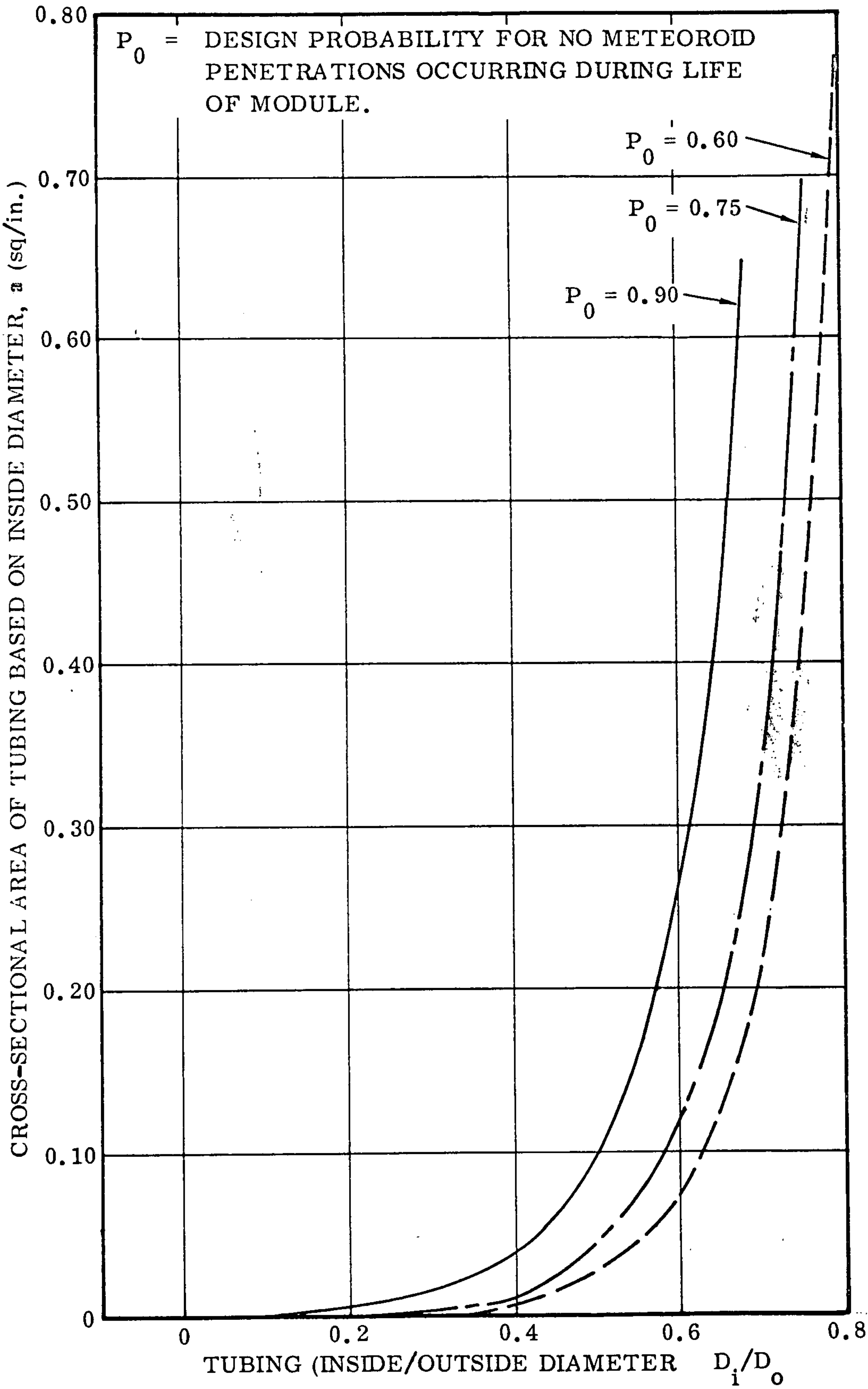

Figure 3-21. Tubing Area vs. Tubing Diameter Ratio, CM-4

SECTION 4

STABILIZATION AND CONTROL SUBSYSTEM

The experiment module considered is an unmanned separate spacecraft operating in a space station attached or detached mode. We are concerned with determining the requirements and providing design technique for experiments operating in conjunction with the zero g space station in the 1975 time period in regard to the stabilization and control system (SCS). Figure 4-1 is a representative* space station configuration. The noted mass properties are used herein.

It is expected that the experiment module will draw support from the space station by interface with space station onboard systems. For reference, Figure 4-2 is representative of the space station guidance, navigation, and control subsystem. The interface to the experiment module SCS is shown as maneuver, attitude, rendezvous and dock commands transmitted to the detached experiment module from the space station. Rendezvous and dock commands are also transmitted to the normally attached experiment module for initial delivery only.

In regard to space station orientation, there are several possibilities encompassing earth, solar, or celestially fixed orientations. A promising selection is earth fixed with the long axis along the orbit normal.

The nominal space station altitude/inclination are 270 n.mi./55 degrees.

4.1 EXPERIMENT REQUIREMENTS ANALYSIS

The most stringent requirements placed upon the experiment module SCS are those of fine point stability and maintenance of a low acceleration environment.

The low acceleration requirement is directly specified in units of earth surface gravity, g. The attitude control specification is usually more complex. The terminology pointing error, pointing stability, jitter, and resolution are used. Figure 4-3 aids in definition of this terminology. As shown, the attitude error time history is drawn with reference to an absolutely perfect point condition. The time "average" of the deviation from the perfect point condition is denoted. As used herein, and implied by most others in the field, the term stability refers to the attitude deviation from the "average" whereas pointing accuracy refers to the maximum deviation from the perfect point condition. The method of specifying stability is apparently variable. In some cases the stability specification gives a maximum deviation from the "average" usually for a specified length of

* Figure 4-1 shows the use of panels for electrical power. Other configurations replace the panels with a nuclear power source.

time, presumably the experiment time duration. In other cases the maximum rate only is specified or the maximum rate is specified in addition to the maximum deviation. This maximum rate is usually termed jitter. A further stability specification is resolution. When resolution is specified, the maximum change in point direction during the experiment exposure time is limited to less than the resolution figure.

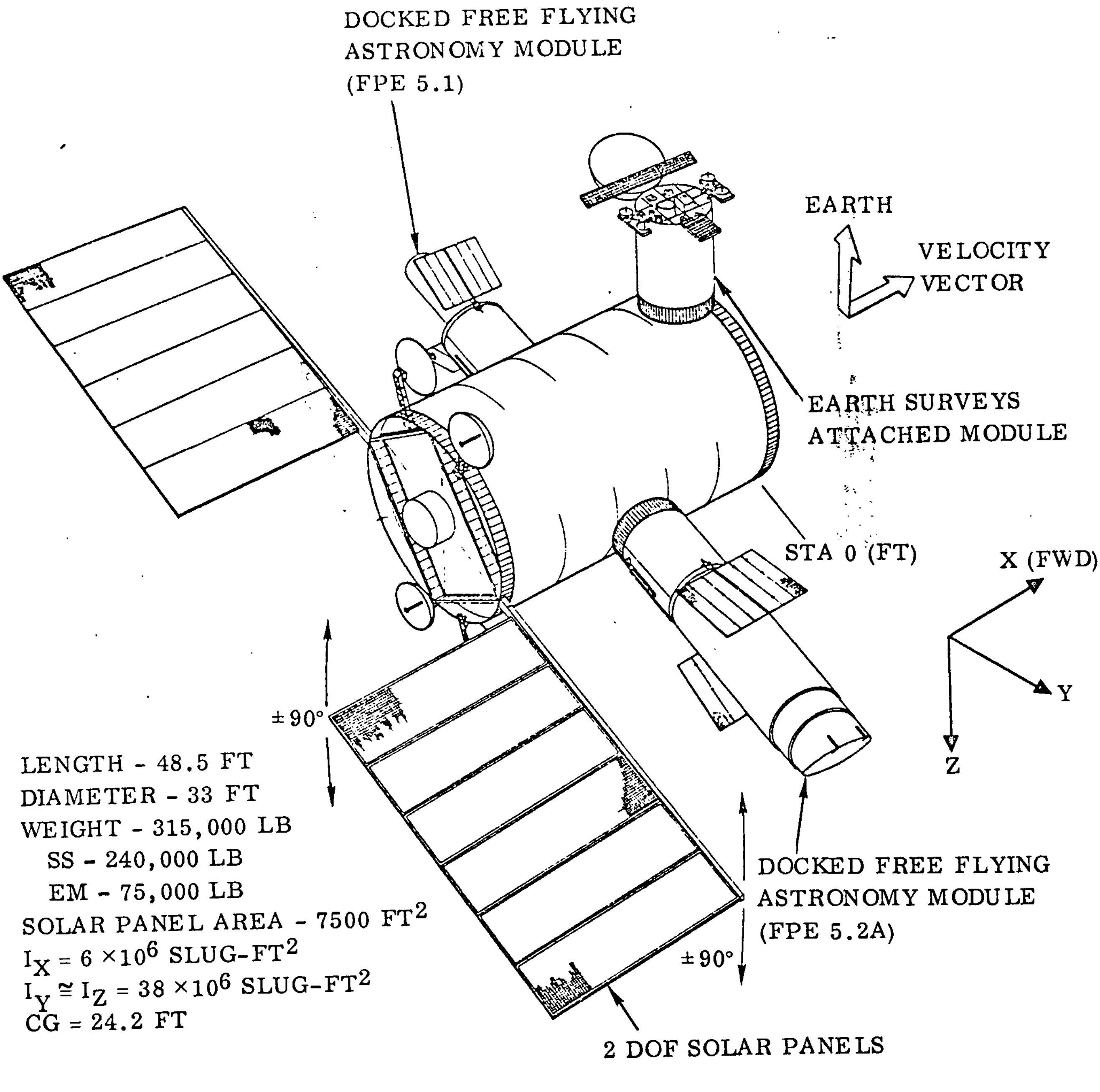

Figure 4-1. Possible Space Station Configuration (Zero G)

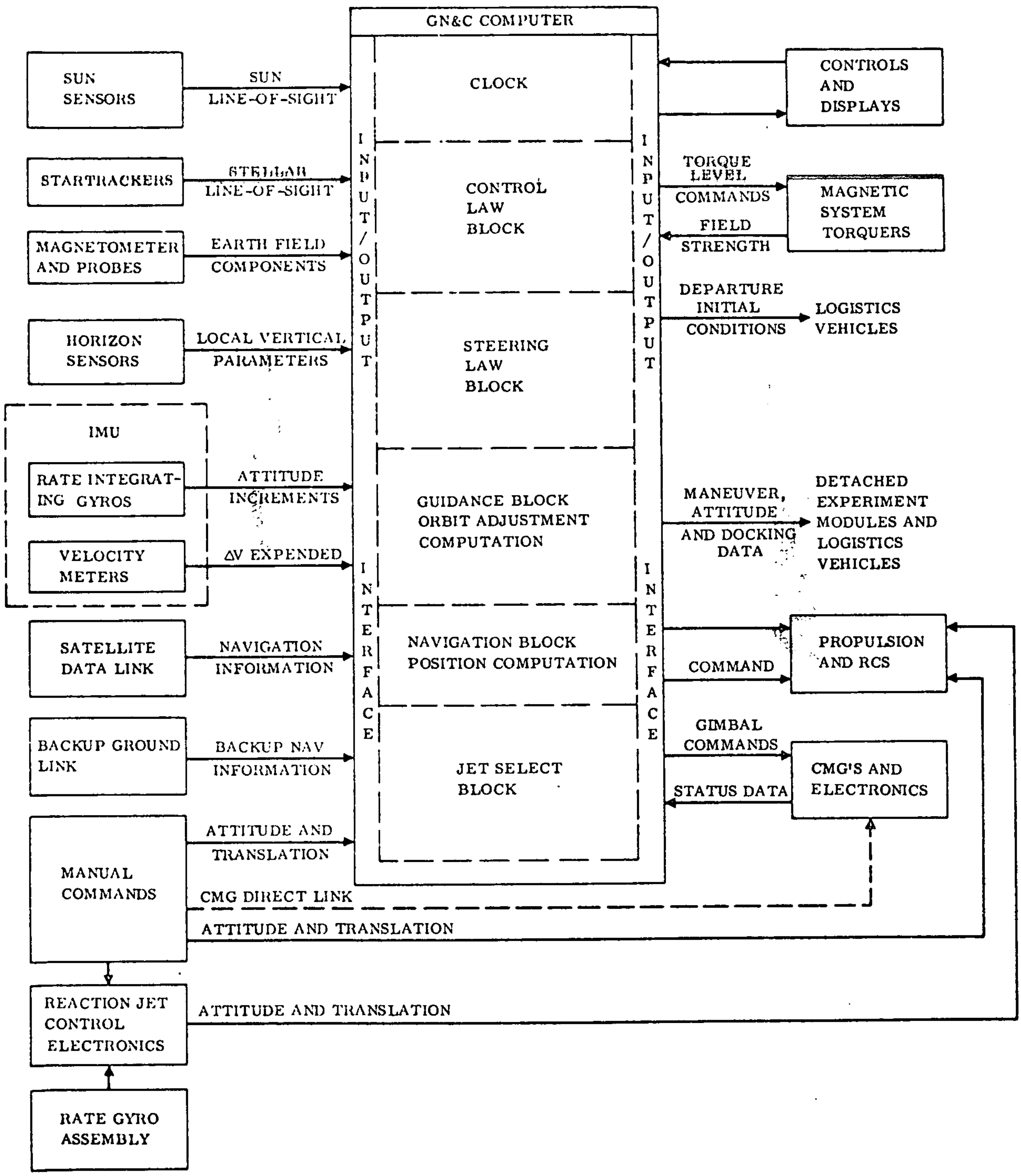

Figure 4-2. Space Station Guidance, Navigation and Control Subsystem Block Diagram

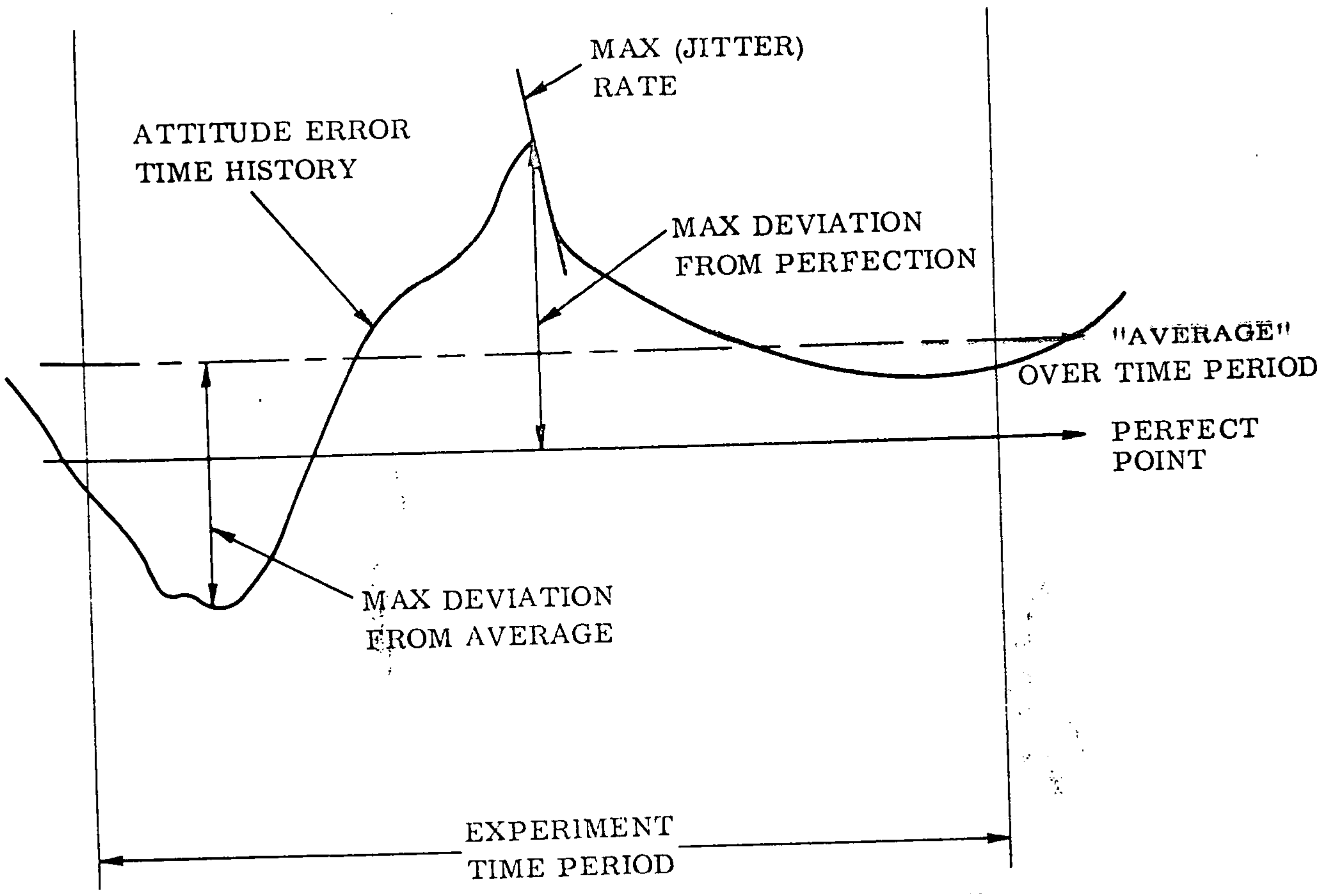

Figure 4-3. Attitude Control Pointing Definitions

Usually it is much less to a limit of 0.1 times the resolution figure. The basic limitation on resolution of "perfect" or diffraction-limited optics is the Rayleigh limit. The smallest light spot or "blur circle" that can be produced from an ideal point source of light (a distant star) has the diameter

$$\alpha = \frac{1.22\lambda}{D}$$

where

λ is the wavelength

D is the primary collector diameter

α is the angular diameter of the point source image (the blur circle or Airy disk diameter).

If the angular distance between the centers of two point sources is equal to the blur circle diameter, it is assumed that it will be discerned that two bodies exist. For example, if a one meter telescope is imaging in the visual band ($\lambda = 0.55$ microns) then the blur circle diameter is 0.67×10^{-6} rad or 0.137 arc-sec. If 0.237 arc-sec resolution is specified, a pointing stability of 0.1 arc-sec during the experiment exposure time is required. More likely the stability requirement will be one-tenth the blur circle radius to conserve the resolving power of a given telescope, 0.0137 arc-sec in this case.

The control requirements for the various experiment modules applicable to the space station are given in Table 4-1. These requirements were derived from the "Blue Book," Reference 4-1. The first four experiments are concerned with stellar or solar astronomy over a wavelength range extending from visible to gamma and X-ray frequencies. These usually involve fine pointing a telescope to fractional arc-sec. The most stringent requirement is the stability requirement of 0.005 arc-sec for the three-meter diffraction limited telescope of experiment 5.2.

For comparison purposes it is noted that earth-based capability is between 1.0 (best seeing) to 2.0 arc-sec (normal) resolution (page 123 of Reference 4-2) at visible (0.55 microns) and above wavelengths. The big ground telescopes (Palomar 200 inch, Lick 120 inch, etc.) usually imply pointing capability at a few arc-secs.

Also for reference, it has been estimated that the space station will yield a pointing of 0.25degree and a stability of 0.001 deg/sec (Reference 4-15). These values are well above the astronomy experiment requirement precluding use of a hard mount of the astronomy experiment module to the space station.

A low g requirement is noted in the Space Biology (5.9/10/23), Materials Science and Processes (5.16), zero g Fluid Physics (5.20-1), and Physics and Chemistry (5.27) FPEs where the requirements range from 10^{-3} to 10^{-5} g maximum.

The remainder of the requirements listed in Table 4-1 are either less stringent or listed as not required (NR). Where the requirement exists, it appears that the space station can provide it by a hard mount.

In addition to the fine point and low g requirements given above, the usual SCS requirements also exist. The module operating mode, either attached or free flying, is the major driver. The most complex SCS is required for the free flyer. A worst case (maximum amount of experiment module SCS on-board equipment) is illustrated in Figure 4-4. As shown, only the command function is aboard the space station. The module contains the following SCS elements:

a. Coarse Pointing — Overall module attitude control system involving sensing, momentum actuator, dumping, and controller electronics.

b. Fine Pointing, Low g — Possibly a separate or vernier fine sensing and actuation system. In the case of pointing, the entire experiment module could be pointed using the primary actuation system operating off an experiment boresighted fine sensor.

Table 4-1. Experiment Control Requirements

Expt. No.	Title	Orientation/Range	Point Accuracy	Stability	Installation
5.1	G.I. X-Ray Telescope	Stellar/Spherical	2 arc-min	1 arc-min, 1 arc-sec/sec	CM-1
5.2	Adv. Stellar Astronomy (3-M Telescope)	Stellar/Spherical	10 arc-sec	0.005 arc-sec	CM-1
5.3	Adv. Solar Astronomy				CM-1
	1.5-M UV-Visible Tele.	Solar/0.5 deg	2.5 arc-sec	0.01 arc-sec	
	0.5-M G.I. X-Ray Tele., 0.25-M XUV Tele. and Coronagraphs	Solar/0.5 to 15 deg	2.5 arc-sec	0.1 arc-sec	
5.5	Hi-Energy Stellar	Stellar-Spherical	10 arc-min	3 arc-sec, 1 arc-sec/sec	CM-1
5.7/12	Plasma Physics/RMS	NR/NR	0.5 deg	0.1 deg/sec	CM-3
5.8	Cosmic Ray Lab	Zenith/± 30 deg.	NR	NR	CM-3
5.9/10/23	Space Biology	NR/NR	NR		
	Plants & Sm. Vertebrae			10^{-5} g max. 95% of time, 10^{-4}g max.	CM-4
	Centrifuge			10^{-3}g max. 90% of time, 10^{-2}g max.	Exper. Peculiar
5.11	Earth Surveys	Earth/hemispherical	0.5 deg	0.03 deg/sec	CM-4
5.13	Manned Centrifuge	NR/NR	NR	2×10^{-3} g max, 0.03 deg/sec^2 max.	Exper. Peculiar
5.16	Matls. Science & Proc.	NR/NR	NR	10^{-3} - 10^{-5} g max.	CM-3
5.20-1	Fluid Physics (zero g)	NR/NR	NR	10^{-4} g max.	CM-3
5.20-2	Fluid Physics (low g)	NR/NR	NR	NR	CM-1 + prop. slice
5.22	Component Test & Calib.	Earth/NR	± 2 deg	0.02 deg/sec	CM-4
5.27	Physics & Chemistry	NR	NR	10^{-3} g max.	CM-3

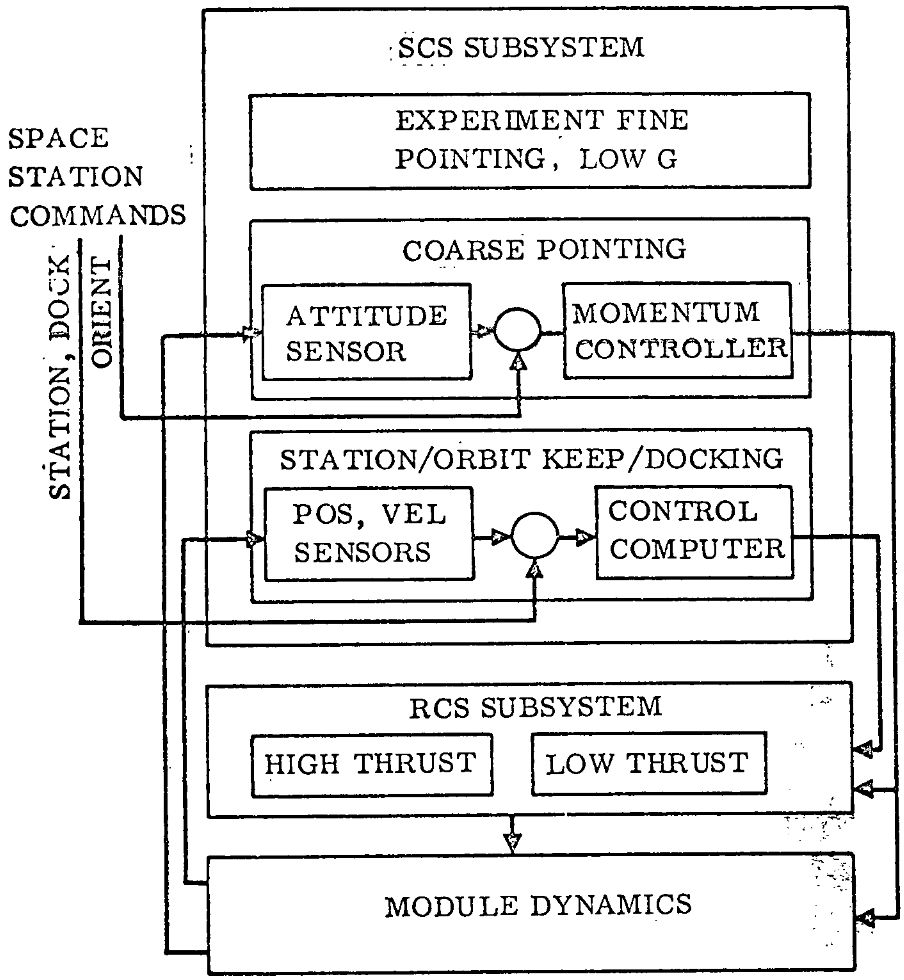

Figure 4-4. Detached Experiment Module SCS Configuration

c. Station, Orbit Keeping, and Docking — Station or orbit keeping and docking require sensing of module position by space station mounted sensors and computer implementation of a control law to deliver appropriate orientation and thrusting commands.

As shown, the SCS interfaces with the reaction control subsystem and communication/data subsystems.

Modules normally operating in an attached mode still are required to free fly for delivery to orbit from the shuttle or an expendable launch vehicle. The most demanding situation is currently delivery from a 100 × 270 n.mi. parking orbit to the 270 n.mi. space station orbit. Rendezvous is required and also docking. This requirement naturally also applies to the free flyer. For the attached module an infrequent change in space station docking port also may be a requirement. Thus, the attached module can contain all the functional requirements of the free flyer (except for the momentum controller and dumping functions) as a result of the delivery requirement. Although this function can be supplied by a separate space maneuvering system or tug, it has been decided from the results of a trade study reported in another volume, to retain the delivery capability aboard the experiment module.

Figure 4-5 shows the most complex on-board control situation during attached operation. This particular situation would apply to an experiment module requirement for an independent orientation and better stability than available from the space station. Removing the independent orientation requirement removes the need for the motorized articulated boom. For less stringent stability requirements, such as appear in many experiments, the fine point (or low g) system would be deleted.

As mentioned previously, the above requirements were derived starting from the Blue Book. Paragraph 1.3 of Volume II of this report covers changes in requirements as a result of anticipated experiment growth or possible changes in study ground rules and assumptions. In regard to control, the only growth requirement identified was an increase in pointing accuracy for FPE 5.1 (X-ray) from the current value of 2 arc-min to 1 arc-sec. This inherently changes the stability requirement to 1 arc-sec maximum deviation because pointing accuracy encompasses stability. It was elected to accept this requirement rather than term it abnormal because this capability must exist in the module design to accommodate other experiments. However, the pointing signal must be provided by experiment equipment.

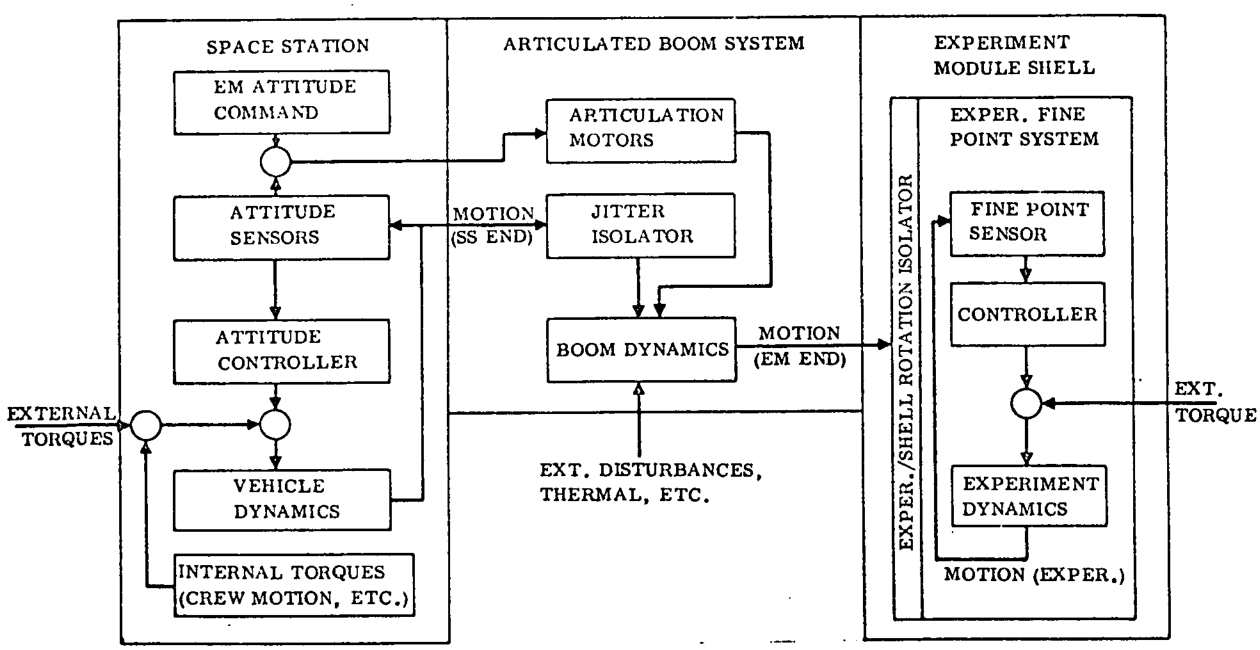

Figure 4-5. Attached Experiment Module SCS Configuration

4.2 SUMMARY OF RESULTS

The primary results of the SCS study are considered to be

a. Definition of the baseline SCS configuration.

b. Scaling data for the selected SCS.

c. Recommended alternates for further study.

These items are covered in the following paragraphs.

4.2.1 BASELINE CONFIGURATION. The baseline or currently selected configuration reflects accommodation of experiment requirements including growth, system maintenance, commonality, and modularity considerations.

4.2.1.1 Free-Flyer. For the free-flying module CM-1, delivery to orbit, rendezvous and dock, stationkeeping, and fine pointing are provided by the SCS configuration shown on Figure 4-6. Star trackers provide a highly accurate reference to an inertial measuring unit (IMU) which serves as the source of continuous attitude and linear motion data. All guidance is from external sources (space station) and is received in the form of attitude and ΔV commands. In a typical application, the module is maneuvered in attitude with control moment gyro (CMG) actuators. Subsequently the control is shifted entirely to three orthogonally oriented reaction (or inertia) wheels (RW) whose actuation is based upon sensor signals derived from the experiment sensor or a separate boresighted fine-point sensor. Reaction wheel momentum dumping is provided by a double-pivoted bar electromagnet reacting against the earth's magnetic field. All ΔV applications for initial delivery, stationkeeping, and dock-undock operation are by command from external source and executed via the module reaction control subsystem.

Recommended redundancy to meet FMECA or module recovery criteria is illustrated on Figure 4-7. The elements within solid lines are those components needed to satisfy performance objectives only. The dashed lines enclose additional components (sometimes fractional to indicate an internal partial redundancy) needed to meet the fail-nominal, fail-safe requirement. An operating redundant item must be immediately and automatically (no external commands) brought into action, whereas standby redundancy implies sufficient time to reach operational readiness.

The horizon scanner and sun sensor units are functionally identical to the star trackers but less accurate (0.5 degree) such that they are not generally sufficient for experiment operation. However, they are sufficient for module recovery and are used as backup in the event of star tracker failure.

The basic inertial measuring unit (IMU) contains the requisite three rate-integrating gyros and accelerometers together with operating electronics. One more rate gyro and accelerometer are provided to cover a single failure in any of the three basic units. Another gyro and accelerometer are used in the event of a second failure.

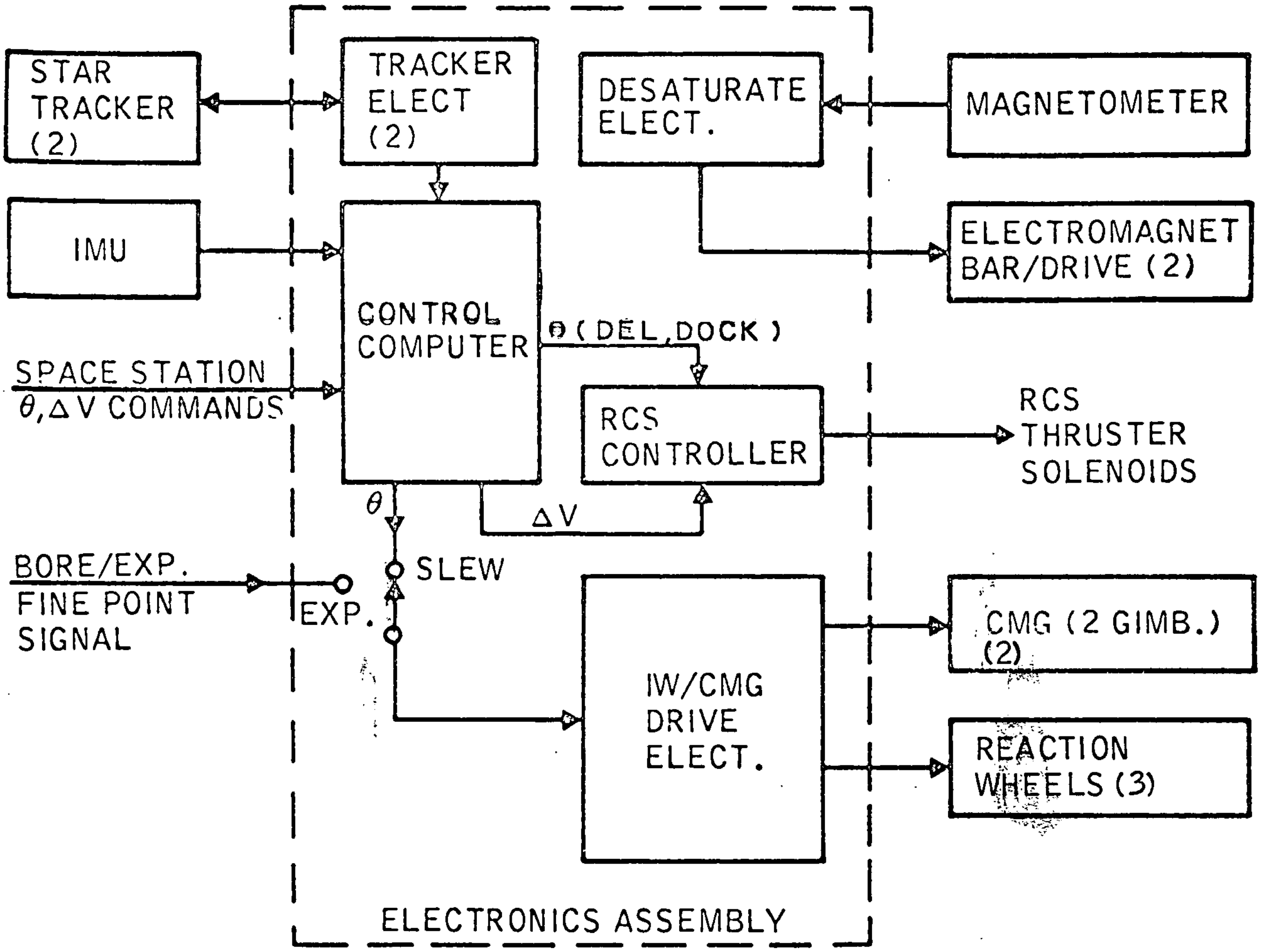

Figure 4-6. Free-Flyer, Stability and Control Subsystem, Current Selection

The control computer is currently digital and provides continuous computation of module attitude and ΔV based upon IMU sensing. A maneuver computer compares commands and current module state to implement an error signal to either the RW/CMG drive electronics or the RCS controller. This element is critical to module recovery as well as experiment operations, so a double failure is accommodated by adding two more units. Active redundancy to accommodate the first failure is shown with the third unit in standby.

The RCS controller provides the electronics necessary to drive the RCS thruster solenoids. Since the RCS is also required to have double-failure capability, so must the controller electronics. The RCS requires the addition of 8 thrusters to the basic 16-thruster system to cover two failures. The remaining components are not critical to module recovery and have no added redundant items pending analysis of experiment operations.

Additional redundancy beyond that resulting from the module recovery requirement is desirable to improve subsystem reliability (reduce failure rate). The rationale used

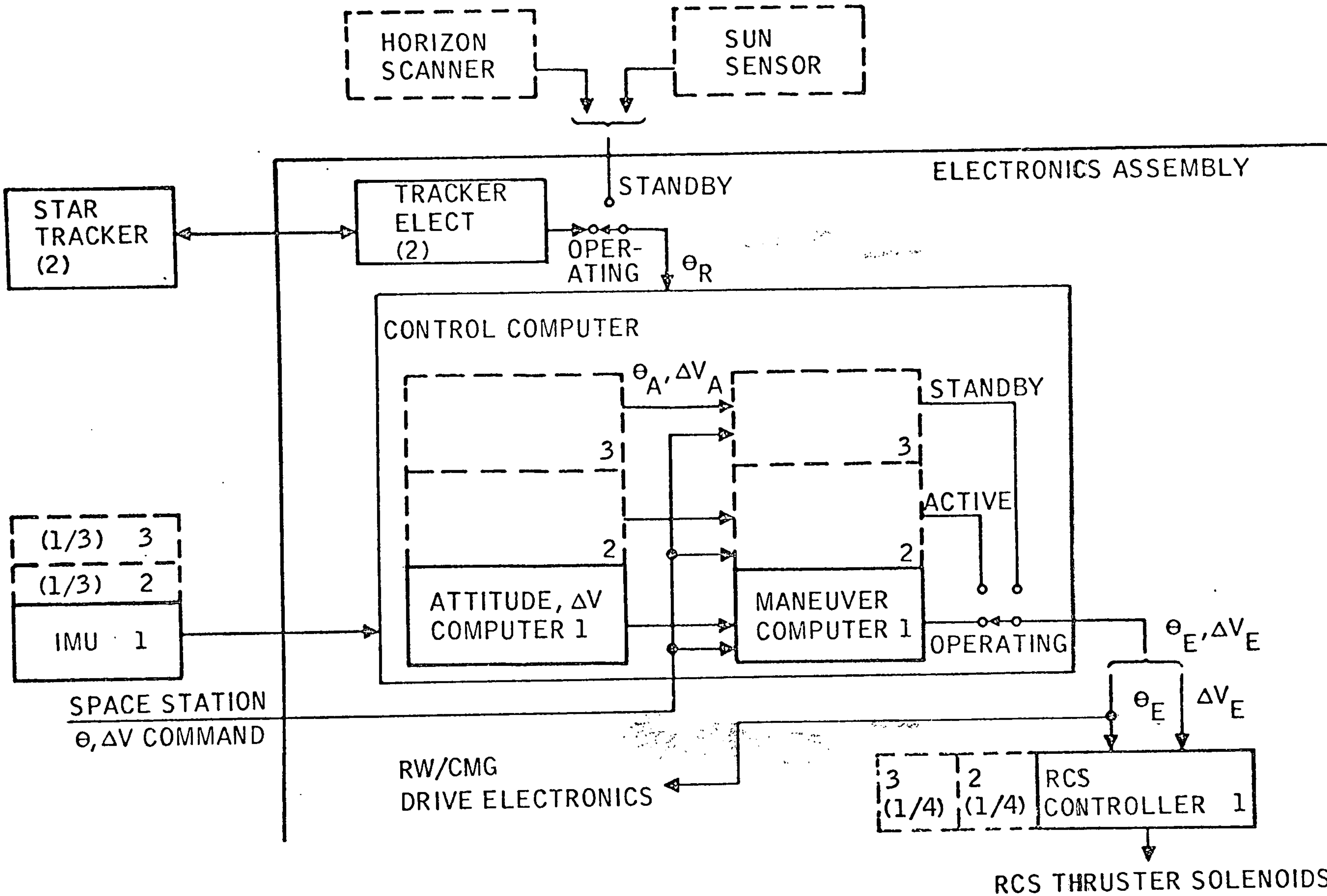

Figure 4-7. Free-Flyer, Stability and Control, FMECA Result

to determine the amount of additional redundancy was to minimize the cost of the installed subsystem plus the cost of returning the module to the space station for repair. A cost minimum at 0.5 failure/year occurs — a desirable point for the SCS subsystem. Table 4-2 gives the final result in the form of a listing of parts needed to accomplish the free-flyer SCS function plus redundancy to meet FMECA and failure rate requirements for each experiment.

The parts listing for the attached modules and propulsion slice are also shown on Table 4-2. They are discussed later.

Referring to Table 4-2, it is noted that the reaction wheels and associated drive amplifiers are left off for experiment 5.1. This is because the module support fine pointing requirement (arc-min) is not as stringent for this experiment as it is for the others (arc-sec) and can therefore probably be supplied by the two double-gimbal-CMGs operating from the module IMU. Reaction wheels can be added later to accommodate growth to 1 arc-sec capability.

Again referring to Table 4-2, note that for the fluid physics FPE 5.20-2 the inertia wheels, CMGs and bar electromagnet are all left off. This experiment requires 10^{-3} to 10^{-6} g thrust levels which are provided by an experiment peculiar propulsion slice element attached to the free-flyer CM-1. The propulsion slice element contains two gimballed thruster assemblies, which supply both thrust level and attitude control. Signals to drive the propulsion slice gimbal motor drive amplifiers are available from the control computer on CM-1.

The maximum requirement for momentum dumping is the three-meter telescope (FPE 5.2). This installation has a pitch/yaw inertia of about 300K slug-ft^2. To dump worst case gravitational impulse a 800-pound bar electromagnet is provided. The required electromagnet bar weight is proportional to module inertia. For design reasons this bar is split into two identically driven parts. Each part consists of five 80 pound bars about 8 feet long, some of which are left off depending on the integrated module inertia. This modular approach saves considerable weight for the other installations. This same approach in theory applies to the inertia wheels and CMGs, but it is not cost effective to provide a number of smaller units in this case so the oversize condition is accepted for the other modules.

The sizing of the two CMGs at 300 ft-lb-sec and the reaction wheels at 900 ft-lb-sec is based on meeting requirements for the 3-meter telescope installation, the largest astronomy experiment installation. The CMGs are sized to provide adequate maneuver capability. Figure 4-8 illustrates their operation. As shown the normal position is with the two momentum vectors opposed, producing zero net momentum. To roll, the two units are scissored through an angle B_2 to produce net momentum change along the module roll axis. To command a vehicle rotation about any desired transverse rotational axis both units are first rotated through an angle α. Then they are again scissored an angle B_1 to command the maneuver rate in an identical manner as for roll.

Table 4-2. Stability and Control Subsystem Experiment Complement

COMPONENT	SIZE (FT^3)	WEIGHT (LBS)	POWER (WATTS)	CM-1						CM-3					CM-4		PROP. SLICE	COMMENTS
				Stellar X-Ray (8)	3-M Stellar (8)	Solar Astronomy (8)	High-Energy (8)	Fluid Physics (3)	Plasma Physics, RMS	Cosmic Ray	Mat'ls. Science(2)	Fluid Physics (2)	Physics & Chem.	Earth Surveys	Component Test	Space Biology (2)	Fluid Physics	
				5.1	5.2	5.3	5.5	5.20-2 (3)	5.7/12	5.8	5.16	5.20-1	5.27	5.11	5.22	5.9/17/23	5.20-2	
Star Tracker	1.8	20	30	2	2	2	2	0	0	0	0	0	0	0	0	0	0	
Sun Sensor	0.1	2.5	5	1	1	1	1	2	2	2	2	2	2	2	2	2	0	
Horizon Scanner	0.15	8.0	10	1	1	1	1	2	2	2	2	2	2	2	2	2	0	
Magnetometer	0.15	7.0	2	1	1	1	1	0	0	0	0	0	0	0	0	0	0	
IMU	0.25	20.0	75	2-1/3	2-1/3	2-1/3	2-1/3	2-1/3	1-2/3	1-2/3	1-2/3	1-2/3	1-2/3	1-2/3	1-2/3	1-2/3	0	
Bar Electromagnet	0.16	80	6	3	10	5	2	0	0	0	0	0	0	0	0	0	0	ℓ = 8.2 ft, L/D = 50
Bar Drive	0.5	10	30	2	2	2	2	0	0	0	0	0	0	0	0	0	0	
CMG	1.76	73	20	2	2	2	2	0	0	0	0	0	0	0	0	0	0	300 ft-lb-sec
Reaction Wheel (RW)	6	160	(6)	0(7)	3	3	3	0	0	0	0	0	0	0	0	0	0	900 ft-lb-sec
Electronics																		
Tracker Drive	0.25	20	(1)	2	2	2	2	0	0	0	0	0	0	0	0	0	0	
Control Computer	0.3	40	75	3	3	3	3	3	3	3	3	3	3	3	3	3	0	
RW Drive Amp.	0.10	10	(6)	0(7)	5	5	5	0	0	0	0	0	0	0	0	0	0	
CMG Drive Amps.	0.10	10	35	2	2	2	2	0	0	0	0	0	0	0	0	0	0	
Desaturate	0.1	10	10	1	1	1	1	0	0	0	0	0	0	0	0	0	0	
RCS Controller	0.2	23	30	2	2	2	2	2	1-1/2	1-1/2	1-1/2	1-1/2	1-1/2	1-1/2	1-1/2	1-1/2	0	
Programmer	0.1	10	15	3	3	3	3	3	0	0	0	0	0	0	0	0	0	
Thruster Gimbal (5)																		
Motor	0.5	10	20														4	
Drive Amp.	0.1	5	5														4	
Total Weight (lbs)				776	1866	1466	1226	266	210	210	210	210	210	210	210	210	60	
Total Size (ft^3)				12.	31.6	30.8	30.3	2.68	2.11	2.11	2.11	2.11	2.11	2.11	2.11	2.11	2.4	
(4) Total Power (watts)				591	927	761	649	325	295	295	295	295	295	295	295	295	100	

(1) Included in star tracker power.
(2) Low g isolators are part of experiment equipment.
(3) CM-1 plus propulsion slice.
(4) Power total does not include those units on standby.
(5) These are located on the propulsion slice.
(6) Proportional to vehicle pitch/yaw inertia. Average power for reaction wheel and drive amp is 1 watt/1000 slug-ft^2.
(7) Added later for growth to 1 sec pointing from current 1 arc-min.
(8) Fine point sensor signal is assumed derived from experiment equipment.

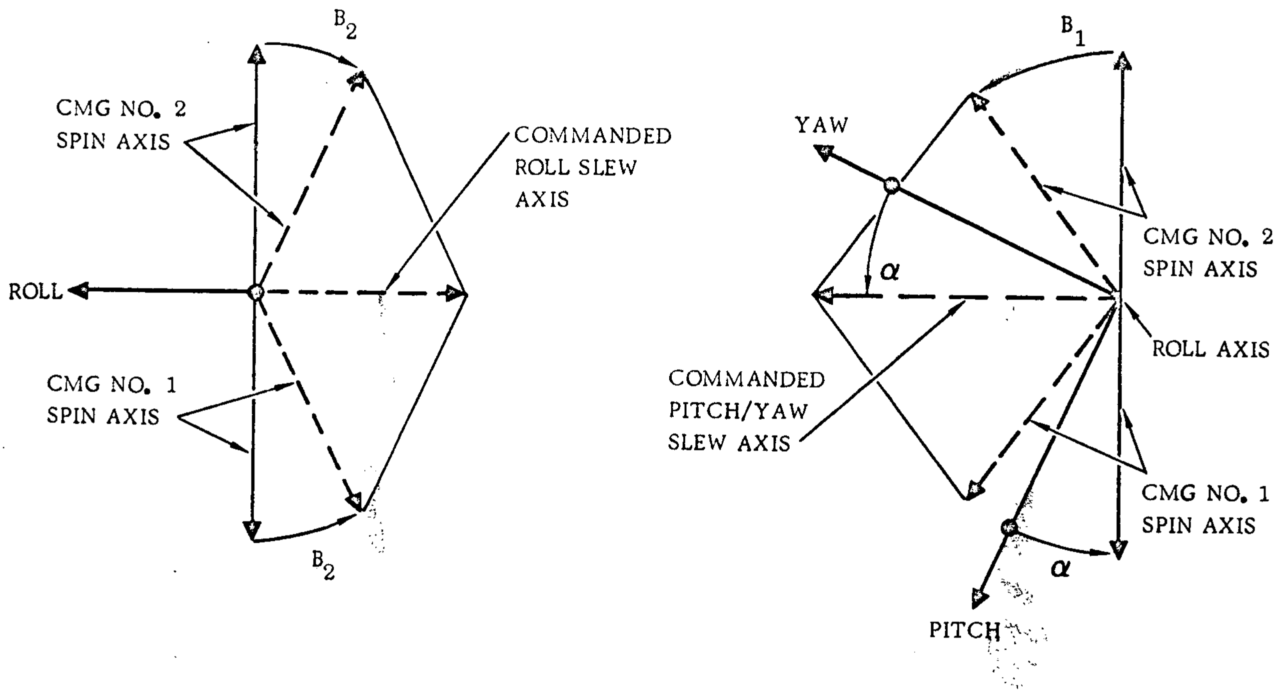

CMG MOMENTUM - 300 FT-LB-SEC
α RANGE ± 90 DEGREES
B_1, B_2 RANGE ± 60 DEGREES
INERTIA (SLUG-FT^2)
PITCH/YAW 300K
ROLL 40K
MANEUVER RATE MAX. (DEG/MIN)
PITCH/YAW 6.0
ROLL 45

3 M TELESCOPE
(FPE 5.2)

Figure 4-8. Free-Flyer CMG Maneuvering System Operation

Ignoring the small amount of environment-generated torque during the slew, completion of the maneuver or stopping the module at its new target direction returns the CMGs to the initial zero net momentum state. At this time the control would typically be shifted to the reaction wheels operating from the fine point sensor for the duration of the experiment. This means that the wheels must react the orbit environment and they are sized to do this under worst case conditions (pointing 45 degrees from the orbit plane).

Note that a fine point sensor is not included in Table 4-2 although such equipment is needed for most of the astronomy experiments. In the current selection or baseline system, the experiment is required to provide this function because it is believed best to utilize the available high quality large aperture experiment optics rather than attempt to duplicate the capability by a boresighted sensor.

4.2.1.2 Attached Module. The attached module SCS is required for orbit delivery and subsequent infrequent change in docking port. The system illustrated in Figure 4-9 provides this capability.

In essence, it is a stripped down version of the free-flyer SCS. The quantity indicated on Figure 4-9 is that needed to meet FMECA requirements during the delivery free-flying period. No further redundancy is required to improve failure rate so the same number is indicated on the previously given Table 4-2 part listing by experiment.

Some experiments require isolation from space-station jitter. Figure 4-10 illustrates an approach to providing this environment as a function of requirement stringency. As shown, passive systems are expected to produce isolation from space-station jitter (10^{-3} g) to the extent of 10^{-5} g. Adding precise acceleration sensing and an actuator is expected to completely eliminate jitter. However, air drag and gravity gradient

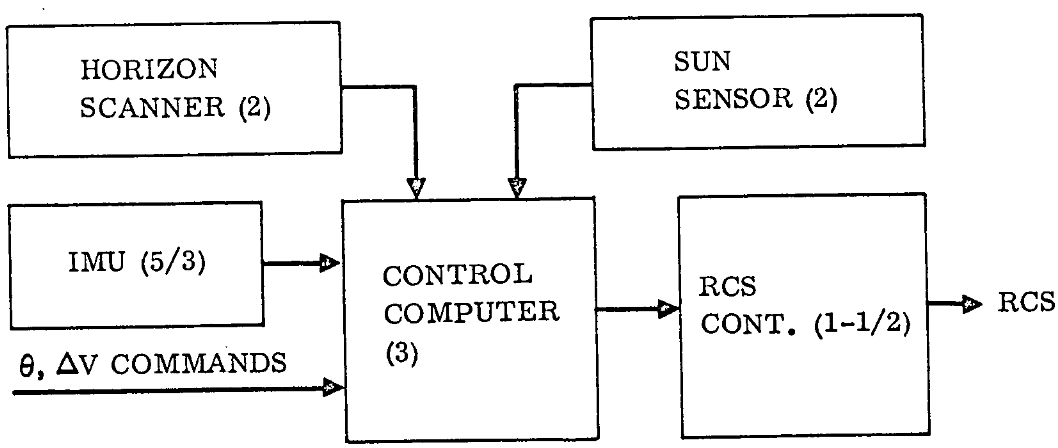

Figure 4-9. Attached Module SCS

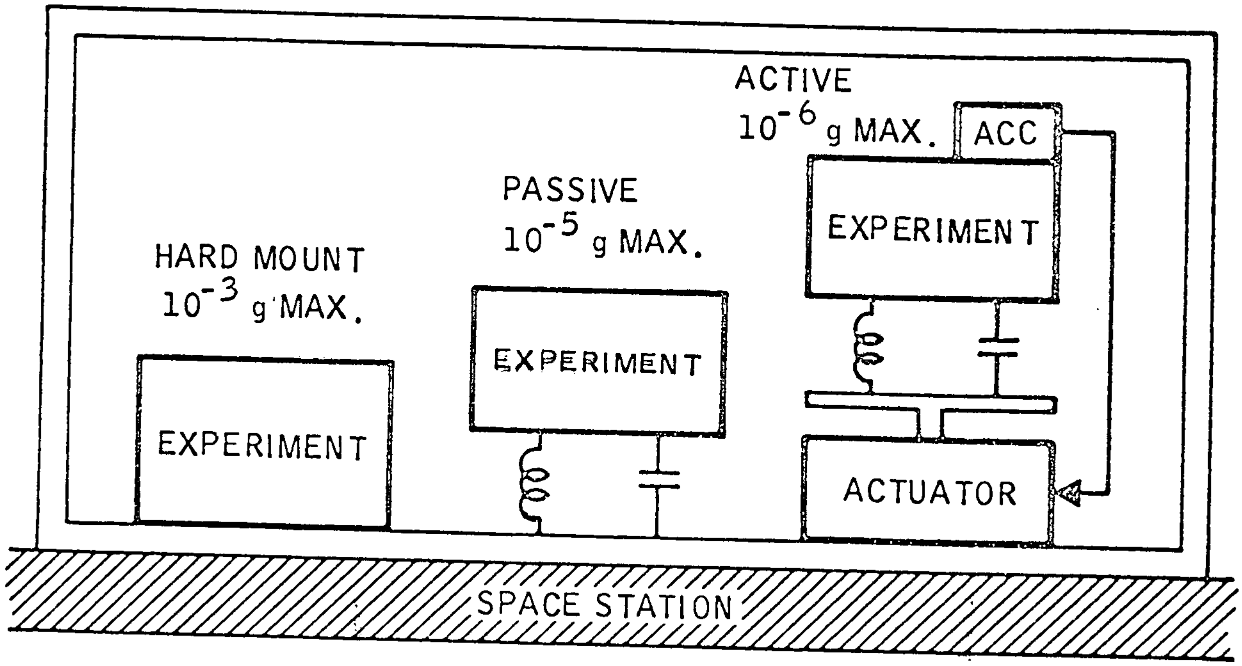

Figure 4-10. Experiment Jitter Isolation Concepts

acceleration levels at about 10^{-6} g remain. Elimination of these g-levels is not feasible because of the large inherent clearance required. For 10^{-6} g and lower, a free-flyer is apparently required. Current plans are for the experiment to supply the appropriate isolation.

4.2.2 SCS SCALING DATA. Weight and electrical power for the selected free-flyer SCS is provided to show:

a. Sensitivity to module parameters.

b. Relative contributions of major elements to the total system weight and power interface.

The attached module SCS is not sensitive to the particular experiment installation. The weight and power was given previously in Table 4-2. The free-flyer weight and power are primarily sensitive to the module inertia and the astronomy fine pointing requirement. Figure 4-11 relates weight and power to module pitch/yaw inertia breaking out the contribution of:

a. Sensors, electronics, CMGs

b. Bar electromagnet

c. Reaction wheels

The reaction wheels supply fine pointing so their contribution to the system weight and power is attributable to that requirement. For reference the astronomy experiment installation weight and power points, taken from Table 4-2, are indicated on Figure 4-11.

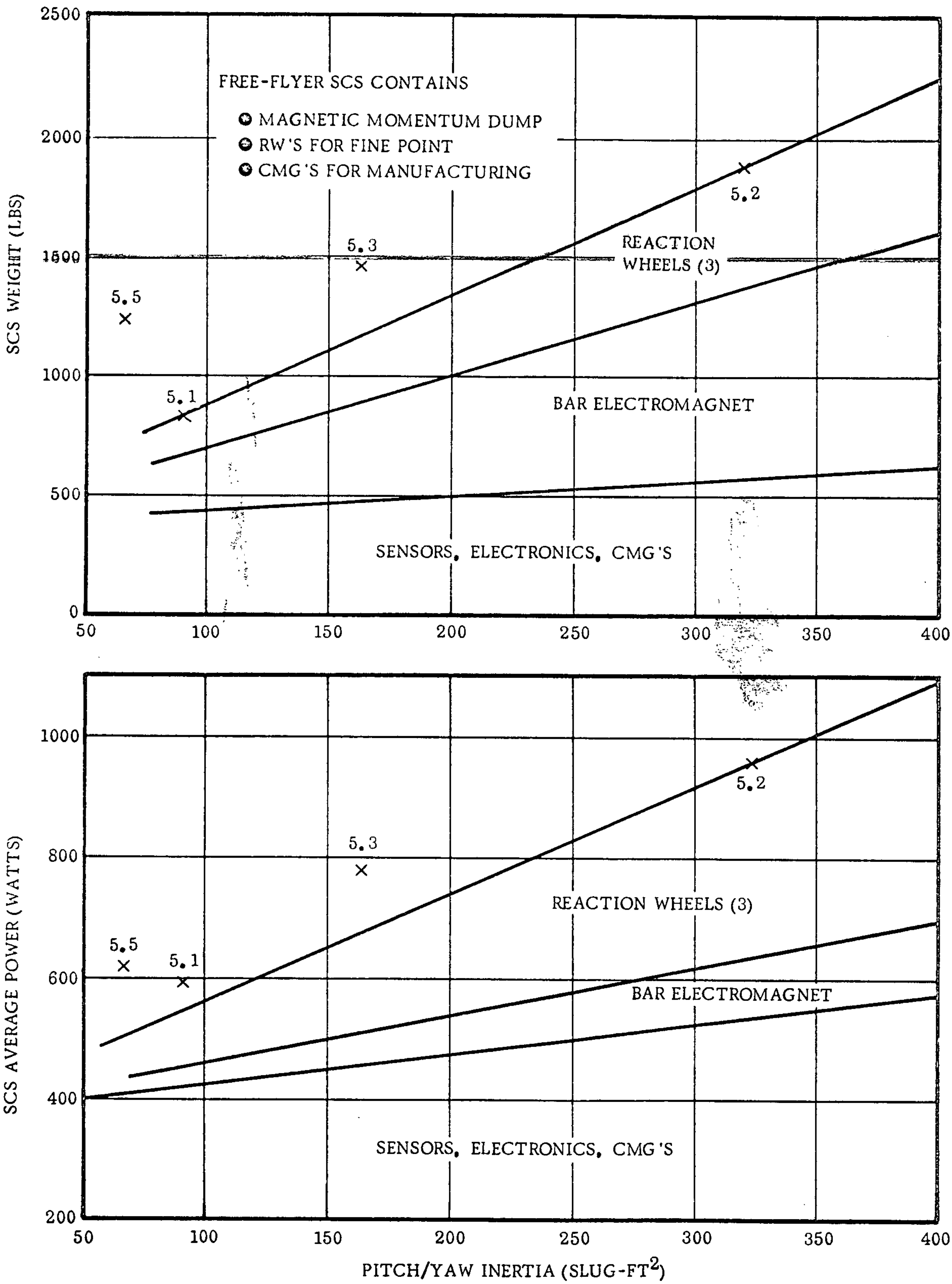

Figure 4-11. SCS Scaling Data

Note that the scaling curve agrees with the current design for the largest module only (5.2). For the smaller modules, 5.3 and 5.5, the weight and power are greater than that given by the scaling curve because only the magnet dumping bar is modular – the CMGs and RWs are not and they are sized for the largest installation of 5.2. The 5.1 installation shows a lesser weight because it does not contain reaction wheels.

4.2.3 RECOMMENDED SCS DESIGN ALTERNATES. In regard to the SCS, the main design issues or alternates recommended for Phase B study are in the following areas:

a. Astronomy fine pointing

b. Momentum dumping.

These areas have been identified as SRT items and appropriate descriptions are contained in Volumes I (Summary) and IV (Detail) of this report. A brief discussion follows.

Figure 4-12 illustrates fine point alternates. The simplest telescope suspension, a hard-mount with no internal vernier, is shown first. This system requires pointing the entire telescope/spacecraft body to satisfy pointing requirements. This places a high demand on the module stability and control system reaction wheels or CMGs but is the simplest mechanical telescope interface. Where reaction wheels are used for fine pointing, CMGs are added to provide module maneuvering. Where CMGs are used for fine pointing, they are also used for maneuvering.

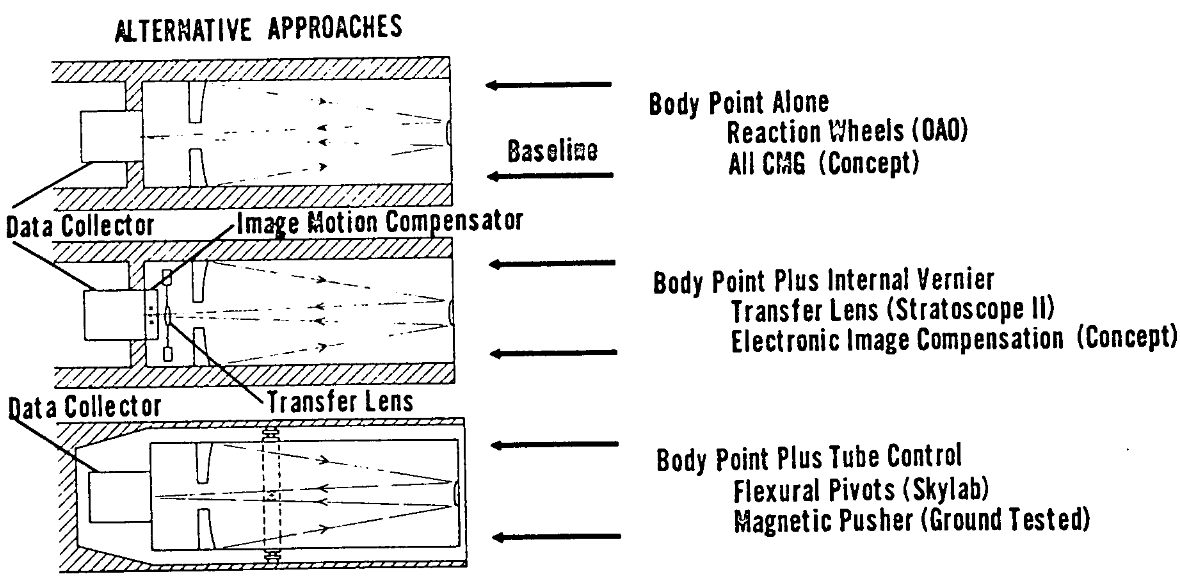

Figure 4-12. Astronomy Fine Pointing Alternates

The second approach relieves the module stability and control subsystem of the total problem by providing an internal vernier pointing system involving either a transfer lens or electronic image compensation. That is, the experiment internal complexity is increased to lessen the stability demand on the module pointing subsystem. In this case the module would use CMGs rather than reaction wheels to obtain the well-known CMG electrical power advantage.

The third approach is regarded as the most complex and probably should be used only when internal vernier techniques are not available. For this approach a module CMG control system is used and the entire telescope body is moved to provide the same compensation afforded by the internal verniers. As indicated, candidate suspension systems are flex pivots and magnetic pushers.

The current selection or baseline is the first approach using the OAO technique of body point alone with reaction wheels as the momentum actuators. The electrical power penalty of reaction wheels relative to CMGs was accepted to gain the fine point capability credited to reaction wheels. However, low output torque (no gimbal drive gearing) single degree of freedom CMGs show promise of comparable fine point capability and could replace the reaction wheel. If four CMGs are used, their capacity would be 900 ft-lb-sec each. Each would weigh about 110 pounds, consume about 30 watts, and have a diameter of about 26 inches. The two CMGs and three reaction wheel plus their drive amplifiers are deleted in this case.

Momentum dumping preliminary studies contained herein evaluate two basic alternate approaches,

a. On-board magnetics
    1. Three large diameter coils
    2. One double pivot bar electromagnet
b. RCS
    1. Hydrazine millipound thrusters
    2. Ammonia resistojet

The current selection is the double pivot bar electromagnet. RCS is, however, somewhat more flexible because there is no dependence on earth magnetic field. Also, some experiments may be sensitive to magnetic fields but not to the RCS exhaust product. For other experiments, the reverse condition may apply. In addition, the magnetic system has high initial weight but avoids RCS resupply. While this expended RCS fuel weight equals the bar weight in about six months of use, shuttle initial launch weight limitations could favor the RCS system.

The gravity gradient approach or reorienting specifically to dump momentum is a possibility but at this time the reorientation is considered to be too much of a restriction on module experiment operations.

4.3 SCS CONCEPT DEVELOPMENT

The stability and control system studies were directed toward selection of a suitable concept to meet the experiment module control requirements. Only those technical areas considered to require conceptual study are covered here. These areas are identified to be:

a. Fine point stability in an attached or detached experiment module.

b. Orbital low acceleration systems in an attached or detached experiment module.

c. Momentum actuation and unloading system selection and sizing for the detached experiment module.

Reference 4-3 is a major source of information presented herein. For brevity, only the study elements and major results are given where Reference 4-3 applies.

4.3.1 FINE POINTING STUDIES. The fine point state of the art is briefly described to establish an initial point of reference. Sources of attitude perturbation for both attached or detached experiment operation are briefly described. The subsequent pointing study is subdivided into that applicable for attached and detached* experiment modules. This subdivision is natural because the first tendency is to attach the experiment module so it can draw support from the space station. The problem then becomes analysis to determine the feasibility of fine pointing an attached experiment module. Failing to meet requirements can force the experiment module into a detached mode. In the detached mode, the required functional capability jumps to include what could be termed a "coarse point" and a separate "fine point" or vernier system. The detached module "fine point" system is configured and analyzed. A fine point concept is selected for the experiment module.

4.3.1.1 State-of-the-Art. The Orbiting Astronomical Observatory, OAO, spacecraft is a current example of a stellar oriented detached module with fine pointing capability. Reference 4-4 gives a coarse pointing mode (operation from vehicle star trackers) accuracy of one arc-min. When operating from an experiment derived (e.g. Princeton 1 M telescope) or boresighted attitude sensor driving reaction wheel actuators, a stability capability of 0.1 arc-sec is given.

Stratoscope II is an unmanned balloon borne 36 inch aperture telescope operating at about 80,000 feet altitude (Reference 4-5). A motorized coarse (mercury and ball) bearings and fine (flexure pivots) gimbaling system permit ground commanded

---

*Detached and free-flyer designations are used interchangeably.

pointing by reference to coarse (10 degree) and fine (50 arc-min) TV picture fields. Ultimately two guide or reference stars are brought into the fine field of view. Attitude sensing signals are derived from the two guide star images and are used to drive a lens in the main optical path to compensate for motion of the telescope body. The net result is that the image of the stellar area including the guide star remains stationary. Flight results indicated a stability of 0.015 arc-sec on 5th magnitude and 0.05 arc-sec on 7.5 magnitude stars.

The Apollo Telescope Mount, ATM, of the Apollo Applications Program, AAP, has not been flown as yet. This system uses narrow range pitch and roll torquer driven flexural pivots to fine point a telescope at particular angles relative to the earth-to-sun line. Boresighted fine sun sensors are used to provide the attitude error signal. References 4-6, 4-7, and 4-8 contain study results indicating pointing accuracy of a few arc-sec, stability at a few arc-sec maximum deviation, and rate at 1 arc-sec/sec.

4.3.1.2 Attitude Perturbation Sources. Attitude stability perturbation sources applicable to attached or detached operation are:

Orbit Environmental Torques - Gravity gradient (GG), air drag and on-board magnetic moment are the principal sources. Of these the GG torque is typically the major source. In general, the GG torque is composed of a secular and sinusoidal (twice orbit frequency) components. The maximum cyclic component is the worst case for pointing stability and occurs when the long axis (line of view of the telescope) is in the orbit plane. Herein, the maximum cyclic GG torque is used to represent the orbit environment torque. For the assumed worst case situation, a long slender body, the GG torque is dependent upon the body maximum moment of inertia. This is illustrated on Figure 4-13 for a low altitude orbit of 2 -300 nautical miles. For reference experiment FPE designations at various inertia values for the detached (total experiment module) and attached (experiment only) modes are marked.

Sensor Noise - A diffraction-limited (all aberrations removed) sensor of specific primary aperture area and field-of-view (FOV) operating off a guide star near the desired pointing direction is assumed. Photon fluctuation noise, detector dark current and efficiency, sensor optical efficiency all enter into a calculation of a signal-to-noise ratio (S/N). The spectral distribution of this noise is assumed to be that of white noise. These factors with values believed to be typical or conservative, are listed in Table 4-3, for all but the sensor primary characteristics of aperture and FOV. Curves are later generated showing the relationship of pointing stability to these sensor primary characteristics.

A guide star brightness rating of 12 (minimum brightness, mv = 12) assures existence of a guide star near the desired pointing direction (say within 30 arc-min.) A typical phototube bandwidth corresponding to 0.1 micron at visible wavelength of

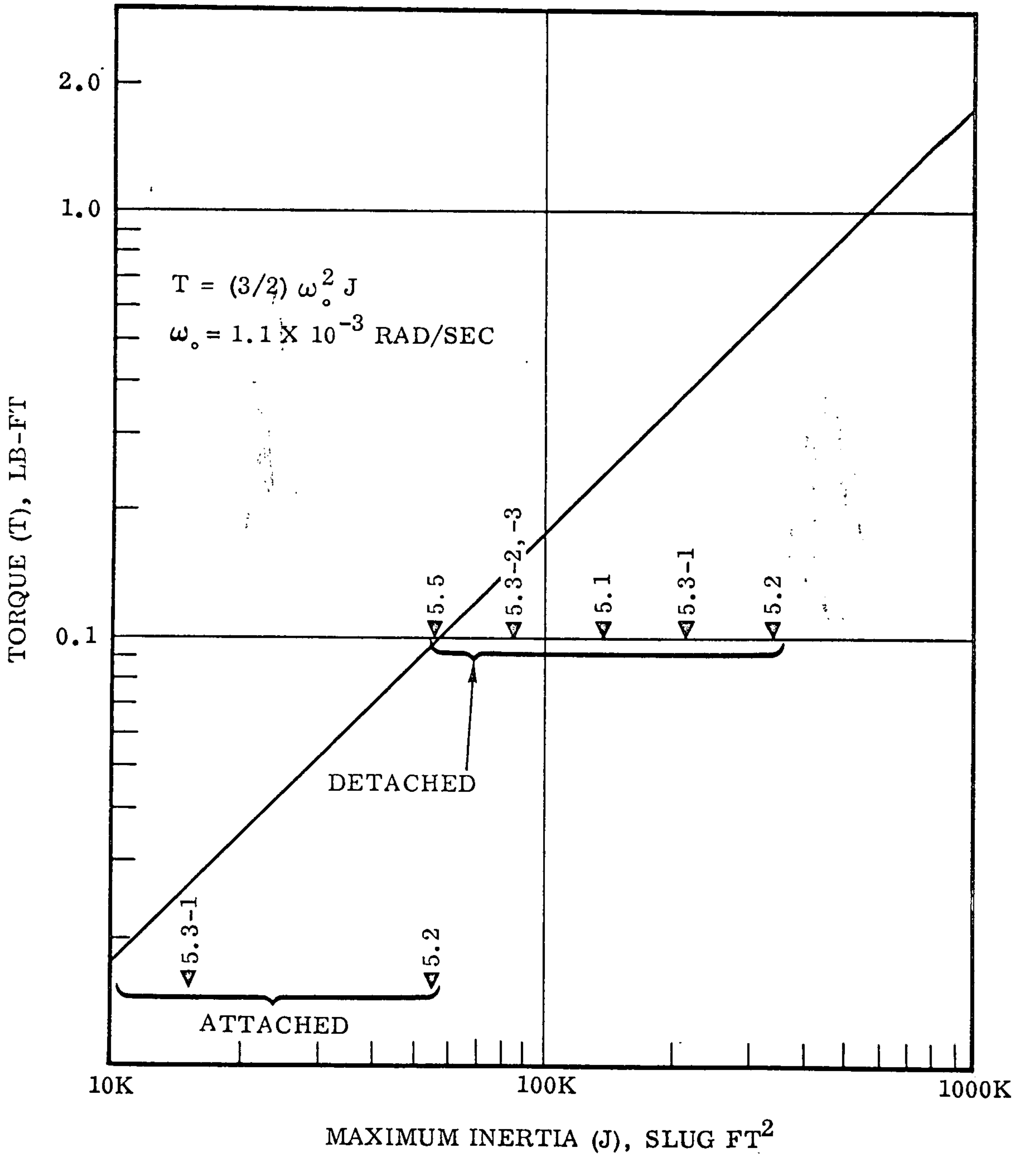

Figure 4-13. Maximum Gravity Gradient Torque vs. Experiment Module or Telescope Maximum Inertia

Table 4-3. Tabulation of Sensor Noise Parameters

Guide Star Brightness Minimum	mv		12
Detector Dark Current Equivalent Brightness	mvd		12
Optical Efficiency	η_o	$\eta_o \eta_q = 0.01$	
Detector Efficiency	η_q		
Phototube Bandwidth	-		0.1 micron
Background Noise			
Orbital Nighttime			
Equivalent Brightness	mvb		11
Field-of-View Factor	f_b		16 arc-min^2
Orbital Daytime			
Equivalent Brightness	mvb		5
Field-of-View Factor	f_b		36 arc-min^2

0.55 microns gives a star irradiance of 3.8×10^{-8} watts/meter^2 for a zero mv star. The efficiencies, η_o and η_q, occur as a product and a typical value (Reference 4-9) is given as $\eta_o \eta_q = 0.01$. Typical detector dark current noise is implied to be equivalent to a 12th magnitude star. Reference 4-9 also gives values for typical background noise as equivalent to one 11 magnitude star per 16 arc-min^2 guide star FOV area during orbital nightime and one 5th magnitude star per 36 arc-min^2 during orbit daytime. The implication of the much higher background noise during orbit daytime is incident solar radiation reflected into the telescope aperture.

For the case where experiment derived sensing is applicable, it is emphasized that the above tabulation refers to the guide star optics which, while using the same primary telescope aperture, usually parallels the main optics. Figure 4-14 illustrates a typical situation. The total field of view is typically 15 to 30 arc-min. It is constrained to be at least big enough to bring a guide star and the area of interest simultaneously into view. The area of interest is smaller, perhaps 5 arc-min diameter, and is centered in the telescope field. The guide star optics FOV is typically much smaller than the total FOV to minimize the effect of background noise on pointing. Typically 1-5 arc-min diameters are used.

The error due to noise is inversely proportional to S/N. The S/N is in turn adversely affected by sensor FOV. This could affect the choice of attach or detach because, according to present estimates, capture from an attached situation would require a 15 arc-min FOV to accommodate space station stability, whereas a detached situation would require a 1 arc-min FOV to accommodate the experiment

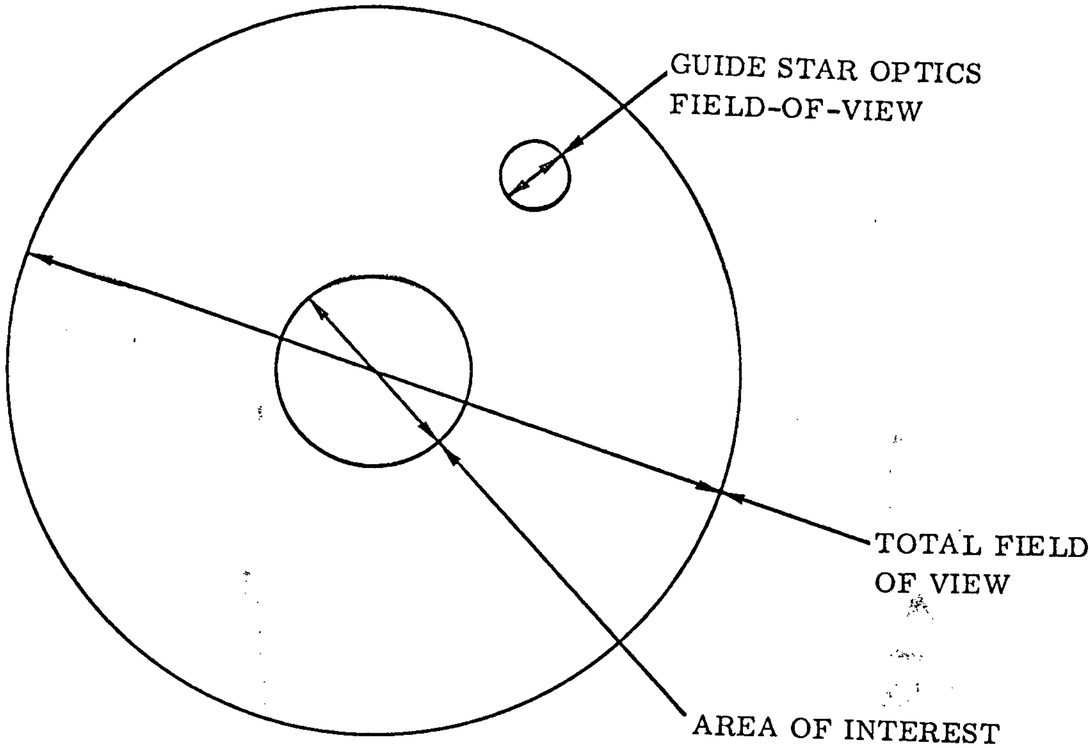

Figure 4-14. Telescope Field of View Identification

module coarse point stability. Figure 4-15 plots the effect of FOV on a sensor S/N. For zero FOV the highest possible actual S/N occurs and hence the best angular stability. A one arc-min FOV has negligible effect on stability during nighttime operation and about a 4 times degradation in daytime. At 15 arc-min the degradation factor at night is 6.65 while during the day it is 62 times worse. A daytime degradation factor of 15 apparently can be directly attributed to attached operation.

Space Station Environment (Attached Only) - There are two deleterious effects of attachment. One is jitter at the telescope mount induced by the space station crew. This jitter is described in Reference 4-10 as equivalent to that of white noise passed through a filter with a second order lead break at 0.5 Hz and a third order lag frequency break at 3 Hz. In Reference 4-3, a 12 man crew is appropriately distributed throughout the space station (see Figure 4-1) and the resultant RMS linear and angular jitter calculated at a telescope mount position. The calculation was based upon rigid body but was increased by a factor of 40 to produce a conservative estimate including flexural effects. In addition, the jitter was concentrated at 1 Hz, a frequency midway between 0.5 and 3 Hz. The result was a ± 0.1 inch maximum displacement. This amount produces 1×10^{-2}g peak acceleration and is considered conservative by perhaps an order of magnitude.

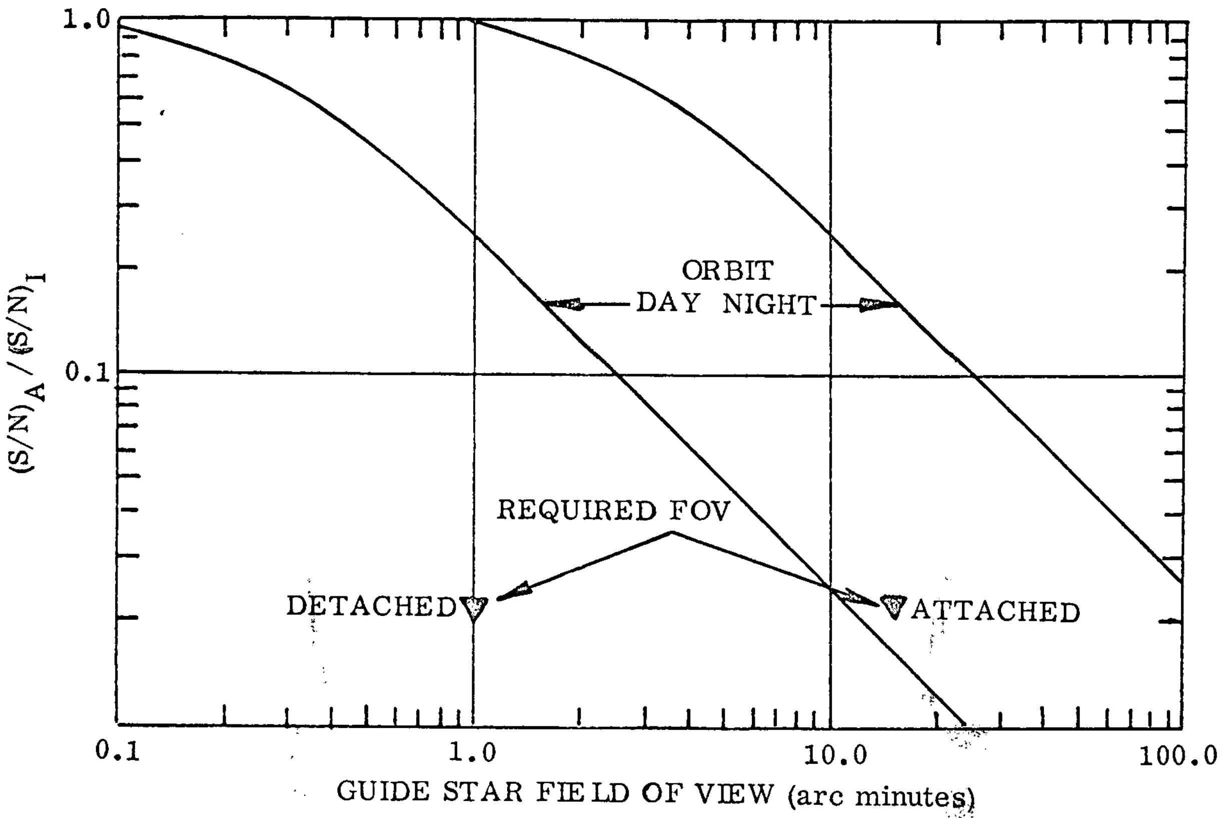

Figure 4-15. Field of View Effect on Signal to Noise Ratio

A second effect of attachment is sustaining those forces due to air drag deceleration and gravity gradient. The air drag deceleration was estimated at 10^{-6} g maximum. The gravity graidient acceleration/deceleration depends upon the offset of the telescope from the space station center of mass and is 1.1×10^{-7} g's per foot offset. Herein an offset of 40 feet was assumed giving a maximum accelerate/decelerate amount of $\pm 4.4 \times 10^{-6}$ g varying sinusoidally at orbit frequency.

Thermal Shock - Whether attached or detached, orbit sunrise and sunset introduce a rapid change in thermal environment. Thermal expansion-contraction is expected but has been assumed controllable by the experiment module environmental control system. Thermal shock has not been included thus far. Its inclusion is recommended.

4.3.1.3 Fine Pointing, Attached Experiment Module

4.3.1.3.1 Alternate Concepts. Figure 4-16 illustrates various concepts for a vernier fine pointing system operating in an attached mode. Note that it is assumed that any gross module orientation relative to the space station has been accommodated and it now remains to improve upon the space station pointing stability. To ease explanation, an imaging telescope with a photographic plate storage of a star pattern example is used. As illustrated the options are:

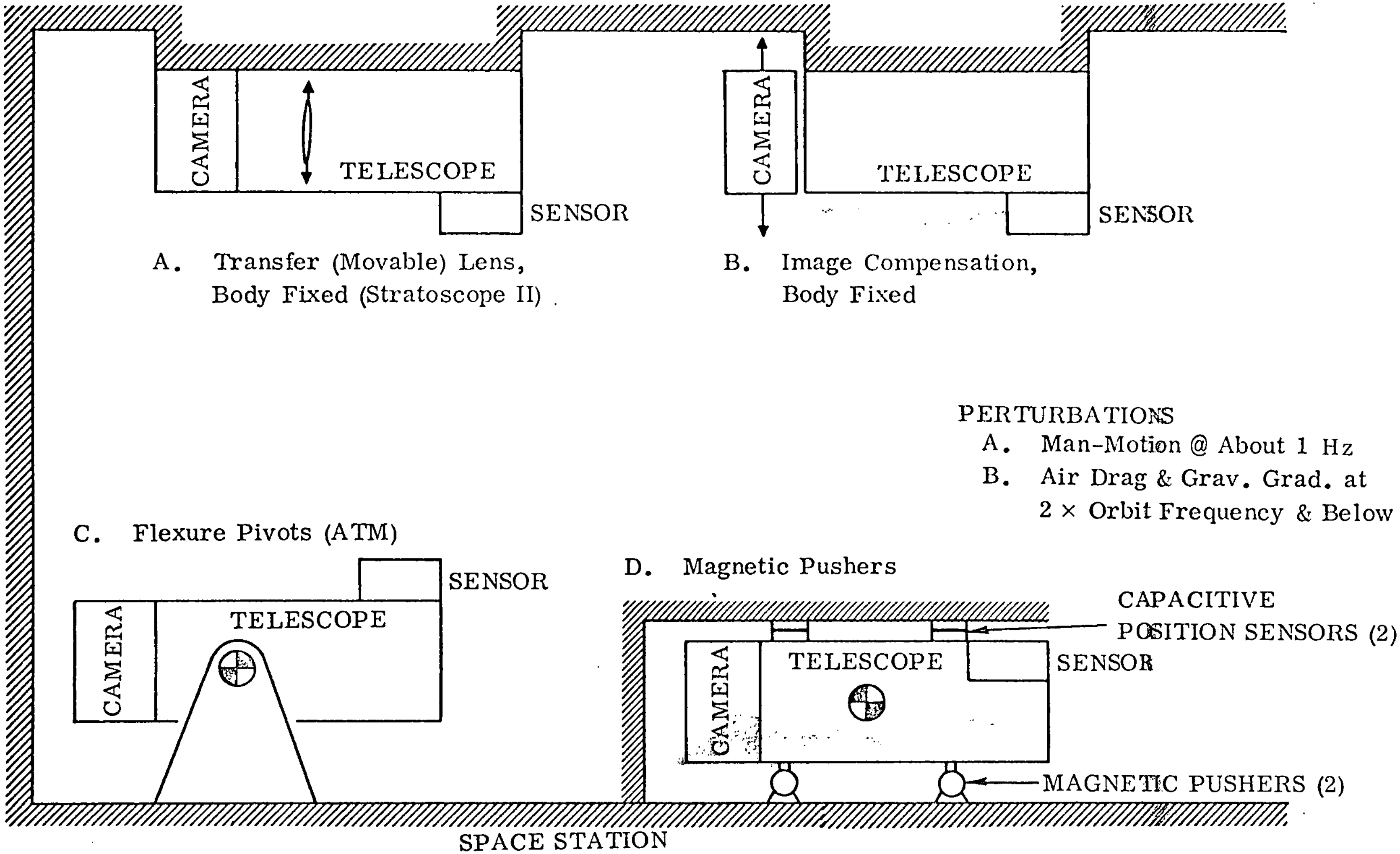

Figure 4-16. Vernier Fine Pointing Alternate Concepts, Attached Module

a. Transfer (movable) Lens, Body Fixed - In this method, the telescope tube and camera are hard mounted but any space station motion local to the experiment is sensed by an experiment derived signal or from a suitably accurate boresighted sensor. This signal is used to move a lens in the telescope main optical path exactly opposite to the telescope body so the image on the camera plate does not move. This transfer lens approach was used in Stratoscope II.

b. Imaging Compensation, Body Fixed - This method is identical to the transfer lens technique except that the photographic plate is moved such that the image is again stationary on the plate.

c. Flexure Pivots - These are "zero" stiction, low spring constant, narrow angular range flexural rotation couplings placed "exactly" at the experiment center of mass. By so doing, space station translation forces are directed through the experiment body center of mass and therefore do not introduce a perturbative torque. The remaining coupling torque is from the flexural pivot spring gradient. Perfect rotary isolation results if the flexural pivot spring gradient is zero. That is, the space station can jitter angularly and in translation with no motion of the telescope. The idea is to approach this ideal suspension by precise mechanization and compensate for residual coupling by use of sensor derived error signals driving torquers paralleling the flexural pivots.

d. Magnetic Pushers - In principle, this technique is identical to the flexural pivot approach. Isolation from space station motion is provided allowing the telescope body to float (not contact the space station) within narrow limits (about an inch). A linear centering system of two position sensors driving two identical magnetic pushers (similar to the common radio speaker voice cone drive) maintain centering in the gap. Rotational telescope motion results in zero displacement error signal due to the signal hookup of the two displacement sensors. The angular position of the telescope is maintained by the pointing sensor producing equal and opposite forces at each pusher to generate the correcting torque. Departure from ideal mechanization results in errors. The errors result from the centering system acting to constrain the telescope natural floating motion in the space station due to gravity gradient and air drag perturbations. The reaction force magnitude together with the available displacement sets the gain of the centering system at some minimum value. Subsequently man-motion jitter at 1 Hz in combination with off-centering of the telescope center of mass and unbalance of the pushers and displacement sensors result in a coupling torque inducing an error.

Of the four schemes presented in Figure 4-16, A and B are poor candidates because typically telescope primary optics full field-of-view is in the 15 to 60 arc-min range and only the image center of a few arc-min may be used. Recognizing that the space station stability will be about 0.25 degree or 15 arc-min would cause considerably loss of telescope useful FOV. Schemes C and D ultimately are limited by the need to move the entire telescope but do not suffer any loss of FOV. Herein scheme A and B are discounted immediately but it is observed that either can be used as a further vernier on schemes C and D with their actuation systems operating from the same sensor.

Scheme C has been evaluated at length (References 4-6, 7 and 8) with the result that the stability is limited by the suspension system to a few arc-secs. It is not covered further herein.

Scheme D is the subject of major analysis herein. The magnetic pusher concept has been treated earlier in connection with a 1 meter diffraction limited telescope in a detached (OAO) mode by Perkins-Elmer in References 4-9, 11, and 12. Herein it is desired to extend the technology to include the perturbative environment of the space station and to provide parametric pointing data relating stability to guidance optics aperture diameter and field of view under typical orbital conditions.

4.3.1.3.2 Pointing Analysis, Perfect Isolation. It is initially assumed that the mechanization provides perfect rotary isolation. After analysis of this ideal condition for pointing error, the added effect of mechanization errors will be determined.

With perfect mechanization the perturbation sources are sensor noise and orbit environment torque. Figure 4-17 is the appropriate analysis diagram. As shown the sensor noise corrupts the input error signal in an amount evaluated by the signal-to-noise ratio. The disturbance torque T_D, taken to be the worst case gravity gradient torque, is the other perturbation input. The control circuit includes a gain factor K, a stability lead network providing a rate signal derived from the displacement error signal, the assumption being that an inertial rate sensor will not have the required resolution or will introduce local mounting perturbations due to thermo-elastic deformation. The displacement plus integral addition of "n" stages is optional at 0, 1 or 2. That is in addition to noting the effect of the loop gain factor K, the effect of n is also desired. Note that the integral addition is:

$$\left(\tau_n + \frac{1}{S}\right)^n = \left(\frac{\tau_n S + 1}{S}\right)^n$$

Figure 4-18 gives the appropriate open loop Bode diagram for n = 0, 1 or 2. For n = 0, that gain $(K/J)_0$ was selected minimizing the sum of worst case attitude error due to gravity torque disturbance (twice orbit frequency) and that due to sensor noise.

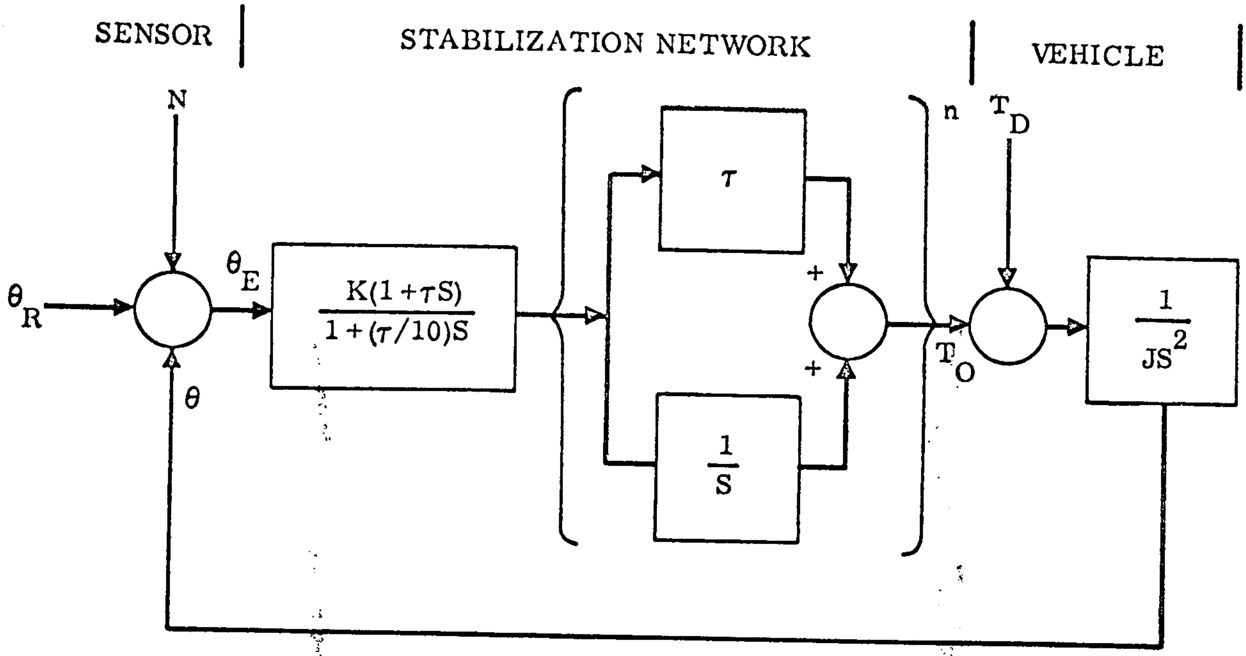

θ_R, θ_E, θ are respectively the reference, error and actual vehicle attitude, rad

S/N is the sensor signal-to-noise ratio, nd

K is the system gain factor, lb-ft/rad

τ is stabilizing network time constant, sec

n is 0, 1, 2 or number of integral type compensation stages

T_O, T_D are respectively the system actuator and environment disturbance torque, lb-ft

J is the telescope moment of inertia, slug-ft^2

Figure 4-17. Stability Analysis Diagram, Attached Telescope, Perfect Rotary Isolation

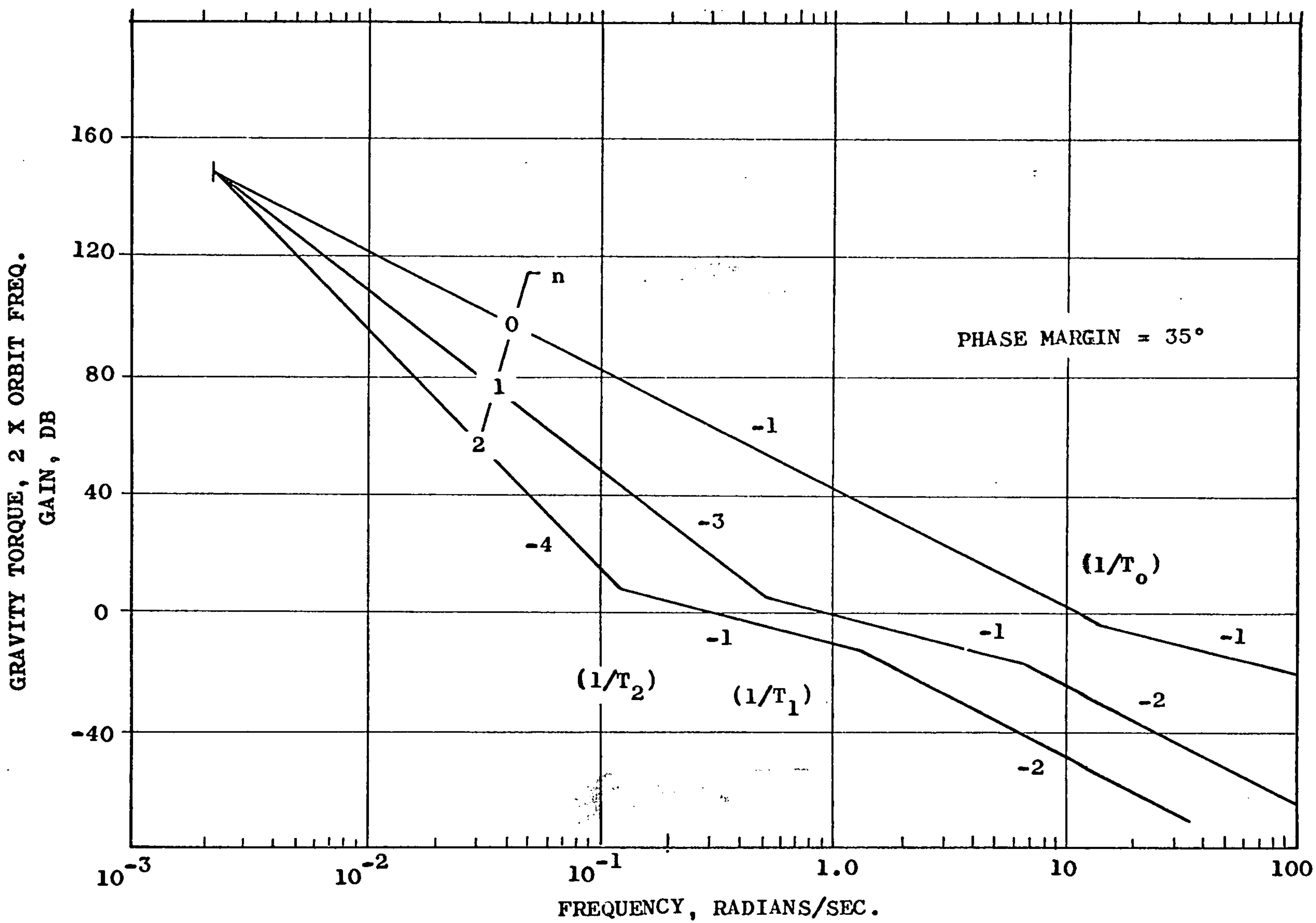

Figure 4-18. Fine Point Stability Bode Diagram, Attached Mode

As $(K/J)_0$ increases, the gravity torque disturbance decreases but that due to sensor noise increases because the system bandpass increases. Adding the stability network for n = to 1 or 2, while keeping the same gain at twice orbit frequency, makes the gravity gradient error the same but reduces the system bandpass, thereby reducing the error. Therefore as n increases the total error diminishes to that due to gravity gradient.

The pointing stability results for n equal to 0, 1 and 2 are shown in Figures 4-19, 4-20 and 4-21 respectively. The value of (K/J) is given as well as the total pointing error. For reference the diffraction limit blur circle diameter and the probable stability requirement at 0.1 times the blur circle diameter are also drawn on Figures 4-19, 4-20 and 4-21. The 3 meter telescope can be used as an example of the requirement feasibility, 0.005 arc-sec. Table 4-4 tabulates the effect based on control system n, FOV and day, night operation.

As shown the 0.005 arc-sec requirement (1/10 the diffraction limit) would be met during orbit nightime for any field-of-view and for n equal to zero. During orbit daytime it is just met for a guide star FOV of 1 arc-min at n equal zero but increasing n to 2 allows increasing the FOV to almost 5 arc-min. However, the space station may only give 15 arc-min of stability which could cause a problem unless a variable FOV, greater than 15 arc-min for initial capture but smaller than 5 arc-min during operation, is used.

Recall that the stability calculated above assumes a perfect suspension system. The following analysis considers imperfections in the suspension system.

Table 4-4. 3 Meter Aperture Stability (Arc-Sec)
(Specified Stability Equals 0.005 Arc-Sec)

n	FIELD-OF-VIEW (arc-min)					
	NIGHT TIME			DAY TIME		
	1	3	5	1	3	5
0	0.001	0.0015	0.002	0.005	0.012	0.02
1	0.0009	0.001	0.0013	0.0025	0.006	0.009
2	0.0007	0.0009	0.001	0.0015	0.004	0.006

4.3.1.3.3 Centering System Analysis. Figure 4-22 illustrates the analysis model. As implied by the illustration, the space station is normally jittering or undergoing rotational or translational vibrations. These vibrations, induced from various sources but mostly from man-motion, were conservatively sized at ±0.1 inch at 1 Hz. The clearance needed for short period motion isolation would not be a serious problem. Also the frequency is high so isolation can be provided by a low natural frequency or low force centering system.

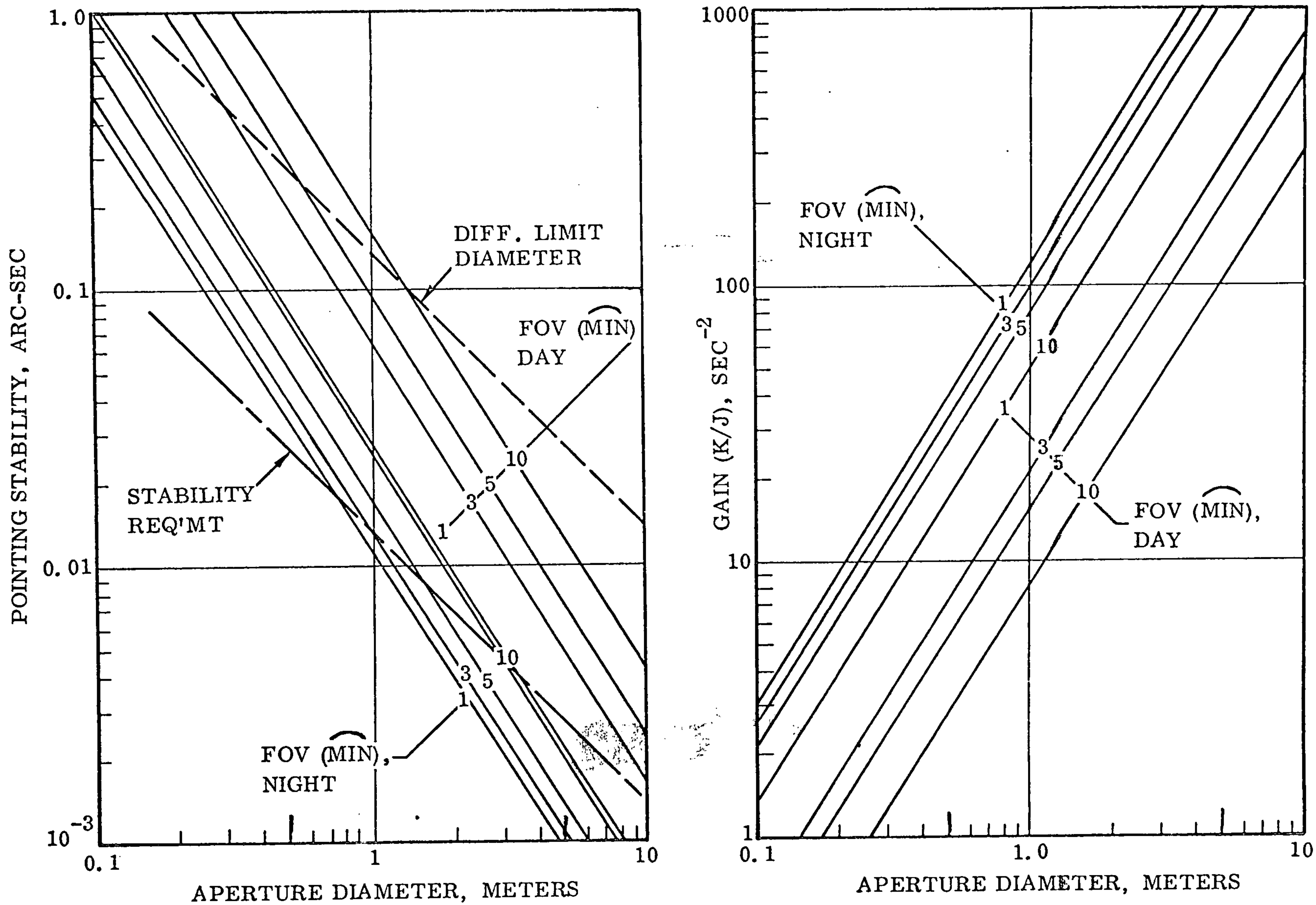

Figure 4-19. Typical Point Stability and Gain, No Control System Integrations

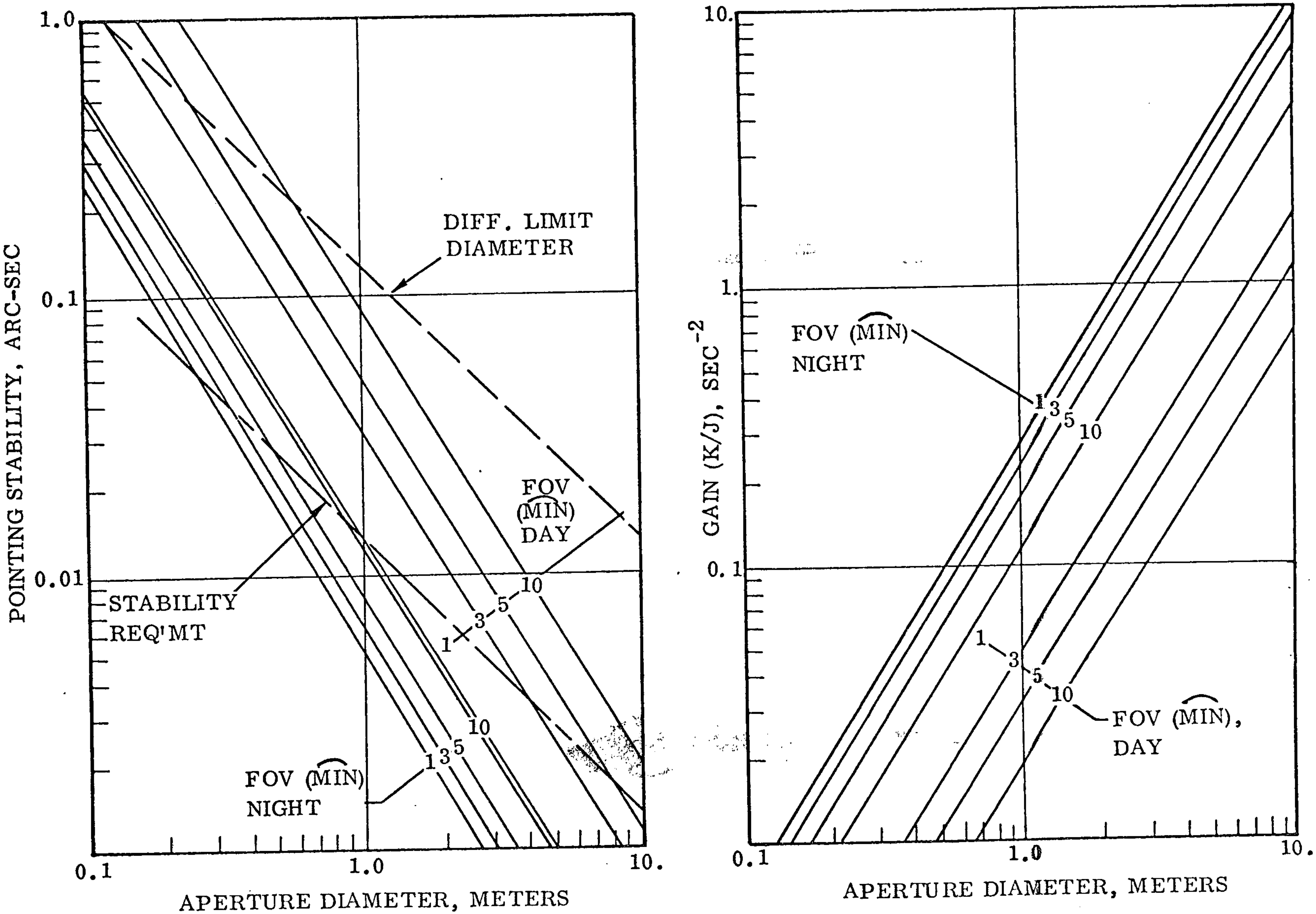

Figure 4-20. Typical Point Stability and Gain, One Control System Integration

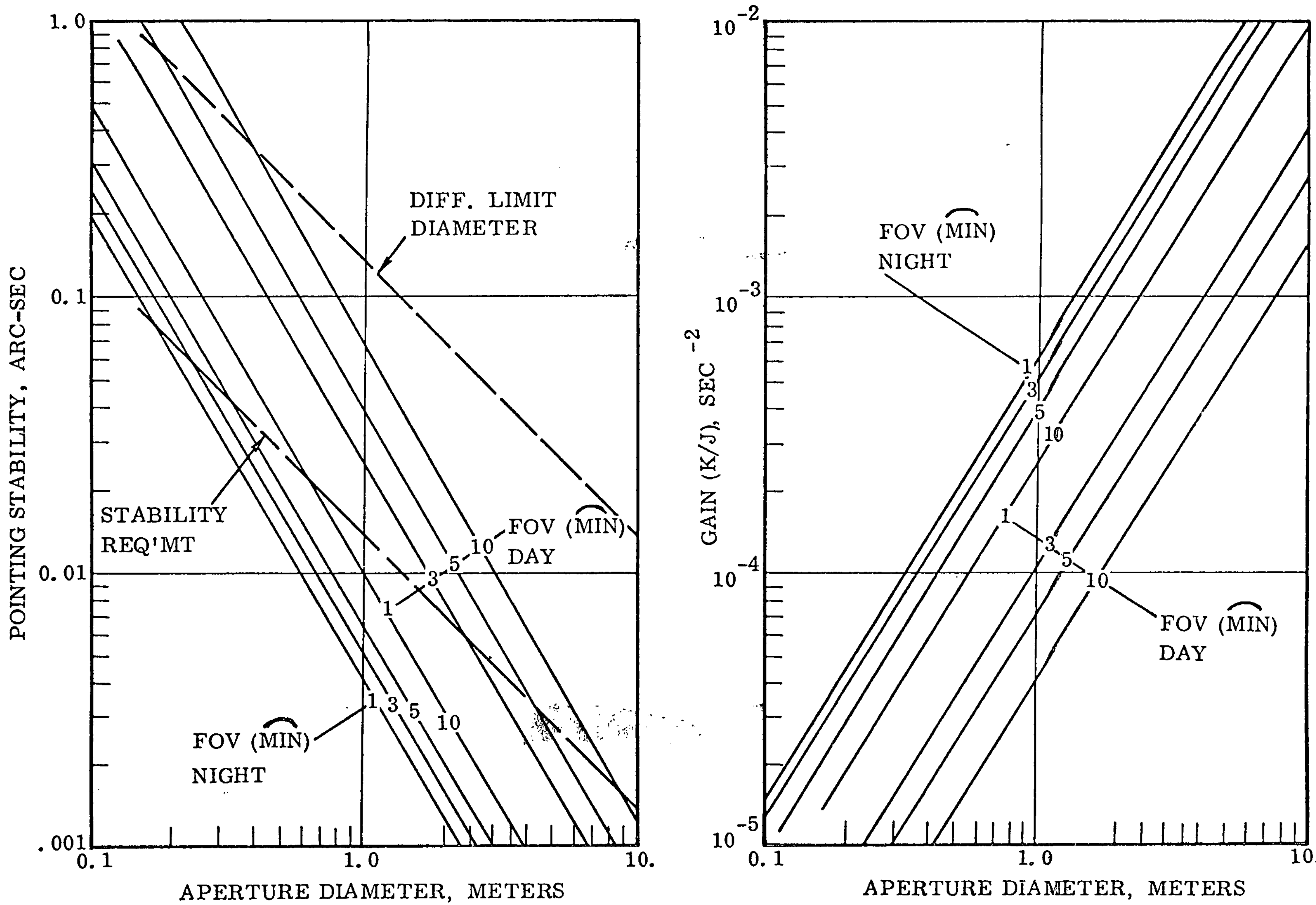

Figure 4-21. Typical Point Stability and Gain, Two Control System Integrations

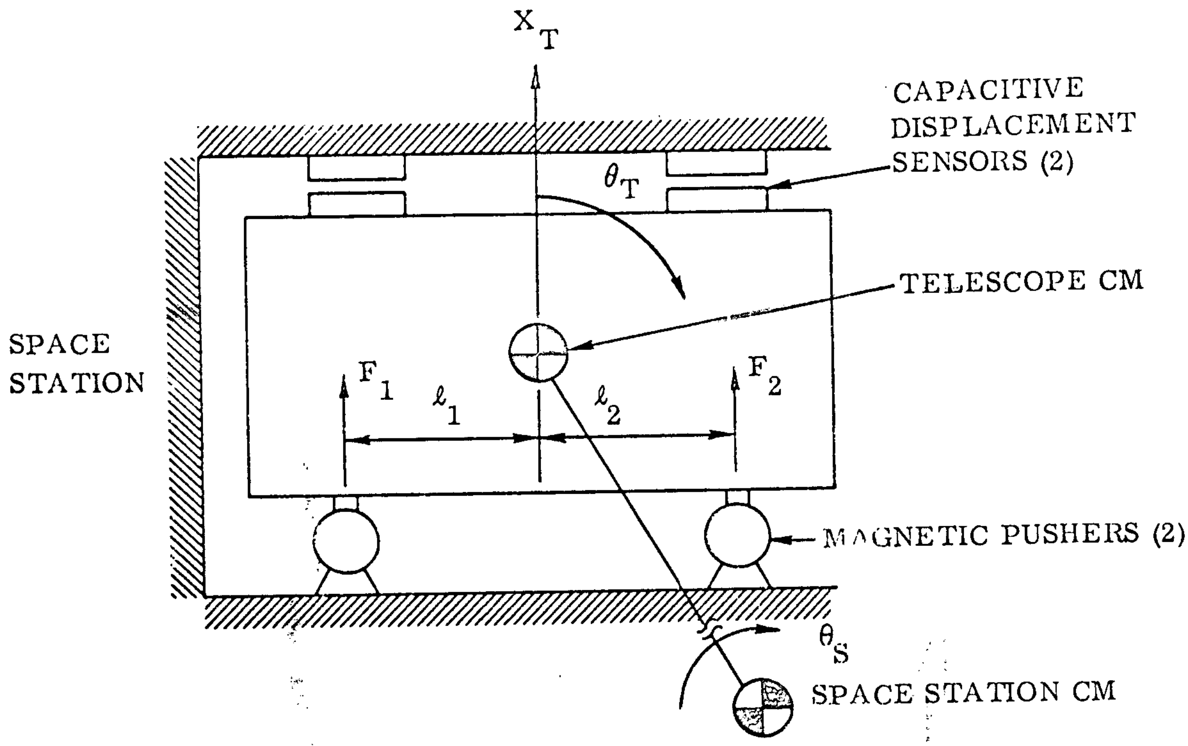

Figure 4-22. Centering System Analysis Model

The telescope is of course inertially pointed and assuming the space station is inertially oriented the telescope could be considered to be in a co-orbiting mode of equal period. If the telescope were 40 ft. above the space station at one point in the orbit, and 40 ft. below it one-half orbit later, it would be in a slightly different orbit about the space station with a semi-major axis of 80 ft. and semi-minor axis of 40 ft. (Reference 13). A centering system is then required to reduce this ±40 to 80 ft. to a practical amount.

To center the telescope the force due to gravity gradient (GG) must be reacted via the magnetic pushers in response to an off-center displacement signal. If the force is applied right through the telescope cm, the problem is solved. If it is slightly misaligned, a moment which tends to cause an attitude error results. The same would be true for the man-motion displacement of ± 0.1 inch at 1 Hz but it is better to simply allow the clearance. Assume a small misalignment (1 inch). The resultant pointing stability due to reacting GG considering telescope misalignment is illustrated in Figure 4-23. As shown a sensor FOV of 3 arc-min is used and appropriate gains (daytime values of K/J for the n equal zero case, Figure 4-19) for various size sensor apertures are given. While the n equal zero case is used herein, the results roughly apply for the n equal 1 or 2 because the gain around orbit frequency is about the same. As illustrated by Figure 4-23, the stability improves linearly with the telescope moment of inertia to mass ratio (same as radius of gyration squared). For reference most of the astronomy telescope values are noted against the FPE designation. As an example use the 3 meter telescope (FPE 5.2). Because of its high gain and radius of gyration the error due to GG is negligible (1.1×10^{-4} error compared to 5×10^{-3} arc-sec requirement). This would be the expected situation if the error signal were derived from the telescope experiment itself. If we use another example where a boresighted fine point sensor is used, with 0.25 meter aperture, the stability degrades by a factor of 50 (5.5×10^{-3} arc-sec) due to the decreased sensor aperture and could drop by another factor of five for other experiments with lower radii of gyration (0.027 arc-sec).

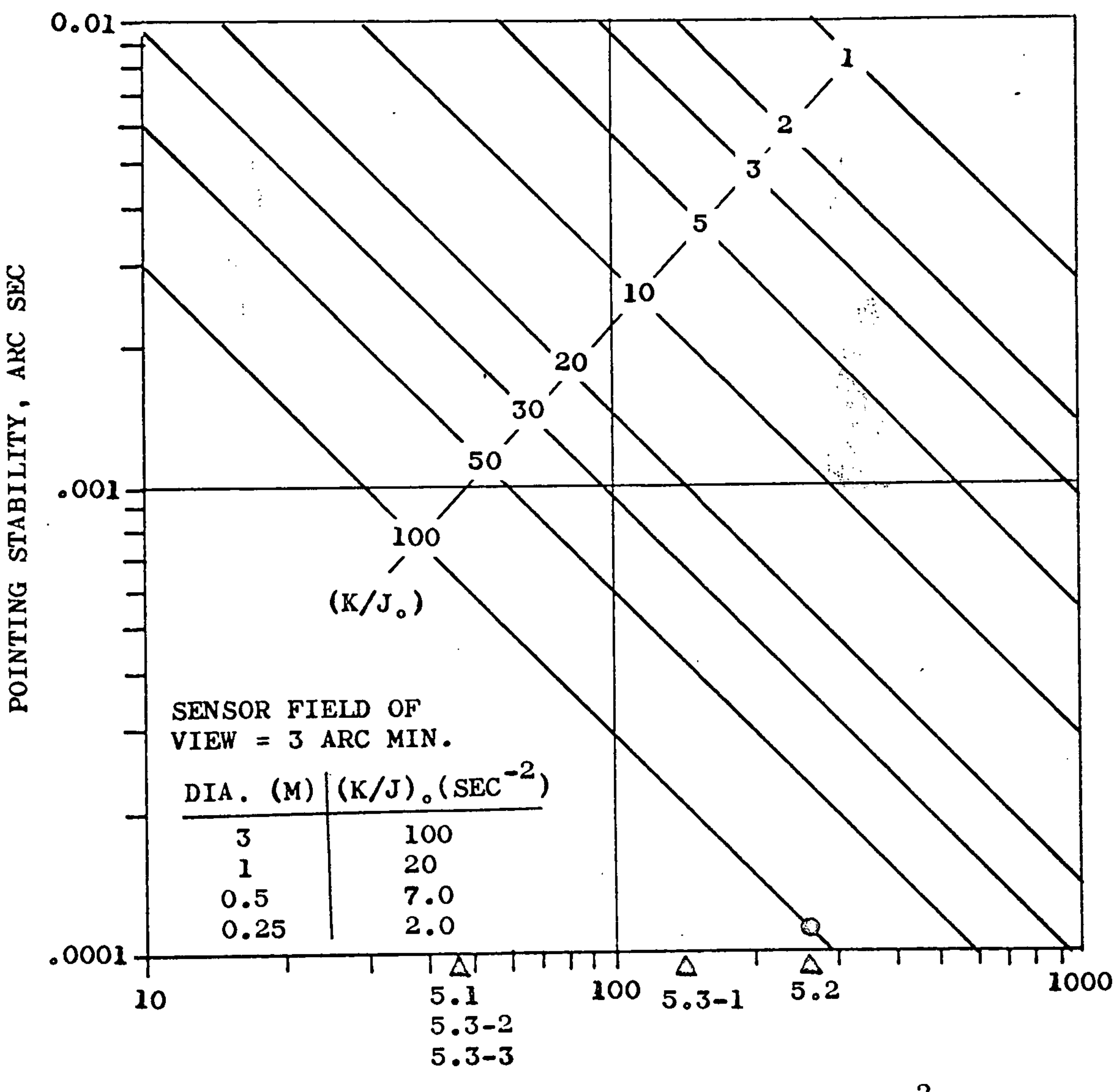

Figure 4-23. Attached Fine Point Suspension Error Due to GG

The overall effect of GG in comparison to the experiment requirement is significant but generally does not pose a serious problem especially if large optics are used for the sensor signal. Evaluation of a more serious error source, that caused by coupling of space station jitter (±0.1 inch at 1 Hz) via the telescope suspension centering system is evaluated next.

Off centering forces due to GG and air drag equivalent to accelerations of about 1.45×10^{-4} ft/sec^2 sinusoidal at orbit frequency are to be reacted while suppressing the uncontrolled values of displacement of 40 to 80 feet to a small amount, say 0.1 inch. Figure 4-24 illustrates the control loop block diagram and Figure 4-25 the corresponding control system Bode diagram accomplishing this function. The control gain, or system crossover frequency is the noted value of 0.021 Hz or period of 47.5 seconds. If the frequency were lowered, more displacement of the telescope "tube" must be allowed. If the frequency is raised, more jitter (X_s) is coupled into the telescope pointing control loop via the same telescope center of mass misalignment discussed previously (1 inch) and unbalanced force outputs from the positioning actuators (herein set at 2%). The resultant stability error is shown on Figure 4-26 where the jitter output at 1 Hz is plotted against inertia to mass ratio for two bounding values of pointing control loop gain (the n equal zero values are used). One boundary is the uncontrolled or $(K/J)_o$ equal to zero case. The stability is better than this. The other limit shown corresponds to the previously used daytime maximum value of gain appropriate to the current largest aperture of 3 meters. Again, for reference the telescope inertia to mass values are noted and the extremes used to establish an area of pointing stability. As noted the stability range is from about 0.002 to 0.02 arc-sec. As an example the error due to space station jitter for the 3 meter telescope of FPE 5.2 is about an order of magnitude greater than that due to GG and about the same as that due to sensor noise (see Figure 4-19).

4.3.1.3.4 Attached Fine Point Summary. Pointing stability in an attached mode is about equally dependent upon sensor aperture and suspension system capability in isolating the telescope "tube" from space station jitter. The suspension system is complex. The telescope cannot be hard mounted but is required to be continuously monitored by positioning sensors and gently centered by force actuators. In addition a rather complex capture mode is required. First the entire telescope must be moved by a two-axis pivot arrangement to the guide star location by space station guidance. Then the fine point sensor (boresighted or experiment derived) with a FOV greater than the space station stability (herein assumed at 15 arc-min) must be used to capture the guide star. Subsequently the sensor FOV might need to be reduced to a few arc-min to obtain the required stability.

4.3.1.4 Fine Pointing, Detached Module. Detaching the experiment module inherently increases the fine pointing potential because space station perturbations no longer apply. In addition, there is no need for space station-operated articulated joints between the experiment module and the space station to enable coarse pointing

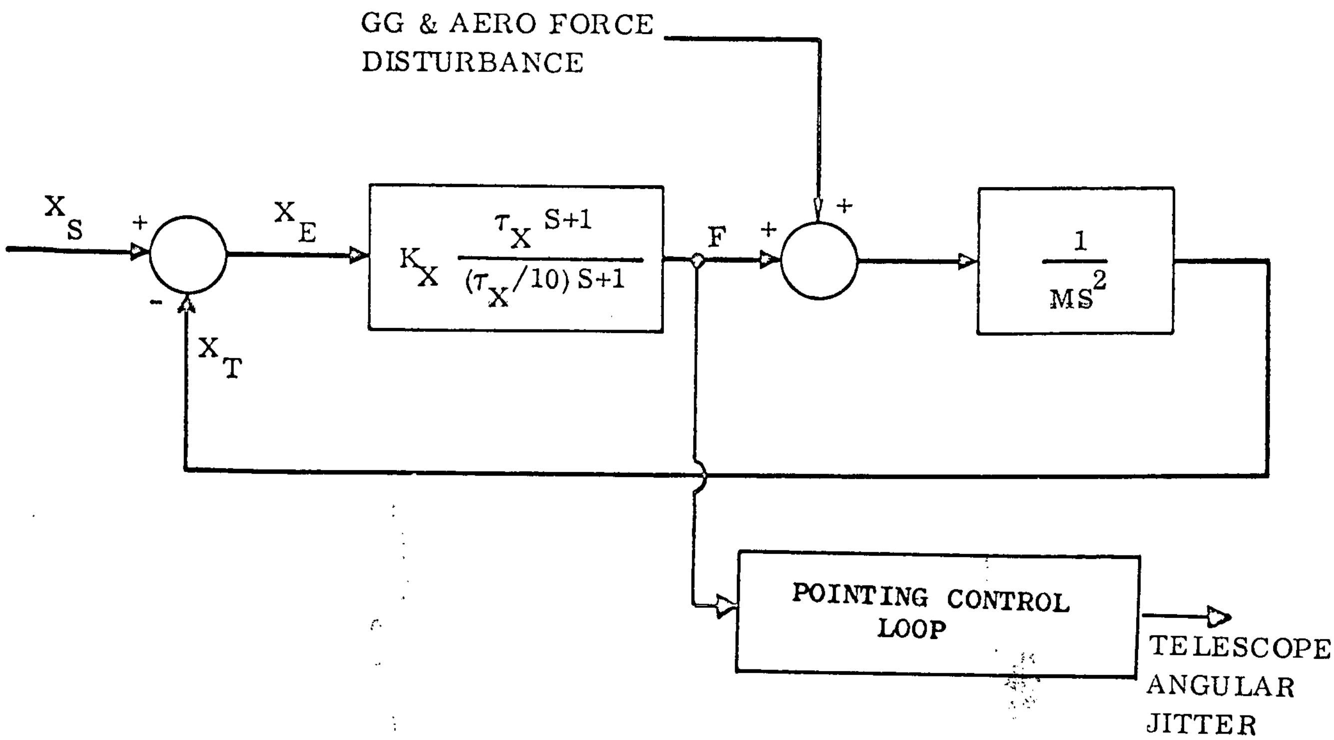

Figure 4-24. Centering System Block Diagram

the experiment module. However, the functional requirements of the detached experiment module SCS greatly increase relative to the attached. Figure 4-27 illustrates a current concept. As implied, the all-attitude vectoring of an experiment (presumably a telescope), docking to the space station, stationkeeping, and fine pointing are all contributed to by the experiment module SCS. In this system the stability is limited by the star all-attitude trackers to estimated values of 0.5 to 1 arc-min values,well above the required. The stability is greatly improved by switching to an experiment derived sensor signal or a suitably accurate (large) boresighted sensor operating off guide stars in the immediate vicinity of the celestial observation. However, depending upon choice of experiment module attitude actuation system (momentum absorption), the stability is estimated at a few arc-sec maximum for CMGs and negligibly small for inertia wheels. If CMGs are used because of their better operating characteristics for maneuvering torque and electrical power usage, then as Figure 4-27 implies, a vernier pointing actuation system local to the experiment is needed. The estimated values of stability resulting from CMGs actuation error and all-attitude sensors were taken from References 4-2 and 4-14.

Regardless of the technique, tracking on a guide star is fundamental. In some cases, one guide star may be tracked with roll (along view axis) controlled by basic experiment module all-attitude sensors because of the inherent lesser need for accuracy in roll. Otherwise two guide stars may be used. Figure 4-28 illustrates the use of a single guide star. A requirement of ± 0.005 arc-sec pitch-yaw control

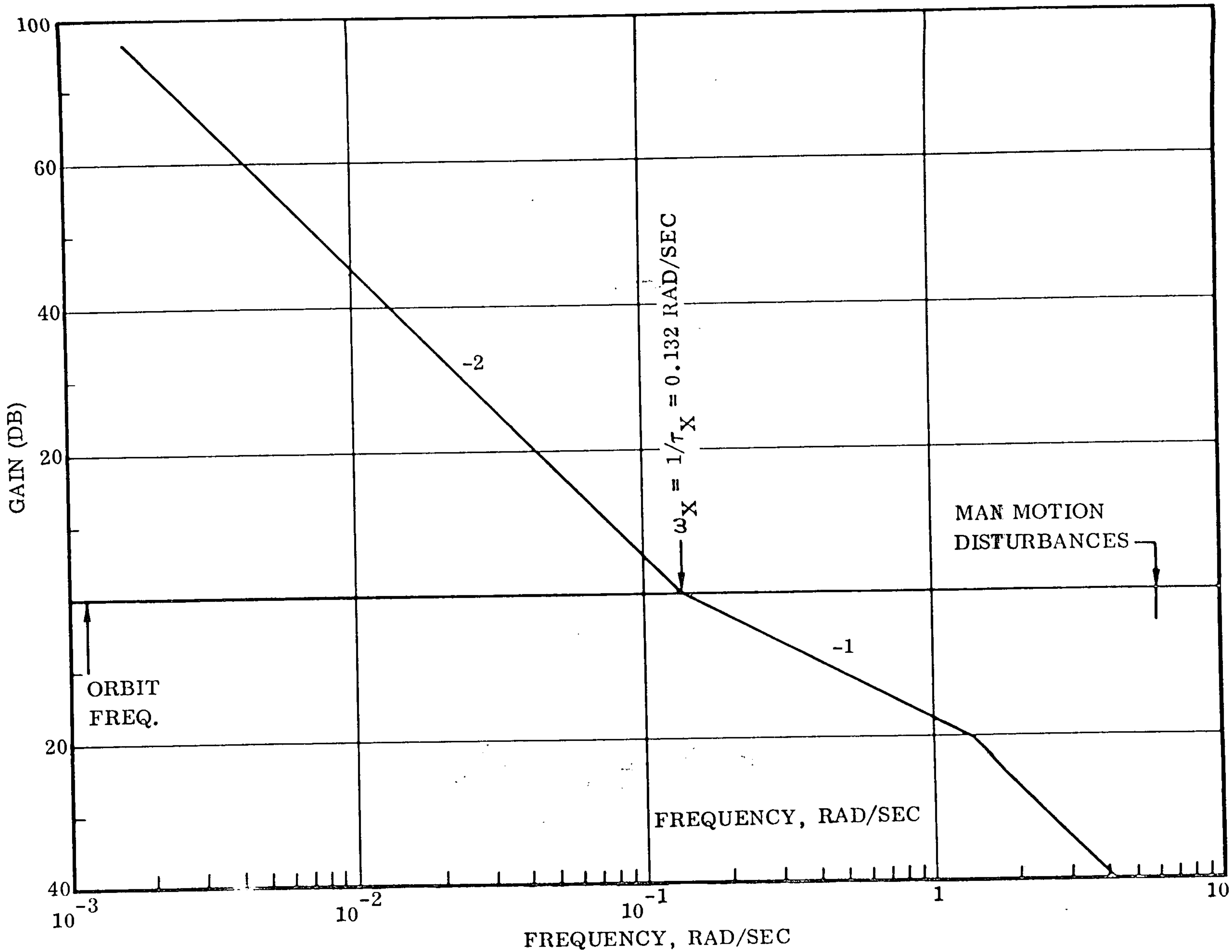

Figure 4-25. Centering System Open Loop Gain Transfer Bode Diagram

is assumed with a guide star off axis by 15 arc-min. The resultant roll angle control needed is 1.146 arc-sec as shown. While the roll requirement is considerably less stringent, in this case two guide stars would be required because basic module sensor system accuracy is currently estimated at 30 arc-sec. If the fine point stability requirement were 0.015 arc-seconds or greater then a single guide star could be used.

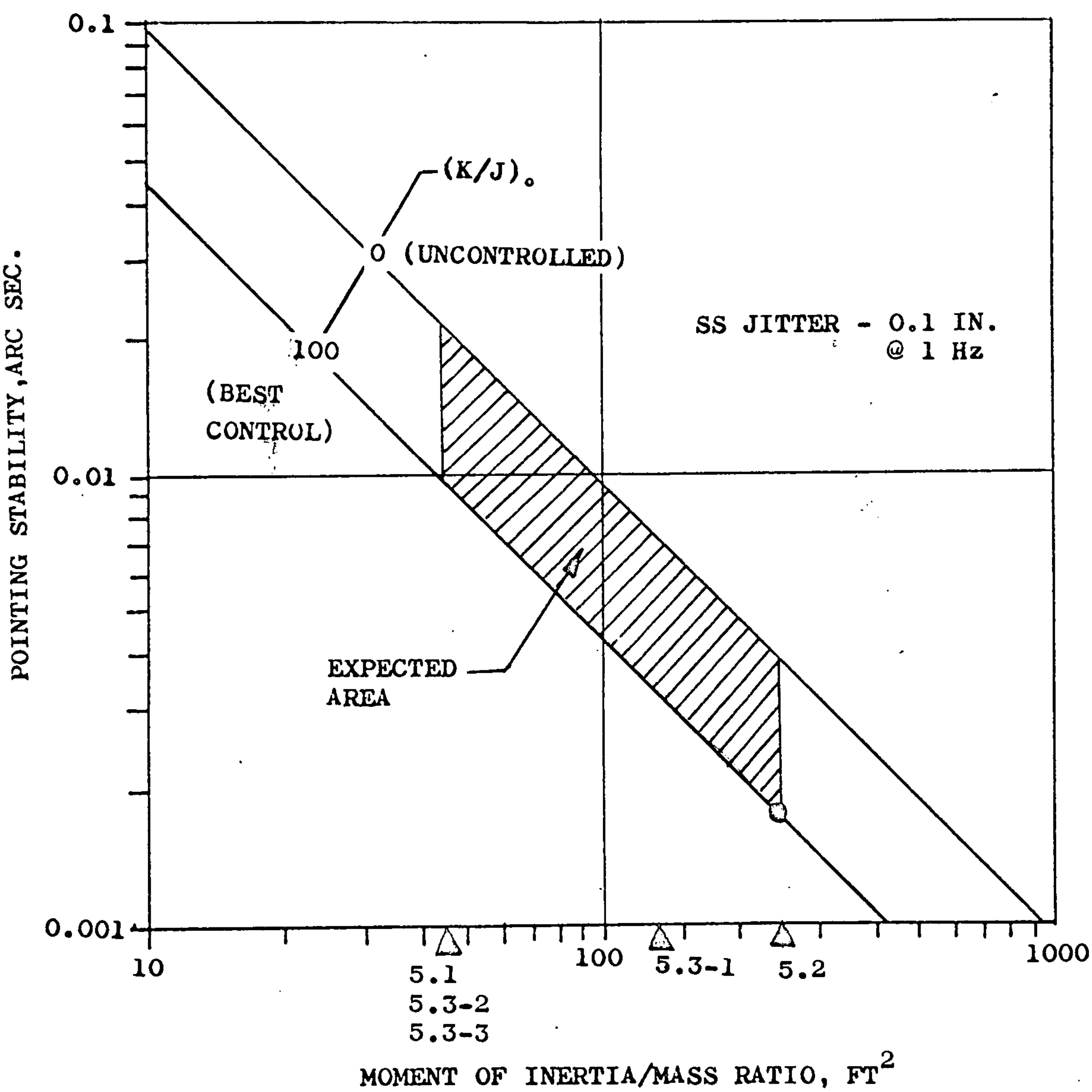

Figure 4-26. Attached Fine Point Suspension Error Due to Space Station Jitter

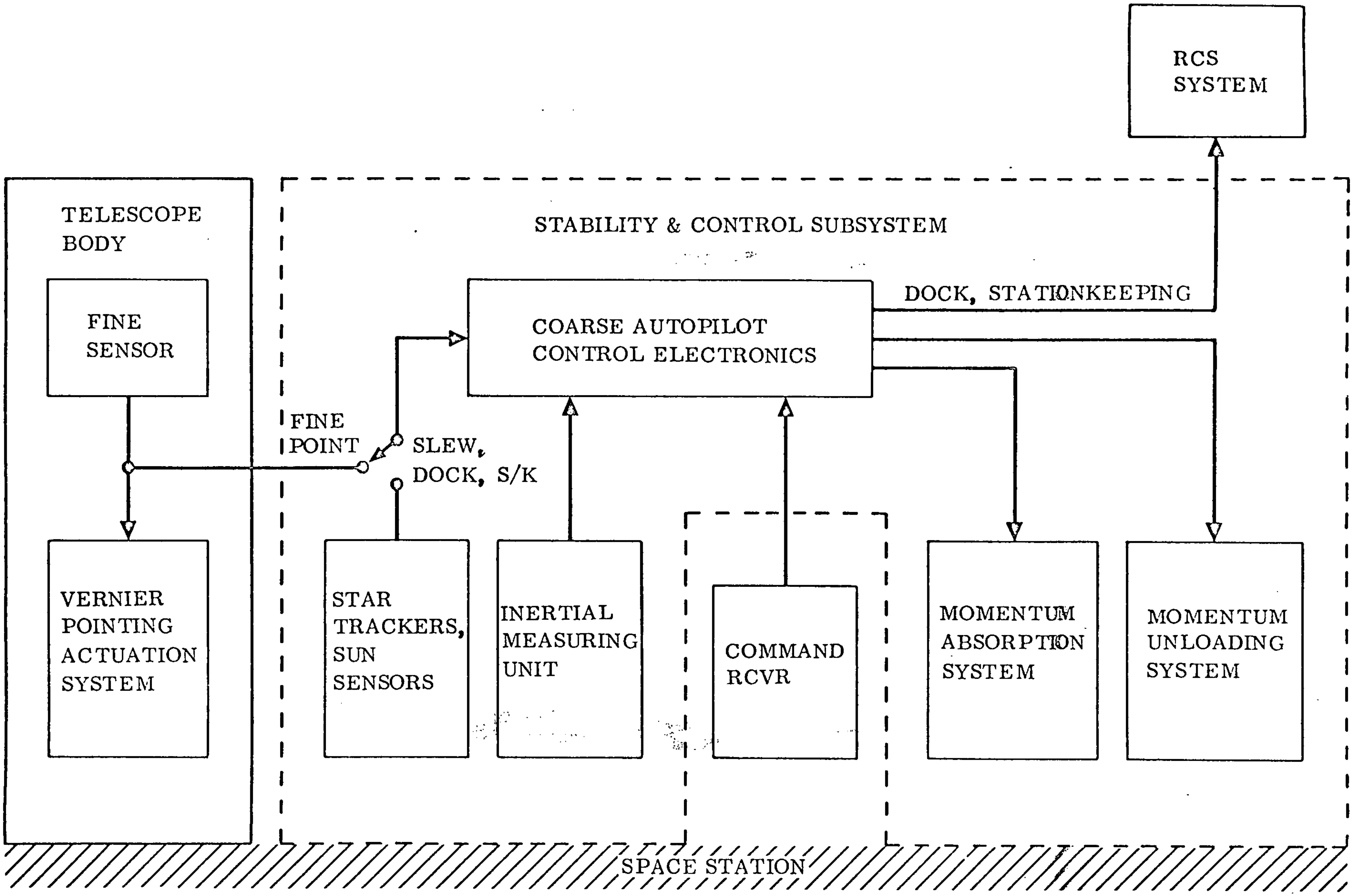

Figure 4-27. Detached Module Stabilization and Control System Concept

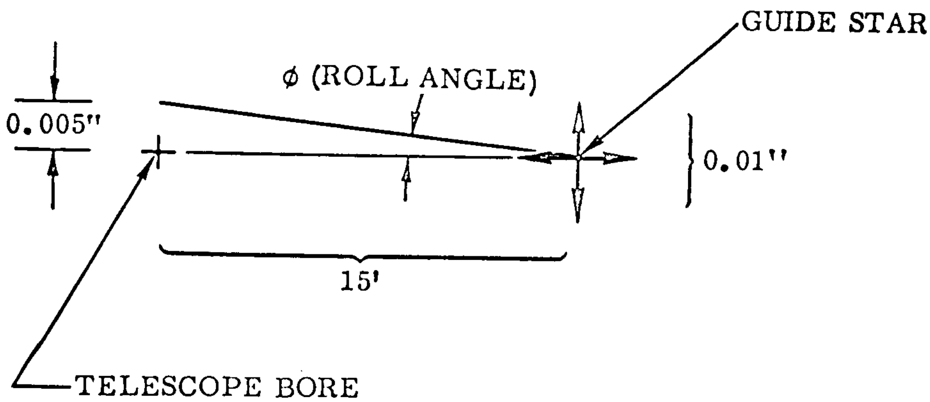

$$\phi = \frac{0.005''}{15' \times 60} \quad \text{Rad.} = 1.146 \text{ arc-sec}$$

Figure 4-28. Roll Control Requirement

4.6.1.4.1 Body Point. The analysis for fine pointing the entire experiment module is almost identical to that for the attached module magnetic pusher (paragraph 4.3.1.3). That is, sensor noise and gravitational torque act the same way. However, a major source of error, space station jitter, no longer exists and, instead of pushing or torquing against the space station, the experiment module primary actuation system is used. Figure 4-29 is the appropriate stability analysis diagram for the detached module. It is almost identical to that for the attached telescope with perfect rotary isolation (Figure 4-17). Indeed the only difference is the added element labeled "actuator dynamics". If the effective actuator time constant τ_M is infinite then there is no difference.

For an experiment module actuation system using single degree of freedom CMGs a value of τ_M less than infinity arises from an inherent feedback torque on the CMG gimbal due to experiment module angular rate. For an experiment module using inertia wheels the same effect occurs due to the inherent drive motor emf feedback in series with the input signal. These control system details are explained fully in Reference 4-3.

A Reference 4-3 recommended value of τ_M equal to 40 seconds is used for either CMGs or inertia wheels. For reference the value in the OAO inertia wheel system is 60 seconds. The actuator has a gain of zero at low frequency which increases to unity at frequencies above 0.025 rad/sec. Recalling that gain at twice orbit frequency is important because gravity gradient is at that frequency, this inherent loss of gain is undesirable and significant.

The analysis procedure is identical to that for the attached telescope with perfect isolation. The resultant optimum gain and pointing stability are given on Figures 4-30 and 4-31 for the calculated cases of n equal zero and 1 respectively. Comparison to the corresponding attached situation (Figures 4-19 and 4-20) shows that

58

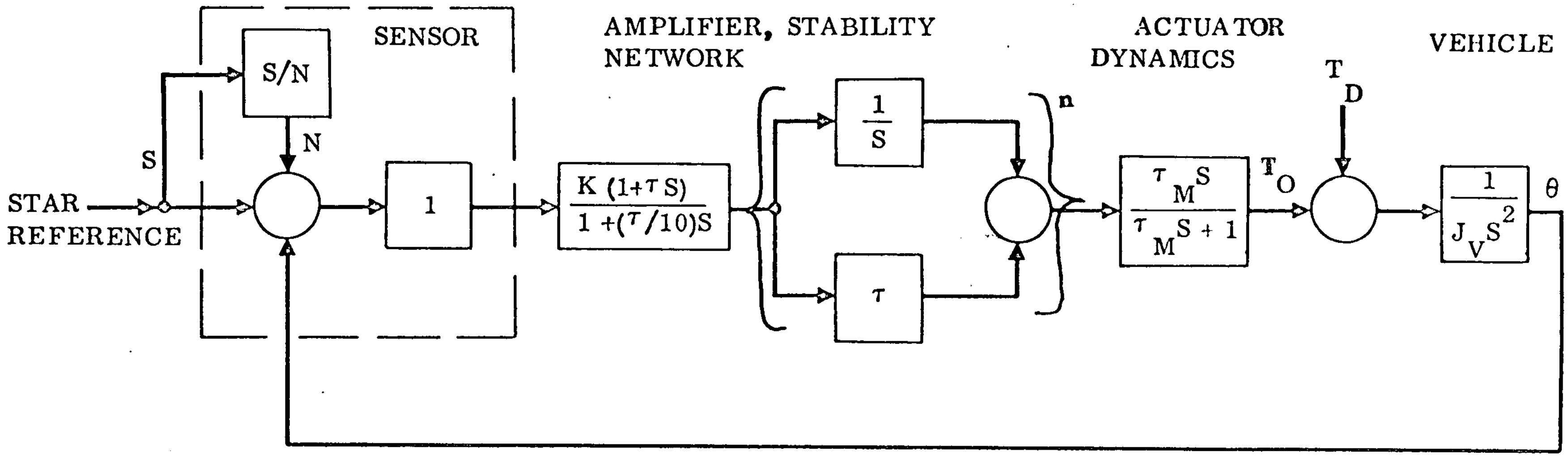

S/N	-	SIGNAL S, TO NOISE N, RATIO
τ	-	STABILITY CIRCUIT TIME CONSTANT, sec
K	-	SYSTEM GAIN, lb-ft/rad
J_V	-	VEHICLE INERTIA, lb-ft-sec^2
T_O	-	OUTPUT TORQUE, lb-ft
T_D	-	ORBIT ENVIRONMENT TORQUE, lb-ft
T_M	-	EFFECTIVE ACTUATOR TIME CONSTANT, Sec.

Figure 4-29. Stability Analysis Diagram — Detached Module

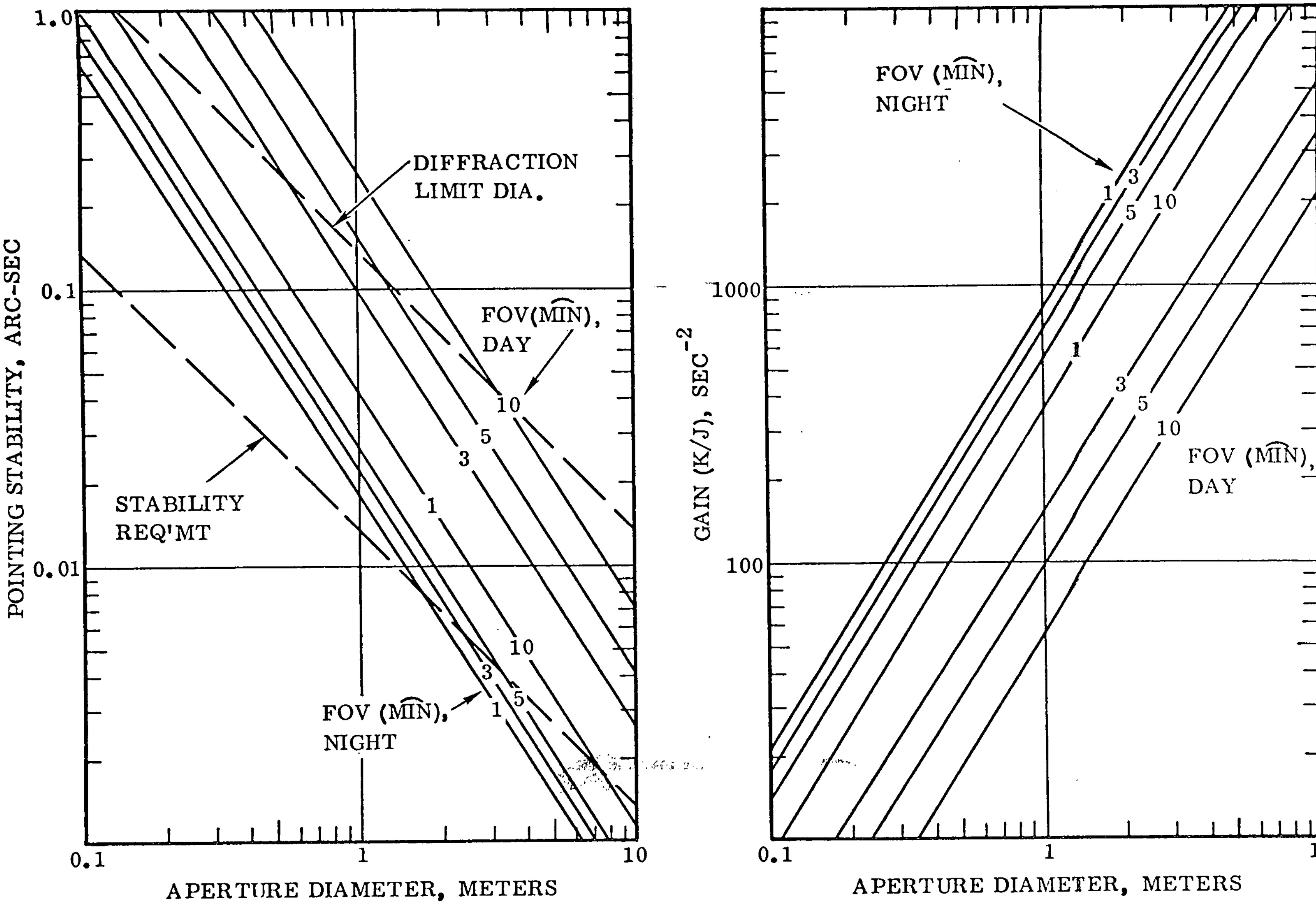

Figure 4-30. Typical Point Stability and System Gain, Detached XMOD, No Control System Integration

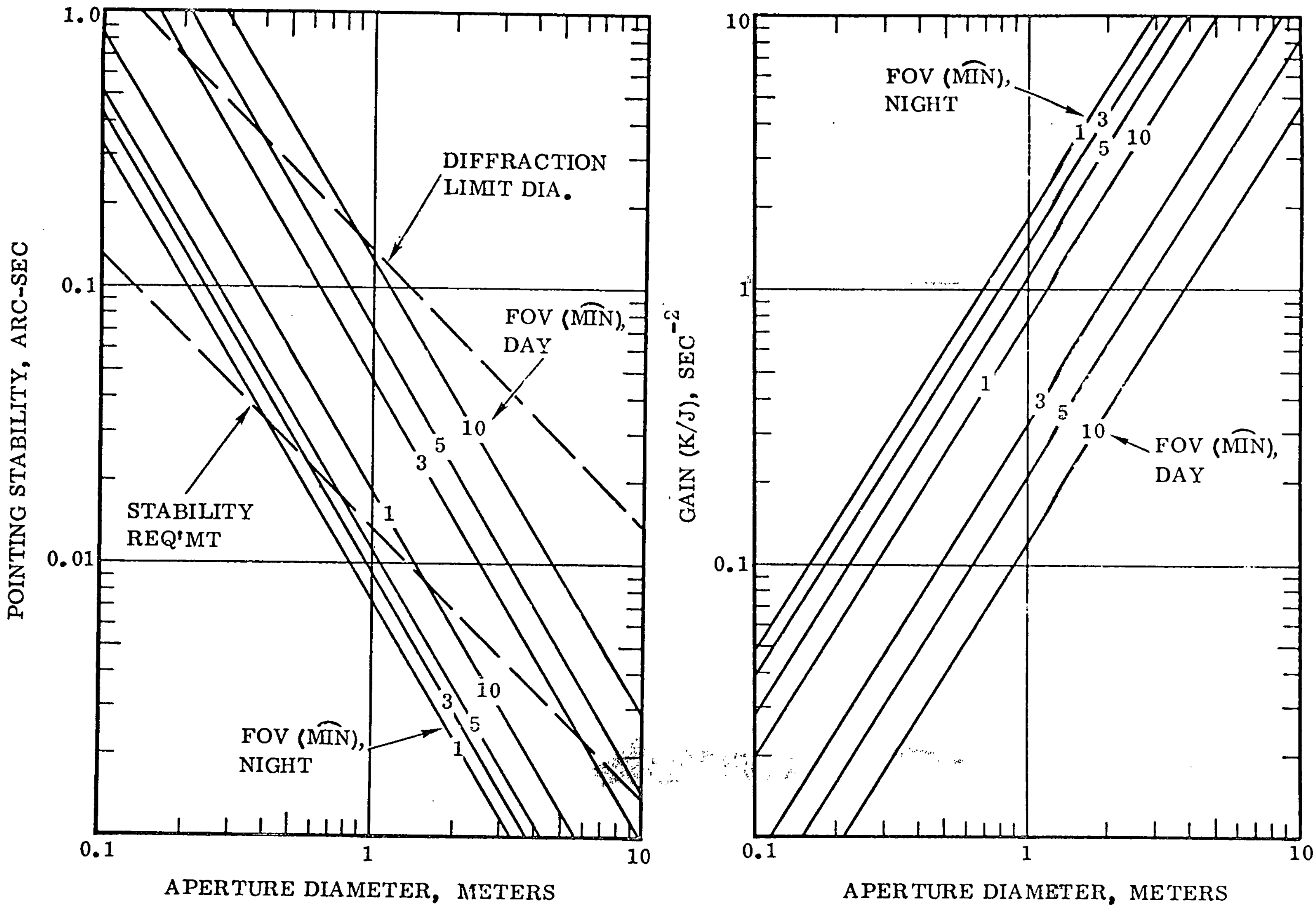

Figure 4-31. Typical Point Stability and System Gain, Detached XMOD, One Control System Integration

the detached mode error is perhaps 50% higher than the attached mode (with perfect isolation). This is directly due to τ_M being less than infinity. As the value of τ_M increases the detached results become equal to that given for the attached situation.

For the detached situation the limitation on guide star FOV for initial capture is estimated at 1 to 5 arc-min as provided by the basic experiment module startracker referenced pointing system. With n equal zero and a final 1 arc-min sensor FOV, the stability requirement, assumed at one-tenth the diffraction limit, is met only for the 3 meter sensor for daytime operation, and 0.7 meter sensor during orbit nighttime. For n equal 1, the situation improves to 0.8 meter during daytime and 0.25 meter during nighttime.

4.3.1.4.2 Vernier Fine Pointing Techniques. No detail work has been done as yet in regard to evaluation of vernier system "on top" of the "body point" system. The motivation for the work is based on a prognostication of CMG actuation errors in the few arc-sec range. If this is true, the weight increase caused by the use of inertia wheels rather than CMGs must be accepted to obtain fine pointing. However, a vernier actuation system "on top" of an experiment module CMG system could be a better choice if the system is not too complex or heavy.

The previously identified alternates for a vernier system on an attached module (see Figure 4-16) also apply for the attached mode. For reference these alternates are:

a) Transfer (movable) Lens
b) Image Compensation
c) Flexure Pivots
d) Magnetic Pushers

Methods (a) and (b) offer the best potential because only a small mass is moved rather than the entire telescope (c and d methods). Study of these methods is recommended starting from a predetermined attitude limit cycle induced by CMG actuation error.

4.3.1.5 Selected Concept. The selected concept for fine pointing is a detached reaction wheel actuated module. The fine point signal is preferably experiment derived. Alternately a large aperture fine point optical sensor boresighted to the experiment line-of-sight would be used.

The detached mode is preferred because:

a) The isolation system required to fine point the telescope in an attached mode is considered complex.

b) If the space station is earth oriented, pointing for astronomy may be incompatible.

c) The space station guided two axis articulation system required to independently orient the experiment module/telescope to a particular target is considered complex.

Reaction wheel actuation was selected to give the experiment module a fine point capability without depending upon an experiment actuation system. The inherent penalty in usage of electrical power by inertia wheels relative to CMGs was accepted to gain this capability.

4.3.2 DETACHED EXPERIMENT MODULE CONTROL ACTUATION. The detached experiment module housing the astronomy experiments will require a control actuation system featuring momentum absorption and unloading because of the long duration missions expected (1 to 2 months). Others, namely material science and possibly earth surveys, will use RCS because of the short duration mission (less than a few days). The fluid physics experiments requiring 10^{-5} to 10^{-3} g acceleration levels are also detached but will use thrust vector control. RCS and thrust vector control systems are well established concepts and no studies of a conceptual nature were performed. However, the development of a momentum actuation and unloading system concept and sizing data, suitable for the detached long duration astronomy experiments, was considered pertinent to phase A experiment module SCS studies.

4.3.2.1 Momentum Actuation System

4.3.2.1.1 Capacity Requirement. The momentum actuation system requirement is to react the environment and possibly supply maneuvering torque (if maneuver is not better supplied some other way, e.g. RCS).

At 200 n.mi. and above (say less than 1000 n.mi.) the environment torque is mainly gravity torque. In general, this torque is composed of a secular and cyclic component. The maximum cyclic impulse and secular impulse per orbit is plotted against experiment module pitch/yaw inertia in Figure 4-32. Inertia about the roll axis is assumed much smaller than pitch/yaw. This is the case for the astronomy experiment modules. For reference the inertias for each astronomy FPE installation in the common module CM-1 are noted.

The momentum transfer system must be sized to absorb the cyclic plus that portion of the secular not yet unloaded by the unloading system. That portion (termed the residual secular) depends upon the unloading system period and duty cycle as illustrated by Figure 4-33. The area corresponding to a duty cycle of 0.25 and period 0.25 to 0.5 orbits (2 to 4 cycles/orbit) is identified as appropriate to magnetic dumping. The area of duty cycle equal to 0.5 and period 0.25 to 0.5 is identified as appropriate to dumping by millipound thrusters, e.g., NH_3 resistojets. Either way, dumping is somewhat continuous, and uses small torques. This concept is appropriate to the fine point requirement, and minimizing momentum system storage requirement. If high thrust RCS were used infrequently to unload, say

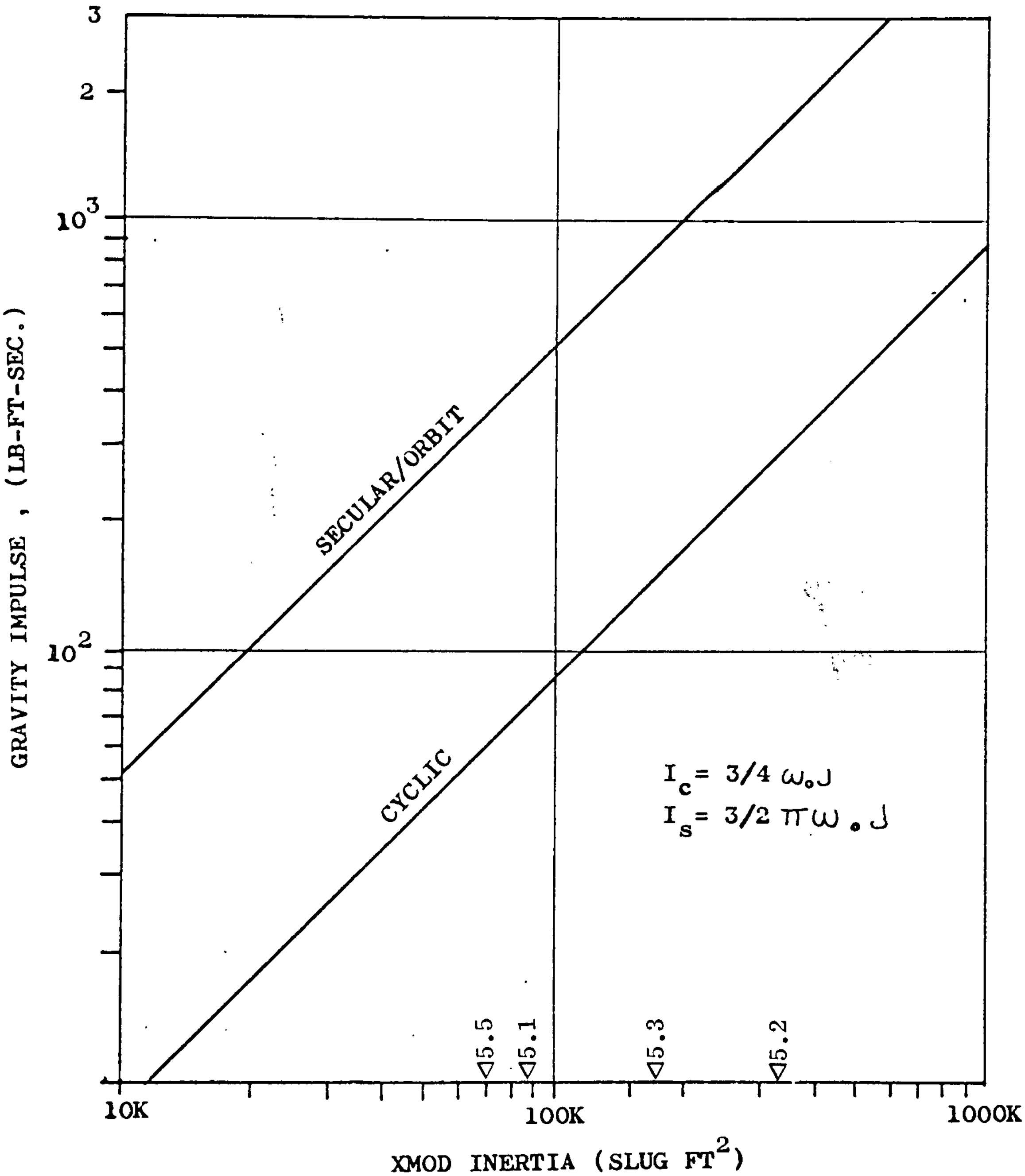

Figure 4-32. Maximum Secular and Cyclic Gravity Gradient Impulse vs. Experiment Module Inertia

every 5 orbits, the residual to secular ratio is naturally 5 rather than roughly 0.3 for the low continuous torque systems. Since some of the larger modules have secular values of 1000 ft-lb sec per orbit, infrequent use of high thrust RCS is not considered advisable.

Herein a value of 0.4 residual/secular is used. The value is sufficiently conservative to cover both the magnetic and millipound thruster technique. Adding this amount to the maximum cyclic gives the required amount to react the environment. If, in addition to environment reaction, maneuvers are to be performed by the momentum system, then additional capacity in an amount dependent upon maneuver rate is needed. This is shown on Figure 4-34, which gives the experiment module momentum capacity needed for a specified maneuver rate and vehicle size.

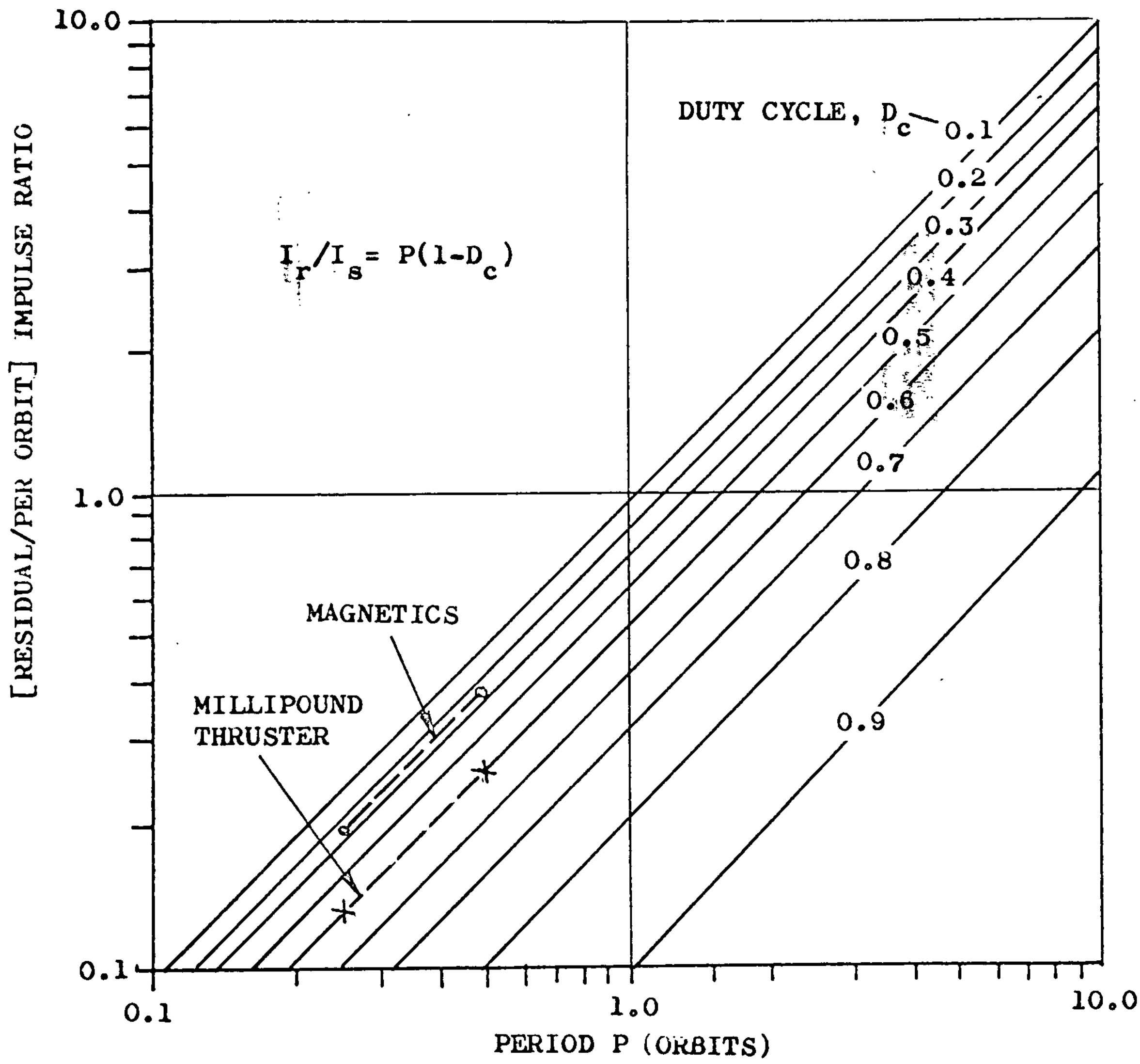

Figure 4-33. Residual/Secular Momentum Ratio vs. Unloading System Period and Duty Cycle

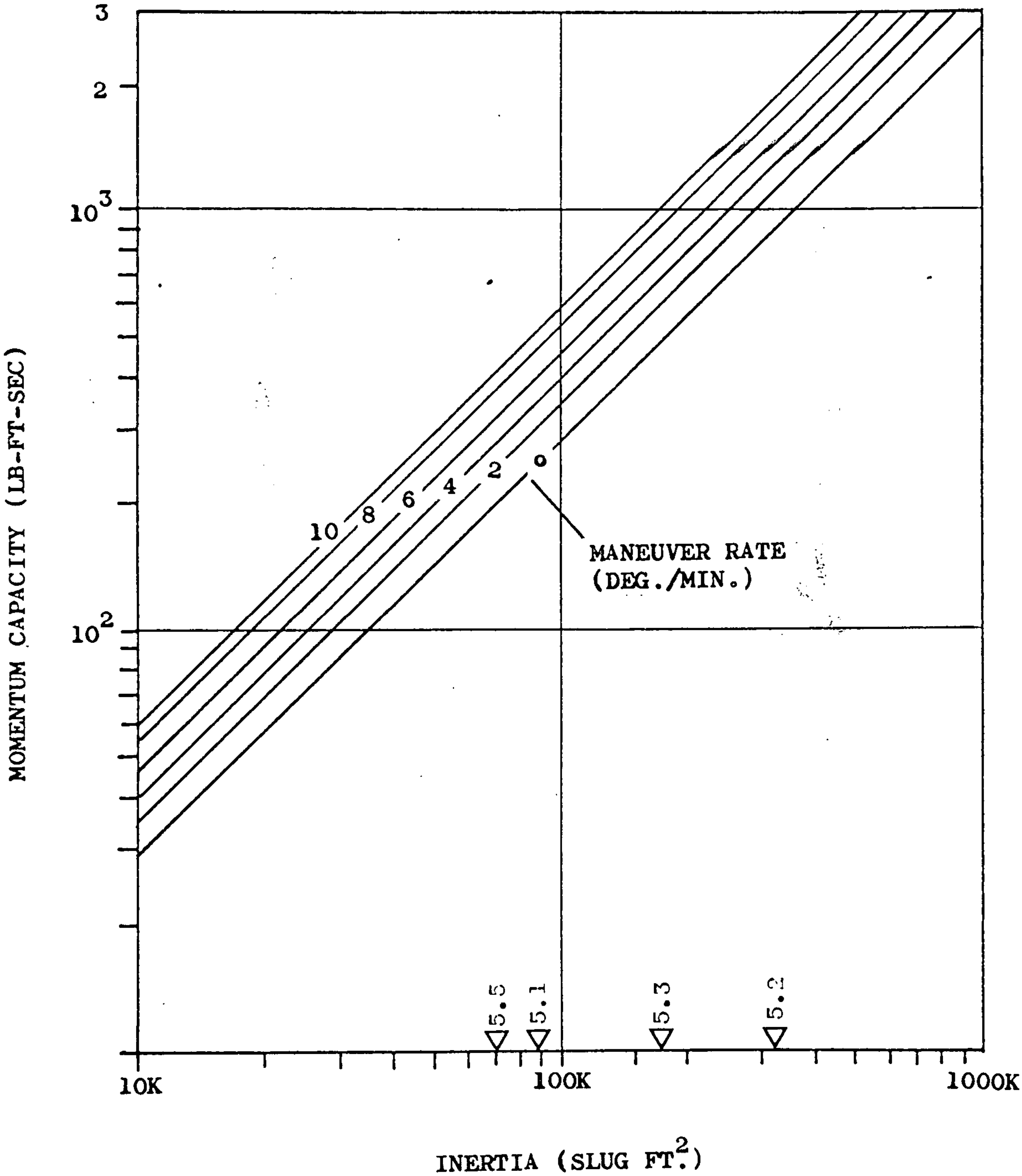

Figure 4-34. Experiment Module Required Momentum Capacity vs. Inertia, Maneuver Rate

4.3.2.1.2 Momentum System Implementation. A selection of maneuver rate is needed. The OAO maneuver rate is believed to be 2 deg/min whereas values of up to 10 deg/min have been informally expressed as desirable from experimentor sources. Herein a value of 6 deg/min is used.

Three alternate techniques are considered to supply the environment reaction and 6 deg/min maneuver rate. These are:

a) Three inertia wheels for environment reaction and hydrazine fueled RCS for maneuvers.

b) Three inertia wheels for environment reaction and two scissoring two-gimbal-CMG's for maneuvers (see Figure 4-8).

c) Four single-gimbal-CMGs supply both environment reaction and maneuvers.

For (a) or (b) above the inertia wheel capacity is that for zero maneuver rate on Figure 4-34. For (c) above each of the four CMGs is canted 15 degrees from absolute saturation*. Each of the four gyros is then required to have a wheel momentum of 0.596 times the 6 deg/min line on Figure 4-34. For each of the two-gimbal-CMG's used exclusively for maneuvers, the required size is simply the maneuver impulse imparted to the vehicle to perform the 6 deg/min maneuver for a ±60 degree scissoring gimbal angle. The unit sizes are plotted on Figure 4-35.

Weight, size and power data for the momentum actuator is available from Table 4-5. For the single or double-gimbal-CMG the electrical power required to react the environment and maneuver the experiment module is included in the operating power. However, the tabulation does not include the electrical power needed to react the environment for the inertia wheels. This was calculated separately and is given in Figure 4-36. It is noted that this inertia wheel power penalty, applied to concept (a) and (b), is accepted to obtain the fractional arc-sec stability attributed to inertia wheels.

For concept (a) the maneuver rates would be established by a RCS system (hydrazine, I_{sp} = 220 sec, thruster leverage typically about 5 feet). Then each time the spacecraft is maneuvered, an angular rate is established and then terminated (say 1 to 10 deg/min in range of interest). The weight of the RCS fuel required per maneuver is given on Figure 4-37. Assuming 6 deg/min as an acceptable rate, about 1.0 lb for the large and 0.25 lb for the small vehicles is needed per maneuver. While the per maneuver fuel is not alarming, if one figures on about 5 maneuvers/ day average, the fuel rate per month is 150 lb for the large and 37.5 lb for the small vehicles. It is assumed that the inertia wheels are braked to a fast stop to save time with appropriate RCS reaction. Otherwise additional RCS fuel is expended in the maneuver.

---

* Saturation is assumed to occur at a gimbal angle of 30 degrees.

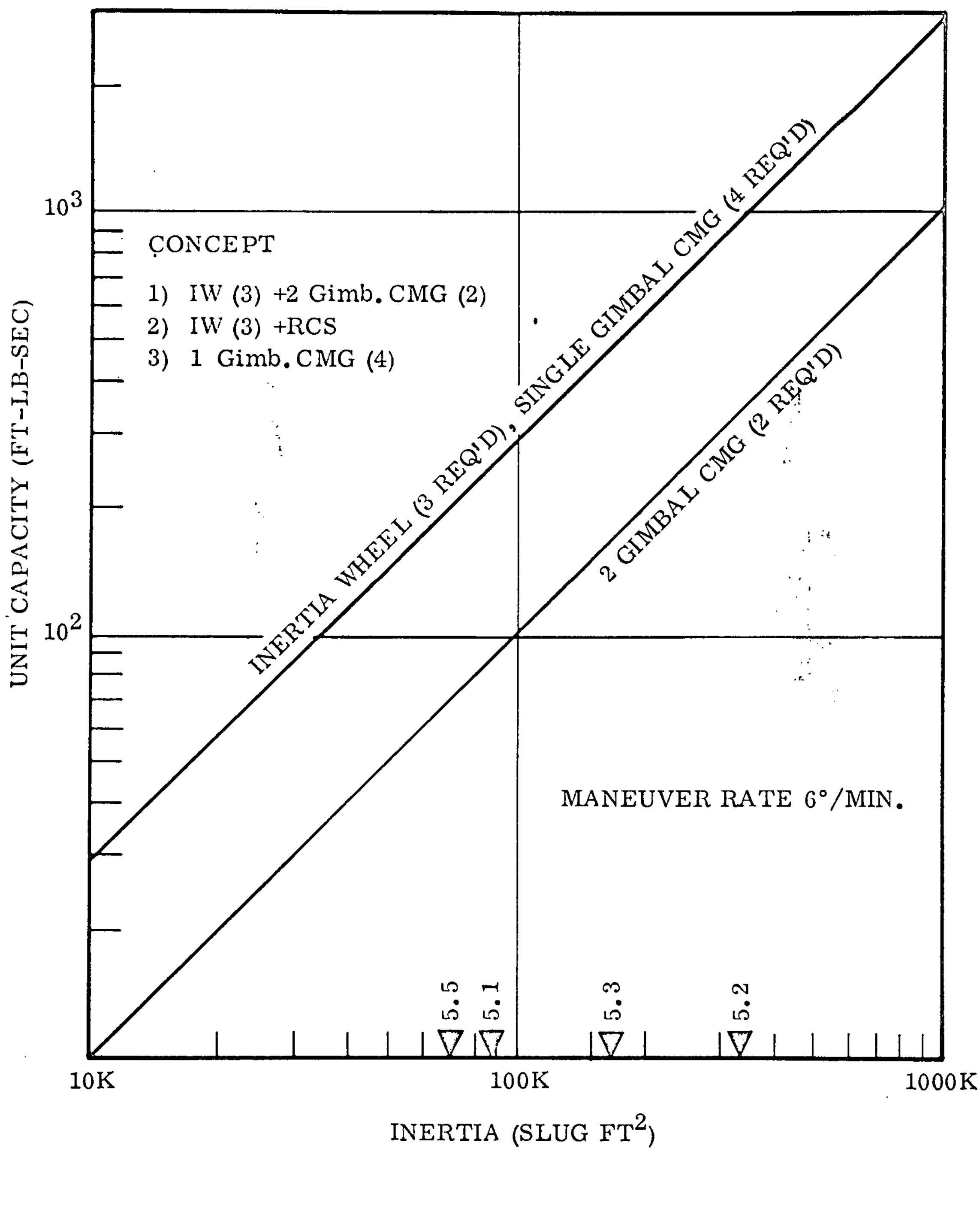

Figure 4-35. Momentum Unit Capacity vs. Vehicle Size

Table 4-5. Reaction Wheel, CMG Sizing Data Listing

REACTION WHEEL ASSEMBLY DATA

H	Equivalent Wt.	Actual Wt.	Rotor Wt.	Steady Running Power	Outside Diameter	Height	RPM	Bearing Number
20	22.1	18.7	7.8	3.0	12	5.64	5000	38H
50	29.3	24.2	11.2	4.6	14	6.17	6000	38H
75	33.8	26.7	11.4	6.4	16	6.78	7000	38H
100	38.2	28.8	11.8	8.5	17	7.07	8000	38H
150	51.0	38.0	18.0	11.9	18	7.37	6459	100H
200	62.3	48.6	24.6	12.2	20	7.93	4919	200H
300	73.3	56.5	28.3	15.0	22	8.47	5285	200H
400	88.9	69.8	32.2	16.2	26	9.52	4472	201H

CONTROL MOMENT GYRO DATA

H	Equivalent Wt.	Actual Wt.	Rotor Wt.	Average Operating Power	Envelope Diameter (Inches)	RPM	Bearing Number	Program
30	29	23	8.5	4.8	19.88	5142	100H	Single Gimbal CMG 11
60	35	28	12.4	6.2	19.88	5999	100H	
90	41	33	17.1	6.5	19.88	5999	100H	
120	46	35	16.5	8.2	22.40	6750	100H	
200	60	45	21.4	12.3	18.00	6666	200H	
300	72	57	28.0	11.7	20.00	6000	200H	
500	99	77	38.4	15.7	24.00	5000	202H	
700	128	99	44.6	16.8	30.00	4000	203H	
900	144	110	60.3	27.1	26.00	4615	105H	
1100	161	125	65.1	24.1	30.00	4000	105H	
30	38	31	10.1	5.8	19.88	5000	101H	Two Gimbal CMG 21
60	45	38	12.4	6.3	19.88	5999	100H	
90	52	44	17.1	6.6	19.88	5999	100H	
120	58	47	16.5	8.2	22.40	6750	100H	
200	74	59	21.4	12.3	18.00	6666	200H	
300	88	73	28.0	11.8	20.00	6000	200H	
500	120	98	38.4	15.8	24.00	5000	202H	
900	169	134	60.3	27.1	26.00	4615	105H	
1100	190	154	65.1	24.1	30.00	4000	105H	

Note: 1. Supplied by Sperry-Phoenix.

2. Torque less than 0.1 momentum (CMGs only).

In scheme (b) or (c) CMGs are used for maneuvering at a small power penalty. No RCS fuel (Figure 4-37) is expended.

4.3.2.1.3 Selected Concepts. Initially the four CMG system was selected with the condition that fine pointing be supplied by an actuation system internal to the experiment identical in concept to that employed in Stratoscope II (Reference 4-5). This amounted to placing a fine point requirement on the experiment to save reaction wheel electrical power (350 watts for the worst case experiment module, 5.2) and slewing RCS fuel (150 lb/month for five 6 deg/min manouvers/day of 5.2).

Subsequently the reaction wheel power penalty was accepted in the interest of fine pointing. The reaction wheel system, with two two-gimbal-CMG's for maneuvering was selected. The four-CMG system is however retained as a highly promising alternate.

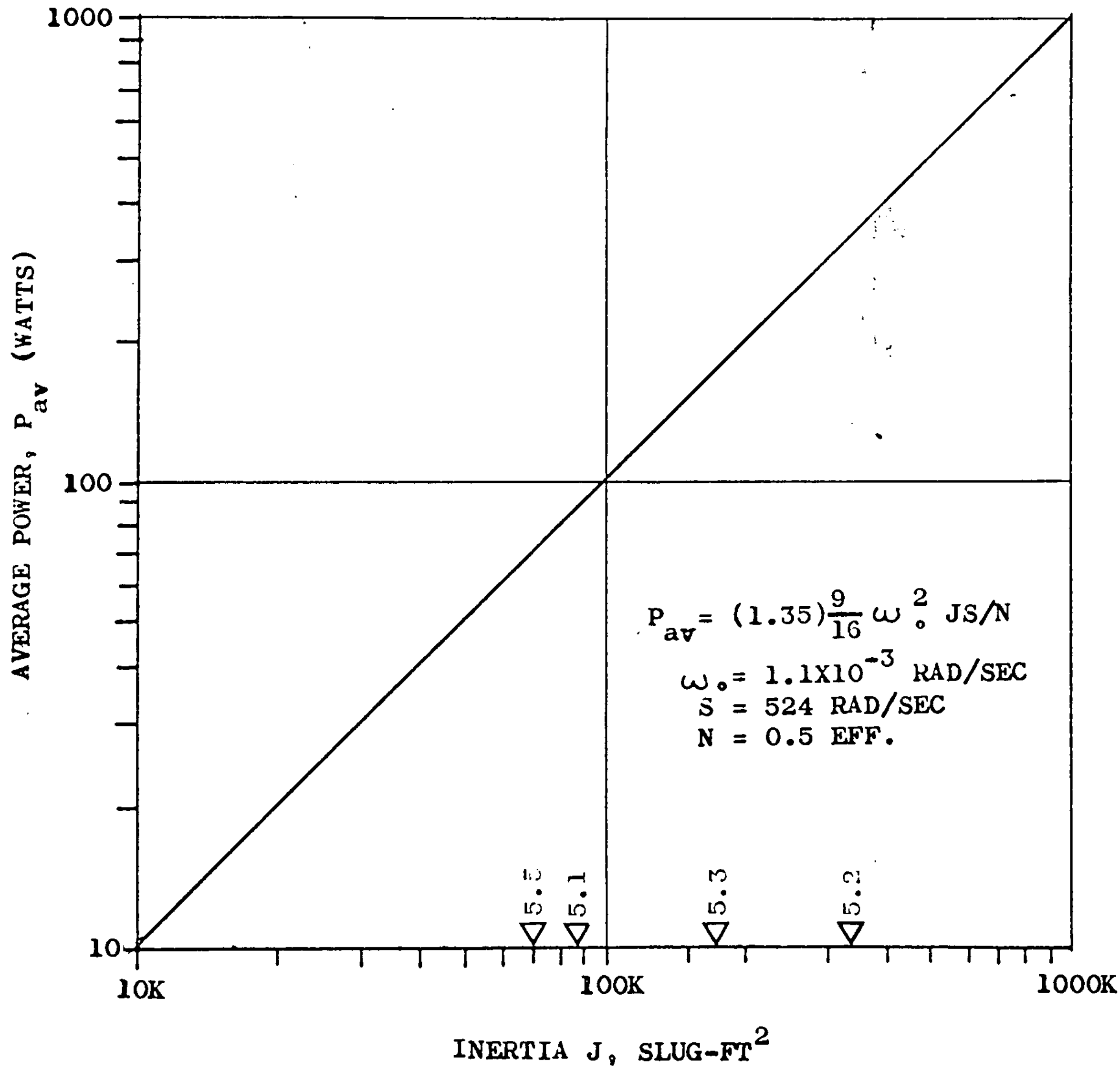

Figure 4-36. Inertia Wheel Average Power to React Environment vs. Vehicle Size

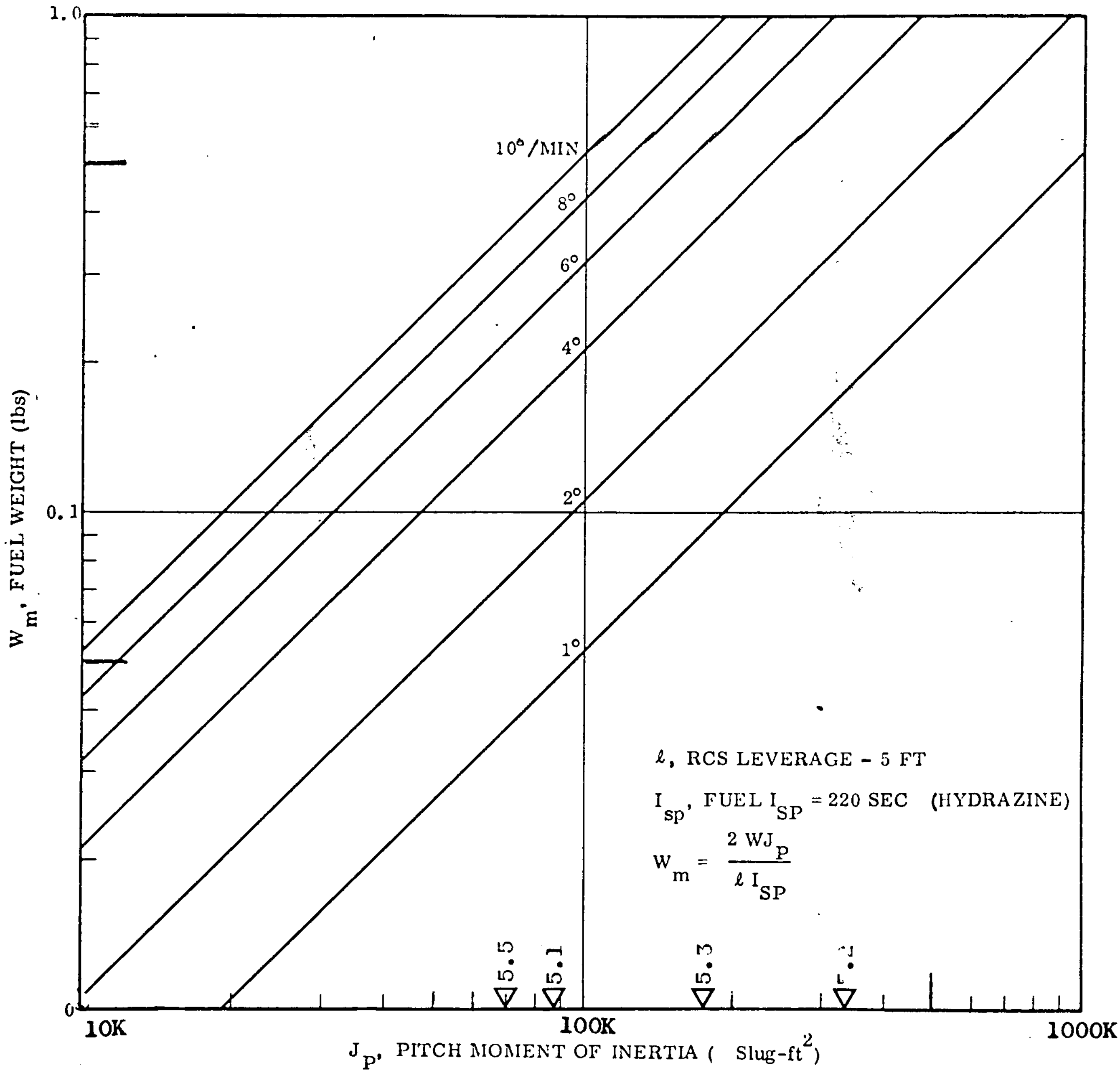

Figure 4-37. Fuel Weight vs. Vehicle Size Per Maneuver

4.3.2.2 Momentum Dumping System. The objective of the study is to compare desaturation (momentum dumping) techniques. Specifically an RCS system is compared to an on board magnetic coil system energized appropriately to interact with the earth magnetic field. The RCS system used was an ammonia resistojet with specific impulse at 350 seconds and leverage at 7.5 feet. Several magnetic coil concepts were considered. A large diameter flat coil was compared to a long slender iron core (bar) electromagnet (50:1 length to diameter ratio). Variations on the bar electromagnet concept were 3 fixed orthogonally mounted units, two single-rotation-pivoted units, and one two-rotation-pivoted unit. All three variations accomplish the same purpose, establishing a dipole moment vector.

Regardless of technique the requirement is the same, that of reacting the average gravitational torque. The maximum amount is used to size the system and occurs when the spacecraft long axis is 45 degrees from the orbit plane. Figure 4-38 evaluates the torque. The previously mentioned duty cycle of 0.25 is used to size the required magnetic torque at four times the average. The maximum instantaneous gravitational torque is also shown for reference.

4.3.2.2.1 Earth Magnetic Field Discussion. A rough characterization of the earth magnetic field is shown on Figure 4-39. The field actually moves in a complicated way but for present purposes, it is sufficient to observe that it roughly cones about the orbit normal two times per orbit. It is desired to generate the opposite directed or unloading torque, $\bar{T}_M$, magnetically by waiting until the spacecraft is at the proper position in orbit such that energization of the spacecraft onboard coil produces the dipole moment, $\bar{M}$ (shown perpendicular to the spacecraft long axis). Two earth field positions are appropriate and each occurs twice/orbit making a total of four opportunities. Each time,

$$\bar{T}_M = \bar{M} \times \bar{B}_E$$

where $\bar{M}$ is the dipole moment
$\bar{B}_E$ is the earth magnetic field vector
$\bar{T}_M$ is the magnetically induced torque

For most applications, the location of the spacecraft long axis with respect to the orbit is arbitrary. Further, it is presently intended that unloading be accommodated while the experiment is in progress. As implied in Figure 4-39, the spacecraft dipole moment (coil axis) will not in general be at the ideal position, 90 degrees from the earth field vector. The torque that results will be reduced as given by the above equation.

Herein, the overall result of the above earth field considerations was an estimated duty factor of 0.25 and a period of four times per orbit. No degradation or loss was added for non-perpendicularity of dipole moment and earth field. In

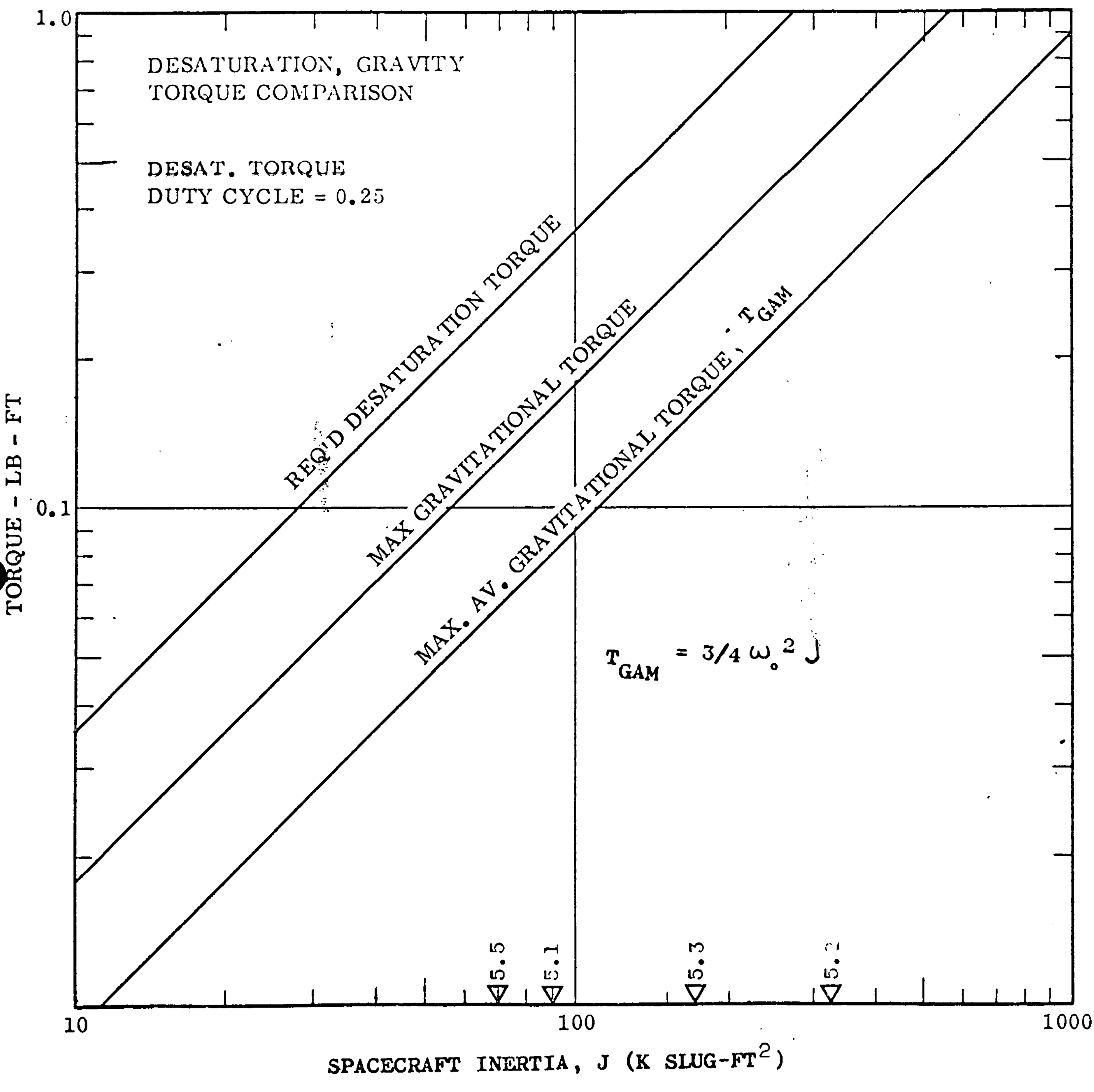

Figure 4-38. Desaturation, Gravity Torque Comparison

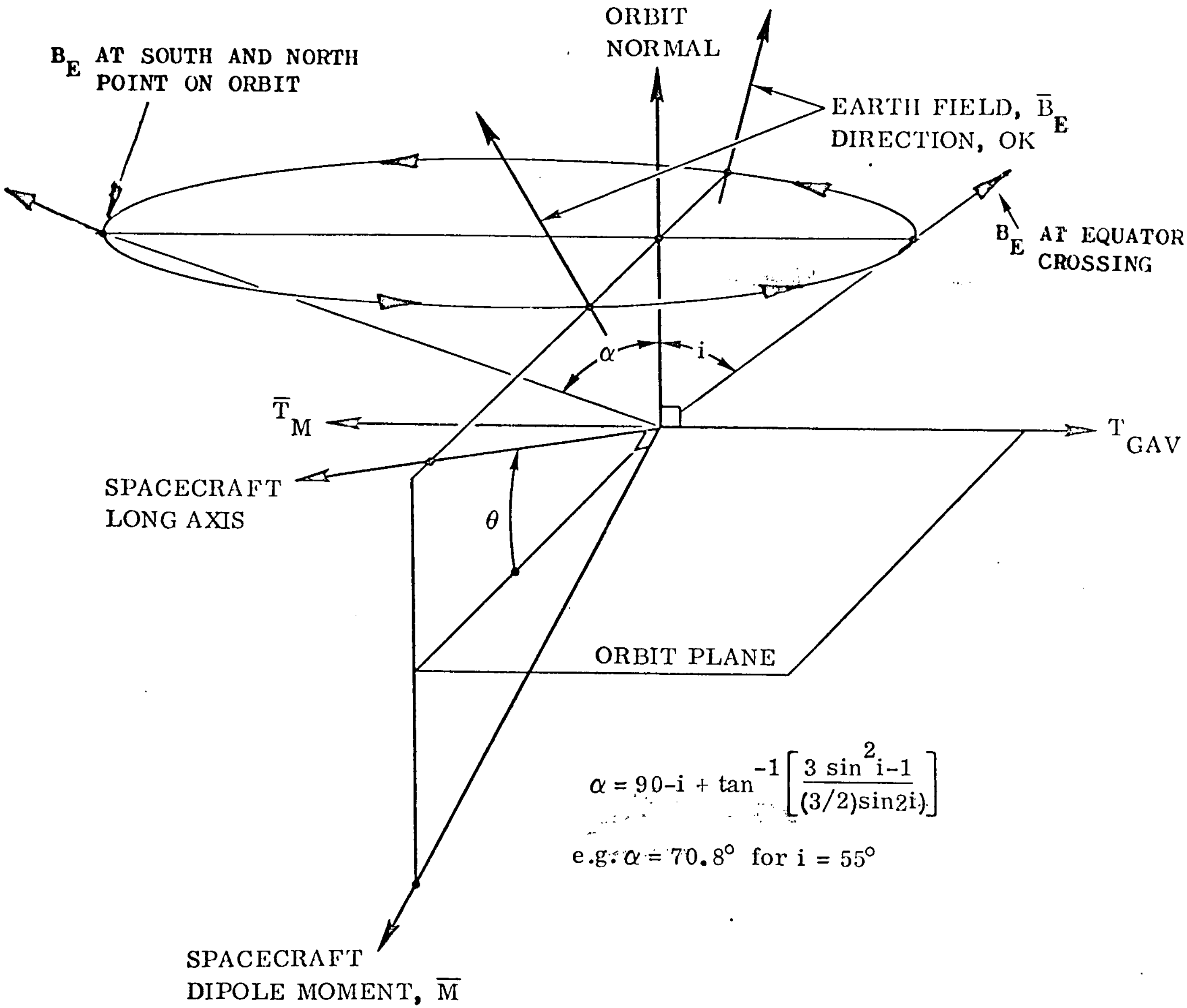

$$\alpha = 90 - i + \tan^{-1}\left[\frac{3\sin^2 i - 1}{(3/2)\sin 2i}\right]$$

e.g. $\alpha = 70.8^\circ$ for $i = 55^\circ$

Figure 4-39. Orbit Positions for Magnetic Unloading addition, the magnitude of the earth field intensity varies throughout the orbit. Herein the value was assumed constant at 0.4 gauss.

4.3.2.2.2 RCS Fuel Rate. The RCS fuel rate is calculated based upon the following ground rules and assumptions:

a) The angular offset from the orbit plane is equally likely to be in any position.

b) The unloading control law will be sophisticated enough to direct the thrust in the direction of the accumulated secular momentum vector rather than along the secular plus cyclic component.

c) Vectoring losses in RCS fuel are excluded.

All three assumptions tend to reduce the fuel usage from the worst possible, that of a continuous spacecraft long axis offset 45 degrees from the orbit plane. The resultant fuel rate is given on Figure 4-40. For reference the worst possible fuel rate is a factor of 1.57 higher in value.

4.3.2.2.3 Magnetic Unloading. Sizing relationships for a flat large diameter coil and bar electromagnet relating physical characteristics to torque output is given in Reference 4-3. Figure 4-41 gives the resultant bar magnet and flat coil design data.

Assume a 1.06 ft-lb output torque corresponding to the maximum requirement of experiment 5.2, the 3 meter telescope. Table 4-6 gives design data for each technique.

Table 4-6. Bar Magnet, Flat Coil Comparison
(Torque equal 1.06 ft-lb)

	Bar Electromagnet (1)*	Flat Coil
Size	18 ft long	14 ft coil diameter
Weight	800 lb	115 lb
Peak Power	120 watts	1950 watts

(1) Saturation flux of 10,000 gauss or 1 weber/meter^2
* One bar electromagnet is used here. In the actual design 10 modular shorter length units are used.

Comparison of the two type magnetic torquers shows that the bar magnet is much heavier but does not require nearly as much electrical power as the bulkier, lighter flat coil. This is the essential difference. As indicated the flat coil is sensitive to diameter, its physical characteristics becoming worse as diameter is reduced. For the bar magnet a saturation flux of 1 weber/meter^2 was used because this value is readily obtained. It is believed to be the OAO design value. However,

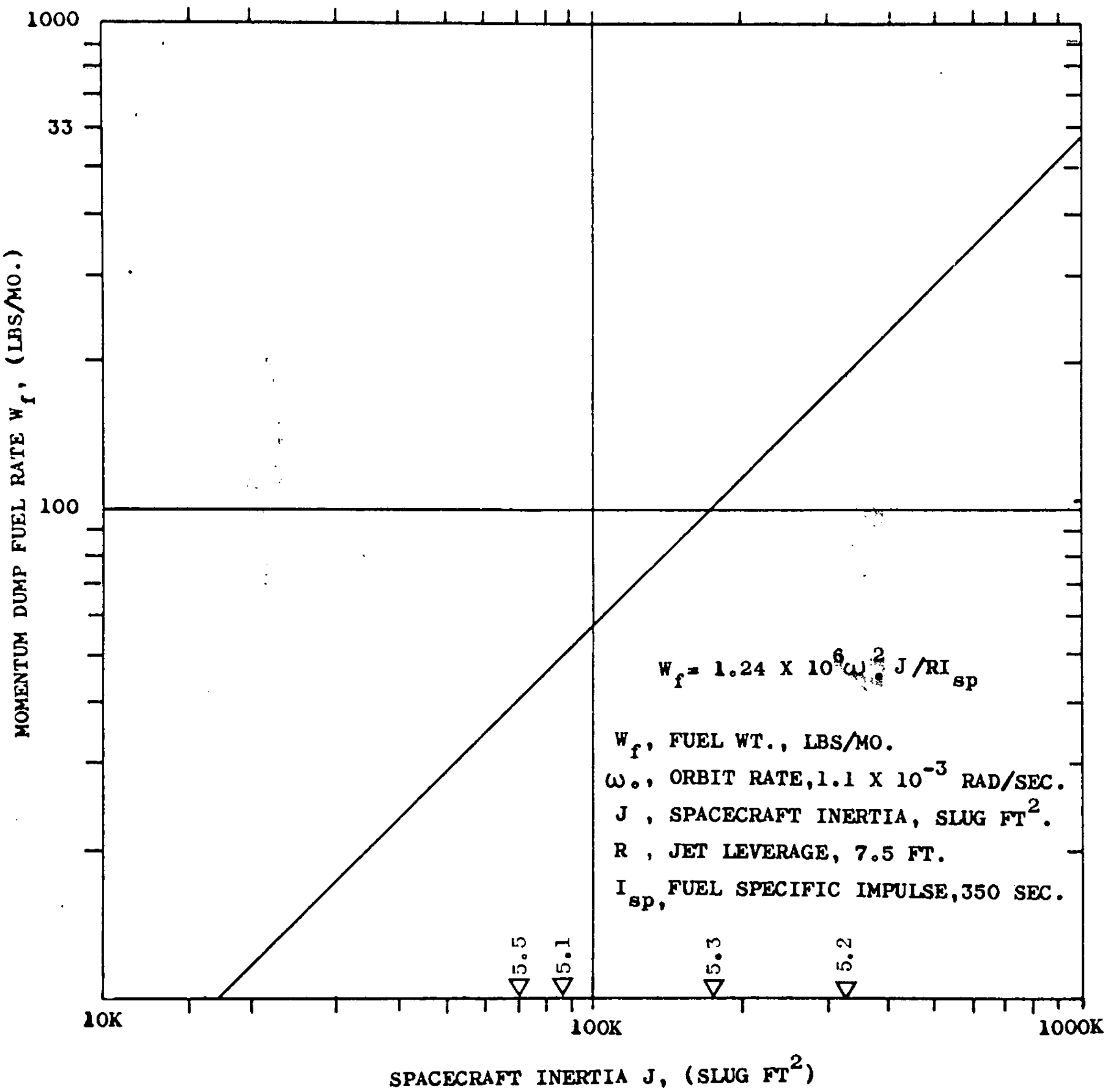

Figure 4-40. Fuel Rate vs. Spacecraft Inertia for RCS Unloading

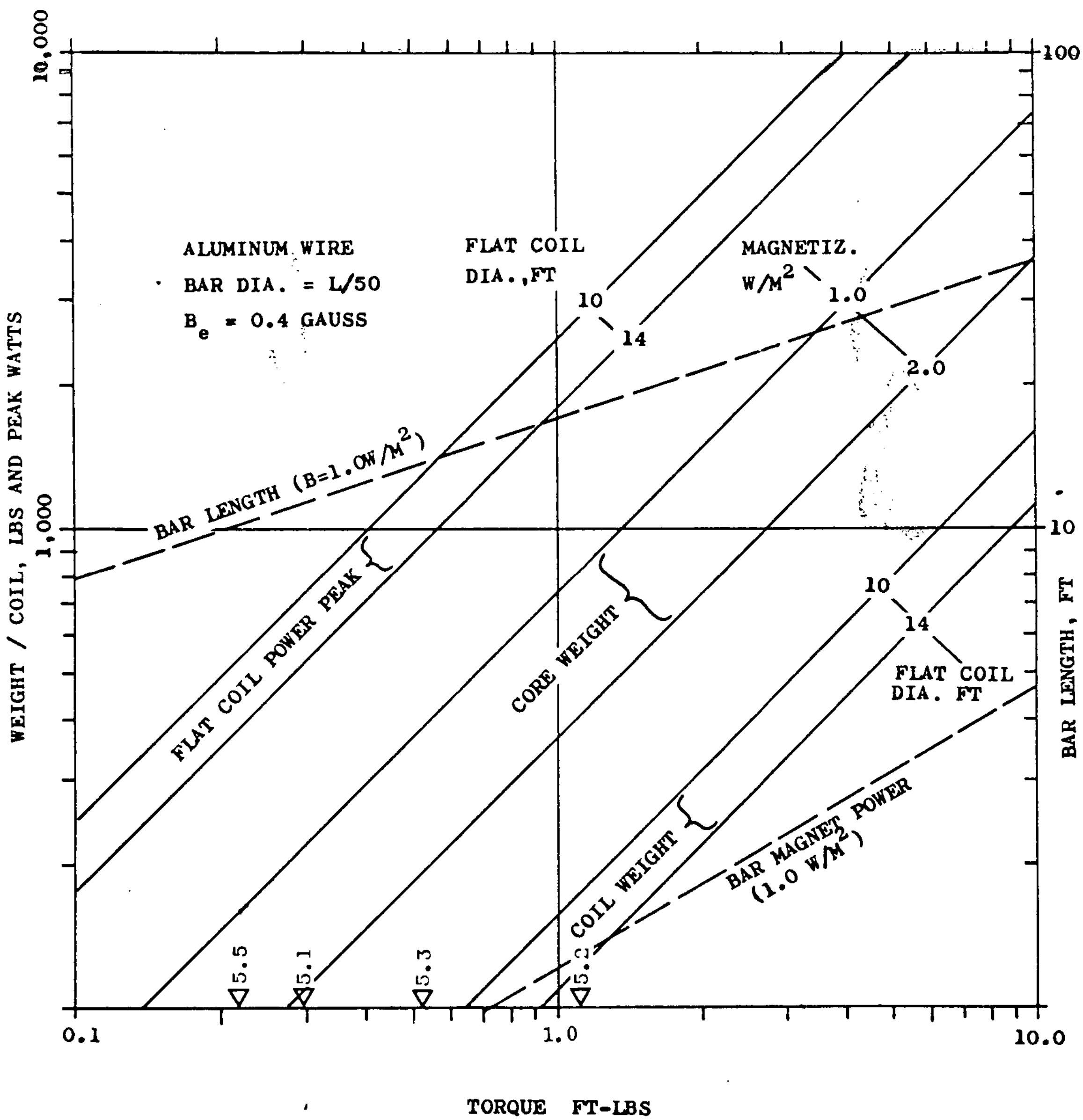

Figure 4-41. Bar Magnet, Flat Coil Design Data

it is noted that materials exist which perhaps can yield 2 weber/meter^2 in a practical situation. Further study is recommended in this area because increasing the maximum magnetization proportionately reduces the weight.

Comparison of the bar magnet with the flat coil requires inclusion of a power system penalty for the flat coil. The kind of power needed is dc on demand with no special regulation requirement. This power is available from solar panels and appropriate electronics. Power system weight penalty estimates have ranged from 0.5 to 1.0 lb/watt (average power). The current value is 0.77 lb/watt. Note that the duty cycle of 0.25 implies that the peak power is four times the average. For the flat coil the "system weight" is defined to be weight of three coils plus the weight of power system to drive it. For the bar magnet, drive power is negligible, the weight is simply that of one, two or three cores. This comparison is illustrated on Figure 4-42. It is seen that the large diameter flat coil has the weight advantage unless the number of bar magnets are reduced to one by providing a two axis gimbal.

It is emphasized that system weight is an important but not all-important criteria for system selection. Dollar cost for example favors the bar magnet relative to the 3 flat coils with increased power system capacity.

For comparison to the RCS system, the time in which the initial weight of the magnetic system is equaled by the RCS fuel is:

t (flat coil) = 86.4 days

For jet leverage equal to 7.5 ft.

t (3 iron core) = 420 days
t (2 iron core) = 280 days
t (1 iron core) = 141 days

Considering mission times of 2 to 10 years, the use of magnetic torques for unloading is advantageous weightwise.

4.3.2.2.4 Selected Concepts. Neither the resistojet or the magnetic system is regarded as eliminated by Phase A study. The current preference is a two-axis gimbal bar electromagnet because of less complex installation, compatibility with use of modularity, and lower cost.

Based upon this same dollar cost analysis, the magnetic concept was eventually selected over that of the resistojet. The resistojet was the initial selection because of its flexibility. That is, there is no dependence on earth magnetic field and it can also be used to provide stationkeeping with high specific impulse and gentle thrusting. Also some experiments may be sensitive to magnetic fields but not to the ammonia exhaust product. For other experiments, the vice-versa condition may apply.

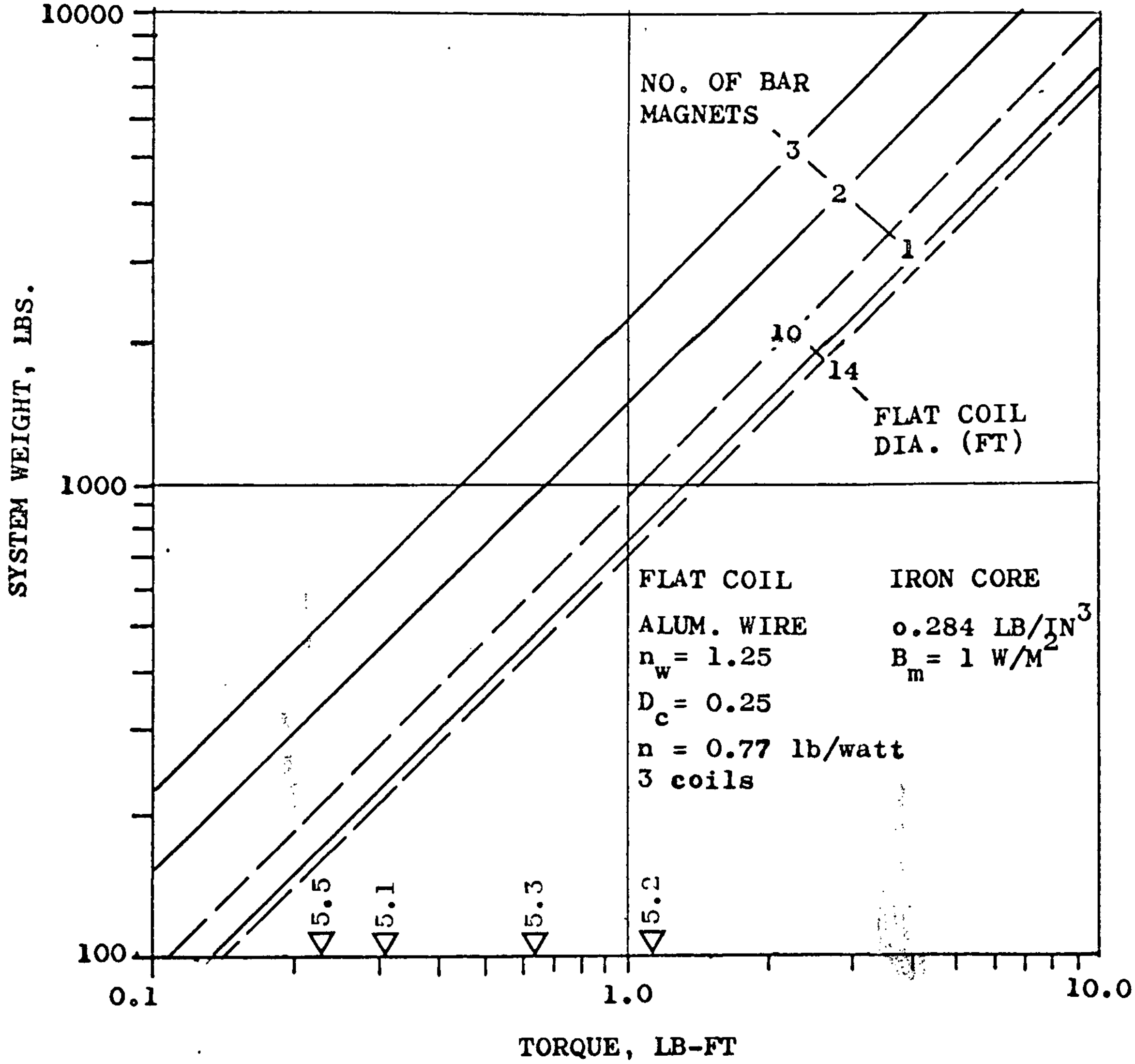

Figure 4-42. Bar Magnet, Flat Coil System Comparison

4.3.3 ORBIT LOW ACCELERATION SYSTEMS ANALYSIS. As for the pointing analysis, the material herein is a summary of more detailed work in Reference 4-3.

4.3.3.1 Attached Low Acceleration Systems. Figure 4-43 illustrates orbital low-g system concepts for attached configurations. Three control concepts are identified which generally increase in complexity as lower maximum g levels are required at the experiment. As discussed under pointing perturbation sources (paragraph 4.3.1.2) space station jitter at 0.5 to 3 Hz and gravity gradient (GG) plus air drag, at orbit frequency and below, are the sources of perturbation which tend to degrade the orbital zero g environment.

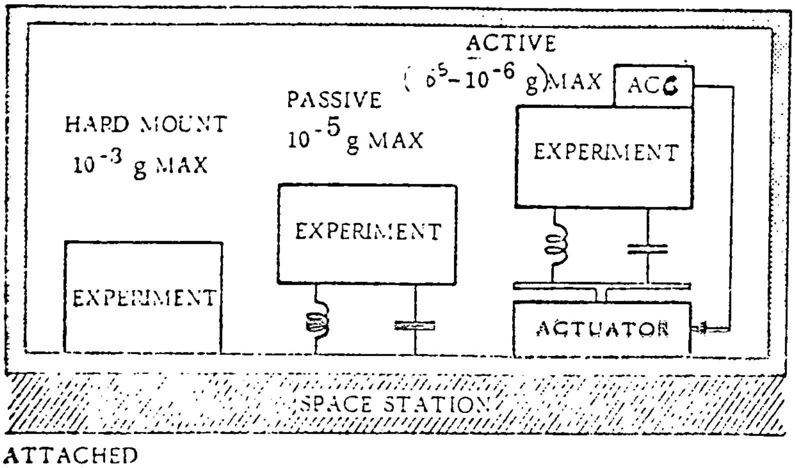

Figure 4-43. Attached Low-g Concepts

For a representative space station configuration, the magnitude of acceleration experienced by the vehicle as a result of crew activity was evaluated for a twelve man crew in an assumed distribution and level of activity ranging from sleep to moderate exercise. The resultant force and moment, translational and rotary accelerations are given in Table 4-7.

The jitter is at about 1 Hz. Assuming concentration at this frequency, and a maximum displacement of the experiment from the space station center of mass equal to 40 feet, the peak value is 2.58×10^{-4} g's. This value is based upon rigid body analysis. An estimate including flexural effects, but based on rigid body analysis, is 1×10^{-3} g's for a space station hardmount.

For many experiments this g level maximum is not low enough. The initial technique to improve upon this hardmount value of 10^{-3} g's is to use a passive spring-dash pot arrangement shown in Figure 4-43. The experiment is constrained by the spring to react a 10^{-6} g equivalent force without excessive deflection. The damping ratio or viscous constant provided by the dashpot should be very low to enhance isolation. However, it cannot be zero because no reduction in initial oscillation will occur. Assume that the damping is set to a negligibly small but finite value. Then the calculation of spring constant versus experiment weight and required maximum g level shown in Figure 4-44 applies. In Figure 4-44 a 1×10^{-3} g input jitter at 1 and 0.5 Hz is assumed and the spring constant needed to reduce this jitter to 10^{-4} and 10^{-5} g's is shown.

For reference the weight, g requirement points for fluid physics (5.20-1) and space biology (5.9/5.10) are plotted for a 10^{-3}g input at 0.5 Hz. The required spring constants are 0.1 lb/inch for 5.9/5.10-3 and 1.7 lb/inch for 5.20-1. The 0.1 lb/inch spring constant is low but is considered feasible.

Table 4-7. 12 Man-Crew Activity Levels (RMS Values)

Direction	Force lbs.	Torque lb-ft	Acceleration Linear g's	Acceleration Rotary rad/sec^2
X	13.25	93	5.52×10^{-5}	0.91×10^{-4}
Y	6.62	446	2.76×10^{-5}	1.085×10^{-5}
Z	6.76	301	2.82×10^{-5}	0.733×10^{-5}
Vector Totals			6.8×10^{-5}	0.92×10^{-4}

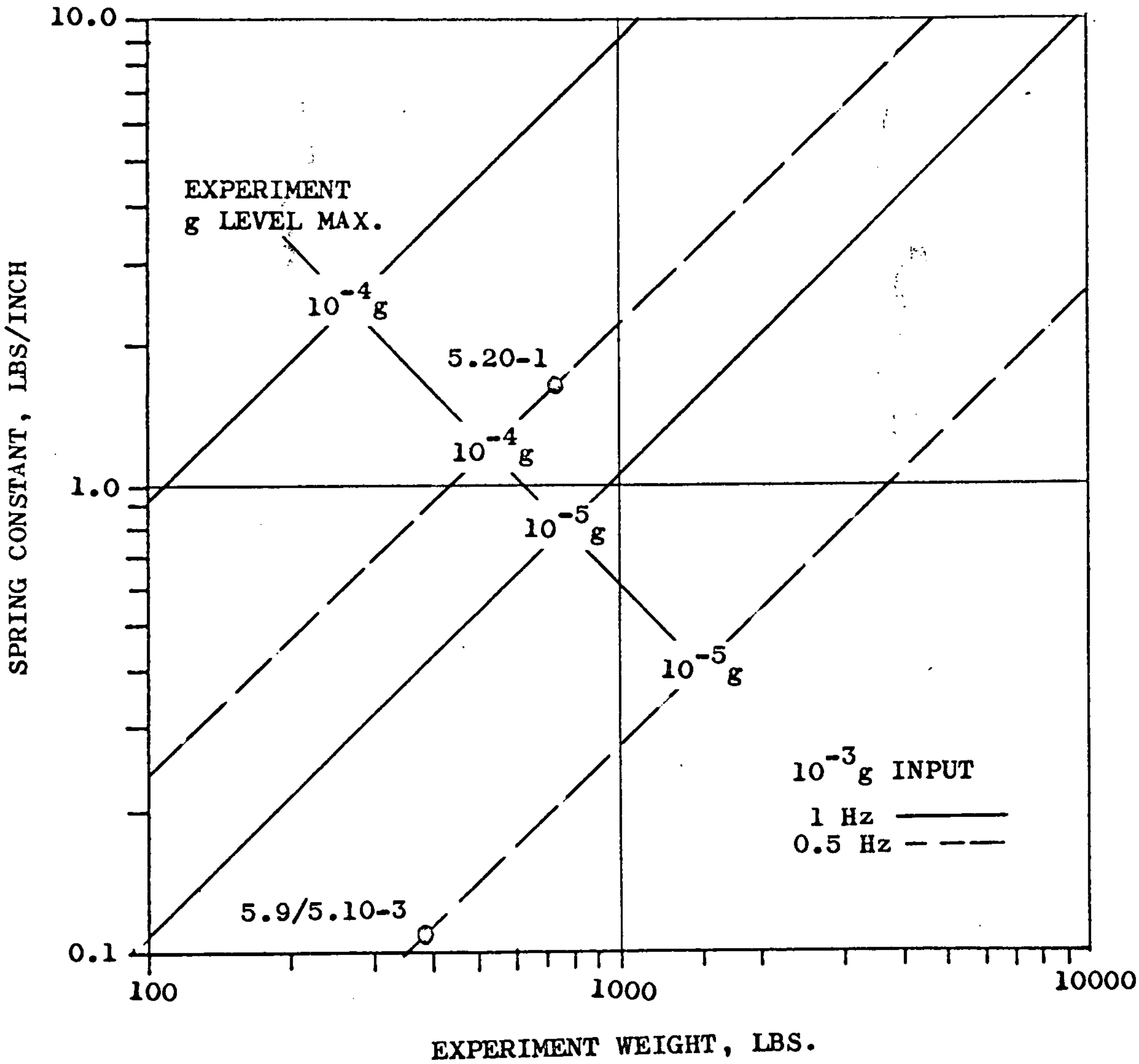

Figure 4-44. Passive Isolation Spring Constant vs. Experiment Weight

The attached-active system shown on Figure 4-43 is regarded as a backup for the simple passive spring-dashpot isolator. Note that the same passive isolator is part of the active system and still accomplishes isolation at high frequency. However an accelerometer monitors experiment residual acceleration not removed by the passive isolator. This residual acceleration would be at low frequency because the passive isolator is very effective at high frequency. As shown the residual low frequency acceleration signal is used to actuate the platform on which the experiment is mounted in a compensating manner.

Table 4-8 lists the numerical rationale leading to a 10^{-6} g maximum estimate for air drag. The tabulation reflects the use of maximum solar activity and maximum diurnal effect. A space station area of 9000 ft^2 and weight of 315,000 lb were assumed (see Figure 4-1).

Figure 4-45 gives an evaluation of the g level induced by gravity gradient. This is dependent upon the displacement of the experiment from the space station center of mass. As shown a 10^{-6} g environment occurs beyond a 10 foot displacement.

4.3.3.2 Detached Low Acceleration System. As the low g requirement becomes more stringent (herein estimated at 10^{-6} g), eventually the experiment is forced into a detached mode. If the experiment is free floated aboard the space station, jitter is no longer present but the long period nature of GG and air drag forces causes a requirement of large experiment to space station wall clearances. For example a 10^{-6}g maximum sinusoidal time history at orbit frequency (1.1×10^{-3} rad/sec) corresponds to about a 30 foot maximum displacement also at orbit frequency. Such is the nature of the motion induced by air drag and GG forces. There is little gained by separating the experiment from the space station and hard mounting it to a free-flying experiment module because air drag perturbations will still be present and can be (in extreme case) as high as 10^{-6}g. However, if as illustrated in Figure 4-46, the experiment module shell to experiment clearance is monitored and the experiment module shell is flown around the experiment, extremely low g levels will be obtained.

Table 4-8. Space Station g Level Induced by Air Drag

Altitude nm.	Air Pressure, lbs/ft^2	Maximum Drag Force, lbs.	Maximum g Level, g's
200	10^{-5}	0.09	0.28×10^{-6}
270	3.5×10^{-6}	0.0315	0.98×10^{-7}

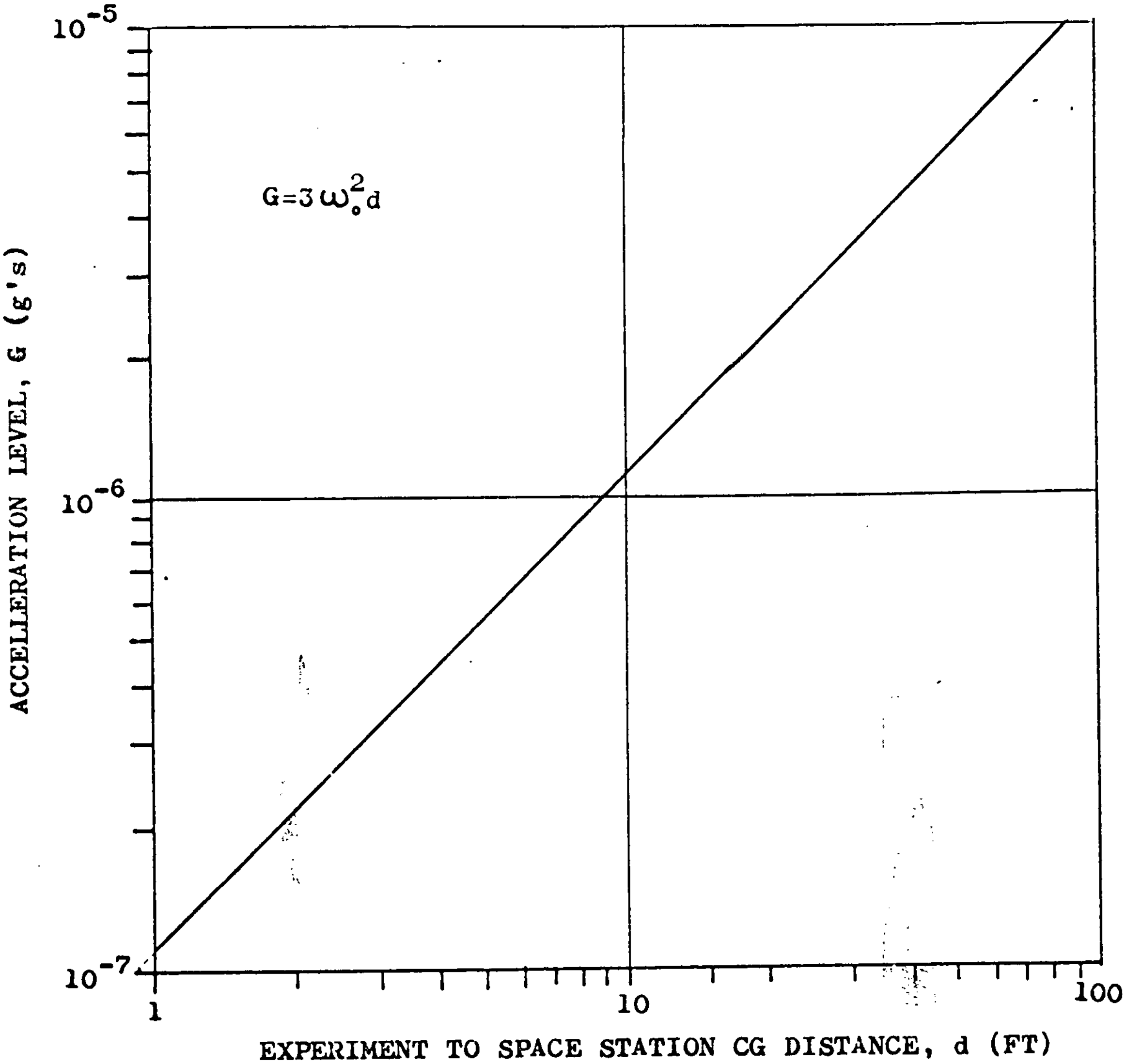

Figure 4-45. Gravity Gradient Induced G Levels on Space Station

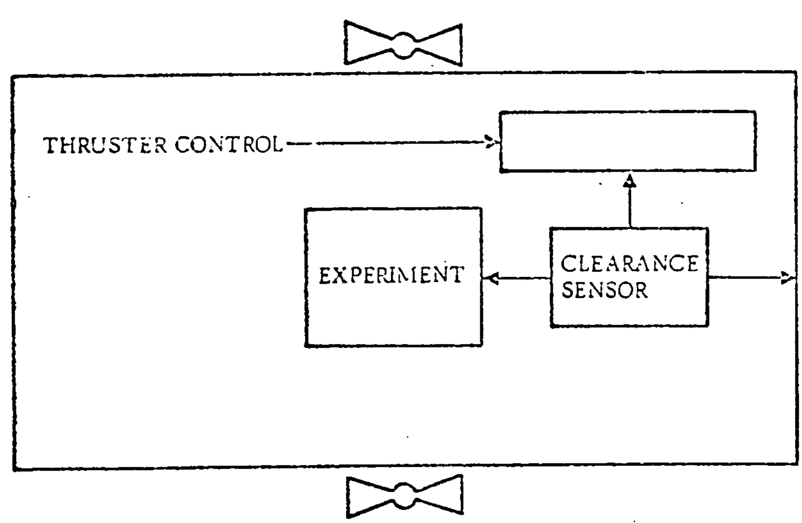

Figure 4-46. Detached Low G System, Drag Free Concept

4.4 REFERENCES (SCS)

4-1. Candidate Experiment Program for the Manned Space Stations, NASA MSFC NHB 7150. XX, September 15, 1969.

4-2. Orbital Astronomy Support Facility (OASF) Study, McDonnell-Douglas Report DAC-58144. June 28, 1968, Vol. IV, Task C. Book 2 of 3.

4-3. D. J. Chiarappa. R. M. Smith. Attitude Pointing and Stability of Space Station Experiments, General Dynamics Convair ERR-1448, December 1969.

4-4. OAO News Reference Handbook, GAEC and NASA Goddard.

4-5. Daniel J. McCarthy, Operating Characteristics of the Stratoscope II Balloon-Borne Telescope, IEEE Transactions Vol. AES-5, No. 2, March 1969.

4-6. Conceptual Design and Analysis of Control System for Apollo Telescope Mount, LMSC-A842157, March 1967.

4-7. Apollo Applications Program (AAP) Payload Integration, Technical Study and Analysis Report, Single Axis Hard Mounted ATM Control System Study, Martin-Marietta Report ED-2002-80, April 20, 1967.

4-8. W. B. Chubb, D. N. Schultz and S. M. Seltzer, Attitude Control and Precision Pointing of the Apollo Telescope Mount, AIAA Paper 67-534, 14-16 August 1967.

4-9. Princeton Advanced Satellite Study, Final Report, NGR-31-001-044, March 1965 to May 1966, Perkins-Elmer Report No. 8346.

4-10. D. M. Eggleston, Statistical Model for Crew Motion Disturbances, General Dynamics Convair Memorandum AD-67-43, November 1967.

4-11. C. Nicita, Fine Pointing Feasibility Study for an Advanced Princeton Experimental Package Hard Mounted to an OAO, Grumman AEC Report GCR-67-1, 23 March 1967.

4-12. Advanced Princeton Satellite Study, Final Report, NGR-31-001-004, Perkin-Elmer Final Report prepared for Princeton University Observatory, PE Report No. 8688, 6 September 1956 to 30 June 1967.

4-13. D. M. Eggleston, Relative Orbital Motion and Stationkeeping, General Dynamics Convair ERR-1440, January 1, 1970.

4-14. Advanced Astronomy Mission Concepts, Vol. III-Subsystems Design, Martin-Marietta Report ED-2002-795, 4/69, NAS8-24000.

4-15. Baseline Program Document, Space Station Program Definition, Phase B, Vol. III, Book 1, Mcdonnell Douglas Report, NASA Contract NAS8-25140, March 16, 1970.

SECTION 5

GUIDANCE, NAVIGATION, RENDEZVOUS, AND DOCKING SUBSYSTEM

5.1 REQUIREMENTS

The guidance, navigation, rendezvous and docking subsystem (G&N) is used to provide attitude angle (θ) and incremental velocity (ΔV) information to the stability and control subsystem during maneuvers of the experiment module relative to the space station. These occur for all modules during initial delivery operations; for free-flying (CM-1) modules (CM-3, CM-4) during moves from one docking port to another.

These requirements are independent of experiment configuration since the G&N subsystem has no function to perform during experiment operation.

The attached module for fluid physics experiments (CM-3/FPE 5.20-1) has the requirement that, while it is docked to the space station, the free-flying fluid physics module (CM-1/FPE 5.20-2) must dock to it for calibration and checkout purposes. Growth versions of other experiments such as FPE 5.22 and FPE 5.27 may have similar requirements.

The functional requirements of the G&N system are to monitor relative range and range rate between the space station and experiment module to generate orders for maneuvering the experiment module. The space station computer is suitable for the necessary calculations. There is no need for a dedicated computer to perform these infrequently required functions. The S-band tracking, telemetry, and command link of the communication and data management subsystem has adequate capacity during the times G&N operation is required to handle all necessary command and data transmission.

Maximum range at which the G&N is required to function is 500 n. mi. Docking maneuver computations ordinarily do not require tracking of the experiment module to ranges greater than a few n. mi.

5.2 SUMMARY DEFINITION

The sensor and computation hardware of the G&N subsystem is housed aboard the space station as shown in Figure 5-1. Equipment aboard the module is limited to that required to enhance the sensor function.

Provision for docking to the CM-3/FPE 5.20 is made by equipping it with a laser radar of the same type as that normally installed at the space station docking port. Other items in the G&N equipment complement are listed in Table 5-1.

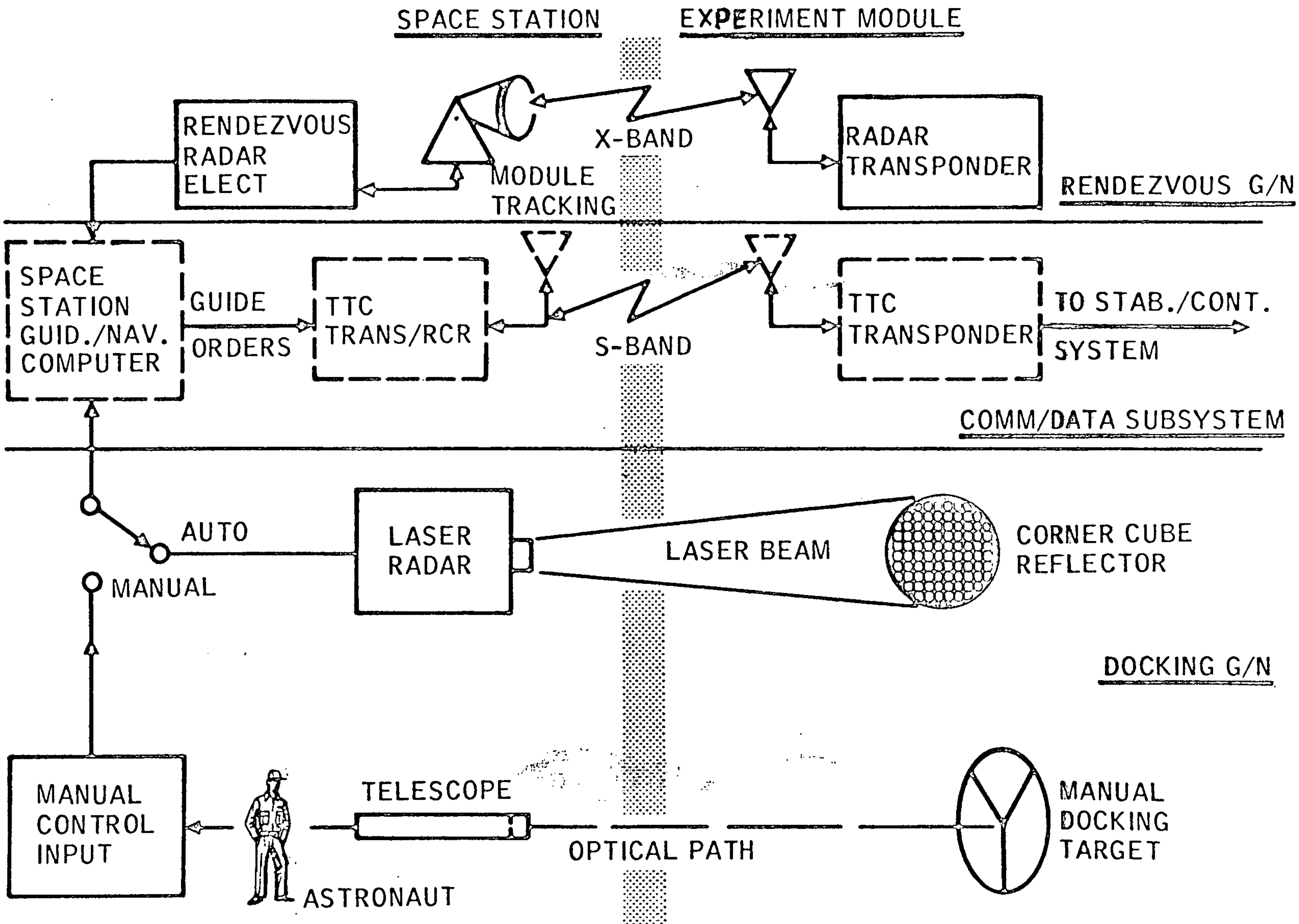

Figure 5-1. Guidance and Navigation Subsystem Selected Concept

Table 5-1. G&N Subsystem Configuration

Component	Size (cu ft)	Weight (lbm)	Power (watts)	Quantity Required*			
				CM-1	CM-3†	FPE 5.20	CM-4
Docking Corner Cube	0.66	2	—	1	1	1	1
Target/Stadia & Illumination	1.25	5.25	100	1	1	1	1
Omni-directional Antenna	1.0	3	—	1	1	1	1
Antenna Diplexer	0.66	1	—	1	1	1	1
Transponder	1.0	9	20	2	2	2	2
Laser Radar	1.36	28	30	0	0	1	0
Total		Size	(cu ft)	5.57	5.57	6.93	5.57
		Weight	(lbm)	27.25	27.25	57.25	27.25
		Power	(W)	140	140	170	140

*FPE Allocation By Modules

CM-1: 5.1, 5.2A, 5.3A, 5.5, 5.20-2

CM-3: 5.7/5.12, 5.8, 5.16, 5.20-1, 5.27

CM-4: 5.9/5.10/5.23, 5.11, 5.22

†Except FPE 5.20-1 module which is shown in next column.

For the selected orbits of the remotely operating modules, the module position and velocity (as functions of time) will be measured by means of the tracking, telemetry, and control (TTC) loop. From this information, as obtained at the space station, orders for the initiation of rendezvous are calculated via the space station computer and transmitted to the experiment module over the same TTC loop. Details of the TTC loop and the position/velocity mode of operation are given in Section 7, Communication and Data Management Subsystem. During the rendezvous maneuver, tracking of the module is carried out from the space station by the microwave rendezvous radar, and corrections to the rendezvous maneuver derived from measurements of range and range rate. Orders for correction are transmitted over the omni-directional TTC. Angle measurement achieved by the rendezvous radar could serve as a redundant check on the validity of the midcourse corrections required. Orbital stabilization and docking are served by a docking radar bore sighted to the desired docking port.

The rendezvous instrumentation that has been selected is a relatively low-powered X-band microwave radar with a range limitation, in a skin tracking mode, of approximately 50 miles. Extension of this range to approximately 500 miles will be obtained by means of experiment module borne radar transponder. The module position and trajectory are monitored by this radar, and midcourse corrections made based upon space station computation.

A skin tracking mode of operation for the rendezvous instrumentation has been considered in sizing the radar in order to allow space station operation with other, as yet undefined, non-cooperative vehicles. This mode of operation further reduces the amount and complexity of additional equipment in the Experiment Module as well as reduces the power loading on the module power source. The operating characteristics of this radar are given in Table 5-2.

Table 5-2. Rendezvous Radar Characteristics

Frequency	X Band
Range	50 n.mi. Skin Track 500 n.mi. Transponder
Range Accuracy	1.0%
Range Rate	0-1500 fps
Range Rate Accuracy	2.0 fps
Angle Coverage	0-180° Elevation, ±20° Azimuth
Angle Accuracy	±0.11 Degrees

A light weight scanning laser radar has been selected as the primary instrumentation for the automatic docking system with an optical system as a manual back-up. The choice of the laser radar has been made because of the ability to make range measurement to zero range, and to increase angle accuracy due to the very small beam angle. The back-up system consists of a telescope fitted with the proper cross hairs and reticules mounted on the space station. This telescope would be used to optically track an experiment module mounted stadia. For remote docking of an unmanned transporter module to an orbiting experiment module, a television vidicon bore sighted to the telescope could be employed and the video transmitted to the space station for operation and control.

The laser radar requires that the target being tracked be cooperative; a four inch corner reflector mounted on the experiment module will allow acquisition and tracking to ranges far in excess of the range at which docking will normally be initiated. The equipment on the space station consists of a laser transmitter-receiver positioned and oriented relative to the space station axes.

The space station laser radar transmitter-receiver package would weigh about 20 pounds, and the electronics package associated with it about 8 pounds. The radar transmitter uses a semiconductor laser about the size of a package of cigarettes. The beam of the transmitter is steered by means of solid state piezoelectric crystals and optical lenses. The receiver consists of lenses, filters and an image dissector.

The system selected for the space station/experiment module complex is the radar currently under development by the Aerospace/Optical Division, ITT. This effort is under the sponsorship of NASA under contract number NAS8-20633. The major subsystems and associated key components that make up the radar are:

Laser Transmitter - Diffraction limited GaAs semiconductor laser.
Beam Steerer - Piezoelectric beam deflector and amplifying optics.
Receiver Optics - High speed, narrowband, refractive receiver optics.
Scanning Optical Detector - Image dissector.
Electronics - High speed integrated circuits.
Cooperative Target - Optical corner cube.

The two basic radar functions of the target acquisition and tracking are accomplished by scanning the laser transmitter-receiver. The full raster acquisition scan pattern covers 30° x 30° in steps of 0.1° x 0.1° but can be logically programmed to scan smaller areas, if experiment module navigation data indicate better a priori knowledge of the relative positions of the space station and the module. In the track mode, the angle scanner is deflected in a cross pattern around the target location. Angle and angle rate readings are obtained from the angle scanner electronics, while range measurement is obtained by a precise measurement of the elapsed time between transmitted and received signals. Range rate is obtained through differentiating successive range readings. A listing of the estimated system performance characteristics is shown in Table 5-3.

Table 5-3. Estimated Docking Radar Performance Characteristics

Range	0-120 km (75 miles)
Range Accuracy (3σ)	±0.02% or ±10 cm (whichever is greater)
Range-rate	0-5 km/sec (28,800 mph)
Range Rate Accuracy	±1.0% or ±0.5 cm/sec (whichever is greater)
Angle Coverage without Gimbals	±15° pitch, ±15° yaw, ±90° relative roll
Angle Accuracy	
Pitch and Yaw	±0.2°
Roll index	±1.0°
Acquisition Scan Time	Less than 150 sec
Angle Rate	
Acquisition mode	0-0.4°/sec
Track mode	0-10°/sec
Angle Rate Accuracy	±1.0% or ±0.01°/sec (whichever is greater)

The space station has been selected as the primary site for location of both the rendezvous and docking equipments, with docking equipment also being placed aboard transporter modules for the purpose of transporter/module rendezvous remote from the space station. This selection is based on a consideration of: docking frequency requirements of each vehicle; numbers and characteristics of units involved as a function of distribution; effects of distribution on the ancillary equipment aboard the experiment module; orbital constraints; manual docking back-up requirements; stabilization and attitude requirements on the rendezvous and docking mounting platforms; and crew safety and human factors. Having evaluated the above factors, sites were selected which yielded minimum impact on total system cost, best time utilization of equipment, and most reliable operating characteristics with proper maintainance and repair.

Manual docking back-up will be provided both through monitoring the laser radar outputs and the orders transmitted to the module, and through an optical docking system similar to the optical docking used in the Apollo. A schematic of this system is shown in Figure 5-2.

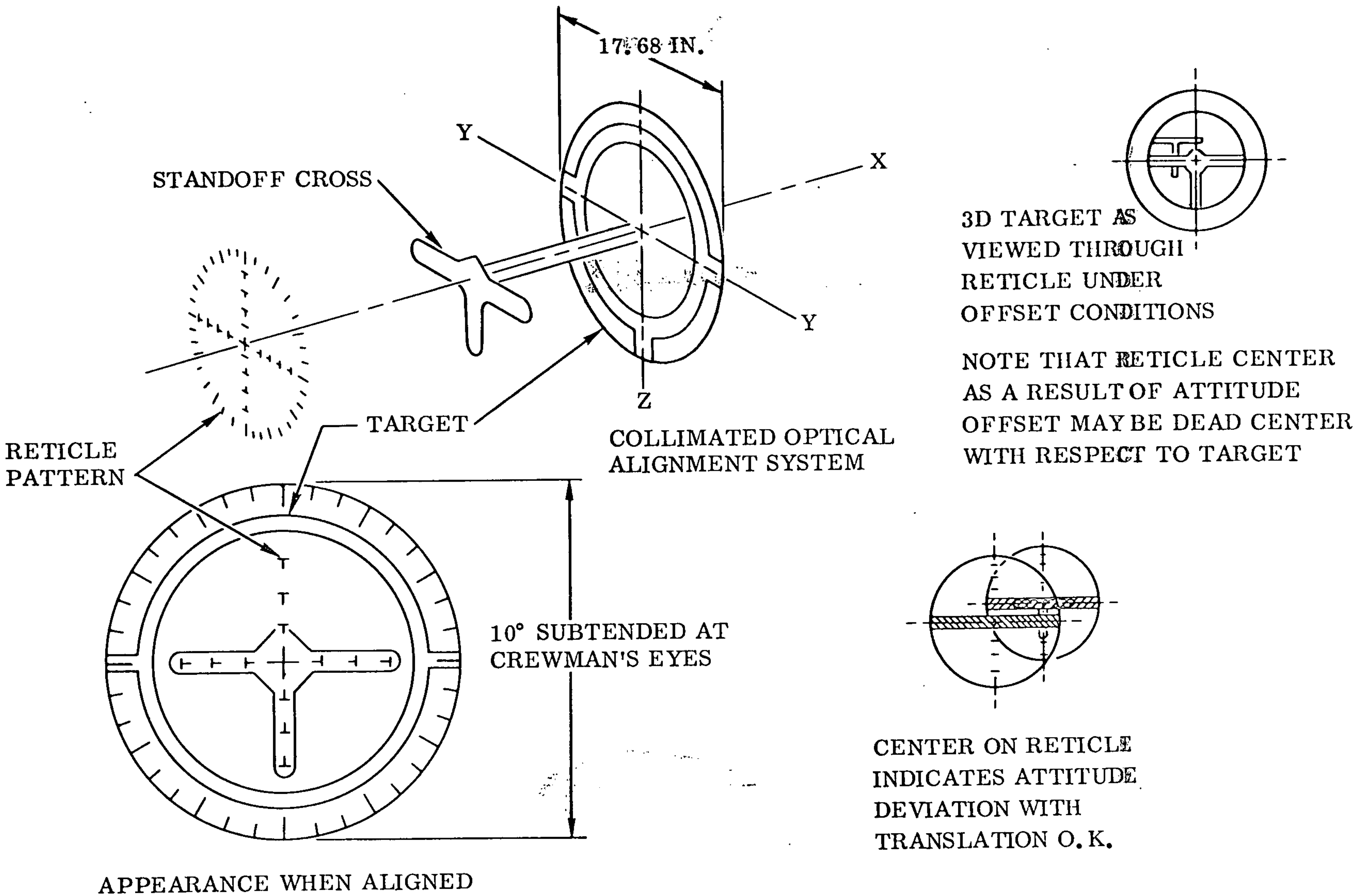

Figure 5-2. Optical-Manual Docking Schematic

In addition to the above mentioned instrumentation, the guidance and navigation system includes the software required to calculate the maneuver order for the experiment module. This software would become a permanent routine of the space station computer in which the module orders would be calculated and formated for transmittal. Information for calculations of orders would be derived either from the instrumentation sub-systems discussed above or from consideration of the particular experiment being addressed. Formating of orders would include the address of the particular module to which such orders apply. A block diagram of the total G&N system is shown in Figure 5-3.

Alternative approaches to the instrumentation for the G&N system would include: a navigational quality IMU on the module from which position and velocity could be generated and relayed to the space station for action; an omni-directional TTC of increased power to be used for measurement of range and range rate information independent of the relative space station/module positions; the use of the radar/transponder system developed for Apollo; and docking of the module to the space station via the rendezvous radar with final approach being accomplished with a purely manual system.

5.3 CONCEPT DEVELOPMENT

The spectrum of vehicles and docking requirements considered in equipment distribution studies include: an experiment module docking to the space station or to a second module permanently attached to the space station; an unmanned transporter* module docking to the space station either with or without an experiment module in tow; an unmanned transporter module docking to an orbiting module; and a space shuttle docking to any of the above.

A summary of considerations made in selecting the space station as a site for the rendezvous radar is given in Table 5-4. The orbit of one vehicle with respect to another may be characterized by tracking from either vehicle, or from some third point, by tracking alternately both vehicles involved. The rendezvous can be accomplished by rendezvous instrumentation attached either to the space station or to each of the other vehicles involved. Location of such instrumentation only on the transporter module assigned to the station was not considered since this would mean, in some instances, that the space tug would have to be orbited from the station in order to have an unocculted view of the module. Location on more than one vehicle (both on the space station and on the module, for example) was not considered since such dual location is unnecessary to fulfill the function of rendezvous initiation.

From Table 5-4 it can be seen that location on the space station will have minimum impact on the experiment module. Further, this location makes the unit readily

*The unmanned transporter is not currently a part of the baseline system but is considered to be a possible future addition.

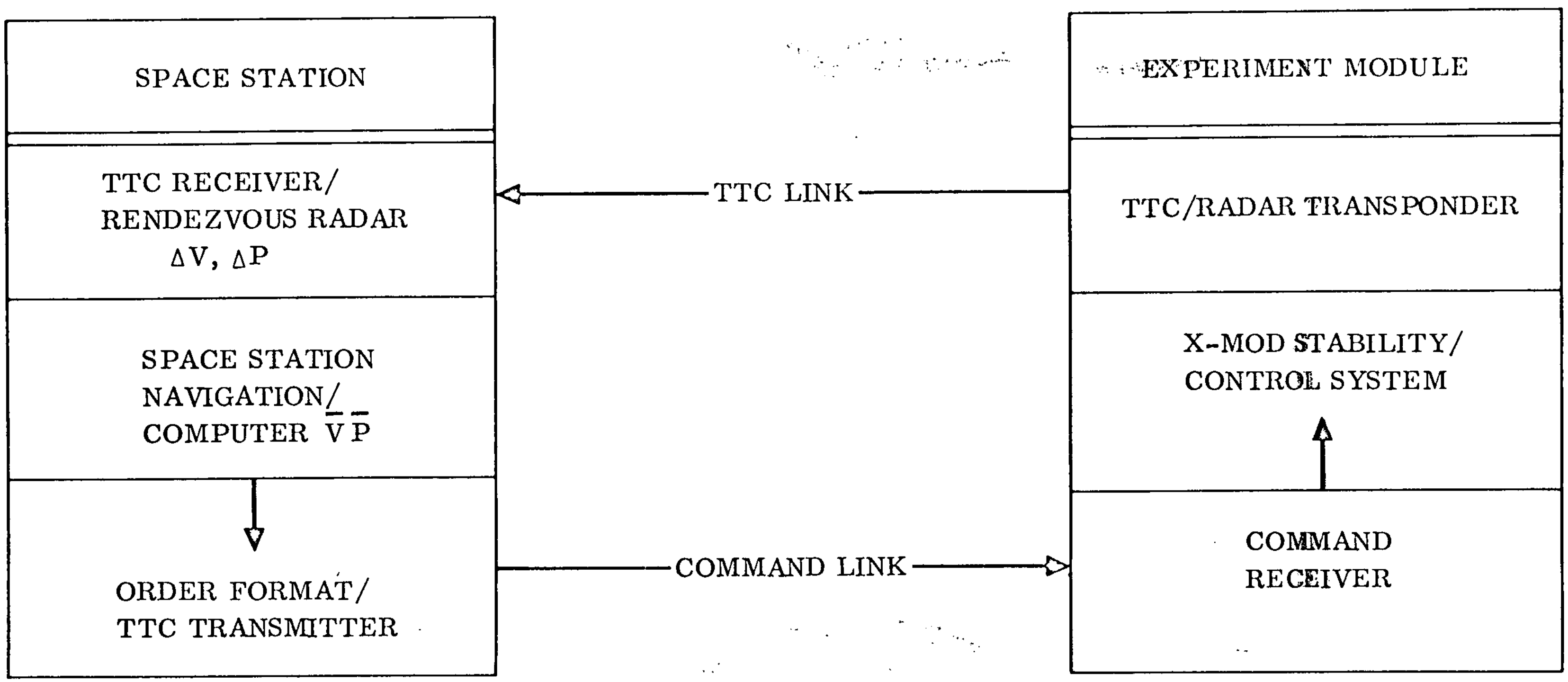

Figure 5-3. G&N System Configuration

Table 5-4. Rendezvous Instrumentation Considerations

INSTRUMENT LOCATION	NO. REQUIRED	EFFECTS ON X-MOD/S.S.	EFFECTS ON INSTRUMENT	ADVANTAGES/ DISADVANTAGES
X-Mod	1/Detached Mod. Total of Seven	1. Increase Power Required 2. Increase Nav. Computer Capacity 3. Increase RCS Propellant Required to Point Sensor 4. Increase Telemetry Requirements for Monitoring/Backup 5. S.S. Computer Required for Backup	1. Reduce Gimbaling Requirements 2. Required Cooperative Device/s on Spacecraft to Assure Point Tracking 3. Higher Reliability Required due to Non-Availability for Maintenance/Repair Except when EM is Docked	<u>Advantages</u>: 1. Reduce S.S. Load <u>Disadvantages</u>: 1. Increased Cost/Unit, Total System 2. Increased Load on EM Ancillaries 3. Poor Time Utilization of Equipment 4. Possible Antenna/ Solar Panel Shadowing
Space Station	2 Units	1. No Effect if Instrument Capable of Skin Track. Require Cooperative Device/s (active or passive) if not. 2. With Cooperative System, RCS must be used to Align Mod. Alignment not Critical 3. Orders Developed in S.S. Computer/Transmitter to EM.	1. Fully Gimballed for Operation +90° in track, ±20° Cross Track 2. Power Reliability Allowable due to Availability for Maintenance/ Repair 3. Cold Skin Track without Wander due to "Small" Size of Target.	<u>Advantages</u>: 1. Reduced Cost/Unit, Total System 2. No Increase on EM Ancillaries over Normal Experiment Requirements 3. Good Time Utilization of Equipment <u>Disadvantages</u>: 1. Increased S.S. Load

available for test, periodic maintenance and repair, thus reducing the design constraints brought about by the necessity of long periods of unattended stand-by followed by short periods of unattended operation as would be the case if the instrument were located on the module. The number of units required as a function of location can also have considerable impact on system cost. As a point of reference, the development of the rendezvous radar for the Apollo system cost in the neighborhood of $100M and the production units cost approximately $20M each.

Characterization of the orbit of the experiment module with respect to the space station will require tracking only over a short time span of a single orbit, since much a priori knowledge of the orbit will be at hand. Best tracking conditions can be obtained when the effects of background interference are minimized. Thus, if an optical tracker is used, tracking a flashing light on the module, better accuracy can be obtained against the black background of space than against the earth-shine which would be present in tracking modules below the station. In a microwave system tracking against a space background would allow the use of a low noise receiver (such as a parametric amplifier) and thus considerably lower transmitted power would be required in order to achieve desired accuracy. For this reason, a location top-side on the space station has been selected as the instrumentation site.

In selecting a generic type for the rendezvous instrumentation, the possible sets of data that could be used for orbital characterization were defined and instrumentation capable of providing each such set examined. Further, as specified earlier, the growth potential associated with inclusion of new tasks to the space stations function was also considered. Table 5-5 summarizes these considerations. Since the microwave radar can obtain both sets of data required, through proper design, and since its growth potential appears best, particularly for medium to long range uses, this concept is recommended.

Placement of the docking instrumentation on the space station and on the transporter rather than on the module has been selected on the basis of number of units required, the necessity for manual back-up for docking, effects on experiment module design, and possible hazardous effects to space station personnel. Since extremely low power is required for this application, the instrumentation may be made very light and compact, thus allowing it to be portable so that it can easily be moved from port to port within the space station or carried into an attached module or transporter for operations involving these vehicles, thus the number required can be limited to three or four at most depending on station activity. Portability however, requires precise mounting guides at each port in order to maintain system alignment and bore sight.

As previously mentioned, a microwave radar system has been selected as the instrument for tracking the experiment modules in order to characterize their orbits for rendezvous initiation. A study has been conducted to size a radar for the rendezvous task of the space station/module system. Three possible modes are envisioned: an active cooperative mode in which the module is equipped with active

Table 5-5. Rendezvous Requirements, Instrumentation Trade-offs

Measurements Required to Initiate Rendezvous	Instrumentation Alternatives	Effect On X-Mod	Operational Consideration	Growth Potential
Angle vs. Time	Optical Tracking	Requires multiple flashing lights and/or attitude control	Range of operation limited	No long range capability Requires cooperative target
	Laser Radar	Required multiple corner cube reflectors and/or attitude control	Excessive search time to acquire/ limited range	Requires cooperative target
	Microwave Radar	Transponder	Search time minimized	Can skin track other/ new vehicles at short range, cooperative targets to 250 n.mi. or more
Range, Range Rate vs. Time	Laser Radar	Oriented corner cube	Same as above/$\dot{R}$ obtained by smoothing/differentiating range	Same as above
	Microwave Radar	Transponder	Same as above/$\dot{R}$ obtained by differentiating range of or by doppler	Same as above
	TTC	No effect	No search time if omni-directional	Increased block at longer ranges

echo enhancement devices such as repeaters, transponders or beacons; a passive cooperative mode where the module-borne enhancement device consists of a corner reflector or Luneberg lens mounted on a module and requiring only crude attitude control of the module; and an uncooperative module against which only skin tracking may be employed. Of these, the more taxing requirement for the radar sensor is the uncooperative mode. Further, the cooperative mode can certainly be accommodated by any radar capable of meeting the requirements of the uncooperative target.

A specific radar definition has not been attempted here, but rather a representation of a radar sized to meet the preliminary baseline mission requirements with the least demands on power, size, and weight. Some of the more obvious tradeoffs have been considered. Two basic approaches to the space station rendezvous radar have been investigated; namely, a conventional, low-duty cycle pulse modulation scheme and an interrupted CW (I.C.W.) modulation whose pulse repetition frequency is automatically locked to the target range. Results have shown that the XMTR power requirements for the fixed modulation are prohibitively high for present solid state technology, while the low ratio of peak to average power facilitated by the I.C.W. modulation permits the use of solid state transmitters of present (or very near future) capabilities.

The present rendezvous requirements have been employed to size nine I.C.W. radar configurations differing in antenna size and operating frequency. Estimates were made for the weight and prime power for each of the nine configurations as constrained by a somewhat arbitrary assumption of high noise temperature (e.g., diode mixer front-ends). Even under this pessimistic assumption, it is shown that the baseline requirements can be met with either a 6-ft. C-band antenna or a 5 or 6-ft. X-band antenna, the best overall performance probably being provided by the X-band radar. S-band may be unsatisfactory primarily for reasons of angle accuracy. The 6-ft antenna X-band radar is estimated to require 12 watts of prime power and weigh 30 pounds.

Certain general studies, applicable to either a conventional radar or an I.C.W. radar were initially undertaken. These included: a study of the optimization of the power-aperture product vs. search and detection geometry and range; an evaluation of range differentiation vs. doppler measurement as methods of extracting range rate information; error relations for both range and range rate; and angle tracking methods and error relations. Accuracy requirements for the system were set by consideration of the transfer orbits for the various modes of operation, and the accuracy of module location desired at the end of the rendezvous phase for the initiation of docking maneuvers.

Since the volume of uncertainty of the experiment module when orbited from the space station would be relatively small, power-aperture product requirements were based on the condition of module delivery by means of an expendable launch vehicle.

Under these conditions, lack of relatively long periods of ground tracking of the launched module would result in a fairly large volume of uncertainty of module position with respect to the space station. These power operative studies were carried out under the assumptions that the antenna would scan the volume of uncertainty in some particular pattern and that a cumulative probability of detection of 0.997 was required. The results of this study provided optimal total scan power-aperture product, best relative module/space station geometry for search, and optimal dwell time for each incremental volume in the total search volume to obtain the required detection probability. The results were then compared with the case of fixing the radar angle and allowing the natural drift between the space station and the module to perform the scan function. While slightly higher total scan power is required to obtain the same probability of detection since dwell times on any incremental volume are increased.

For short signal pulse, the evaluation of doppler vs. range differentiation showed range differentiation to provide better range rate accuracy, whereas for pulse lengths exceeding about 10 microseconds, doppler measurement was superior. In the interrupted C.W. systems, since ranges less than the range equivalent of 10 microseconds (approximately 5,000 feet) will rarely be made, doppler measurements will provide range rate.

In the studies of the application of a conventional radar system to the rendezvous requirements, the effects of pulse compression techniques, spread spectrum, and frequency diversity on system parameters, particularly power requirements, were considered.

A comparison of the conventional pulse radar with the I.C.W. radar showed the I.C.W. radar power requirements to be slightly smaller (in the practical case) because of better utilization of the energy on target. This fact, combined with the ability for full solid state implementation of the I.C.W. system, resulting in larger mean times between failure, reduced cooling requirements and lower weight have led to the selection of the I.C.W. approach as the rendezvous radar to be used with the experiment module program.

Operating parameters for nine I.C.W. radars were determined as previously mentioned, and the results of these are shown In Table 5-6. Operation of the radar in the search mode would place the radar at a fixed angle and allow the relative space station/module motion to provide for scanning the volume of uncertainly. It is recommended that the operating frequency of the system be 10 GHz and that the antenna size be either 4 or 6 feet, whichever appears most feasible for mounting on the space station.

Table 5-6. Parametric Radar Designs

Carrier Frequency	3 GHz			5 GHz			10 GHz		
Antenna Diameter (ft)	2	4	6	2	5	6	2	4	6
(Acq.) RF Power Watts	58	9	2.6	39	6	2	23	4	1.5
No. of Beam Positions	5	18	39	12	49	112	49	195	450
Antenna Gain (db)	23	29	32.5	27.5	33.5	37	33.5	39.5	43
Antenna Beamwidth (deg)	12	6	4	7	3.6	2.4	3.6	1.8	1.2
Ti (seconds)	16.5	4.15	1.85	7.4	1.85	0.84	1.85	0.46	0.024
L (N) (Ratio)	8.3	5	3.3	5.5	3.3	2.3	3.3	2.1	1.9
$\Delta\phi$ (0.1 sec data rate)	4.6°	1.5°	0.82°	2.2°	0.73°	0.4°	0.73°	0.23°	0.11°
% Range Error (Unambiguous) (0.1 sec data rate)	38.4	24.8	20.4	31.6	20.4	16.4	20.4	12.7	8.95
PRF Multiple for 1% Ranging (0.1 sec data rate)	130	72	56	100	56	42	56	30	15
Prime Power (watts)	150	30	15	105	25	15	65	20	12
Total Weight (lb)	35	32	34	20	22	32	20	20	30

Figure 5-4 shows a block diagram of the I.C.W. radar. Angle tracking, not shown in the figure, would be provided through a monopulse feed for the antenna, and measured angles would be smoothed over 0.1 seconds to provide required data accuracy.

The selected type of docking equipment is a laser radar. This selection has been made because of the ability to make range measurement to zero range, and to increase angle accuracy due to the very small beam angle as discussed in the mid-term report.

Major considerations in the selection of the laser radar over a microwave system included the directive gain and size of the antenna systems in the two cases, the almost total lack of side lobes in the laser system (60-70 db below main lobe) as compared to the microwave system, the ease of scanning and the field of view that can be scanned relative to the beamwidth, achievable angular accuracy, and minimum range to which a target may be tracked.

In regard to possible hazardous effects of the laser system on space station personnel, worst case analysis conducted by ITT has shown that for the power levels required for accurate tracking, no danger is involved to any part of the body other than the eyes. Direct exposure of the eyes to the laser beam with ranges of two miles or less could be injurious. While the likelihood of such exposure is very low due to the narrowness of the laser beam and the almost total lack of side lobes, all possible precautionary measures to prevent accident must be taken. Thus, filters eliminating radiation above 7000 angstroms should be employed on all space station windows from which exposure to the reflected signal may occur. To protect station personnel operating in an extra-vehicular mode, such filters should be built into the space suit view plates. These filters, while eliminating the harmful laser radiation may be built so as to have no effect on personnel visibility or color rendition.

5.4 OPERATING CONSIDERATIONS

Five operational sequences involving the use of the guidance, navigation, rendezvous and docking instrumentation exist and are considered in this section. These are: delivery of the experiment modules to the space station, orbiting of the detached modules from the space station, experiment dictated attitude and station keeping, rendezvous of the remote modules with the space station, and docking attached to the station.

The primary delivery mode is via the shuttle orbiter. The use of expendable launch vehicles is a considered alternative. With either delivery vehicle there are experiment modules whose weight exceeds direct payload capacity to space station circular orbit. In these cases an elliptical parking orbit having apogee altitude equal to the space station altitude is set up, and at apogee and in proximity to the space station to the module integral propulsion capability is used to circularize the orbit.

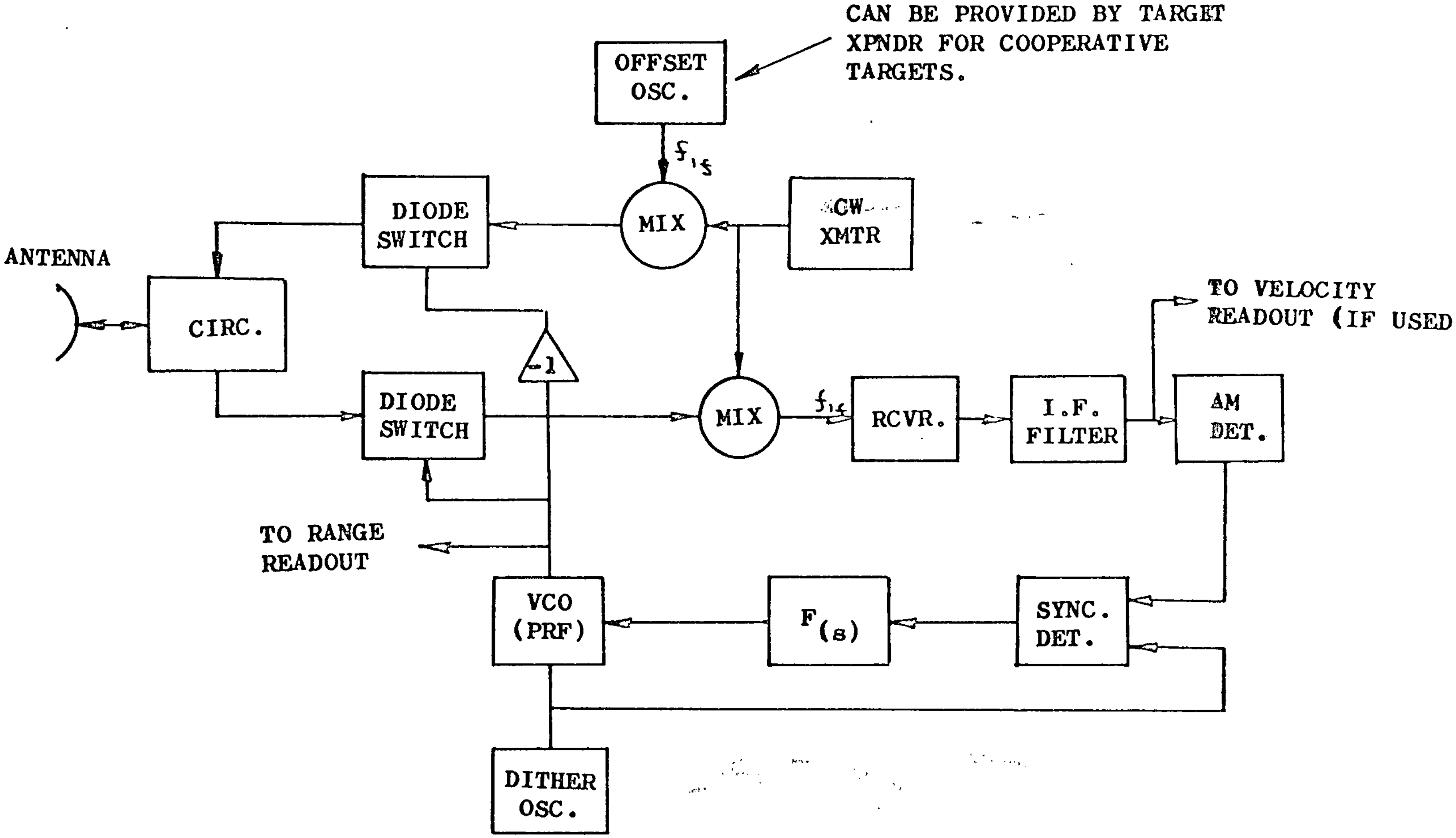

Figure 5-4. Simplified Block Diagram, ICW Radar (PRF Tracker)

Direct Delivery

If the modules are delivered directly to a point near the space station, docking is accomplished by the space station - experiment module docking system. The module will be maneuvered into a position trailing the space station and stabilized in the orbit of the space station. These maneuvers will be made utilizing the reaction control system of the module and on command from the space station.

In the case of delivery of a module which will be permantly attached to the bottom side of the space station, such as the earth survey module, the module will be given a small incremental velocity normal to its orbital path trailing the space station and in a downward direction. This will place the module in an elliptical path relative to the space station such that it will be carried downward and forward from its initial position, and at perigee of this path, the orbit of the module will be recircularized. Proper control of the incremental velocity will cause the point of recircularization to occur below and just aft of the assigned docking port. In this position, the module will be rotated so as to align its docking mechanism with the docking port. Being below the space station, the module will drift forward so as to come in line with the assigned port. After acquisition by the docking instrument boresighted to the assigned port, docking operation will proceed.

Docking to a top-side port may be accomplished by giving the module a somewhat greater incremental velocity normal to and down from its initial position trailing the space station, such that the module will take an elliptical path relative to the space station which will carry it down under and up in front of the station. At the point of crossing the stations orbit, a small velocity increment downward will modify the orbit of the module such that it will reach apogee above and just forward of the assigned port where its orbit will be re-circularized at an altitude slightly above the station. In this orbit, the module will drift backward along the station toward the assigned port. Alignment of the module axis for docking will be made and upon acquisition by the docking instrument, docking will proceed.

More direct approaches to docking on top or below the space station may be taken by moving the module from its initial position aft of the station by just the brute force of its engines against the natural orbital effects. This might save some time, particularly in the case of top-side docking, but would require considerably larger expenditure of fuel and somewhat closer monitoring of the maneuvers. The procedures described have been suggested because of the relative ease with which they may be carried out and because of the saving of fuel that will result through the use of the more or less normal orbital characteristics.

Parking Orbit Delivery

In the event that the parking orbit technique is used, the module will be placed in a circular orbit above and leading the space station, guidance and navigation systems activated and aligned, and the attitude of the module stabilized. While an orbit below and lagging the station could also be used, consideration of the placement or rendezvous instrumentation for all phases of the space station/experiment module activity, as well as the impact of placement on background noise effects on equipment design and operation, have led to the selection of a space station top-side site for this equipment. Thus to utilize this instrumentation in capture of the delivered module, a higher orbit is desirable.

Prior to the beginning of rendezvous procedures, the experiment module in its orbit above and leading the space station will be acquired and tracked by the rendezvous radar in order to characterize its orbit relative to the space station. Further, outputs from the navigational computer associated with the module's on-board IMU will be telemetered to the space station in order to maintain a check on the module's continued progress during this rendezvous phase.

From this orbit above and leading the space station, the station will overtake the module and the addition of a properly timed velocity increment along but opposing the orbital path of the module, will bring the module into position for top-side docking. For docking to the general port area of the space station, the same sort of velocity increment, delayed in time from that required for top-side docking, will cause the module to pass aft of the station where its orbit can be re-circularized in the orbit of the space station but trailing the station in position for docking. If the initial maneuver for the end docking were executed and allow to continue, the module would pass under the space station and reach a perigee somewhere below the station. By slowing the module as it passes behind the station, however, the module can be made to reach a perigee close to the station and aft of an assigned bottom-side port. Recircularizing at this perigee will allow the module to overtake the assigned port and be docked. These maneuvers are shown in Figure 5-5.

Co-orbital Maneuvering

The orbit selected for the remote operating modules is shown in Figure 5-6. Motion in this orbit will result from module drag. Deployment into this orbit will be made to a point in close proximity to the space station, at which point the module velocity will be adjusted to circular. It will then follow the outward path below the projected orbital path of the space station. This deployment may be accomplished by one of three methods. By giving the module an initial downward increment of velocity, it will move in an elliptical path below and in front of the space station. Adjustment of the module velocity when it reaches the desired point in the orbit will then be accomplished. This method of deployment is shown in Figure 5-7.

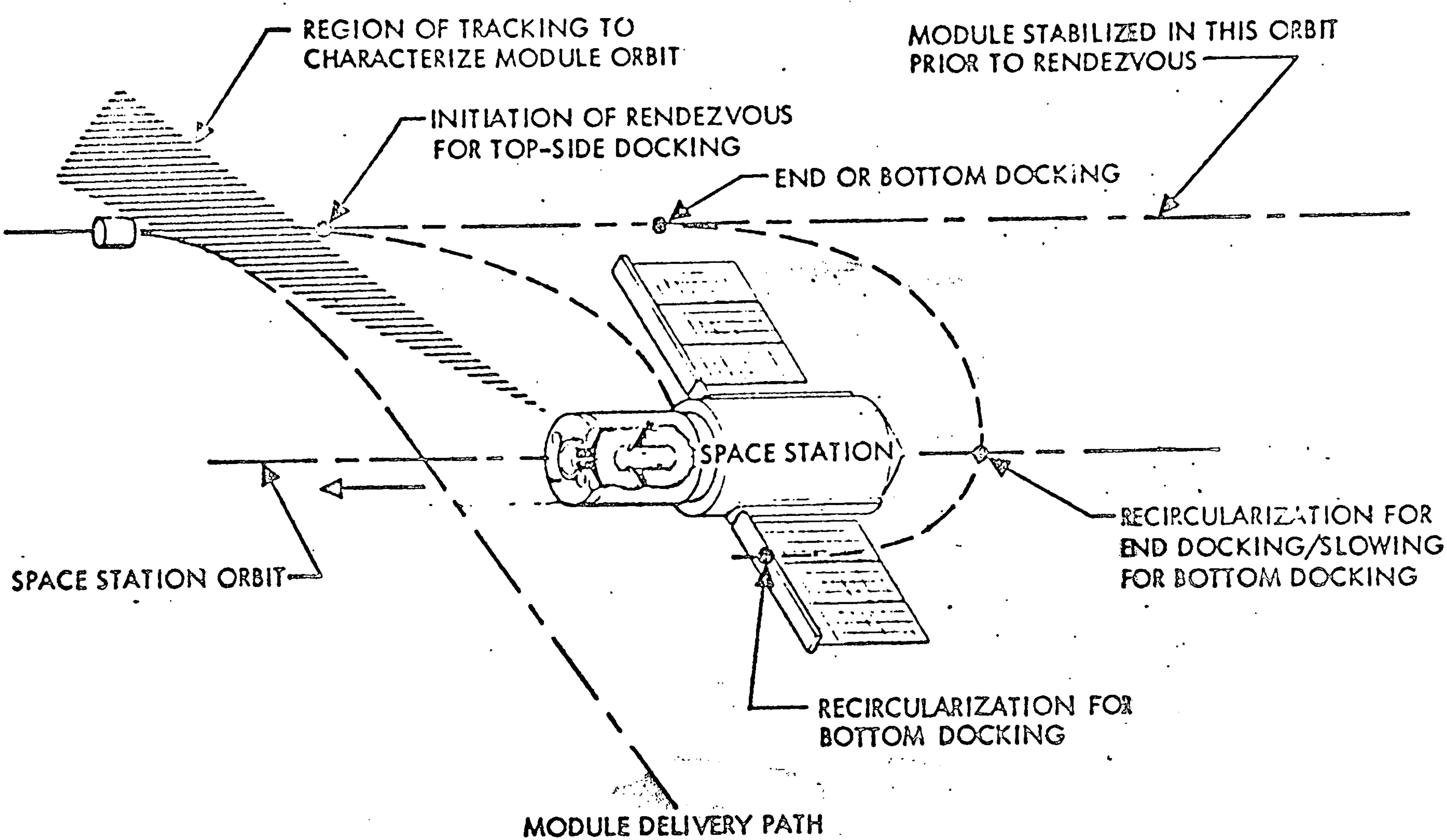

Figure 5-5. Rendezvous Maneuvers for Expendable Launch Vehicle Delivered Modules

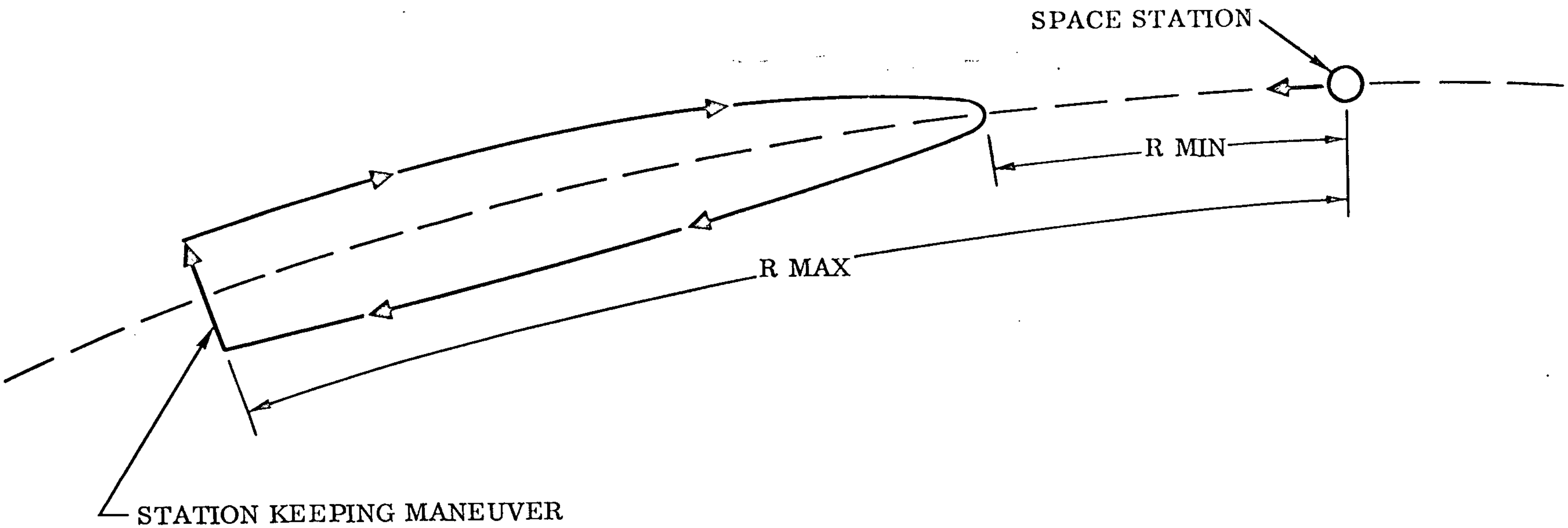

Figure 5-6. Experiment Module Orbits

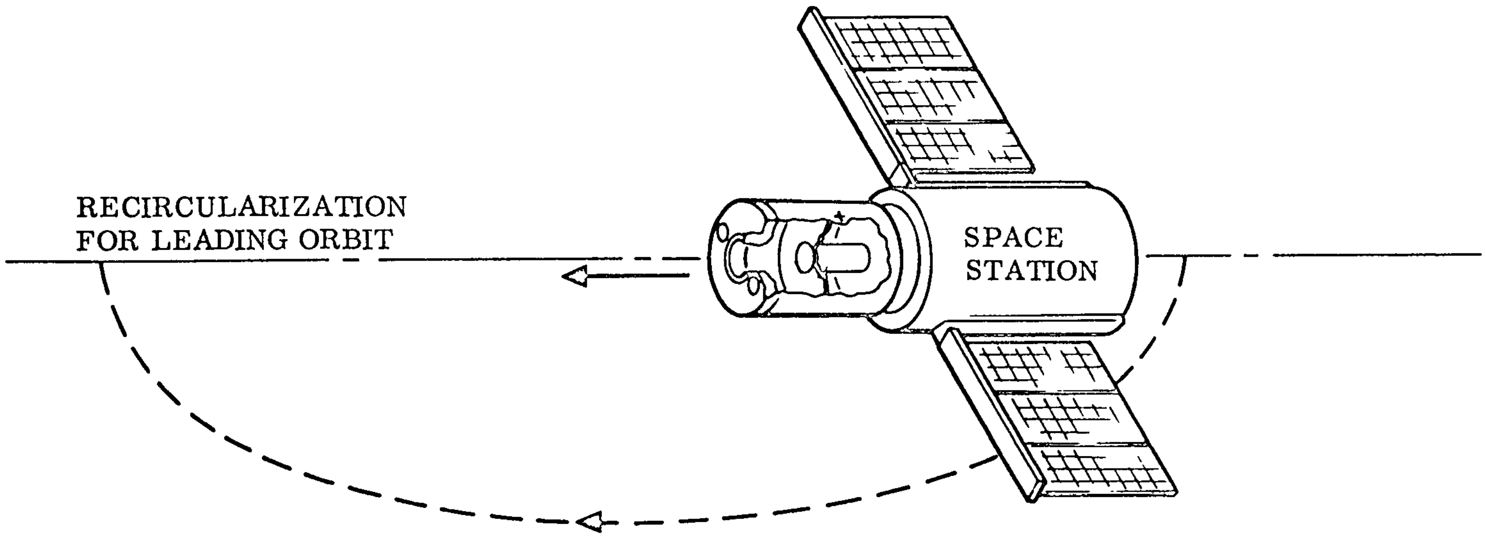

Figure 5-7. Experiment Module Launch Geometry

A second method requires an initial increment of velocity in the same direction (downward) but of smaller magnitude than that for the first method will cause the module to start in an elliptical path relative to space station, and if at the perigee of this path, the orbit of the module is re-circularized, the module will drift forward, relative to the space station. Re-circularization may be accomplished by means of an increment of velocity backward along the new circular orbit. At the proper time, an increment of velocity forward along the circular orbit of the module will cause the module to rise in to the required experimental orbit where velocity adjustment must be made as previously. This second method takes less velocity increment but more time relative to the first.

A third method would require an initial velocity increment backward along the space station orbit. This would cause the module to fall back and downward from the space station and then move forward, rising and looping over to continue with its forward motion, finally crossing the desired path at which time the velocity of the module must be re-adjusted.

Tradeoffs between these three methods of delivery would depend on allowable time to station, total magnitude of the velocity increments required, and minimum safe distance at which the module may pass the space station.

Orbits by which experiment module rendezvous may be accomplished are essentially the inverse of those required for deployment of the module initially.

Having brought the remote module into docking position, control of the module will be taken by the docking instrumentation system. This system will measure the relative range and range rate between the module and the space station, as well as the angle between the line of sight of the module from the space station and the bore-sight line of the assigned docking port. Commands to correct off bore-sight error will be computed in the inertial reference frame of the space station and transmitted via the command link to the module. These commands will be in the form of incremental velocities, direction and time of application. In the computer on board the module (part of the stabilization and control subsystem) these commands will be transformed to local module coordinates and correction initiated on command from the space station. After aligning the module with the docking port, commands from the space station will roll the module around its docking axis in order to align the docking pins/cones with their mating pairs on the space station. The module will then be commanded toward the station at a controlled rate, maintaining its alignment with the port. This procedure will be carried on automatically by means of the IMU/navigation computer system in the module and be monitored with the docking instrument. Override of the module control during this phase can be made at any time monitoring of the module motion indicates necessity. Manual back-up to the docking system will be available both by monitoring the output of the docking instrument and by a visual system similar to that used on the Apollo spacecraft.

SECTION 6

PROPULSION AND RCS

6.1 REQUIREMENTS DESCRIPTION

The reaction control system (RCS) assists in implementing the following module functional requirements:

a. Orbit Circularization

b. Docking and departure

c. Station keeping (i.e., correction of orbit decay due to drag)

Modules may require orbit circularization at 270 n.mi. after being placed by the space shuttle into a 270 x 100 n.mi. parking orbit, in addition to docking. Additional propellant is provided to change docking position on the space station. The propellant increments for these maneuvers are listed in Table 6-1. The propellant weight is determined from a maximum design weight and a system specific impulse.

In order to achieve maximum propulsion system commonality, the same total propellant tankage capacity (i.e., 1920 lb. N_2H_4) was required for the detached module (CM-1). The tank capacity provided roughly represents a one-third increase over the requirement that is related to the delivery to the space station, where propellant for the module operations would be resupplied. The vehicular operational requirements are listed in Table 6-2. The stationkeeping propulsion requirements is time dependent. The tankage capacity is adequate for a considerable number of docking cycles without refueling.

Table 6-1. Module Delivery Requirements

	Maneuver	ΔV - ft/sec
	Circularize	300
	Docking	30
	Departure	10
*	Docking	30
	Contingency	55
	Total	425
	Module Design Weight	32,000 lb
	Hydrazine Monopropellant Performance	220 lbf-sec/lb
	Propellant Tank Capacity Requirement	1,920 lb N_2H_4
	Propellant Tank Capacity Provided	2,560 lb N_2H_4

* This represents a docking port position change.

Table 6-2. Detached Vehicular Operations

Maneuver	ΔV-ft/sec
Departure	10
Stationkeeping	10 to 20/month
Docking	30

The docking capability requires adequate control response of the RCS. The level provided in the Apollo and LEM programs was about 0.25 ft/sec^2 of linear acceleration. The same level is provided for the module. The corresponding angular control authority depends on the thruster leverage arm (~7.5 ft. radius) and module moment of inertia. The resultant angular authority is about 0.5 degree/ sec^2 acceleration, a value below Apollo and LEM, but considered acceptable.

Stationkeeping, or drag makeup, at a nominal 270 n.mi. altitude will be performed at intervals of 30 days or more depending on the prevailing atmospheric density and available communications range. Accelerations imposed on the module by RCS operation are low enough to obviate the need for solar panel retraction during maneuvers. Optical surfaces that are subject to degratation by propellant effluent are covered during these periods.

The fluid physics experiments (FPE 5.20-2, -3, and -4) have a requirement of four artificial gravity levels: 10^{-3}, 10^{-4}, 10^{-5}, and 10^{-6}. Table 6-3 contains a list of the propulsion requirements in terms of vehicle ΔV for each thrust level. There is a tolerance of ±10% on the gravity level to be delivered.

6.2 SUMMARY OF RCS/PROPULSION RESULTS

Monopropellant hydrazine propulsion systems were selected for the following applications:

a. RCS for the free-flying module (CM-1)

b. RCS for the attached modules (CM-3 and CM-4)

c. Thrust for the propulsion slice to provide 10^{-3}, 10^{-4}, and 10^{-5}g levels. An ammonia propellant resistojet system is used on the propulsion slice to provide the 10^{-6}g acceleration level.

A functional diagram of the RCS is presented in Figure 6-1. It consists of pressurization, propellant, and thruster systems. This minimum thruster system, which involves four thruster assemblies each containing four thrusters, can be used to produce three-axis displacement and three-axis control.

Table 6-3. Fluid Physics Experiments - Propulsion Requirements

FPE GROUPING	EXPERIMENT NO.	THRUSTING TIME & ΔV REQUIREMENTS PER FLIGHT							
		10^{-3} g		10^{-4} g		10^{-5} g		10^{-6} g	
		TIME (HRS)	ΔV (FPS)	TIME (HRS)	ΔV (FPS)	TIME (HRS)	ΔV (FPS)	TIME (HRS)	ΔV (FPS)
5.20-2	5.20.4.1	0.27	31.4	0.27	3.14	0.27	0.314		
	5.20.4.4	1.14	132						
		1.44	167						
	5.20.4.3	1.47	171	1.47	17.1			1.47	0.17
	5.20.4.7	2.0	232			2.0	2.32		
		1.0	116			1.0	1.16		
	5.20.4.8			1.04	12				
				2.76	32				
	5.20.4.6	0.5	58					0.5	.058
TOTAL ΔV			907.4		64.24		3.794		0.228
5.20-3	5.20.4.2	17.8 in 5 flights	2064 in 5 flights	33.5 in 2 flights	389 in 2 flights	144 in 4 flights	167 in 4 flights	51.8 in 2 flights	6 in 2 flights
	5.20.4.9	1.65	192						
				1.65	19.2				
						1.65	1.92		
	5.20.4.12	7.0	812						
				80.0	928				
						120	139		
TOTAL ΔV			3068		1336.2		307.92		
5.20-4	5.20.4.10			50.0	580				
		10.0	1160						
		12.2	1417						
		1.15	134	100	1161				
		5.4	626			476	552	2000	232
		0.5	58	5.0	58				
TOTAL ΔV			3395		1799		552		232

The actual RCS design resulted from FMECA and maintenance analyses that are reported in Volume V, Appendix C, Section 6. The minimum requirement was to provide for free flying module recovery (i.e., safe rendezvous and docking to the space station) after two failures in the same or different types of components. This degree of redundancy in critical components (those required for module recovery) would require abandoning the experiment after the first failure, and returning to the space station. The maintainability analysis showed that redundancy to provide for an additional failure would be economically justified in terms of reducing the cost of unscheduled returns to the space station. The resulting RCS design is shown in Figure 6-2. Basically there are four parallel lines; each line includes pressurant, propellant, and a thruster module. An interconnect system is provided between the modules, and this is shown in Figure 6-2 and in Figure 6-3. The associated solenoid valves are normally in the closed position. However, any propellant line can be fed into any thruster assembly by opening two appropriate valves. This is done in the event of a propellant feed failure.

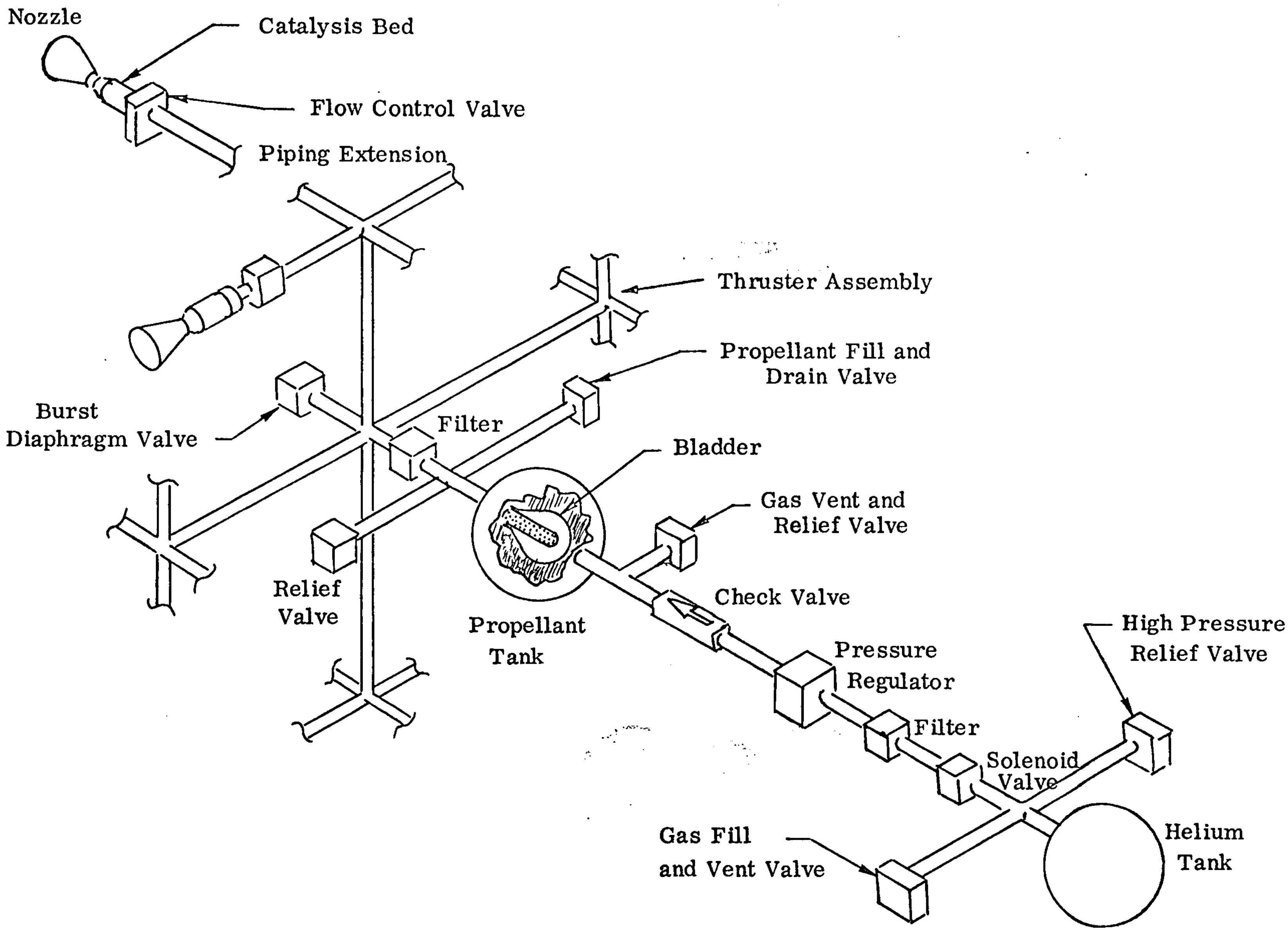

Figure 6-1. Monopropellant RCS System

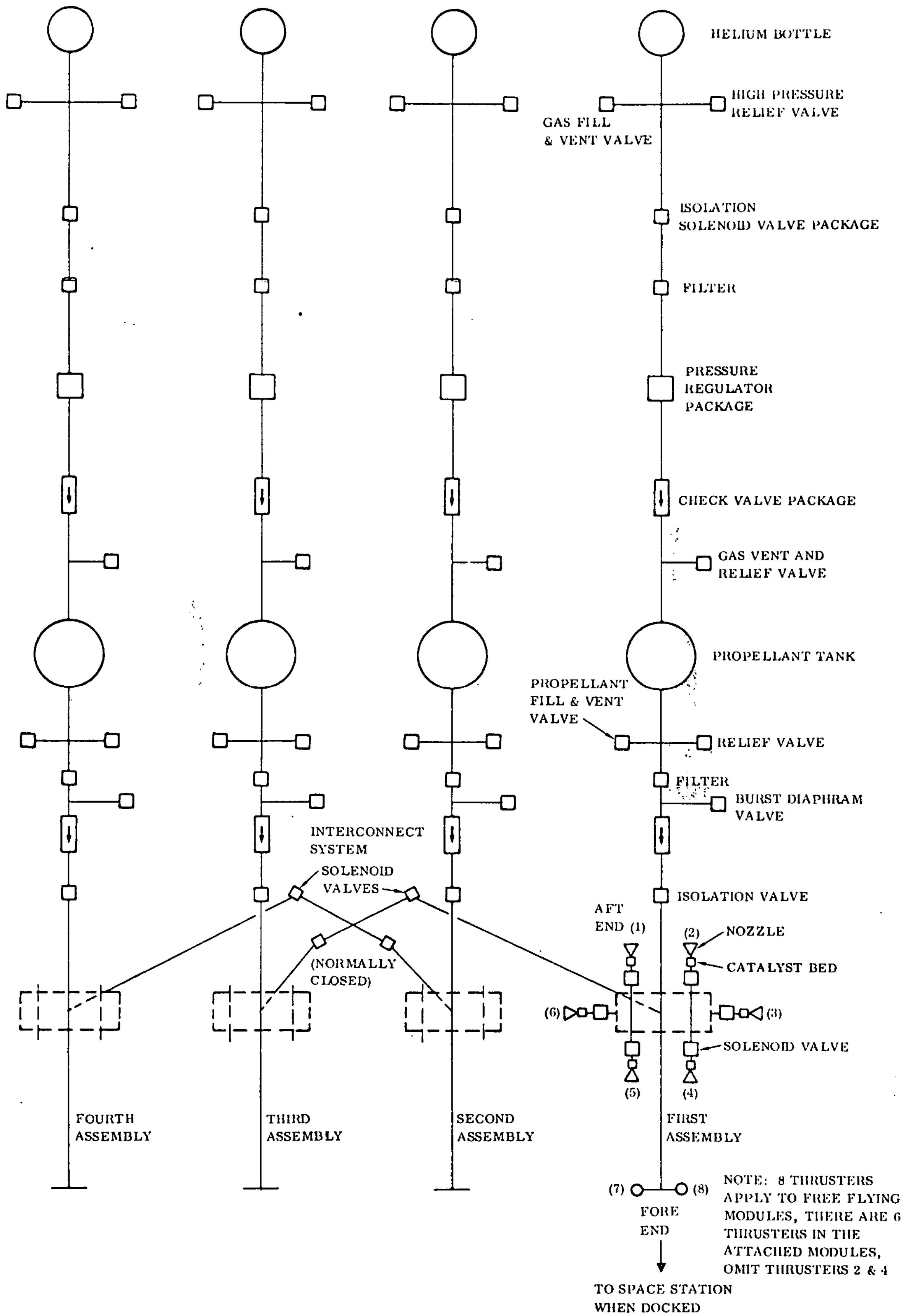

Figure 6-2. Redundant RCS System

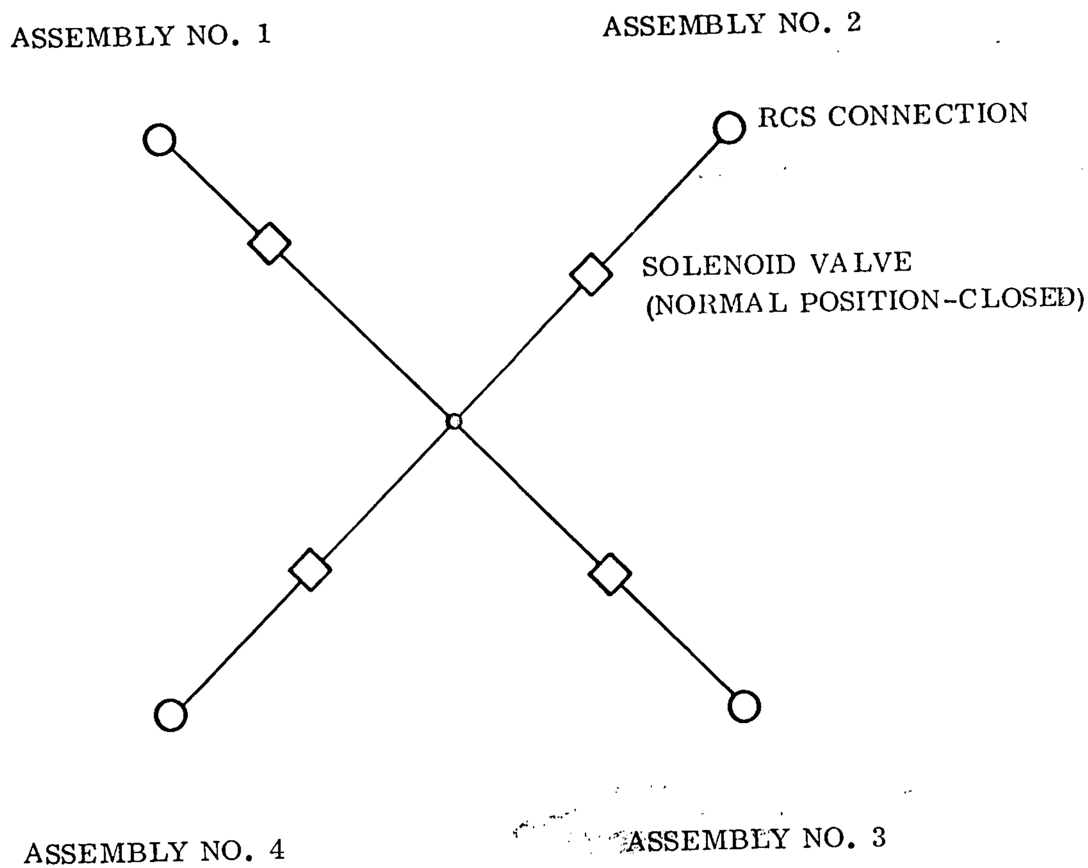

Figure 6-3. Cross Connect for RCS Assemblies

The RCS system for the attached modules was made common with the free flying module except that the eight thrusters indicated in Figure 6-2 are deleted. Redundancy to provide for two failures results in the 24-thruster system while retaining full control and displacement capability.

The delivery of the attached and free flying modules from a shuttle or expendable launch vehicle are similar. The major propellant requirement is to provide for orbital circularization of the vehicle. Three tanks provide the propellant for the maneuver given previously in Table 6-1. A fourth tank provides sufficient propellant capacity for the loss of one line just after release from the delivery vehicle.

The thruster valves received particular attention. A fail-open mode could result in a serious situation while docking to the space station. A series redundant valve would be utilized to prevent this situation.

Table 6-4 lists the resultant RCS component makeup for each installation. The characteristics of the propulsion slice system are presented in Table 6-5. Three pairs of hydrazine monopropellant thrusters are provided, and each pair provides a given thrust level. The lowest thrust level is provided by resistojet thrusters. Each of the two sets of thrusters is mounted on a plate that can be gimballed to provide fine vehicular attitude control during the low gravity experiments. Some thrust flexibility can be obtained by operating more than one pair of thrusters at the same time. The hydrazine thrusters are used in the continuous mode and require long operating life. A thermal decomposition type of hydrazine thruster would be compatible with this application. A catalyst type of thruster would be used in the RCS in order to produce high response pulsing operation.

The propulsion slice is not a critical subsystem and is not subjected to redundancy criteria as was the RCS system. The six tanks and two bottles for the hydrazine system and the two tank ammonia resistojet systems resulted from structural design analysis and not from redundancy requirements. The hydrazine propulsion slice system would be similar to the RCS except for the thruster arrangement. The resistojet system would be similar to that shown in Figure 6-12.

6.2.1 RCS SCALING DATA. The RCS/Propulsion subsystem is substantially affected by the mass of the vehicle and the equivalent velocity increment of the mission. The scaling curves presented in Figures 6-4 and 6-5 are based on the hydrazine monopropellant RCS previously given in Figure 6-2. The data presented in Figure 6-4 is for a 32-thruster system, a 24-thruster system is represented in Figure 6-5. The thrust level selected will impart a longitudinal acceleration of 0.25 ft/sec^2.

The RCS dry weight was synthesized in connection with the major component scaling curves presented in Section 6.3. The tank weights are consistent with the use of teflon or elastomeric bladders. The use of metallic bladders will approximately quadruple the dry propellant tank weight. For example, the design point of 929 lb would be increased to about 1330 lb dry weight if a metallic bellows tank were used.

Table 6-4. Hydrazine Monopropellant RCS Component Definition

Component Function	Size (cu ft)	Weight (lb)	Power (watts)	Quantity of Comp Required CM-1	CM-3	CM-4
Helium Tank	1.90	66.5	0	4	4	4
Gas Fill & Drain Valve		0.4	0	4	4	4
High Pressure Relief Valve		0.4	0	4	4	4
Solenoid Valve		2.0	30	4	4	4
Pressure Reg. & Filter		2.4	0	4	4	4
Check Valve		0.2	0	4	4	4
Vent & Relief Valve		0.4	0	4	4	4
Prop. Tank & Bladder	12.0	32.0	0	4	4	4
Relief Valve		0.6	0	4	4	4
Filter		0.2	0	4	4	4
Check Valve		0.2	0	4	4	4
Isolation Valve		1.5	30	4	4	4
Interconnect Valve		1.5	30	4	4	4
Burst Diaphram		1.5	0	4	4	4
Thruster (140 lbf)	0.13	15.3	90	32	24	24
Total Size, cu ft				59.6	58.6	58.6
Total Dry Wt, lb				928.8	806.4	806.4
Power: None Required During Experimentation				—	—	—
Propellant, lb				2560	2560	2560
Pressurant, lb				20	20	20
Total System Weight				3508.8	3386.4	3386.4

FPE Location

CM-1: 5.1, 5.2A, 5.3A, 5.5, 5.20-2

CM-3: 5.8, 5.7/12, 5.16, 5.20-1, 5.27

CM-4: 5.11, 5.9/10/23, 5.22

Table 6-5. Propulsion Slice System Characteristics

	10^{-3}g to 10^{-5}g	10^{-6}g
Thrusters		
I_{sp}	230	350
Number	2 + 2 + 2	2
Type	Monopropellant	Resistojet - NH_3
Thrust (lbf), (each of 2 engines firing)	15 ~ 10^{-3}	0.015
	1.5 ~ 10^{-4}	
	0.15 ~ 10^{-5}	
Propellant	Hydrazine	Ammonia
Propellant Tanks		
Capacity lb/Pressure psi	6800/400	690/350 psi
Number & Type	6	2
Gas Pressure Vessels		None Required
Capacity lb/Pressure psi	46#/4000 psi	
Number & Type	2	
Weights		
Propellant	6800	690
Gases/Fluids	45	None
Dry System	1000	170
Wet System	7845	545

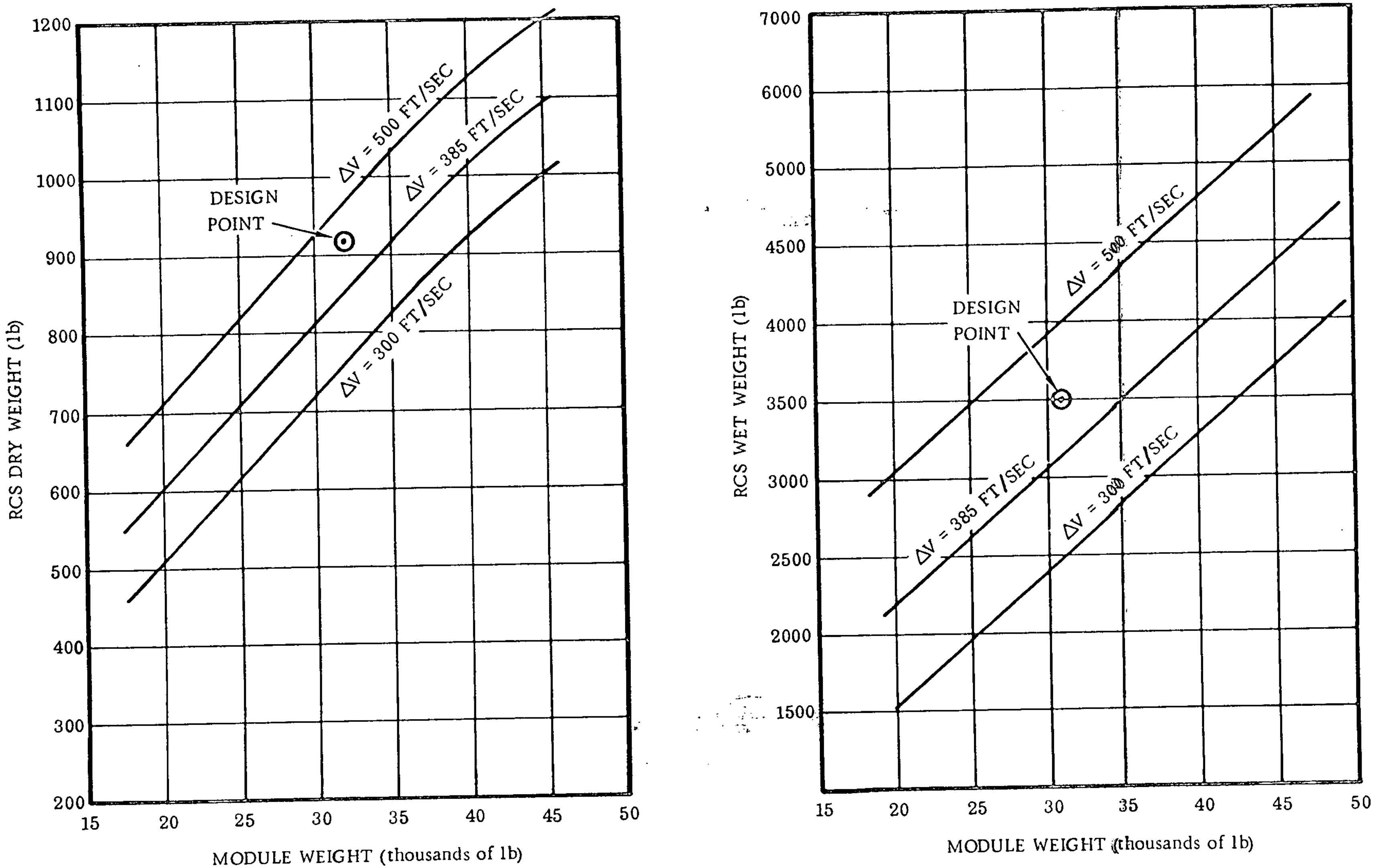

Figure 6-4. RCS Scaling Curves for CM-1

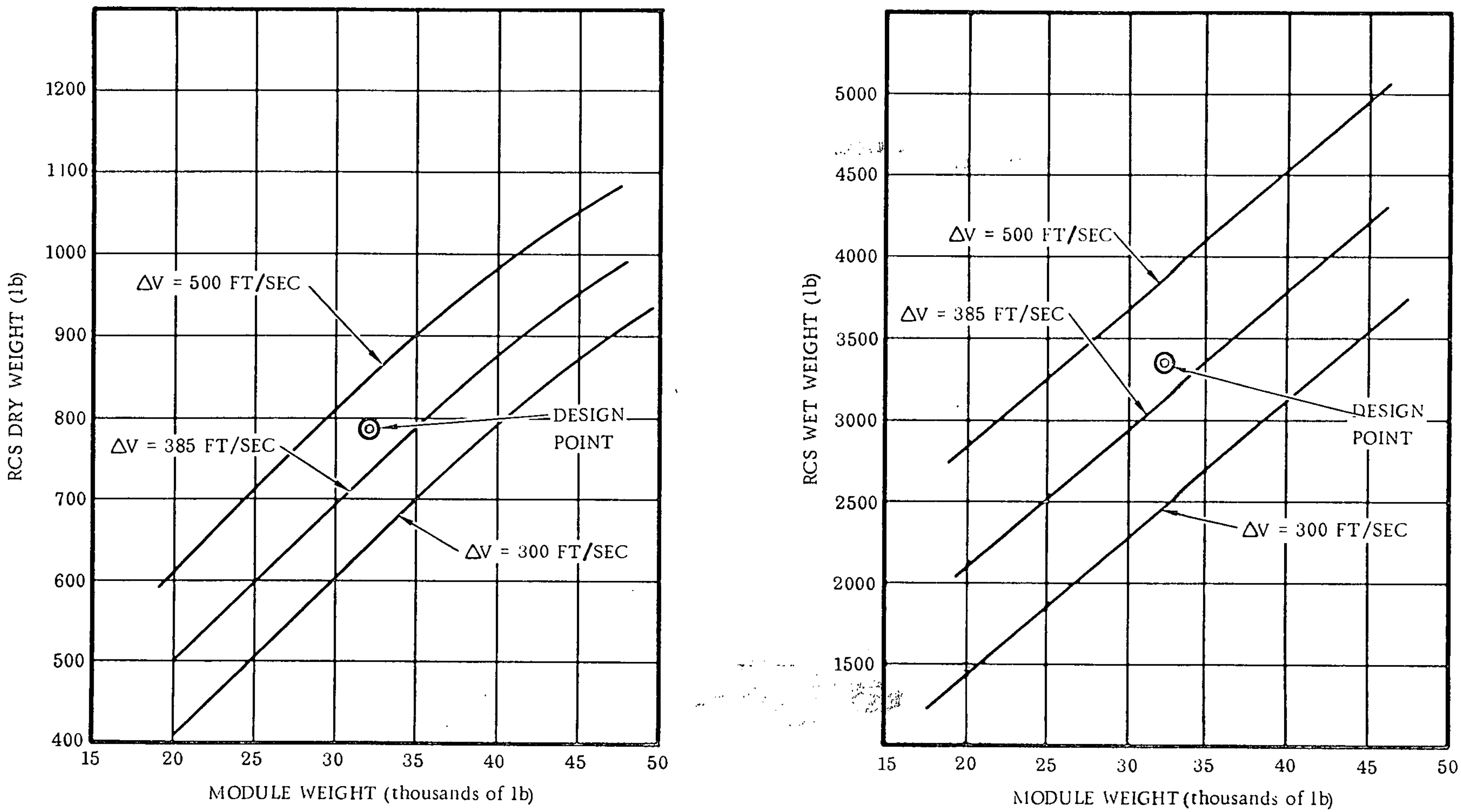

Figure 6-5. RCS Scaling Curves for CM-3 and -4

6.2.2 <u>RECOMMENDED ALTERNATES AND DESIGN ISSUES</u>. The monopropellant propulsion system approach is currently selected over the higher performance storable bipropellant approach due to the following considerations:

a. Substantial explosive hazards associated with N_2O_4 - MMH.

b. More serious contamination and heating effects of N_2O_4 - MMH exhausts.

c. More difficult 10-year material life with N_2O_4.

d. Substantially simpler system approach with monopropellant.

e. Logistics simplified with single propellant.

Cryogenic bipropellant has an almost twofold specific impulse advantage over monopropellant hydrazine, but the following disadvantages are substantial:

a. Propellant boiloff, particularly for free flying mode.

b. Large hydrogen tank volume and weight for supercritical storage.

c. Cryogenic propellant transfer potentially difficult.

d. Significant explosive or combustion hazards.

The catalyst associated with the monopropellant system is recognized as a negative factor, particularly from the standpoint of operating life. The large propellant consumption associated with long term low acceleration experiments indicates the desirability for higher performance. The effluent of hydrogen-oxygen thrusters probably has the lowest contamination potential of the three propellant systems considered.

For the propulsion slice element only a resistojet thruster system was added primarily because the combination of catalyst attrition and small nozzle throat in a hydrazine millipound thruster could cause plugging of the small nozzle throat area. Also the resistojet performance is substantially higher than the standard hydrazine system. The hydrazine resistojet should be evaluated. The catalyst problem would be avoided, and the performance would be comparable to the ammonia resistojet. The status of the thruster technology for hydrazine resistojet would be a key item for consideration. A satisfactory hydrazine vaporizer will have to be evolved in order to make the hydrazine resistojet approach practical.

The major design issues associated specifically with the hydrazine system are discussed below. More detailed trade studies and technology evaluations are recommended in these areas to optimize the hydrazine system.

Helium was selected as the RCS pressurant because the weight is about one seventh that of nitrogen. However, helium has a greater tendency to leak. A preliminary review of helium systems that have been developed indicates that the problem is significant but can be resolved by proper component selection, development, and providing moderately excess capacity.

Elimination of the high-pressure gas system by use of a vapor pressure system would avoid potentially troublesome components and high-pressure system hazards. Pressurant resupply would also be avoided. However, the technology of vapor pressurization for the size of the current application is not nearly as advanced as that of the high-pressure system approach. The requirement of an associated thermal control system and operational considerations could obviate the use of a vapor pressurization system.

Chief requirements of a propellant tank bladder are low fluid permeability, high reliability, adequate recycle capability, and low weight. Bell Aerosystems has reported a Teflon bladder that could be recycled 50 times. Elastomer bladders have a higher recycle capability, but permeability characteristics may not be acceptable. Metallic bellows bladders have a high recycle capability and the least permeability, but the tank weight is about four times that of the elastomers or teflon approaches. A detailed analysis of current vendor technology data is required to make the best compromise selection for the attached and free-flying module applications. The bladder problem was included as part of the SRT on propellant transfer.

The thermal, pressure, and contamination plume effects on the module and space station surfaces require parametric analyses that would importantly contribute to the desired thruster arrangement and orientation for avoiding the associated problems. Another important consideration is the inherent variability of the module center of gravity position with experiment FPE. Additional balancing thrusters, movable thruster assemblies, or some propellant inefficiency result when producing vehicular lateral and vertical displacements.

6.3 PROPULSION AND RCS CONCEPT DEVELOPMENT

6.3.1 CANDIDATE PROPELLANT SYSTEMS. Emphasis was placed on the following propellant systems.

Type	Material	Specific Impulse (sec)	Thrust-lbf
Bipropellant	MMH-N_2O_4	280 - 310	Above 2
Monopropellant	N_2H_4	180 - 235	Above 0.050
Resistojet	NH_3	~350	Above 0.001

BIPROPELLANT-MMH-N_2O_4. The storable bipropellant system is a strong competitor for higher thrust levels because of the high specific impulse steady and/or pulsed mode operation, and substantially advanced technology that was developed in connection with the Apollo program. A typical flow diagram of the system is presented in Figure 6-6. The arrangement of the components represents functional

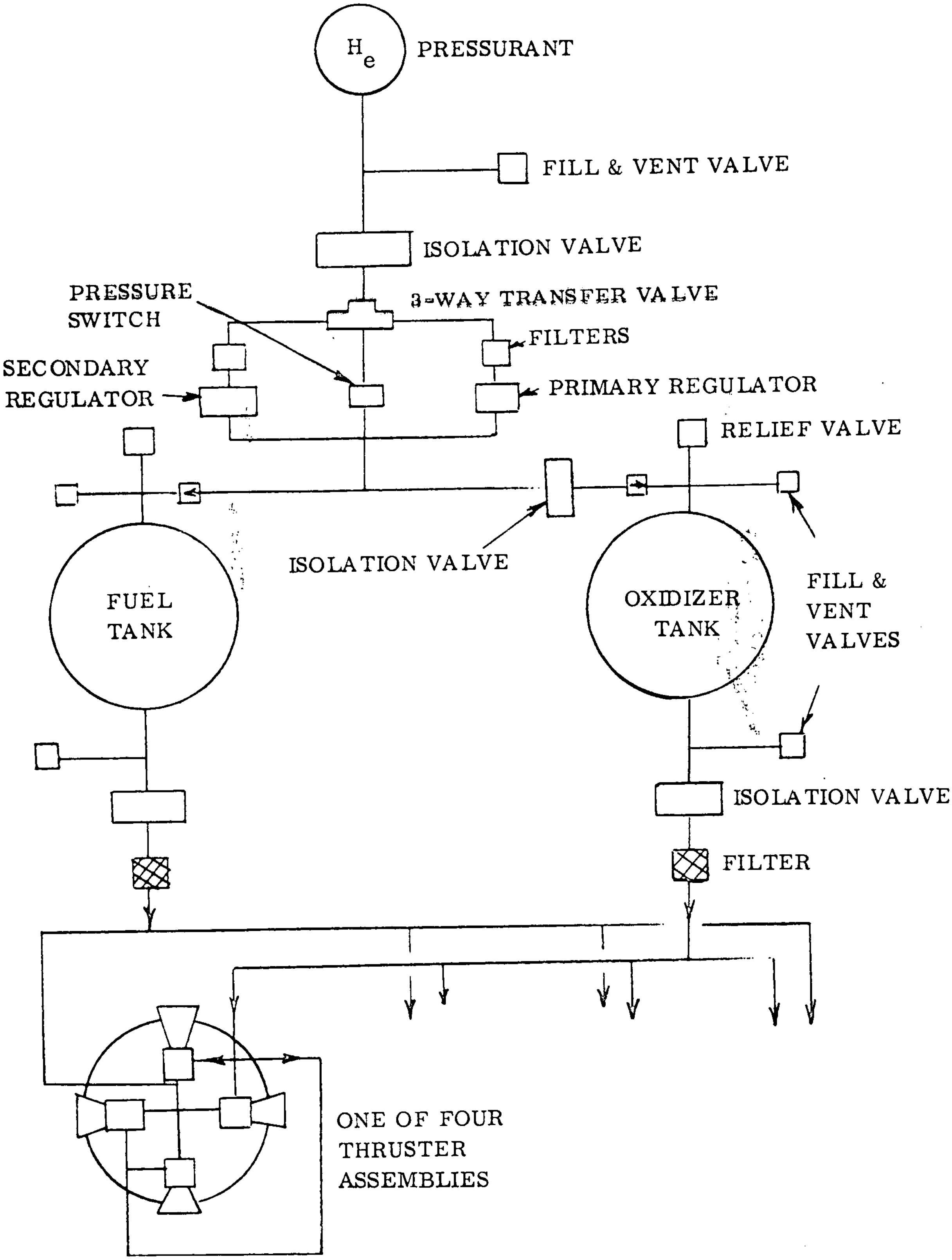

Figure 6-6. N_2O_4 - MMH Bipropellant RCS System

operation, but maintainability and reliability considerations could substantially alter redundancy and arrangement of the components in later studies. A high pressure nitrogen or helium supply could be provided to pressurize the propellant tanks for thruster operation. The much heavier nitrogen gas represents a considerable portion of the system weight. However, helium gas tends to leak at a much higher rate than nitrogen through the valves. A resupply schedule in the order of six months to one year is envisioned. Helium leakage in a closed system has been demonstrated not to be an important problem, and the approach is used in current programs. However, if the system is to be used intermittently there is a possibility that valve closing may not be adequate to reduce leakage to an acceptable extent. It is anticipated that the solenoid isolation valve shown in Figure 6-6 would provide reuse capability with only minor helium leakage. However, the official test data should be reviewed, if it can be provided prior to making a final recommendation. Current ground rules call for the resupply of helium by line rather than by bottle replacement. The details and cost for doing this will be part of the maintainability study. The transfer of high pressure gas tends to be inefficient due to adiabatic compression and expansion effects. However, it is anticipated that this type of problem can be avoided by thermal control equipment.

Reliability considerations indicate the need for regulator redundancy as shown in Figure 6-6. The N_2O_4 and MMH tanks are equal in size because an oxidizer to fuel ratio of 1.6 is used. Maximum propellant specific impulse is also delivered with this mixture ratio. An isolation valve is provided at the tank outlet line largely to prevent leakage during thruster system shutdown. Although control valves are integral with each individual thruster, the high cycling characteristics utilization could produce a significant leak in at least one of the thrusters.

The propellant tanks could contain either a bladder or a surface tension device to assure a liquid effluent from the tank. It is important to avoid two phase flow to the thrusters. A bladder also has the potential of preventing the gas pressurant from dissolving in the propellant. The dissolved gas could later form bubbles in the propellant at reduced pressure prior to entering the injector. This does not tend to be a serious problem in practice, but it is not desirable. Teflon bladders have been largely used to date. Although some gas and propellant diffusion has been experienced through earlier versions of this material, later technology involving composite materials, of which a metal film comprises one or more layers, showed substantial improvement in the Lunar Orbiter and Comsat programs. In addition, since there is a ground rule to resupply propellants by umbilical cords rather than as new tank systems, bladder recycle capability is necessary. Single use missions such as Apollo and Lunar Orbiter impose a ten cycle specification on teflon bladders. Investigation is required to verify a higher reuse capability such as a twenty cycle design. Metallic bellows bladders have a high recycle capability and essentially impermeable to fluids. However, they have low reliability, are expensive, heavy and involve high residual propellant. It is anticipated that either a teflon based bladder or surface tension expulsion system will eventually be selected after maintainability studies.

In the case of the RCS system, 16 engines would be arranged in clusters of four engines space at 90° apart on the outside periphery of the assembly and preferably at the module center of gravity longitudinal position. Lateral movement could be more efficiently provided in this manner. This arrangement provides versatility for individual engine firing or pure force couples in yaw, pitch, and roll. If the thrusters are located away from the longitudinal center of gravity, such as in the case of a space tug moving a module, lateral movement would require an additional couple, and this approach would increase the propellant requirement. It is clear that the 16 thruster configuration provides complete redundancy for the roll control thrusters. Commonality of the thruster modules is also achieved. The loss of a pitch or yaw thruster is partially redundant in that a couple could be created by the operation of three thrusters. For example, two yaw thruster operation could compensate for the loss of a pitch thruster. This may not be entirely satisfactory, and a 24 thruster system may be required to attain complete redundancy. Such considerations would be pursued in a reliability and maintainability study.

Radiation cooled thrust chamber assemblies are recommended for use on the RCS and propulsion for the bipropellant system. The Marquardt R-4D-7 engine represented in Figure 6-7 is considered typical of this approach. Substantial experience has been developed with the system on the Apollo program which would accrue to the experimental modules. Engine life development is in progress. One current objective is to verify a 2 x 10^6 pulse engine. The burn time could be extended substantially by increasing film cooling at a modest performance reduction. However, the maximum burn time characteristics of the bipropellant thrusters is not presently available.

The mass properties of the bipropellant propulsion system are to be described in order to document the assumptions and physical constants that were used. Attention was focused on the principal items: pressurant tank, propellant tanks, and thrusters.

Pressurant Tank Characteristics:

Material	Ti 6 Al-4V
Ultimate Tensile Strength	155,000 lb/sq.in.
Material Density	0.160 lb/cu.in.
Safety Factor on Skin Thickness	1.8
Weight Factor Allowance for Misc. Items	1.2
Volume Allowance Factor for Leakage	1.2
Operating Pressure	4,000 psi
Maximum Pressure	5,000 psi

Residual Pressure	600 psi
Nominal Operating Temp.	530°R
Maximum Operating Temp.	660°R
Minimum Operating Temp.	460°R

Bottle System Weight, LBM=5.7 x Volume of Propellant (cu.ft.)

Table 6-6 contains a summary of mass properties and size results for the pressurant system. The data are plotted in Figure 6-8.

Propellant Tank Characteristics:

Material	Ti 6Al-4V
Minimum Thickness	0.02 inches
Safety Factor on Ultimate Strength	1.4
Factor for Mfg. Tolerance & Construction	See Table 6-5
Ullage Volume Allowance	10%
Design Pressure	400 psi

Table 6-7 contains a summary of the design data, and these are plotted in Figure 6-9.

Thruster Data:

A plot of RCS (16 thrusters, 4 thrusters per module, 4 modules) weight is presented in Figure 6-10. The thruster weight was determined in connection with the Marquardt radiation cooled engines such as represented in Figure 6-7. Additional weight, about 20% of the engine weight, represents the structural portion of the modules.

MONOPROPELLANT - N_2H_4. The monopropellant hydrazine propulsion system technology has been of particular interest because of its long term space storability, system simplicity, and good propellant performance.

A typical monopropellant system is shown in Figure 6-11. The system is similar to the bipropellant system previously described. The characteristics of the system are shown in Figures 6-8, 6-9, 6-10 and Tables 6-6, 6-7 and 6-8 with the bipropellant data.

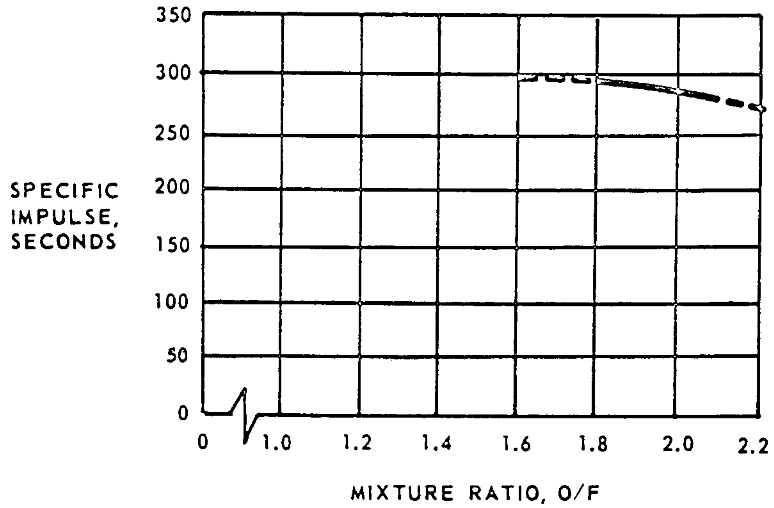

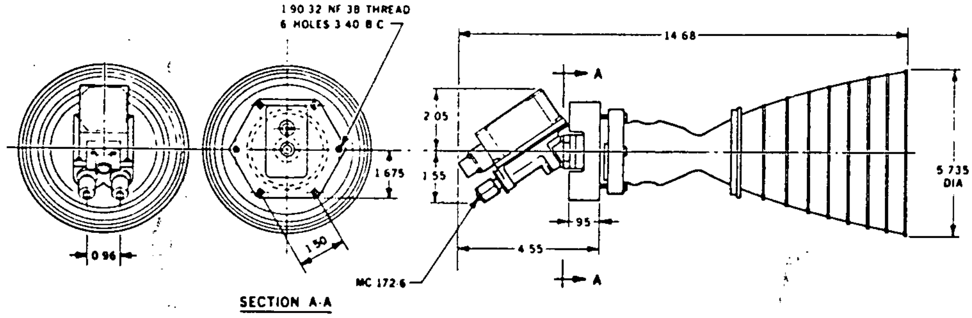

GENERAL DESCRIPTION

Total Weight: 4.83 lbs.
Moog Bipropellant Valve with mechanically linked poppets.
Extended Pulse Width Injector
Fuel Film Cooled Combustor
40:1 Expansion Bell
Valves can be furnished with pigtails or mechanical connectors as required.

PERFORMANCE

Operating Life:	Unlimited
Pulse Width Range:	0.006 sec. to Continuous
Thrust Operating Range:	80 to 160 lbs.
O/F Operating Range:	1.6 to 2.2
Minimum Impulse:	0.20 lb-sec.

RATING CONDITIONS

Propellant Pressures:	180 psia @ 100 lbs. Thrust + O/F = 2.0
Propellant Temperatures:	30 to 110°F
Valve Voltage:	21 to 33 Volts DC
Valve Power: (Primary & Secondary Coils)	26 Watts @ 28 Volts DC

PROPELLANTS

Oxidizer:	N_2O_4
Fuels:	MMH or A-50
Pressurants:	N_2 or He

Figure 6-7. Marquardt Model R-4D-7 Rocket Engine, 100 lb Thrust

Table 6-6. Pressurization System Characteristics

Propellant Tank Volume cu. ft.	Pressure Bottle Volume cu. ft.	Pressure Bottle Weight LB	N_2 Pressurant Weight LB	He Pressurant Weight LB	Hydrazine Propellant Weight Equivalent	N_2O_4 - MMH Propellant Weight Equivalent
0.455	0.0741	2.60	1.26	0.18	25	28.8
0.91	0.1482	5.19	2.24	0.32	50	57.5
1.82	0.296	10.40	4.48	0.64	100	115.0
3.64	0.594	20.60	9.66	1.38	200	230.0
7.28	1.188	41.5	19.3	2.72	400	460.0
14.56	2.37	83.0	38.6	5.44	800	920.0
29.12	4.74	166.0	77.0	11.50	1600	1,840
58.24	9.50	332	154	23.00	3200	3,680
116.48	19.00	664	308	46.00	6400	7,360
174.72	28.50	996	462	69.0	9600	11,100

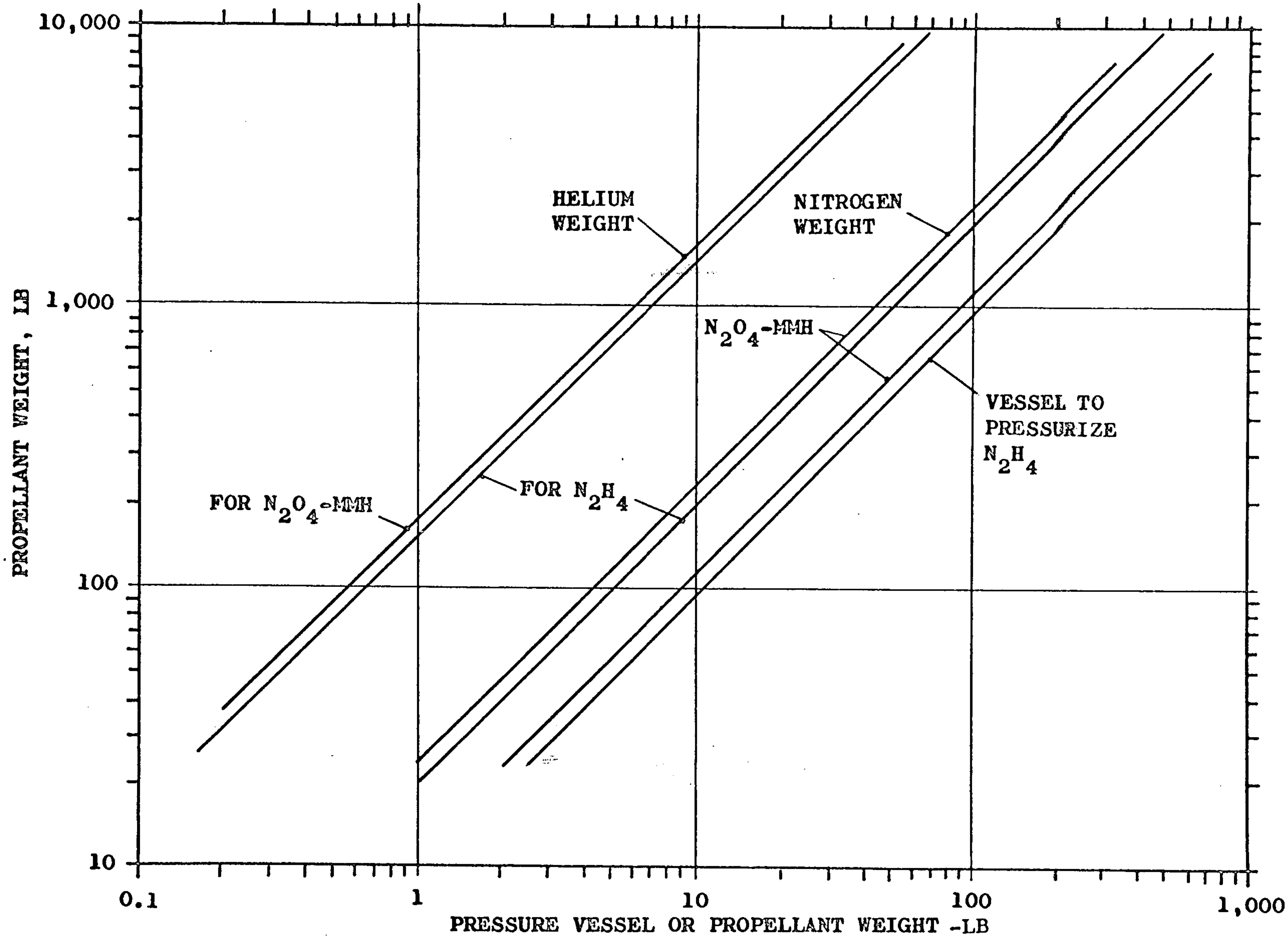

Figure 6-8. Pressurant Component Weight

Table 6-7. N_2O_4 — MMH Propellant Tanks Design Data

Propellant Weight LB	Volume of Each Tank cu. ft.	# F ---	Tank Diameter Ft.	Tank Weight LB	Bladder Weight LB	Total Weight
59.5	0.455	1.8	0.951	4.72	0.90	5.62
119	0.91	1.7	1.203	7.10	1.50	8.60
237	1.82	1.6	1.513	10.60	2.40	13.00
*						
476	3.64	1.5	1.91	16.4	3.60	20.00
955	7.28	1.4	2.40	30.6	5.40	36.00
1910	14.56	1.3	3.02	56.8	10.00	66.80
3810	29.12	1.25	3.80	109.0	16.00	125.0

Factor for manufacturing tolerances and construction.

* Numbers above refer to minimum gauge tanks.

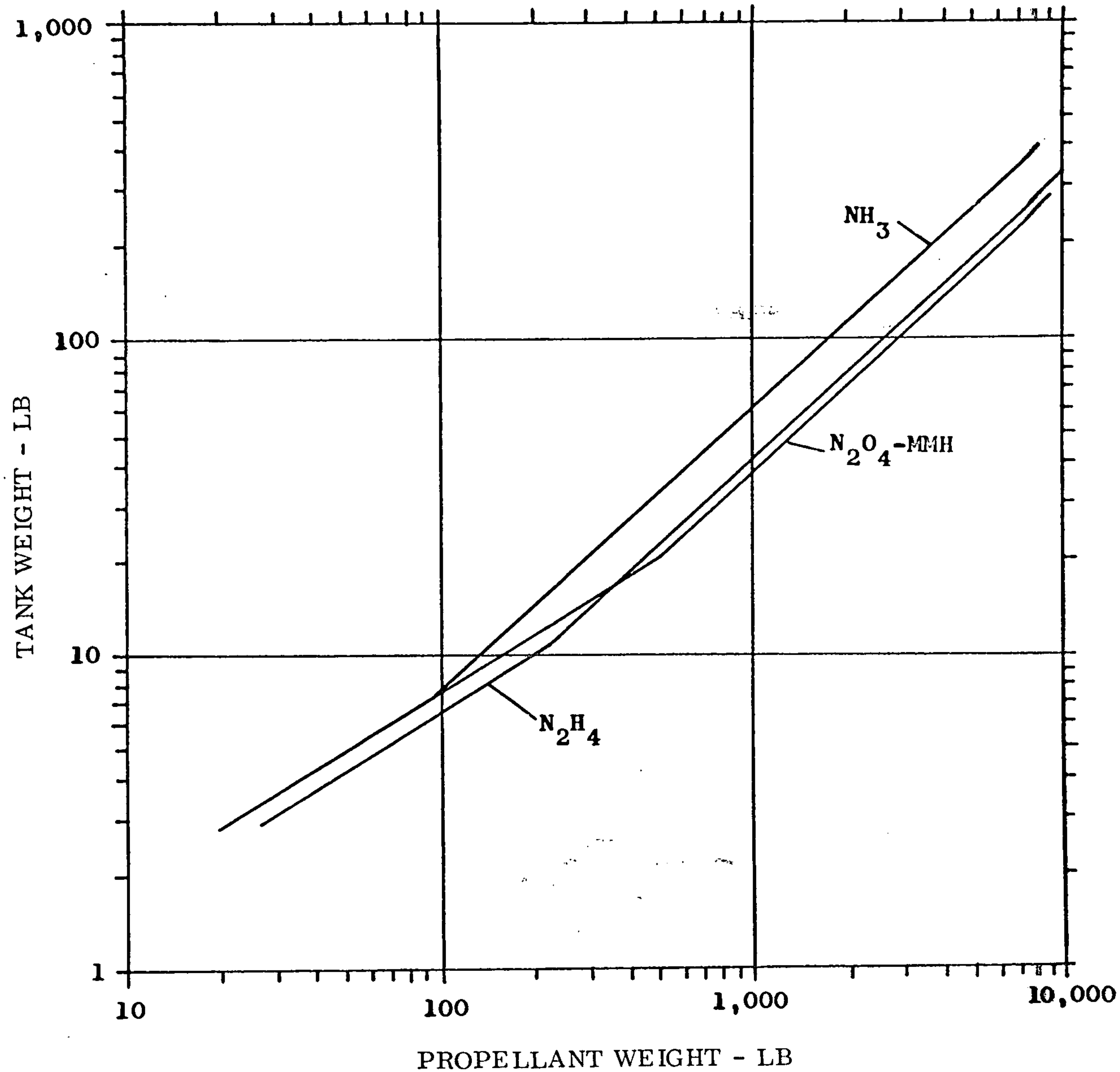

Figure 6-9. Propellant Tank Weight

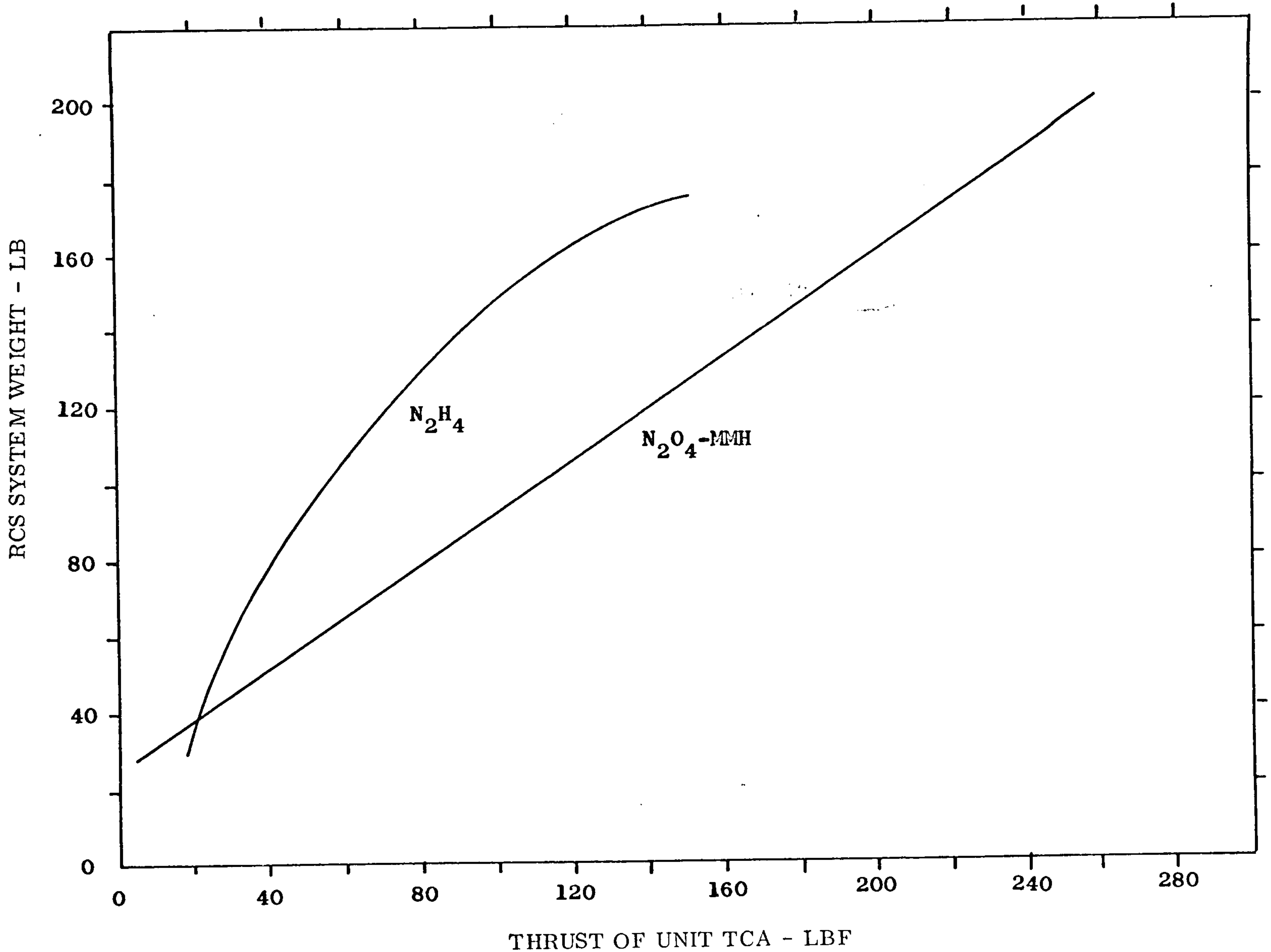

Figure 6-10. Reaction Control Thruster System Weight

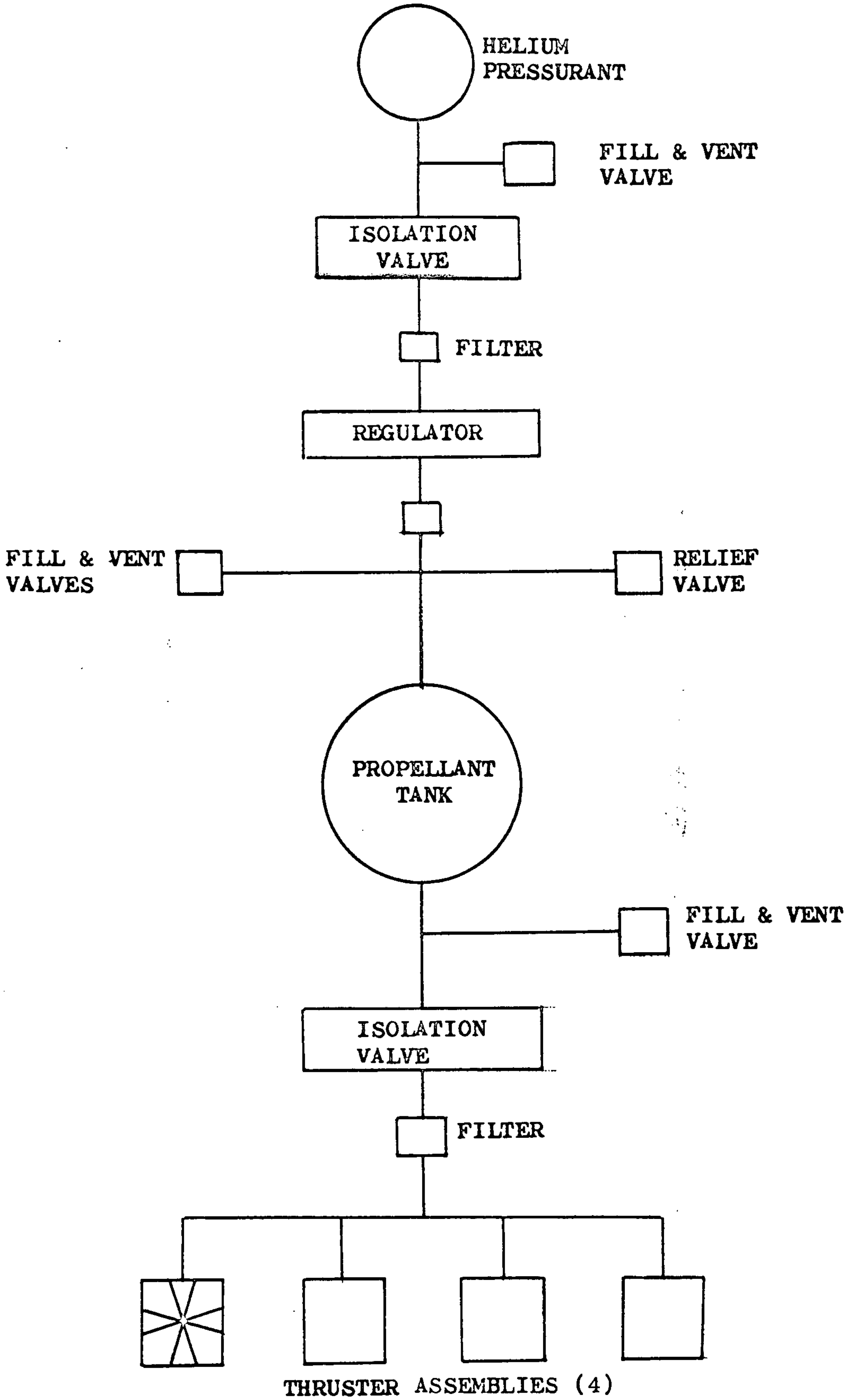

Figure 6-11. Monopropellant RCS

Table 6-8. Hydrazine Monopropellant Tank Characteristics

Monopropellant Weight (lb)	Volume (cu ft)	F	Diameter (ft)	Tank Weight (lb)	Bladder Weight (lb)	Total (lb)
25	0.455	1.8	0.951	2.36	0.45	2.81
50	0.91	1.7	1.203	3.55	0.75	4.30
100	1.82	1.6	1.513	5.30	1.20	6.50
200	3.64	1.5	1.91	8.20	1.80	10.0
400	7.28	1.4	2.40	15.30	2.70	18.0
800	14.6	1.3	3.02	28.40	5.00	33.4
1600	29.1	1.25	3.80	54.50	8.00	62.5

RESISTOJET - NH_3. The ammonia resistojet is applicable for very low thrust levels (e.g., 1 to 50 millipounds) where high total impulse requirements imply high specific impulse. They are applicable for gyro desaturation, stationkeeping, and low "g" (e.g., 10^{-6}) accelerations. A typical system is shown in Figure 6-12.

The resistojet involves nozzle thermal expansion in order to generate thrust as in the case of combustion rockets. However, the heat is supplied electrically prior to the expansion process in contrast to combustion in chemical rockets. The requirements of the combustion process, such as adequate injector performance, limits the minimum feasible thrust level attainable. The resistojet thruster avoids this limitation without sacrificing propellant performance. Specific impulse is not the only factor in selecting a propellant for the resistojet. Although gaseous hydrogen has a much higher specific impulse than ammonia in the temperature limited device, the tank weight required for gaseous hydrogen storage is excessive. Ammonia propellant has very favorable vapor pressure characteristics that can be appreciated in connection with the flow diagram in Figure 6-12. Ammonia is a liquid at moderate temperatures (below 100°F) and pressures (below 200 psia). However, it can be vaporized by waste heat, therby avoiding the need for a gas pressurization system and a bladder. The propellant tank effluent can then be completely vaporized by exchange with a liquid that is carrying waste heat. The resulting gas is then regulated by a typical sequence of pressure regulators, and valves. A summary of characteristics is presented in Table 6-9.

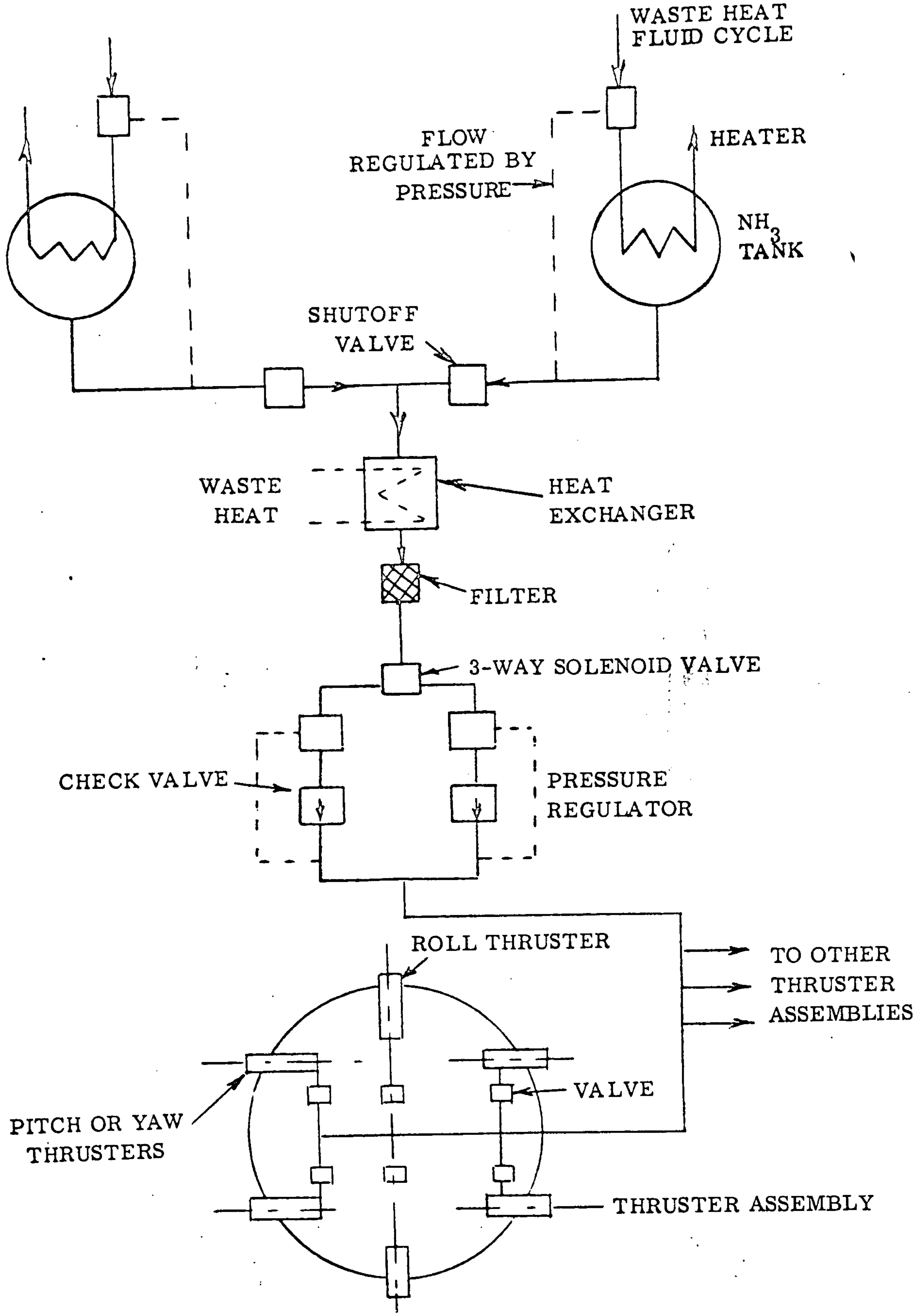

Figure 6-12. NH_3 Resistojet RCS

Table 6-9. NH_3 Resistojet Propulsion System Summary

OPERATING CHARACTERISTICS	
Thrust Level Per Unit	0.015 lbf
Chamber Pressure	30 psia
Tank Pressure	325 psia
Tank Temperature	124°F
Design Specific Impulse	350 lbf-sec/lbm
Electrical Power Per Thruster	225 watts

The characteristics of the system are:

High propellant specific impulse

Liquid propellant storage

Self-pressurizing propellant, no bladder required

About 150 watts of power required per 0.01 lbf.

The weight of the propellant tank is represented in Figure 6-9 above (along with hydrazine and bipropellant tank weights). Additional weight must be provided for tank insulation, heaters, valves and lines. This is roughly 40% additional weight based on the tank. The weight of the thruster system was determined as follows:

10^{-2} lbf Thrusters	Weight
Thruster Modules (4)	40
Valves	5
Power Switches	10
Mounting Brackets, Lines, Misc.	20
	75

6.3.2 DOCKING, DEPARTURE & STATIONKEEPING. Considerable latitude exists for selecting thrust levels to supply adequate control for docking experiment modules to the space station. As mentioned previously the thrust size was based upon a 0.25 ft/sec^2 translational acceleration with two engines firing.

The RCS system can also be used for stationkeeping. However, the thrust level required for adequate accuracy in producing the needed small ΔV's is about one-tenth that required for docking. This dual thrust capability could be incorporated into a single thruster.

The bipropellant or monopropellant RCS are applicable for docking, departure, and stationkeeping. The following considerations were used for making a preliminary selection:

1. Contamination of spacecraft surfaces and cloud formation from propellant exhausts.
2. Performance; i.e., system weight on a comparable basis.
3. Reliability, safety, maintainability, and life.
4. Flexibility, commonality, and projected growth.

The performance or weight of the N_2O_4 - MMH bipropellant is favored by about 27% over that of the monopropellant. The fourth consideration is mildly in favor of the monopropellant.

The third consideration strongly favors the monopropellant. This is substantially a direct result of a single liquid feed system that is characteristic of the monopropellant. The bipropellant is a potential hazard in operation, maintenance and resupply conditions. An explosive gaseous mixture can be generated at pressure conditions corresponding to a range of 75,000 to 250,000 feet (see Ref. 6-3 and 6-4). This property is to be translated into a weight penalty in using this system. Also, the use of welded joints would be emphasized in the bipropellant system thereby reducing system maintainability.

The technology of contamination effects of propellant exhausts in orbital research vehicular systems is in a rudimentary status (Ref. 6-2), but tests have been performed at AFRPL and are being initiated at NASA-Lewis. The principal surface contaminant of the bipropellant engine is a compound resulting from the combination of oxidizer and fuel. The quantity produced is considerable, and the thick and adhesive nature indicate that it could be a major problem. The monopropellant exhaust can produce a slight haze on a surface. The source or composition of this is not known. However, it has not hampered the performance or properties of spacecraft surfaces to date. Consideration of this problem could take precedence over performance in propellant system selection.

The initiation of bipropellant thruster operation is accompanied by the production of a cloud of liquid droplets that could obstruct astronomical observations. The same problem in a monopropellant thruster is easily avoided by a preheat cycle avoiding such a startup condition. Further study is required to determine if liquid or solid particles could be formed or avoided in plumes in either one of the propellant exhausts under steady state conditions.

The foregoing considerations led to selection of the monopropellant system on both the detached and attached modules.

The quantity of propellant required for docking and separation was estimated to be equivalent to a velocity increment of about 40 ft/sec. Stationkeeping was found to involve a velocity increment of about 20 ft/sec per month.

6.3.3 MOMENTUM DUMPING — Momentum dumping of the detached module momentum absorption actuator system is performed by a magnetic technique but dumping by millipound thrusters (10-15 millipound thrust) is an alternate. Design data covering this technique is presented.

The propellant requirement was determined by the following equations:

$$W_f = 4.12 \times 10^4 \left(\frac{W_o^2 \, I_p \, t \left[1 - \frac{I_r}{I_p} \right]}{R \, I_{sp}} \right)$$

where W_f . Fuel lb

t Time in Days

R is Moment Radius (ft)

I_{sp} Fuel Specific Impulse (350 $\frac{\text{lbf-sec}}{\text{1 bm}}$ for NH_3)

I_p main inertia (slug-ft^2)

I_r rotational inertia (slug-ft^2)

W_o 1.1×10^{-3} radians/sec

The equation was simplified to

$$W_p = 0.094 \frac{I_p}{D}, \quad W_p \text{ is } NH_3 \text{ (lb) required per year}$$

The power equivalent to ammonia propellant is 0.167 watt-years per pound mass. The power assigned to the resistojet was increased by about 50% to 0.25 watt-years/pound to account for:

Power and heat losses

Non-ideal thrusting schedules

Safety factor on theoretical estimates.

A summary of the results is shown in Table 6-10.

6.3.4 LOW LEVEL THRUSTING (FLUID PHYSICS) — A major portion of the Fluid Physics experiment (FPE 5.20-2, 3, 4) requires thrusting to produce acceleration

Table 6-10. NH_3 Resistojet System Characteristics for Momentum Dumping

FPE Module	Moment Arm (ft)	I_p Moment of Inertia (Slug-Ft^2)	Propellant Reqmt (lb/year)	Average Power (Watts)	Force (Milli-pounds)	Tank + Aux. (lb)	Thruster + Aux. (lb)	Dry Weight (lb)
5.1	15	130,800	812	203	15	75.4	75	150
5.2A	15	353,000	2,200	550	15	205	75	280
5.3A-1	15	212,000	1,550	410	15	140	75	215
5.3-2, 3	15	84,600	530	140	15	47.5	75	122.5
5.5-1, 2	15	53,200	388	96.5	15	40.5	75	115.5

levels of 10^{-6} to 10^{-3}g. The experiments are housed in CM-1 with appropriate propulsion supplied by the integral addition of the propulsion slice element. The propulsion slice contains a propulsion subsystem yielding 10^{-6}, 10^{-5}, 10^{-4} and 10^{-3}g thrust levels.

Propellant must be supplied to such experiment modules for two purposes: (1) to provide vehicle acceleration to produce artificial gravity forces; (2) to provide for module docking to and departure from the space station.

An increase in the amount of propellant carried on the module decreases the number of dockings required for propellant resupply. The required amount of propellant for docking is thereby reduced for a given total experiment program. However, the amount of propellant required for providing gravity forces is increased in order to accelerate the larger propellant inventory and storage system. A parametric study was made in order to evaluate the effect of storage propellant capacity on total propellant requirements for a given total experiment program.

In order to form a basis for a tradeoff, the requirements for a typical fluid physics study were developed involving (1) slush propellant behavior, (2) propellant transfer, and (3) boiling heat transfer. The estimate of vehicular propulsion requirements for these experiments is summarized in Table 6-11. The durations required for the experiments are only roughly estimated. Therefore, a liberal (34%) allowance over the estimate requirement was made.

The dry weight of the experiment module is comprised of a fixed weight plus a weight that is a function of the quantity of propellant storage capability. The propellant tank and feed system dry weight was generally found to be about 20% of the propellant capacity.

$$\text{Dry Weight of Module} = M + 0.20\ (G+D)$$

where M is the dry weight of module minus propellant system (lb)

G is the weight of propellant for artificial "g" forces (lb)

D is the weight of propellant for docking (lb).

The amount of propellant required for docking was assumed to be equivalent to a velocity increment of 40 ft/sec. The propellant required per docking is therefore:

$$D = \frac{[M + 0.20\ (G+D) + D]\ \ 40}{g\ I_d}$$

Table 6-11. Fluid Physics Detached Experiment Module Requirements

Module No. 5.20-3		No. of Tests per Flight	No. of Flights per Experiment	"G" Level	Duration Per Flight -Hours-	ΔV Per Flight Ft/sec	Total ΔV Ft/sec
Experiment No.	Type						
5.20.12	Slush Propellant Behavior	4	1	10^{-3}	7.0	812	812
		4	1	10^{-4}	80.0	929	929
		4	1	10^{-5}	120.0	139	139
5.20.9	Propellant Transfer	9	3	10^{-3} to 10^{-5}	4.98	214	642
5.20.2	Boiling Heat Transfer	1	1	10^{-3}	3.0	348	348
5.20.2.1	↓	1	1	↓	2.4	278	278
.2	↓	1	1	↓	2.0	232	232
.3	↓	1	1	↓	2.0	232	232
.4	↓	1	1	↓			
.5	↓	1	1	10^{-4}	9.4	109	109
.6	↓	1	1	"	7.4	86	86
.7	↓	1	1	10^{-5}	26.1	30.2	30.2
.8	↓	1	1	↓	21.8	25.3	25.0
.9	↓	1	1	↓	11.8	13.7	13.7
.10	↓	1	1	↓	10.0	11.6	11.6
.11	↓	1	1	10^{-6}	33.9	3.93	4.0
.12	↓	1	1	"	16.6	1.93	2.0
.13 thru 16	↓	2	2	10^{-3}	1.0	116.0	232.0
TOTAL							4126.0
*VALUE USED							5380.0

*Basis - 1 Year

where I_d is the specific impulse of the docking propellant (lbf-sec/lb). The propellant required for the acceleration load could be a large fraction of the module weight, and this propellant weight can be determined implicitly from the following equation:

$$\frac{\Delta V}{N} = I_g \, g \, \ln \left(\frac{[M + 0.20 \ (G+D) + D] \ + G}{[M + 0.20 \ (G+D) + D]} \right)$$

where ΔV is total mission requirement ft/sec (5380 in Table 6-10)

N is total number of dockings (also module excursions to accomplish total experiment)

I_g is propellant specific impulse required for artificial "g" forces (lbf-sec/lbm)

The total propellant requirements is (ND + NG). Some calculated results are given in Table 6-12 and plotted in Figures 6-13 and 6-14. A propellant specific impulse of 220 lbf-sec/lb was used for the study, and this propellant is typical of hydrazine monopropellant. For this study the module dry weight, excluding propulsion-system dry weight, M, was assumed to be 20,000 lb. The results are scalable with this weight.

The frequency of docking is plotted against the capacity for the propellant per excursion that is to be used to provide artificial gravity forces (see Figure 6-13). The total propellant requirement is plotted as a function of acceleration propellant tank capacity in Figure 6-14. The integral number of excursions or dockings is also given for reference. The minimum amount of propellant consumption is obtained just above a 2,000 lb tank capacity by inspection of Figure 6-14.

The results of the type presented in Figure 6-14 represent an aspect of the selection of propellant tank capacity. The results are based on one year of operation (i.e., ΔV = 5380 ft/sec). Since the experiment program is to be repeated in the second year, the mission would be obtained by doubling the numbers on the ordinate (docking, acceleration and total propellant consumption, the number of dockings), but the acceleration propellant tank capacity would remain the same. Also the propellant requirement scales directly with dry weight, M.

The number of dockings (N) also implies that the propellants are also replaced each time. The problems of propellant transfer and bladder reuse would tend to bias the selection of the propellant tank size larger than that indicated by the results of Figure 6-14. A 6,000 lb capacity tank would result in about 8% more propellant consumption than the weight optimum size indicated. The bladder recycles

Table 6-12. Total Mission Propellant Weight Requirement

G Propellant Tank Capacity for "g" Forces (lb)	D Propellant Tank Capacity for Docking (lb)	N Number of Dockings	NG Total Propellant for "g" Forces (lb)	ND Total Propellant for Docking (lb)	NG + ND Total Propellant Consumption for Mission (lb)
300	114.1	51.3	15,400	5,850	21,250
600	114.3	25.7	15,400	2,940	18,340
1,000	115.0	15.9	15,900	1,830	17,730
2,000	116.0	8.18	16,350	948	17,298
3,000	117.0	5.61	16,940	656	17,496
4,000	118.3	4.34	17,350	523	17,873
5,000	119.5	3.55	17,750	425	18,175
7,000	122.0	2.70	18,900	330	19,230
10,000	125.0	2.05	20,500	256	20,756

M = 20,000 lb $I_d = I_g = 220$ sec $\Delta V = 5380$ ft/sec

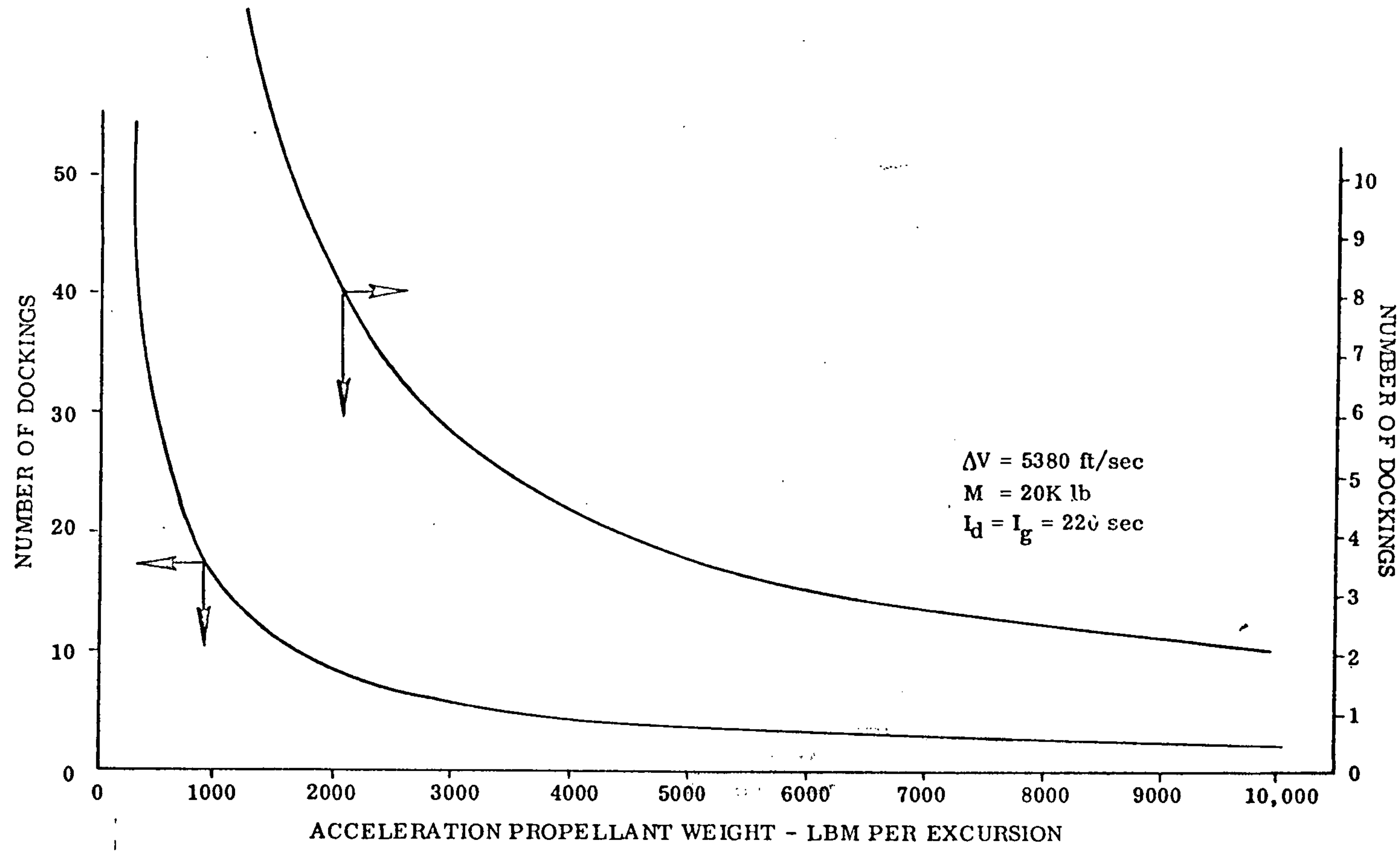

Figure 6-13. Docking Frequency and Propellant Relationship

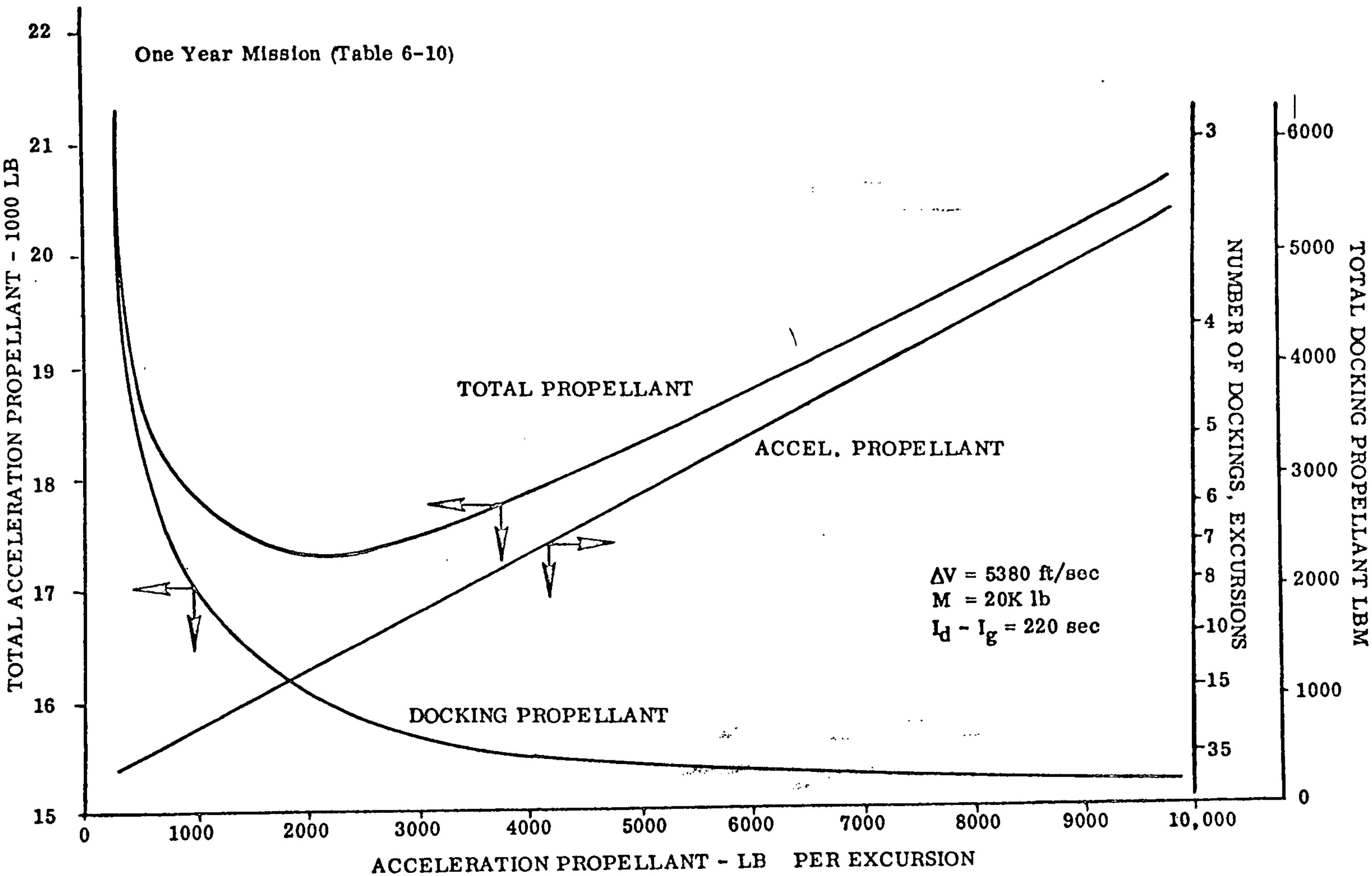

Figure 6-14. Propulsion and RCS Propellant Optimization

would be substantially reduced from 7 to 2 (one less recycle than the number of dockings). This approach is reasonable although further study of the propellant transfer and bladder reuse characteristics is justified.

6.3.5 THRUSTER ARRANGEMENT. The docking maneuver is to be accomplished with three axis controls (yaw, pitch, and roll) and three axis displacements (longitudinal, vertical, and lateral) in the current concept. It would be feasible to dock without the vertical or lateral displacements capability by steering into position. However, the more complete control would be more efficient and it was the specified approach on the orbital space shuttle.

The fail-nominal, fail-safe specification on critical components implies that two failures could take place in the same type or different types of components, and the docking capability of the RCS would be retained. The requirement can be implemented by placing eight thrusters in each module. See Figure 6-15. This was evaluated by listing the six control or displacement modes (yaw; pitch; roll; lateral; vertical; longitudinal) and enumerating all the thruster combinations to accomplish these requirements. It was also considered to make each module identical so that there would be module interchangeability. This approach would also produce symmetry in deployment, thereby simplifying the control system logic. The 32 thruster system produces more redundancy than the minimum requirement of fail-nominal, fail-safe in some of the displacement or control modes. An important case of this is the thrusters associated with longitudinal displacements. These thrusters will involve much more operating time than the other thrusters since they provide vehicular propulsion for circularization and stationkeeping. It was also found that more than the minimum redundancy is economical because a thruster failure could be tolerated without abandoning the experiment mission in the free-flying modules. However, this justification is not applicable for the attached modules, and two thrusters are deleted from each module as indicated previously in Figure 6-2.

The selection of a 32 thruster system for the free-flying module and 24 thrusters for the attached modules results from application considerations.

The thruster modules should be located near the longitudinal center of gravity, and they are spaced ninety degrees apart. If the thruster modules are not at the longitudinal center of gravity position, lateral and vertical displacements can be obtained by operating two additional thrusters to produce a compensating torque. However, the required torque and the associated propellant consumption becomes excessive as a result of a substantial center of gravity offset. The two thrusters that fire in the radial direction are placed on the opposite longitudinal position as that of the thruster assemblies. This change is represented in Figure 6-15. The radially firing thrusters that were removed from the module are shown as blank triangles. The darkened thrusters are the final position selections for the attached modules. This arrangement yields two failures to normal operating capability and one additional failure to a safe operating condition.

REDUNDANCY CHARACTERISTICS

SELECTED ARRANGEMENT : THREE WORST CASE FAILURES
SELF CONTAINED ASSEMBLIES: TWO WORST CASE FAILURES } TO LOSE ONE OF 3-AXIS DISPLACEMENT OR CONTROL CAPABILITY OF RCS

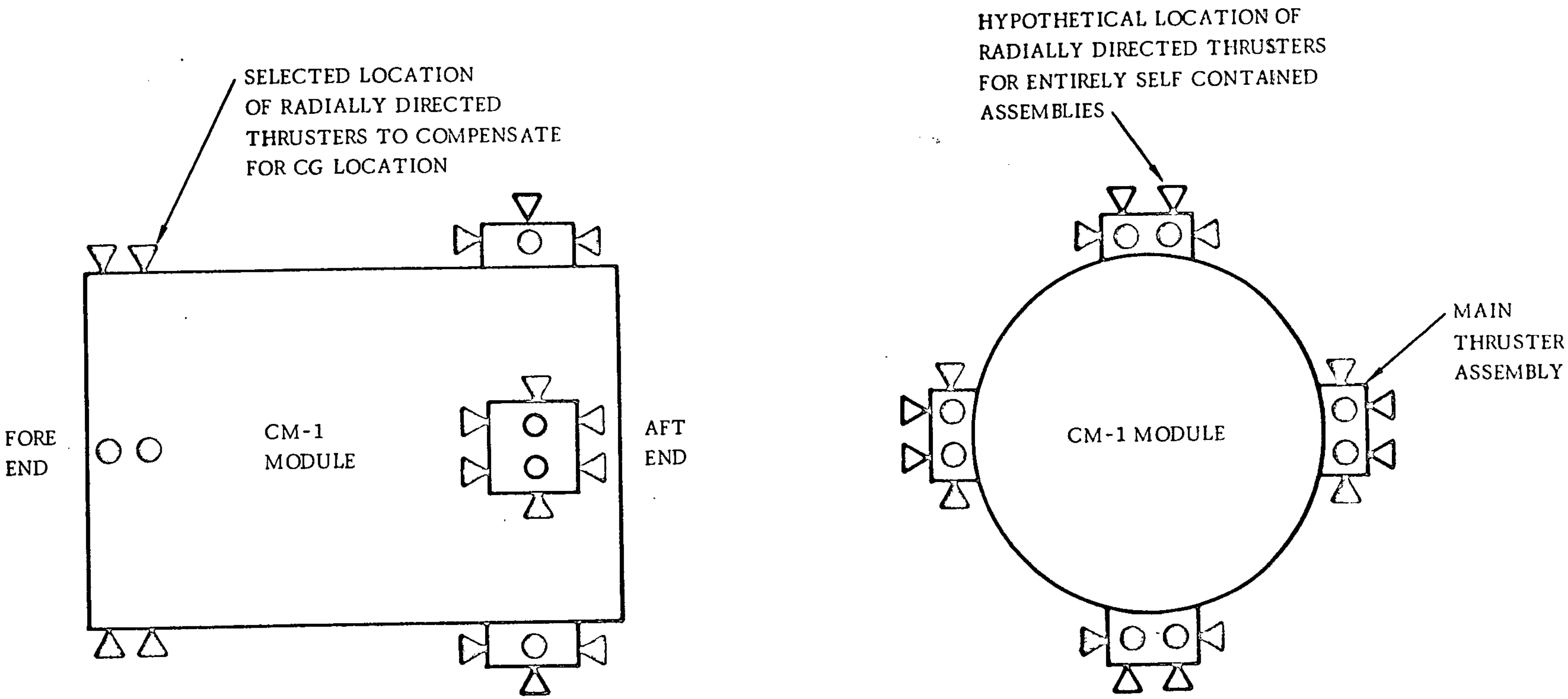

Figure 6-15. RCS Thruster Arrangements (Redundant System)

The center of gravity positions for the CM-1 vehicles are shown in Figure 6-16. It is desired to locate the main thruster modules at the extreme end of the module to minimize plume effects on the space station. The lateral and vertical vehicular displacements can be made by properly adjusting the duty cycle and/or the pulse width of the appropriate thrusters on either side of the center of gravity.

6.3.6 PRESSURANT AND PROPELLANT SYSTEM ARRANGEMENT. Figure 6-2 contains a schematic of the redundant RCS. The functional pressurant and propellant systems are shown in Figure 6-1. Essentially, there are four propellant feed lines, and an interconnect is provided between the thruster modules. Normally the valves in the interconnect lines are closed. However, any propellant feed line can be connected to any thruster module by the opening of two appropriate valves. An interconnect system is not provided between the pressurant tanks. Redundancy is more efficiently provided in this case by adding redundant critical components.

The system provides for three worst case failures in any one type or different types of components before loss of the subsystem capability. Therefore, at least one failure can be tolerated while experiments are being performed without returning to the space station for repair. The cost of providing this extra redundancy is more than compensated by saving the repair trip.

The propellant capacity of 1,920 lb for the system is substantially dictated by providing a vehicular circularization capability on delivery. This capacity is placed in three of the propellant lines. A fourth line provides 33% additional capacity so that the loss of one line after release from the delivery vehicle can be tolerated. This was considered adequate in that RCS checkout could be performed before the experiment module is released.

The four propellant lines allows each line to be individually connected to each thruster assembly. Manifolding, which would result in loss of all propellant in some cases, is thereby avoided.

6.3.7 PROPELLANT & PRESSURANT RESUPPLY. The propellant and pressurant can be resupplied to the experimental module by fluid transfer through an umbilical line, or by replacing the tanks. This consideration is principally related to the free-flying modules.

The total capacity of the propellant tanks for the RCS is currently specified as 2,560 lbm. If this were to be replaced by a man, a weight limitation of 80 lbm is generally imposed. This would involve the use of 32 tanks. This would not be a reasonably efficient approach.

The transfer of the high pressure vessels would be feasible since a four tank system would be involved. However, the mechanical manipulations involved in replacing high pressure vessels manually would be substantially more costly in man hours than

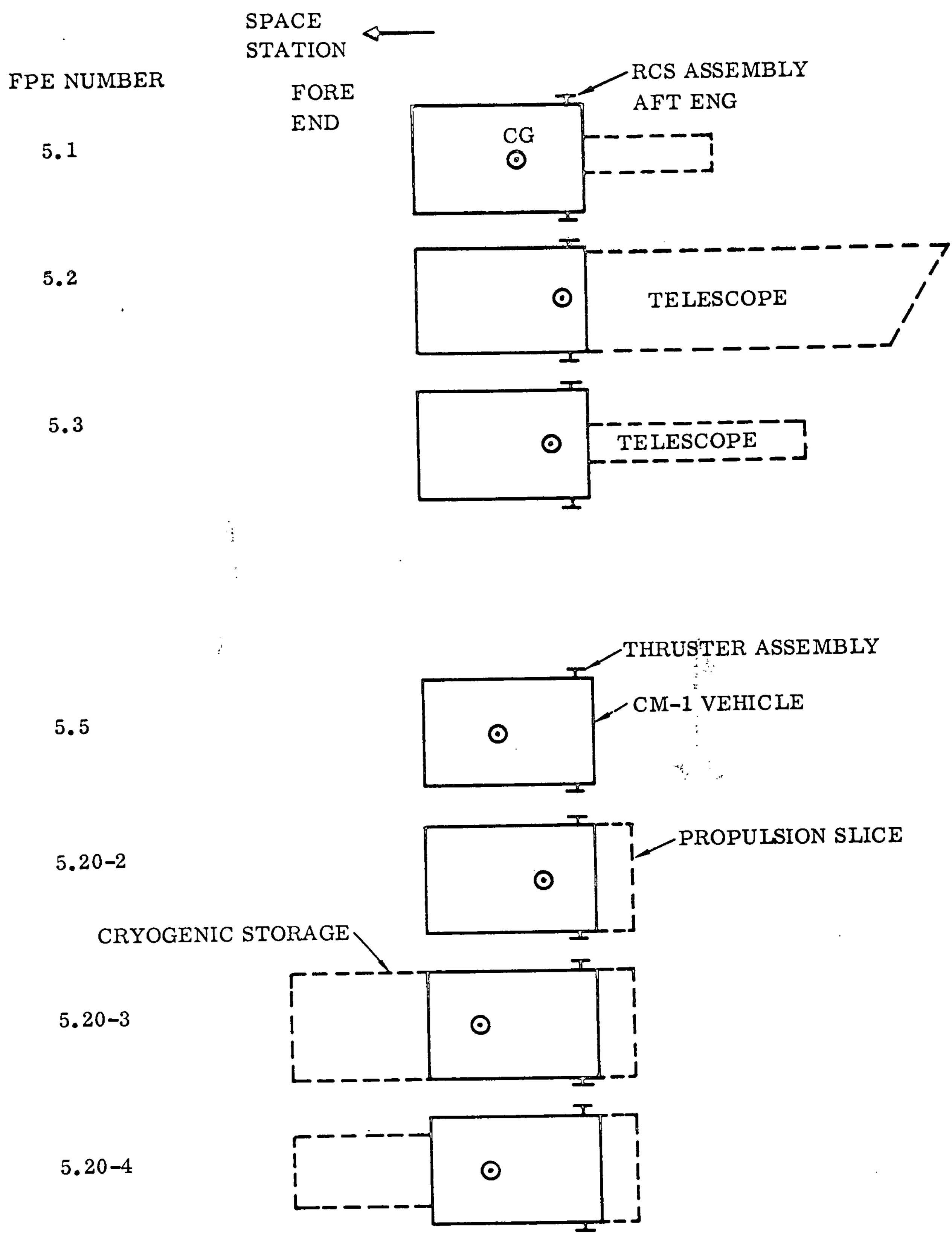

Figure 6-16. Center of Gravity Locations of CM-1 Modules

in making an external umbilical connection. In addition, the hazard potential is inherently lower in the fluid transfer approach as compared to a man manipulating the high pressure vessels in a space environment.

Figure 6-17 contains a schematic diagram of a pressurant and a propellant resupply system for the RCS. The hydrazine monopropellant supply in a space station or logistics vehicle is stored in a tank containing a positive expulsion bladder. A helium pressurization system is used to effect the transfer. The flow control of the liquid propellant is aided by the use of a cavitating venturi during the transfer process. The pressurant and propellant isolation valves on the RCS are closed during the transfer process. The helium in the RCS propellant tank can be vented as the propellant tank is filled. This approach is quite simple and no serious developmental problems are anticipated.

The cold gas transfer system approach is also illustrated in Figure 6-17. Cold helium is supplied from an insulated tank in the shuttle vehicle and delivered to the experiment module. When the pressures between the two tanks become equalized, heat is applied to the supply tank to increase the pressure and drive out some of the residual gas into the receiver tank. The transfer process is initially controlled by a pressure regulator, and later by a control valve.

The cold gas approach has a number of advantages. The required capacity of helium can be stored in a smaller tank. A cooling loop in the RCS tank can be avoided. However, it must be recognized that the materials problems associated with the range of operating temperature is an important consideration. A parametric analysis of the total system (RCS and resupply system) must be made to determine the optimum approach.

The umbilical connectors for the pressurant and propellant transfer system are key components that require advanced development. Bladder recycle capability is an implied requirement, and selection of this component should receive special emphasis.

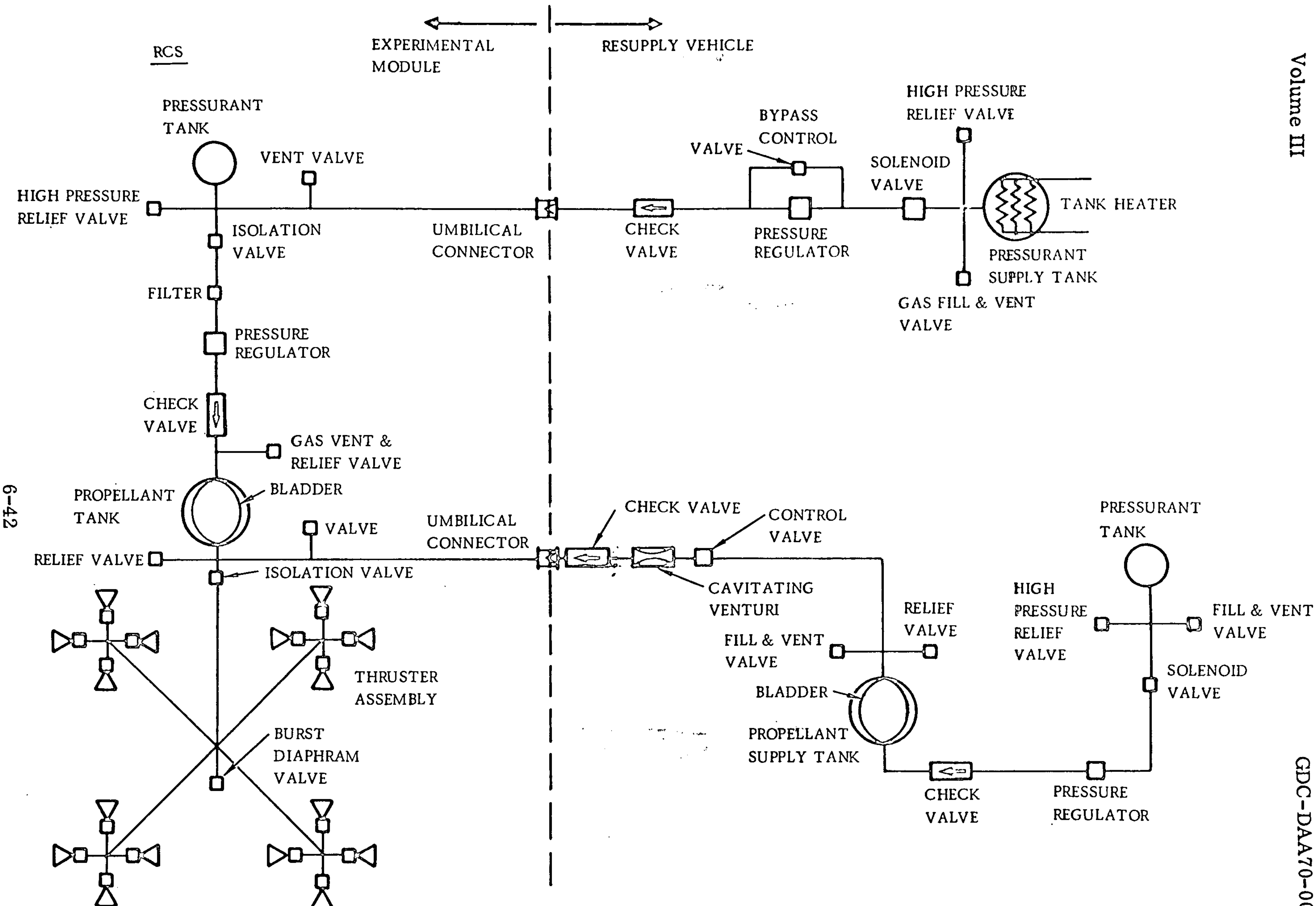

Figure 6-17. RCS Pressurant and Propellant Transfer Systems

6.4 REFERENCES

6-1 D. Eggleston, Relative Orbital Motion and Stationkeeping, GDC-ERR-1440, January 1970.

6-2 Bipropellant Attitude-Control Rocket Plume Contamination Investigation, B. J. Martinkovic, AFRPL-TR-251, October 1969.

6-3 Space Vehicle Propulsion Compartment Fire Hazard Investigation, AFRPL-TR-64-170, December 1964.

6-4 Space Vehicle Hazards, P.J. Martinkovic, AFRPL-TM-64-60, December 1964.

6-5 Attitude Control Rocket Exhaust Plume Experiment, Technical Report AFRPL-TR-67-3, February 1967.

6-6 Mid-Thrust Hydrazine Engines, Hamilton Standard HSPC 67R06, March 1967

6-7 Orbital Workshop Reaction Control System, Marquardt Report (Preliminary) 1970.

6-8 Study of Propulsion System Concepts for Space Station, Marquardt Report (Preliminary) MIR #367, February 1967.

6-9 Space Engine Design Handbook, Rocketdyne Report R-8000P-1, January 1969.

6-10 In-Flight Maintenance Study, Martin Marietta, Contract NAS9-8144, December 1969.

6.5 BIBLIOGRAPHY

1. Apollo Operations Handbook, Subsystems Data; LMA790-3-LM5.

2. Propulsion and RCS Subsystem Study Guide for Lunar Module LSG-770-154-9-LM-5.

3. Definition of a Resistojet Control System for the Manned Orbital Research Laboratory, Final Report, NASA CR-66600, May 1968.

4. Monopropellant Hydrazine Rocket Technology, Status Report RRC-67-R-88, Rocket Research Corp., 1967.

5. Aerospace Fluid Component Designers' Handbook, Air Force Rocket Propulsion Laboratory, Report No. RPL-TDR-64-25.

6. Monopropellant Exhaust Contamination Investigation, P. J. Martinkovic, Technical Report AFRPL-TR-69-72, April 1969.

7. Long Life 5 LBF Hydrazine Engines for Endurance Requirements, Hamilton Standard Report SP 13R68, August 1968.

8. Ammonia Propulsion System Study, TRW Systems, Report No. TRW 14294.000, 1330.5-3162, July 1969.

9. Life Test of Attitude Control and Station Keeping Subsystem, (NH_3 Resistojet) Technical Report AFAPL-TR-69-116, February 1970.

10. Conversion of Spacecraft Crew Wastes and Cabin Wastes to Propellant, General Dynamics Report, GDC-ERR-AN-909, December 1966.

11. Model R-4D 100 Pound Thrust Liquid Bipropellant Rocket Engine, Marquardt Report V6848-3B.

12. Model R-1E 22 Pound Thrust Liquid Bipropellant Rocket Engine, Marquardt Report V7535-7.

13. Design Study for Precision Control Rocket Engine of 1300 Pounds Thrust and 500 psia Chamber Pressure, Marquardt Report S-928, April 1969.

14. Low Thrust Propulsion Study (Hydrazine), Hamilton Standard Report HSPC 68R07, June 1968.

15. Basic Data Package for Flight Weight Hydrazine Monopropellant REA (0.1 Pound Thrust), August 1969.

16. Valve/Thruster Performance, 0.1 LBF Hydrazine Engine, Hamilton Standard Report SVHSER 5447, July 1969.

SECTION 7

COMMUNICATIONS AND DATA MANAGEMENT SUBSYSTEM

7.1 DEVELOPMENT OF REQUIREMENTS

Each of the experiments within the FPEs uses a variety of sensors and instruments that produce raw data in the form of digital, analog, and film. The communications and data management subsystem's role in handling this data aboard each experiment module is to:

a. Provide the means of sequencing, controlling, and adjusting experiments and subsystems.

b. Gather the data from the experiment packages and module subsystems.

c. Perform data accumulation, correlation, transformation, and other processing associated with experiments and subsystems.

d. Format the data for either transmission to the space station and/or ground stations or for further processing and delivery in hard-copy form to the Principal Investigator.

e. Perform on-board checkout and redundancy control of experiments and subsystems.

The ground rules that influenced the communications and data management subsystem (CDMS) design are as follows:

a. Free-flyer experiment and subsystem data are to be transmitted to the space station. Control of experiments and subsystems aboard free-flyers is to be via the space station.

b. Space station/free-flyer maximum separation during experiment operation is 500 n.mi.

c. Command and telemetry links between the space station and modules must be capable of operating at a maximum line-of-sight distance of approximately 2600 n.mi.

d. One modular CDMS design should be applicable to all experiment modules with the possibility of leaving off equipment where not required.

e. Attached modules will contain all the subsystem elements to perform rendezvous and docking. This implies that the CDMS aboard the attached modules must perform the necessary subsystem control and telemetry functions as in the case of the free-flying modules.

f. Experiment and subsystem data and control will be hardwired to the space station while the module remains attached.

7.1.1 REQUIREMENTS ANALYSIS. Eight of the 13 experiment module configurations operate attached to the space station as a primary mode. Five of the configurations free-fly. All modules must be capable of free flight to accomplish delivery from the shuttle or expendable launch vehicle to the space station.

The current concept for free flying modules calls for orbits that are coplanar with the space station at distances ranging from 10 to 500 miles. It is, therefore, necessary that the experiment data be transmitted by a radio frequency link from the module to the space station or ground station.

A major requirement imposed on the subsystem during attached operation is crew safety and monitoring. All modules will be manned when they are attached to the space station for experiment operation, routine maintenance, calibration, or replenishment of expendables. The safety of man and his ability to communicate verbally and via television are paramount considerations. A wideband analog signal distribution system must, therefore, be provided between the module and the space station even when links are not required for the transfer of primary experiment data. This system will probably be hardwired from the module to the station, but safety considerations preclude use of the air-lock as a pathway for cables. Means must be provided, therefore, for maintaining the highly reliable wideband analog signal path through the docking assembly without interfering with hatch operation. This requirement is not exclusive to the crew safety function since primary experiment data must also be transferred during attached module operation phases.

Table 7-1 shows the FPE assignment to the three common module types. Of special interest is type CM-1, the free-flyer, where experiment data must be transmitted via rf link to the space station or stored on-board (e.g., film, tape) and retrieved at regular intervals by docking the module to the space station.

7.1.2 EXPERIMENT DATA COLLECTION RATES. Because the "sizing" of the CDMS will be determined primarily by the required data collection rates, it is important that reasonable estimates be made concerning the amount of data that will actually have to be managed as a function of time by the CDMS. These estimates are difficult to obtain and a continuing requirements analysis is needed to determine the specific objectives of each experiment, the time-phasing of experimental operations, and the requirements in each case for the necessity of real-time processing versus the adequacy of data storage for later analysis.

With these factors in mind, expected data rates have been estimated and used to conceive and analyze a baseline CDMS design.

Table 7-1. FPE/Common Module Type Assignment

Common Module Type	FPE
CM-1 Free Flying	5.1 X-Ray 5.2 Stellar 5.3 Solar 5.5 High Energy 5.20-2 Fluid Physics
CM-3 Attached	5.7/12 Plasma Physics 5.8 Cosmic Ray Lab 5.16 Materials Science 5.20-1 Fluid Physics 5.27 Physics & Chemistry
CM-4 Attached	5.9/10/23 Biology 5.11 Earth Surveys 5.22 Component Test

The analog, digital, and film data accumulation rates were derived during the study from Candidate Experiment Program for Manned Space Stations, NASA NHB-7150-XX, 15 September 1969. Each of the FPEs was analyzed to determine the experiments' communications and data management requirements; the results are given in Tables 7-2 and 7-3.

7.1.3 COMMAND, TELEMETRY AND MONITORING DATA RATES. For the purpose of this study, it was assumed that the housekeeping telemetry requirements for the experiments and engineering subsystems would be modeled after typical scientific payloads of unmanned satellites of 1970 vintage. Experiments on satellites like the Orbiting Geophysical Observatory (OGO), the Synchronous Meteorological Satellite (SMS), and Earth Resources Technology Satellite (ERTS) average approximately 20 housekeeping telemetry monitoring points per piece of equipment. The module with the largest number of individual experiments is FPE 5.11, which has 21 experiments listed, so the expected number of housekeeping telemetry points is 420. Telemetry sampling requirements range typically from one sample per minute for non-critical temperature and pressure measurements to ten samples per second for event sensitive or dynamic measurements. Considering all measurements, the average is approximately one sample per second. A typical telemetry word is roughly six bits in length excluding frame synchronization and parity, which add approximately 1.7 bits per word. Applying this standard to FPE 5.11 yields the following rate:

$$\text{bit rate} = 420 \times 7.7 \frac{\text{bits}}{\text{sample}} \times \frac{1 \text{ sample}}{\text{second}} = 3240 \text{ bps}$$

Table 7-2. Experiment Data Requirements Summary
Attached Modules

FPE	Title	Mod Proc & Displays	Rate	Data Volume/Day
5.8	Cosmic Ray Physics Lab	On-board processing/ data compression	20 kbps	1.7×10^9 bits + tape
5.9/5.10	Bio (D & E)	Data Compression	10 kbps	6.9×10^8 bits and analog tape
5.16	Materials Processing	Strip chart or equivalent	1 Hz Analog	10 channels plus film & paper
5.20-1	Fluid Physics	TV Monitors		8.7×10^7 bits/200 min
5.11	Earth Surveys	Quick Look	26.4 Mbps +3.6 MHz Analog	9.5×10^9 bits/6 min plus film & tape
5.7/12	Plasma Physics, RMS	TV & Ephemeris	80 kbps	1.4×10^8 bits/day plus tape
5.22	Component Test	---	20 kbps	Film & Tape
5.27	Physics & Chemistry Lab	---	Negligible	Film

Table 7-3. Experiment Data Requirements Summary, Free-Flying Modules

FPE	Title	Maximum Data Volume	Duty Cycle	Rate	Bandwidth
5.1	Grazing Incidence X-Ray Telescope	7.3×10^{7} + Film	Continuous	8 kbps	8 kHz
5.2A	Stellar Astronomy	$> 10^{11}$ Bits/Orbit	1 Frame/orbit	10 Mb/Frame in 5.4 minutes, or 1 Mbps for 54 min.	1 MHz
		Television	Intermittent	Plus film	1 MHz (RF Bandwidth)
	Solar Astronomy Telescope	3 Channels 1.3 MHz Analog for 7.5 min.	Once/Month	1 MHz for 160 min. plus film	1 MHz
5.3A	Spectroheliograph	712 Frames/day (Film)	50%	Film	
	Solar Coronagraph	7200 Frames/day (Film)	50%	Film	
	0.5m X-Ray Telescope	Television	Intermittent		1 MHz
5.5	High Energy Stellar Astronomy	6.6×10^{8}	50%	16.4 kbps	16.4 kHz
5.20-2	Fluid Physics	Insignificant	-	-	-

The current estimate of telemetry rate for engineering subsystems aboard a typical module indicates that there will be approximately 250 monitoring points. Applying the same standard used above, the rate is:

$$250 \times 7.7 \ \frac{\text{bits}}{\text{sample}} \times \frac{1 \ \text{sample}}{\text{second}} = 1925 \text{ bps}$$

The total housekeeping telemetry rate in the detached mode is, therefore, approximately 5 kilobits/second.

The availability of a telemetry and command function aboard the module allows with little additional complexity the inclusion of a range and range rate measuring capability by using the radio frequency reception/transmission equipment as an active transponder. NASA's Apollo unified S-band (USB) and Goddard range and range rate (GRARR) and the USAF space ground link subsystem (SGLS) transponders all combine telemetry tracking and command (TT&C) as integrated functional elements utilizing common rf components.

It should also be mentioned that for the attached module several other signals may be required for monitoring purposes:

a. Television (full duplex NARTB standard color TV for each module crew station for external visual monitoring and coordination)

b. Voice communications (two or more redundant duplex channels for each crew station)

c. Physiological monitoring circuits (including EKG, EEG, blood pressure, and respiration rate)

d. Environmental monitoring (air quality including humidity, aromatic vapors, duct, dangerous gasses, life support housekeeping)

e. Emergency Warning (including highly redundant trigger circuits for visual and aural warning devices, perhaps with preprogrammed instructions on desired action)

7.2 SUMMARY OF RESULTS

7.2.1 BASELINE SUBSYSTEM LINK GEOMETRY AND FREQUENCY CHOICE. The S-band communication link geometry for the free-flyer module is shown in Figure 7-1. It is assumed that the proposed 15-ft antennas on the space station, which are to be used to communicate with the data relay satellite system (DRSS) at K_u-band, have a dual-feed that permits operation with the free-flyer modules at S-band. The choice of S-band for experiment module baseline communication links was made after careful consideration of several factors.

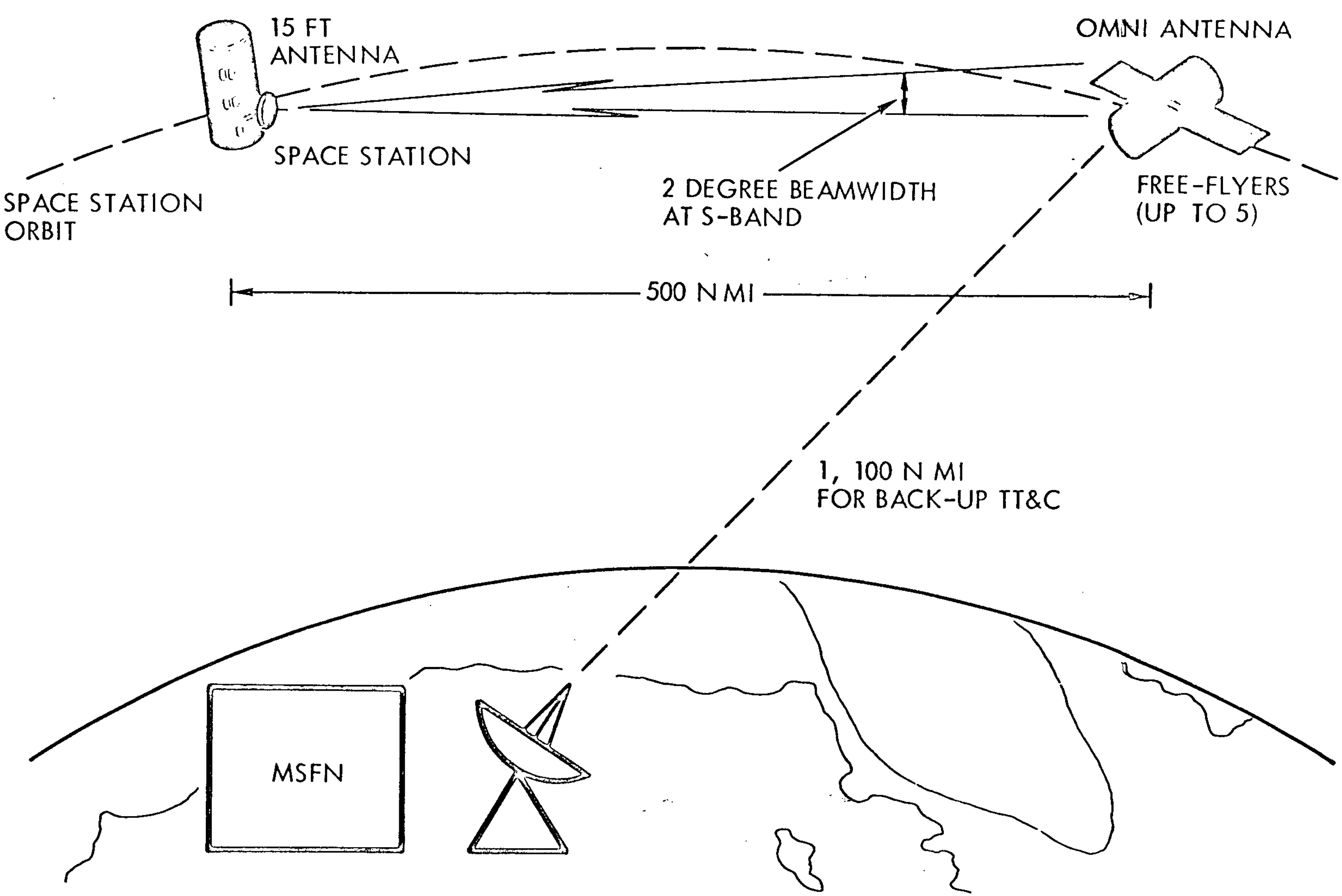

Figure 7-1. Communications/Data Management System Module - Space Station Link Geometry Phase A Baseline

a. The experiment module program may precede the space station and DRSS. In this event, communication links will have to be direct to the ground, using the MSFN without extensive modification.

b. The astronomy modules have a stringent attitude stability requirement; therefore, it is undesirable to have a communications link that requires moving antennas -- at S-band, omniantennas may be used.

Baseline Configuration. The overall CDMS baseline configuration is shown in Figures 7-2 and 7-3 for the free-flyer and attached modules respectively.

A small aerospace computer is chosen as the preliminary processing element of the CDMS. In this way, the required flexibility to accommodate the various sensors and experiment configurations is achieved through software modification. The cost effectiveness of this small standardized computer architecture must be demonstrated in a Phase B cost tradeoff study. In general, however, the capability for mission independence will save non-recurring costs. It should be borne in mind that the computers considered in this study are not large bulky machines, but miniaturized (LSI), highly reliable data processors. Their physical requirements are modest for the capability gained, and their per unit cost is reasonable when purchased in quantity. A unique feature of the baseline concept is the use of a common data bus for internal communications.

The data bus is a time division and/or frequency division multiplexed, single line (possibly consisting of several conductors), shared by all elements of the CDMS. Special interface terminals, called bus interface units (BIU), are required to connect the bus to a data source. Depending on design, a single BIU may interface with numerous signal sources. The number of BIUs required is a function of the module complexity and configuration. The location of data sources, the numbers of signals, and the degree of subsystem autonomy determine the actual number.

As seen in Figures 7-2 and 7-3, the experiments are divided into high data rate and low data rate categories, with only the latter connected exclusively to the data bus. High rate data, which may have a dedicated communications link or hardline, is provided with a direct path to the high rate data formatter. This data may be preprocessed by experiment peculiar equipment and is not provided a processing capability using the CDMS computer, but is simply converted to digital form, formatted, and transmitted. By keeping this data off the bus, the mechanization of the data bus is simplified and less constraints on its use are imposed. Also, the computer is not burdened with non-computational repetitive input/output tasks. For FPE 5.11, data rates over 30 kbps are considered high rate. A nominal 100 foot long data bus should satisfy the 35 ft x 15 ft diameter common module providing two lengthwise and two diameter traverses. For this length, a 0.5 Mbps bit rate can easily be achieved on a single twisted pair line.

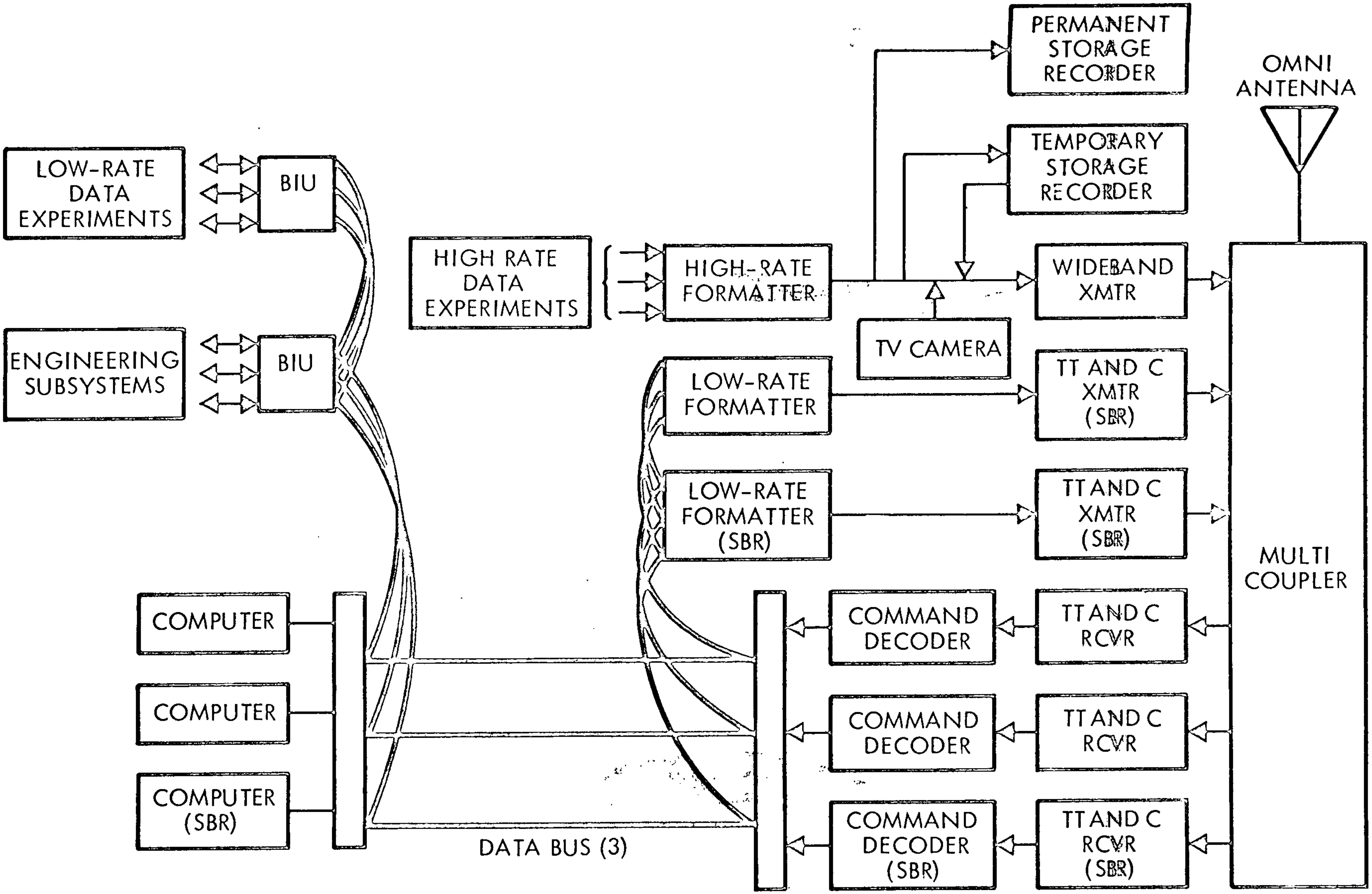

Figure 7-2. Baseline Communications/Data Management Subsystem Free-Flyer Modules

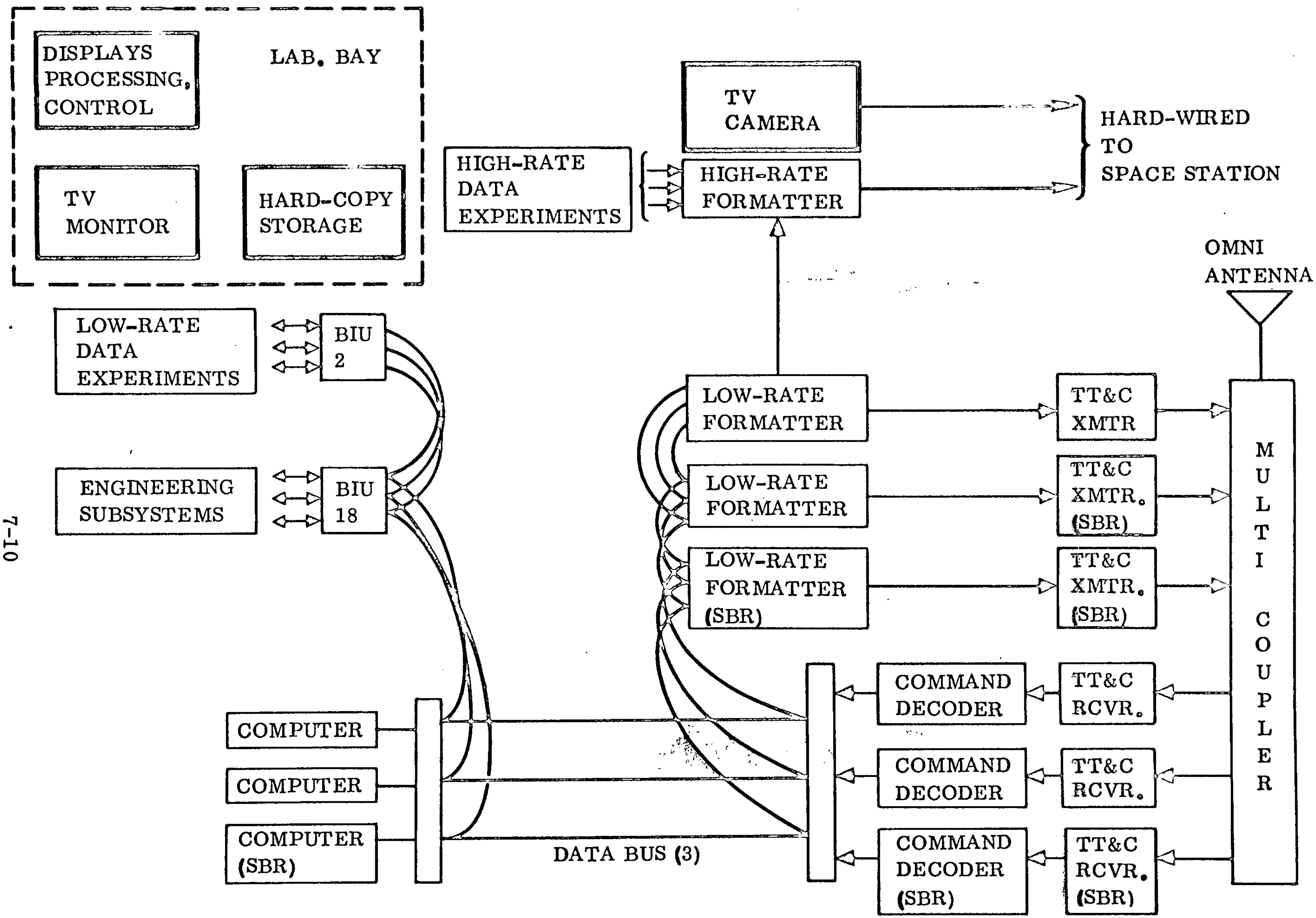

Figure 7-3. Baseline Communication/Data Management Subsystem Attached Modules

The computer is required to interface directly only with the common data bus. The computer/bus interface unit is similar to a BIU, but will be inherent in the computer design. Several functions are required of the computer/bus interface unit. It must:

a. Provide timing and control of the data bus

b. Provide data buffering and word formatting capability

c. Provide error detection for the data bus

d. Handle status and interrupt information from the subsystems to the computer

e. Multiplex and demultiplex data.

The computer/bus interface unit will interface both with the CPU and the memory.

The computer will use a fixed CPU with an 8000 word modular memory and it will be a nominally fast machine (4 μsec add time). A 16-bit word is considered large enough to fit the data requirements of the experiment modules. Elaborate calculations are not required so that a fairly simple 20-30 instruction set should suffice.

A major task is to size the memory requirements for the common modules. The following major software tasks may be identified as follows:

a. Computer diagnostic routines

b. Common subroutines for processing

c. Engineering subsystem control

d. Engineering subsystem checkout

e. Experiments processing

f. Experiments calibration and control

g. Command generation

h. Data bus management

i. Telemetry and wideband data formatting

j. Adaptive experiment data sampling

k. Data storage system control

l. Display generation for console

Although numerous, many of these tasks are routine. Also, higher language capability is not required; i.e., all programming will be in machine language.

The purpose of the formatting and switching units is to prepare data for storage, display, or for transmission external to the module. As all inputs and outputs are digital, the units consist almost entirely of switching circuits.

The high rate data is buffered and combined with low rate data frame synchronization and timing added, and clocked to the wideband digital transmitter or space station. This straightforward handling allows high rate data to be treated serially. It is required that each experiment be instrumented to produce the high rate data in a standard digital form. Multiplexing is performed by the unit if there are multiple high rate channels.

Narrow band data for the telemetry link is made up of inputs from the computer and other sources via the common data bus.

The low rate formatter must pick off the appropriate data from the bus (through suitable addressing), perform addressing and formatting, and enter the data in a buffer. The buffer contents are clocked out to the high rate formatter and/or to the TT&C transmitter. The latter forms a back-up mode in the event of wideband data system failure.

The command decoder receives serial, digital command data from the TT&C uplink. The decoded command is then forwarded to the computer via the data bus. Reasonableness checks and/or retransmission by telemetry are performed by the computer. Upon receipt from the command decoder of the "execute" command, the proper sequence of control words is transmitted to the addressed subsystem by the computer via the data bus.

For emergency backup, in case of computer or data bus failure, some dedicated command decoder to subsystem paths are required. It is considered a crew safety requirement for the space station that the module be commandable in some modes at all times. For example, station-keeping must be maintained to prevent possible collisions with other vehicles. For this reason, redundancy is necessary for the command decoder and data bus.

For the free-flyer modules a dual-purpose 5-watt solid state S-band wideband transmitter provides the capability to transmit 1 Mbps data or 0.2 MHz video bandwidth TV/analog data to the space station at a distance of 500 n.mi. The dual capability is obtained by switching modulators - a biphase modulator is used for digital data and a frequency modulator is used for TV/analog data. Wider bandwidth data may be transmitted with correspondingly higher transmitter power; e.g., the 2.9 MHz video bandwith TV originally required for the astronomy modules would require 80 watts rf. In this case a high power TWT would be necessary and would require 320 watts prime power assuming 25% efficiency. It was for this reason that a slower scan TV (with the same resolution) was proposed for the astronomy modules.

All of the modules require telemetry, tracking, and command (TT&C) equipment to provide the control capability during rendezvous and docking. For free-flyer modules telemetry data is normally interspersed with the experiment data and transmitted via the wideband transmitter. In case of failure of the wideband transmitter, the telemetry data is transmitted using the TT&C transmitter. Turn-around ranging capability is also provided by the TT&C equipment as back-up to the rendezvous and docking radar.

Sufficient redundancy or inherent reliability has been incorporated in the baseline (see Figures 7-2 and 7-3) to allow module recovery in the event of two independent failures. Specifically, the redundancy rationale is as follows:

a. Computer — Three computers are incorporated in the CDMS. Two of the computers are in a standby mode and may be activated through the command link or through failure detection by means of internal self-check features.

b. Engineering Subsystems BIUs — Each engineering subsystem, e.g., RCS, is monitored and controlled through access by any of the three data busses. The interface between the engineering subsystem and each of the three data busses is through a BIU.

c. Experiment BIU — No redundancy is incorporated at present in the experiment/data bus interface.

d. Telemetry and Wideband Data Transmission — For free-flyer modules, telemetry and low-rate data transmission are accomplished by means of the low-rate data formatting and switching unit, the high-rate formatting and switching unit, and the wideband transmitter during normal operation. Two TT&C transmitters serve as backup for module recovery operations and permit retransmission of the ranging code for redundancy of the tracking function.

   For attached module three TT&C transmitters are used; one operational and two for backup.

e. Command Receivers and Decoders — Three each of these units are incorporated in the design, thus providing fail-operational, fail-safe capability. Two are operated in an active redundancy mode; one in standby. The receivers are each on different frequencies, and each command decoder has its own address. Cross-strapping is accomplished by a passive summing network; no single-point failure modes are thus incurred. The receivers incorporate turn-around ranging capability as a backup mode to the rendezvous radar when operated in conjunction with the TT&C transmitter.

f. Multicoupler — To provide a means of coupling the omni antenna system to the representative transmitters and receivers, a multicoupler is used. The ports of the multicoupler provide isolation between all transmitter inputs and receiver outputs. Since this component is not only passive but protected in a sheltered environment, redundancy is assumed to be unnecessary.

g. Omni Antenna System — Five cavity-backed, broad-band, crossed-dipole antennas distributed around the module cylinder provide omnidirectional coverage with circular polarization. With five antennas arranged in this manner, sufficient inherent redundancy exists to make physical redundancy unnecessary.

Common Module Equipment Complement. The objective of the communications/data management subsystem (CDMS) design is to provide a common configuration that could almost universally meet the experiment and subsystem requirements. The baseline design meets this objective by satisfying the most stringent requirements and by providing flexibility to leave off equipment where not required by less demanding modules. Table 7-4 lists CDMS equipment requirements including redundancy by FPE and indicates the approximate size, weight, and power for each unit.

7.2.2 SCALING. The baseline communications/data management subsystem has been sized to meet the requirements established in Section 7.1. Recognizing that these requirements are fluid, particularly at this stage in the development program, important communications system parameters (e.g., module transmitter power, digital data rate, video bandwidth, module-space station separation, and carrier frequency) have been graphed parametrically. They are presented herein as an aid to scaling to establish the impact of requirements change.

7.2.2.1 Required Module Transmitter Power vs. Data Rate (S-Band). Two of the most likely system parameters to change are digital data rate and analog/video bandwidth. The effect on the communications system of changes in these parameters is a proportional change in the module effective radiated power (ERP). For an omni-antenna (0 dB gain) the transmitter power equals the ERP neglecting transmission line loss. Use of Figure 7-4 permits the establishment of the required module transmitter power for other digital data rates and analog/video bandwidths assuming S-band operation and 500 n.mi. separation between the module and the space station. The supporting link power budget is shown in Section 7.4.3. The current baseline ERP at 5 watts is denoted. The impact of TV video bandwidth at 2.9 MHz on required ERP (71 watts) is also noted because this bandwidth is also of interest.

7.2.2.2 Required Module Transmitter Power vs. Separation (S-Band). The cost per module return to the space station warrants extending the time between returns. This implies that the separation between the module and space station be optimized with regard to atmospheric drag and weight of expendables to supply the ΔV for station-keeping. Currently, this separation is 500 n.mi. Changing this separation represents a large impact on the communications system design since the required

Table 7-4. Common Module Communications/Data Management Subsystem Equipment

Component	Size (ft^3)	Weight (lb)	Power (watts)	Quantity per Module												
				CM-1 (Free-Flyer)					CM-3 (Attached)					CM-4 (Attached)		
				5.1	5.2	5.3	5.5	5.20-2	5.7/12	5.16	5.20-1	5.27	5.8	5.11	5.9/10/23	5.22
TV camera	0.1	5	10	1	1	1	1	1	1	1	1	1	1	1	1	1
Analog/video tape recorder	1.65	35	100	-	1	-	-	-	1					1		
Digital tape recorder	1.5	35	100	-	-	-	-	-		1			1	1	1	
R/W recorder - analog/video	1.65	35	100	-		1	-	-	-	-						
R/W recorder - digital	1.5	35	100	-	1	1	-	-		-					1	
High-rate formatter	0.1	5	5	1	1	1	1	1	1	1	1	1	1	1	1	1
Low-rate formatter	0.05	2.5	5	2	2	2	2	2	3	3	3	3	3	3	3	3
Command decoder	0.1	2	1	3	3	3	3	3	3	3	3	3	3	3	3	3
Computer	0.2	8	40	3	3	3	3	3	3	3	3	3	3	3	3	3
BIU - experiments	0.05	1	0.75	2	2	2	2	2	2	2	2	2	2	2	2	2
BIU - subsystems	0.05	1	0.75	21	21	21	21	21	21	21	21	21	21	21	21	21
Data bus	-	2	-	3	3	3	3	3	3	3	3	3	3	3	3	3
Wideband transmitter	0.2	9	25	1	1	1	1	1	-	-	-	-	-	-	-	-
TT&C transmitter	0.1	8	15	2	2	2	2	2	3	3	3	3	3	3	3	3
Remodulator	0.05	2	1	2	2	2	2	2	3	3	3	3	3	3	3	3
TT&C receiver	0.1	15	9	2	2	2	2	2	3	3	3	3	3	3	3	3
Multicoupler	0.05	5	-	1	1	1	1	1	1	1	1	1	1	1	1	1
Omni antenna system	0.7	10	-	1	1	1	1	1	1	1	1	1	1	1	1	1
Total Size (ft^3)				3.8	6.95	6.95	3.8	3.8	5.45	3.95	3.95	5.45	5.45	6.95	6.95	3.95
Total Weight (lbs)				148	218	218	148	148	194	159	159	194	194	229	229	159
Total Power (watts)				163	363	363	163	163	263	163	163	263	263	363	363	163

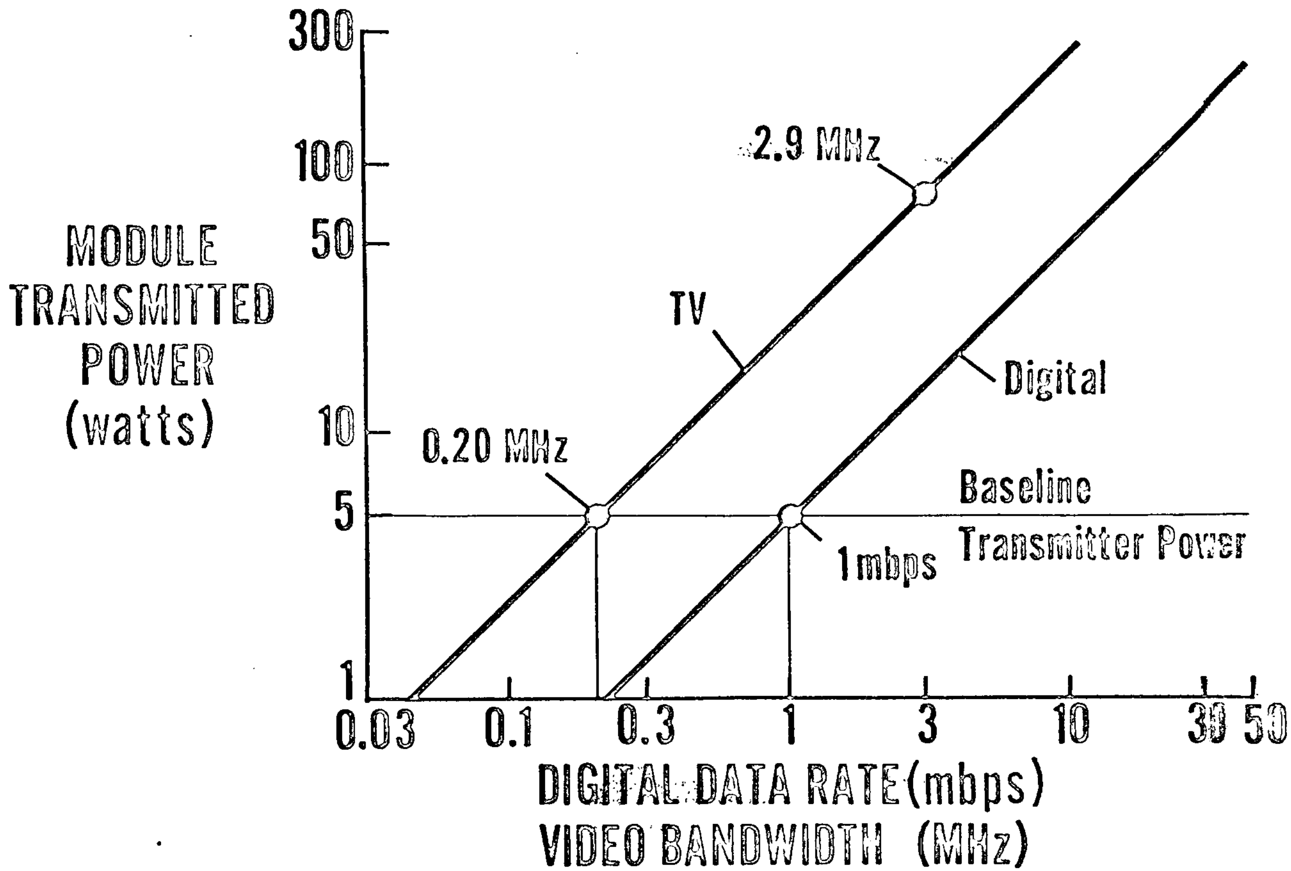

Figure 7-4. Required Module Transmitted Power vs. Data Rate (S-Band)
500-N. Mi. Range, 15-ft. Space Station Antenna

transmitter power varies as the square of the separation distance. Other factors are involved such as antenna size, antenna beamwidth, and data rate. Figure 7-5 shows the required transmitter power vs. module-space station separation for various data rates and antenna configurations. Supporting link power budgets are given in 7.4.3.

7.2.3 COMMUNICATIONS/DATA MANAGEMENT SUBSYSTEM ALTERNATIVES

7.2.3.1 Communication Link to Space Station. Other frequencies were considered for the module-to-space station link; e.g., Ku-band (13.5 GHz) and V-band (60 GHz). The principal advantage of operating at higher frequencies is the availability of large bandwidths in the event realtime transmission of unprocessed data from imaging type sensors is required.

The Ku-band configuration assumes that the space station antenna has a 10-degree beamwidth, which according to one space station conceptual design is the acquisition horn of one of the four 15-foot dishes used to communicate with a data relay satellite at Ku-band. On the module a 4-foot steerable antenna is used -- actually two will probably be required to prevent shadowing by the module in certain orientations. At a range of 500 n.mi, 24 watts transmitter power is required for a transmission rate of 100 Mbps. Figure 7-6 shows parametrically the transmitter power requirements for other transmission rates and antenna size (two-foot dish).

The V-band configuration uses one-foot steerable antennas on both the space station and the common module. Approximately 15 watts are required to transmit 100 Mbps at a range of 500 n.mi. The power required for other data rates is also shown in Figure 7-6.

7.2.3.2 Data Mangement Subsystem. The alternative to the data bus concept is the conventional fixed-format, non-addressable system shown in Figure 7-7. It is typified by the data handling scheme used on earlier (and considerably smaller) spacecraft.

A basic deficiency of the conventional data management concept, and the principal reason for adopting the data bus approach is its inability to control experiments. For each of the common modules, experiments are generally interrelated and the sampling and processing requirements of the sensor data differ dynamically according to observed experimental and environmental conditions. In any mechanization of the data management subsystem for the experiment modules, this capability for a periodic sampling, adaptive control, and flexible processing is mandatory. The data bus approach offers these capabilities with the added advantage of modularity. Thus with the addition or deletion of bus interface units (devices which interface subsystems and experiments with one another) and computer

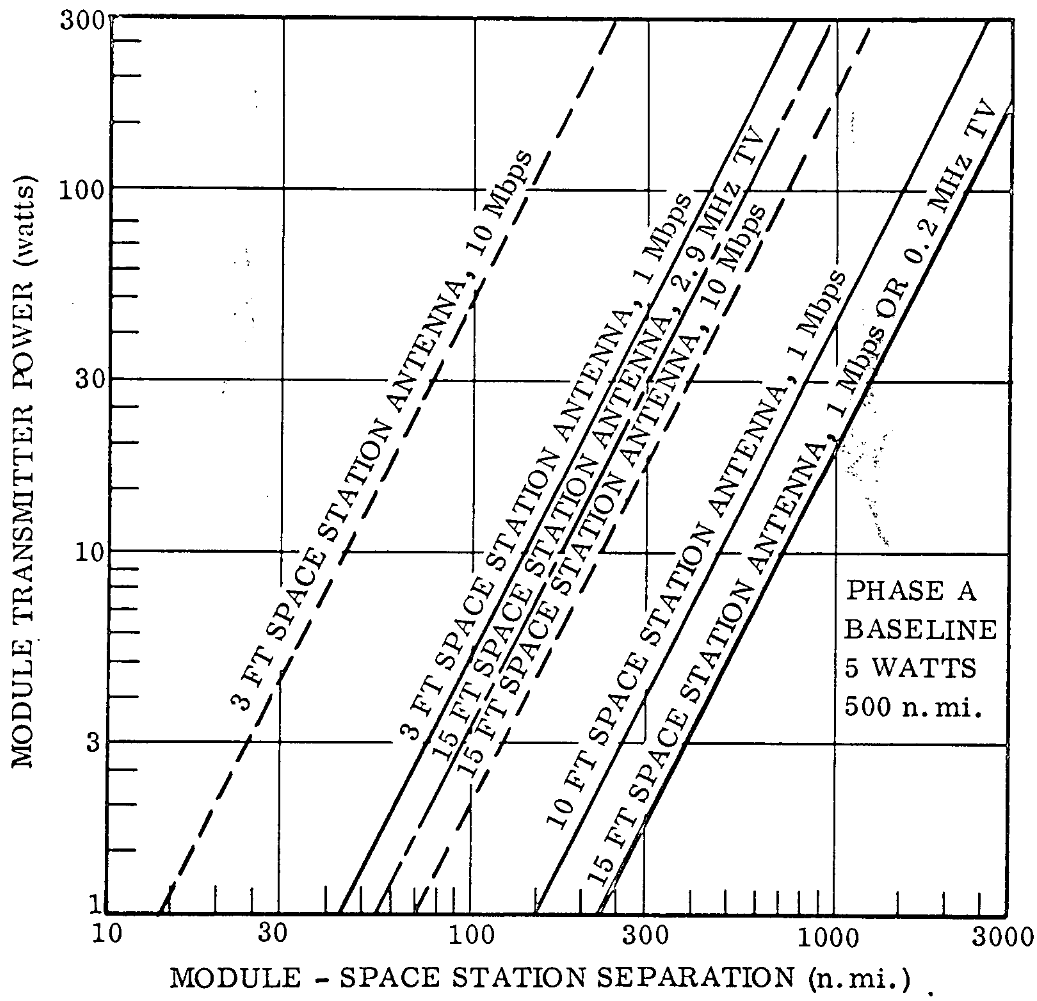

Figure 7-5. Required Module Transmitter Power vs. Separation (S-Band)

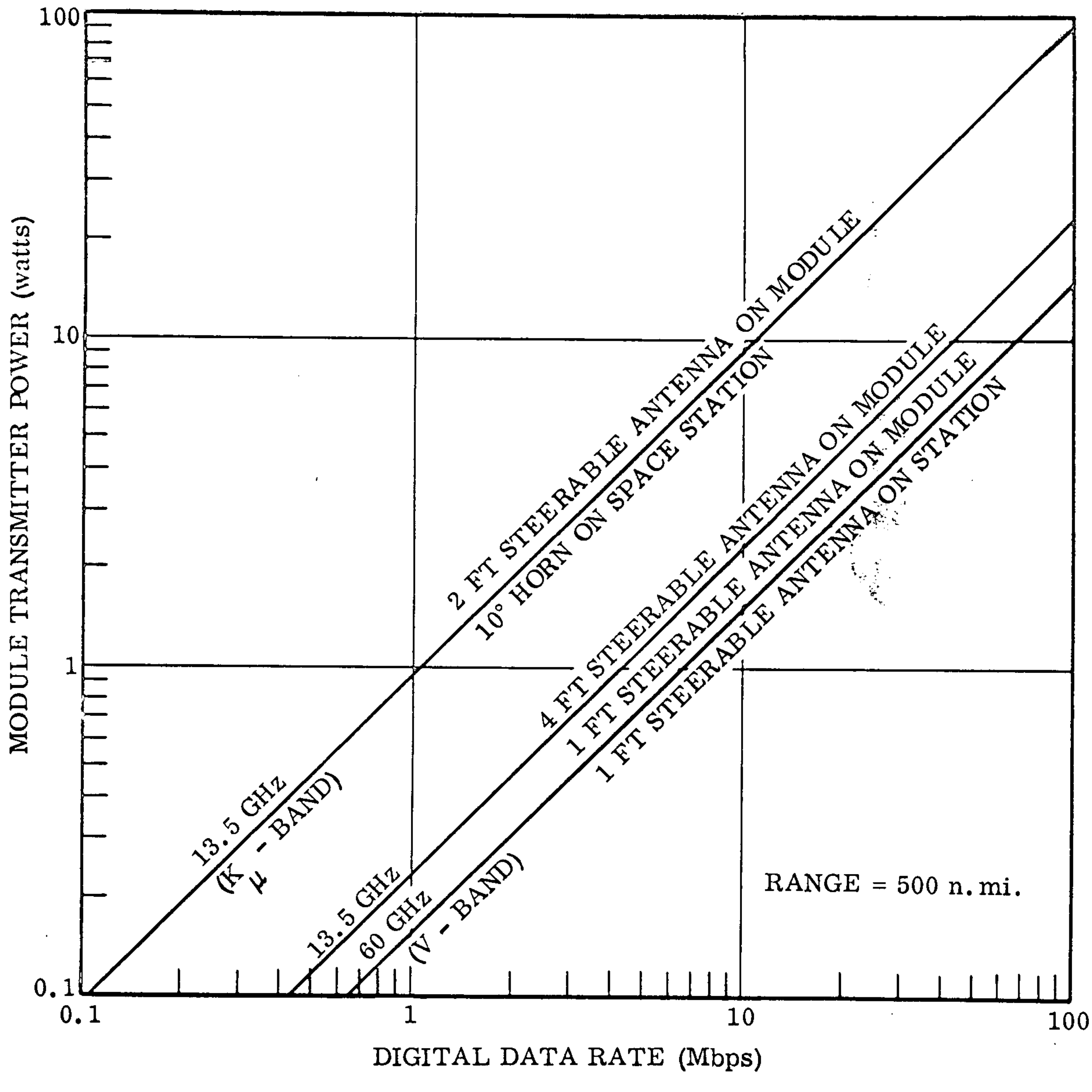

Figure 7-6. Alternate Communication Link Frequencies

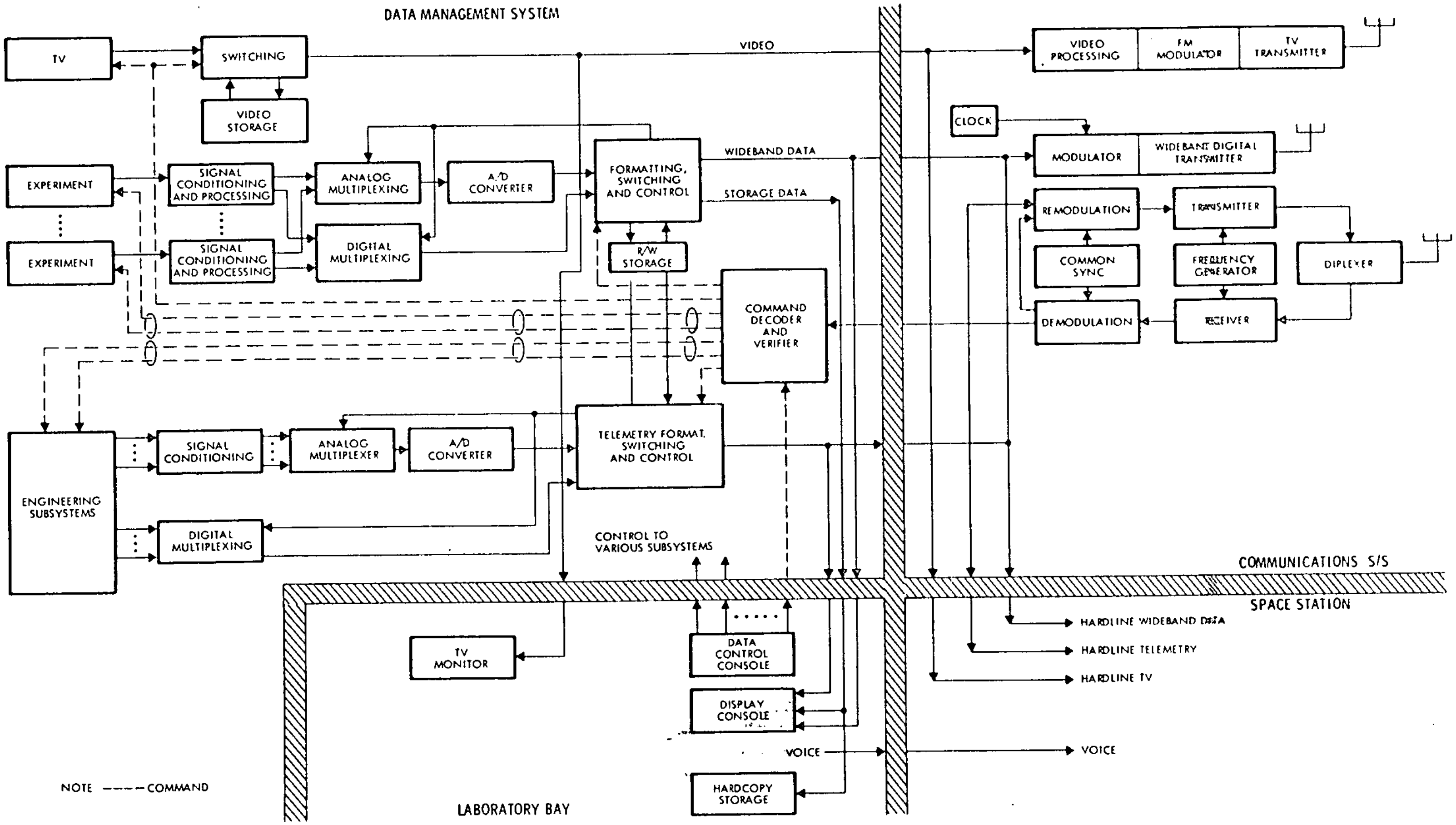

Figure 7-7. Conventional Communications/Data Management Subsystem

reprogramming the data management subsystem may be easily reconfigured to support a variety of experiments.

A great deal of interconnection is seen to be associated with the Command Decoder and the Data Control Console in the Laboratory Bay. The internal communication function is very complex in the conventional CDMS. For example, the baseline command system for FPE 5.11 requires four commands per experiment for 20 experiments. These 80 signals must be transmitted from the command decoder to each experiment interface. With a similar command repertoire for engineering subsystems, and a possibly even more complex parallel function from the control console, just the cabling problem may be so severe as to impose restrictions on the CDMS.

It is seen that the conventional CDMS configuration provides very little checkout capability since there is no provision for limit checking or other diagnostic procedures. Calibration of sensors may be performed, but laboriously, through the command system and additional expensive, specialized formats in the data formatter. A checkout and calibration feature is considered an important requirement for experiment modules as the module is to provide facilities for changing numbers and types of experimental sensors. Despite the periodic servicing of the module (maximum 60-day intervals) the ability for on-board checkout must be highly automatic for such high complexity systems. These considerations, coupled with the previously mentioned limitations of the conventional CDMS concept, make it rather unattractive as a baseline system.

A data bus concept can alleviate some of the above disadvantages but several alternatives still exist for the CDMS architecture.

The throughput of the computer depends on the data bus organization as this is its entire interface with the various subsystems. A number of separate data buses may be employed, organized by function or subsystem. For example, all of the experiments may be connected to a dedicated bus, the engineering subsystems to another, etc. This approach has the advantage of clear division of control of buses and ease in design and checkout, but has the drawback of burdening the computer with interbus data traffic and bus-related hardware.

Another approach is to put all subsystems onto one data bus except for a few high data rate subsystems which communicate with the computer through a dedicated interface. Here the advantage of integrated design and optimum data flow is obvious, but there is a disadvantage of complex configuration control.

Yet another approach is to connect all subsystems according to physical location, consideration being given to the prevention of possible mechanical damage. This approach may result in shorter cables, but it may also result in more complex data traffic control and equipment. The baseline approach is simply to organize the data bus by function.

7.3 CONCEPT DEVELOPMENT

There are many ways to organize a communications and data management system (CDMS) for an experiment module. Several conceptual designs are documented in this report, and a baseline system chosen as a basis for design tradeoffs. With further definition of all requirements, it will be possible to determine accurately the extent to which the CDMS can be standardized for a number of different module types. Because of the highly preliminary nature of the experiment definitions, however, it is possible that there will be unique requirements that will exceed the capability of the selected, or any other CDMS. From the present knowledge of the experiments (detailed in Section 7.4) these exceptional cases will probably be few in number. In any event, the study effort has been directed towards a highly flexible concept adaptable to a wide variety of scientific experiments with different analog/digital data mixes, data format bandwidths and control requirements.

7.3.1 FUNCTIONAL CDMS DESIGN CONSIDERATIONS. A basic aim of the common module concept is to provide a facility for the scientific experiments. This implies that a service be provided to the investigators which imposes minimum restrictions on their experiments and allows for modifications or exchanges for the duration of a program.

7.3.1.1 Functional Requirements. The basic requirements for the experiment module CDMS can be translated into functional subsystem blocks as indicated in Figures 7-8 and 7-9. These requirements fall into the categories of:

a. External communications

b. Internal communications

c. Processing and formatting of data

d. Command generation, sequencing, and control

e. Data storage

External Communications. The functions of the external communications links are simply to transfer the experimental data from the free-flyer modules to the space station and to provide for telemetry, tracking, and command signal exchange between the modules and the space station. The implementation of these functions was discussed in Section 7.2 with the main design decisions being to maximize the desirable experiment data flow, and to select carrier frequencies to be used for the contemplated links.

Internal Communications. Basically, there are six system elements with which the CDMS must interface.

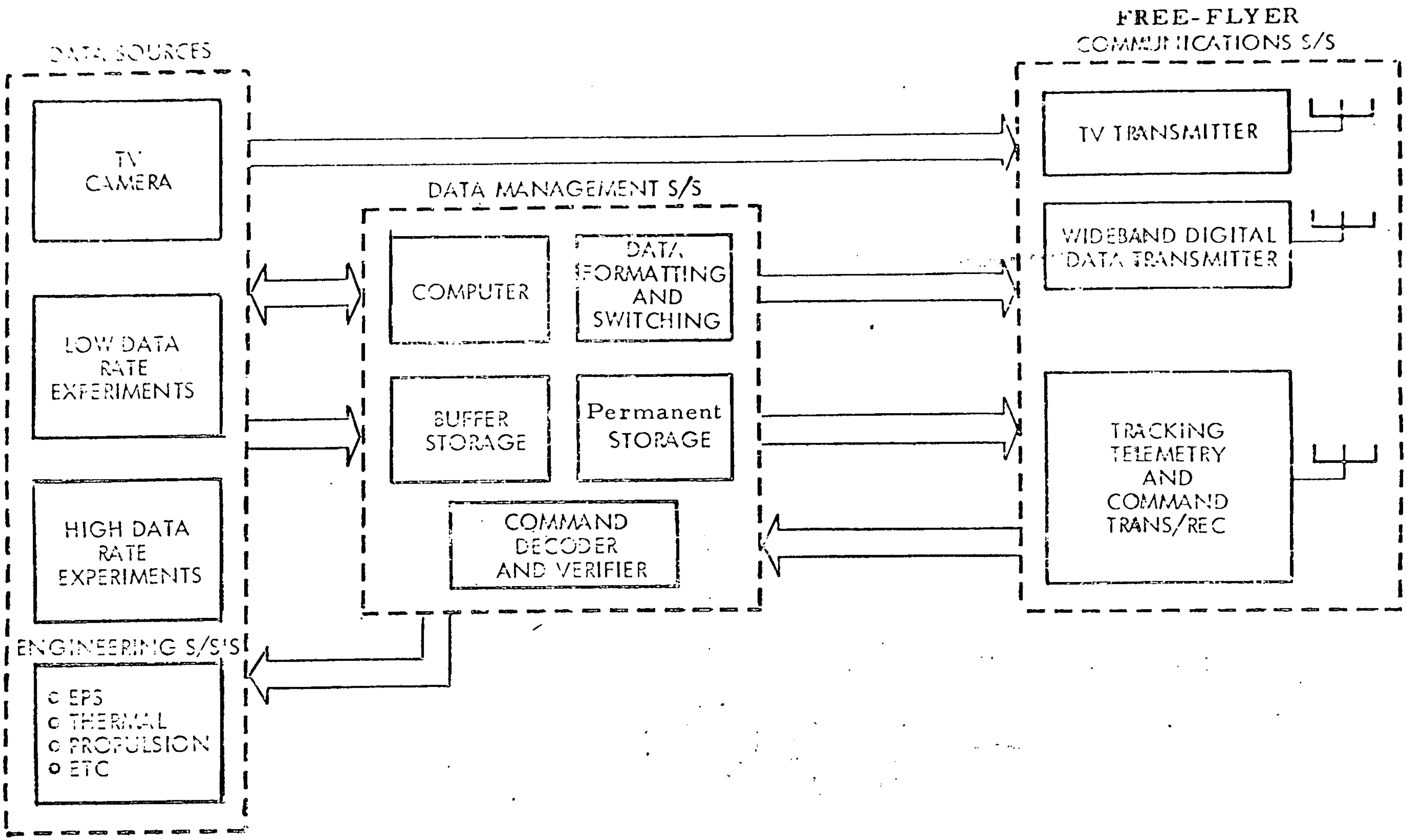

Figure 7-8. Functional CDMS Design Configuration – Free Flyer Modules

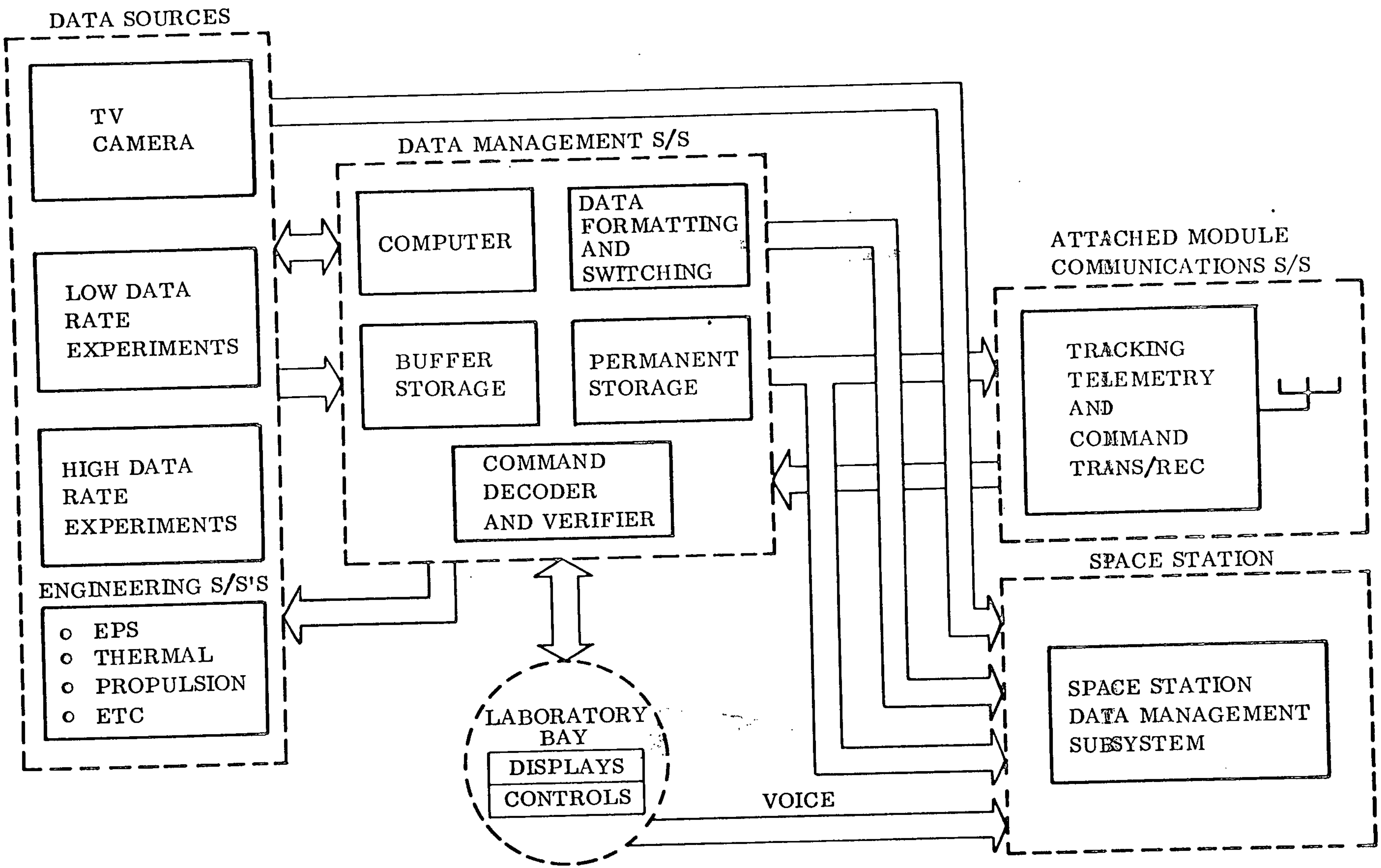

Figure 7-9. Functional CDMS Design Configuration – Attached Modules

a. Engineering subsystems (7)
   1. Electrical power
   2. Stabilization and control
   3. Guidance/navigation, rendezvous/docking
   4. Environmental control/life support
   5. Propulsion/RCS
   6. Thermal control
   7. Communications/data management
b. Experimental subsystem, including TV
c. Laboratory bay displays and controls
d. Data communications, wideband, and telemetry
e. Command decoder
f. Data storage

The baseline data rate between these subsystems is estimated to be 200 kbps. This rate represents a worst-case value and would not normally occur continuously. However, the CDMS must provide such internal communications paths.

Processing and Formatting of Data. The prime function of an experiment module is to provide accurate, timely, and relevant experimental data. Typical processing and formatting functions required are multiplexing, analog-to-digital conversion, addressing, timing, computation, framing, and switching. For each of the experiment modules, the following processing and formatting tasks have been identified.

a. Experimental data
   1. Accumulation (pulse counters)
   2. Analog multiplexing
   3. Analog-to-digital conversion
   4. Digital buffering
   5. Digital multiplexing
   6. Timing of above functions
   7. Provide clock and frame synchronization for wideband data link
   8. Switching data to/from storage

70

Table 2-3. Experiment Module Weight Summary, CM-1 Systems Summary & Nominal Dry Weight (1)

Item Condition	FPE 5.1 X-Ray	FPE 5.2A, 3-Meter Stellar	FPE 5.3A Solar	FPE 5.5, High Energy Stellar	FPE 5.20-2, Fluid Physics — Non-Cryogenics	FPE 5.20-3, Fluid Physics — Intermediate Term Cryogenics	FPE 5.20-4, Fluid Physics Long Term Cryogenics
Experiment — Cargo	3,300	8,685	6,875	7,800	5,141	5,776(2)	7,568(2)
Structure	7,749	10,629	9,162	7,911	6,579	9,979	9,979
Propulsion — Dry (3)	—	—	—	—	4,412	4,412	4,412
Reaction Control — Dry	1,161	1,161	1,161	1,161	1,161	1,161	1,161
Electrical Power	1,859	2,084	1,934	1,859	1,519	1,673	1,365
Guidance & Navigation	45	45	45	45	45	45	45
Stabilization & Control	1,061	2,172	1,908	1,468	285	285	285
Communications & Data Management	343	343	381	343	343	343	343
Environmental Control & LSS	177	177	177	177	177	177	177
Thermal Control & Environmental Protection (1)	2,604	2,604	2,604	2,604	2,604	2,604	2,604
Total (1)	18,299	27,900	24,247	23,368	22,266	26,455	27,939

Notes: (1) Includes Radiator Fluid & EC/LSS Expendables
(2) Includes 2,316 Lb. Dry FPE 5.20-2 Experiment Equipment
(3) Propulsion Slice, See Table 2-35
(4) The same CM-1 Basic Module is used for all Detached Mode Fluid Physics Experiments

Table 7-5. Data Preprocessing/Compression Candidates

FPE	Title	Sensors/Sources	Preprocessing/ Compression Types
5.1	X-Ray Astronomy	Polarimeter Spectrometer Detector Status	Pulse rate counter Pulse rate counter Redundancy removal Redundancy removal
5.2	Stellar Astronomy 3 Meter Telescope	Videograph Spectrograph Status	Image processing Image processing Redundancy removal
5.3	Solar Astronomy	Spectrograph Status	Image processing Redundancy removal
5.5	High Energy Stellar Astronomy	X-Ray Imager Spectrometer Spark chamber Status	Pulse rate counter Pulse rate counter Pulse rate counter Redundancy removal
5.8	Cosmic Ray Physics Lab	Spectrograph Status	Pulse rate counter Redundancy removal
5.9/ 5.10	Space Biology	Specimen measurements Environmental measurements	Redundancy removal Parameter extraction
5.11	Earth Surveys	Multi-spectral scanner IR sounder UV spectrometer Vidicon Status	Redundancy removal Redundancy removal Redundancy removal Image processing Redundancy removal
5.12	Remote Maneuvering Subsatellite	Electron/ion traps Spectrometer Status	Parameter extraction Parameter extraction Redundancy removal
5.16	Materials Science and Processing	Instruments Status	Parameter extraction Redundancy removal
5.22	Component Test and Sensor Calibration	Instruments Status	Parameter extraction Redundancy removal
5.27	Physics and Chemistry Lab	Instruments Status	Parameter extraction Redundancy removal
Engineering Subsystems		Status	Parameter extraction, alarm

b. Engineering data

1. Analog multiplexing
2. Analog-to-digital conversion
3. Digital multiplexing
4. Telemetry formatting changeable with mode
5. Switching telemetry to and from storage.

A significant reduction in the volume of data to be handled may be achieved by applying pre-processing and data compression techniques to the sensor outputs. An examination of several of the FPE's revealed certain sensors and other data sources where preprocessing would be particularly beneficial. These are shown in Table 7-5 together with applicable techniques of preprocessing and compressing the data.

Command Generation, Sequencing, and Control. Receipt of commands may occur via the space station communications link, hardline from the station, from the laboratory bay of the module, or from the MSFN-USBS when the module is operating autonomously in a back-up mode. The MSFN-USBS, for example, has an uplink command capacity of 200 bps and therefore the space station rf command link and hardline command link should be compatible.

Numerous onboard command, sequencing, and control requirements are envisioned. One of the more important of these is a provision to allow certain events occurring within the experiments to change the data processing and formatting modes. Similarly, engineering subsystem events, particularly critical failures, may require internal issuance of command sequences. Command instructions are required for sequencing and controlling the experiments, engineering subsystems, and the CDMS.

When operating autonomously in the free-flyer mode some degree of control may be required of the CDMS, depending upon the level of autonomy within the particular experiments and engineering subsystems. This is a fundamental design tradeoff affecting costs, both recurring and nonrecurring, reliability, maintainability, and overall system performance.

Data Storage. There are two basic requirements for data storage on experiment modules. First, there is the requirement to match communications bandwidths to experiment rates; that is, buffering storage. This may arise from both varying experiment data rates due to fluctuations in measurables, and from varying communications rates as visibility periods open and close. Buffering storage is herein referred to as read/write (R/W) storage since eventual playback over the communication link is planned. Both engineering and experimental data may use R/W storage.

The second storage requirement is termed permanent and is used principally for high data rate experiments. In most cases, the experiments will have to provide their own permanent storage; e.g., film cameras. However, for some modules a common permanent storage facility such as a digital film recorder is desirable. This stored data is removed or read out only upon servicing of the module by the space station.

7.3.1.2 Flexibility Considerations. The individual scientific/experiment packages have highly differing requirements; i.e., some experiments produce extremely high data rates, others very low rates. Some modules may require a large number of external commands while others may operate nearly autonomously. These considerations lead to a basic cost tradeoff, the cost of one basic flexible system versus the nonrecurring costs of many individually optimized systems. Although flexible systems are generally more complex and have a high one-time recurring cost, their complexity and high cost can be offset by the multiplicative costs of many individually tailored systems as would be required for the experiment modules.

A primary requirement of a CDMS for a multi-mission scientific satellite is the ability to interface with a variety of experiments. With such satellites, the experimental interface changes constantly, and may in fact be drastically altered late in the program. Experiment packages may also be changed during the life of a module. This consideration demands an ability to easily change the experiments/CDMS interfaces on short notice. Therefore, an ability to modify formatting, processing, and control functions through some form of programming is obviously desirable.

Failure mode switching considerations also demand a high degree of flexibility of the CDMS. If an experiment should fail in the "off" mode for example, the bandwidth or time slot assigned to it would be wasted if a fixed format were used. With a programmable format, however, this bandwidth could be profitably reassigned to a higher sampling rate of another experiment or an engineering subsystem. Reassignment of experiment data between storage and transmission may be required in other equipment failure modes. For example, in the case of a transmitter power drop, it may be desirable to modify the data format or to reassign the data to storage so as to avoid data loss.

7.3.1.3 Common Data Bus and Bus Interface Units (BIUs). Much experience gained in previous aerospace and aircraft applications of the common data bus concept will find direct application here. The bus concept permits a very flexible system approach. However, along with flexibility goes the increased complexity in developing an optimum control and management technique. Some of the more promising techniques must be traded off against such criteria as ease of reconfiguration, efficiency of bus utilization, equipment complexity, and compatibility with the overall common module philosophy.

Data bus management can be effected through use of central control, federated control, or a combination of both. Central control has the advantage of simplifying subsystem hardware; however, software is very complex and inefficient use is made of the data bus (raw data parameters occupy the bus that might better be pre-processed in the subsystems). Federated control, with computational capability at the subsystem, has the advantage of permitting improvement in realtime response, more efficient data bus utilization, and permits the implementation of sophisticated self-test within the subsystem. However, this is done at the expense of added complexity in both hardware and software at the subsystem level.

There are numerous ways to mechanize a common data bus configuration. The best mechanization is probably the one most compatible with the computer word size and timing scheme. However, in order to develop a basic configuration for future trade-off studies a sample configuration was prepared for four-bit parallel word byte transmission and is shown in Figure 7-10. The purposes of the lines are:

a. Four parallel data lines for transmitting both instructions and data.

b. One BUS BUSY line to indicate the bus is being used.

c. One GET READY line to inform the recipient of the data that information is to appear on the data lines.

d. One INFORMATION PRESENT line to tell the recipient of the data when to read the information.

e. One LOGIC RESET line to allow all logic in the BIUs to be reset by the computer. (This is normally only done when the system is first turned on.)

A twisted shield pair was chosen for each signal line in order to increase common mode rejection and to reduce electromagnetic interference. The total number of twisted shield pairs for the mechanization scheme is eight. The wide bandwidths and consequent high data rates that can be achieved through use of coaxial lines, waveguides, and fiber optics are unnecessary in light of the relatively low data rate requirement for each data bus. Shielded, twisted-pair data lines will handle these data rates satisfactorily and will simplify the problems of implementation.

The 200 kHz clock is generated in the computer interface unit (CIU), and is used for INFORMATION PRESENT. Biphase (Manchester) coding may be used on this line. For the low data rate assumed, and the short physical length of the bus, clock skew may be ignored.

The BIUs will be coupled to the lines through the use of transformers. Lines may be terminated as necessary to obtain proper impedance matching and reduce reflections. By presenting the characteristic line impedance when receiving, the BIU also will reduce possible line reflections.

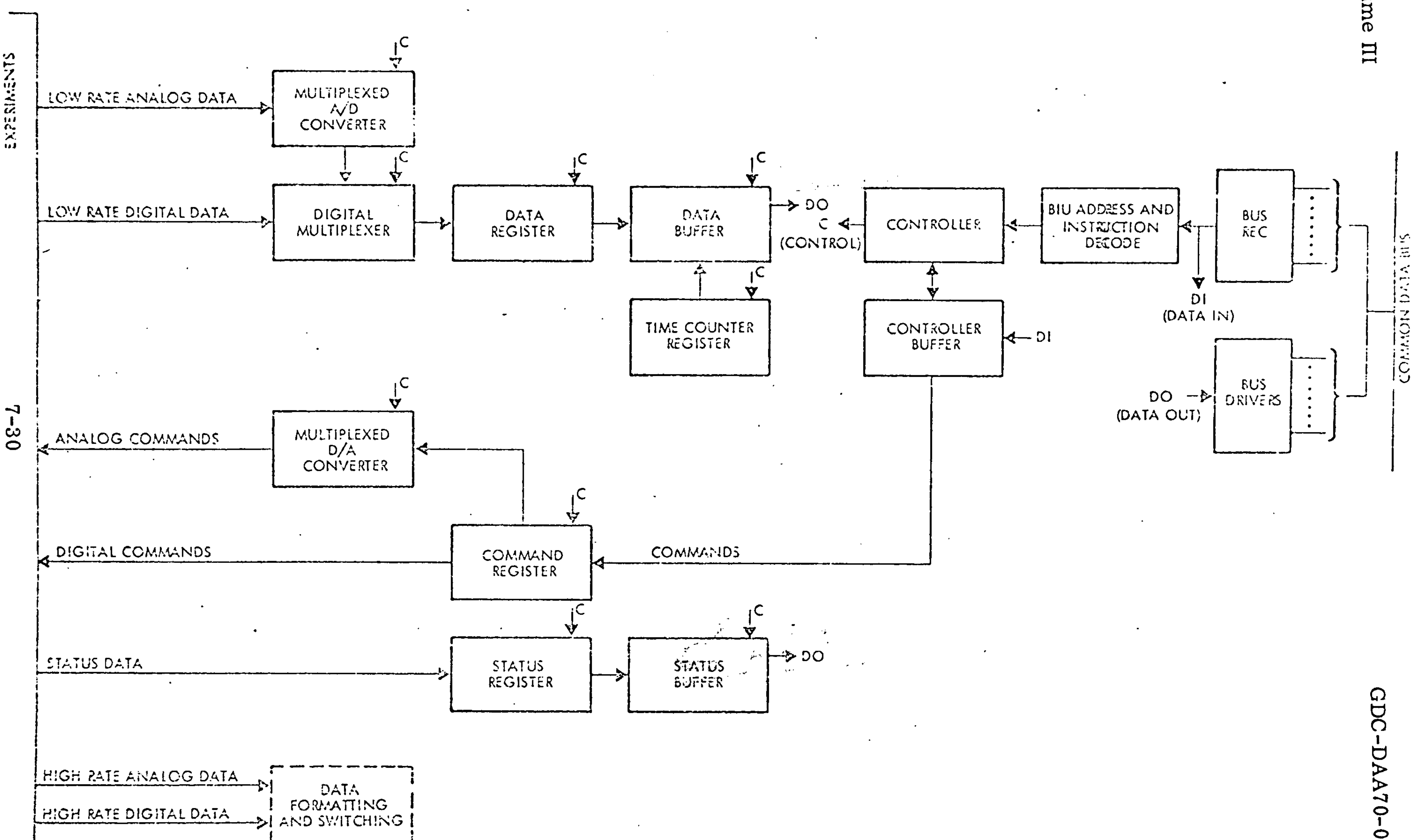

Figure 7-10. Experiment/Common Data Bus Interface

A flexible time division multiplex format is used for command, data, and synchronization. This simplifies the hardware required to implement the CDMS as compared to that required by; e.g., frequency division multiplexing with its attendant filters, oscillators, etc. Clocking information will be extracted by each BIU receiver. The TDM system to be used employs relatively simple BIUs having a high degree of commonality, operating in conjunction with a central computer that controls and manages the utilization of time on the bus.

The computer utilizes software to perform general housekeeping and data gathering functions on the bus. The housekeeping program provides the computer with logic to: (1) command all devices on the bus by transferring command routines to the device BIU, (2) monitor the health of each device by reading their status, (3) receive commands from telemetry, and (4) rearrange the software to reflect commands received through a command link. The data management program provides the computer with the necessary logic to: (1) query the BIUs for filled data buffers, (2) transfer the contents of filled data buffers to the computers, (3) assemble the collected data, and (4) send the assembled data to the Data Formatting and Switching network.

BIU Characteristics. A most important function of the CDMS is to interface with the experiments. To properly perform this function, data must be gathered continuously, intermittently, or randomly depending upon the particular experiment. The data may be analog or digital with differing accuracy. Similar command requirements exist. To perform such diverse functions and remain flexible demands some complexity within the BIU. A BIU conceptual design is presented in this section with the emphasis on the experiment interface.

The BIUs will:

a. Provide a means for each experiment to receive/transmit information on the bus.

b. Decode computer instructions into functional commands for the experiment or subsystem (examples are "Turn Absorption Spectrometer ON," "START MW Scanner," etc.)

c. Provide a buffer for data generated by the experiment sensors.

d. Provide a buffer for data and instructions sent to the BIUs.

The BIU contains:

e. Bus drivers/receivers for driving and receiving information on the bus.

f. A data buffer for storing low rate data, device status, and control commands to the experiments.

g. An experiment controller for decoding and executing the control commands sent to the experiment.

Figure 7-10 shows each of the functional blocks. A description of the role of each component follows·

a. Bus Drivers/Receivers: provide the device with a means of sending/receiving information on the common bus

b. Data Buffer: stores information and commands

   1. Buffer Address and Instruction Decode: decodes instructions and BIU addresses received from the computer

   2. Data Buffer No. 1 and 2: separated to allow the device to fill data in one buffer while data from the other is being transferred to the computer

   3. Control Sequence Buffer: stores control instructions from the computer

   4. Status Buffer: stores status words from the device

   5. Clock: provides BIU clock pulses

c. Experiment Controller: decodes command instructions and adds required time and address notes to data

   1. Device Instruction Decode: decodes instructions from the data buffer

   2. Command Register: sends command signals to the sensors and A/D – D/A converter via switches

   3. Device Status Register: monitors status signals from the device

   4. Time Counter Register: stores required time notes with data

   5. Data register: transmits device data to the data buffer

   6. Switches: gate housekeeping signals to the experiments and the multiplexed A/D – D/A converter.

   7. Multiplex A/D – D/A converter: converts analog data and status signals from the sensors to digital signals. Converts digital commands to the sensors to analog signals.

7.3.1.4 Computer. Numerous studies have been made of the use of small general purpose computers in scientific satellites. In many cases, these have not proven feasible due to stringent reliability conditions or severe physical restrictions. With the advent of LSI computers, these restrictions become less important. For the experiment modules, the flexibility requirement is an overriding consideration as previously mentioned.

Technology Considerations. It is unreasonable, in fact unfeasible, to require that components for the module DMS be available today (1970). This would be disregarding highly useful developments in a period of rapid expansion in these fields. For this study, 1972 space qualified technology baseline has been selected. General purpose LSI computers are today in hardware development stages. Miniaturized memories (Microbiax or plated wire) already exist and have been used in space. Although these choices could not have been made five years ago, a brief survey is included below to support the assumptions.

Computer Requirements. In order to perform a preliminary design of the computer subsystem, the accuracy, computational speed, storage, and data transfer requirements must be estimated.

Complex experiment calculation requirements are completely unknown at this time. If greater than 15 bit accuracies are required, double precision will be used. Speed requirements are equally vague. Based on other programs, a 50 times per second interaction would be fast enough for even the most complex control functions. This imposes no severe speed requirement and nominal LSI computer speeds are more than adequate.

The data transfer rates are set by (1) the data bus traffic and (2) the dedicated path to the data formatter. A 16-bit I/O word rate could exceed 25,000 per second. For this reason direct memory access is recommended for the CIU.

Computational Requirements. The software functions can be put into basically 3 classes: command programming, data processing, and checkout.

a. Command Programming. The computer must initiate command action at pre-set times and sequences. An internal realtime clock, stored programs, and count-down programs are used. As several different sequences might be required for different modes, 2K words of memory are allotted.

b. Data Processing. Formatting of data is not a particularly busy task but the transformation or correlation of experimental data may be. These requirements are not estimated here. Storage of telemetry formats and switching functions, display generation and other requirements are allotted 2000 memory words. Additional requirements (or deletions) may be met by adding or subtracting memory modules. Memory modularity is a definite requirement on the computer.

c. Checkout. The primary checkout requirement is limit checking of the estimated 250 engineering system monitors. As previously mentioned, these are sampled 10 times per second. Limits must be stored for each and a sequencing program chosen. This requires approximately 600 words. In addition, similar requirement exists for some experiments. Assume 100 experiment monitors which take an additional 200 words of memory. Calibration functions may also be performed but these are not yet defined. A computer diagnostic program may be allotted 200 words, which is more than enough for simple health data.

Table 7-6 summarizes the computer storage requirements and indicates a total of 8000 words is required.

Candidate Computers. The baseline is designed to use a computer that employs:

a. Binary 2's complement, parallel arithmetic.

b. Sixteen bit word or greater.

c. Sufficient instruction repertoire to perform control and data management tasks.

d. Directly addressable 1k memory.

e. Modular memory in 2k increments up to 16k

f. At least one interrupt

The required computer will have the following major building blocks:

1. Memory/computer interface
2. Arithmetic unit
3. Control unit
4. Serial I/O
5. Memory and associated electronics
6. Power supply

Although a significant number of interrupts has not specifically been identified, a minimum of one (external) should be provided.

Table 7-6. Summary of Computer Storage Requirements

Function	Storage Requirements in Words
Spare	3k
Command Programming	2k
Data Processing	2k
Checkout	1k
	8k words

Seven, of a large number of computers considered, are compared in Table 7-7. This number is sufficient for establishing the possibility of using an LSI computer for the module application using 1972 technology. The selection of a specific computer satisfying desired characteristics will have to follow further definition studies in later study phases.

7.3.1.5 Conceptual Data Storage and Recording Methods. One objective of the study has been to consider means to record the data collected aboard the modules, and to determine how much of it can or should be stored aboard the space station. In general, the data can be handled in at least three ways:

a. It can be recorded on film for later processing if the data rate is high (e.g. over 1 megabaud per second), or if film is necessary to maintain fidelity (e.g. in the case of a metric camera).

b. It can be transmitted in PCM form via a radio link or hard line to the station for recording and handling.

c. Or it can be transmitted as a separate video stream for human viewing.

The emphasis during the study has been placed on the use of PCM, but the film recording technique was also considered. The conclusions to date are:

a. Onboard storage of even the sub-megabaud data requires many hundreds of thousands of feet of digital film; magnetic tapes (digital or analog) are, therefore, not applicable except on a short term basis, and a better storage medium is needed.

b. The space station will probably need a formal data library.

c. The image data for some experiments, such as ERTS, does not seem to be excessive, but other data, such as that involved in the astronomy experiments, would be much too high unless severe restrictions were placed on the required use of the available data.

d. It would not be practical to store the video data or other very high data rate outputs.

There is, therefore, a clear need for additional requirements analysis on video and imaging sensor data handling. More analysis would also be beneficial to "timeline" the other sensors to determine what the total data rate would actually be in practice.

7.3.1.5.1 Digital Storage. The PCM data is to be recorded in digital form for later analysis and for transmission to the space station via a data link. The volume of required physical storage is analyzed in this section.

Table 7-7. Prospective Spaceborne LSI Computers

NAME / DATE INTRODUCED	DATA FLOW	DATA TYPE	NO. OF INSTRUCTIONS	COMPUTING TIME, μSEC			MEMORY						IN/OUTPUT		PHYSICAL CHARACTERISTICS				MTBF (HRS)	COMMENTS
				ADD	MULT	DIV	TYPE	WORD SIZE (BITS)	CAPACITY (WORDS) MIN	CAPACITY (WORDS) MAX	ACCESS TIME (μSEC)	CYCLE TIME (μSEC)	NO. OF CHANNELS	NO. OF INTERRUPTS	TYPE OF HARDWARE	WEIGHT (LBS)	SIZE (CU. FT)	POWER (WATTS)		
ARMA PORTABLE MICRO D EARLY 1968	P	Fx	36				CORE ROPE	18	4K				2		1C	14	0.195			ALSO CALLED CELESTIAL DATA PROCESSOR. WEIGHT AND SIZE INCLUDE BATTERIES AND I/O DEVICES
HONEYWELL H-437 LATE 1968	S	Fx	32	9	103	193	LSI ROS LSI ROS LSI	12 18 18	1K 128 32				2	2	10	4	0.13	20	17,522	HAS HARDWARE SQUARE ROOT. MEMORY IS EXPANDABLE TO 8K. MEMORY SHOWN HAS 1K INSTRUCTIONS, 128 CONSTANTS AND 32 SCRATCH PAD WORDS
ARMA ADVANCED MICRO D DEVELOPMENT	P	Fx	36	6.6	25	25	CORE	18	4K	32K	0.7		2	1	1C	6.6	0.096	55		
AUTONETICS D-200 DEVELOPMENT							MOS	24	4K	32K						9	0.116	10		WEIGHT, SIZE, AND POWER ARE GIVEN FOR 4K MEMORY
CONTROL DATA MOS-LSI DEVELOPMENT	P	Fx	44	2.4	10.4	30	PLATED WIRE	16	4K	64K	1.0	1.6	4	4	MOS-LSI	2.5	0.1	10	25,000	
NORTH AMERICAN D-200	P	Fx	35	8	108		CORE	24	4K	32K		2	4		MOS-LSI	6	0.1	10		
BUNKER RAMO ASM COMPUTER	P	Fx	25	6	25		FILM-MOS	16				2	1	1	MOS-LSI	8	0.1	25		

Digital Magnetic Tape Storage. A convenient baseline storage media is channel digital magnetic tape. While not the only medium, it provides a good reference point since it is well developed, will interface with most data handling devices, and is easily visualized.

The capacity of a tape (in bits) is derived by:

a. 8 bits per data frame

b. 800 bits per inch (1600 BPI and higher may be too high)

c. 1800 foot tape length

d. 80% blocking factor (blocks of 300 bytes)

This yields $8 \times 800 \times 1800 \times 12 \times 0.8 = 11 \times 10^7$ bits, which translates to:

a. 10^8 bits of storage

b. 1.3 kBPS for 24 hours

These values have been applied to the known data rates for the "under 1 megabaud" experiments, and the results summarized in Table 7-8.

An examination of the data leads one to conclude that:

a. Tape is a rather poor medium for some experiments (e.g., 5.2 Stellar, 5.8 Cosmic Ray Physics).

b. Anything but short term storage (1 to 2 days) aboard the spacecraft would require an impressive size tape library.

Table 7-8. Digital Tape Storage

Experiment	Tapes/day
5.1 Stellar	16
5.2 Stellar	305
5.5 High Energy Stellar	6-7
5.20 Fluid Physics	3-4
5.8 Cosmic Ray Physics	384
5.9, 5.10 Bio D/E	<1
5.11 Earth Surveys	17
5.12 Remote Maneuvering Satellite	1

c. One could reasonably anticipate 10 to 30 tapes per day with several modules operating.

Digital Film Storage. Film may be written with a digital code. The capacity sized for 70 mm film is:

a. Useful width of 60 mm for data.

b. 40 bits/mm across film (scan direction).

c. 20 bits/mm (500 lines/inch) along film.

Using a 100 foot spool of 70 mm film as a standard, one has:

$$100 \times 12 \times 500 \times 40 \times 60 = 1.44 \times 10^9 \text{ bits}$$

To a first order, a 100 foot spool of 70 mm digital film is equal to 13 spools of digital tape.

Alternatively, 1 kilobaud for 24 hours is 6 feet of film.

Table 7-9 summarizes the capacities required to store data for the various experiments.

Two facts are quite evident:

a. There are some experiments whose data simply cannot be stored by this means, at least for very many days.

b. For everything else, digital film storage appears to be quite attractive.

Video Tape. Digital signals can be modulated onto video tape. A 2200-foot spool of 1-inch tape can handle 30 minutes of recording at 6MHz. With a simplistic view of S/N and modulator-demodulators (Modems), this leads to:

$$6 \times 10^6 \times 1800 = 10.8 \times 10^9 \text{ bits/tape}$$

This is roughly equal to 100 digital tapes which, in turn, is roughly equal to 750 feet of digital film.

Trading 750 feet of 70 mm film for the need for a Modem and 2200 feet of 1-inch tape does not seem to be a good trade, and the use of video tape is not, therefore, desirable.

Table 7-9. Digital Film Storage (70 mm)

Experiment	ft/day
5.1	126
5.2	2400
5.5	50
5.20	30
5.8	3000
5.9, 5.10	3.5
5.11	132
5.12	480

Storage Requirements. To handle all sub-megabaud data in digital form, at least two orders of magnitude improvement are needed over the capabilities of digital film:

a. Present film postulate: 5×10^5 bits/in^2.

b. Requirement for experimental module: 5×10^7 bits/in^2. (60 day storage on board)

The storage of "over megabaud" data is, therefore, not feasible from a digital point of view. A summary of tape storage devices and archival equipment is shown in Tables 7-10 and 7-11.

7.3.1.5.2 Film Handling. Many sensors, e.g., the stellar camera, record directly on film for final use. Others record on film for further processing (optical in this case). To determine the quantity of film to be processed, stored, retrieved, etc., "equivalent frames" were analyzed by considering the strip records to be sliced up into squares. The results (to this date) given in Section 7.4.1 indicate that some of the experiments, such as 5.11, pose little difficulty, while the amount of film required to handle other experiment data outputs is obviously excessive.

7.3.1.6 CDMS Redundancy Inclusion Techniques. As described previously, the CDMS incorporates redundancy to meet prescribed reliability requirements. The resulting complex of interconnected and standby units requires a set of systematic switching rules for use under every anticipated failure possibility. Available techniques for employment of redundancy fall broadly into the categories of majority (voting) techniques, switching techniques, or combinations of these. Initially, numerous candidate redundancy inclusion concepts may be conceived but few provide

Table 7-10. Survey of Magnetic Tape Storage Devices

MFG.	MODEL	NO. OF TRACKS	DATA CAPACITY (IN BITS)	PACKING DENSITY (BPI/TRACK)	TAPE LENGTH & WIDTH	WEIGHT	SIZE (IN INCHES)	POWER (IN WATTS)
BORG-WARNER	R215	8	5×10^{8}	1100	5000'x1/2"	18	11x11x4	> 30 W
KINELOGIC	LS2	5	2.6×10^{7}	1350	1100'x1"	< 12	9x11x6	22 W MAX
KINELOGIC	RSL	24	2.9×10^{8}	1350	400'x1"	5.5	6x5x5	6 W
LEACH	2000 SERIES	7	5×10^{8}	2000	3000'x1/4"	10	5x7x7-1/2	15 W
RCA	ERTS VIDEO TYPE	1	24×10^{9}	1×10^{6}	2000'x2"	74	T 22x15x7 E 17x16x7	280 W START-UP 90 W STEADY-STATE
RAYMOND	APOLLO EM 11 TYPE	18	10^{8}	853	550'x1"	18	9-3/4Dx8	20 W MAX

Table 7-11. Summary of Archival Equipment Characteristics

Equipment Type	Medium	Bits/in^2 X10^6	Bits/in^3 X10^8	Medium Cost X10^{-7} ¢	Equipment Cost	Data Life	Data Rate	Access Unit
Magnetic								
IBM-2401	tape	0.0256	0.0424	20	40K	limited	180K byte	3.5×10^8
Ampex-1900	tape	0.25	1.0	0.03	50K	unknown	15M bit	3.0×10^{10}
Ampex-1928	tape	0.5	2.0	0.015	60K	unknown	30M bit	6.0×10^{10}
Ampex-1932	tape	0.64	2.56	0.013	60K	unknown	38M bit	7.5×10^{10}
G. D. -Unidar	tape	1.0	4.0	0.007	150K	unknown	115M bit	1.5×10^{11}
Optical								
IBM-1360	diazo chip	1.2	0.38	84.5	-	permanent	2M bit	3.2×10^5
P. I. C. -Unicon	metal strip	20	0.8	0.25	200K	permanent	4M bit	2.0×10^9
SYN. -PDR-5	silver	0.5	0.55	2.0	-	permanent	10M bit	1.0×10^9
F. M. -390	film coated plastic card	0.42	0.084	0.25	-	permanent	0.8M bit	1.0×10^7

the desired reliability. This may be shown by using relative reliability figures to form an accurate basis for comparison of the concepts and insuring that the reliability of every switching or majority operation is properly included in the analysis.

If the experiment module is to be capable of control after two independent failures, many critical subsystems, including the data bus, must be triply redundant. The simplest way to implement this redundancy is with three independent data management systems including computer, BIU, command decoders, and data bus. Mean time-to-failure of each unit in the series-string must be sufficiently high to achieve the overall target reliability. In addition, care must be taken to eliminate "sneak" paths which could compromise independence and to account for the reliability of all switching elements.

If the single-thread reliability number is not sufficiently high, then the individual elements must be improved through device improvement, internal redundancy, or through interconnection of the three systems in some way so as to pool spare elements between threads.

Consider the three computers in Figure 7-2, which must interface with the three data buses. In one switching concept, the interface may be a 3 by 3 switching matrix allowing full interconnection capability with any computer capable of being connected to any data bus. This course obviously leads to rather complex switching software and hardware. Similar possibilities exist at the BIUs and command decoders where multiple buses may be connected to a single unit or multiple BIUs used, one for each bus. Due consideration in choosing a scheme must be given to system philosophy, to the overall reliability and to the operational checkout plan.

An alternative to switching redundancy is the majority technique. This technique has been studied both from a mathematical and from an implementation standpoint, and has been used in some high-complexity data bus applications. Well known, for example, is TMR (triple modular redundancy). In the present case, three data buses could be operating simultaneously with voting between them at the computer, the BIUs and the command decoder. Suitable majority circuits would be required at each unit and their reliability included in the MTBF calculations. Other options exist such as utilizing voting between computers and command decoders.

7.3.2 DETAILED ANALYSES

7.3.2.1 Maximum Link Distances

Multipath. Because of the possibility of low grazing angles with respect to the earth for space station-to-module transmission link, particularly for larger separation distances, there exists a potential for multipath fading. In order to have a sufficiently solid communication link, i.e., one without fading, the space station-to-module distance must be less than some value that is determined by the space station antenna pattern (the first null). (A less restrictive limitation is maximum line-of-sight.)

In the following analysis, the above distance limitation is taken as that which allows a particular hypothetical ray to be received by the module. This ray originates at the space station and reflects from the earth's surface at equal incidence and reflection angles (Figure 7-11). The angle of this ray with respect to line-of-sight is the space station antenna half beamwidth to main lobe null as shown in Figure 7-12 and is given by

$$\theta_{\text{first null}} \simeq \frac{70\lambda}{D}$$

By solving the geometrical problem shown in Figure 7-11 for L as a function of $\theta_{\text{first null}}$ and the orbit altitude A_s, the distance at which multipath fading would occur is determined. The relationship is

$$L = E \sin 2\theta \pm \sqrt{E^2 \sin^2 2\theta + (A_s^2 + 2EA_s)4 \cos^2 \theta}$$

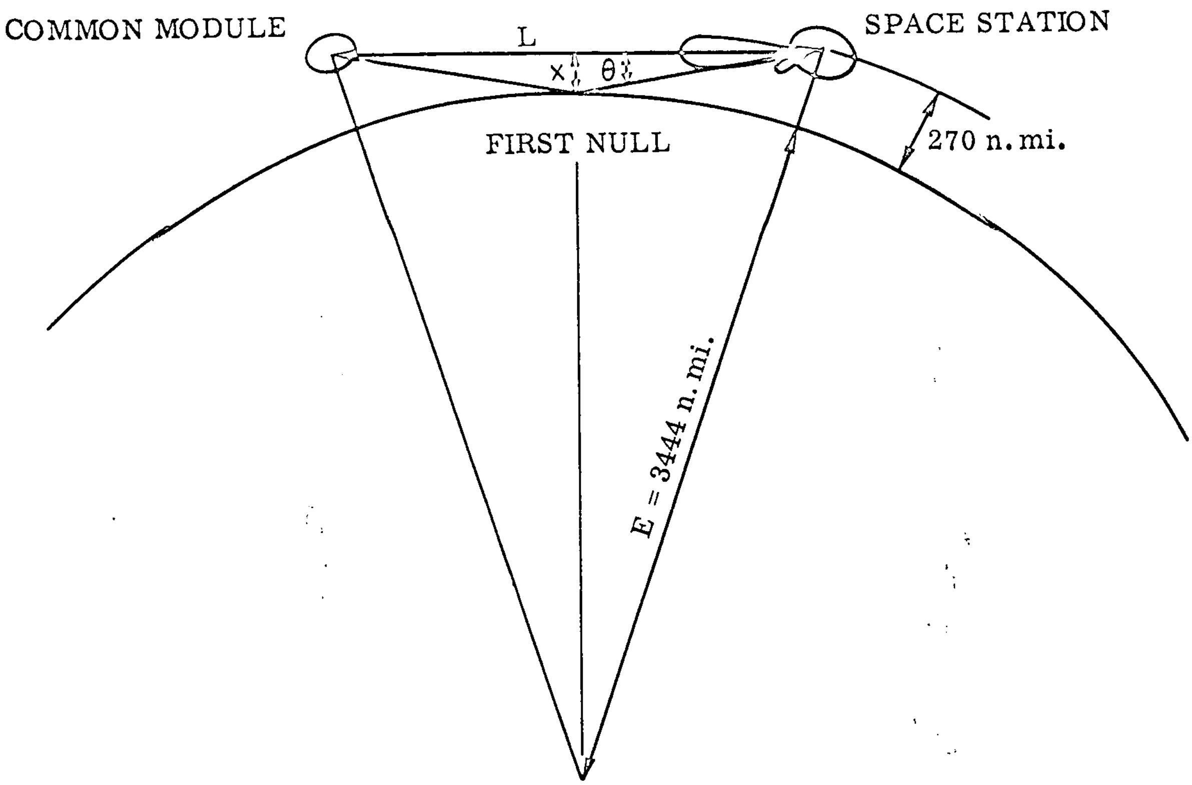

Figure 7-11. Space Station-Module Maximum Link Distance Geometry

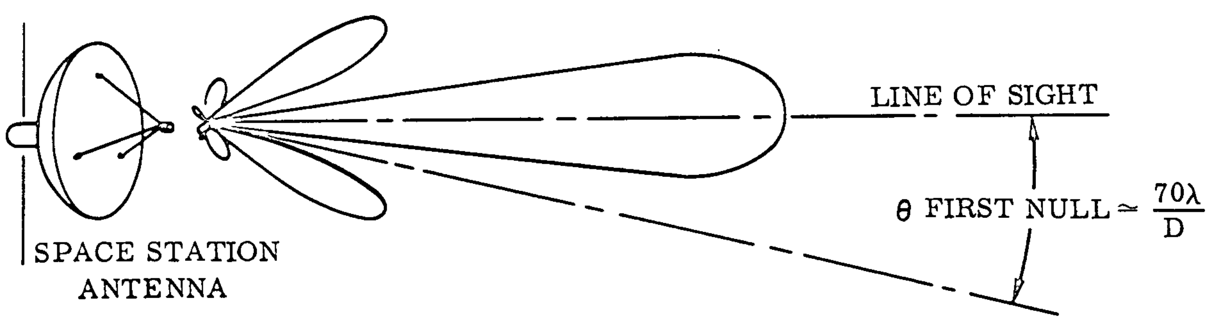

Figure 7-12. Space Station Antenna Pattern Null

If the space station S-band antenna is a 15-foot dish, for example, the half beamwidth to main lobe null is approximately 2.7 degrees for the lowest S-band frequency considered (1.7 GHz). The above limitation on space-station-to-module propagation distance is in this case 2456 n.mi.

Module-to-Ground Slant Range (Back-up Mode). For module-to-ground transmission in a back-up mode, the distance between a ground station and a module at 270 n.mi. altitude is 1120 n.mi. at an elevation angle of 5 degrees.

7.3.2.2 Link Power Budgets. Tables 7-12 through 7-17 are power budgets for communication links from the experiment module to the space station, to MSFN (backup mode only) and to the DRSS (Reference only).

Table 7-12 applies to the experiment-module-to-space-station baseline S-Band systems ERP of 5 watts and 1 MHz transmission bandwidth or 0.2 MHz video bandwidth. Table 7-13 applies to the same situation but with the ERP increased to 71 watts to accommodate an increase in video bandwidth to 2.9 MHz.

Tables 7-14 and 7-15 apply to a 100 MHz wideband communication link from the module to the space station at Ku (13.5 GHz) and V (60 GHz) band respectively.

Table 7-16 applies to a backup operating mode of the experiment module baseline system directly transmitting to MSFN at S-band. An excess S/N margin of 12 db is noted.

Table 7-17 is for reference only and illustrates a high module ERP (100 watts) transmission at Ku band directly to DRSS with a 4-foot antenna on the module.

7.3.2.3 Common Data Bus Flow Analysis. A common data bus is used to interconnect engineering subsystems and experiments as well as all of the major elements of the CDMS. One of the fundamental design parameters of the data bus is the traffic on the bus and the total data rate required. The traffic and data rate on the bus is dependent upon the particular experiments carried aboard the module; therefore, as an example, flow analysis FPE 5.11 Earth Surveys is used. Experiment data flow, consisting of sensor outputs, sensor command and control, and experiment status and monitoring, is analyzed first. Next, engineering subsystem traffic and data rate for a typical module is examined and finally miscellaneous other traffic is estimated.

7.3.2.3.1 FPE 5.11 Experiment Data Flow Analysis

Sensor Data. Table 7-18 shows the estimated data rate for each of the sensors contemplated for FPE 5.11. (Those sensors whose output is recorded on film are not listed.) Two of the instruments, the UV imager/spectrometer and the IR spectrometer/radiometer, are arbitrarily classed as high data rate devices and their outputs

Table 7-12. Baseline Common-Module-to-Space Station Digital Data Link

(500 nmi Separation, 1 Mbps)	
Transmitter Power (5 watts)	+ 7.0 dbW
Line Loss	- 1.5 db
Common Module Antenna Gain (Omni)	0
Free Space Loss (2250 MHz, 500 n.mi.)	-158.8
Space Station Antenna Gain (15-ft dish, 2° Beamwidth)	+ 38.0
Pointing Loss (Off Beam Allowance)	- 2.5
Line Loss	- 1.5
Received Signal Level	-119.3 dbW
Boltzmann's Constant	-228.6 dbW/Hz-°K
System Noise Temperature (1200°K)	30.8 db-°K
Bandwidth (1 MHz)	60.0 db-Hz
Noise Power	-137.8 dbW
Threshold for BER = 10^{-6}	+ 12.5 db
Margin	6.0
Required S/N	+ 18.5 db

Table 7-13. Common Module-to-Space Station Wideband TV Link Power Budget

(Carrier Frequency 2263 MHz, Video Bandwidth = 2.9 MHz)	
Common Module Transmitter Power (71 watts)	+ 18.5 dbW
Line Loss	- 1.5 db
Common Module Antenna Gain (Omni)	0
Free Space Loss (500 n.mi.)	-158.8
Space Station Antenna Gain (15-ft dish, 2° BW)	+ 38
Pointing Loss (Off Beam Allowance)	- 2.5
Line Loss	- 1.5
Received Signal Level	-107.8 dbW

(Continued)

Table 7-13. Common Module-to-Space Station Wideband TV Link Power Budget (Continued)

Boltzmann's Constant	-228.6 dbW/Hz-°K
System Noise Temperature (1200°K)	30.8 db-°K
*Bandwidth (16 MHz)	72 db-Hz
Noise Power	-125.8 dbW
FM Improvement Threshold	12 db
Margin	6
Required S/N	18 db
Min. Predetection S/N (Improvement Threshold)	12 db
Peak-Peak/RMS Factor	9
**FM Improvement (β = 1.75)	14
Video S/N (pk-pk/rms)	35 db

$$*B_{IF} \approx 2f_m(1+\beta) = 2(2.9)(1+1.75) = 16 \text{ MHz}$$

$$**R = \frac{3}{2}(\beta^2)\frac{B_{IF}}{f_m}$$

Table 7-14. Common Module-to-Space Station Wideband Digital Link Power Budget, Ku Band

(Carrier Frequency = 13.5 GHz, Data Rate = 100 MBPS)	
Common Module Transmitter Power (23.4 watts)	- 13.7 dbW
Line Loss	- 1.5 db
Pointing Loss	- 1
Common Module Antenna Gain (4 ft dish)	+ 42
Free Space Loss (500 n.mi., 13.5 GHz)	-174.3
Space Station Receive Antenna Gain (10° BW)	+ 25.4
Pointing Loss	- 1
Line Loss	- 1.5
Received Signal Level	- 98.2 dbW

(Continued)

Table 7-14. Common Module-to-Space Station Wideband Digital Link Power Budget, Ku Band (Continued)

Boltzmann's Constant	-228.6 dbW/Hz-°K
System Noise Temp. (F = 8dB T = 1540°K)	31.9 db-°K
Bandwidth (100 MHz)	80 db-Hz
Noise Power	-116.7 dbW
Threshold for BER = 10^{-6}	12.5 db
Margin	6
Required S/N	18.5 db

Table 7-15. Common Module-to-Space Station Wideband Digital Link Power Budget - V-Band

(Carrier Frequency = 60 GHz, Data Rate = 100 Mbps)	
Common Module Transmitter Power (15 watts)	11.8 dbW
Line Loss	-1.5 db
Pointing Loss	-1
Common Module Antenna Gain (1-ft dish)	43
Free Space Loss (500 n.m. - 60 GHz)	-187.3
Space Station Receive Antenna Gain (1-ft dish)	43
Pointing Loss	-1
Line Loss	-1.5
Received Signal Level	-94.5 dbW
Boltzmann's Constant	-228.6 dbW/Hz-°K
System Noise Temperature (F = 11 dB → T = 3360°K)	35.6 db/°K
Bandwidth (100 MHz)	80 db-Hz
Noise Power	-113.0 dbW
Threshold for BER=10^{-6}	12.5 db
Margin	6
Required S/N	18.5 db

Table 7-16. Back-up Common Module-to-MSFN Digital Data Link

(Carrier Frequency 2250 MHz, 1 Mbps Data Rate)	
Transmitter Power (5 watts, Baseline)	+ 7 dbW
Line Loss	- 1.5 db
CM Antenna Gain (omni)	0
Free Space Loss (2250 MHz, 1120 n.mi., 5° El)	-165.8
MSFN Antenna Gain (2250 MHz, 30-ft dish)	+ 44.1
Line Loss	- 1.5
Received Signal Level	-117.7 dbW
Boltzmann's Constant	-228.6 dbW/Hz-°K
System Noise Temperature (110°K 5° El)	20.4 db-°K
Bandwidth (1 MHz)	60.0 db-Hz
Noise Power	-148.2 dbW
Threshold for BER = 10^{-6}	+ 12.5 db
Margin	6.0
Required S/N	+ 18.5 db
Excess Margin	+ 12 db

Table 7-17. Common Module-to-DRSS Digital Data Link

(Carrier Frequency 13.5 GHz, 10 Mbps Data Rate)	
Common Module Transmitter Power (100 watts)	+ 20.0 dbW
Line Loss	- 0.9 db
Common Module Antenna Gain (4 ft)	+ 43.0
Free Space Loss (23,000 n.mi., 13.5 GHz)	-207.6
DRSS Antenna Gain (4.5 ft)	+ 43.0
Line Loss	- 2.0
Required Input Signal Level for Saturated Output	-104.5 dbW

(Continued)

Table 7-17. Common Module-to-DRSS Digital Data Link (Continued)

<u>Noise Power Density Contribution of Repeater</u>	
Boltzmann's Constant	-228.6
Repeater Noise Temperature (2300°K)	+ 33.6
Repeater Gain (for 6w output)	+112.3
Transmitter Antenna Gain	+ 30.0
Free Space Loss (21,000 n.mi., 14 GHz)	-207.1
Atmospheric Attenuation	- 2.0
Ground Antenna Gain (85 ft dish, 14 GHz)	≈+ 54.0
Noise Power Density	-207.8 dbW/Hz
<u>Noise Power Density Contribution of Ground Station</u>	
Boltzmann's Constant	-228.6
Ground Receiving System Noise Temperature (150°K)	+ 21.8
Noise Power Density	-207.8 dbW/Hz
<u>DRSS to Ground</u>	
DRSS Transmitter Power (6W)	+ 7.8 dbW
DRSS Antenna Gain	+ 30.0
Free Space Loss (21,000 n.mi., 14 GHz)	-207.1
Atmospheric Attenuation	- 2.0
Ground Antenna Gain (85 ft dish, 14 GHz)	≈+ 54.0
Received Signal Level	-117.3 dbW
Noise Power for 10 MHz Bandwidth	-134.8
Received S/N	+ 17.5 db
Required S/N (BER = 10^{-6})	12.5
Margin	+ 5.0 db

Table 7-18. FPE 5.11 Experiment Sampling Requirements and Data Rate Estimate

Sensor	Number of Analog Channels	Sample Rate	Period	Bits/ Sample	Bit Rate
*UV Imager/Spectrometer	2	5000 sps	continuous	8	80k*
*IR Spectrometer/Radiometer	2	1900 sps	continuous	10	20k*
IR Atmospheric Sounder	41	150 sps	9-13 sec intervals	12	4k (peak)
IR Interferometer/Spectrometer	(Digital)	4300/frame	13 sec interval	12	4k
Active/Passive Microwave Radiometer	(Digital)	400 sps	continuous	8	3.2k
Radar Altimeter/Scatterometer	(Digital)	400 sps	continuous	8	3.2k
Data Collection Set	(Digital)	10 sps	Random; <1000 in 10 min.	200	2.4k
Absorption Spectrometer	3	50 sps	continuous	8	1.2k
Multifrequency Microwave Radiometer	5	8 sps	continuous	12	480
UHF Spherics	(Digital)	10 sps	continuous	10	260
		20 sps	continuous	8	
Visible Wavelength Polorimeter	16	1 sps	continuous	10	260
Microwave Atmospheric Sounder	5	2 sps	continuous	10	100
Microwave Scanner Radiometer	(Digital)	34.4 sps	continuous	9	310
Laser Altimeter	(Digital)	20 sec	continuous	24	480

*Data from these sensors are not put on the data bus but are connected directly with the high rate data formatter.

would be directly wired to the high data rate formatter and subsequently recorded or transmitted via the space station link to ground. Excluding these two high rate devices, the total data rate produced by the sensors is estimated to be 90 kbps.

Experiment Command and Control. Most of the units have their own sequencing facilities; the commands are simply on/off as far as data collection goes. A few devices require timing signals, but they are of a rather trivial nature.

There are no closed loop controls, per se. There is an interesting possibility that the astronauts may command the devices through the common data bus. This would give rise to a few samples per second on the line.

A total 1 kbps bus data rate is assigned to command and control of experiments.

Experiment Status and Monitoring Data. All 20 sensors have some housekeeping. Assuming each has perhaps five bit variables per second, the peak housekeeping load is 600 bps.

Experiment Data Flow Summary. The experimental system sampling load, at a peak moment, is shown in Table 7-19.

7.3.2.3.2 Engineering Subsystems Data Flow Estimate. A total complement of engineering subsystems measurements, their data rates, and modes of operation are not available at this time. However, 250 monitoring points have been identified and a sampling rate of 10^6 bit samples per second arrived at as a worst case condition. This results in 15 kbps to flow on the common data bus to the computer.

Command rates to the engineering subsystems will not be very high, say less than 1 kbps. Closed loop control, however, may be quite high if the computer is used actively. Based on other programs, even for propulsion periods, this data rate probably will be on the order of 10 kbps unless some unusual demands are imposed. For this baseline, such exceptional cases are deemed to be closed loop within the subsystem and only monitoring is required by the computer.

Table 7-20 summarizes the engineering subsystem rates in bits per second.

Table 7-19. FPE 5.11 Data Flow Summary

Sensor Outputs	90 kbps
Command and Control	1.0
Status and Monitoring	0.6
Total	91.6 kbps

Table 7-20. Engineering Subsystems Data Flow Summary

Monitor Data	15 kbps
Command Data (Maximum)	1 kbps
Control Data (Maximum)	10 kbps
Total	26 kbps

7.3.2.3.3 Miscellaneous Common Data Bus Traffic. The computer is also required to control the switching, formatting, data storage and display systems. Switching and data storage require only intermittent data and then in the form of low bit rate discrete signals. Hence, these contribute very little to the bus traffic. Formatting, both at the BIUs and at the data formatters, is performed intermittently. A particular format might involve several hundred bits, but would be changed so infrequently and over such a long period (say, one second), that the average bit rate from this source is vanishingly small.

An unknown quantity, however, is the data requirement for the laboratory displays. If generated entirely by the computer, a very high data rate would result. For the baseline, it was assumed that the prime data source for any displays was the wideband data stream or telemetry data. Otherwise, the displays could be driven by the computer via a dedicated channel. The data bus is here used only for homing on particular measurements or console control functions. The result is that 1 kbps is considered a sufficient bandwidth for all of the above requirements.

7.3.2.3.4 Processed Data. In addition to the primary data on the bus, there will be data that is the result of computer processing of some experiment and subsystem outputs. This processed data is routed to its destination via the data bus. Its destination may be short-term storage, permanent storage or the low rate data formatter.

As an estimate of the rate of the processed data resulting from the 90 kbps experiment sensor outputs, assume that 1/5 is processed at compression ratio of 4:1. Thus, the processed data on the bus from experiments is approximately 4.5 kbps.

For the contribution of processed engineering subsystem data, assume that all the data (15 kbps) is compressed at 5:1. In this case, the processed data on the bus from engineering subsystems is 3 kbps.

The total processed data on the bus is then approximately 7.5 kbps.

7.3.2.3.5 Data Bus "Overhead." A final important source of traffic is the control of the common data bus itself. For a fixed format, i.e., highly structured information format on the data bus, the "housekeeping" data may be a fairly low percentage of the information data. However, for more flexible formats, this percentage increases, often by 100% or even 200%. For this conceptual study, no particular format was chosen. An average 100% overhead will be imposed for housekeeping data on the data bus. This includes BIU addresses, internal subsystem addresses, functional codes, error control coding, etc.

7.3.2.3.6 Summary Data Flow on Bus. The above results are summarized in Table 7-21. It is seen that a total serial bit rate of 252 kbps has been determined.

Table 7-21. Common Data Bus Traffic Summary - FPE 5.11

Total Experiment (FPE 5.11)	91.6 kbps
Engineering Subsystems	26
Processed Data	7.5
Miscellaneous Bus Traffic	1
Subtotal	126.1
Data Bus Overhead @ 100%	126.1
Total Peak Bus Bit Rate	252.2 kbps

SECTION 8

ELECTRICAL POWER SUBSYSTEM

The electrical power subsystem supplies the electrical power required by the experiments and the other functional subsystems within each module. Prime power is supplied by the space station during attached modes of operation. During free-flying modes of operation power is supplied by batteries or solar panels. Normally attached modules require a minimal amount of power for relatively short periods of time during rendezvous and docking. This power requirement is most suitably supplied by batteries. Modules in which the normal mode of experiment operation is free-flying need larger amounts of power for longer periods of time, a condition best met by a combination of solar panels and batteries. Power conditioning equipment consisting of voltage regulators, dc-dc converters, and dc-ac inverters is provided for the module subsystems. Experiment power conditioning is not specifically provided. Power distribution (harnessing and buses) and control are provided in all modules for both subsystem and experiment power requirements. An important control function is switching on of redundant components upon failure of the primary component.

8.1 REQUIREMENTS ANALYSIS

Each experiment module generally houses more than one experiment. Experiment power requirements within each FPE were analyzed. Analysis results are given in Tables 8-1 and 8-2 for free-flying and attached modules respectively. The tables list the maximum experiment power required within the FPE. FPEs 5.17, 5.18 and 5.X (suitcase) experiments are grouped in a logical manner with other FPEs.

Power is assumed to be distributed to the experiments as equivalent 28 Vdc as no detailed information concerning further definition of power type (voltage, frequency) is currently available. In addition, it will be necessary to conduct a trade-off study of the advantages of centralized versus decentralized power conditioning after such information is available. Power conditioning is discussed in further detail in Section 8.3.3.

The experiment modules have subsystems, each of which has power requirements. The module configurations at the commonality study conclusion resulted in the subsystem power requirements also included in Tables 8-1 (free-flyer) and 8-2 (attached). In the case of the attached modules the subsystem power requirement is primarily for data equipment. Also required is power for crew support such as lighting and atmosphere quality monitoring. The biology group FPE 5.9/10/23 has a life support system separate from the space station for the experimenters.

Table 8-1. Power Requirements Analysis — Free-Flyer

FPE	Experiment (kW)	Comm. (kW)	Stab & Reaction Control (kW)	TCS (kW)	Total (kW)
5.1	Avg. 0.193	0.259	0.621	0.074	1.147
	Peak 0.36	0.259	0.830	0.074	1.523
5.2A	Avg. 0.743	0.259	0.957	0.074	2.033
	Peak 1.050	0.259	1.200	0.074	2.583
5.3A	Avg. 0.503	0.359	0.939	0.074	1.875
	Peak 0.850	0.359	1.200	0.074	2.483
5.5	Avg. 0.510	0.259	0.909	0.074	1.752
	Peak 0.66	0.259	1.100	0.074	2.093
5.20-2	Avg. 1.0	0.259	0.355	0.074	1.688
	Peak 1.4	0.259	0.510	0.074	2.243
5.20-3	Avg. 1.4	0.359	0.355	0.074	2.188
	Peak 4.0	0.359	0.510	0.074	4.943
5.20-4	Avg. 0.165	0.259	0.355	0.074	0.853
	Peak 1.20	0.259	0.510	0.074	2.043
CM-1 Design Requirement	Average				2.188
	Peak				4.943

Table 8-2. Power Requirements Analysis — Attached Modules

FPE	Experiment	Total Average	Total Peak
CM-3 Power Requirement (kW)			
5.7/5.12	1.28	1.8	2.0
5.8	3.1	3.7	4.5
5.16	2.0	3.05	5.3
5.20-1	0.4	1.0	1.2
5.27	1.6	2.35	2.55
CM-3 Design Requirement		3.7	5.3
CM-4 Power Requirement (kW)			
5.9/5.10/5.23	3.95	5.2	5.5
5.11	1.04	1.65	7.0
5.22	1.0	1.75	2.0
CM-4 Design Requirement		5.2	7.0
Free-Flying (Docking) Mode Requirement		0.64	0.8
Attached Module Design Requirement		5.2	7.0

8.2 SUMMARY OF RESULTS

This section presents the selected hardware configuration for each FPE/module design. Pertinent parametric or scaling data for extending the design concept are presented and alternative approaches are identified.

8.2.1 ELECTRICAL POWER SUBSYSTEM SELECTED CONFIGURATION. Table 8-3 lists the characteristics of the building block components from which the electrical power subsystem configuration for a specific module is constructed.

Configuration summary of electrical power subsystem design for the free-flying modules is given in Table 8-4. The maximum power rating of 2.4 kW is used for the FPE 5.2A module. The other modules use leave-off tailored versions of this design. The FPE 5.20 module (fluid physics) design has requirements for short time power resulting in additional batteries. Further discussion of this module is given in Section 8.3. Rating is based on the multi-orbit capability of the installed electrical power subsystem. Actual dissipation or heat load is also tabulated and exceeds rating in the fluid physics application because of the use of stored energy.

Table 8-3. Characteristics of Electrical Power Subsystem Components

Component	Weight (lb)	Volume (cu ft)	Power Dissipation (watts)
Solar Panel (27.5 Square Feet)	30.0	4.2	
Sun Sensor	1.2	0.01	2
Deploy/Retract/Orient Mechanism	58.8	0.55	
Deploy/Retract Motor (Brushless dc)	3.4	0.03	20
Orientation Motor (Brushless dc)	3.4	0.03	20
Motor Dr[illegible]	1.4	0.03	2
Battery ([illegible]	140.0	0.85	200
Battery Charger	20.0	0.3	70
Regulator (1 kW)	40.0	0.8	120
Inverter (250 VA)	18.0	0.4	70
Power Control and Distribution (7 kW Peak)	60.0	1.7	10

Table 8-4. Electrical Power Subsystem Configuration of Free Flying Modules

Component \ Quantity per FPE	5.1	5.2A	5.3A	5.5	5.20 -2	5.20 -3	5.20 -4
Solar Panel	18	24	20	18	6	6	6
Sun Sensor	2	2	2	2	1	1	1
Mechanism	2	2	2	2	1	1	1
D/R Motor	4	4	4	4	2	2	2
Orient Motor	4	4	4	4	2	2	2
Amplifier	3	3	3	3	2	2	2
Battery	4	4	4	4	5	6	4
Charger	4	4	4	4	5	6	4
Regulator	2	2	2	2	1	1	1
Inverter	4	4	4	4	2	3	3
Distribution	1	1	1	1	1	1	1
Totals							
Weight, lb	1543	1723	1603	1543	1210	1370	1050
Volume, cu ft	85.6	110.8	94	85.6	35.4	36.5	34.2
Rated Average Pwr, kW	1.8	2.4	2.0	1.8	1.8	2.2	1.0
Heat Load, kW	1.4	2.4	2.3	2.1	2.0	2.5	1.1
Array Area, sq ft	495	660	550	495	165	165	165
Array Weight, lb	691	871	751	691	256	256	256

Table 8-5. Electrical Power Subsystem Configuration of Attached Modules

Component \ Quantity Per FPE	CM-3 5.7/ 5.12	5.8	5.16	5.20 -1	5.27	5.9/ 5.10/ 5.23	CM-4 5.11	5.22
Battery	3	3	3	3	3	3	3	3
Charger	3	3	3	3	3	3	3	3
Regulator	1	1	1	1	1	1	1	1
Inverter	3	3	3	3	3	3	3	3
Distribution	1	1	1	1	1	1	1	1
Totals								
Weight, lb	634	634	634	634	634	634	634	634
Volume, cu ft	7.15	7.15	7.15	7.15	7.15	7.15	7.15	7.15
Rated Avg Pwr (Heat Load), kW	1.93	3.7	3 05	1.0	2.35	5.2	1.65	1.75

The attached module configuration is given in Table 8-5. A common design was chosen for all the modules. This approach is largely attributable to the common power requirements during the free-flying mode of rendezvous and docking. Rated power or heat load represents the demand on the space station

Block diagrams typical of the electrical power subsystem configurations for the free-flyer and attached module are shown in Figures 8-1 and 8-2, respectively. A few details included in Table 8-4 are not included in Figure 8-1 for clarity such as the standby redundant motor drive servoamplifier.

8.2.2 SCALING DATA. Pertinent characteristics of the selected design concept for the free-flying module electrical power subsystem are shown in Figure 8-3.

Total electrical power subsystem weight versus average output or load power is plotted from 0.5 kW to 6.0 kW as 250 lb constant plus 710 lb per kW. All the weights of Table 8-4 fall within 15% of this curve with the greatest deviation occurring below the curve (i.e., the selected design is lighter than the parametric design). The curve appears to be useful for preliminary design purposes. Deviations are attributable to the necessarily discrete manner in which components are added to the configuration. As an example, the FPE 5.2A electrical power subsystem at 1723 lb is 13% below the curve but adding an additional battery and charger would bring it to 1883 lb or 4% below

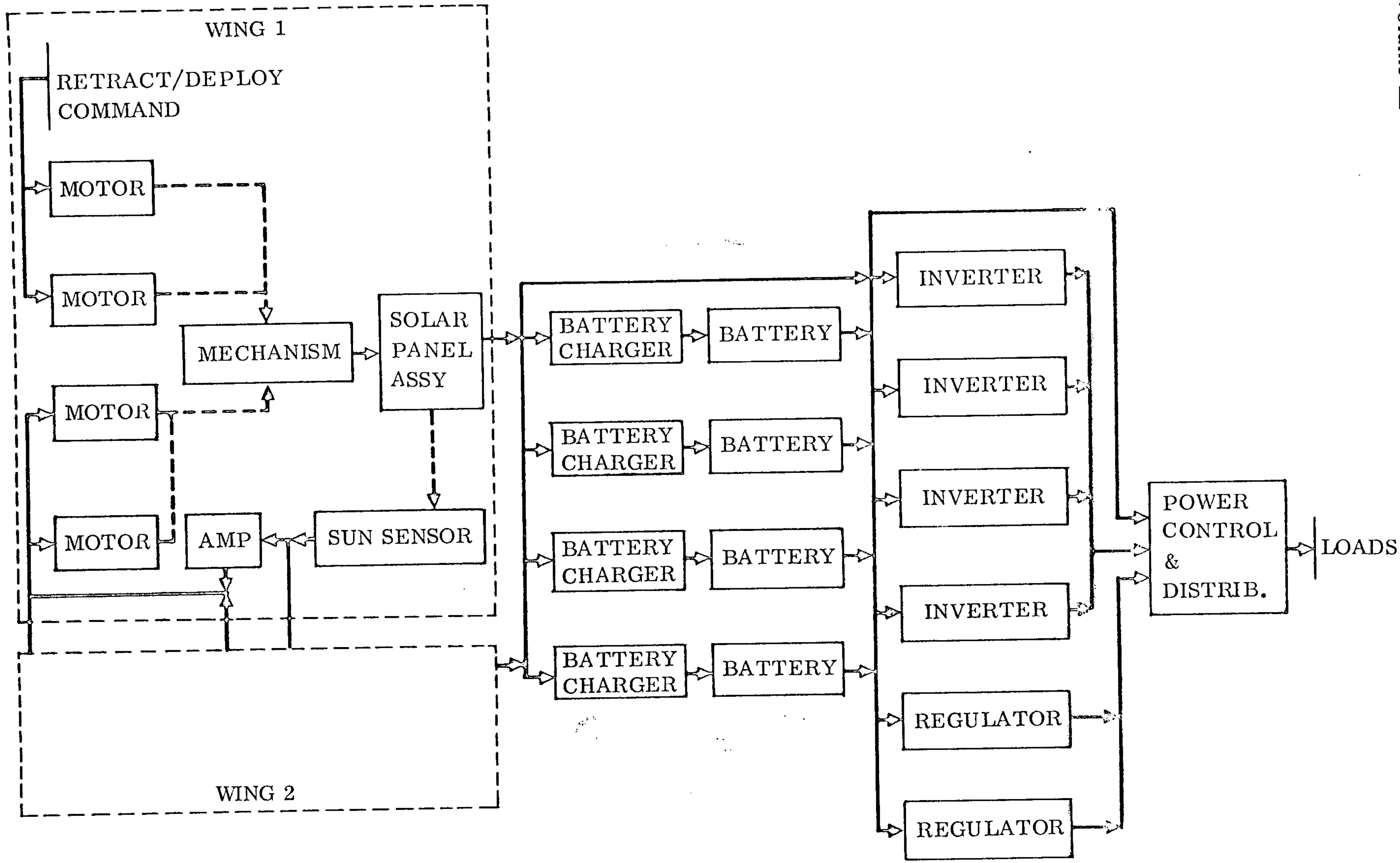

Figure 8-1. Free Flyer Electrical Power Subsystem Block Diagram

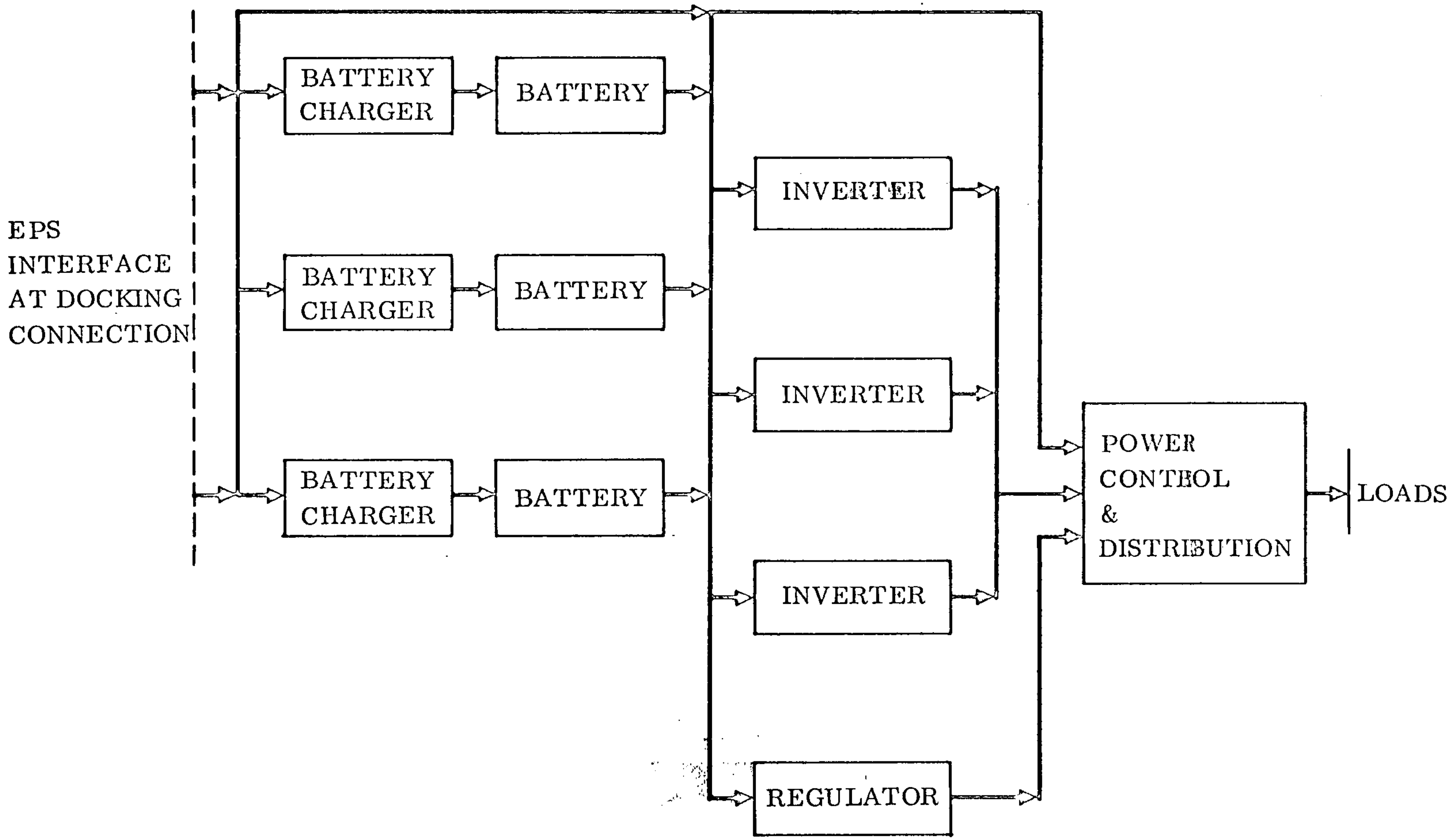

Figure 8-2. Attached Module Electrical Power Subsystem Block Diagram

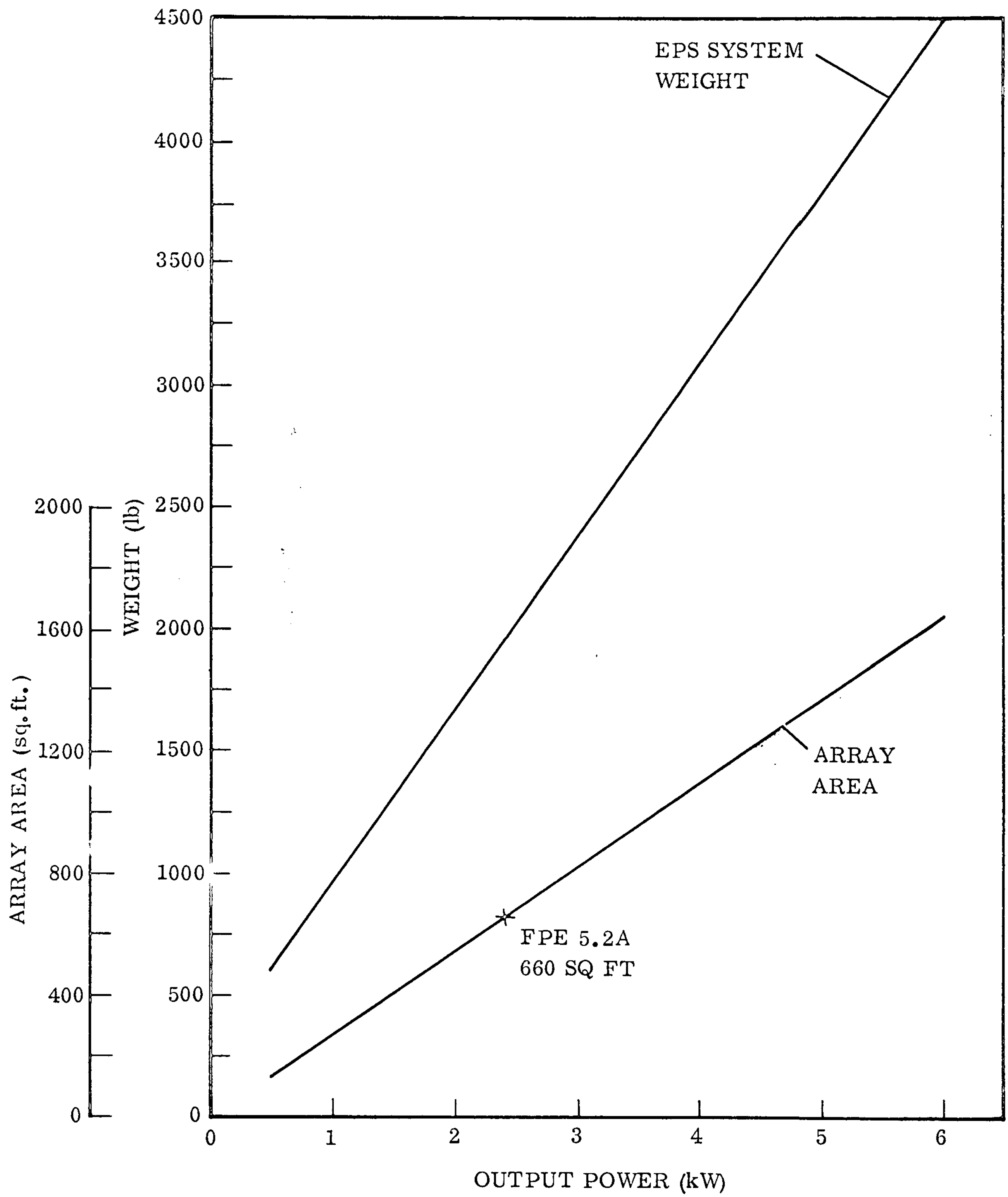

Figure 8-3. Electrical Power Subsystem Scaling Line

the curve. This selection might have been made during the conceptual design had only slightly more pessimistic data been used.

Solar array area is the second parameter plotted in Figure 8-3. It is presented linearly as 275 sq ft per kilowatt. This curve agrees with Table 8-4 for the astronomy modules but not for the fluid physics modules. The curve is not applicable to the fluid physics modules because the array design for these modules is essentially capable of handling the subsystem load only. Power for the experiments is supplied from energy stored in the batteries during the attached periods of operation. The parametric curve should be used only for designs where the entire orbit average load power is to be supplied from the module solar array for long periods of time and not for those cases of short duration missions where stored energy from the space station power source is used as a supplement to the module array power.

Weight data factors were used for preliminary comparisons of various configurations. These factors are:

	Weight	Volume	Area
Solar Array	8.35 watt/lb	50 watts/ft^3	8.35 watts/ft^2
Battery	8.2 W-hr/lb	780 W-hr/ft^3	
Power Conditioning Equipment	30 lb/kW	0.53 ft^3/kW	
Power Distribution Equipment	25 lb/kW	0.5 ft^3/kW	

8.2.3 RECOMMENDED ALTERNATES. There are alternatives to some of the conceptual design selections that need to remain open for consideration into program definition activities.

A continuing task of documenting power requirements for experiments and subsystems will provide useful data for further design refinement. Peak and average power requirements over several pertinent time intervals are required. Time-line studies can be used to maximize the economical and reliable use of available power. Trade-offs of dc versus ac, regulated versus unregulated, and centralized versus distributed power distribution will minimize conditioning and distribution equipment weight and cost.

Alternative battery selections could include the use of Ag-Cd or Ag-Zn batteries replacing the conceptual design selection of Ni-Cd batteries for some of the specific applications requiring energy densities and charge-discharge cycles more suited to these alternates. An important consideration is commonality of battery or cell type and size used in other portions of the total space program. The resulting lower total life cycle costs are the primary reason Ni-Cd batteries were selected for all configurations even though some weight advantages were identified if Ag-Cd or Ag-Zn batteries were to be used for short-term energy storage requirements. Another advantage to the selection of Ni-Cd batteries for the attached module design is that they may be left installed and used during experiment operations after the short-term need of rendezvous and docking has been satisfied.

Battery charger design and battery thermal control for maximum charge and discharge efficiencies are required. Separate chargers for each battery are provided. Further evaluation of the requirements and available techniques may lead to consideration of such alternates as a single charger for all batteries or of integrated charger-battery-regulator modules.

8.3 ELECTRICAL POWER SUBSYSTEM CONCEPT DEVELOPMENT

8.3.1 ALTERNATE CONCEPTS. The electrical power subsystem selection depends upon the experiment module operating mode: free flying or attached. The power for all attached modules experiments is to be supplied from the space station. Only a power distribution system is provided for during normal operation. However, power for subsystem standby and operation from launch to docking is provided by a battery since the energy requirement is relatively small. These requirements have been previously identified in Table 8-2. The power requirements for the experiments and subsystems for the free flying modules have been previously listed in Table 8-1.

Three types of primary power supplied were considered for free flying operation regardless of eventual operating mode

a. Solar cell arrays

b. Fuel cell (H_2-O_2)

c. Secondary batteries

Typical application regimes for these types of power supplies are shown in Figure 8-4. These are approximations only and are subject to a number of other considerations in making a final power source selection. An example of a necessary consideration is that of supplying power during the dark portion of an orbit if a solar array is used. This requirement is usually met by a hybrid battery - solar array approach in which the battery is recharged during each orbit light period by the solar array. Batteries are also often conbimed with fuel cells to meet emergency and peak load requirements.

Table 8-6 contains a summary of power performance on batteries and fuel cells. In comparison a 1 kW solar array- Ni-Cd battery system weighs 960 lb. This weight in secondary batteries would provide electrical energy of 38.4 kW-hr for Ag-Zn type and 17.3 kW-hr for the Ag-Cd electrode system. If the maximum energy required between dockings were less than these capacities, a secondary battery system that is recharged by the space station could be the more efficient approach. The number of

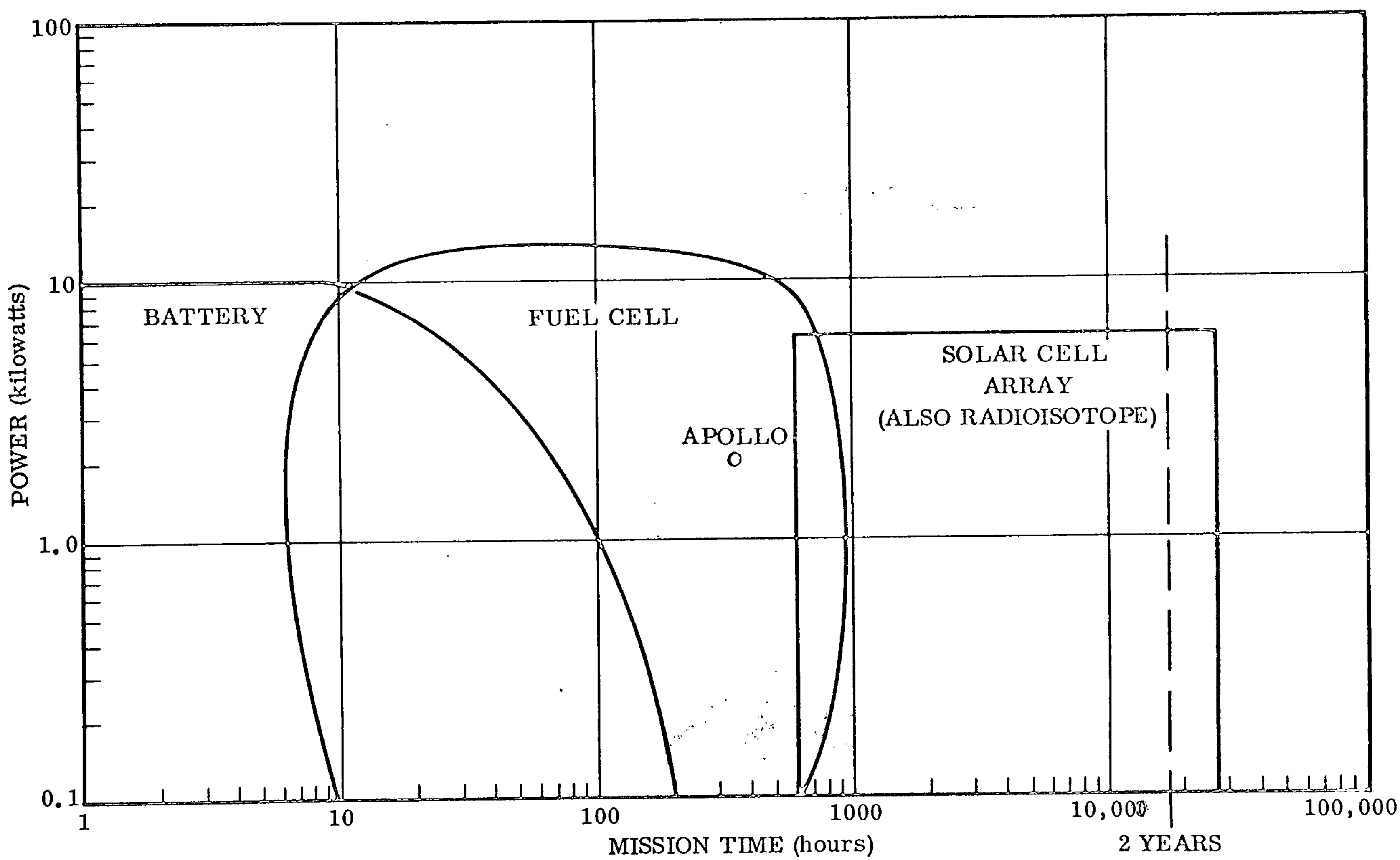

Figure 8-4. Application Regimes of Candidate Power Source Subsystems

Table 8-6. Characteristics of Battery and Fuel Cell Power Sources

BATTERIES	CAPACITY W-hr/lb	MAXIMUM % DEPTH OF DISCH.	CYCLE LIFE
Secondary Nickel-Cadmium	9 to 12	50	@ 25% depth of disch. to 20,000
Secondary Silver-Cadmium	18	50	@ 25% depth of disch. to 10,000
Secondary Silver-Zinc	40	100	20 to 40
Primary Silver-Zinc	70	100	few (nominally one, 2 or 3 possible)

Fuel Cell Weight Equation $W_s = 52\, P_k + 30 + 1.022\, \frac{P_t}{E_a}$

where

W_s = system weight in pounds	E_a = delivered voltage — volts	
P_k = peak power in kW	Cell operating life 90 days	
P_t = energy requirement kW-hr	Fuel (H_2 - O_2)	0.9 lb/kW-hr

recharge cycles required would also have to be considered, particularly for the Ag-Zn type which has a limited recycle capability (see Table 8-6). The salient characteristic of the fuel cell performance is the weight of fuel required for the life of the mission. For example, the power available from 960 lbm. of fuel (i.e., H_2-O_2) is roughly 960 kW-hr. A 960 lbm solar array-Ni-Cd electrical power system can generate 1 kW for 2 years, the life of the batteries, and this is equivalent to 17,500 kW-hr. Therefore, in order to consider a fuel cell for a one kW average requirement, the energy requirement would have to be less than 960 kW-hr. The problem of handling and storage of the cryogenic fuels, the high cost of developing fuel cells and their limited life (i.e., ~ 90 days) are deterrents from using the approach even when performance is competitive.

Radioisotope systems are weight and reliability competitive with solar arrays as indicated on Figure 8-1. However, these systems are not cost competitive. Boretz* in a recent article analyzing various power systems found the solar-array/secondary battery system to have the lowest in-earth-orbit cost for 260 n. mi. altitude and two year mission duration. Extrapolating his data to a 2 kW experiment module yields $600,000 as the cost of a solar-array system and $4,100,000 as the cost of an isotope system. This large ratio in cost justifies exclusion of the radioisotope approach.

*Boretz, Jonathan E., "Large Space Station Power Systems," Journal of Spacecraft and Rockets, Vol. 6, No. 8, August 1969, pp. 929-936.

The above power system concepts were applied to the power system requirements previously given in Tables 8-1 and 8-2. Table 8-7 is a summary of the initial electrical power subsystem selections and rationale. The analyses that led to these results are presented in the following sections.

8.3.2 POWER SYSTEMS ANALYSIS - DETACHED MODULES. The basic system for providing electrical power for long term missions in low earth orbit (270 n. mi.) and 55° inclination is solar arrays, supplemented by secondary batteries for the dark portion of the orbit. A flow diagram of the system is shown in Figure 8-5. A power balance shows that the solar array must provide 2.12 kW power while exposed to the sun so that a continuous load requirement of 1.0 kW can be satisfied. The electrical energy provided by solar radiation per orbit is therefore 2.12 kW-hr, of which 1.57 kW-hr is utilized by the load. The difference, 0.55 kW-hr, which represents 35% of the load, represents power loss in components shown in Figure 8-5. The corresponding capacity of the battery utilized is 0.645 kW-hr. The actual capacity of the secondary battery would be much greater than this because a low depth of discharge is used in order to attain high cycle life.

As shown in Table 8-6 the Ag-Cd type of secondary battery has a much higher capacity than that of the Ni-Cd. However, the Ni-Cd battery has the higher cycle life at the same depth of discharge as given in Table 8-6 and Figure 8-6. As indicated, a slight improvement in the state-of-the-art of Ni-Cd batteries is necessary in order to be able to operate for two years at a 25% depth of discharge. More test data are required to establish the performance of such batteries to a reasonable accuracy.

The charge acceptance characteristics for Ni-Cd and Ag-Cd batteries are shown in Figure 8-5. The Ni-Cd battery is favored at high charge rates (i.e., short charge times) and the Ag-Cd batteries are favored by long charge times.

The selection of batteries for orbiting missions involves the trade-off comparisons of the following parameters:

a. Depth of discharge

b. Altitude and inclination

c. Allowable charge and discharge rates (1/H)

d. Cycle life (number of cycles)

e. Capacity (watt-hr/lbm)

Some standard terms and relationships must be defined before the battery comparison can be continued.

Table 8-7. Power System Selection for Experiment Modules

Function	Selection	Reason
5.1 X-Ray, 5.2A Stellar, 5.3A-1,-2,-3 Solar 5.5 Hi-Energy, 5.9/10 Bio-Plants Independent long term power duty requirements for low earth orbit, 55° (60 min. light, 34 min. dark).	Silicon solar arrays supplemented by Ni-Cd secondary batteries.	Minimum weight and cost system for low earth orbit, 55° inclination, long term duty cycle. Ni-Cd batteries have high cycle life required for 2 years in low earth orbit with 60 min. light, 34 min. dark exposure to solar rays.
5.16-2 Materials Science 5.20-2 Fluid Physics Low energy requirement between dockings, many dockings.	Ag-Cd batteries recharged at space station while docked.	The Ag-Cd batteries have the most efficient combination of capacity (>Ni-Cd), adequate cycle and shelf life for 2 years. An awkward design and configuration problem associated with solar arrays is avoided. Weight, simplicity, reliability and low maintenance favor this approach.
5.20-3 Low Energy requirement between dockings, moderate number of dockings.	Ag-Zn secondary battery recharged from space station.	Large capacity of Ag-Zn battery can be exploited because of relatively low number of recharge cycles.
5.20-4 Independent long term power requirement in low earth orbit plus a few relatively high energy peaks.	Silicon solar arrays supplemented by Ni-Cd batteries for extended duty and secondary Ag-Zn second-battery for high energy peaks.	The high capacity of Ag-Zn secondary battery can be exploited because of the low number of recharge cycles required for high energy peaks.
Attached modules deployment and operating power.	Primary Ag-Zn battery for post launch subsystem power, space station for operating power.	Ag-Zn primary battery has a very high capacity that can be exploited due to the single major energy requirement, and a minor subsequent requirement for position change.

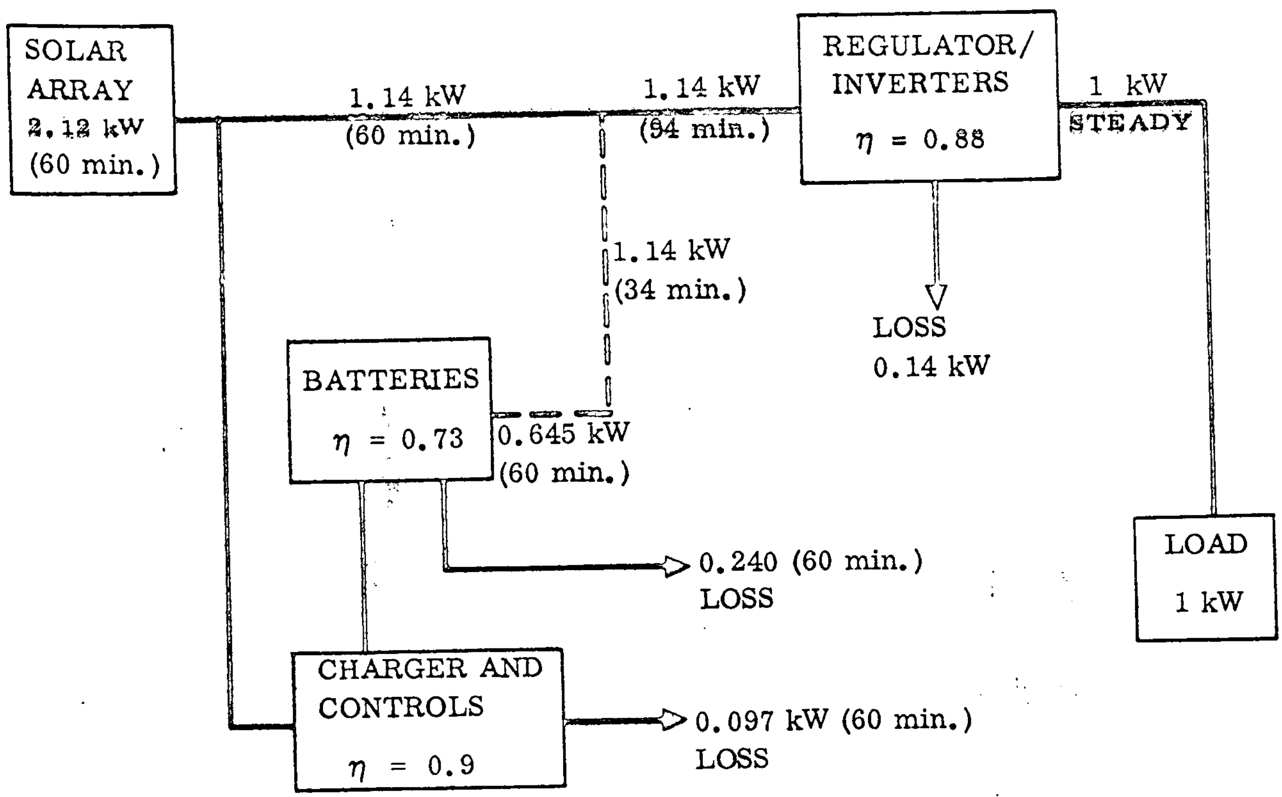

Basic Space Power System for Detached Experiment Modules

270 n. mi., 55° Orbit; 94 min. /Orbit
60 min. light; 34 min. dark

Figure 8-5. Baseline Electric Power Supply

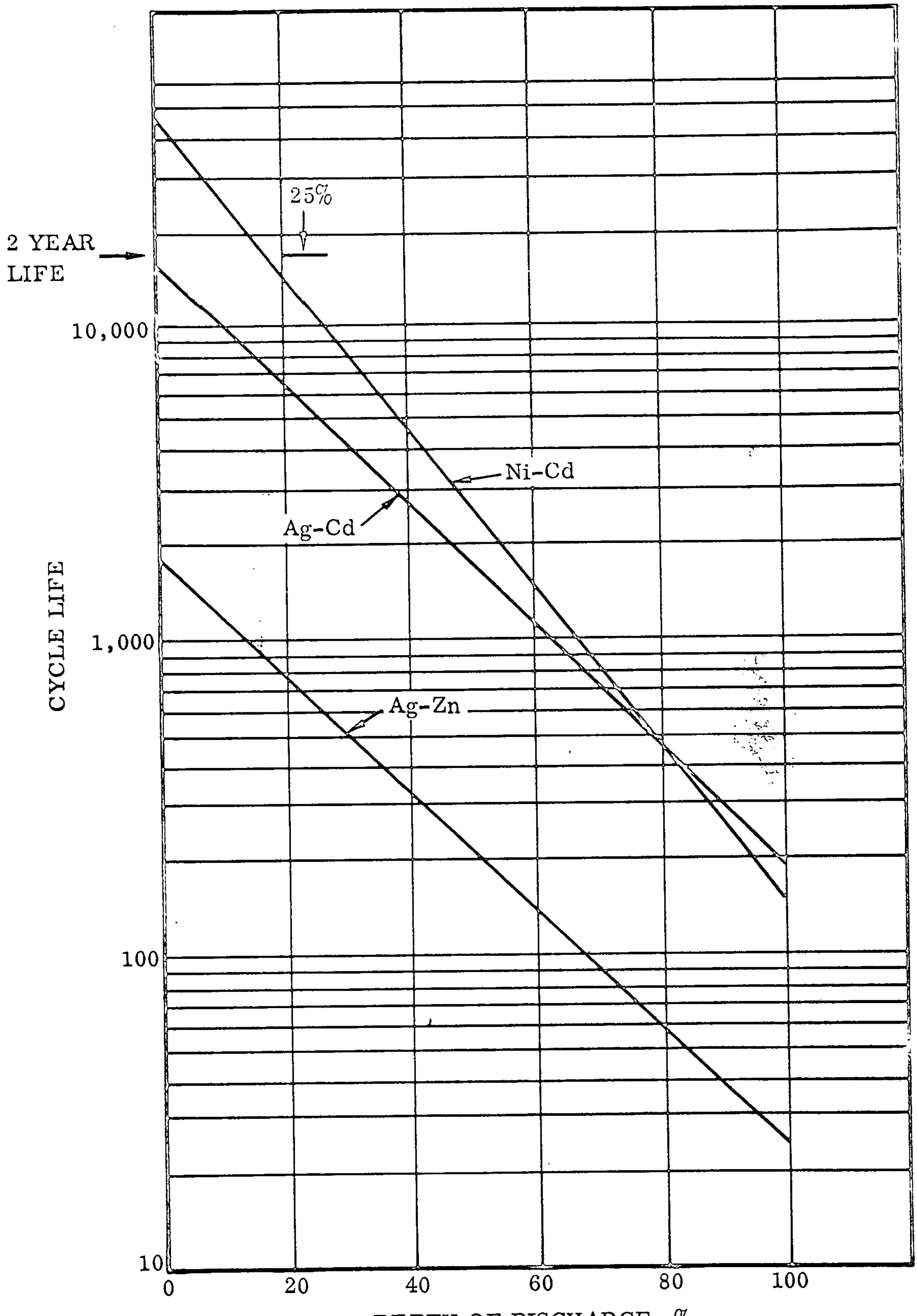

Figure 8-6. Cycle Life of Secondary Batteries

e_b is the battery ampere-hour charge efficiency factor shown in Figure 8-7.

Q is the amount of battery discharge, in ampere-hours

I_{ch} is the orbital average value of the added source current which must be maintained to fully recharge the battery within the available charge time.

H is the average relative charge time in hours

C is the required battery capacity in ampere-hours.

d is the depth of discharge factor

a is the fraction time the solar array is exposed to the sun (see Figure 8-8).

τ is the orbital period in hours (see Figure 8-9).

The following three relationships result from the preceding definition of the terms:

$$e_b = \frac{Q}{a \tau I_{ch}} \tag{1}$$

$$H = \frac{C}{I_{ch}} \tag{2}$$

$$C = Q/d \tag{3}$$

Equation (4) is derived from the preceding three relations:

$$d = e_b \frac{a \tau}{H} \tag{4}$$

Equation (4) together with the data in Figures 8-5 through 8-9 can be used to construct curves of depth of discharge factor versus altitude for maximum dark time orbital inclinations. In Figures 8-10 and 8-11, each solid curve is for a constant charge time. The curves for Ni-Cd and Ag-Cd are not identical because they do not have identical charge acceptance characteristics (i.e., e_b vs. H).

The data in Figures 8-6, 8-8 and 8-9 are used to obtain the constant total life curves shown as dashed lines in Figures 8-10 and 8-11. The curves of Ni-Cd batteries reflect their superior cycle life characteristics.

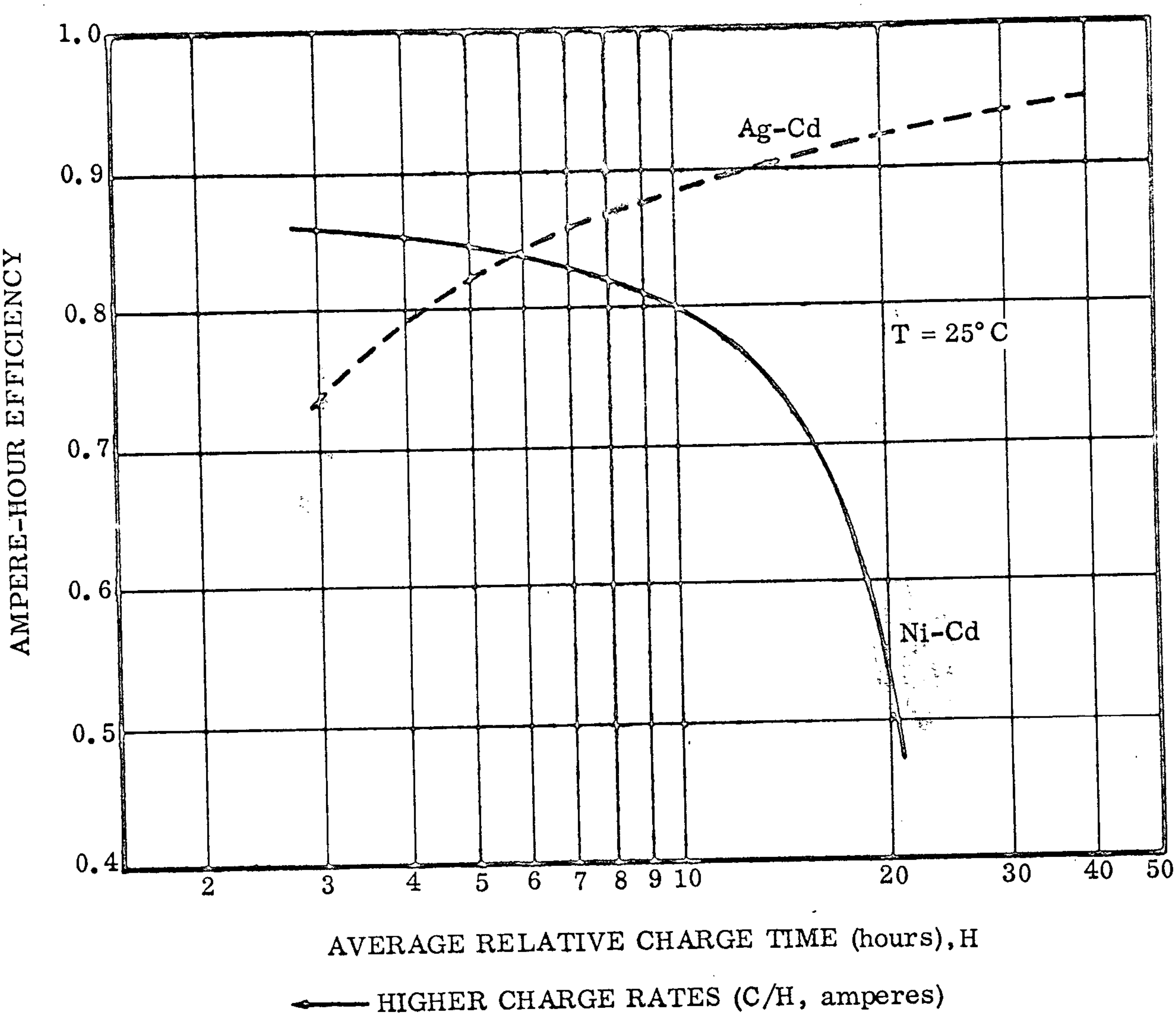

Figure 8-7. Battery Charge Acceptance

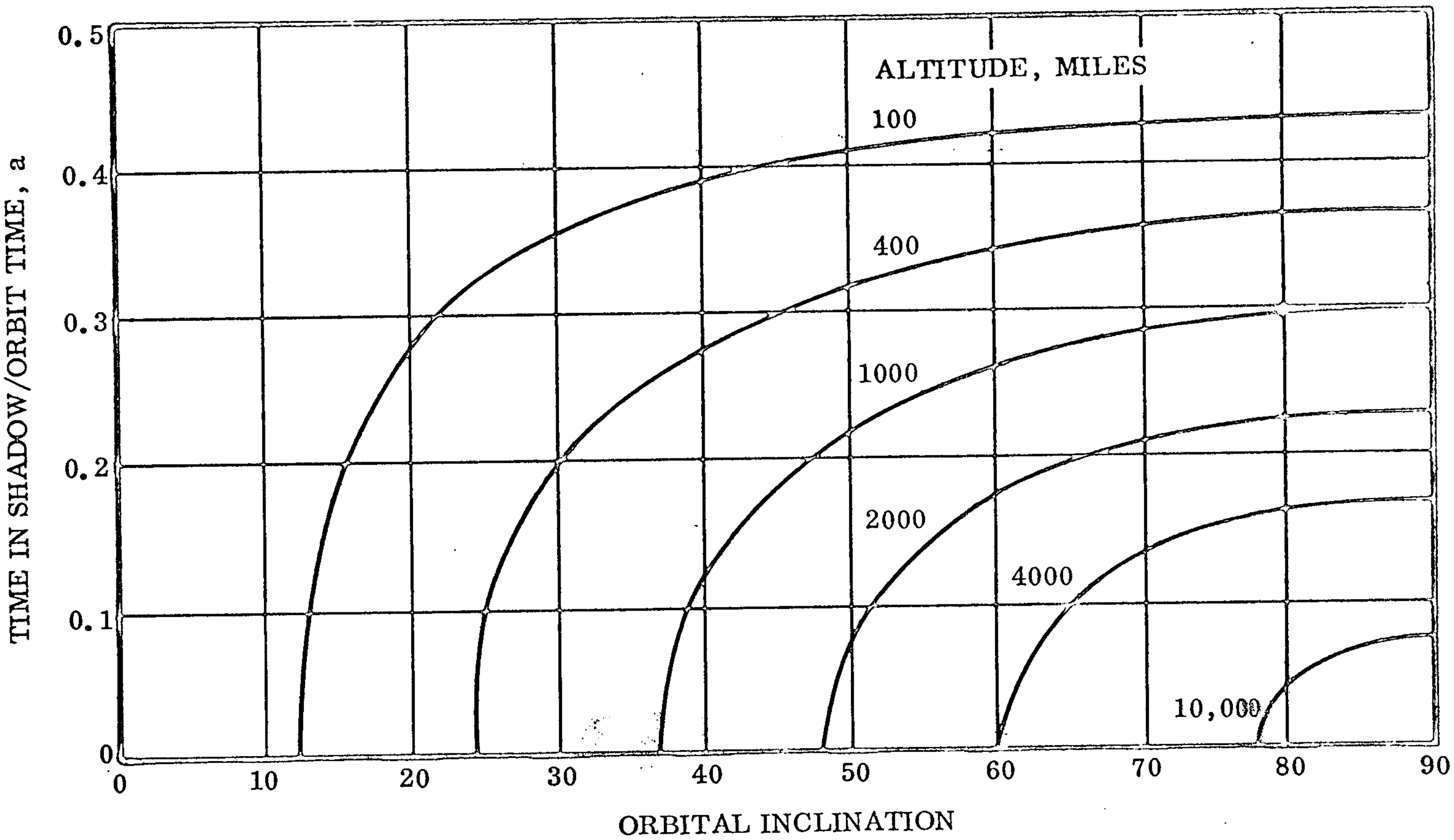

Figure 8-8. Shadow Time in Earth Orbit

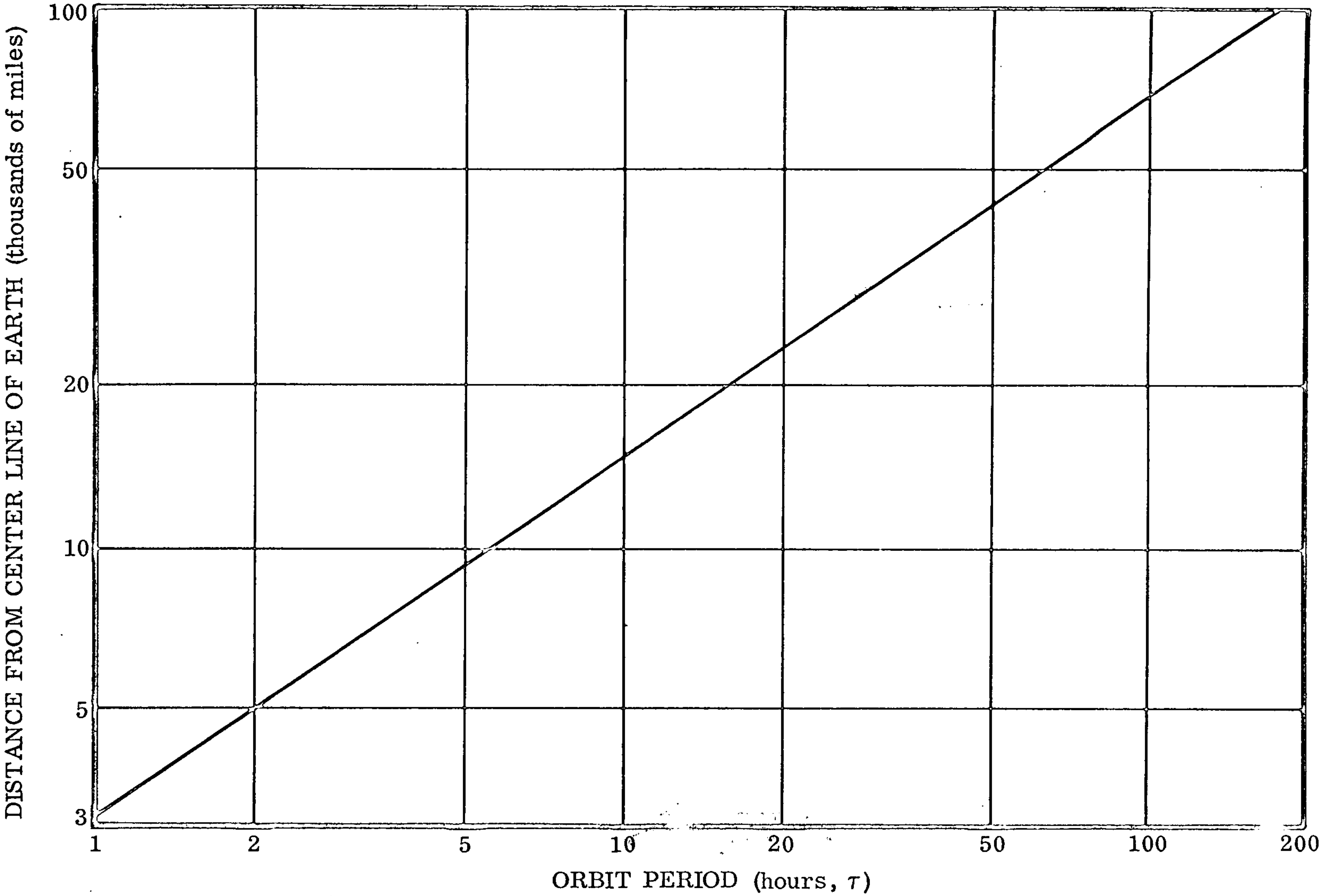

Figure 8-9. Total Time Per Orbit

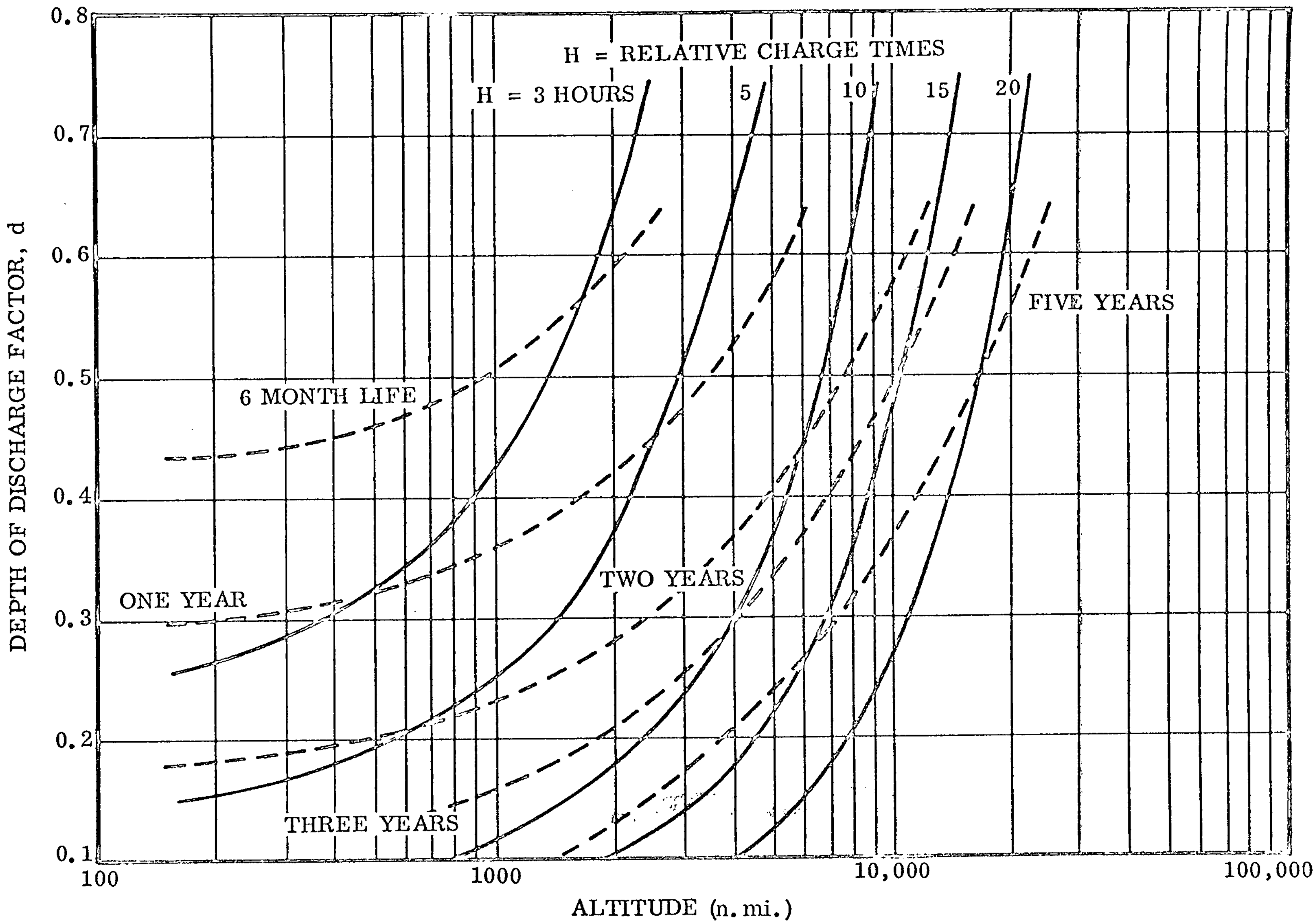

Figure 8-10. Ni-Cd Battery Characteristics

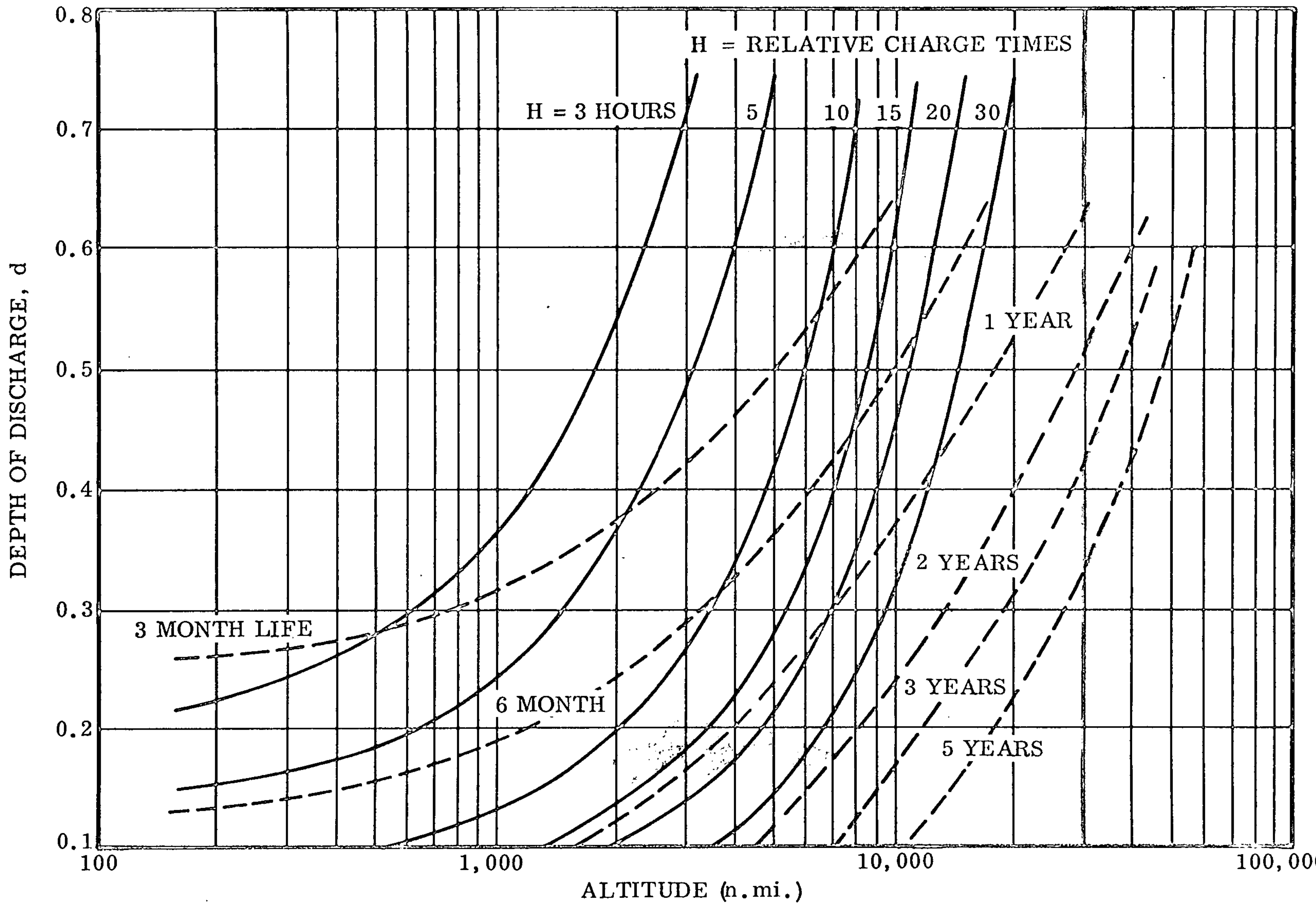

Figure 8-11. Ag-Cd Battery Characteristics

The utility of the curves presented in Figures 8-10 and 8-11 becomes evident by considering three of the limitations imposed on depth of discharge:

a. Total life time requirement

b. Maximum allowable charge rate on battery

c. Maximum allowable depth of discharge for the batteries.

The first limitation is imposed by mission requirements. A wet life limitation independent of cycle life must also be considered. This limitation is 1.5 to 2 years for Ag-Cd batteries, and over five years for Ni-Cd system.

The second limitation depends upon the nature of the charger as well as on the battery. The status of the technology is not clearly defined and improvement for high rates appears to be in progress. For the current analysis, a conservative C/5 rate is used.

A maximum depth of discharge of 0.50 to 0.60 is generally stated in the literature for Ni-Cd and Ag-Cd secondary battery applications. The allowable depth of discharge is determined by the minimum value of the above requirements or criteria.

In order to obtain weight comparisons for Ni-Cd and Ag-Cd batteries in the application represented by Figure 8-5, capacity per unit weight as found in Table 8-6 is used in addition to the foregoing data. The chosen values are 10 watt-hours per pound for Ni-Cd and 18 watt-hours per pound for Ag-Cd. The ratio of weights for Ni-Cd and Ag-Cd batteries as a function of mission life and altitude (maximum dark time at the altitude) is plotted in Figure 8-12. The results show that for longer mission times and low earth orbits, the Ni-Cd battery is far superior in performance for providing power during the dark period due to the high cycle life characteristics. The three and five year curves are dashed and presented for reference only. As pointed out previously, Ag-Cd batteries currently have a wet life of less than two years.

It follows that Ni-Cd type of secondary battery is applicable for the 270 n.mi. orbital application. Projections of battery cycle life show that a two year life at a 25% depth of discharge is a reasonable design point. Figure 8-13 contains some Eagle-Picher data relating Ni-Cd battery temperature to cycle life. Thermal control is obviously a sensitive design factor in achieving long battery life.

The long term steady power requirements of the astronomy modules in low earth orbit are clearly best satisfied by the solar array - Ni-Cd battery power system just described. The power requirements for these systems was presented in Table 8-1.

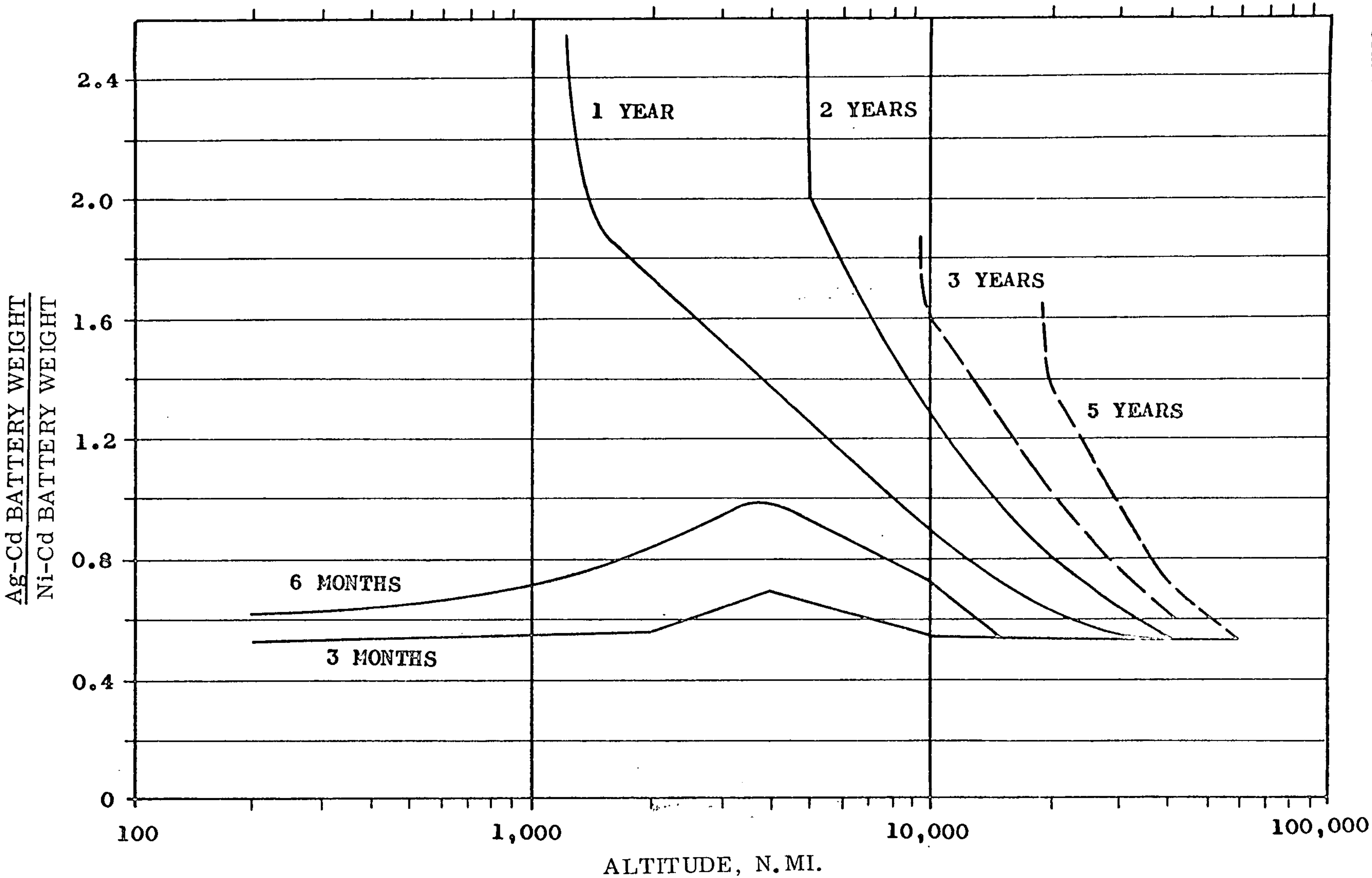

Figure 8-12. Ni-Cd vs Ag-Cd Battery Comparison for Earth Orbital Missions

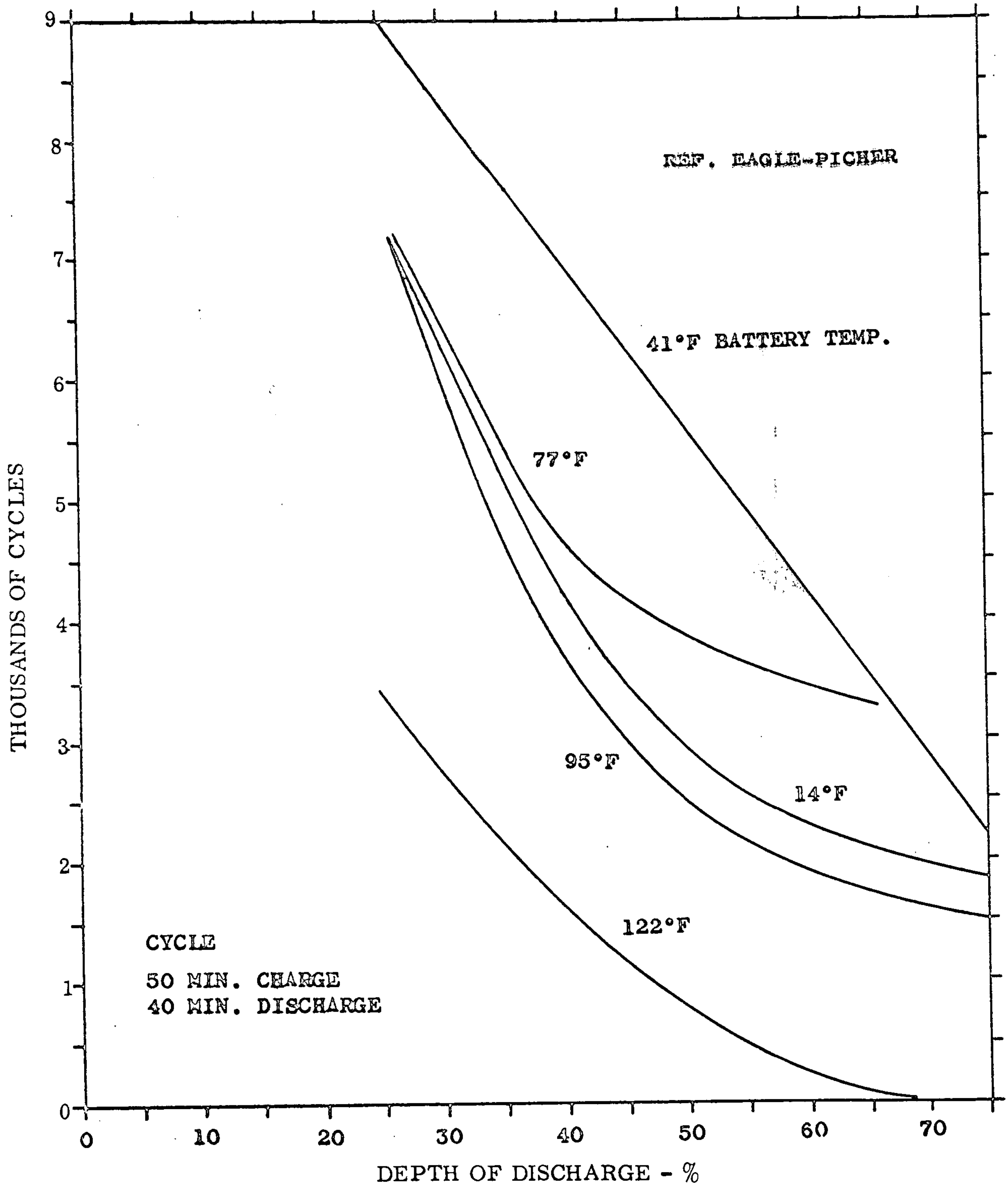

Figure 8-13. Results of Cycle Life Tests, Ni-Cd Batteries

The fuel requirement alone for a fuel cell at a 1 kW level for two years would be approximately 17,500 pounds, an order of magnitude more than the weight of the recommended system. The use of a high capacity secondary battery system (e.g., Ag-Zn) to be charged once a month from the space station would involve 18,000 pounds of battery and would have to be replaced twice a year.

8.3.3 FLUID PHYSICS MODULE ANALYSIS. Power requirements analysis includes study of time variation of load in order to evaluate peak and total energy requirements. Figure 8-14 includes a typical experiment profile. Experiment requirements are combined with subsystem requirements in a module power time line analysis such as shown in Figure 8-14 and 8-15. A summary of power characteristics obtained from the time line charts is presented in Table 8-8. Again, the weight of fuel alone for a fuel cell system would be roughly 5,000 pounds for two years, and this would not be competitive with a solar array-battery system. The weight of a secondary battery power system that is recharged by the space station would also be prohibitive. The three power peaks shown in Figure 8-13 could be serviced by batteries supplementing the solar array-battery system instead of sizing the basic system to meet these loads. These batteries would not be kept up to charge by the solar array but would need recharging at the space station between flights.

The power requirement characteristics for the 5.20-2 module are shown in Table 8-8. Nickel cadmium batteries were used for this mission because the energy requirement between dockings (i.e., 2.59 kW-hr) allowed recharging from the space station with a system that would perform for a two-year period (40 flights/year). Silver zinc batteries were not used because they would have to be resupplied two or three times due to cycle life and wet life limitations. The fuel cell system weight determined from the equation in Table 8-6 was 210 lb. However, this result requires qualification in that it assumed that the same fuel cell would last two years and neglected the long term boil-off of the fuel. These considerations at least double the two year weight requirement, making the fuel cell system noncompetitive with the selected approach.

Silver-zinc batteries were considered for use in 5.20-3 due to the low cycle life requirement (up to 25 flights per year). The wet life of the battery possibly could be extended for a two-year duration by maintaining them at a low temperature between the infrequent flights (three per year). This system was found to weigh about 672 pounds. Nickel-cadmium batteries were retained in the conceptual design for cost and design commonality reasons as well as the fact that no special techniques would be required to meet the requirements. A fuel cell system was estimated to be about 500 pounds for the two year period according to the equation mentioned in connection with FPE 5.20-2. However, after making allowance that the fuel cell would have to be replaced and cryogenic boiloff would be substantial in the period, the working fuel cell system weight associated with the two-year period would exceed that of the recommended secondary battery system.

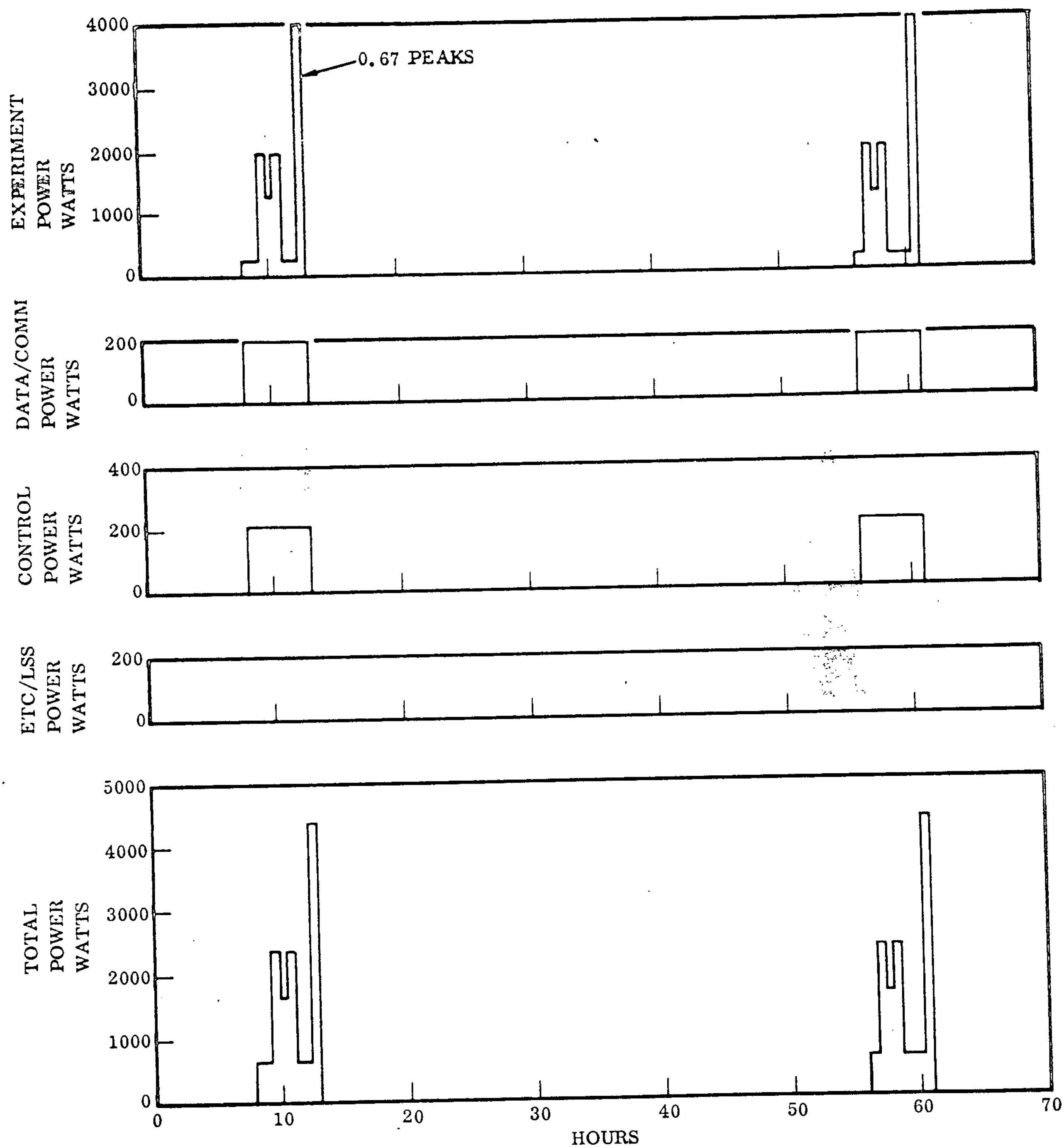

Figure 8-14. Power Time Line — Fluid Physics (Propellant Transfer)

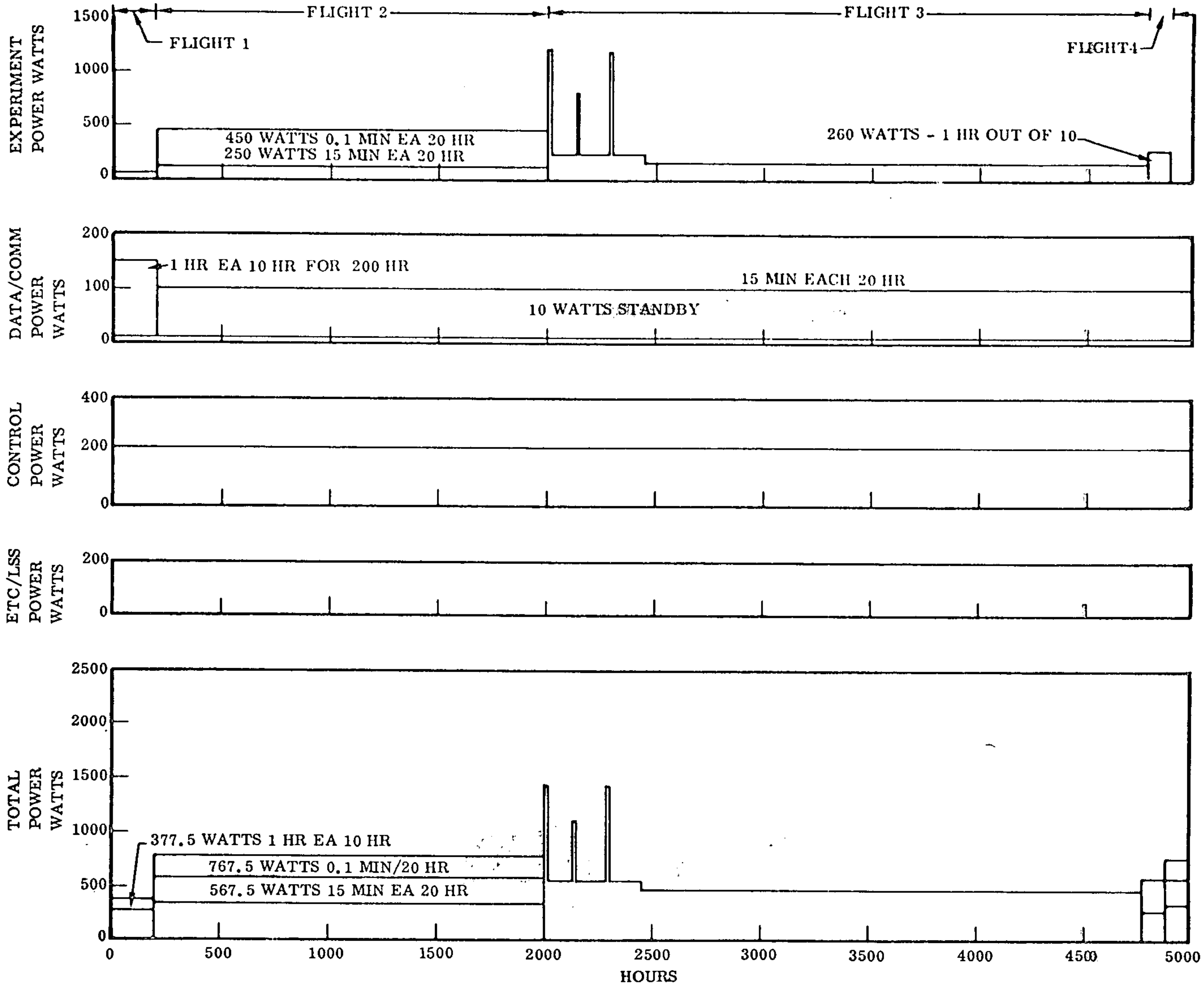

Figure 8-15. Power Time Line — Fluid Physics (Long Term Storage of Propellants)

Table 8-8. FPE No. 5.20-2, -3, -4 (Fluid Physics) Module Power Characteristics Summary

-2 Module

Energy Required for 2 Years = 80.96 kW-hr

Peak Power = 2.243 kW where Energy/Flight = 1.12 kW-hr

Max. Energy/Flight = 2.59 kW-hr

-3 Module

Energy Required for 2 Years = 372.7 kW-hr

Peak Power = 4.943 kW where Energy/Flight = 8.68 kW-hr

Max. Energy/Flight = 21.95 kW-hr

-4 Module

Energy Required for 2 Years = 5332 kW-hr

Peak Power = 2.043 kW where Energy/Flight = 1032.4 kW-hr

Max. Energy/Flight = 1032.4 kW-hr

8.3.4 POWER SYSTEM ANALYSIS — ATTACHED MODULES. These modules derive their power from the space station. The basic module system is a power control and distribution system. A battery in each module provides the power to dock the modules to the station during the launch phase. Each attached module is capable of docking itself. To perform this function, subsystem power is required. An analysis of the requirement results in the following.

System	Power: Active Watts	Power: Standby Watts
G & N	120	0
Telemetry & Command	160	40
Controls	180	100
Gyro	100	75
Propulsion	80	0
	640	215

10 hr. standby, 10 min. docking

This system requirement results in 2256 watt hours of energy required to perform the docking. A safety factor was added raising the requirement to 4200 watt hours. This is provided by Ni-Cd batteries because this is the most economical power source available for this application considering commonality and capability for later use.

The power conditioning equipment required consists of inverters to provide 400 Hz power to the stability and thermal control systems. The other subsystems will operate directly from the battery voltage.

During experiment operation while attached to the spacecraft, the stability and control subsystem and the propulsion/reaction control subsystem have no function to perform. The rf data and command transmission function is no longer required as data transmission is by hardwire connection during attached operations.

The inverters used for the docking phase could continue to supply ac power during attached operation thus reducing the electrical power interface with the space station to one for dc power only. Alternatively, the inverters could be reallocated to experiment power conditioning with required ac power for the thermal control subsystem being supplied from the space station. Another alternative is to remove the inverters from the module and allocate them as support spares for the free-flying modules. Similar alternatives apply to batteries and battery chargers. If the batteries remain in the attached module, they can meet local peak power demands at lower line voltage drops, thus reducing electromagnetic compatibility problems. In addition, they can serve as a source of emergency power in the event the electrical connection to the space station is disrupted.

8.3.5 <u>POWER CONDITIONING AND DISTRIBUTION.</u> The types of power required by the experiments could not be determined from the Blue Book or other sources. They are assumed to use power at +28 Vdc. (This is the experience of the OV1* satellite, which may be described as a miniature common module.)

The data and communications system will use its power as +28 Vdc regulated.

The stability and control system power requirements are for +28 Vdc and +26 Vac, 400 ±0.04 Hz. The system is assumed to use 50% of its total power as dc and 50% as ac.

The thermal control system is assumed to use 100% of its power as +26 Vac, 400 ±4 Hz primarily for pump motors.

The reaction control system will use 100% of its power as unregulated dc.

---

*The OV1 (Orbital Vehicle - 1) is a current USAF/General Dynamics Spacecraft Program.

8-9

Alternatively, a completely centralized power conditioning system could be devised with increased efficiency. This requires definition of load requirements. As an example of a typical situation, the OAO* uses 20% of its power as ac and 80% at five different dc levels.

As noted, the central conditioning systems offer efficiency. The price for this in regards to the common module concept is that each new FPE would require custom design of this equipment. Thus, the concept of a central power conditioning system to supply all of the various voltage levels and frequency which may be required for a particular FPE does not seem to offer any gain as the equipment would have to be changed with the next FPE. The common module concept is best followed if much of the power conditioning is done in a decentralized manner. It is proposed then that the module power conditioning provide regulated +28 Vdc to the experiments, unregulated dc to certain subsystems and +26 Vac, 400 Hz to certain subsystems and that any other voltage or frequency be generated within the using system starting at +28V dc regulated and/or unregulated dc.

8.3.6 SYSTEMS INFLUENCE ON ELECTRICAL POWER SUBSYSTEM DESIGN — Power systems designs and characteristics were developed for numerous common module designs concepts during the custom module development and commonality studies. However, only the final common module definitions are documented in this section.

Experiment growth provisions do not affect the electrical power subsystem except in the case of the driving experiment (i.e., that experiment requiring the largest amount of power). In the CM-1 module this is FPE 5.2A for sizing the power source equipment and FPE 5.20 for sizing the power distribution equipment. As previously noted, power source equipment (solar arrays, batteries) can be expanded modularly. It appears that the power distribution equipment is presently sized to cover the most likely growth in experiment requirements.

An analysis was made which compared electrical power demands of each FPE/common module application versus the design capabilities of each of the common modules. CM-1 was analyzed for the detached operating mode and for the docked mode. The analysis was conducted for the attached operating mode for CM-3 and CM-4. The results of these analyses are plotted in bar graph form in Figures 8-16 through 8-18. The amounts of peak and average power required by experiment equipment and supporting subsystems are identified.

For the CM-1 applications, the supporting subsystems require considerably more power than the experiment equipment, with the ratio of subsystem to experiment average power ranging from 1.5:1 to 5:1. It is evident that the electrical

*Orbiting Astronomical Observatory

FPE	TITLE		TOTAL POWER (kW)
	CM-1 Module	Peak	7.00
		Avg.	2.40
5.1	X-Ray	Peak	1.523
		Avg.	1.147
5.2A	Stellar	Peak	2.583
		Avg.	2.033
5.3A	Solar	Peak	2.483
		Avg.	1.875
5.5	High Energy	Peak	2.093
		Avg.	1.752
5.20-2, -3, -4	Fluid Physics	Peak	4.943
		Avg.	2.188

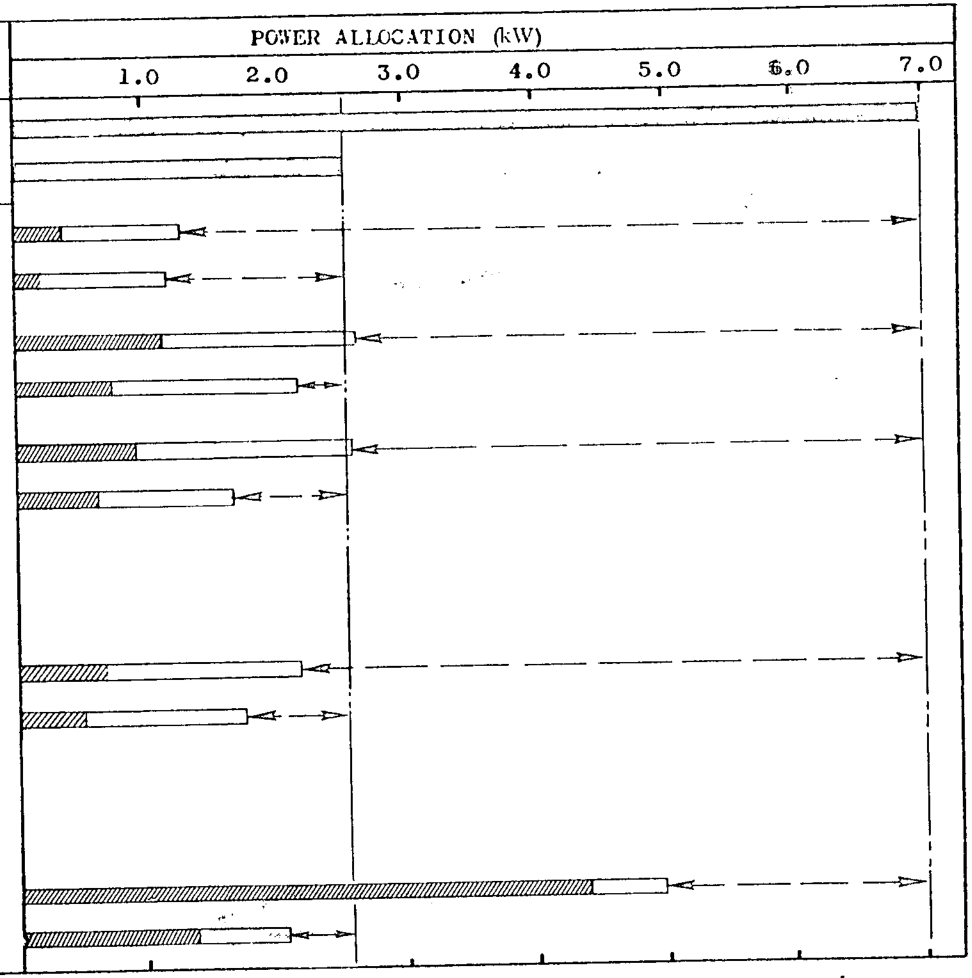

LEGEND: Module Design Capability; Experiment Requirements; Load At Module/SS Interface; Growth Capability; Subsystem Requirements

Figure 8-16. Power Requirements Vs. Module Capabilities (CM-1)

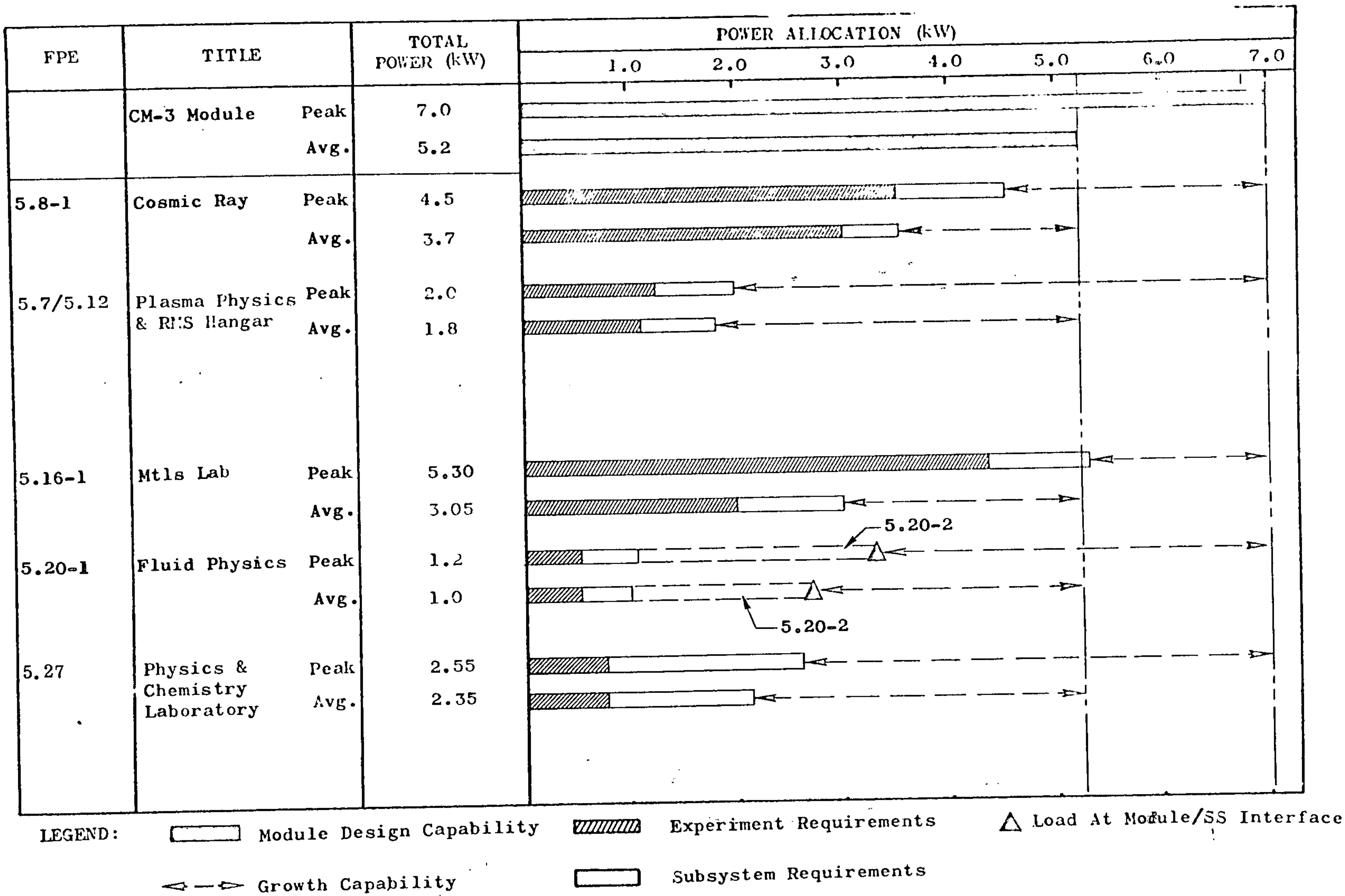

Figure 8-17. Power Requirements Vs. Module Capabilities (CM-3)

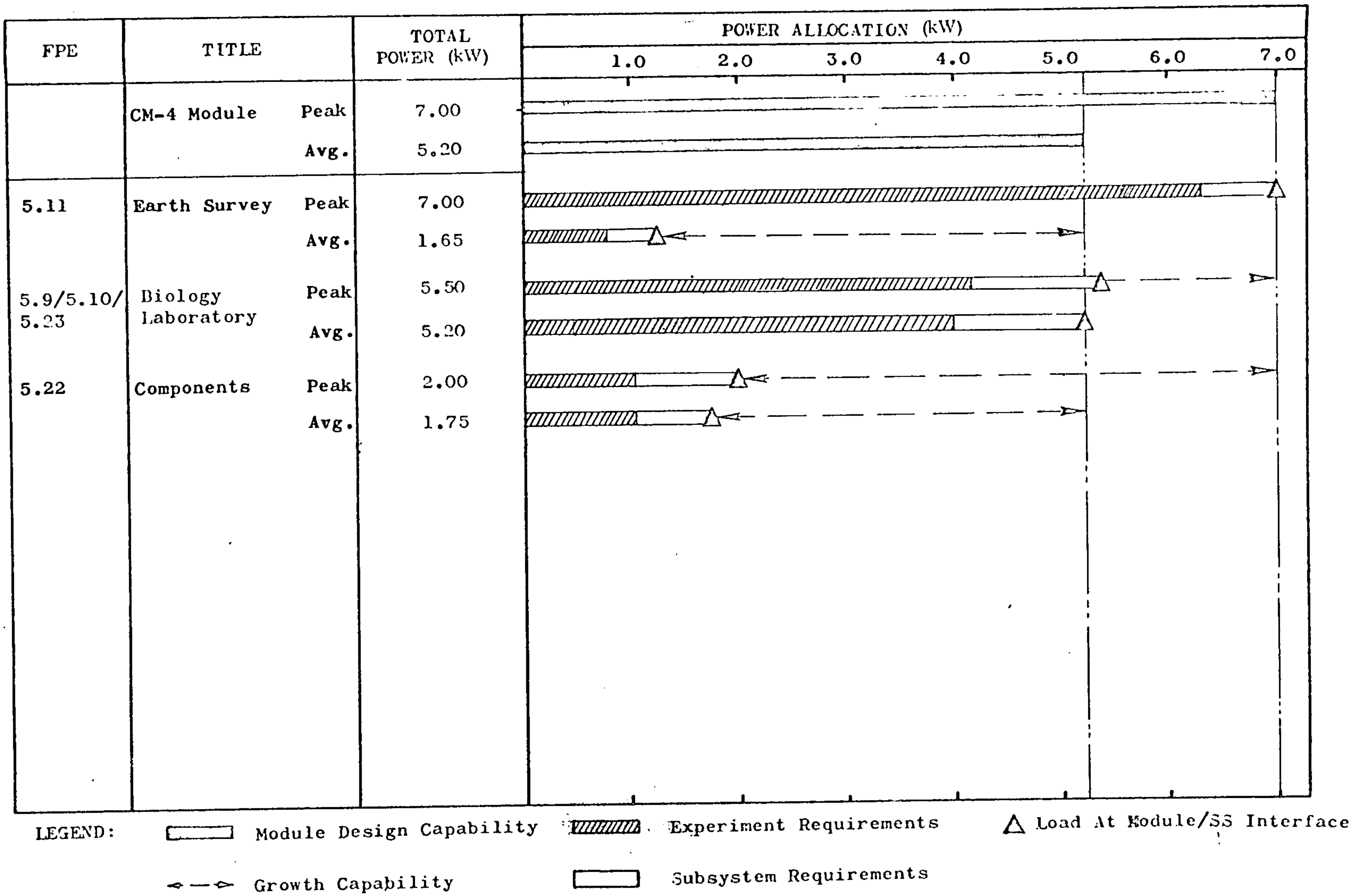

Figure 8-18. Power Requirements Vs. Module Capabilities (CM-4)

power subsystem baseline design could accommodate growth in power demands of about a factor of two for all applications except the FPE 5.2A Stellar Astronomy module, which was the design driver.

For the CM-3 and CM-4 applications, the ratio of subsystem to experiment average power is much lower, in the range of 0.2:1 to 1.5:1.

Since the space station provides the power source for CM-3 and CM-4, the required electrical power system for these modules consists of only the interfacing hardware and the distribution equipment and cabling. In the interest of commonality and interface standardization, the baseline electrical subsystem design is the same for CM-3 and CM-4. Thus, the peak load of 7.0 kW is set by FPE 5.11 (Earth Surveys), and the average power design requirement of 5.2 kW is set by FPE 5.9/10/23. The growth capacity shown in Figures 8-17 and 8-18 indicate a large margin available for growth for all except the design driving FPEs.

The electrical power demands for the CM-1/5.2A, Stellar Astronomy application which govern the CM-1 baseline design capability were analyzed to identify the individual requirements for experiment equipment and supporting subsystems. The results of this analysis are shown in Figure 8-19. The ratio of subsystem to experiment equipment power was 1.7:1, with the Stability and Control Subsystem having the greatest demand at about 50% of the total power.

Any change in experiment power demand would be directly reflected in the total demand, and could have a secondary effect on the thermal control subsystem demand. Data and communication subsystem powers demand is relatively insensitive to changes in data rates where the total bit rate does not exceed 10^6 bps, but would increase if more or higher powered RF links are added. The stability and control subsystem power demand is sensitive to changes in experiment equipment or subsystems mass and location which result in changes in module pitch and yaw plane inertias.

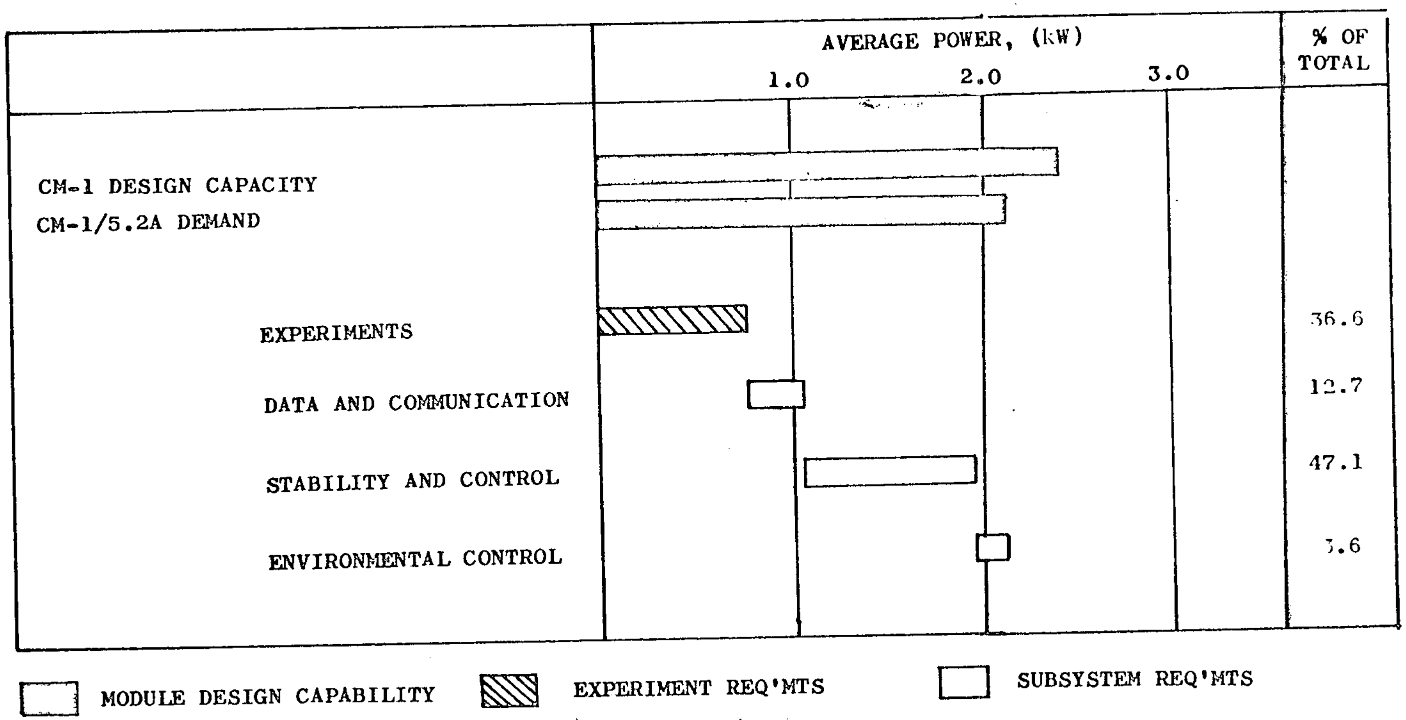

Figure 8-19. CM-1/5.2A Growth Sensitivity - Power

SECTION 9

THERMAL CONTROL SUBSYSTEM

Both active and passive control techniques are employed in current spacecraft to maintain components and the internal environment within acceptable temperature limits. An active control system can be either an open or a closed cycle. In an open cycle a fluid is evaporated and the temperature at which the phase change occurs determines the heat sink. In a closed cycle a fluid loop transports the heat to externally mounted radiators and the radiators reject heat to the space environment. A passive control system requires a judicious selection of internal and external coatings and an optimum wall insulation, in order to reject the exact amount of heat to the space environment.

In general the passive approach is the lightest weight, since very little hardware is employed. This technique is used in many of our satellites such as the OV1 series,* which operate up to a year in space. However, there is very little flexibility in changing components or missions. Any revision of the operating mode or incorporation of different components requires a thermodynamic rebalance and subsequent change of coatings and heat conduction paths. Frequently the vehicles are continuously rotated (2-4 rph) to minimize the time that the external surfaces are exposed to the sun, earth, or deep space and consequently maintain more uniform external surface temperatures.

An open cycle active control system is useful for short missions, such as Apollo. For such missions a few pounds of water provide a significant heat sink in lieu of a heavy radiator and a few problems that accompany the closed cycle.

A closed cycle active control system is employed when mission times are long (months) and there is sufficient variation in operations (heat load, orbits, orientation, etc.). Usually the closed cycle is employed when a higher heat transfer rate is required than available by radiant interchange or conduction.

A heat pipe could be classed as a special form of closed cycle active thermal control system. Problems with the closed cycle are in the form of fluid leakage, fluid toxicity and fluid freeze-up at low loads. Furthermore, fluid circulation requires mechanisms (pumps) and temperature control devices.

---

*OV1 (Orbiting Vehicle-1) is a current USAF/General Dynamics spacecraft program.

9.1 REQUIREMENTS ANALYSIS

Initially the thermal control analysis was directed toward obtaining experiment requirements and support of conceptual designs of individual modules. The analysis consisted of compilation of approximate heat loads with temperature levels and examination of possible means of thermal control with the constraints imposed by the mission and experiment module configuration. Location of experiment and subsystem loads were investigated to determine if radiator (active or passive) surfaces were readily accessible for heat transfer/transport from load-to-radiators. Information from previous studies (References 9-1, 9-2, 9-3) were drawn upon for conceptual design values where applicable. General conclusions were drawn and pertinent ground rules established from the conceptual design approaches to individual modules and experiment requirements to obtain common modules thermal system designs.

9.1.1 EXPERIMENT REQUIREMENTS. The significant experiment requirements affecting thermal control designs are:

a. Whether or not the experiment is attached to space station.

b. Whether the experiment requires a pressurized environment.

c. Level of energy that must be dissipated as heat.

d. Temperature control tolerance that must be maintained.

e. Whether or not experiment components require temperatures at cryogenic levels.

These significant requirements have been derived from Reference 9-4 and are listed in Table 9-1 for each FPE. The environmental atmosphere can be used as a heat transport loop if the experiment can be operated in a pressurized concept. The energy level provides an indication of whether or not an active cooling loop is required. However, specific components because of their combination of size and energy level or particular temperature control can also establish a requirement for an active control loop. Tolerances on the temperature level are also important in selecting a thermal control concept since this establishes the complexity of the thermal control system. A requirement for a cryogenic temperature creates a problem in the overall insulation scheme since this represents a significant heat sink.

9.1.2 MODULE HEAT LOADS. Commonality studies resulted in three module designs, one detached and the other two attached. Primary internal heat loads were derived by a compilation of average power consumption and the assumption that this energy would ultimately be rejected as waste heat from using components. The power requirements along with the experiment groupings for the detached module, CM-1, are listed in Table 9-2.

Table 9-1. Experiment Requirements on Thermal Control Subsystem

FPE	5.1	5.2	5.3	5.5	5.8	5.9/10/23	5.11	5.7/12	5.16	5.20-1	5.20-2,3,4	5.22	5.27
Mode	D	D	D	D	A	A	A	A	A	A	D	A	A
Environment	U	U	U	U	U	P	P	P	P	P	U	P	P
Energy	L	M	L	L	H	L	H	L	M	L	L	M	H
Control	1	1	1	2	1	1	3	3	2	1	1	1	1
Cryogenic	x			x			x		x		x	x	

Mode: A - Attached
D - Detached

Environment: P - Pressurized
U - Unpressurized

Control: 1 - ±5°F
2 - ±50°F
3 - No tolerance

Cryogenics: Blank - No cryogenic temperature required
x - Cryogenic temperature required

Energy: L - <500 watts
M - 500 - 2,000 watts
H - >2,000 watts

Table 9-2. Heat Loads, Detached Module, CM-1

FPE	Experiment Electrical Power (kW)	Subsystem Electrical Power (kW)	Heat Load (Btu/hr)	Radiator Heat Dissipation Req. (Btu/hr-ft^2)
5.1	0.193	1.239	4,890	8.1
5.2A	0.743	1.677	8,250	13.7
5.3A	0.503	1.783	7,800	13.0
5.5	0.510	1.614	7,250	12.1
5.20-2	1.0	0.963	6,700	11.2
5.20-3	1.4	1.103	8,550	14.3
5.20-4	0.165	0.963	3,840	6.4

The power requirements and experiment groupings for the two attached module configurations are listed in Tables 9-3 and 9-4. In all cases the power requirements include the power conditioning losses for experiments and subsystems. Any metabolic heat loads associated with the presence of astronauts in the two attached modules, however, are not included in the module heat loads. It is assumed that these loads will be handled by the space station thermal control system since the space station conditioned air will be that circulated through the experiment module life support system. The heat dissipation requirements for the radiators are based upon the maximum possible amount of side wall integral radiators for each module configuration. These areas are CM-1, 600 square feet, CM-3, 600 square feet, and CM-4, 850 square feet. A more detailed analysis of module heat dissipation capability is presented in Section 9.3.3.

Table 9-3. Heat Loads, Attached Module, CM-3

FPE	Experiment Electrical Power (kW)	Subsystem Electrical Power (kW)	Heat Load (Btu/hr)	Radiator Heat Dissipation Req. (Btu/hr-ft^2)
5.8	3.10	0.60	12,600	21.0
5.7/12	1.28	0.52	6,140	10.2
5.16	2.00	1.05	10,400	17.3
5.20-1	0.40	0.60	3,410	5.7
5.27	1.60	0.75	8,010	13.4

Table 9-4. Heat Loads, Attached Module, CM-4

FPE	Experiment Electrical Power (kW)	Subsystem Electrical Power (kW)	Heat Load (Btu/hr)	Radiator Heat Dissipation Req. (Btu/hr-ft^2)
5.9/10/23	3.95	1.25	17,700	20.9
5.11	1.04	0.61	5,680	6.7
5.22	1.00	0.75	5,970	7.0

9.2 SUMMARY DEFINITION

The concept development studies, commonality, and maintenance analyses resulted in selecting a baseline approach to thermal control.

9.2.1 SELECTED CONCEPT. A completely active thermal control system was selected for both free-flying and attached module concepts. The active thermal control system can be divided into two subsystems: heat absorption and heat dissipation. The heat absorption portion of the system is characterized by the use of "cold plate" heat exchangers to absorb the waste heat from experimental packages and other subsystems. The heat dissipation portion of the system is characterized by the use of low temperature radiators on the external skin of the module to radiate the waste heat to space. The radiator heat transport fluid is Freon 21. The cold plate fluid is water. The two loops are joined together by means of an intercooler heat exchanger at the module pressure shell. The water and Freon pumps and associated controls are actual hardware designs utilized in the Apollo program. The radiators double as the meteoroid protection system. They have a thermal control coating minimizing absorptance of solar radiation and maximizing the emittance of thermal radiation.

Figure 9-1 is a functional flow diagram for the free-flying module. The Freon coolant loop is located outside the pressure shell. There are two systems, each carrying 50% of the total load. Both must be functional during experiment operations. A failure in one system requires shutdown of the experiment and return to the space station for the free-flyer. The standby water evaporation system supplies 24 hours of cooling in the event of a second system failure. The cold plate cabinets housing the critical components have triply redundant cooling loops. Experiment cold plates have a single coolant circuit. Warm Freon is used to prevent the propellant tanks from getting too cold (30°F) in the free-flyer module.

The insulation system chosen for use on the walls of the experiment modules themselves involves the use of layers of high performance radiation shields (superinsulation).

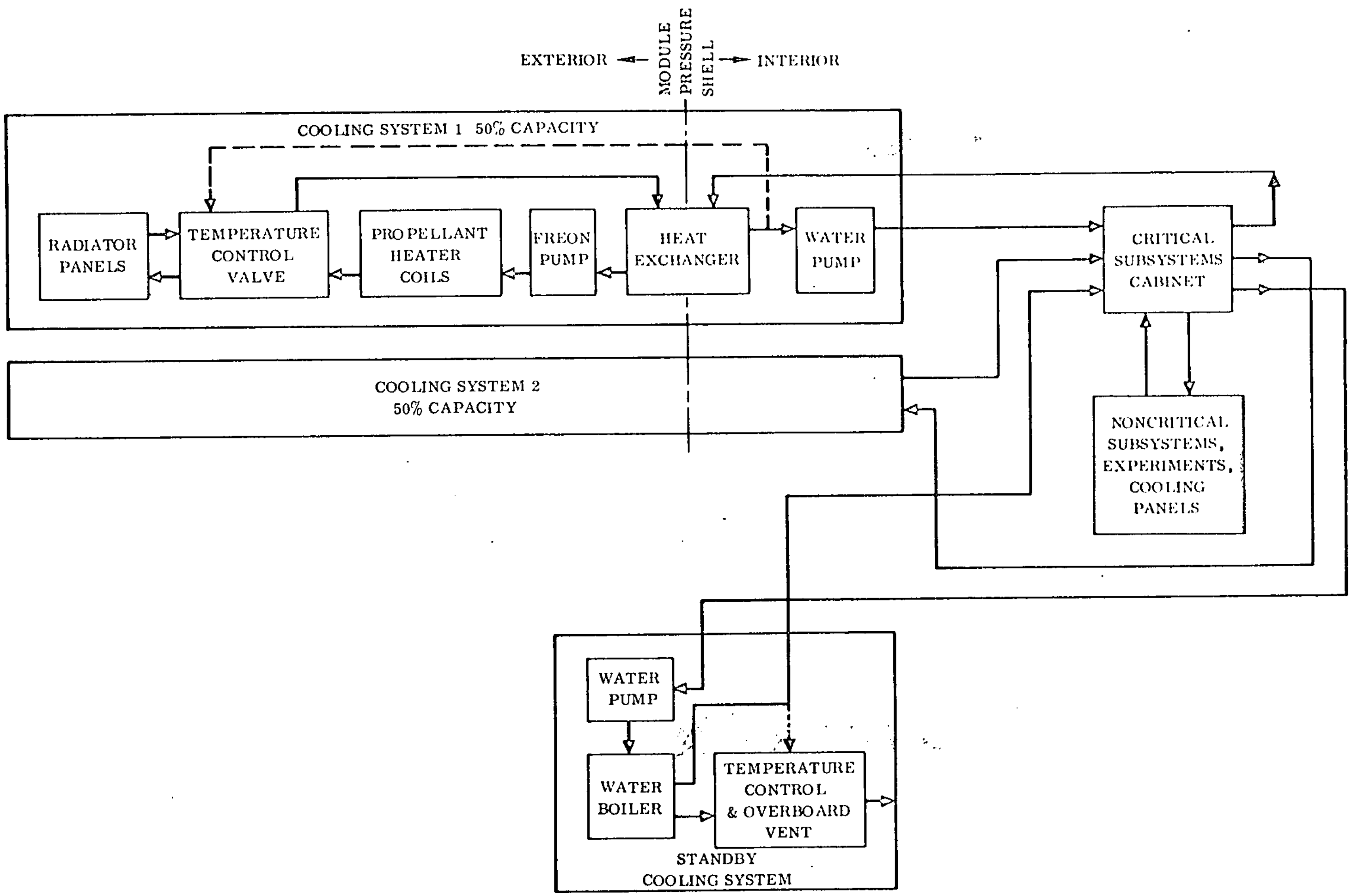

Figure 9-1. Free-Flyer Thermal Control System

The radiators are, with minor exceptions, completely modularized. A typical common radiator panel is shown in Figure 9-2. The use of modular radiator panels will allow the heat rejection subsystem to be tailored to the heat load of each experiment with ease.

Figure 9-3 applies to the attached module. As shown, it is almost identical to that employed on the free-flyer.

The triple redundancy provided allows for safe delivery even after two cooling system failures. This is necessary since critical components in the docking guidance circuit require active cooling.

The major components that make up the thermal control system for both free-flyer and attached modules are shown on Table 9-5. A complete breakdown is given of component weight, volume and electrical power for all experiment module configurations.

9.2.2 THERMAL CONTROL SYSTEM SCALING ANALYSIS. The most useful control system scaling law will include the two critical variables of thermal load and system weight. The analysis of the experiment module thermal control system indicates two separate design areas that can be successfully scaled. These areas are the cold plate heat sinks and associated hardware and the radiator heat rejection system and associated hardware. The cold plate designs consist of three distinct types containing either single, double, or triple flow loops. The multiple flow loop concepts are utilized to provide system redundancy in the event of hardware failure. In addition, the triply redundant cold plates are integral with the mounting cabinets for the electronic boxes and this total structural weight is included as a thermal control system weight penalty. Figure 9-4 is a detailed schematic of the cold plate thermal control system which was analyzed to develop the cold plate scaling equation. It was determined that the form of the scaling equation should be

$$Q_S W_S + Q_D W_D + Q_T W_T$$

where

Q = heat load
W = weight per unit heat dissipation
S = single flow path
D = double flow path
T = triple flow path

Using the system weight summary data from Table 9-5, the heat load data from Figure 9-4, and the guidelines and cold plate design criteria from Section 9.3.2, the cold plate subsystem weight is

$$\text{Weight (pounds)} = 42.2\ Q_S + 222.\ Q_D + 333.Q_T$$

where the heat loads are in kilowatts.

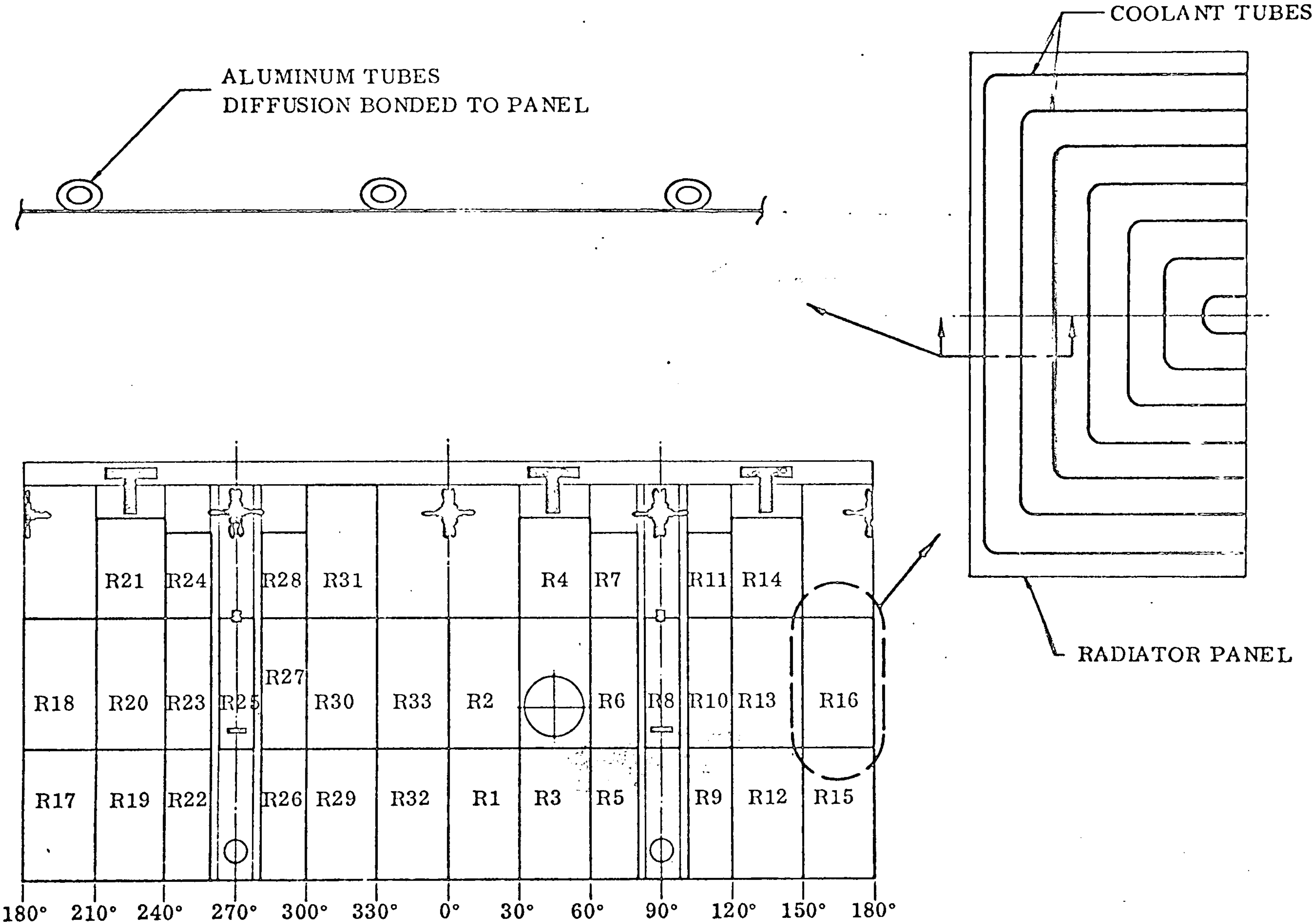

Figure 9-2. CM-1 Radiator Panels Flat Development

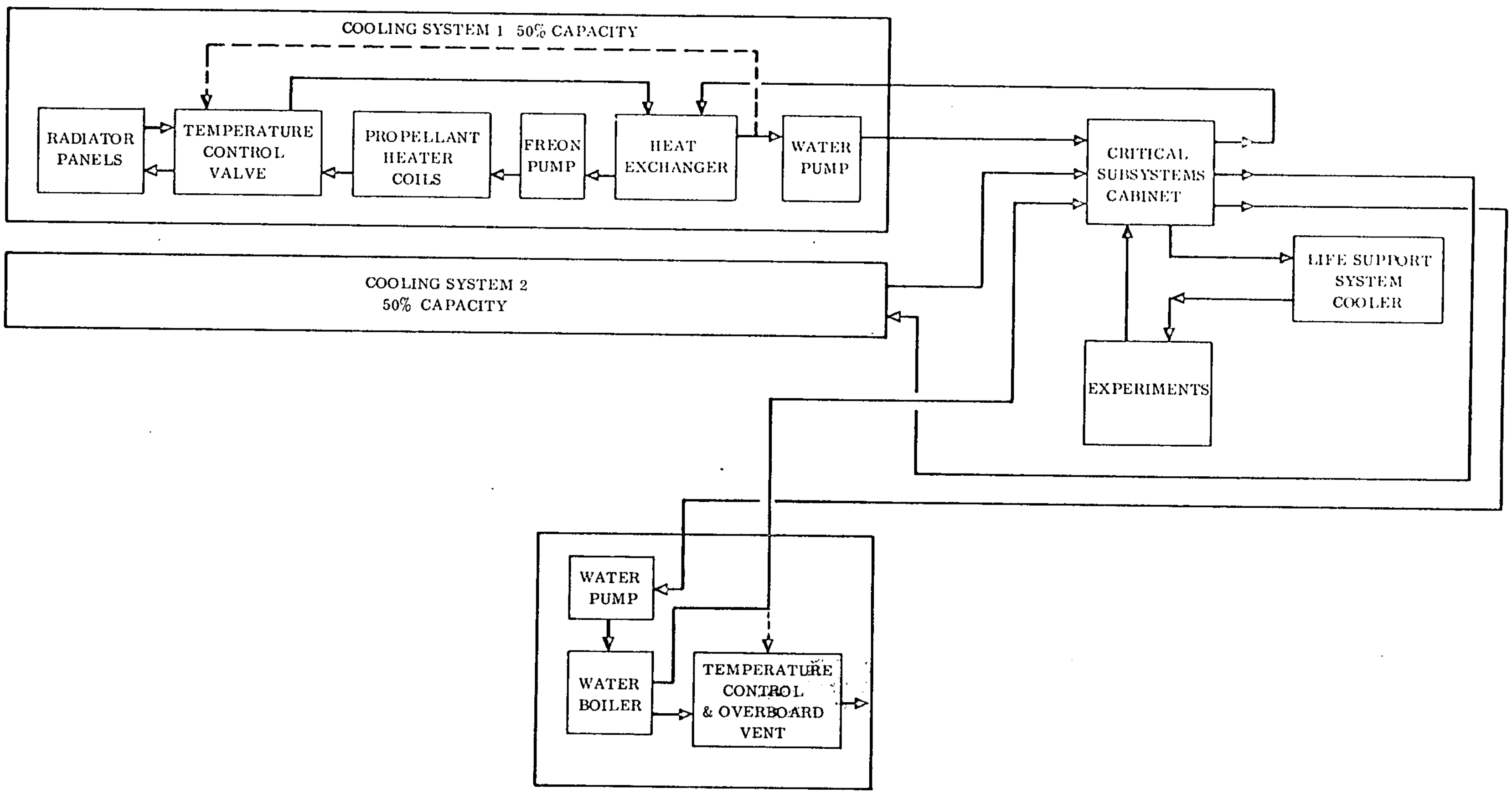

Figure 9-3. Attached Module Thermal Control System

Table 9-5. Thermal Control Systems

Component	Size (Ft^3)	Weight (lb)	Power (Watts)	CM-1 5.1	CM-1 5.2	CM-1 5.3-1	CM-1 5.5	CM-1 5.20	CM-3 5.7/12	CM-3 5.8	CM-3 5.16	CM-3 5.20-1	CM-3 5.27	CM-4 5.9/10/23	CM-4 5.11	CM-4 5.22
Radiator																
600 Ft^2	15.00	600		1	1	1	1	1	1	1	1	1	1			
850 Ft^2	21.30	850												1	1	1
Intercooler	0.50	10		2	2	2	2	2	3	3	3	2	3	3	2	2
Temperature Control (Sensor & Valve)	0.50	20		2	2	2	2	2	3	3	3	2	3	3	2	2
Freon Pump, Motor, Accumulator	0.25	15	25	2	2	2	2	2	2	2	2	2	2	2	2	2
Water Pump, Motor, Accumulator	0.25	15	8	3	3	3	3	3	2	2	2	2	2	2	2	2
Propulsion Heating Coil	0.20	5		2	2	2	2	2								
Evaporator & Reservoir - Standby	0.70	10		1	1	1	1	1	1	1	1	1	1	1	1	1
Temperature Control & Overboard Vent - Standby	0.30	10		1	1	1	1	1	1	1	1	1	1	1	1	1
Fluid Lines	0.50	35		1	1	1	1	1	1	1	1	1	1	1	1	1
Insulation	85.00	120		1	1	1	1	1	1	1	1	1	1	1	1	1
Cold Plate Battery Cabinet	8.00	187		1	1	1	1	1								
Cold Plate SCS Cabinet	10.00	197		1	1	1	1	1								
Cold Plate Communications Cabinet	10.00	197		1	1	1	1	1								
Cold Plate High Temperature Experiment	5.00	14		1	1	1	1	1								
Cold Plate Internal Module Wall	0.50	40		1	1	1	1	1								
Cold Plate Low Temperature Experiment	2.00	11		1	1	1	1	1								
Cold Plate CMG	0.50	3		1	1	1	1	1								
Cold Plate IW	0.05	9		1	1	1	1	1								
Cold Plate Subsystems Cabinet	5.80	117							1	1	1	1	1	1	1	1
Cold Plate Life Support	9.00	36												1		
Weight (lb)						1578			1042	1042	1042	1012	1012	1328	1262	
Size (ft^3)						141.2			111.2	111.3	111.3	110.3	110.3	126.3	116.6	
Power (watts)						74			66	66	66	66	66	66	66	

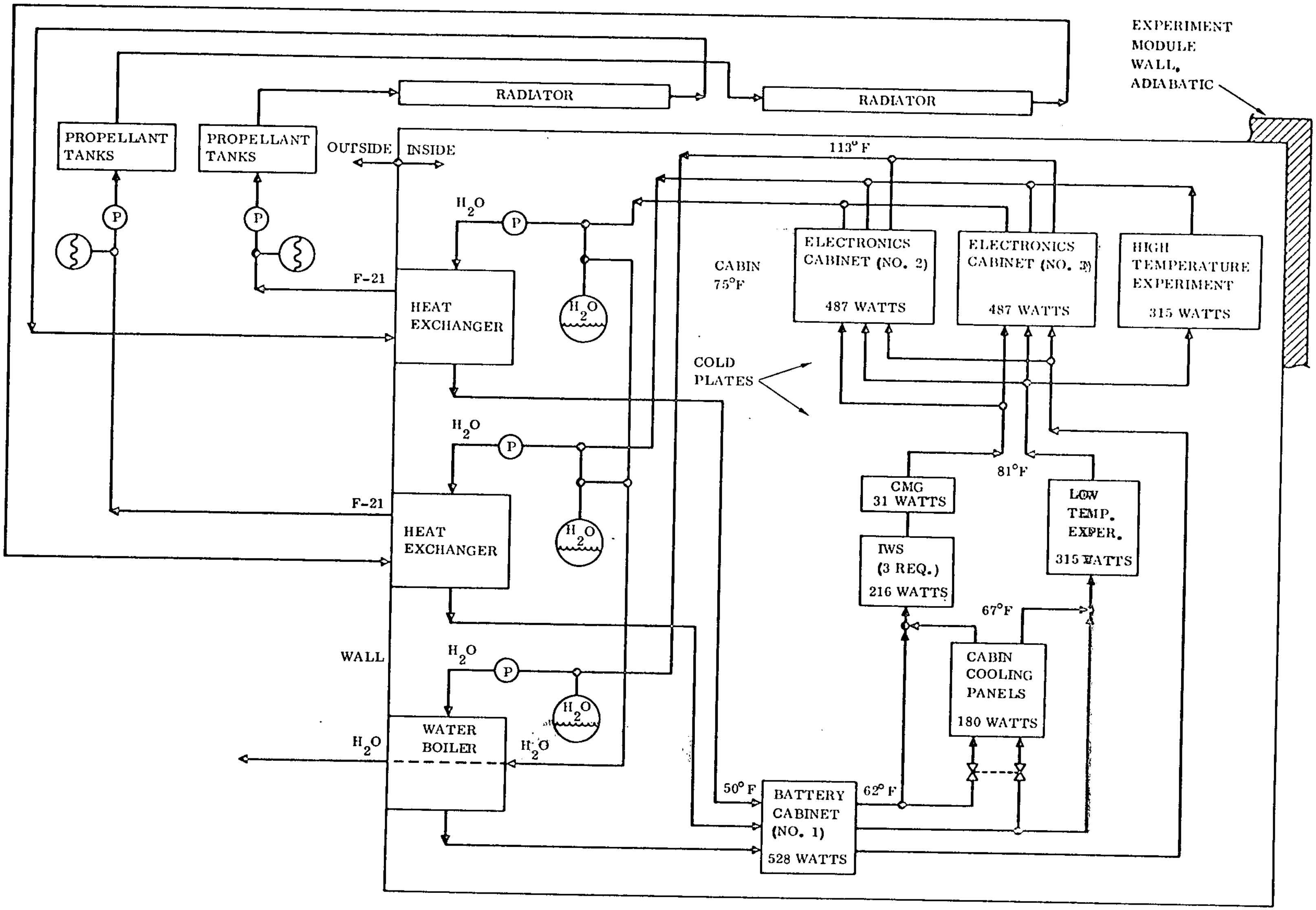

Figure 9-4. Cold Plate Flow Schematic (CM-1/5.2A)

The components included in this weight scaling law include all of the cold plate hardware.

The scaling analysis for the radiator heat rejection part of the subsystem and associated hardware is performed using the technique of linear regression analysis and the data on system definition as contained in Table 9-5. The thermal subsystem designs were made utilizing the configuration of real state of the art hardware as much as possible. In this way a realistic weight scaling law can be constructed with a minimum amount of danger in extrapolation beyond the range of specific point design data. The components included in this scaling analysis include all hardware, including insulation, except the cold plates.

The solution of the normal equations (Reference 9-5) determined the estimator for the regression coefficient to be 239.82. Therefore, as shown on Figure 9-5, the regression line or scaling law for the radiator heat rejection portion of the thermal control subsystem is

$$\text{Weight (pounds)} = 239.82\ Q_{TOTAL}$$

The validity of the regression was reviewed by evaluating the index of determination and the significance of the regression. Both results indicate that the regression line provides a reasonable method for weight/performance scaling for the heat rejection subsystem of the module thermal control system.

A total thermal control system weight scaling equation can be obtained by combining the expressions developed separately for the heat absorption cold plates and the rest of the system hardware usually associated with heat rejection. This total scaling equation is:

$$W_{TOTAL} = 239.82\ Q_{TOTAL} + 42.2\ Q_S + 222.\ Q_D + 333.\ Q_T$$

Weight is in pounds and load is in kilowatts.

9.3 CONCEPT DEVELOPMENT

Various concepts were reviewed to develop an approach to thermal control. In order to establish a basis for these conceptual approaches an analysis was made of the types of components requiring cooling and determining the type of cooling applicable. This analysis provided an insight into the active cooling loop. An analysis was also made on the external coating requirements and wall insulation. Since some experiment sensors require super-cold and cryogenic temperatures, data were generated on characteristics of closed cycle refrigeration systems that produce low temperatures.

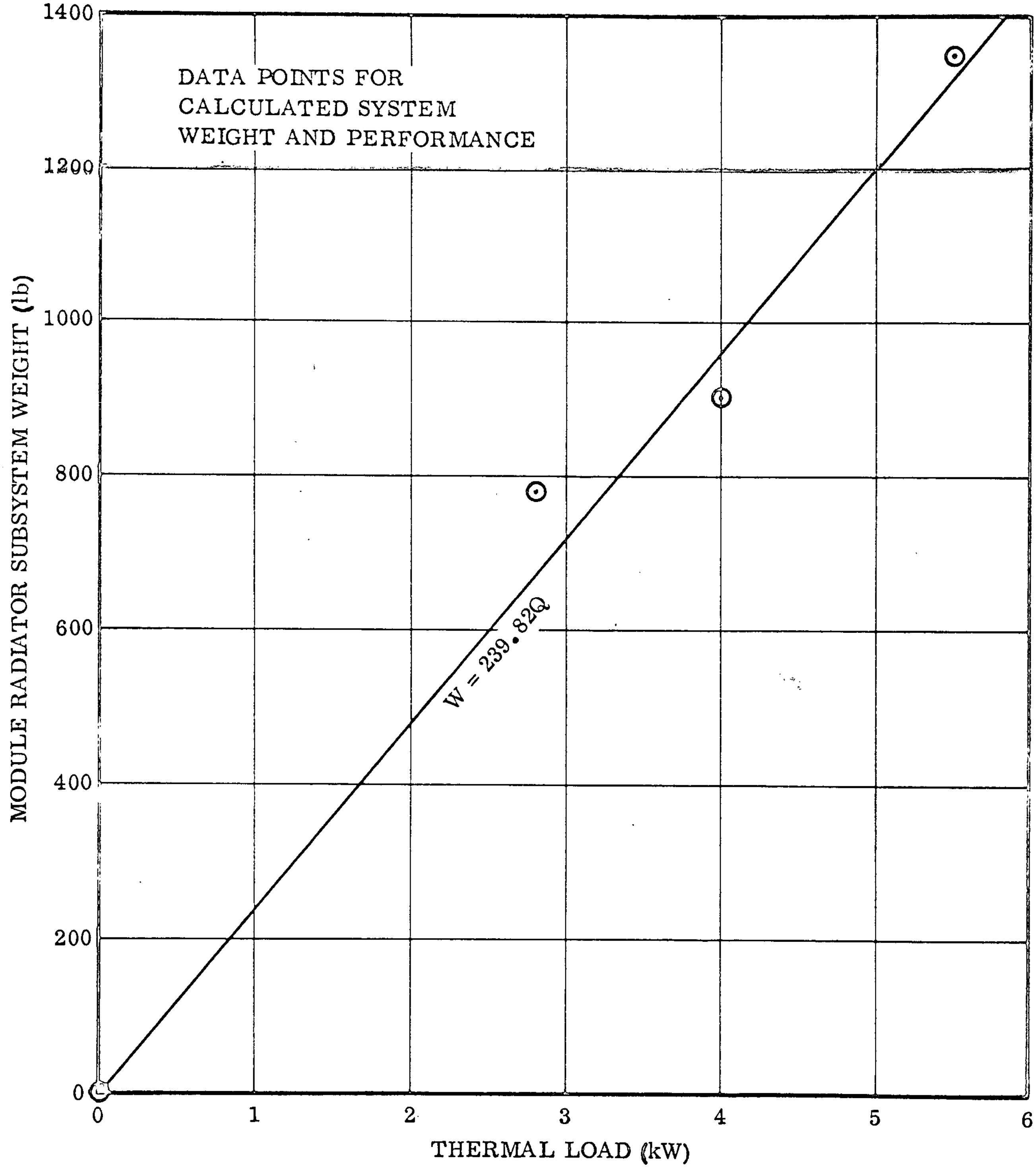

Figure 9-5. Experiment Module Radiator Heat Rejection System Regression Line Scaling Law

A conceptual approach was established to obtain super-cold mirrors for the stellar astronomy experiment to alleviate a temperature tolerance problem.

9.3.1 COMPONENT PASSIVE COOLING ANALYSIS. A survey of subsystem components was made to determine if passive cooling for thermal control is feasible. In order to be passively cooled, the components need to have sufficient area to radiate heat, or dissipate a low quantity of heat. Those components whose operating temperatures would exceed their limit value in order to dissipate heat by radiation require active cooling. Active thermal control loads are centered in the power conditioning system, which requires positive heat removal at relatively low temperature. Another factor is the location of heat producing components relative to possible passive heat sinks. The location must also be compatible with component accessibility for servicing and maintenance. In most cases subsystem components are located in the aft end of the module where the docking end and skirt areas would be used for radiative heat rejection both passively and actively during detached operation.

Table 9-6 lists major subsystem components as originally analyzed, and their heat rejection rates, operating temperature limits, and base mounting areas. Not shown on the table are the experiment required cooling loads. The table shows the required cooling rate for either conduction cooling through the mounting area or radiant cooling through the remaining external area.

The calculated component radiant cooling rate is plotted on Figure 9-6 against temperature limit. As noted in the figure, the interior surface was assumed to be 60°F and to have an emittance of 0.9. A family of curves of available cooling rates vs. temperature for idealized geometric shape factors were also plotted on Figure 9-6. Components with case temperature limits to the left of these curves will require active cooling. Those with limits to the right of the curves can be passively cooled.

The curves of Figure 9-6 were based on radiant energy exchange equation:

$$\frac{Q}{A} = \sigma \epsilon F_A (T_c^4 - T_s^4)$$

where,

T_c = component case temperature

T_s = module interior structure temperature

ϵ = component emittance = structure emittance

F_A = radiation geometric factor

σ = Stefan-Boltzmann constant = 0.1714×10^{-8} Btu/hr-ft^2-°R^4

Table 9-6. Component Cooling Capacity Data

Unit No.	Subsystem	Load (Watts) Avg.	Load (Watts) Max.	Case Temperature °F Min.	Case Temperature °F Max.	Base Conduction Cooling Rate BTU/Hr/Ft^2	Ext. Surface Radiation Cooling Rate BTU/Hr/Ft^2	Base Mounting Area In.^{2}
	Electrical Power							
1	Battery/Charger Modules		530	50°	90°	550	97	518
2	Main Regulator		188	0°	160°	302	130	300
3	Inverter A		56	0°	160°	233	72	74
4	Inverter B		103	0°	160°	372	160	140
	TOTAL							
	Stability and Control							
5	(2) Star Tracker	0	0	-32°	120°			
6	(2) Star Tracker Electronics	30	85	0°	160°	122	44	384
7	Coarse Sun Sensor Elect.	1	1	-20°	160°	12	4	40
8	Panel Sun Sensors	0		-20°	160°	N/A	N/A	N/A
9	(1) Fine Sun Sensor	1	13	-35°	72°	62	16	104
10	Electronics	7	9	0°	160°	34	10	130
11	(1) Inertial Reference Unit	23		-67°	110°	108	28	104
12	(1) Electronics	54		0°	160°	197	89	135
13	(9) CMG/Inertia Unloading Magnet	40	168	-100°	400°	N/A	54	N/A
14	(1) Magnetometer Sensor	2		0°	160°	20	4	50
15	(2) Electronics	6		0°	160°	30	15	100
16	(9) Inertia Wheels	600		0°	90°	13	40	2340
17	Two Gimbal CMG	35		0°	90°	N/A	10	1660
18	(2) Control Computer (1 Redundant)	200		-15°	160°	102	47	1920
	TOTAL							
	Communication & Data							
19	Display	3		0°	160°	10	5	144
20	Intercom	2		0°	160°	33	11	30
21	Test Set	10		0°	160°	35	11	140
22	Cabling	0		N/A	N/A	N/A	N/A	N/A
23	(2) Transmitter Driver	6		0°	160°	35	13	40
24	Hybrid Summer	—		0°	160°	—	—	—
25	Power Amplifier	80		0°	160°	1038	378	24
26	(3) Spectrum Analyzer	30		0°	160°	200	107	48
27	Antenna	0	0	N/A	N/A	N/A	N/A	N/A
28	Diplexer	—		0°	160°	—	—	—
29	Receiver	1.5		0°	160°	26	10	28
30	Decoder	1.0		0°	160°	9	3	57
31	Command Distribution	1.0		0°	160°	12	4	40
32	Digital Control	15		0°	160°	150	48	49
33	Flexible Format Generator	2		0°	160°	16	7	63
34	T.V. Camera	10		0°	160°	103	30	48
35	(12) Remote Data Acquisition	2.4		0°	160°	5	2	300
	Navigation & Guidance							
36	Reflector Target			35°	75°	N/A	N/A	

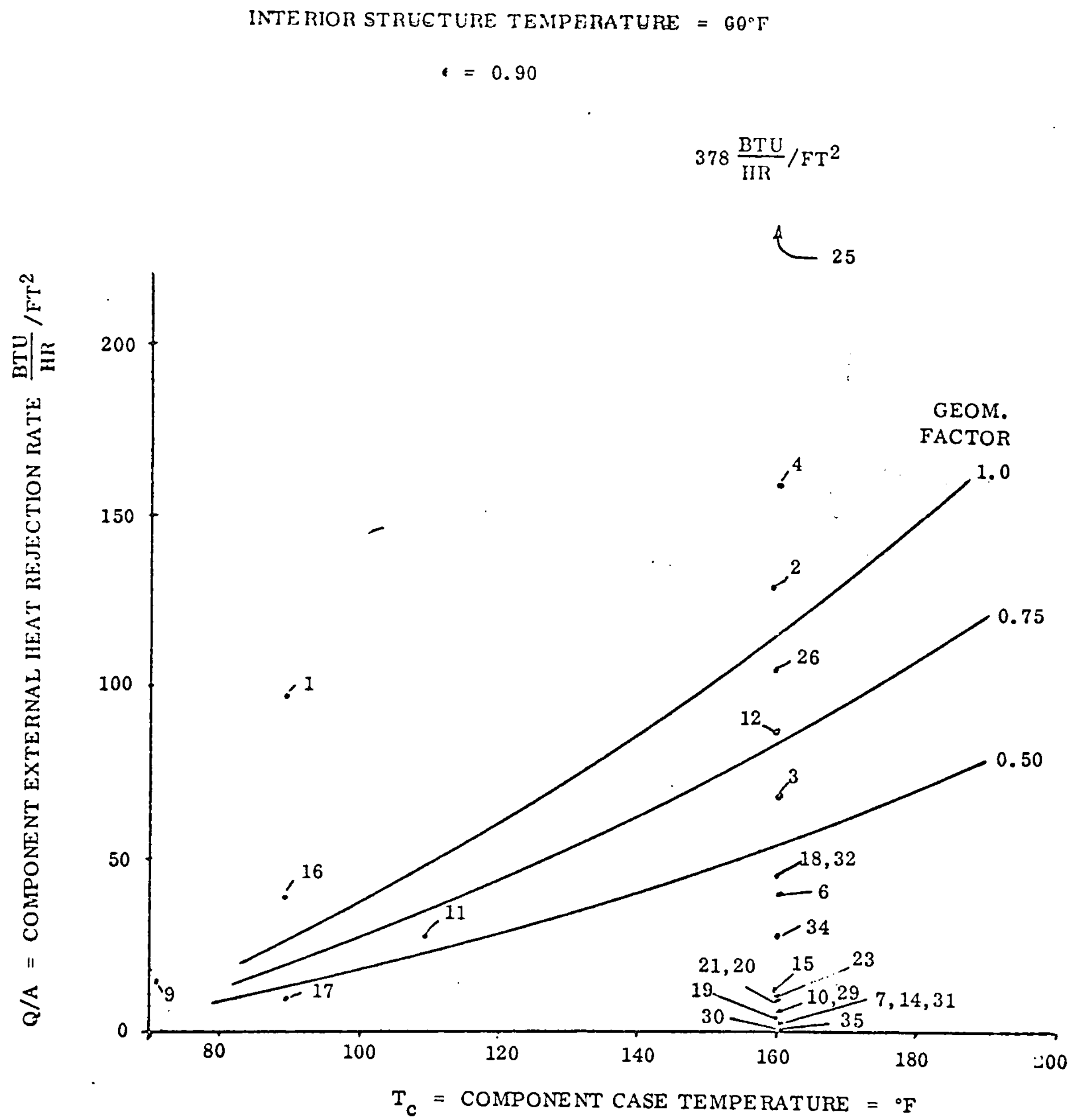

Figure 9-6. Component Case Temperature Vs. Heat Rejection Rate

Since a reasonable geometric factor would be between 0.50 and 0.75, data on Figure 9-6 suggests that the components shown above the 0.75 geometric factor line require active cooling. Thus since a completely passive cooling system is not possible, an active cooling was selected for the experiment modules. A mixed passive-active cooling system was rejected because of the complexity that would ensue since future changes in subsystem or experiment arrangement would require a completely new thermal analysis for each configuration. This requirement would severely limit the versatility of the module designs.

9.3.2 COMPONENT ACTIVE COOLING ANALYSIS. The active component cooling system for the experiment modules was designed to use cold plating for component heat rejection. To assess the general characteristics of the cold plating equipment, the free flying module, CM-1, was utilized to develop a typical component cooling system design. The following criteria were used in the analysis:

a. FPE 5.2A heat loads

b. 100% active module heat rejection

c. Adiabatic module wall

d. 75°F cabin temperature

e. Water as cold plate coolant

f. Cold plate load = 1 watt/in^2

g. Cold plate dry weight:
   Single passage 1 lb/ft^2
   Dual passage 1.75 lb/ft^2
   Triple passage 2.5 lb/ft^2

h. Aluminum cold plate hardware

In addition, the design was based on the failure criteria used in the module study, i.e., (1) any initial failure leaves the module operational excluding experiment functions, and (2) any second failure leaves the module with sufficient function to return to the space station.

9.3.2.1 Subsystem Heat Loads. To determine typical cold plate loads, an updated group of the components listed in the FMECA analysis was reviewed. Components inside the cabin that require cooling belong to the subsystems of (1) stability and control, (2) communications and data management, and (3) electrical power. Components with heat loads of 10 watts or more are listed individually in Table 9-7 by the same number assigned to these components in the FMECA. The table lists the number required, their approximate size, the heat output, temperature requirements, and acceptable location from a subsystem standpoint. Total base area and volume were used in estimating the size and configuration of electronics cabinets to house the components.

Table 9-7. Cold Plate Loads Temperature and Location

Block No.	Item	Total No. Reqd.	Total Base Area (in^2)	Total Volume (ft^3)	Total Steady Load* (watts)	Temperature Control	Temperature Min	Temperature Max	Acceptable Location**
4-2	Star Tracker Electronics	2	144	1.34	40	-	0	160	EC
4-3	IMU	1-2/3	170	0.04	50	90	0	135	EC (rigid mount)
4-4	IMU Elect.	3	405	0.11	30	-	0	160	EC
4-5	SCS Computer	3	900	3.3	50	-	0	160	EC
4-14	CMG	1	1100	13.6	35	90	0	160	On rigid structure
4-15	Inertia Wheels	3	2340	29.5	240	90	0	135	Rigid Orthogonal Surface
4-16	IW Drive Amp	1	300	1.1	120	-	0	135	EC
7-1	TV Camera	1	-	0.1	10	-	0	160	Cabin
7-2/3	Video Tape Recorder	1	-	1.65	100	-	0	160	EC
7-4	R/W Storage Tape	1	-	1.5	100	-	0	160	EC
7-5/6	Rate Data Switching	4	-	0.25	10	-	0	160	EC
7-8	Computer	3	-	0.6	40	-	0	160	EC
7-24	TV Transmitter	1	-	0.2	50	-	0	160	EC
7-25	W.B. Digital Trans.	1	-	0.2	10	-	0	160	EC

*Loads which are on for over about 15 minutes

**EC = Electronics Cabinet

Table 9-7. Cold Plate Loads Temperature and Location (Continued)

Block No.	Item	Total No. Reqd.	Total Base Area (in^2)	(ft^3)	Total Steady Load* (watts)	Temperature			Acceptable Location**
						Control	Min	Max	
7-27	TTSP Trans.	3	-	0.3	15	-	0	160	EC
8-2.1	Batteries (incl. htrs)	3	864	5.0	480	55	50	90	EC
8-2.3	Batt. Charger	3	600	1.38	120	-	0	160	EC
8-2.4	Regulator	1	300	0.87	250	-	0	160	EC
8-2.5	Inverter	3	480	0.84	80	-	0	160	EC
-	Misc. Minor Loads	7	-	-	12	-	0	160	Cabin
-	Misc. Minor Loads	11	-	0.78	16	-	0	160	EC
-	Experiment Loads	-	-	-	350	-	70	90	-
-	Experiment Loads	-	-	-	350	-	0	160	-
	Totals				2558				
	(Totals for EC)			(14.46)	(1561)				

*Loads which are on for over about 15 minutes
**EC = Electronics Cabinet

The loads are generally maximum values, which were assumed to require cooling for 15 minutes or more when they are on. Thus the subsystems average values may be substantially less. Maximum and minimum temperature requirements of the components are also listed. For components with stringent control requirements, the control temperatures are indicated. It was not assumed, however, that the cold plate would provide the precise temperature control since heaters are generally used for this purpose.

The temperature requirements of the 700-watt experiment load was not known. Therefore, this load was assumed to be composed of equal parts of (1) 350 watts of room temperature type components requiring coolant at 70-90°F, and (2) 350 watts of electronic type components requiring 0-160°F.

9.3.2.2 Cold Plate Concept. The general goal of the cold plate system is to maintain component temperatures at their desired values and yet maximize coolant temperatures and thus the efficiency of the space radiator in rejecting heat. The achievement of this goal is enhanced by minimizing parasitic loads to or from the components, generally due to heat transfer from or to the cabin, respectively. Also, the components must be distributed along the fluid circuit according to their temperature requirements. The flow configuration also depends upon the component loads, subject to constraints on physical location. In general, the temperatures shown in Table 9-7 suggest a flow sequence placing the batteries first, the low temperature experiment load and IW's/CMG next, and then the high temperature experiment loads and electronics. Cabin cooling panels to maintain the cabin at about 75°F, require coolant at about 60-70°F and are placed down stream of the batteries.

The number of loops and number of lines running to the cold plate cabinets are based on the system failure rule as applied to the liquid circuits. The system normally operates with both F-21 loops active and the two respective water loops being used to cool internal components. Each F-21/water circuit will pick up approximately half the load. Any failure in either F-21/water loop will leave the remaining loop to cool critical components, with the experiment and associated subsystem loads shut down. In this case, the CMG and IW's will be completely shut down and other loads will be reduced. A second failure of the remaining F-21/water loop will require use of the third water boiler loop to cool critical components.

The triple lines running to the electronics and battery cabinets indicate that these cabinets have the triple loop capability, but not necessarily that each component within has a triply redundant cold plate. Each of the critical subsystem components has back-ups to satisfy the dual failure criteria, and these components may be cooled in various ways so that the critical functions are retained by using any of the three available coolant circuits.

The temperatures on the flow schematic indicate maximum values based on the loads in Table 9-7. At lower loads the components will run at lower temperature but still generally within the acceptable range. The IMU, which must be controlled to 90°F, is located in one of the electronics cabinets receiving coolant at about 85°F. It will have an individual flow control valve and also a heater to provide fine control and added heat if the coolant temperature drops.

9.3.2.2.1 Cabin Cooling Panels. The cabin load is 180 watts, which results primarily from heat losses from components, fluid lines, and cold plated cabinets. These losses were assumed to be 10% of the equipment loads, and the cabin walls were assumed to be adiabatic. In order to absorb this load, radiation panels integral with the cabin wall were designed to operate with a cabin temperature of 75°F and a panel temperature of about 65°F. The rate at which these panels will absorb heat from another surface is given by,

$$q = FA\sigma \left(T_s^4 - T_p^4\right),$$

where

F = the overall interchange factor between panel and surface at T_s
σ = Stefan-Boltzman constant
A = panel area
T_s = surface temperature
T_p = panel temperature (uniform)

The rigorous evaluation of this heat transfer rate is beyond the scope of this analysis; however, an order of magnitude value was computed as follows:

a. Assume a single sink area of 500 ft^2 (panel) at uniform temperature, and the rest of the module interior of about 500 ft^2 at uniform cabin temperature and uniform emissivity.

b. Panel emittance and absorptance = 0.9 (coated).

c. Surrounding emittance and absorptance = 0.2 (aluminum).

d. Each zone has an equal view of itself and the other zone.

For these conditions, F is about 0.15 and the panel at 65°F will absorb the following amounts of heat depending upon cabin temperature:

Cabin Temp (°F)	Watts/Ft^2	Total watts (500 ft^2)
55	-0.41	-205
65	0	0
75	0.45	225
85	0.95	475
95	1.44	720

As indicated, at 75°F the panel should absorb the 180 watt load quoted above and shown in Figure 9-4. The radiation rate to the panel may be improved by locating the panel so that it sees mostly the heat generating components, and coating these component surfaces to increase their emissivities.

The 500 ft^2 area and the assumptions used above were based on using five pressure hull panels of CM-1. The panels are separated by frames spaced 26 inches apart and the resulting effective radiation area would be about 100 ft^2 per panel. The frames are shown in Figure 9-7 as well as a possible coolant tube location and a cross-sectional view of the pressure hull, which must act as a fin to conduct heat to the coolant tube.

The coolant tubes will run peripherally around the module and their spacing depends upon the effectiveness of the wall as a conductive fin. The uniform conductance of this fin is 0.5 Btu/hr-°F per foot of tube length, assuming one dimensional conduction along the fin to the tube. This is comparable to a required radiation design rate of about 2.5 Btu/hr per foot of tube length. Therefore, the fin will cause a temperature drop of 2.5°F along its length, and a single tube located at each frame should be adequate. Fluid convection rates within the tubes should be large compared to the low radiation rates.

When the module is docked to the space station, the cooling panels can be turned off to prevent any possible crew discomfort resulting from the 65°F panels. However, this may not be required. Even though the batteries will not be dissipating heat, the panels will probably not receive 50°F fluid because the performance of the space radiator will be degraded when CM-1 is docked to the space station. Also the air in the module will transfer heat to the panels faster than it can be removed, thus warming the panels to nearly room temperature.

9.3.2.2.2 Cold Plate System Weights. The weights associated with the cold plate system were estimated and are listed in Table 9-8. Tubing weight was based on 1/4-inch O.D, 0.028-inch wall, aluminum. The tubing weight is 0.0235 lb/ft, and the water is 0.0128 lb/ft. The pressure drop in this tube at 70 lb/hr flow is 0.035 psi/ft. Allowing for bends, fittings, and about 5 psi drop in each of the three cabinets, water pumps of the 30 to 50 psi variety will be acceptable.

The CMG and inertia wheels are individually cold plated and insulated. The loads are fairly low and so are the resulting weights. The actual experiment cold plate configurations were not defined in this study, and therefore general weight penalties were applied to arrive at the weights shown.

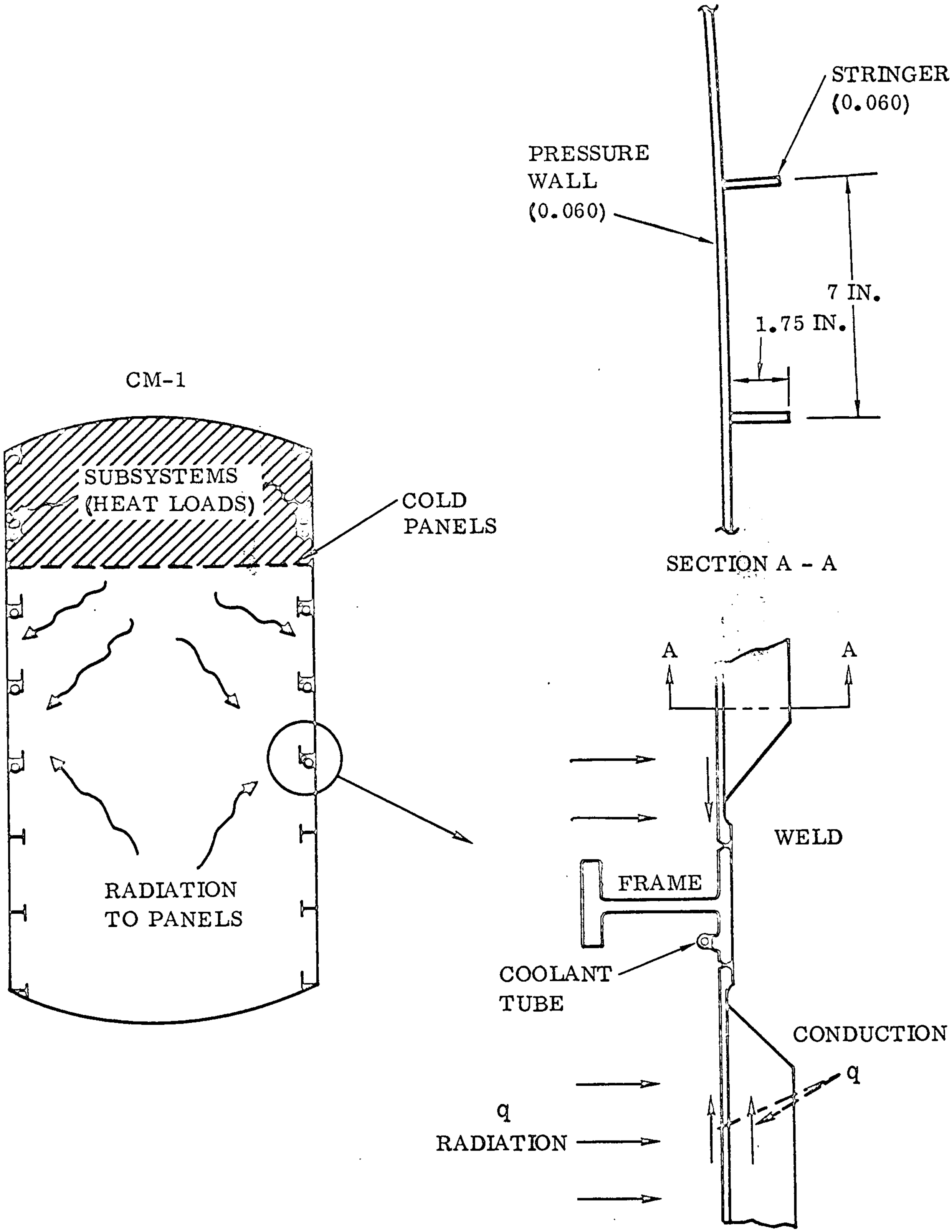

Figure 9-7. Cabin Cooling Panel Configuration

Table 9-8. Cold Plate System Weight Summary

Item	Weight (lb)		
	Dry	Fluid	Total
1. Tubing (460 ft, 1/4 in. Al.), Insulation & Structure Associated with Tubing (Includes Tubing for Radiation Panels)	34	6	40
2. Inertia Wheel Cold Plate & Insulation (3 reqd.)	9	negl.	9
3. CMG Cold Plate & Insulation	3	negl.	3
4. Low Temperature Experiments	10	1	11
5. High Temperature Experiments	13	1	14
6. Battery Cabinet No. 1 Cold Plate & Insulation	35	2	37
7. Electronic Cabinet No. 2 Cold Plate & Insulation	45	2	47
8. Electronic Cabinet No. 3 Cold Plate & Insulation	45	2	47
Total	194	14	208
Cabinet Structural Weight for Items 6, 7 & 8, not required solely for cold plate function	450		450

Three cold plate cabinets, Figure 9-8, are provided to support the components, contain cold plated mounting surfaces, and insulate these black boxes so that they don't reject heat to the cabin. One cabinet generally houses the batteries and associated EPS components. Two cabinets are for the higher temperature electronic components. Some of the experiment components might be placed in these two cabinets as there is some extra available space.

9.3.3 HEAT REJECTION SYSTEM ANALYSIS. A study was conducted to determine the capability of an experiment module to reject the heat generated within the module by the use of low temperature space radiators. This heat rejection would be accomplished without resorting to the use of the space station heat rejection system. To perform the study, a worst and best case analysis was conducted to bracket the extent of the experiment module radiator heat rejection capability. The maximum orbital heating case (maximum solar exposure) and minimum orbital heating case (maximum earth shadow time) were run to obtain the extremes of space radiator heating environment. Since it is not possible to determine, at this time, precisely the spatial orientation of an attached experiment module under exact experimental

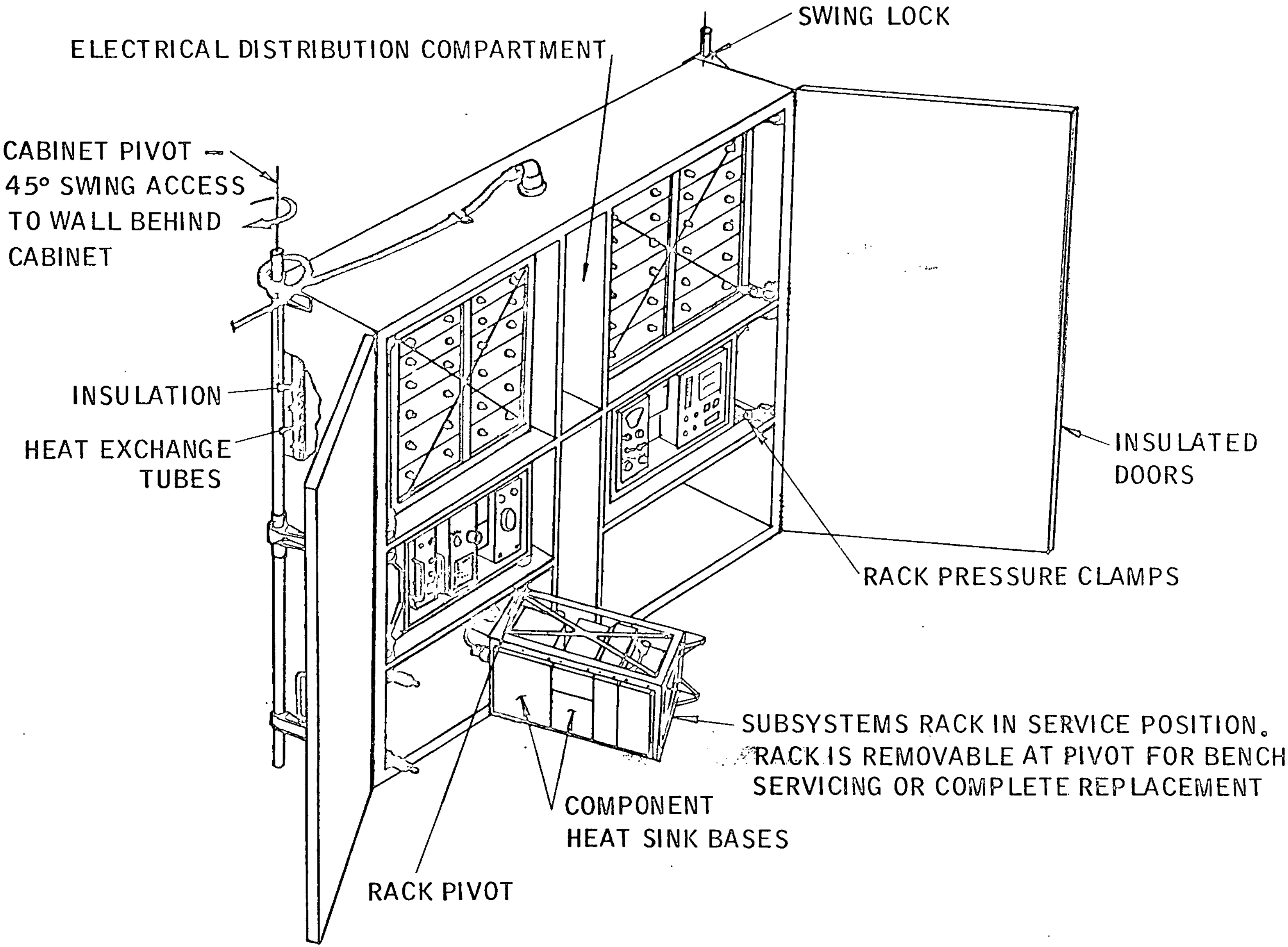

Figure 9-8. Thermally Controlled Subsystems Cabinet

conditions, both earth and solar orientations were analyzed for axial and perpendicular vehicle reference systems. Vehicle orbital inclinations of 55° and 28.5° were utilized. The specific cases analyzed are shown as follows:

Case 1. Maximum shadow; 55° orbit; axis pointed to earth.

Case 2. Maximum sun; 55° orbit; axis pointed to earth.

Case 3. Maximum shadow; 55° orbit; axis pointed to sun.

Case 4. Maximum sun; 55° orbit; axis to sun.

Case 5. Maximum shadow; 55° orbit; broadside to sun.

Case 6. Maximum sun; 55° orbit; broadside to sun.

Case 7. Maximum shadow; 55° orbit; broadside to earth.

Case 8. Maximum sun; 55° orbit; broadside to earth.

Case 9. Maximum shadow; 28.5° orbit; broadside to sun.

Case 10. Maximum sun; 28.5° orbit; broadside to sun.

The calculation scheme for the analysis was to determine the net amount of energy that would leave the module radiators taking into account radiator performance, absorbed solar and earth emitted radiation, and radiative interference with space station and other module hardware. The absorbed radiant energy calculations were made using the Convair Space Vehicle Radiant Energy Program (Reference 9-6). The low temperature radiator structure completely surrounds the surface of the module cylindrical structure. The properties of the thermal control coatings on the radiator were assumed to be solar absorptance (α) = 0.35 and thermal emittance (ϵ) = 0.85. These values account for the expected degradation of the surface properties due to the aging expected over the long mission time. The radiator surface absorbed heat flux was then obtained for a complete orbit for all areas around the module for the mission cases described above.

The energy transferred from the module radiator surface in the ideal case is a function of the surface temperature (T) and the surface emittance (ϵ) and is given by

$$\frac{Q_R}{A} = \sigma \epsilon T_R^4$$

where

$\frac{Q_R}{A}$ = Heat flux

σ = Stefan-Boltzmann constant

For the radiator energy dissipation calculation, the radiator base equilibrium temperature is calculated from the average of the fluid inlet temperature (552°R) and fluid outlet temperature (500°R) minus 15°R (Reference 9-7). The average ideal radiative heat dissipation for these ground rules is 99.4 Btu/hr-ft^2. To account for the fact that a space radiator is not 100% effective, the performance is degraded as a function of the radiator fin effectiveness. The basic subsystem module radiator designs (Reference 9-7) were designed for a maximum heat load fin effectiveness of 0.9. Since the radiator requirements are very similar to those of the experiment module, a fin effectiveness of 0.9 was used to degrade the theoretical radiator performance. The predicted net radiation heat transfer for the experiment module radiators is given on Figures 9-9 to 9-18 for the ten orbital cases discussed above. The data are shown for a complete orbit and present average, maximum section, and minimum section heat flux for each condition. The integrated average values for the maximum, minimum, and average section in each case are shown on the bar chart of Figure 9-19. Here it can be seen that Cases 2, 6, and 8, which are all full sun orbits, have average radiator heat rejection rates of less than 30 Btu/hr-ft^2 and in addition show a very wide variation in maximum and minimum net heat flux for areas around the vehicle.

The integration of the experiment module with a space station poses another problem which must be analyzed before the complete module radiator performance can be predicted. Radiant interaction of docked modules and space station must be evaluated to determine if performance degradation occurs. A computer analysis was made using the Convair radiation configuration factors program (Reference 9-8). The radiation configuration factors were calculated for four space station-module docked geometries. The space station definition was obtained from Reference 9-9. The experiment module analyzed was CM-3. It was assumed that the thermal properties of the surfaces of both the modules and the space station are similar since both will be covered by radiator surfaces or solar cells. The degradation of radiator performance due to station and other module interference is given by the view factor between the module in question (emitter) and the other structural surfaces. The configurations used to input the computer program are given in Figure 9-20.

The view factors from emitter to receiver for the four modules are:

I	0.00059
II	0.100
III	0.1283
IV	0.1633

Thus, in three cases, the reduction in radiator performance can be as much as 10-16% due to experimental module or space station interference.

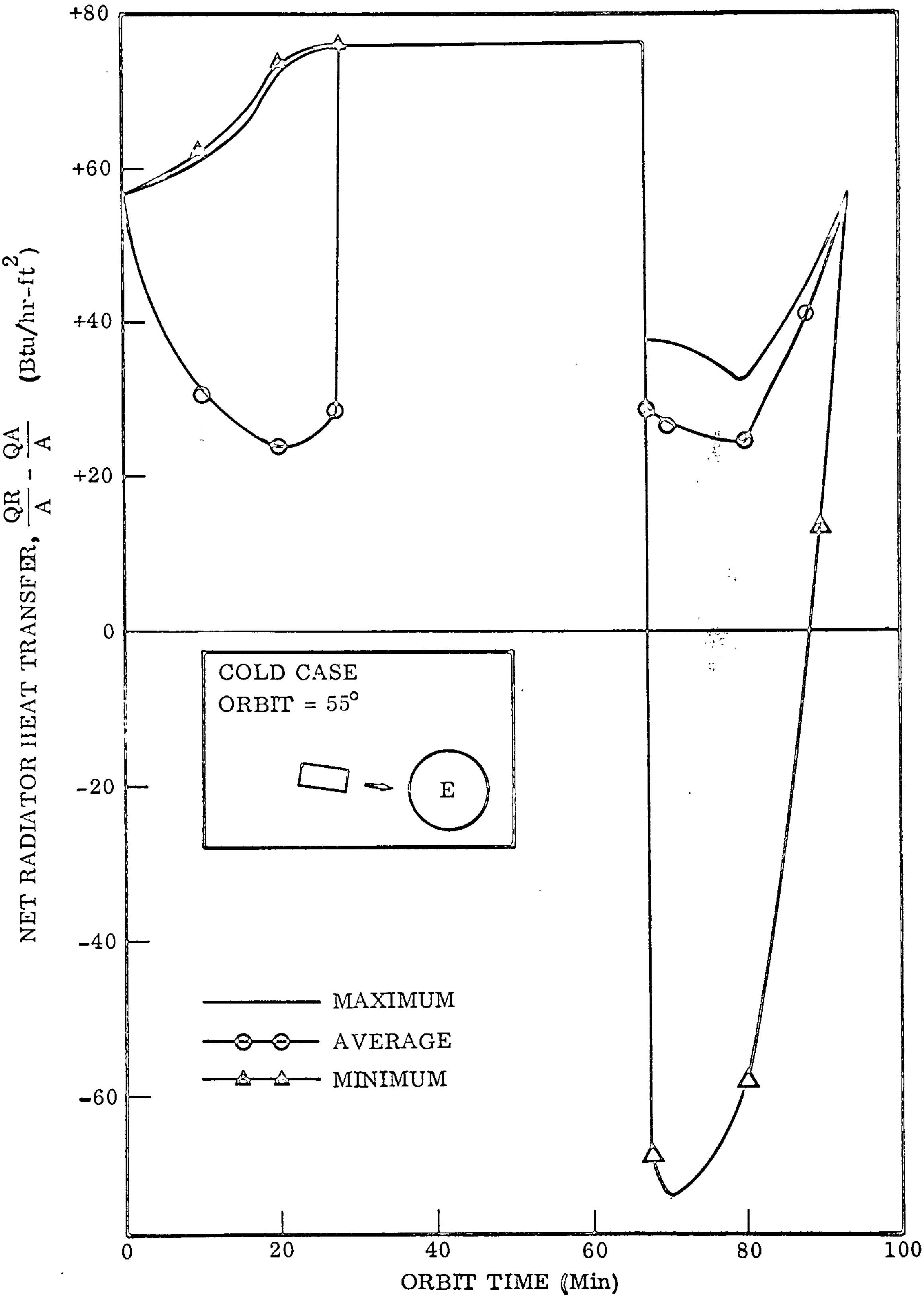

Figure 9-9. Radiator Net Heat Flux — Case 1

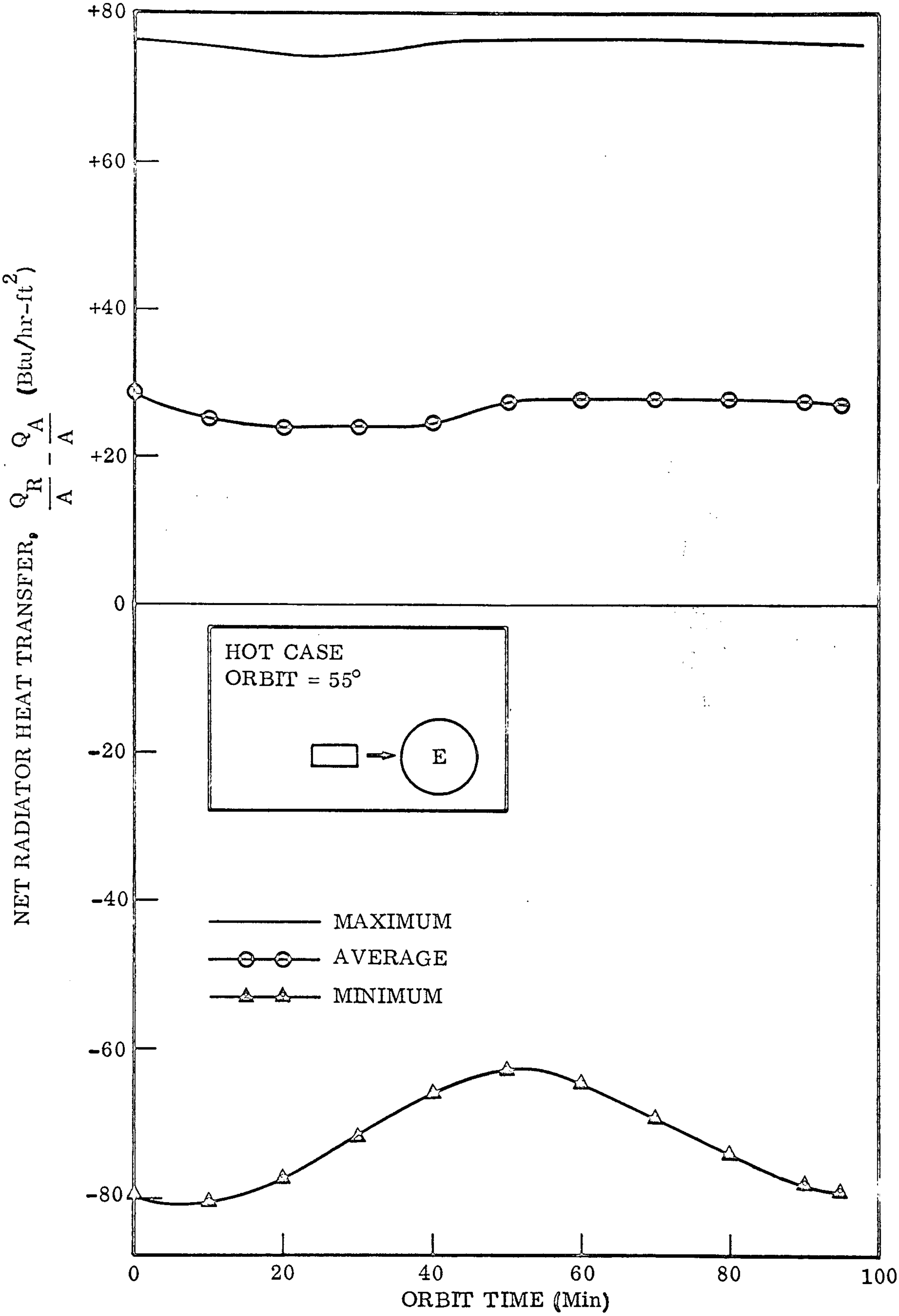

Figure 9-10. Radiator Net Heat Flux — Case 2

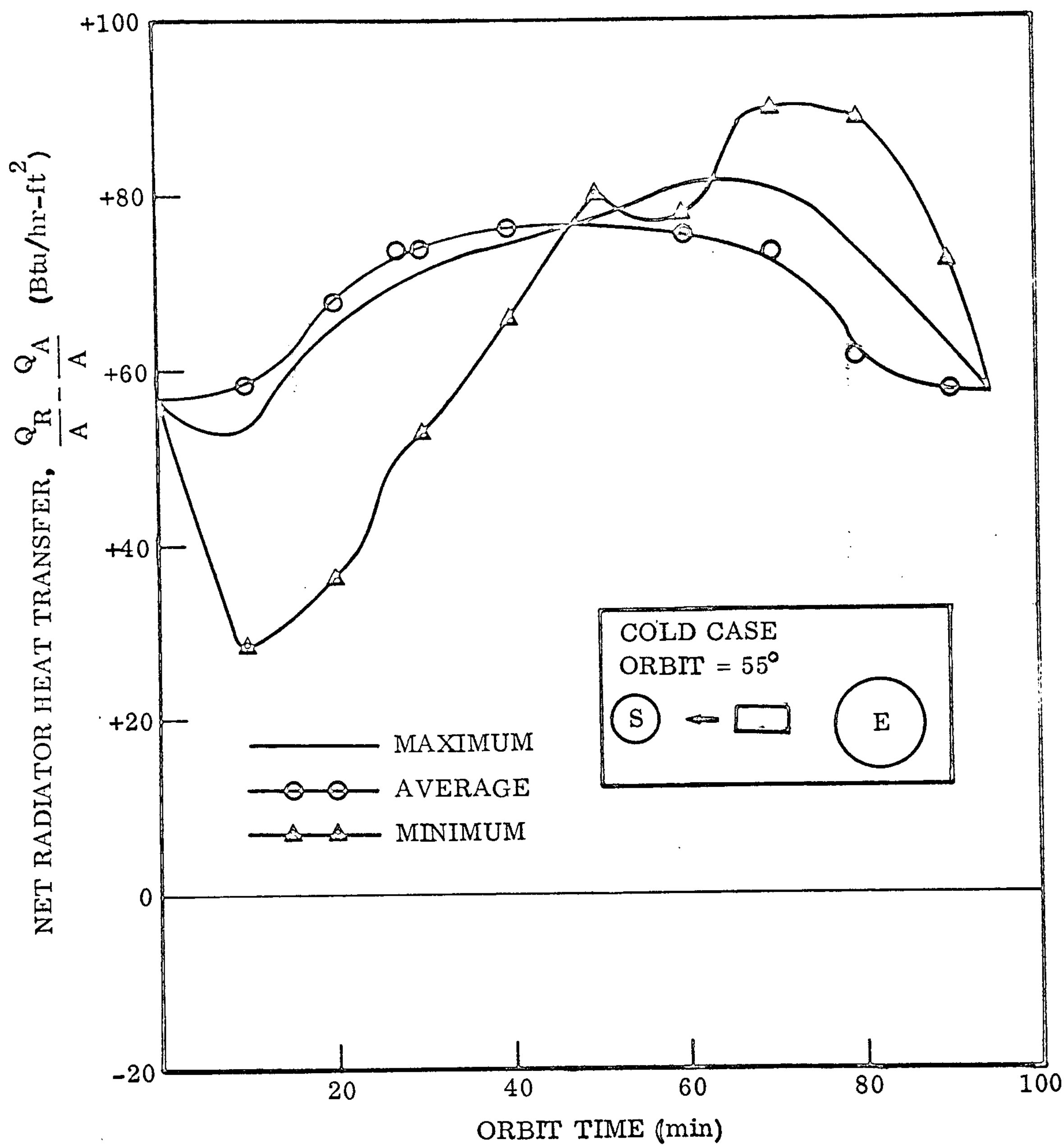

Figure 9-11. Radiator Net Heat Flux — Case 3

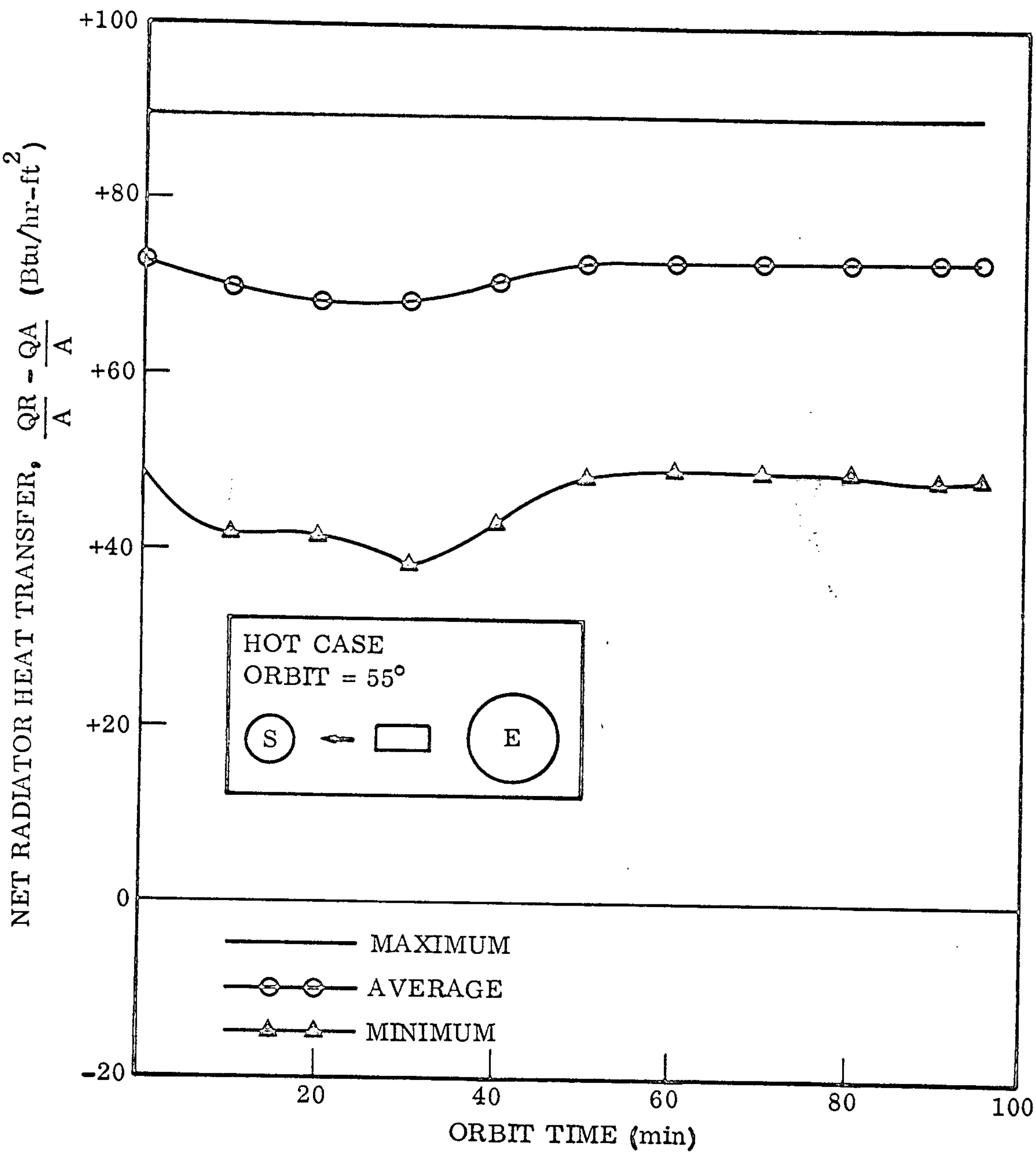

Figure 9-12. Radiator Net Heat Flux – Case 4

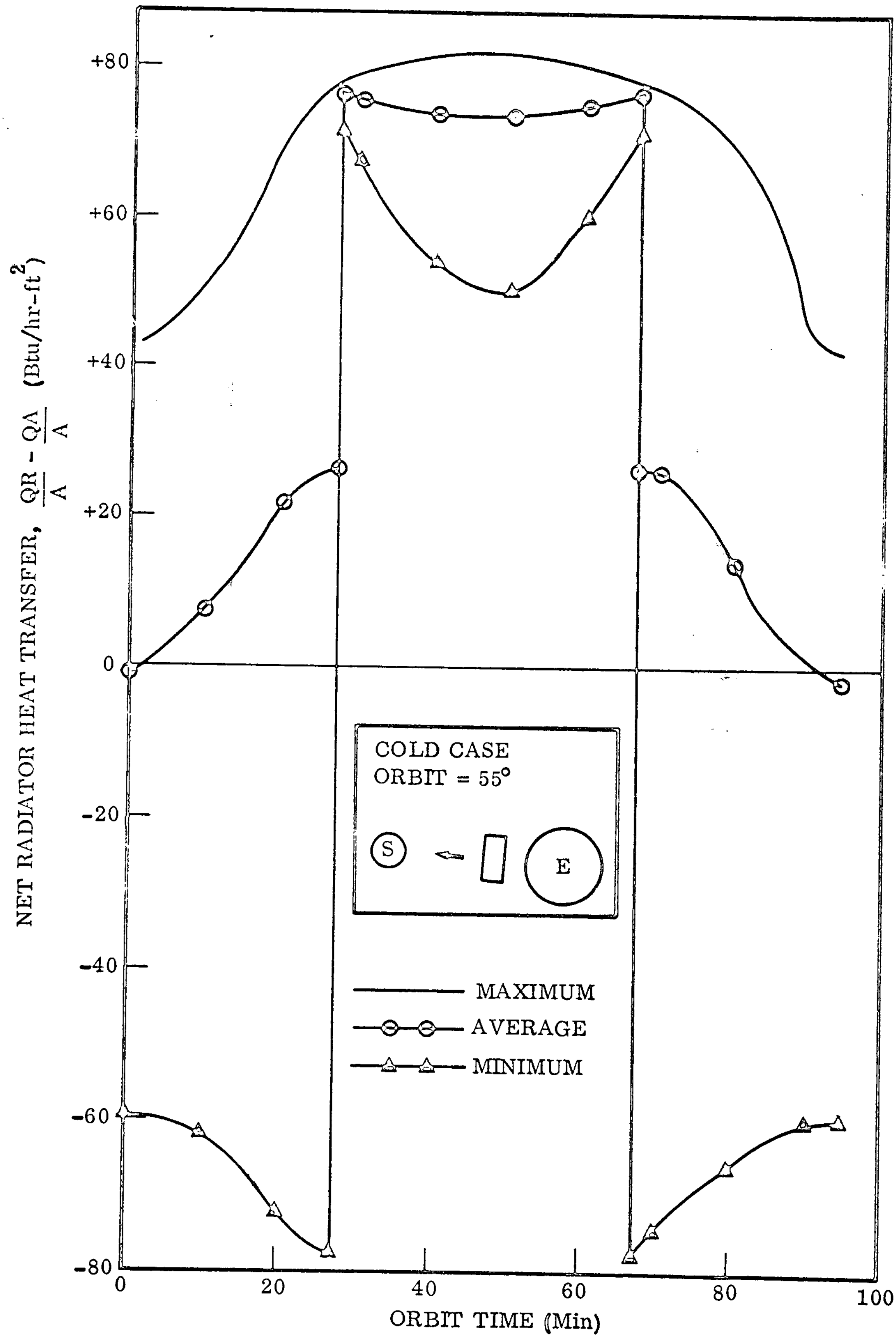

Figure 9-13. Radiator Net Heat Flux – Case 5

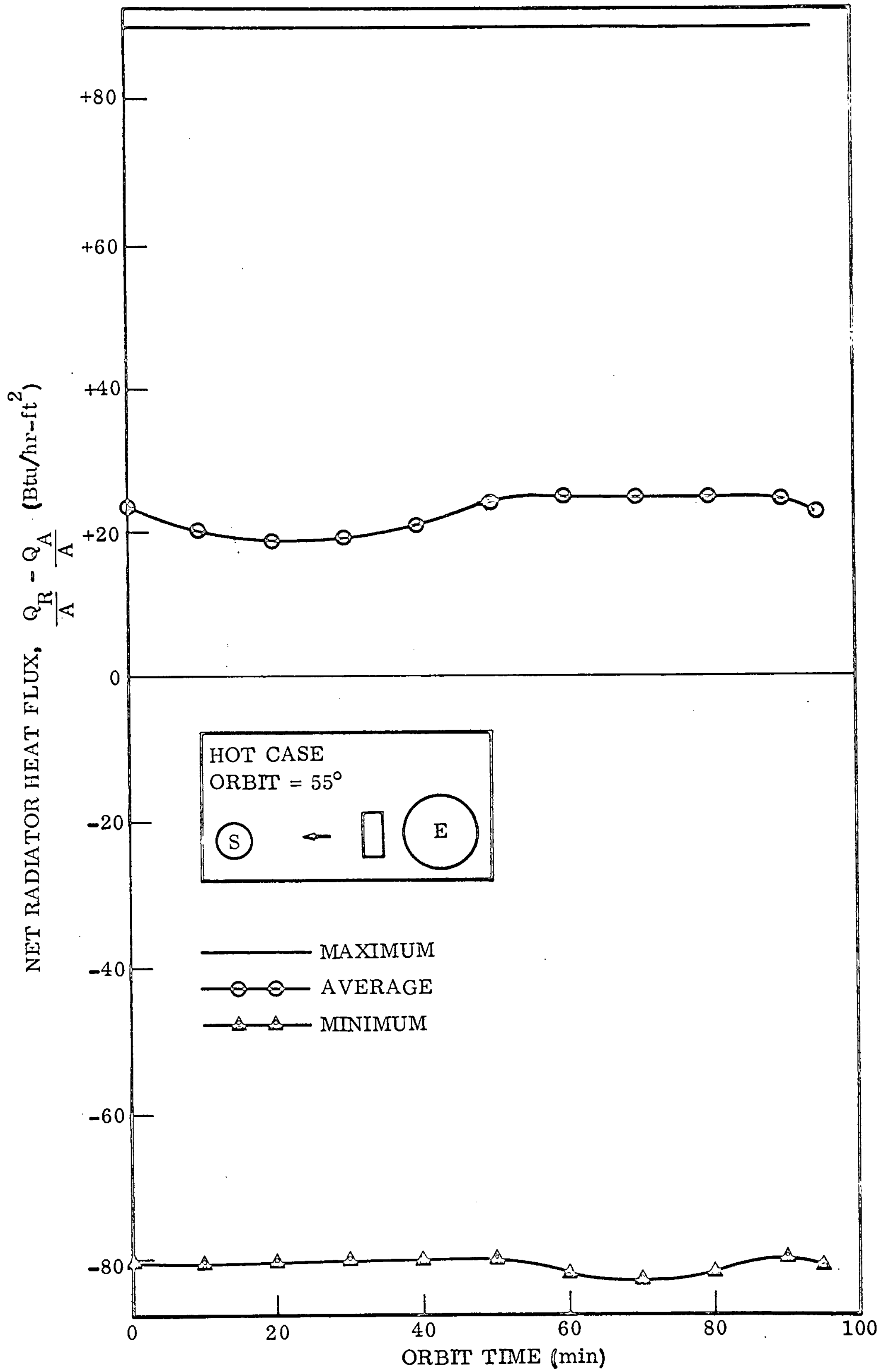

Figure 9-14. Radiator Net Heat Flux – Case 6

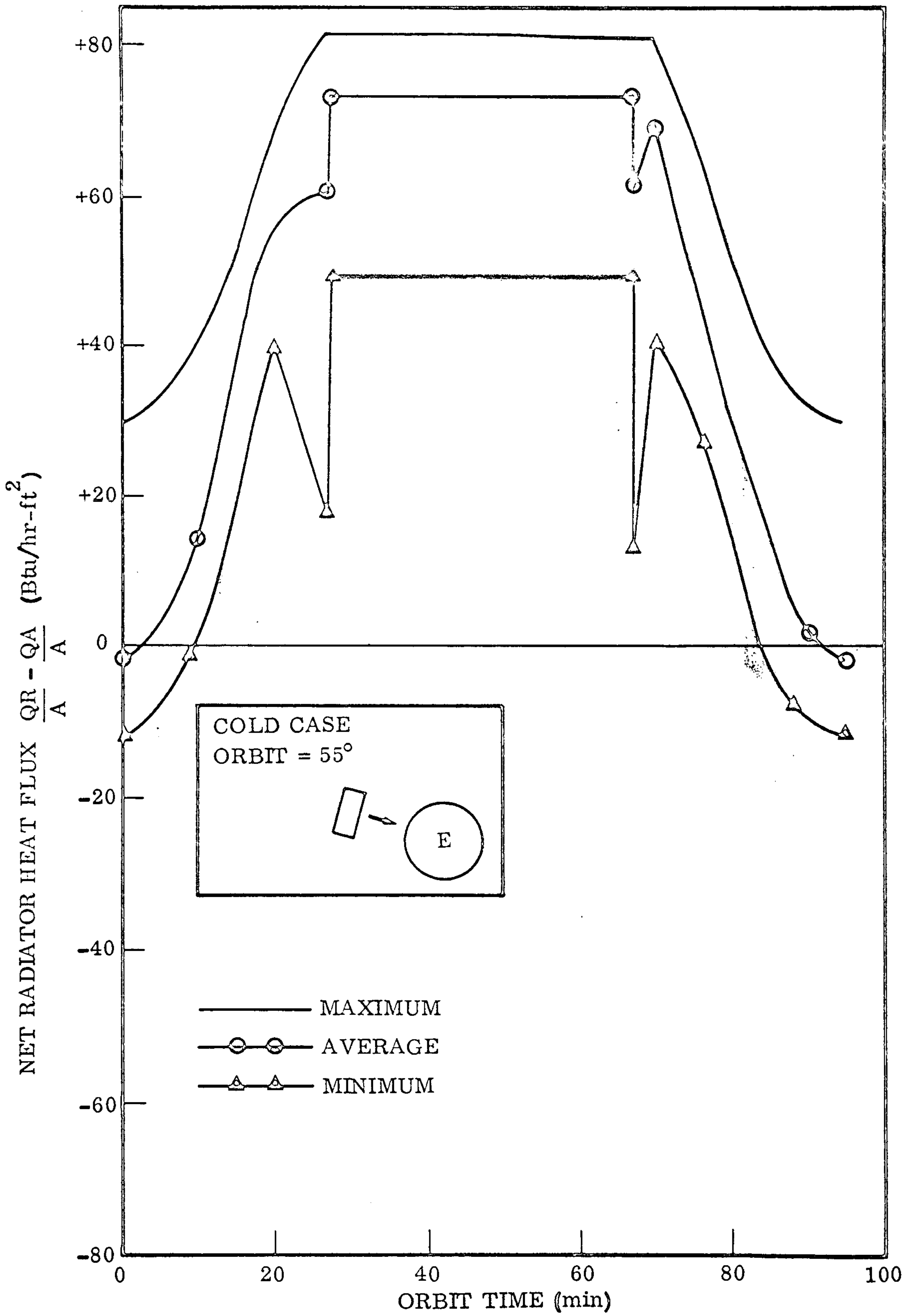

Figure 9-15. Radiator Net Heat Flux — Case 7

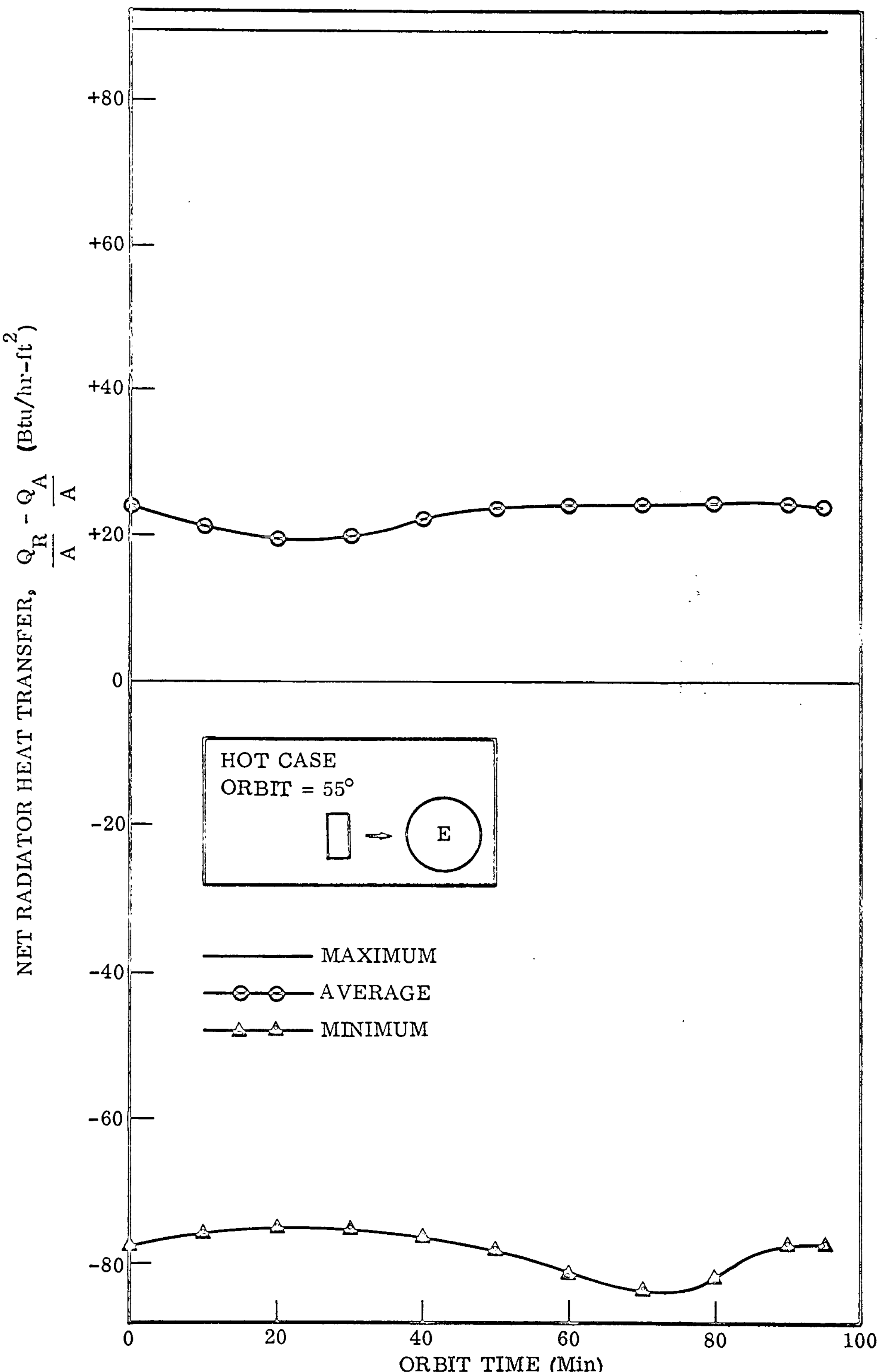

Figure 9-16. Radiator Net Heat Flux — Case 8

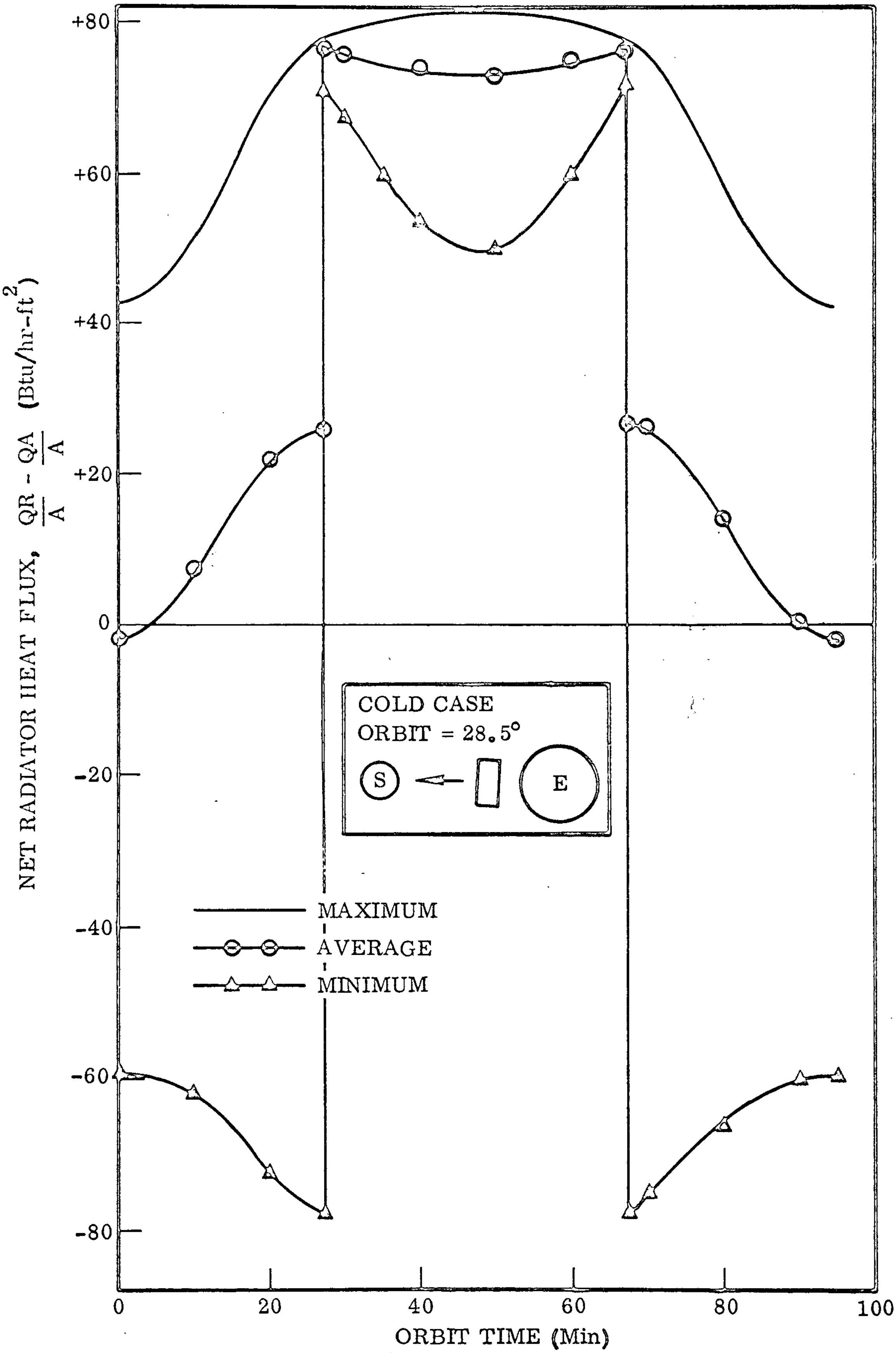

Figure 9-17. Radiator Net Heat Flux – Case 9

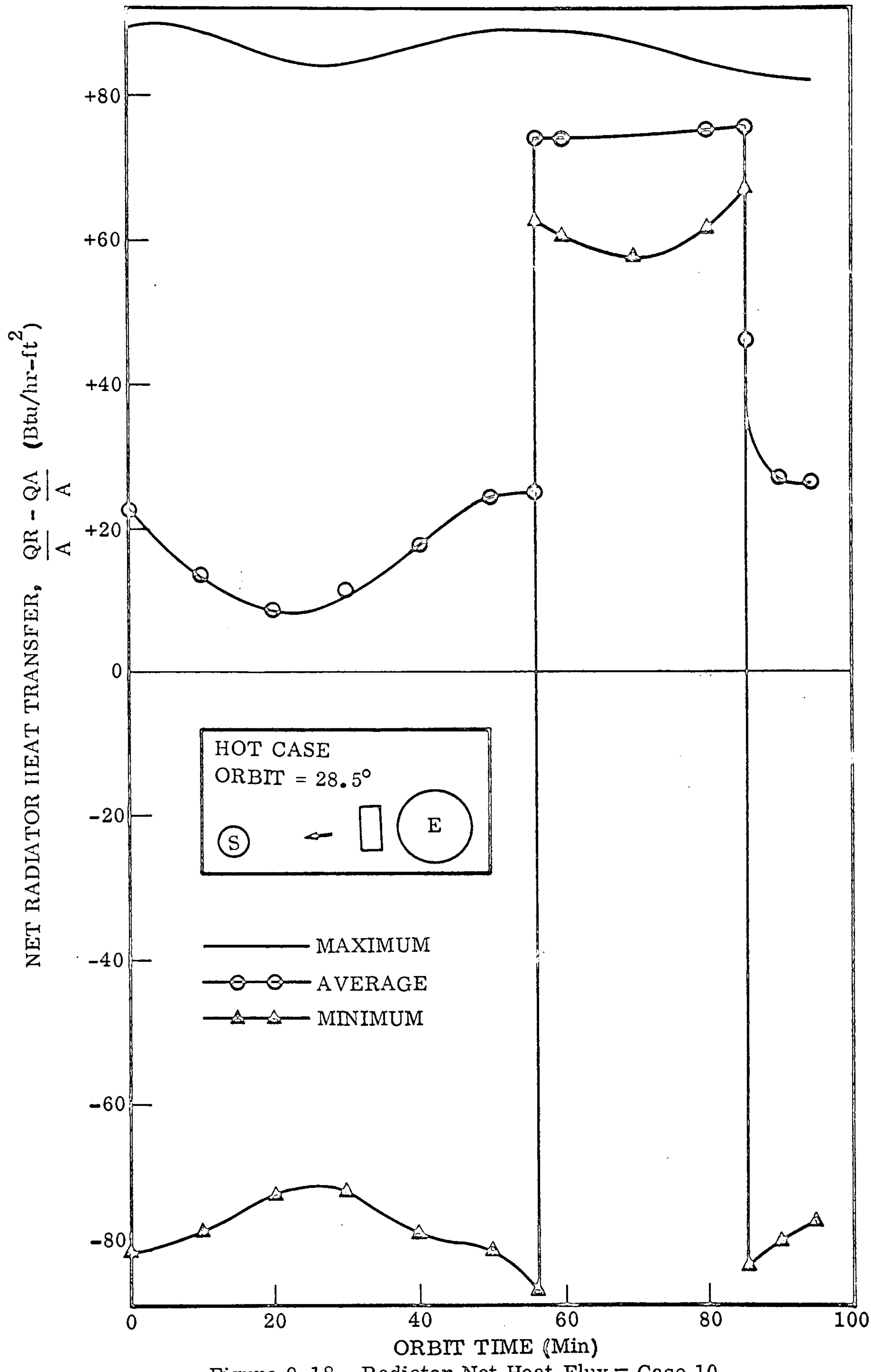

Figure 9-18. Radiator Net Heat Flux – Case 10

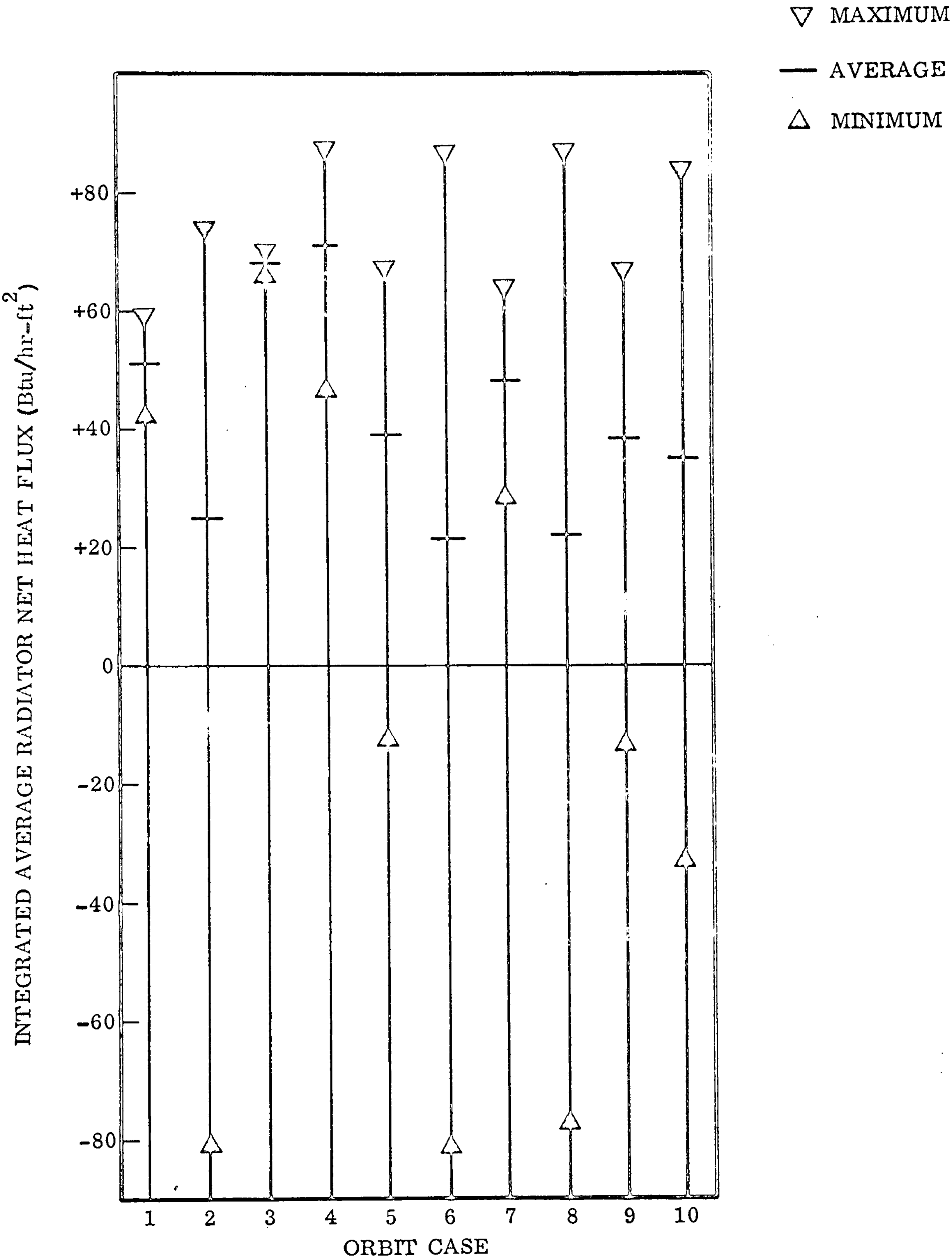

Figure 9-19. Integrated Average Radiator Net Heat Flux

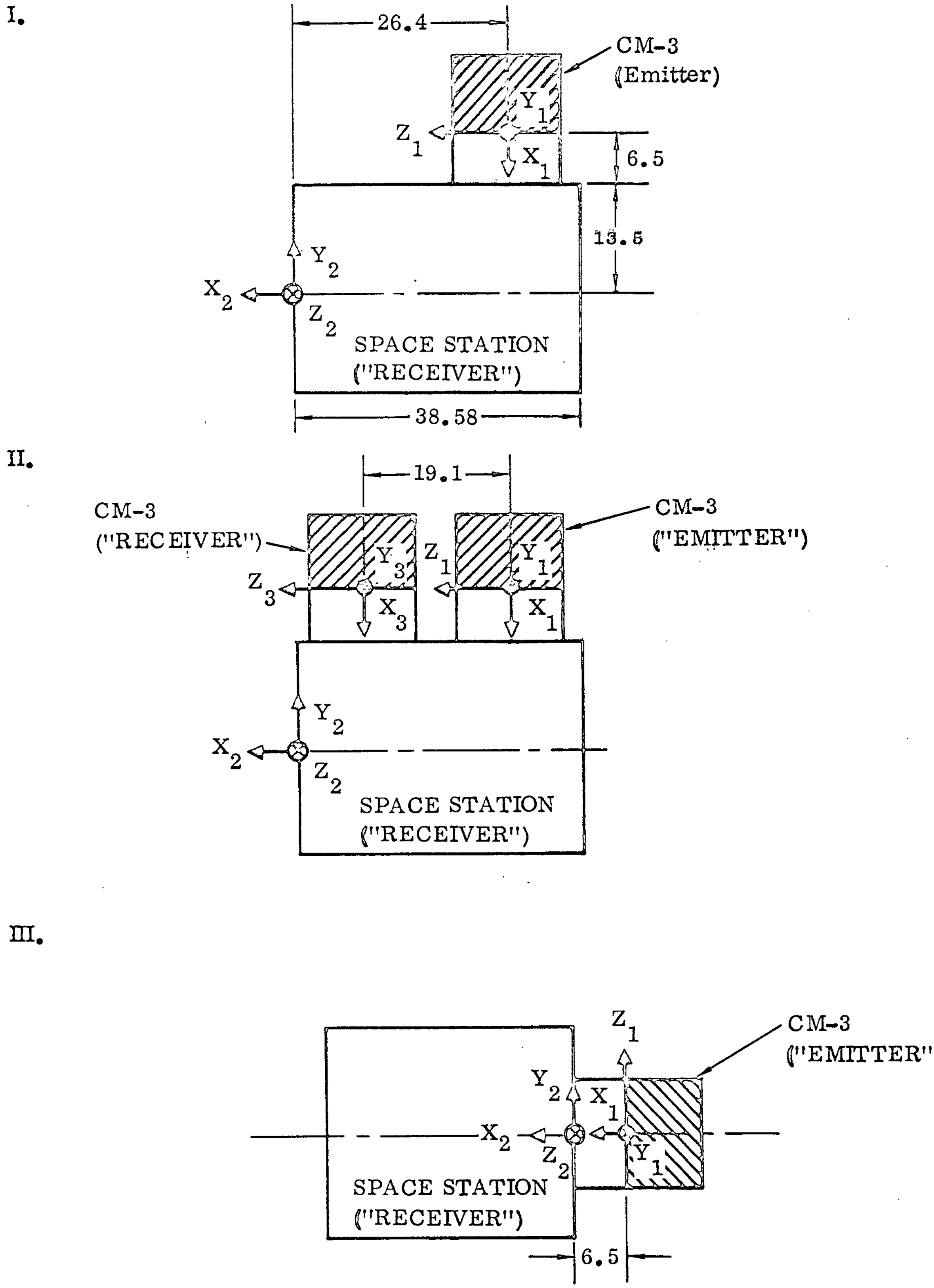

Figure 9-20. Computer Configurations Used for Radiator Interference Effects Analysis (Sheet 1 of 2)

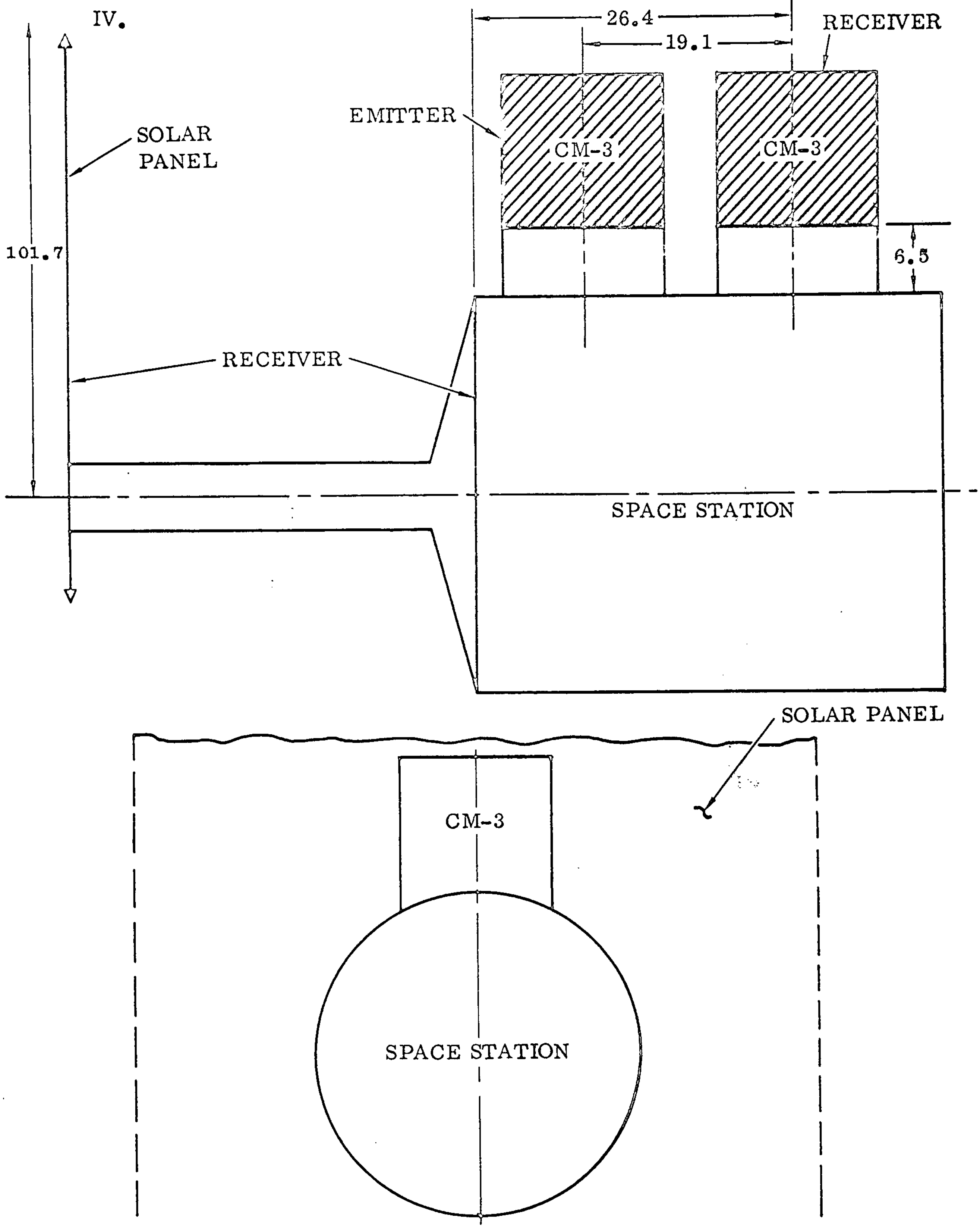

Figure 9-20. Computer Configurations Used for Radiator Interference Effects Analysis (Sheet 2 of 2)

In the nominal case with an average radiator temperature of 526°R and surface emittance of 0.85, the net heat released by the experiment module integral radiators in the worst interference orientation (configuration IV) can be reduced by as much as 14.6 Btu/hr-ft^2.

A potential problem arises when the free-flying modules are docked with the space station. In this situation, deployed solar panels on docked modules could provide a significant amount of radiation interference between the space station integral radiators and the deployed module solar panels. To remedy this situation, the module panels will be retracted as shown on Figure 9-21 to reduce the interference to lowest possible level. The space station configuration shown is taken from Reference 9-10. For the space station configuration shown in Figure 9-20-II, the free-flying modules will be docked with the retracted solar panels parallel to the space station axis. This will assure that there is no interference between the radiators and solar panels of adjacently docked modules.

The calculations discussed previously have all been made using the anticipated degraded radiator thermal control coating performance (Reference (9-11). In addition, all of the analyses were performed using a worst case solar albedo heating environment as determined from Reference 9-12. The value of albedo used was 0.48, which is the nominal value plus three standard deviations. To assess the sensitivity of radiator performance to variation in the value of the radiative properties of the thermal control coatings, a parametric study was run by varying first the solar absorptance value from 0.2 to 0.4 and then the thermal emittance from 0.8 to 0.9. The analysis was run for the worst case orbital heating orientation for the module (Case 6 as described above). The calculations were again made using the Convair Space Vehicle Radiant Energy Program. This program allows the input of the planetary albedo, and calculates the planetary thermal radiation by performing an energy balance on the earth. The calculated value of earth thermal radiation as a function of albedo is given in Figure 9-22 for the nominal solar constant.

The results of the parametric study are presented in Figures 9-23 and 9-24. The decrease in radiator performance with decreasing albedo is due to the fact that a large portion of the integrated average radiator absorbed heat flux is due to earth emission. The data also show rather strongly the value of coating the radiator surfaces with a nondegrading thermal control coating with a low α/ϵ ratio. The search for such a long life coating should be a major item of research for a long life module development. It is a recommended SRT item for the experiment module program.

The three common experiment module configurations (CM-1, CM-3, and CM-4) show maximum heat dissipation requirements ranging from 14-21 Btu/hr-ft^2 of available integral radiator area. Thus, radiator performance may be very marginal under maximum load conditions and under worst case orbital orientation or docking location unless satisfactory schemes are developed and used to effectively utilize

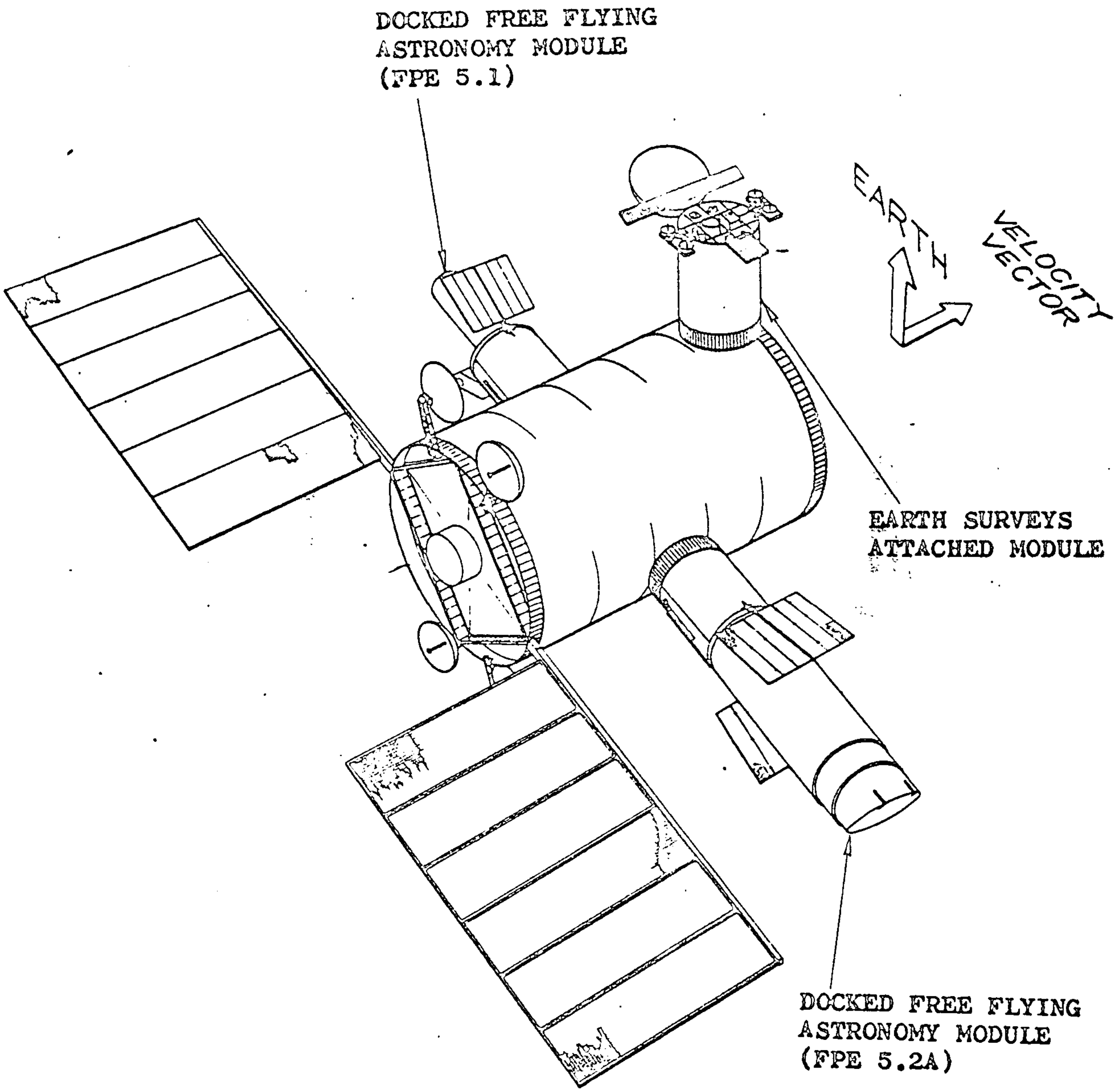

Figure 9-21. Space Station/Experiment Module Complex

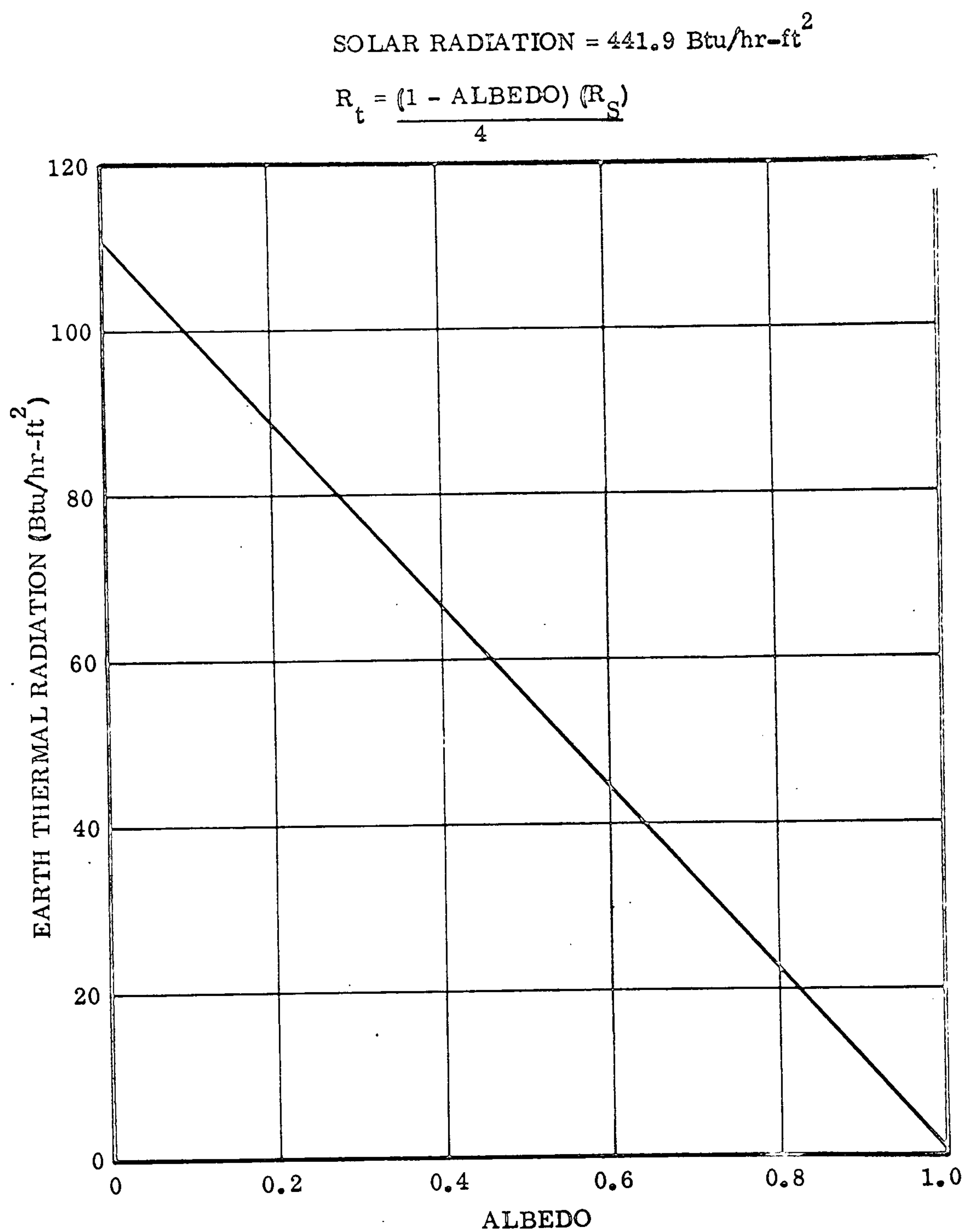

Figure 9-22. St. Nero Calculation of Earth Thermal Radiation

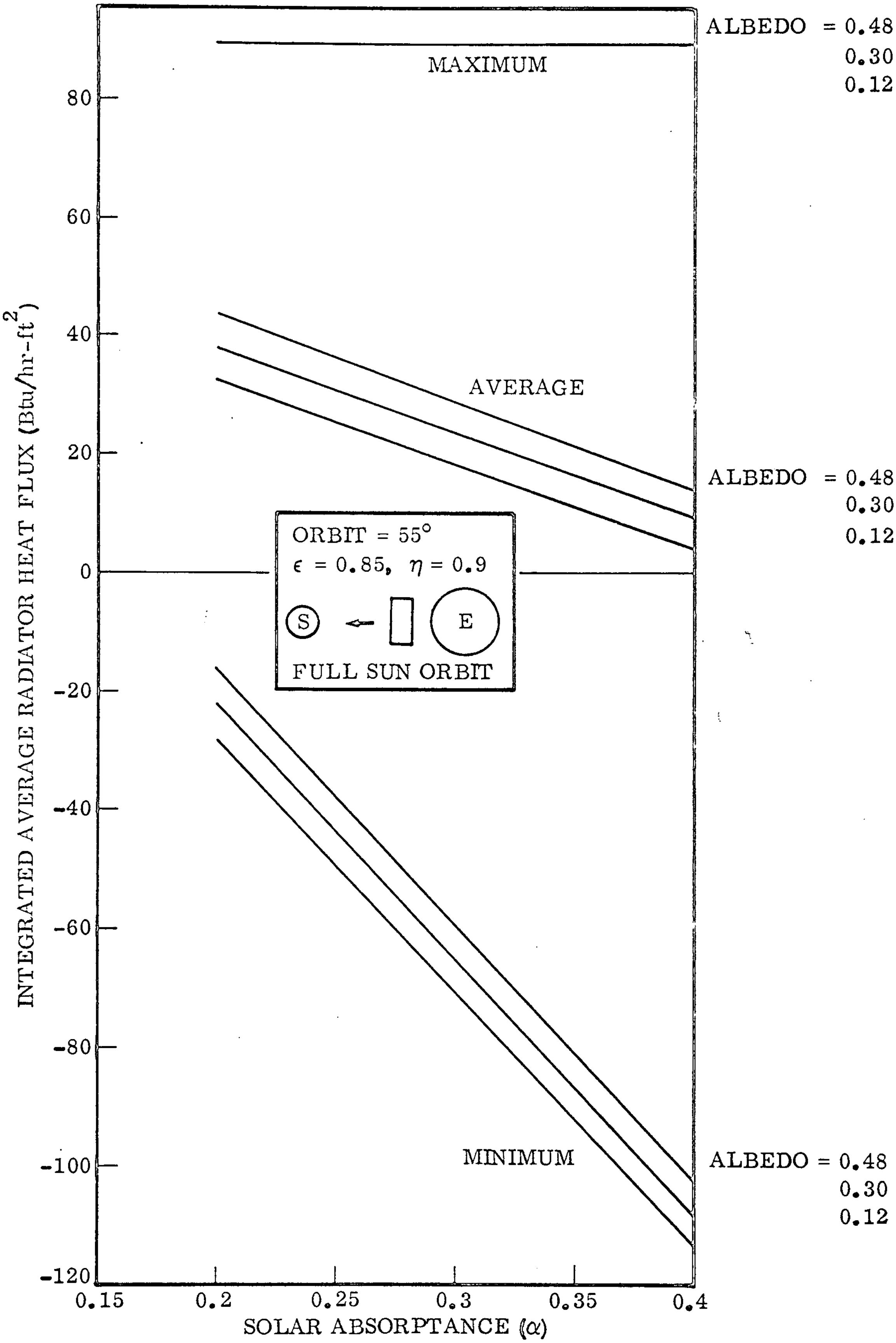

Figure 9-23. Variation of Integrated Average Radiator Heat Flux with Solar Absorptance for Hottest Orbital Orientation of Experimental Module

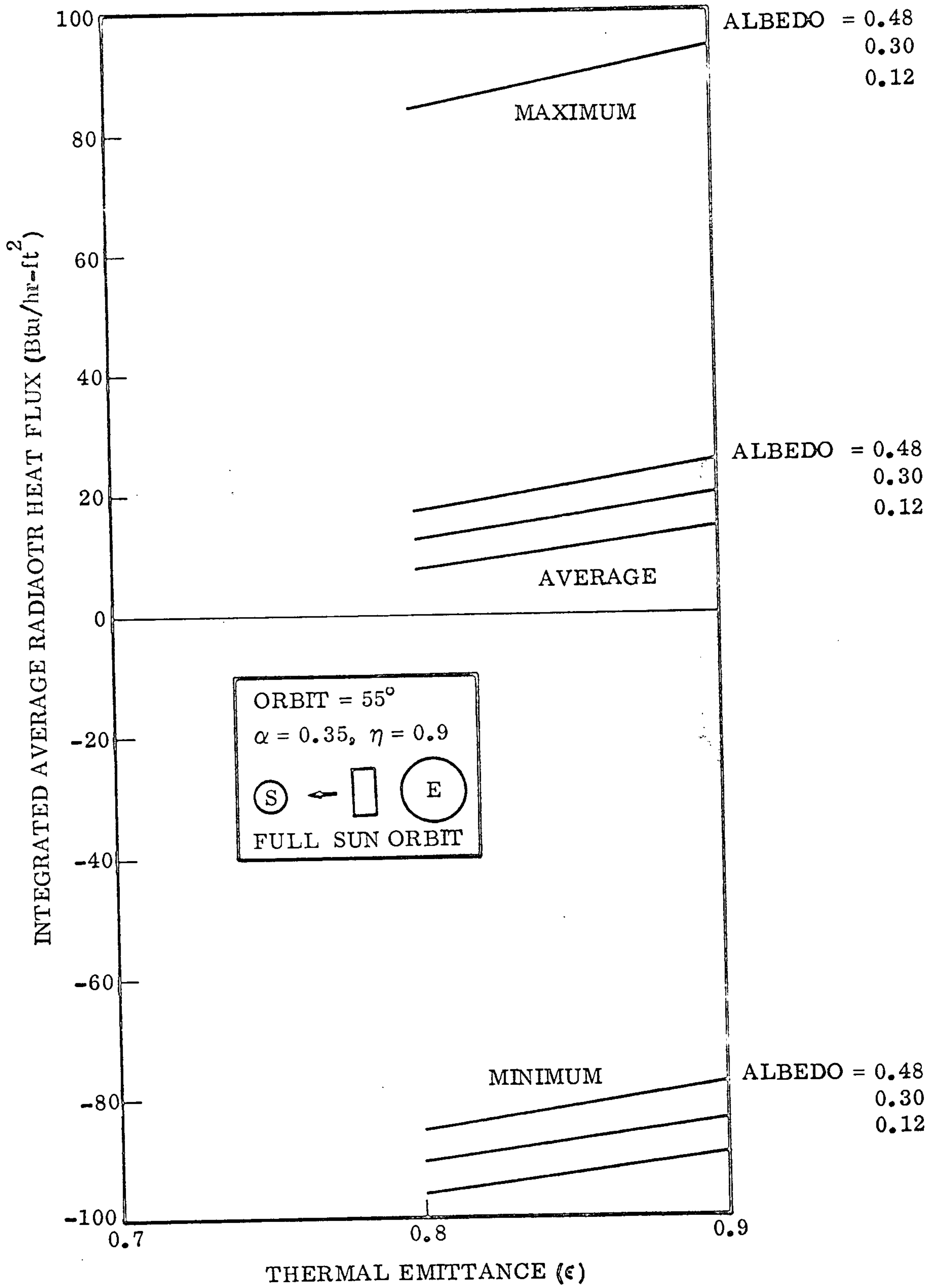

Figure 9-24. Variation of Integrated Average Radiator Heat Flux with Thermal Emittance for Hottest Orbital Orientation of Experimental Module

the radiators in their most efficient manner. Through the use of proper valving and flow control, it may be possible to control the radiator load to those panels which have the greatest heat rejection potential. It may also be possible to schedule mission time and space station docking locations to avoid hot orbits or hardware radiation interference between modules or module and station. Thirdly, it may also be possible to develop deployable radiator kits for attachment to the modules for the high heat dissipation experiments. These latter two alternatives, however, impact the overall module and station operating characteristics and are less desirable than the first alternative. In any event this is a problem area that will require additional work to obtain the optimum solution for module heat dissipation requirements.

9.3.4 THERMAL CONTROL COATING SELECTION. Proper selection of external coatings is required to provide the desired heat transfer rate through the external surfaces of the modules, particularly the space radiators. Untreated metal surfaces usually are unacceptable because of poor absorptance or emittance(α or ϵ) or the ratio of α/ϵ. The effect of various thermal control coating properties on radiator performance was shown on Figures 9-23 and 9-24. It can be seen that radiator thermal performance is very strongly dependent on the coating properties, particularly α. It is obvious from these results that a low α and high ϵ are desirable for the module application. White paint surfaces (usually obtained with titanium or zinc oxide pigments) have the desirable coating properties ($\alpha/\epsilon = 0.2/0.88$). Experience has shown, however, that the thermal control properties of the white paint degrade in space over several weeks and severely degrade with long solar exposure (Reference 9-11). This degradation quickly results in solar absorptance values of 0.35 or greater. On this basis, initial thermal control system calculations for baseline systems were made for $\alpha = 0.35$.

Since the maintenance of the properties of the thermal control coating is very critical to superior module performance, new stable coatings must be developed for use with the module. The desired properties are $\alpha = 0.2$, $\epsilon = 0.9$. This may be accomplished by the use of composite coatings, which are vapor deposited over a suitably prepared substrate. In this way the absorptivity of the surface is determined by the substrate properties and the emissivity by the thickness of the vapor deposited coating.

9.3.5 WALL INSULATION. Foam and multi-foil radiant shields were considered as candidate wall insulations. The analysis task was limited to checking feasibility of achieving temperature control with these materials. The experiment module wall thermal design must consider the experiment bay and the occupied lab area somewhat differently. The occupied compartments must maintain wall temperatures above the dew point of the atmospheric gases at all times. Experiment bay wall design must be based upon maintaining a particular sensor or instrument within certain temperature limits over a given orbit and operating condition. The two concepts analyzed are shown in Figure 9-25.

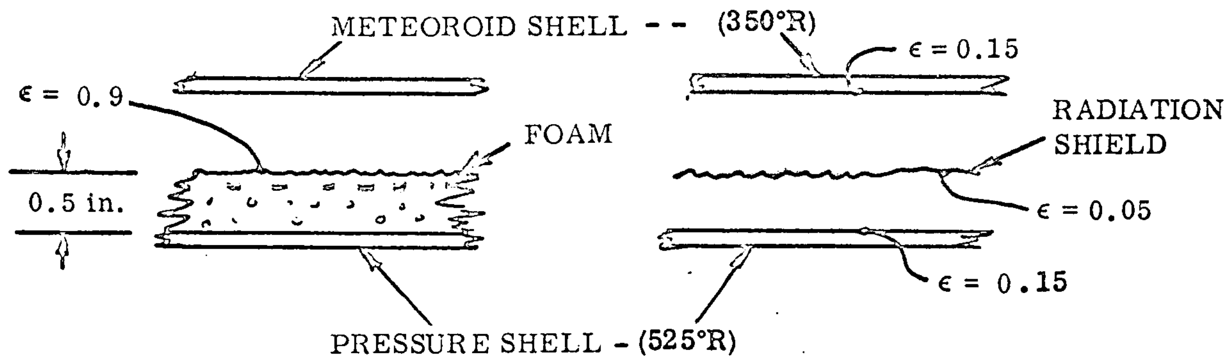

$K = 0.0047$ Btu-ft/hr-ft^2-°R

$W/A = 0.12$ lb/ft^2 $\qquad$ $W/A = 0.014$ lb/ft^2

Figure 9-25. Wall Insulation Concepts

Unit heat transfer rates were determined as follows:

Foam

$$Q/A = \frac{K}{L}\,(525 - T_{Foam})$$

$$= \frac{\sigma(T_{Foam}^4 - 350^4)}{\left(\frac{1}{\epsilon_1} + \frac{1}{\epsilon_2} - 1\right)}$$

$$= \frac{0.0047 \times 12}{0.5}\,(525 - T_F)$$

$$= \frac{0.171 \times 10^{-8}\,(T_F^4 - 350^4)}{\left(\frac{1}{0.15} + \frac{1}{0.9} - 1\right)}$$

$$= 7.6 \text{ Btu/hr-ft}^2$$

Foil

$$Q/A = \frac{\sigma(525^4 - 350^4)}{\left(\frac{1}{\epsilon_1} + \frac{1}{\epsilon_2} - 1\right) + \left(\frac{1}{\epsilon_2} + \frac{1}{\epsilon_1} - 1\right)}$$

$$= \frac{0.171\,(750 - 150)}{\left(\frac{1}{0.15} + \frac{1}{0.05} - 1\right) + \left(\frac{1}{0.05} + \frac{1}{0.15} - 1\right)}$$

$$= 2.0 \text{ Btu/hr-ft}^2$$

The analysis shows that one layer of foil not only has a lower heat transfer rate through the wall, it also has a much lower weight. Therefore the radiation shield insulation concept was selected as the better of the two.

Since the radiation shield (aluminized mylar) has high lateral heat conduction characteristics (Reference 9-14), its insulation performance is drastically reduced at penetrations and at points of contact with the meteoroid shield or pressure shell. Therefore, the wall unit heat transfer rate must be used judiciously.

The installation of the radiation shield is shown on Figure 9-26. To allow for the unknowns of penetrations and contact heat shorts, two shields are shown installed. Schjeldahl X-850 foil is extremely tough. The foils are punched, polycarbonate grommets are inserted, and the layers are hung on the tabs of the pressure shell frames. Since the pressure shell tabs represent a significant heat short, fiber glass frames are required to support the meteoroid shield to minimize this heat leak.

For performance calculations an average wall conductance value is required. A representative value can be obtained by using the heat transfer rate through a foam insulated wall and increasing this value 50% to allow for meteoroid shield supports and other wall penetrations. Thus, a useful value would be

$$\begin{aligned} U &= 7.6 \times 1.5/175 \\ &= 0.065 \text{ Btu/hr-ft}^2\text{-°F} \end{aligned}$$

9.3.6 SPECIAL EMPHASIS STUDIES. During the course of the study, certain critical thermal control problems, particularly associated experiment payloads, were analyzed to establish their effect on module design. The results of some of these special studies are presented in the following sections.

9.3.6.1 Cooling by Refrigeration. Some experiments require very cold or cryogenic temperatures for operation. In many cases these temperatures are obtained by allowing a cryogenic fluid to be vaporized. In the fluid physics experiments the cryogenic fluids are part of the experiment. Obtaining low temperatures in this manner imposes a requirement that the fluid be resupplied. It may be desirable to supply these temperatures with a closed cycle system to eliminate the resupply.

Figure 9-27 provides insight into the problem of attempting to provide a closed cycle system for low temperature requirements. The curve shows the electrical power required to provide the equivalent cooling load in watts. The curve is the inverse of coefficient of performance for refrigeration cycles. As noted on the figure, the performance is only for a refrigeration cycle that rejects heat to a 550°R heat sink. It must be recognized that it is possible to obtain temperatures above 300°R with much less power than shown on Figure 9-27 with a heat transport coolant loop and orientable radiator.

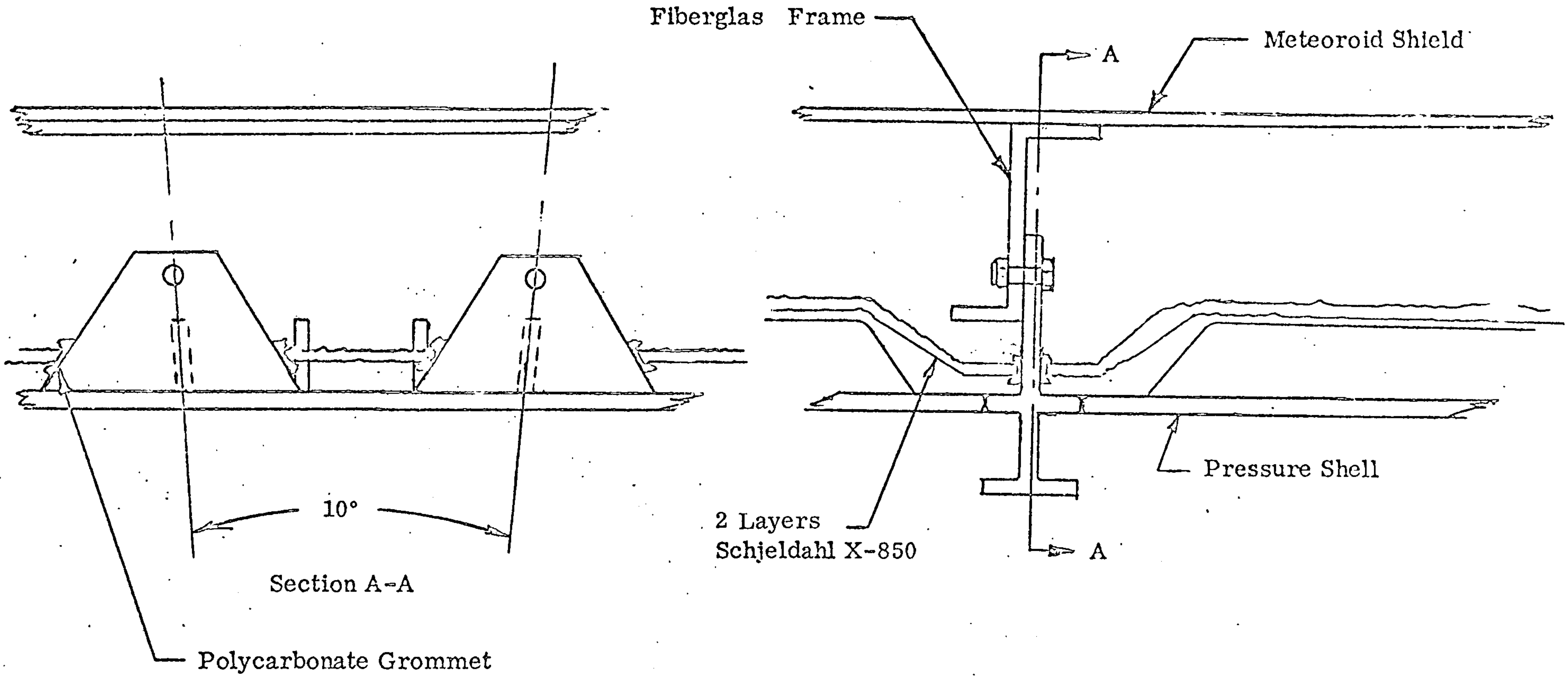

Figure 9-26. Radiation Shield Installation

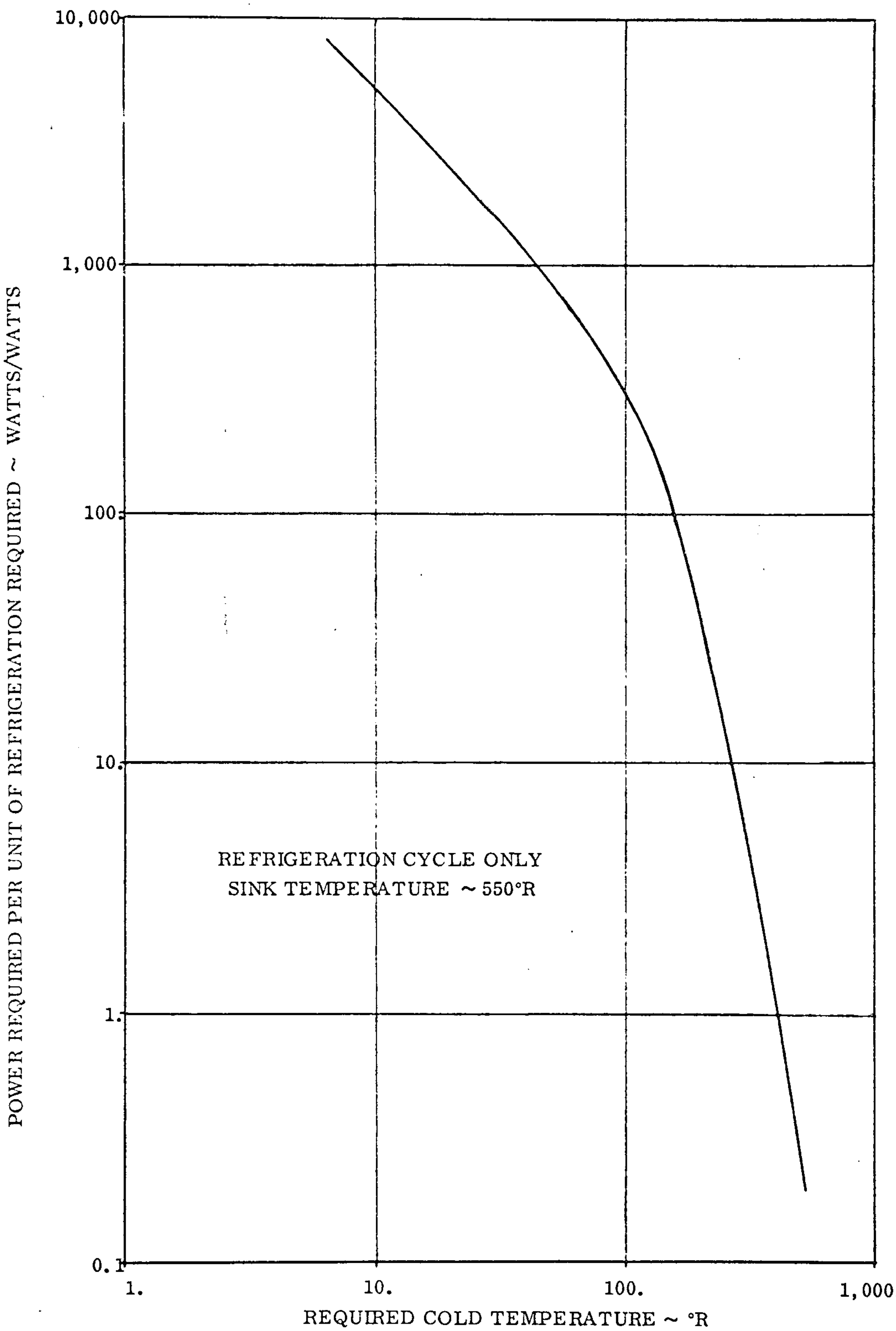

Figure 9-27. Power Required to Obtain Low Temperatures

The power requirement curve, Figure 9-27, shows that a sensor that generates 1 watt of heat (3.4 Btu/hr) at liquid hydrogen temperatures (37°R) will require over 1200 watts of electrical power. Only 0.5 pound of LH_2 per day would be required at this temperature if an open cycle with LH_2 resupply were used. This implies that a closed cycle system would not be practical at LH_2 temperatures unless the sensor cooling loads were considerably less than 1 watt or resupply was totally out of the question. Even at LN_2 temperatures (140°R) cooling loads of 1 to 2 watts impact the module electrical requirements significantly (150/1).

9.3.6.2 Telescope Thermal Control. The critical experiment for CM-1 from a thermal control standpoint is FPE 5.2A for stellar astronomy. The Perkin-Elmer report, Reference 9-3, indicates that to obtain performance from the three-meter telescope, the thermoelastic distortion of the mirror and supports for the secondary mirror must be virtually eliminated. Optically the goals are 1/50 λ (wavelength) or 1/200 arc-seconds resolution. This represents a dimensional tolerance of $<0.4 \times 10^{-6}$ inch.

Perkin-Elmer/Lockheed concludes that this is possible by operating the mirror and its secondary mirror support rod at the temperature where the coefficient of expansion is zero. Their study shows that quartz is the desirable material. The allowable temperature tolerance of quartz is shown on Figure 9-28 (obtained from Reference 9-3). Figure 9-28 shows that a thermal control system that has an 8°F operating band would have to maintain the mirror at -112°F (-80°C). Even a system with a 1°F control band must maintain the mirror at less than -50°F.

Analyses performed in the AM and OTES studies (Reference 9-2 and 9-3) show that a passive thermal control system can provide these super-cold mirrors. The OTES study concluded that:

a. The temperature gradients across the primary mirror segments can be minimized by passive techniques to less than 1°F.

b. The range of temperatures in the primary mirror segments can be controlled from -83° to -107°F in a space-orientation mode using passive thermal control techniques.

c. The maximum primary mirror temperature stabilization time is about 24 hours (from the power off to power on mode).

d. The thermal gradients are uniform along the length of the four quartz spacer rods, so spacing tolerances can be maintained using passive control techniques.

Figure 9-29 shows a thermal control approach that would incorporate the recommendations of the OTES study and provide a super-cold mirror. The objective of this approach is to radiate to space all the heat leaked into the payload chamber.

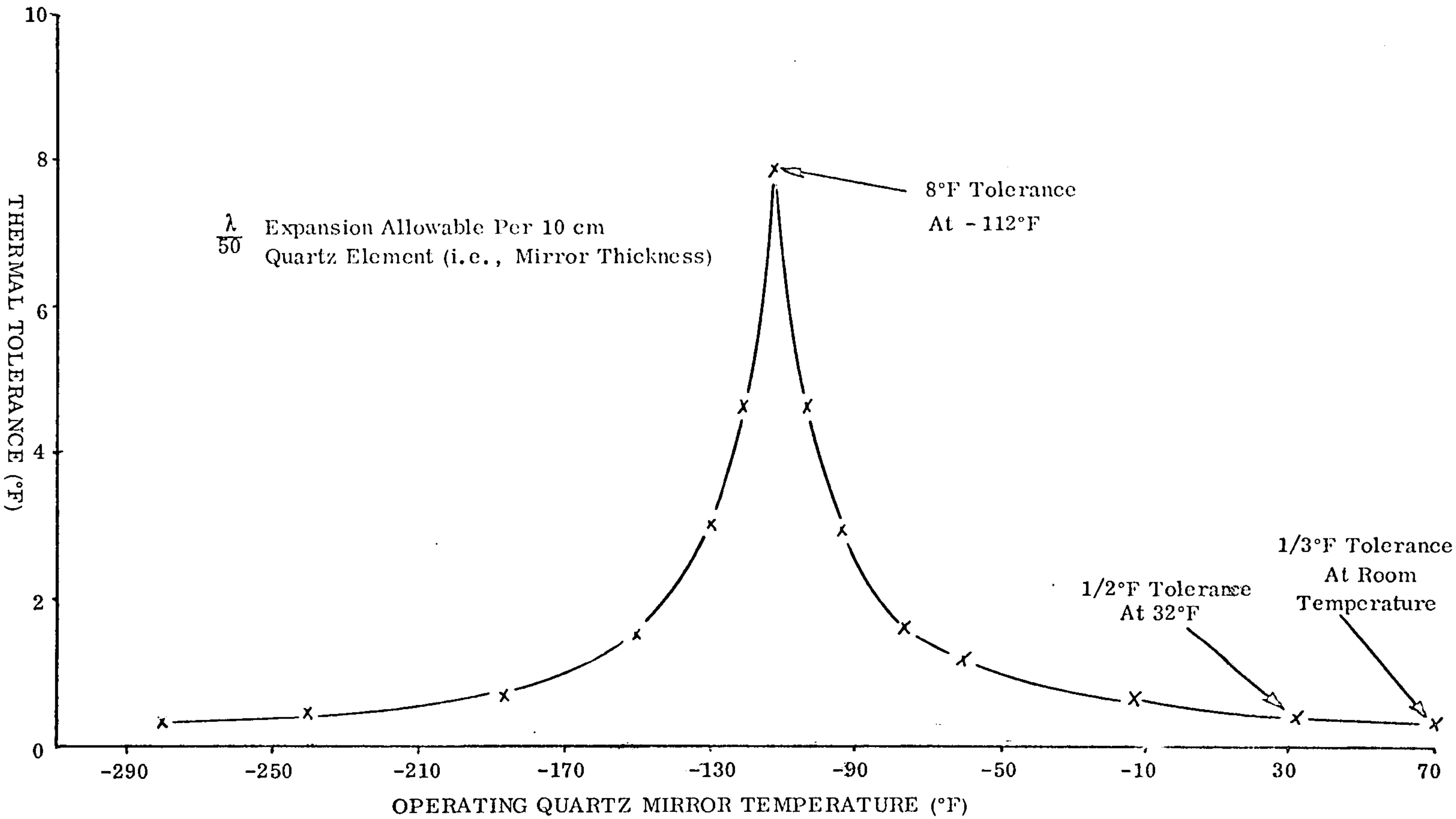

Figure 9-28. Temperature Tolerance Vs. Operating Temperatures for Quartz

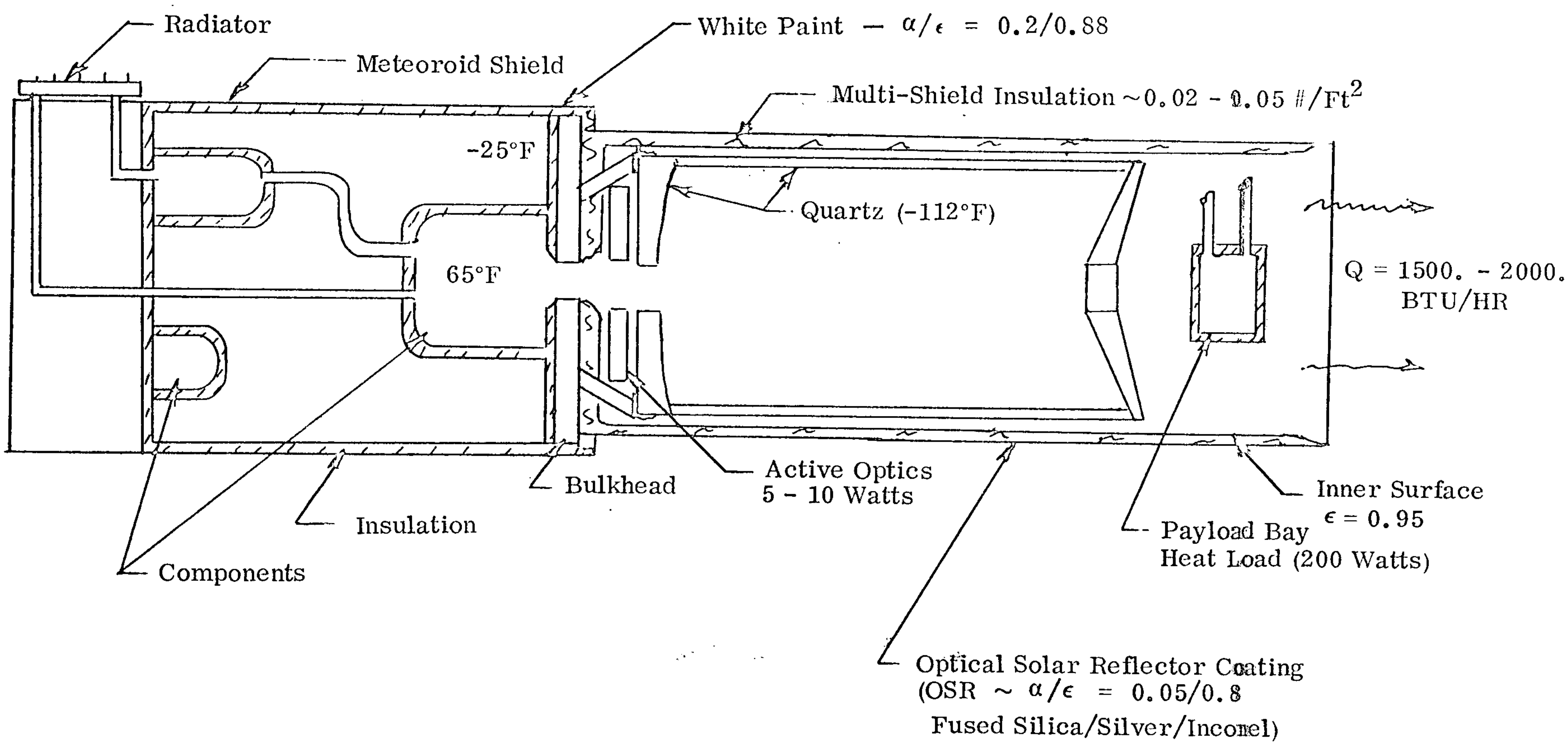

Figure 9-29. Thermal Control Approach for 3-Meter Stellar Telescope

Those components that generate heat would be insulated and their heat would be transported to the radiator. As shown on the sketch, an OSR external surface is required around the telescope to minimize the surface temperatures. This minimizes the heat transfer through the wall and limits the potential heat shorts through structural wall members. The multi-shield insulation virtually eliminates wall heat transfer. Most of the heat enters the payload chamber through the module bulkhead by conduction and radiation from the payload sensors. Therefore, a design approach should include a telescope support designed to minimize heat conduction paths, a bulkhead temperature as low as possible, the sensor equipment well insulated, and low module internal temperatures (possibly -25°F).

It is quite probable that there will be some components in the module that will not permit the low temperature criteria. Furthermore, the module wall construction, including external coatings, may prevent obtaining very low temperatures in the module compartment.

An alternate approach to the design of the stellar astronomy experiment was developed by the Optical Systems Division of Itek Corporation (Reference 9-15). In this case, the optical system is designed to operate at a nominal temperature of 70°F. The use of a "hot" telescope provides a completely different set of experiment peculiar thermal control problems than the "cold" telescope design. With the Itek concept, it is probable that a considerable amount of thermal energy will be necessary to keep the telescope at a uniform 70°F and make up for the energy loss by radiation to space. Schematically, the telescope configuration will be very similar to that previously depicted in Figure 9-29. Because of the required room temperature environment for the optics, however, the module thermal control system must be designed to minimize the radiation heat loss, which in turn will minimize the module power generation requirements. Radiant heat loss from the aperture of the telescope can be reduced by the use of an extended tube section and/or radiation "light baffles" in the tube to reflect energy back to the optics portion of the telescope. The incorporation of these passive cooling techniques, however, will increase the overall weight of the thermal control system. On the other hand, this will also reduce the weight of the power generation system. Thus to optimize the total module weight, a trade study as depicted in Figure 9-30 must be run to determine optimum combination of thermal control and power generation systems to provide minimum module weight.

9.3.7 RECOMMENDED ALTERNATES. There were several problem areas, as noted in the concept development, which require additional studies. The more significant ones are summarized in the following sections.

9.3.7.1 Thermal Control Coatings. Studies should be undertaken to establish cost effective thermal control coatings with a 10-year life. These coatings will be required for the experiment external surfaces, the module surfaces, as well as the radiators. The studies should evaluate maintainability as well as long-life stability.

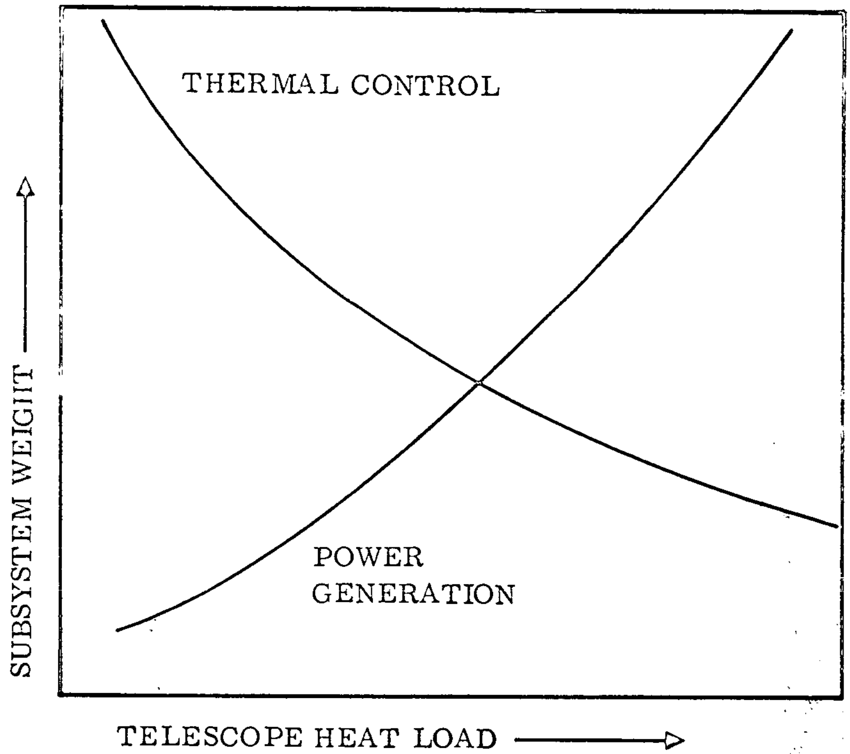

Figure 9-30. Typical "Hot" Telescope Heat Loss Trade Study

9.3.7.2 Radiator Control System. Integral radiators require the maximum use of the external surfaces of the modules. Studies are required to obtain optimum performance from these surfaces. Sizing the thermal control system for the FPE with the highest heat rejection produces excess cooling capacity for FPEs with lower requirements. This may result in very low module temperatures. Alternate systems can be devised that will produce a more consistent temperature value between modules. Special control schemes can be utilized with the heat rejection radiators to offer "fine tuning" thermal control capability for all module configurations. Coolant flow modulation is one technique that must be analyzed. Selective stagnation of various sections of the radiator, thus allowing freezing in portions of the radiator, is another feasible approach to module temperature control that shows promise. A third reasonable method of temperature control that can be utilized is the use of regenerative temperature control in the water loop of the module. In this case, the water is heated to increase the thermal load to the heat rejection system for stable radiator operation.

9.3.7.3 Deployable Radiators. It was noted that deployable radiator kits might be useful for modules with high heat dissipation experiments. Furthermore, studies may show that deployable radiators are more cost effective than integral radiators.

Deployed and properly oriented radiators can reject considerably more heat from either side than integral radiators and at the same time require practically no valves for control. Detail studies are required.

9.3.7.4 Telescope Thermal Control. Additional studies are required to provide efficient thermal control for large orbital telescopes. Thermal control of the telescope optical systems must be very precise to minimize structure distorting thermal gradients. The accomplishment of effective telescope thermal control will involve the imaginative use of passive control techniques as well as the use of active techniques such as heat transfer fluid loops and heat pipe systems.

9.4 SYSTEMS INFLUENCE ON THERMAL CONTROL SYSTEM.

The thermal control subsystem size was based on the experiment with the largest cooling requirement. This method results in a few problems, which are discussed in the following paragraphs.

9.4.1 COMMONALITY. The thermal control system for the free-flying module (CM-1) was sized for the growth version of FPE 5.2A (Stellar Astronomy) which requires 2.85 KW electric power. Hence, it has the capability for rejecting 9720 Btu/hr. The attached modules (CM-3) and (CM-4) are sized to reject 12,600 and 17,700 Btu/hr due to FPE 5.8 and FPE 5.9, respectively.

The cooling systems for the three module configurations are somewhat oversized when utilized for the very low heat rejection experiments assigned to the various modules. The percent variation of heat load dissipation requirements for the experiments assigned to the modules varies from 250% for the CM-1 module to 370% for the CM-3 module. Thus in the low heat load cases, internal module temperatures could become very low, which may be undesirable for any number of reasons. One ideal way to prevent large temperature dispersions among individual payloads is to modularize the thermal control system as much as possible. This is especially effective in the use of a modularized space radiator. A modularized radiator would permit a better match between required cooling and capacity for cooling for the various FPEs.

It is primarily for this reason that a modularized radiator was selected for use on the experiment modules. Also because of the similarity of designs among experiment module configurations, commonality of radiator modules will exist between as well as within experiment module configurations.

9.4.2 GROWTH. Most of the experiment module FPE configurations have the capacity to reject significantly more heat than their current requirements thus providing immediate potential for growth of experiment and subsystem heat load needs. Several of the configurations (those with heat dissipation requirements in excess of approximately 15 Btu/hr-ft^2 of radiator area) (see Tables 9-2, 9-3, and

9-4) are limited in their growth potential. This is due to the physical limitations imposed on the amount of module surface area available for incorporation of integral space radiators. The heat dissipation analysis (Section 9.3.3) on which this conclusion was based was, of course, a worst case analysis. In addition present state of the art thermal control coatings were used for the radiators, and degraded thermal performance characteristics were utilized for the heat rejection analysis. As discussed earlier, improvement in performance and stability of coating characteristics through the development of better thermal control coatings will greatly improve the experimental growth potential of all of the present module designs.

9.5 REFERENCES

9-1 Study for Basic Subsystems Module Preliminary Definition, Vol. VII – Radiators and Thermal Analysis, Report GDC-DAB67-003, Contract NAS 9-6796.

9-2 Advanced Astronomy Mission Concepts, ATM Follow-on Study, ED-2002-795, Vol. III, Contract NAS 8-24000.

9-3 Optical Technology Apollo Extension System (OTES), Vol. II, Contract NAS 8-20255.

9-4 Candidate Experiment Program for Manned Space Stations, National Aeronautics and Space Administration Report NHB 7150.XX, dated September 15, 1969.

9-5 Draper, N. R. and Smith, H., Applied Regression Analysis, John Wiley & Sons, Inc., New York, 1968.

9-6 L. E. Armfield, Space Vehicle Radiant Energy Program (SAINT NERO), Convair Report GDC-ERR-AN-929, November 1966.

9-7 Dietz, J. B., et al, Basic Subsystem Module Space Radiator Study, LTV Report 00.977, 20 August 1967.

9-8 Dummer, R. S. and Breckenridge, W. T., Jr., Radiation Configuration Factors Program, Convair Report ERR-AN-224, February 1963.

9-9 North American Rockwell drawing V030-902116, "Core Module Structure Assembly," June 11, 1970.

9-10 Baseline Program Document, Space Station Program Definition, Phase B, Volume III, Book I, Space Station Program Description, McDonnell Douglas Astronautics Company, 16 March 1970.

9-11 Conceptual Design of a High Energy Astronomy Observatory, NASA TM-X-53967, February 16, 1970.

9-12 Weidner, D. K., Natural Environment Criteria for 1975-1985, NASA Space Stations, NASA Technical Memorandum Report 53865, October 31, 1969.

9-13 Experiment Module Concepts Study Review, Contract NAS 8-25051, Convair Brochure, 28 July 1970.

9-14 Androulakis, John G., Effective Thermal Conductivity Parallel to the Laminations of Multilayer Insulation, AIAA Paper No. 70-846, July 1, 1970.

9-15 Technology Study for a Large Orbiting Telescope, Contract NASw-1925, Itek 70-9443-1, 15 May 1970.

SECTION 10

ENVIRONMENTAL CONTROL/LIFE SUPPORT

10.1 REQUIREMENTS AND DESIGN CRITERIA

The two factors that primarily determine the design of the EC/LS subsystem are (1) the experiment requirements, and (2) the EC/LS support available from the space station. The experiments generally require a shirtsleeve environment for two men for experiment procedures, servicing, and maintenance. While free-flying, the experiment modules are depressurized and unmanned, and therefore require no EC/LS functions.

The modules obtain most of the required EC/LS support from the space station, as indicated in Table 10-1. During attached operation, free air interchange between the module and space station is generally allowed, either through an open hatch or through a duct. The open hatch mode draws air from the space station environmental control (ECS) and returns it through the open hatch. The closed hatch mode similarly draws on the space station air, but requires a return duct that may be routed directly to the space station contaminant control subsystem. The biolaboratory FPEs in CM-4 require an atmospheric loop completely isolated from the space station.

The following list of general design criteria, including the support functions assumed to be available from the space station, were used in establishing preliminary EC/LS subsystem configurations. The design metabolic data were selected based on the crew working at a moderately active level.

a. Docking is performed with an indexing capability of $<15°$ (manual connections of space station/experiment module interface lines are used).

b. Pressure in space station and experiment modules (attached) = 14.7 psia (standard air composition).

c. Crew design O_2 consumption = 3.6 lb/man-day.

d. Crew design CO_2 production = 4.1 lb/man-day.

e. Crew design metabolic rate = 1000 Btu/man-hr.

f. Crew design perspiration and respiration rate = 0.55 lb/H_2O).

g. Potable water = 6 lb/man-day.

Table 10-1. Source of EC/LS Functional Support

EC/LS Functions	CM-1 While Attached*	CM-3	CM-4	
			Nominal	Biolaboratory
Air Flow Control	EM/SS	EM/SS	EM/SS	EM
Air Cooling/Heating	EM	EM	EM	EM
Air Purification & Monitoring	SS	SS	SS	EM
Atmospheric Pressure Control	SS	SS	SS	EM
Atmospheric Gas Supply	SS	SS	SS	SS
Pressure Suit Circuit	EM/SS	EM/SS	EM/SS	EM/SS
Water Processing & Supply	SS	SS	SS	SS
Water Storage & Dispensing	SS	SS	SS	EM
Metabolic Waste Collection	SS	SS	SS	EM
Nutrition, Hygiene, & Waste Management	SS	SS	SS	SS

Notes:

SS = Space Station

EM = Experiment Module

*CM-1 does not require EC/LS support while detached (depressurized and unmanned).

h. Shirtsleeve cabin water vapor partial pressure = 8-13 mm Hg.

i. Design cabin air temperature = 75°F.

j. Selectable cabin air temperature range = 65 to 85°F.

k. Design CO_2 partial pressure = 3.0 mm Hg.

l. Space station subsystems are available for:

1. O_2 supply.
2. N_2 supply.
3. Conditioned air supply.

4. Contaminant monitoring.
5. Pump down and pressurization of modules.
6. Alarm and control functions.
7. Suit circuit O_2 and cooling water.
8. Potable water supply.
9. Waste water processing.

10.2 SUMMARY EC/LS DESCRIPTION

Table 10-2 briefly summarizes the EC/LS subsystems in the three common modules. More detailed descriptions are contained in the following sections.

Table 10-2. EC/LS Subsystem Summary

	CM-1 While Attached)	CM-3 Nominal	CM-4	
			FPE - 5.22	Biolaboratory*
Ventilation Mode	Air Interchange	Air Interchange	Air Interchange	Independent Air Purification
Crew Size	2	2	2	2
Weight, lb	146	223	386	728
Power, watts	200	200	300	930

*Subsystem does not include capacity for biospecimens

10.2.1 COMMON MODULE 1. This module supports the astronomy and fluid physics experiments in a free flying mode of operation. While attached to the space station for servicing, the module must be pressurized, and ventilated to provide a shirtsleeve environment. Pressure suit support is also required for some fluid physics experiment operations, as well as emergency maintenance within the module while depressurized. The space station provides these functions through ducts and lines running into the module. In cases where CM-1 docks to a CM-3 these functions are still provided by the space station, but through plumbing running through CM-3.

A diagram of the equipment included in CM-1 is shown in Figure 10-1, and the estimated weights of these components are listed on Table 10-3. The module is ventilated by means of the ducting shown. Air is assumed to be available from the space station

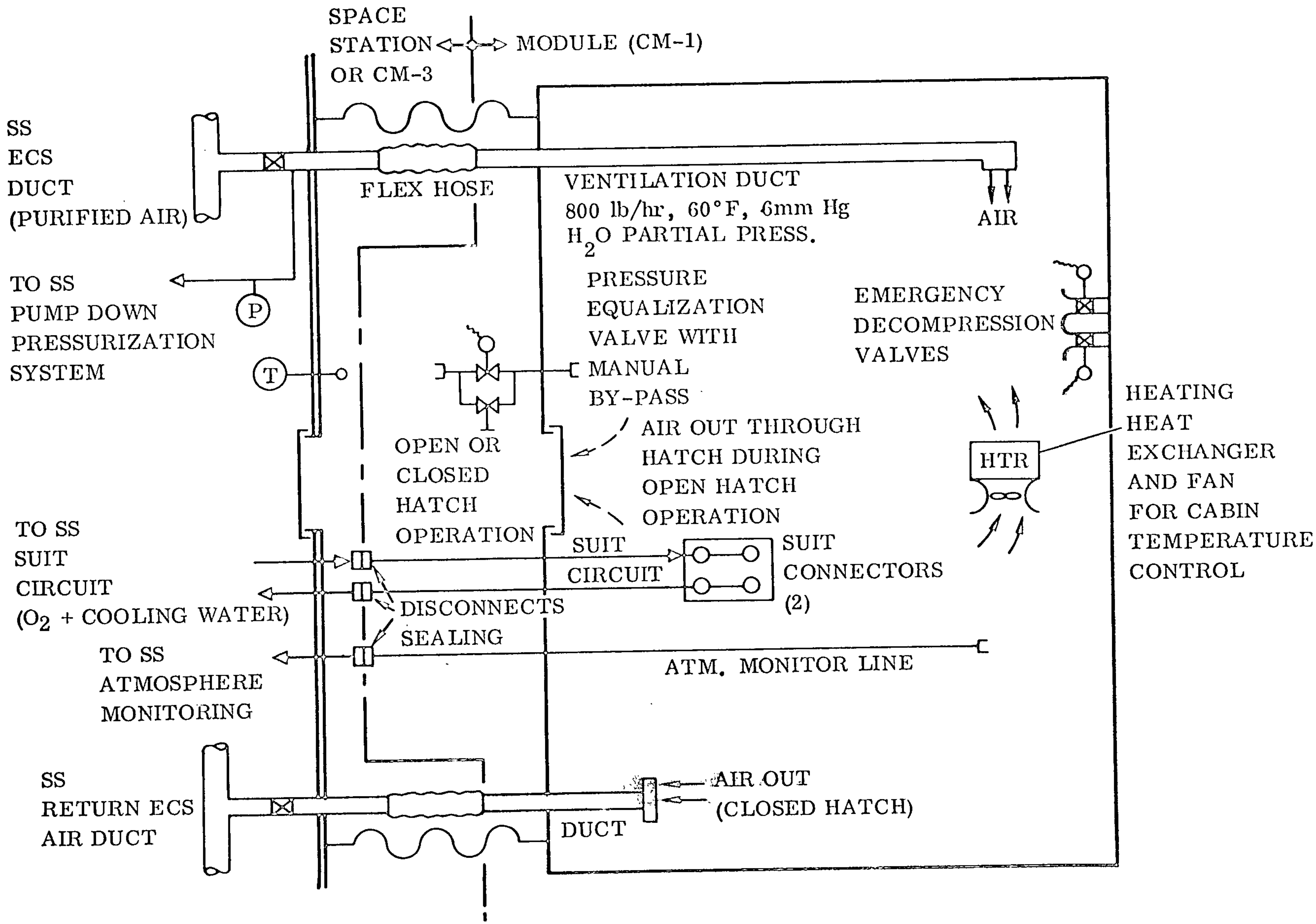

Figure 10-1. CM-1 EC/LS Schematic

Table 10-3. CM-1 & CM-3 EC/LS Components Weight and Power Estimate

Component	CM-1 Dry Weight (lb)	CM-1 Average Power (watts)	CM-3 Dry Wt. (lb)	CM-3 Average Power (watts)
1. Ducting & Supports	32		59	
2. Duct Fittings, Transitions, etc.	12		24	
3. Air Heat Exchanger & Fan	25	50	25	50
4. Pressurization/Pump Down Lines & Hardware	10		36	
5. Gas Sample Lines	3		6	
6. Suit Circuit Lines and Connections	24		24	
7. Light Fixtures	10	150	10	150
8. Decompression Valves	20		20	
9. Fire Extinguisher	8		16	
10. Remote Audible Alarm	2		3	
Totals	146	200	223	200

environmental control system (ECS) downstream of the dehumidifier. This air must be at a relatively constant temperature of 60°F and water vapor partial pressure of 6 mm Hg (see Section 10.3.4 for further discussion). The flow rate required for 2 men is 800 lb/hr, and this air should be at a positive pressure of about 1 to 2 inches of water relative to the space station cabin. The air returns to the space station ECS system one of two ways. During open hatch operation, it returns through the hatch and then enters the space station ECS through the space station air intakes. During closed hatch operation, it enters the space station ECS through the return duct shown in the figure. This return duct also serves as an emergency contamination purge duct for both open and closed hatch operation. In the event of this emergency, the module crew would be evacuated and the hatch closed. If the contamination were not severe, the module air could be processed to remove the contaminants. This would be done by diverting all the return air to the space station contaminant removal system. The allowable process rate for the contaminated air would be quite low but might be adequate to purge the complete module in about 24 hours. This would require that the space station contaminant removal system be capable of processing air from the module at about 7 lb/hr.

Air entering the module is required at 60°F to provide a 65°F to 85°F selectable cabin temperature range. This temperature is achieved and controlled within the module by the heat exchanger (heater) and fan unit. The fan provides air circulation within the module to prevent possible air stagnation.

Atmospheric monitoring of the module air was assumed to be accomplished by the space station system in order to avoid the duplication of this complex equipment. It is anticipated that the space station system will be capable of monitoring a large variety of trace compounds at various locations by drawing air samples from these locations. Thus, one or more of these monitoring lines is run to the module. The lines may be routed within the module to pick up samples at one or more contaminant source areas depending upon the particular experiments being conducted. An exception to this type of monitoring might be the use of local sensors and read-outs for the major constituents such as O_2 or H_2O. Currently, however, no need for such sensors has been identified, especially since free air interchange between the space station and module exists.

Pressurization and module pump-down and venting are provided by the EC/LS equipment in conjunction with the space station. During pressurization, air is supplied from the space station to the service tunnel through the line shown in Figure 10-1. Following pressurization and leak checks of the service tunnel, the pressure equalization valve pressurizes the module via air flow through the service tunnel. The module cabin will be at 70°F prior to docking and therefore raising its temperature to prevent condensation should not be required. Temperature equalization of the service tunnel may be accomplished by air flow through the tunnel. This air flows through the inlet and outlet ducts, valves, and flex hoses. The module side of the duct is sealed by means of caps placed over the duct ends.

Pump down and depressurization of the module is also provided by the space station via the pump-down line. The module is also vented to space vacuum through the space station for final depressurization.

The typical steps of the docking, pressurization, depressurization, and deployment procedure for CM-1 are:

To dock:

a. Pressurize the service tunnel.

b. Leak check the service tunnel by observing its pressure decay and temperature.

c. Open the pressure equalization valve and pressurize the module.

d. Leak check the module by observing its pressure decay.

e. Check the module atmosphere for contamination due to products of outgassing.

f. Open the space station hatch and connect all ducts, fluid lines and electrical lines.

g. Open the module hatch and initiate air ventilation.

To separate:

a. Close the module hatch.

b. Disconnect all lines and cap the ducts on the module side of the service tunnel.

c. Close the space station hatch.

d. Pump down the module and service tunnel.

e. Check for leaks from the space station to module by observing the service tunnel pressure.

f. Vent the module to space vacuum.

g. Separate and deploy the module.

For operation within the module in a pressurized garment assembly, suit circuit lines and connectors are provided. These lines are tied into the space station system to avoid duplication of equipment. The lines and connectors supply both oxygen for breathing and suit ventilation, and water for the liquid cooled garment. The failure of any portion of the suit O_2 circuit while being used can endanger the life of the crew and therefore should be backed up by emergency oxygen units. These units should provide O_2 to the suit for approximately 15 minutes to allow for safe crew transfer to the space station. They are assumed to be part of the space station crew equipment inventory, and would be taken into the experiment modules when required.

10.2.2 COMMON MODULE 3. This common module also has free air interchange with the space station, and supports the FPEs for plasma physics, cosmic ray physics, materials science, fluid physics, and the physics and chemistry laboratory. The EC/LS components for the CM-3 are practically identical to those previously described for CM-1, Figure 10-1. The major difference is that some of the plumbing lines run the full length of CM-3 to provide ventilation and pressurization functions at the end of CM-3 away from the space station. This allows for docking of a CM-1 as in the case of the fluid physics FPE 5.20-2 and for airlock operations such as those required for the remote maneuvering subsatellite. The components for this module are listed in Table 10-3.

The space station EC/LS interface requirements are the same as described for CM-1 in the preceding section, except that 400 rather than 800 lb/hr of ventilating air is acceptable. See Section 10.3.4.

10.2.3 COMMON MODULE 4. This module supports the earth surveys and component test experiments. The latter experiments require airlock operations and therefore, slightly more equipment than for earth surveys. A schematic of this system is shown in Figure 10-2 and the list of components is given in Table 10-4. The components within the nominal CM-4 module perform the same functions previously described for CM-1 and CM-3. These functions rely on space station interfaces for ventilating air (400 lb/hr), pressurization/pump-down, suit circuits, and atmospheric monitoring. Since three separate pressurizable compartments are used in CM-4, three separate air heat exchangers are provided for thermal control of these individual compartments. Also, ventilation ducts, suit circuit lines, and pressurization lines are plumbed to allow depressurized operation of either test cell without affecting the normal shirtsleeve operation of the other test cell or the main cabin.

For the earth surveys experiments, the CM-4 compartments are not individually pressurized and no airlock is included. However, the end dome of the module containing the sensors must be pressurized and pumped down during the servicing cycle. Also, during the removal of sensors in the dome, ventilation air is required. Thus, extension of some ventilation and pressurization lines is required for this FPE.

10.2.4 COMMON MODULE 4 (Biolaboratory Version). The EC/LS design of this module is dominated by the requirement for atmospheric isolation from the space station for the biological experiments (FPE 5.9/5.10, 5.23). The flow schematic and equipment list are given in Figure 10-3 and Table 10-4, and are for support of the crew only. The biolaboratory animal EC/LS system is considered separate and part of the experiment equipment. The crew system is based on a maximum load of two men for 14 hours/day, and a nominal load of about one-half this. The system includes a atmospheric conditioning loop, equipment for waste management and nutrition, washing facilities, and an air heat exchanger and fan for cabin temperature control.

The atmospheric conditioning loop includes contaminant removal filters, a catalytic oxidizer, a condenser/separator, and a vacuum desorbed molecular sieve unit. The flow through this conditioning loop can be diverted for rapid purging and reduction of contaminant levels in the airlock alone. This is done during crew transfer from the module back to the space station. The molecular sieve uses electric heaters and space vacuum for desorption of the CO_2. Thus, CO_2 would normally be vented to space. The amount is less than 10% of the CO_2 being processed for 12 men in the space station oxygen reclamation system. If this loss is not permissable, the space station pump-down system might be designed to operate in conjunction with this unit to provide the required vacuum for desorption. The desorbed CO_2 would then be pumped to the Sabatier reaction oxygen reclamation system aboard the space station. Such a concept would result in weight and power penalties in addition to those shown in Table 10-4. For contaminant removal, charcoal impregnated with phosphoric acid and particulate filters process the main air stream to remove high molecular weight compounds, ammonia, dust particles, and bacteria. The catalytic oxidizer, which oxidizes such compounds as CO and CH_4, is protected by a LiOH pre-filter to prevent catalyst poisoning. A LiOH post filter removes toxic compounds formed in the oxidizer.

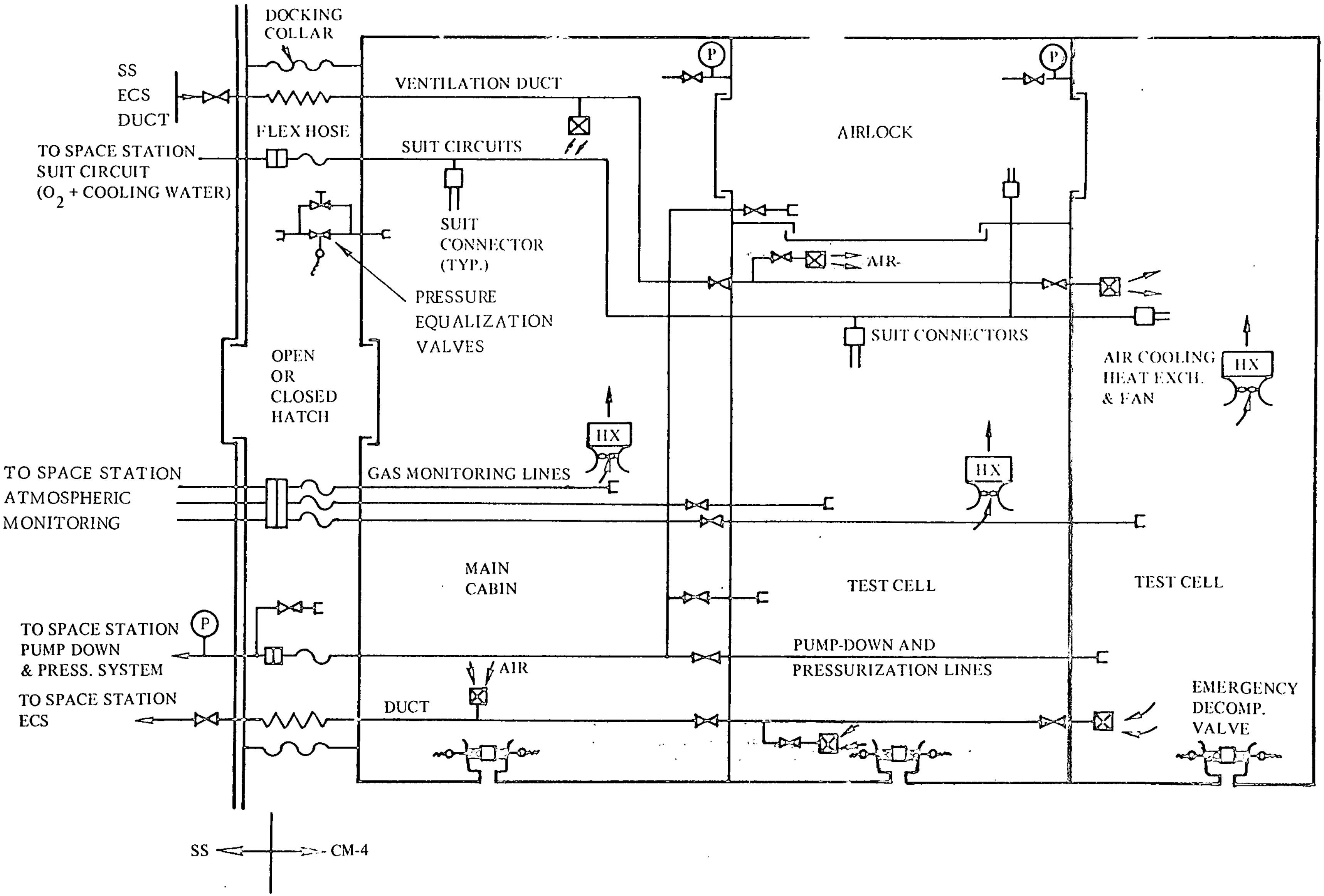

Figure 10-2. EC/LS Schematic for CM-4 (FPE 5.22)

Figure 10-4. CM-4 EC/LS Component Weight and Power Estimates

Component	FPE 5.9/10/23 Dry Wt. (lb)	FPE 5.9/10/23 Average Power (watts)	FPE 5.22 Dry Wt. (lb)	FPE 5.22 Average Power (watts)	FPE 5.11 Dry Wt. (lb)	FPE 5.11 Average Power (watts)
Ducting & Supports	75	0	75	0	90	0
Duct Fittings, & Valves, etc.	22	0	52	0	36	0
Pressurization/Pump-down Hardware	39	0	51	0	40	0
Gas Sample Lines	6	0	9	0	6	0
Suit Circuit Lines & Connections	50	0	50	0	50	0
Light Fixtures	20	200	20	200	20	200
Decompression Valves	20	0	50	0	20	0
Fire Suppression Equipment	19	0	19	0	19	0
Cabin Heat Exchanger & Fan	50	80	60	100	50	80
Subtotals	301	280	386	300	331	280
Molecular Sieve	100	400				
Condenser/Separator	40	0				
Blowers	10	125				
Catalytic Oxidizer	25	125				
Oxidizer Pre-filter (1/2 yr)	8	0				
Oxidizer Post-filter (1/2 yr)	6	0				
Charcoal Filters (1/2 yr)	130	0				
H_2O Holding Tanks & Hardware	6	0				
Waste Collector & Storage	46	(90)				
Water Dispenser	10	0				
Coolant Lines	14	0				
H_2O Transfer Lines & Fittings	12	0				
Wash Facility	20	(40)				
Subtotals	427	650				
Totals	728	930	386	300	331	280

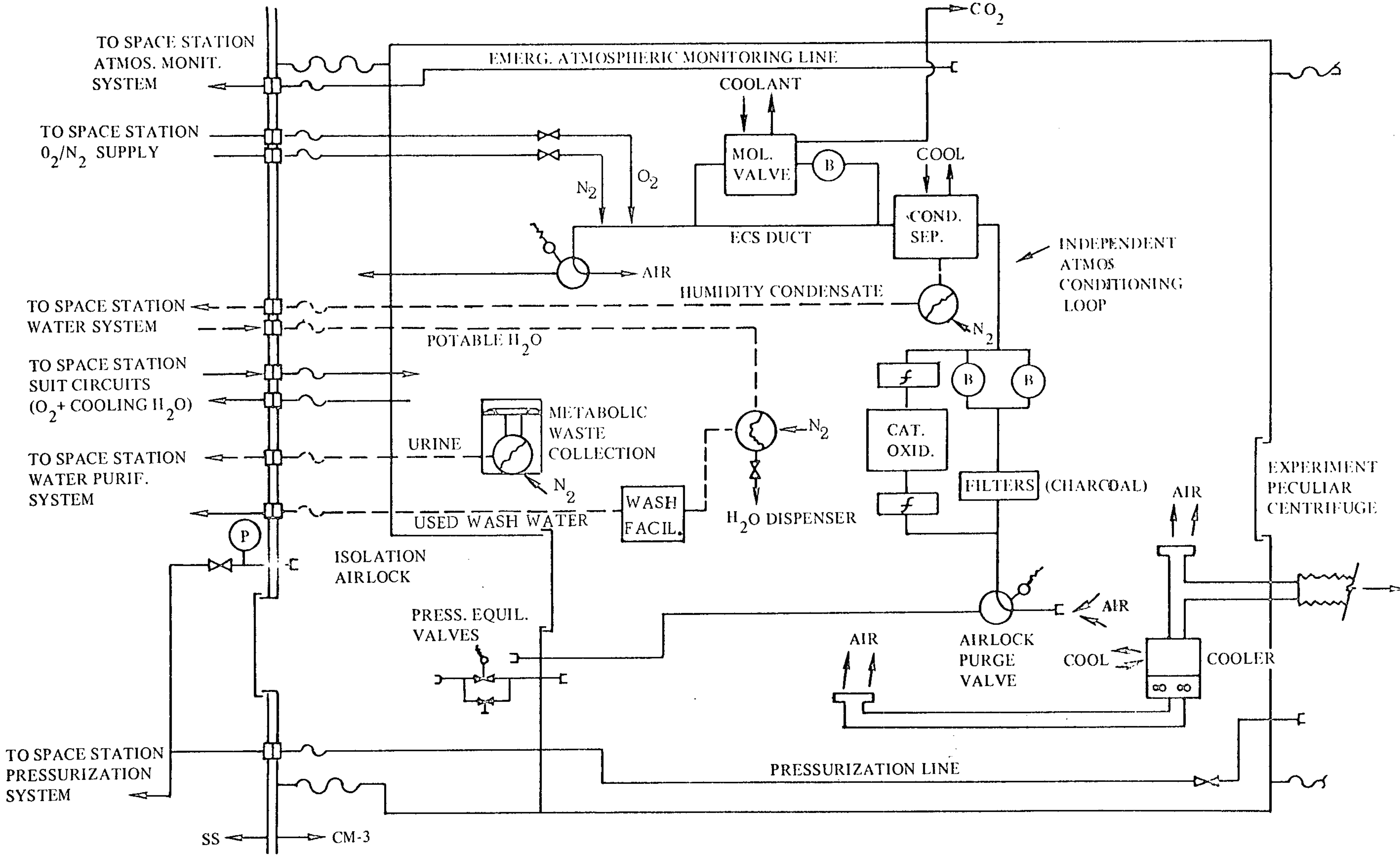

Figure 10-3. EC/LS Schematic for CM-4, Biolaboratory

A waste collection unit is provided for crew micturation and defecation when required. Liquid urine is stored in a batch transfer tank, which is periodically emptied into the space station urine purification system. Dry fecal collection using air entrainment is provided with temporary holding storage planned. Long term fecal management could utilize the anticipated long term waste storage system for the animals in the biolaboratory. The quantity of feces from occasional crew defecation should be small compared to that from the animals, since animal loads equivalent to about four men are anticipated. Also, it is expected that crew duty cycles would be scheduled so that waste management activities would normally take place in the space station.

Potable water is fed to the laboratory for drinking, washing, and occasional food reconstitution. Normal crew hygiene and nutrition will take place in the space station. In the biolaboratory, water is held in a positive expulsion tank and metered to the crew or fed to the wash water facility on demand. The type of wash facility used will depend upon the experiment requirements for hand and body cleansing and sterilization. For the present system, a sponge type unit was assumed, to be used in conjunction with dry wipes.

The biolaboratory system also includes a cooling heat exchanger, fans, and ducting for cabin ventilation and temperature control. Since the centrifuge compartment must also be served by the atmospheric purification loop in the main compartment, the ventilation duct extends into the centrifuge compartment. Air returns from the centrifuge through the interconnecting hatchway.

For the biolaboratory, space station interfaces include supply of both N_2 and O_2. For a total leakage of 2.5 lb/day, the N_2 required would be 2.0 lb/day (some of this would be added through venting of batch expulsion tanks). Oxygen required for leakage make-up is 0.5 lb/day and about 1.5 hr/day estimated for crew breathing and contaminant oxidation. Additional metabolic O_2 for the experiments is estimated at 8 lb/day, maximum. Humidity condensate flow to the space station and crew potable water from the space station are estimated at 10 lb/day. Urine and flush water will be about 12 lb/day. Experiment gas analysis equipment will be normally used to monitor the module atmosphere.

10.2.5 SCALING PARAMETRICS. EC/LS properties for most of the experiment modules are not easily scaled since they depend upon independent variables that are not readily quantitatively stated, such as module configuration. Figure 10-4, however, shows the weight of these EC/LS subsystems as a function of crew size.

The properties of the independent EC/LS subsystem in the biolaboratory are primarily a function of mission duration and crew size. The weight, volume, and power of this system is parametrically plotted in Figures 10-4 and 10-5.

10.2.6 DESIGN ALTERNATES. In general, the module EC/LS is highly dependent on the space station in order to avoid duplication of space station equipment and capacity.

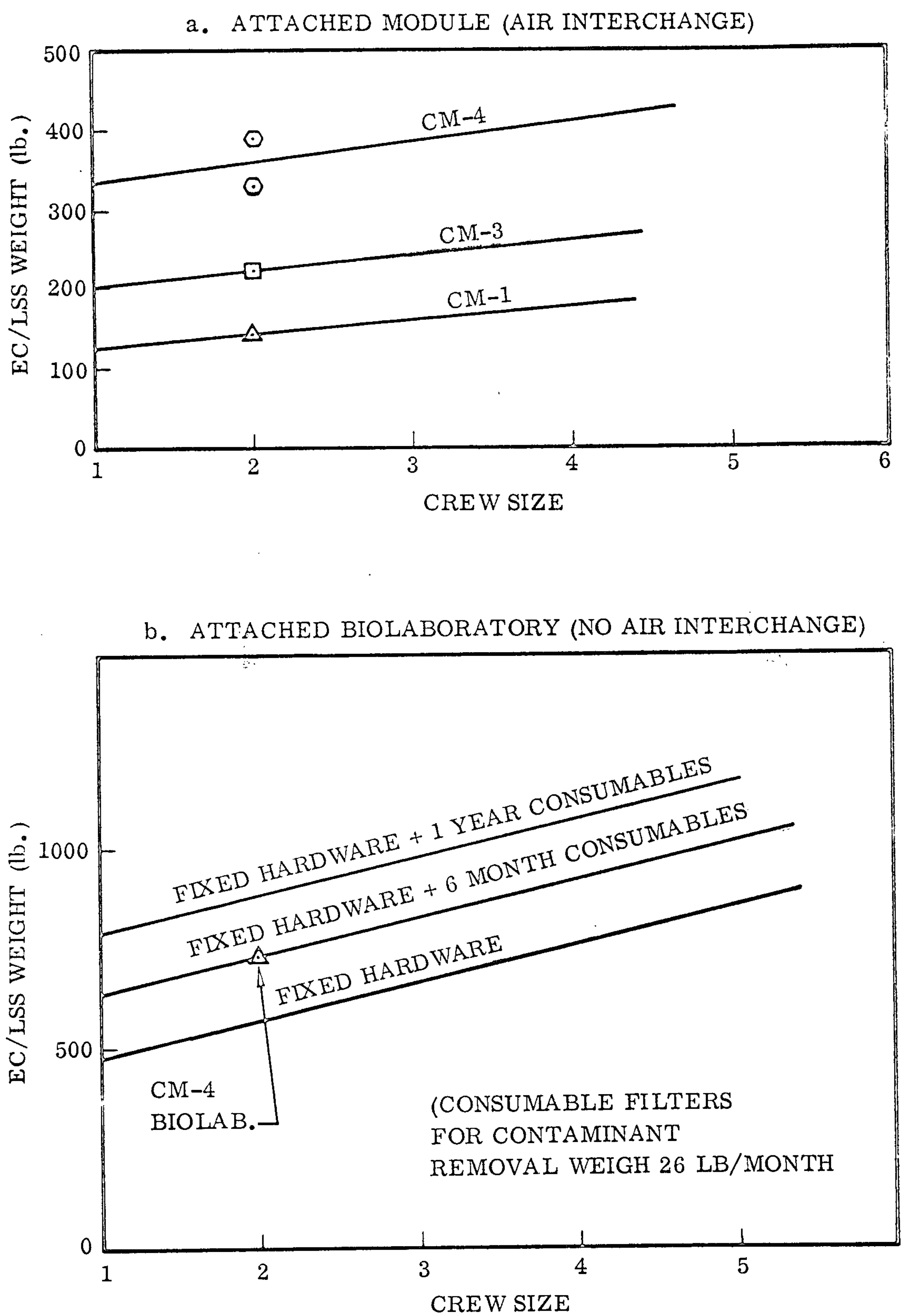

Figure 10-4. Estimated Module EC/LSS Weight Scaling Curves

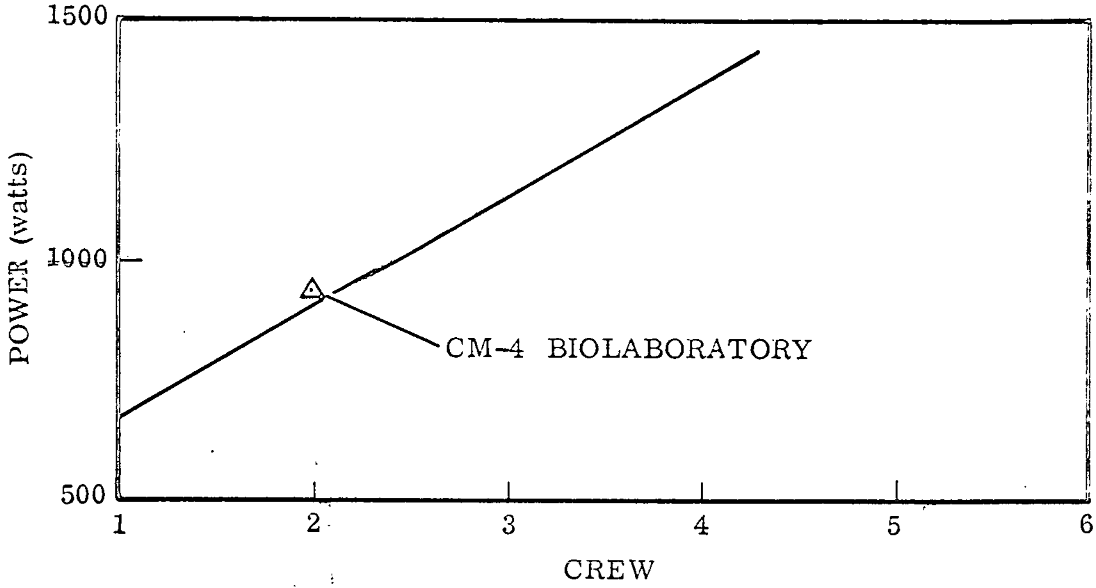

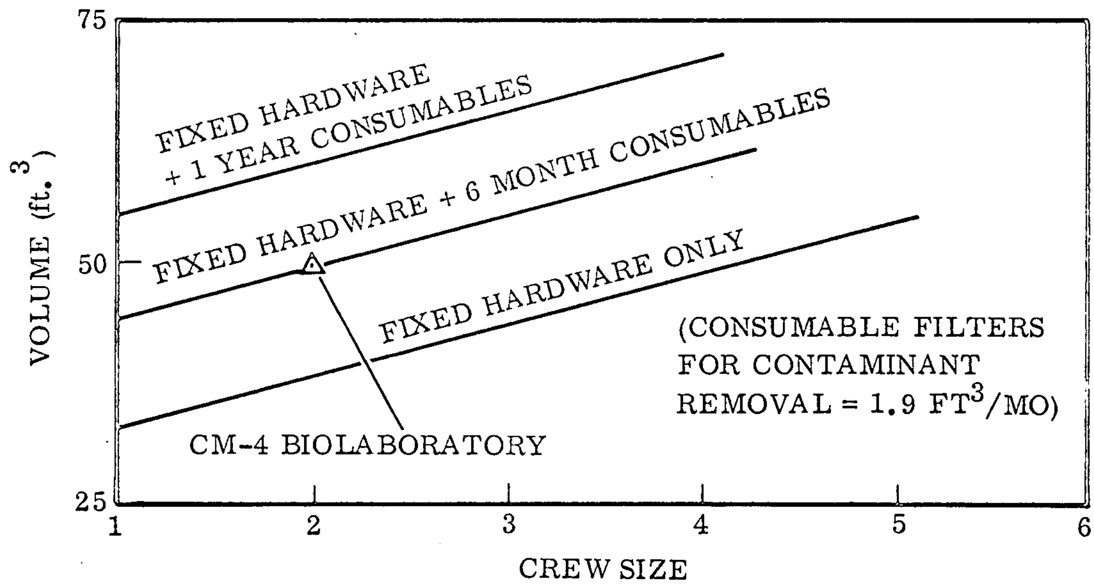

Figure 10-5. Estimated EC/LSS Power and Volume Scaling Curves for the Biolaboratory Module

Most alternate design concepts involve a greater degree of independence from the space station, and might result from expanded FPE requirements or incompatible equipment in the space station EC/LS subsystem.

As in the case of the biolaboratory, independent equipment might be needed for dehumidification, CO_2 removal, contaminant removal, and partial water and waste management. It is likely that some FPE will require pure water or high capacity contaminant removal equipment for certain experiments. Pressurization gas supply and control could also be made independent but at the cost of overall penalties because of equipment duplication. This would include oxygen and nitrogen storage vessels and the pump-down system. Life support functions such as nutrition, personal hygiene, and water purification are not likely to be provided by an independent module system.

Further discussion of the design alternates is contained in the following section on design analysis.

10.3 EC/LS DESIGN ANALYSIS

A discussion of some of the more pertinent EC/LS analyses that are not routine are presented below. These include (1) comparison of module atmospheric pump-down to venting, (2) module decompression times, (3) comparison of a molecular sieve to lithium hydroxide for CO_2 removal, (4) ventilation considerations, and (5) experiment contaminant control.

10.3.1 MODULE PUMP DOWN. The free-flying modules must be depressurized before deployment and repressurized before crew servicing. Two ways of implementing this pressurization cycle were considered. The first assumed air pressurization from the space station cryogenic storage system and subsequent dumping of this gas to space. The second approach was to pump the module down to a relatively low pressure before venting to space, thus conserving most of the gas for re-use.

The primary penalty associated with dumping gas is the make-up cryogenic O_2 and N_2 that must be supplied by the space station. A summary of the weight of this gas is given in Table 10-5. The free-flying FPEs are listed along with currently assumed docking frequency and total weight of gas dumped over two years. For the free-flying non-cryogenic fluid physics experiments (5.20-2) only three months of experiments were assumed to be run over the two-year period (see Table 10-5). The total number of dockings for two years is 124, resulting in 19,600 pounds of gas.

Assuming a 90-day resupply period, the resulting net gas required is 2,450 lb/90 days. The cryogenic storage vessels to hold this gas would weigh approximately 1,000 pounds. These weights represent a large storage and logistics penalty on the space station system.

Table 10-5. CM-1 Repressurization Requirements

FPE	EXPERIMENT	DOCKING FREQUENCY	ASSUMED NO. OF REPRESS. FOR 2 YRS.	TOTAL O_2-N_2* WEIGHT REQUIRED FOR 2 YRS.
5.1	X-Ray Telescope	1/2 mo.	12	1,900
5.2A	Adv. Stellar Astr.	1/2 mo.	12	1,900
5.3A	Adv. Solar Astr.	1/2 mo.	12	1,900
5.3A	Adv. Solar Astr.	1 mo.	24	3,800
5.5	Hi-Energy Stellar	1 mo.	24	3,800
5.20-2	Fluid Physics	40/3 mo.	40	6,300
	TOTALS		124	19,600

Total gas to be resupplied every 3 months = 2450** lb/3 mo.

* Based on a net loss of 2100 ft^3 pressurizable volume of CM-1, or 158 lb per docking.

** Requires about two cylindrical cryogenic vessels, each 3 ft dia. × 8 ft long, to be refilled every three months (approximate weight of vessel is 40% of fluid weight or 1000 lb for two vessels).

The major penalty associated with the alternate pump down procedure is the power required to accomplish the pump down in a reasonable period of time. This was investigated assuming that the module atmosphere could be pumped into the space station without the resulting pressure rise upsetting the station subsystems. This assumption may be invalid and should be investigated further. However, within the assumption the pump down time and power are not prohibitive. The results, as shown in Figure 10-6, indicated that a 1.5 hp vane pump (1100 watts) would provide pump down of 1000 ft^3 to about 1 psia in two hours. This corresponds to about 2.3 kW for two hours for the 2,100 ft^3 net volume of CM-1, which would be required approximately 124 times over two years as indicated in Table 10-5 (286 kW-hr/yr). Considering the guideline value of 25 kWs available on the SS (219,000 kW-hr/yr), the pump down power appeared reasonable and this technique was selected for use.

10.3.2 DECOMPRESSION TIMES. In order to evaluate the times available for emergency engress from the modules into the space station, depressurization times for various hole sizes were computed; see Figure 10-7. The curves are based on a 1000 ft^3 volume but are linearly related to other volumes. The smallest current

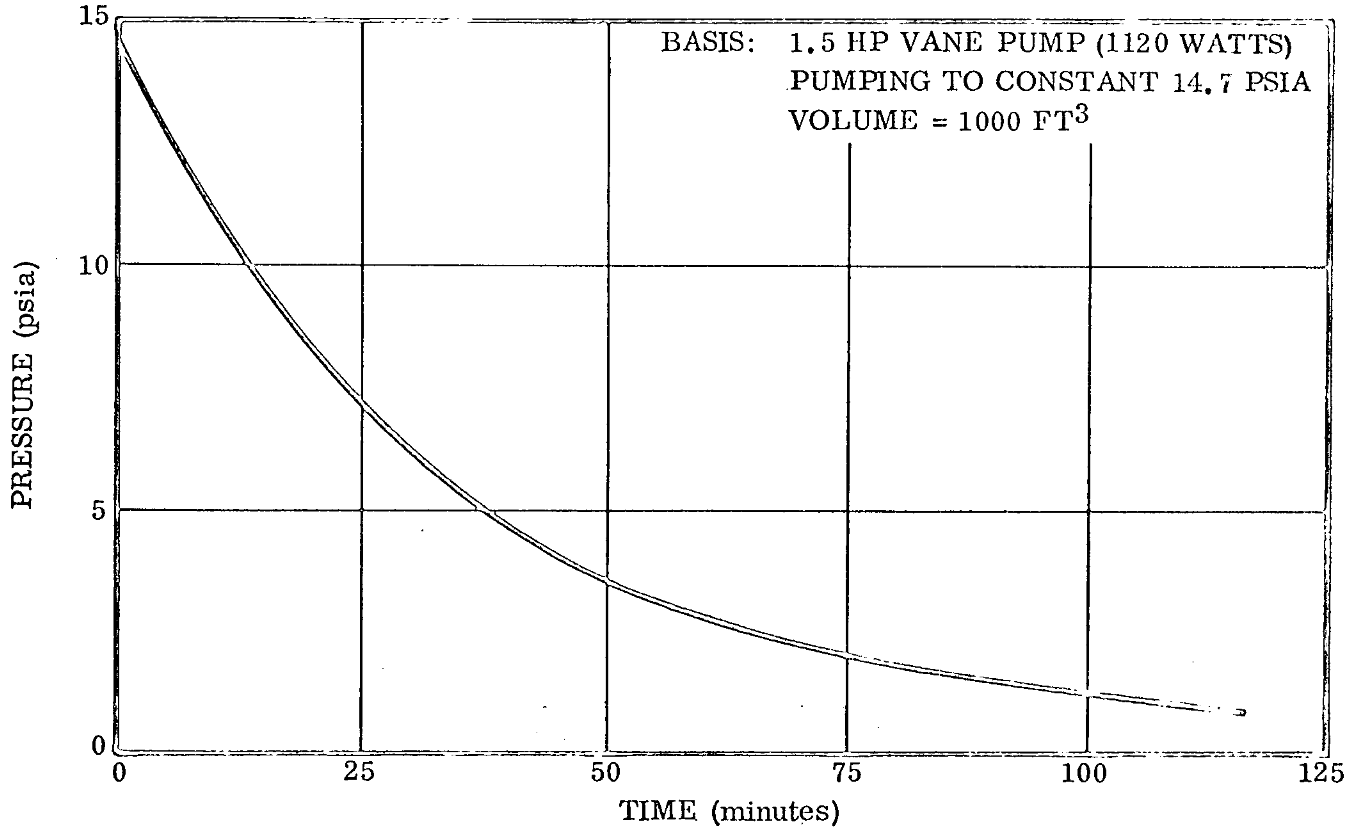

Figure 10-6. Estimated EM Pump Down Characteristic

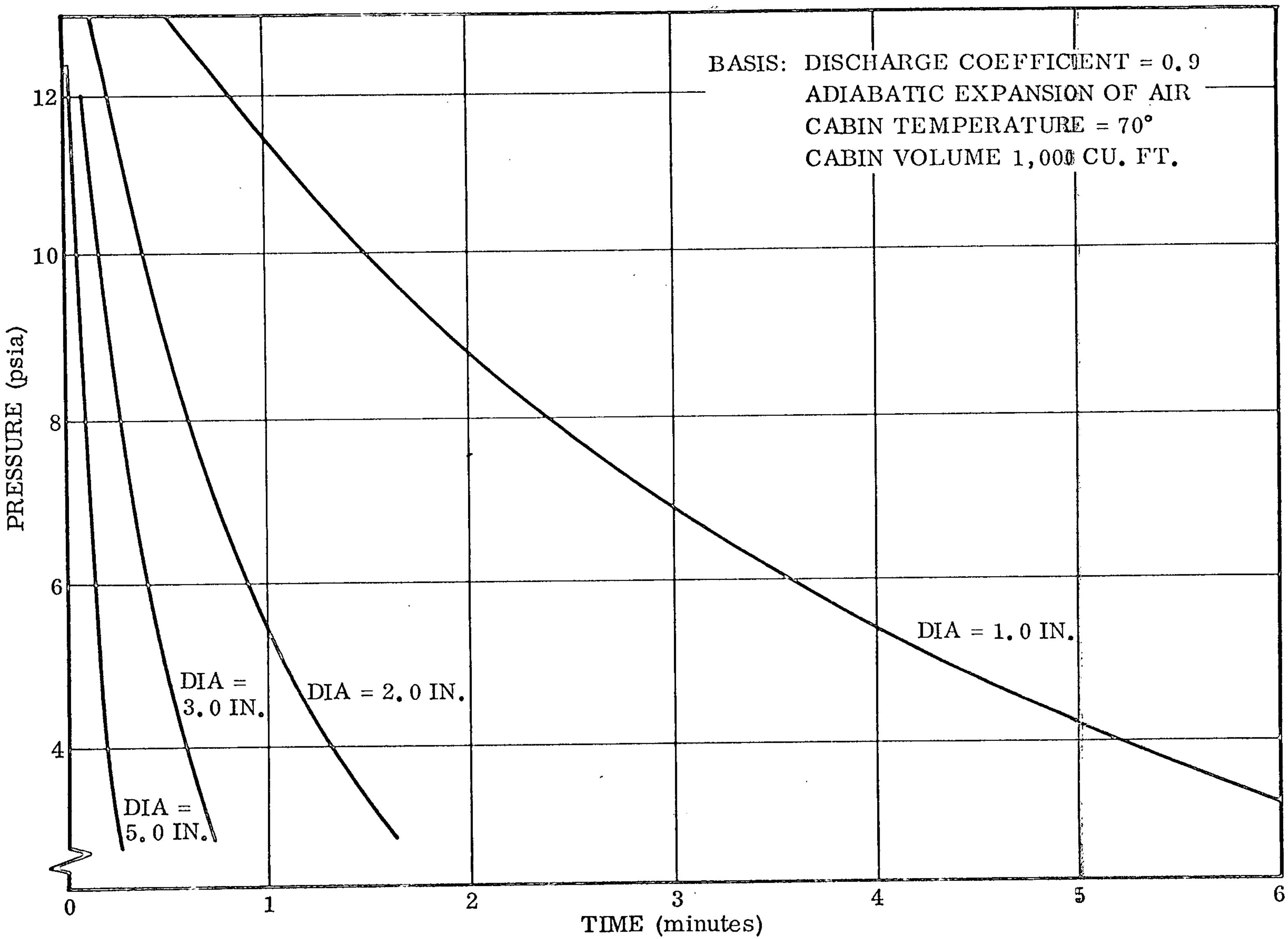

Figure 10-7. Cabin Pressure Decay for Various Hole Sizes

pressurizable module volume is about 2100 ft^3. Thus, a two-inch-diameter hole could be sustained and it would take about two minutes to decay to 6 psia, where positive pressure breathing gear must be used. Also, the modules are ducted to the much larger space station atmosphere and this would tend to increase the decompression times.

10.3.3 CO_2 REMOVAL TECHNIQUE. For the biological FPEs, CO_2 must be removed from the crew compartment within the module, which is atmospherically isolated from the space station. The best known and best developed systems for doing this are those using (1) LiOH and (2) molecular sieve adsorbents.

LiOH is generally favored for shorter missions on the order of 60 man-days because of its simplicity, reliability, and low power requirement. Typical properties of LiOH are shown in Table 10-6, which gives a weight penalty of 2.8 lb/man-day.

For a 16 man-hr occupancy per day of the biolaboratory over two years, this results in 1360 pounds.

The alternate approach is to use a regenerable molecular sieve. A sieve for two men that saves water but dumps CO_2 was estimated to weigh 100 pounds and require 400 watts. Using a solar cell regulated power penalty of 600 lb/kW*, the equivalent weight penalty for power is 240 pounds.

Table 10-6. Properties of LiOH

1.	Reaction $2\ LiOH + CO_2 = Li_2\ CO_3 + H_2O$ $48 + 44 = 74 + 18$	
2.	CO_2 Rate (lb/m-d)	2.12
3.	LiOH Reacted (lb/m-d)	2.31
4.	Approximate Percentage of LiOH Reacted	90
5.	LiOH Required (lb/m-d)	2.57
6.	Weight Allowance for Canister and Filters (%) (lb/m-d)	10 .26
7.	Total Weight Required (lb/m-d)	2.83

*Study for Basic Subsystem Module Preliminary Definition, Final Report, Vol. VI, Convair Division of General Dynamics Report GDC-DAB67-003, October 1967.

Since the total equivalent weight penalty for the molecular sieve (340 pounds) is substantially less than that for LiOH (1360 pounds), it was selected for use. The weight penalty difference is large enough to neglect minor penalties such as blower power for the LiOH, heat rejection penalties for both systems, and water balance penalties. Neither system may be credited with CO_2 conserved for O_2 reclamation.

10.3.4 MODULE VENTILATION. Ventilating air is required from the space station to maintain a shirtsleeve environment in the modules. The air flow must be sufficient to remove CO_2 and water vapor and maintain these constituents within acceptable levels. The air flow must also be sufficient to supply breathing oxygen and remove trace contaminants, but these requirements are generally satisfied if the former two requirements are satisfied. An exception to this would be the gross introduction of trace contaminants from experiments, which is discussed in Section 10.3.5.

Of the two requirements for CO_2 and H_2O removal, the latter will generally dominate in the selection of the air flow.

The air flow to maintain each of these constituents is shown in Figure 10-8. For water vapor removal, the flow depends upon the inlet and outlet H_2O partial pressure and the H_2O introduced into the module. The most stringent requirement is for CM-1, which houses optical equipment requiring a dry atmosphere to prevent contamination of the optical surfaces. Although the specific requirement has not been established, the current guideline being used is to maintain the cabin relative humidity below 40% at 70°F. This corresponds to a water vapor partial pressure of 7.5 mm Hg. To satisfy this requirement, very dry air must be available from the space station. It was assumed that this air would be available at 6 mm Hg. This could be achieved by using a low temperature condenser to obtain air at a dew point of 39°F. Under these conditions, an air flow of 800 lb/hr will maintain the module at less than 7.5 mm Hg with a two-man work crew. This ventilation rate was used for CM-1.

To satisfy the humidity requirements for crew habitability, the limit on outlet partial pressure is 13 mm Hg, much higher than the 7.5 mm Hg required for CM-1. This applies to CM-3 and CM-4, and for these modules a ventilation flow of 400 lb/hr was selected. This will adequately remove the crew latent load while maintaining the cabin humidity between 8 and 13 mm Hg. For these modules air supplied to the modules could contain up to 8 mm Hg of water vapor.

Referring to the plots for CO_2 in Figure 10-8, the air flow required again depends upon the inlet and outlet concentrations and the CO_2 introduction rate by the crew. The CO_2 content of the air leaving the module is limited to the design cabin level of 3.0 mm Hg. This air will either return to the space station cabin, which is designed to contain CO_2 at a partial pressure of 3.0 mm Hg, or enter a space station environmental control return duct where the CO_2 level will also be 3.0 mm Hg. The CO_2 content of the air entering the module will depend upon the removal efficiency of the space station CO_2

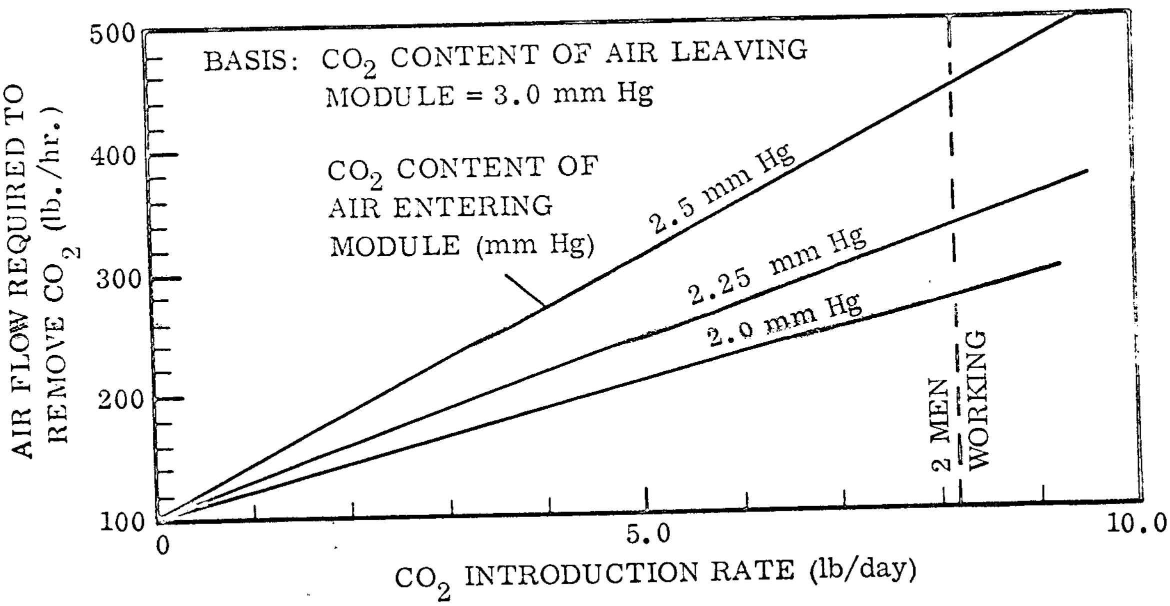

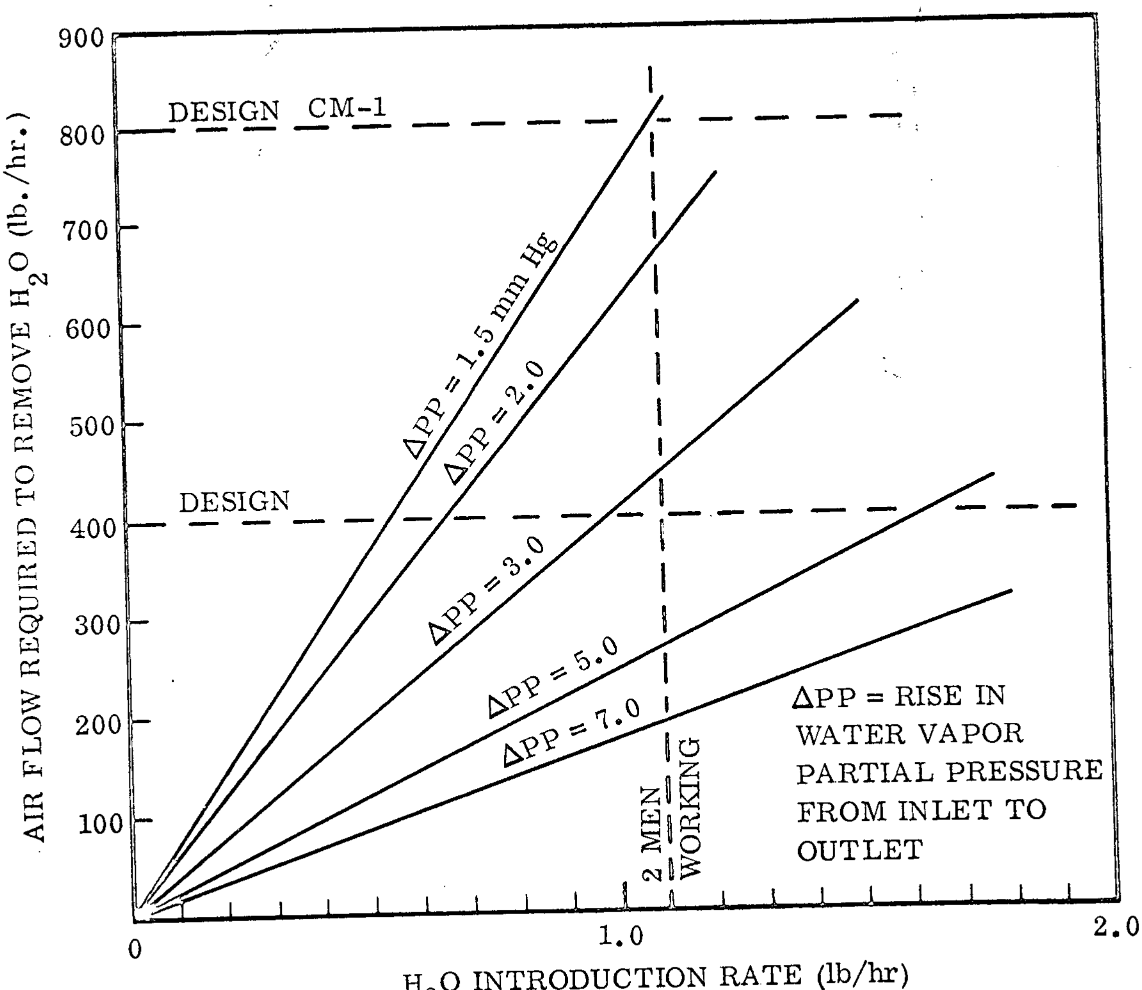

Figure 10-8. Air Flow Required to Remove CO_2 and Water Vapor from the Experiment Module

removal unit, and the bypass flow ratio through this unit. Figure 10-6 indicates that at an airflow of 400 lb/hr, an inlet CO_2 partial pressure of about 2.5 mm Hg would be adequate to maintain the module CO_2 level at 3.0 mm Hg.

Besides the absolute humidity and flow rate of the air entering the module, the temperature was also considered. The two options were (1) to accept air at constant temperature, or (2) specify a variable selectable temperature corresponding to crew desires. The latter choice requires an independent temperature control system in the space station responding to demands of the module. The former approach was considered to be more practical since it places the control requirements on the module and more closely adheres to the philosophy of the module being independent of the space station. It will, however, impose a heat load on the space station heat rejection system. The reason for this is that the air entering the module must be at about 60°F to satisfy the minimum selectable cabin air temperature of 65°F. Thus, if the crew desires a higher cabin temperature, the return air to the space station will be at this higher temperature and will therefore impose a heat load on the space station cabin air circuit. The magnitude of the load depends on the air flow rate and selected cabin temperature and can be determined from Figure 10-9. For example, if the crew on CM-1 with 800 lb/hr of ventilation air selects 70°F (ΔT = 10°F), the heat added to the air would be about 2000 Btu/hr. About half of this is from the crew metabolic heat output. The rest is supplied indirectly from cold plated equipment by means of a cabin heating heat exchanger. In the case of CM-1, the requirement for a heating heat

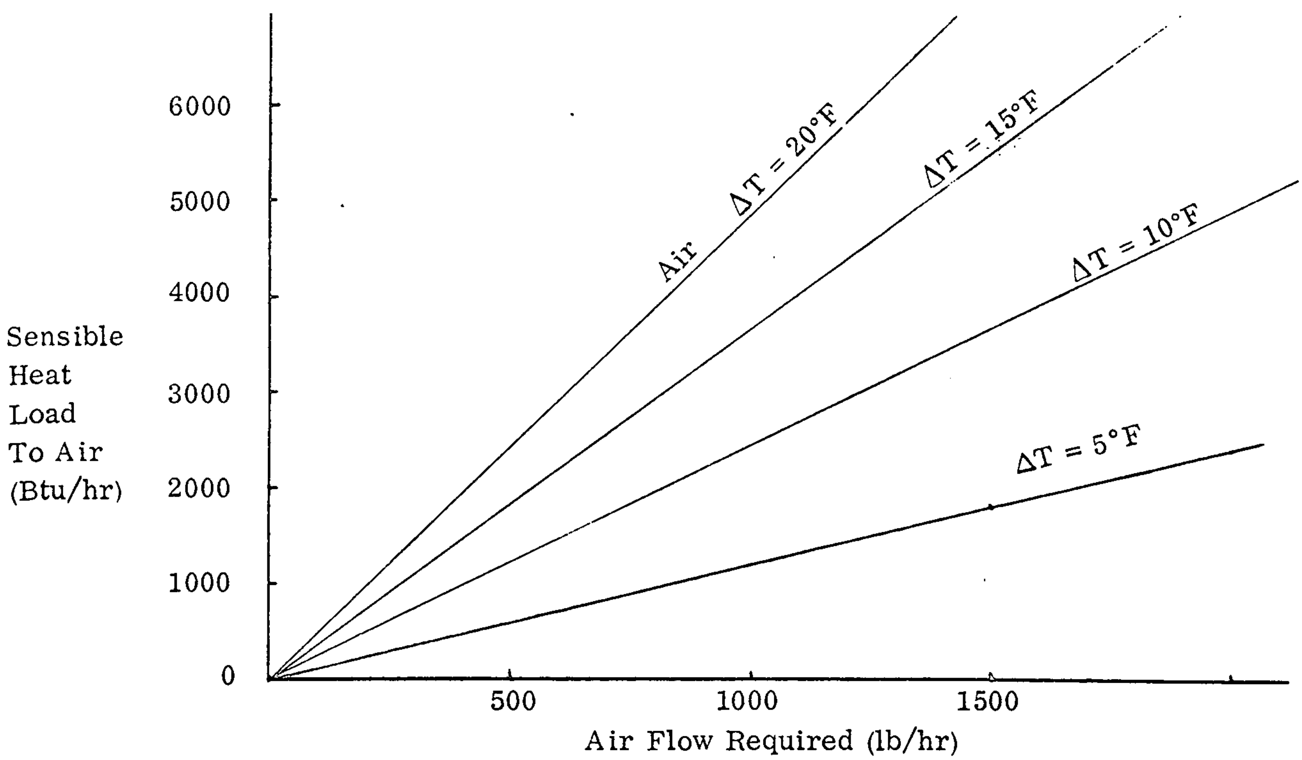

Figure 10-9. Ducted Air Heating Requirements

exchanger is anticipated since the electrical loads in this module are almost 100% cold plated with insulation preventing heat losses to the cabin; see Section 9. This is required because of the depressurized mode of operation while free flying. In the case of both CM-3 and CM-4, the cold plating is not expected to be so thorough and more heat will be rejected to the cabin air. In these modules, a cabin air cooler will probably be required. These requirements cannot presently be precisely stated because module experiment heat loads and their mode of cooling is currently not exactly known. However, when cooling loads on air and liquid circuits are established, heat exchange concepts can readily be adapted to provide adequate temperature control.

Shown in Figure 10-10 are various duct sizes to accommodate the air flow from the space station to the module. Small ducts (high velocities) are desirable to minimize weight and volume within the docking collar. Conversely, large ducts produce less noise and lower pressure drop. A moderate value of about 1400 fpm velocity was used in the modules, resulting in ducts of about 10 to 20 square inches in cross section. Further size reduction in ducts would require condenser/separator hardware to be placed within the modules and this would probably not trade off favorably against the current duct size utilizing the existing condenser system in the space station.

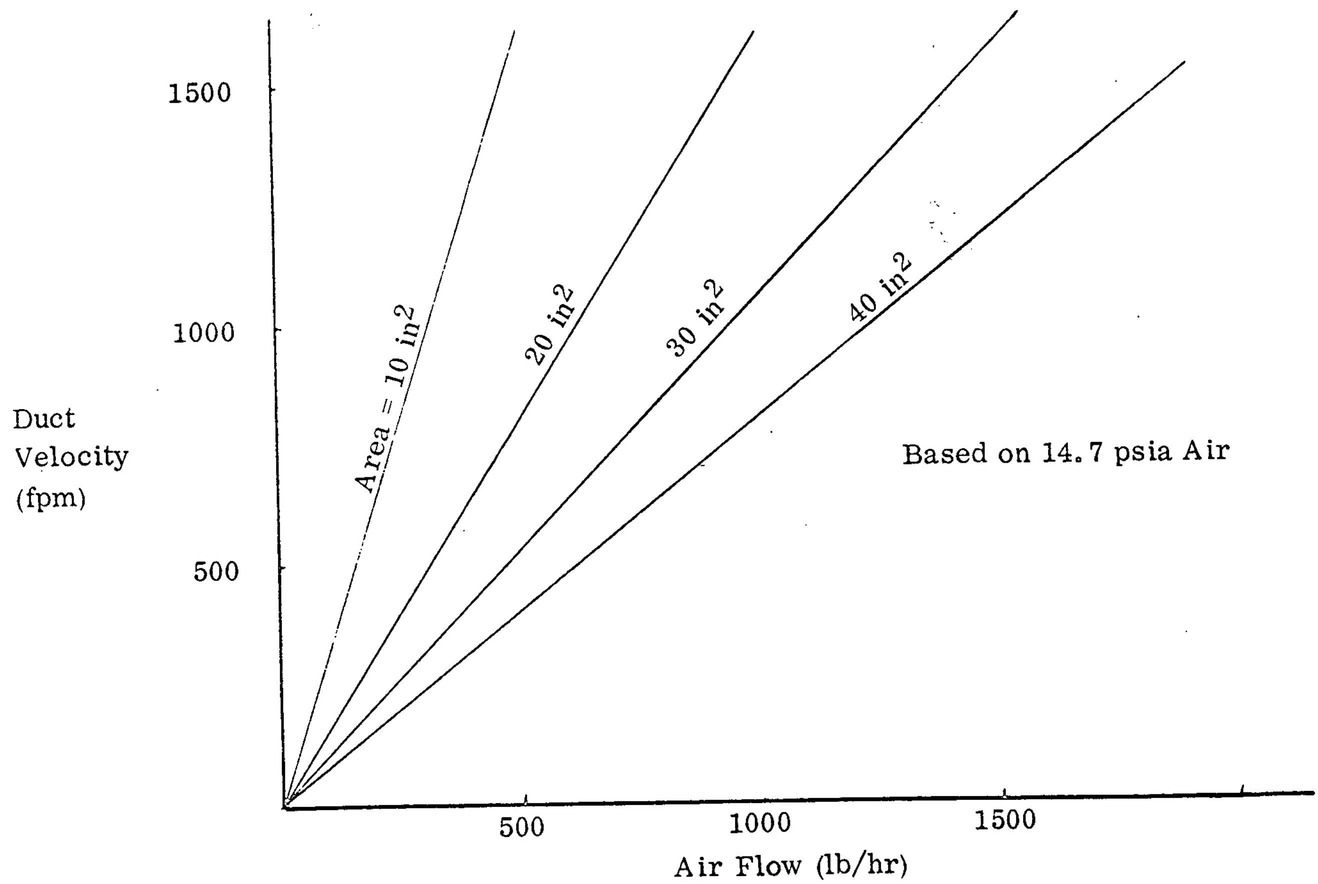

Figure 10-10. Ventilation Duct Velocity

10.3.5 EXPERIMENT CONTAMINANT CONTROL. Control of contaminants generated in various experiments, including high temperature molten materials, presents a problem for further study. This is an identified supporting research technology item. Types and quantities of contaminants should be tabulated and removal techniques should be studied. The resulting system may possibly become quite large since it is currently required that no deleterious contaminants be vented to space from the modules while attached to the space station. Hence, all experiment atmospheric gases including those from a melting furnace must be processed for contaminant removal. Depending upon the various FPE requirements, this equipment might be considered experiment peculiar. Such environments might also be vented to the space station contaminant removal system. This system may be similar to the system used for the biolaboratory and include activated charcoal, particulate filters, LiOH and a catalytic oxidizer. Such a system can remove a very large variety of contaminants, probably including all that might be generated by experiments. However, its capacity would have to be sized to accommodate the increased load.